Vertical Profiles of Radioisotopes, Contaminants, Nutrients and Diatoms in Sediment Cores from the Tidal Christina River Basin: A Historical Analysis

Patrick Center for Environmental Research - The Academy of Natural Sciences

College of Earth, Ocean and Environment - University of Delaware

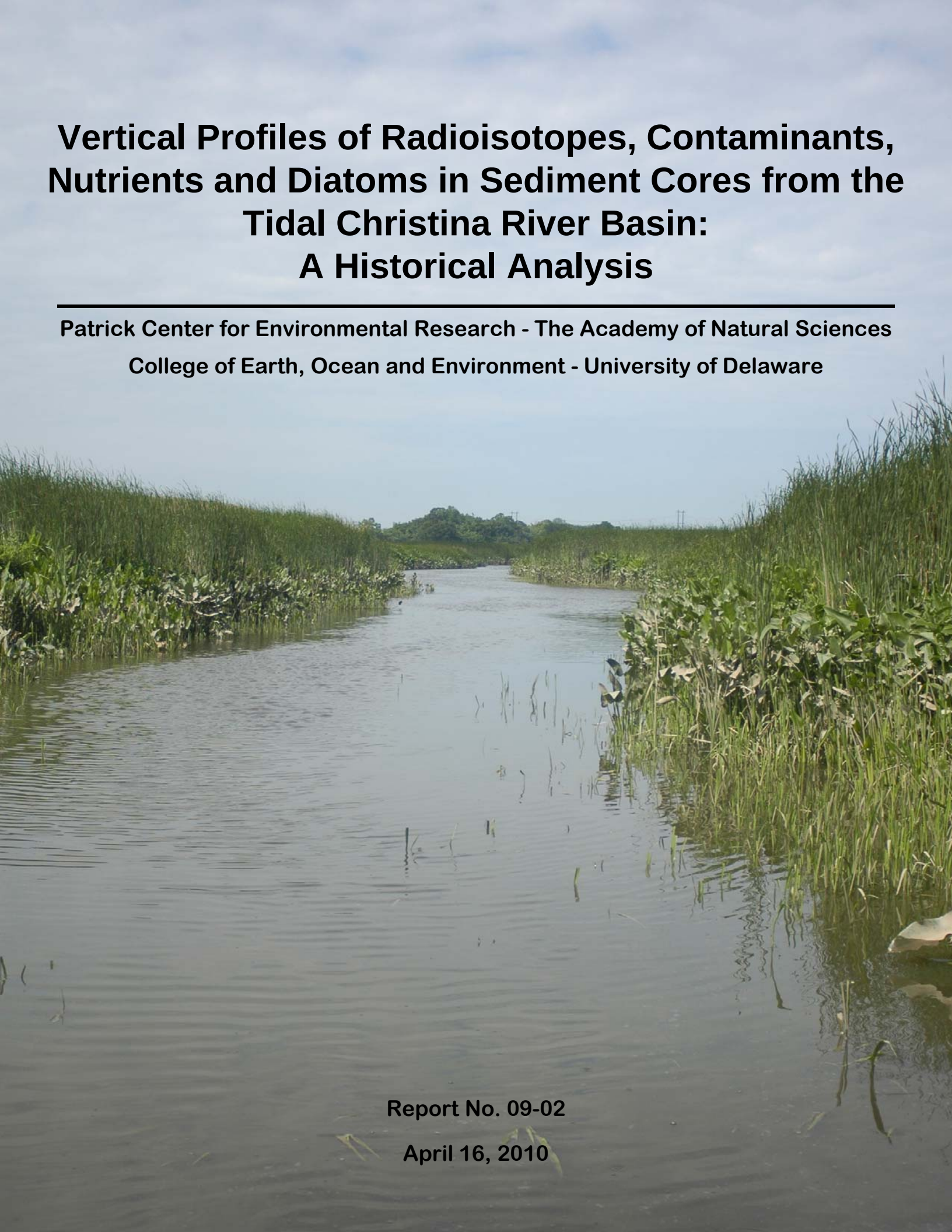

Report No. 09-02

April 16, 2010

FINAL REPORT

to

Dr. Richard Greene
Delaware Department of Natural Resources and Environmental Control
Division of Water Resources
Watershed Assessment Branch
820 Silver Lake Blvd., Suite 220
Dover, DE 19904-2464

Vertical Profiles of Radioisotopes, Contaminants, Nutrients and Diatoms in Sediment Cores from the Tidal Christina River Basin: A Historical Analysis

PCER Report No. 09-02

By
Drs. David Velinsky, Christopher Sommerfield[1] and Don Charles
Patrick Center for Environmental Research
The Academy of Natural Sciences
Philadelphia, PA 19103

[1]University of Delaware
College of Earth, Ocean and Environment
Lewes, DE

April 16, 2010

TABLE OF CONTENTS

Page

List of Tables iii
List of Figures iv
Executive Summary v

A
Introduction **1**
A1 Background 1
A2 Objectives of Study 1
A3 Study Area 2

B
Field and Laboratory Methods 3
B1 Field Sampling 3
B2 Laboratory Methods 4
B2.1 Organic Contaminants 4
B2.2 Iron (Fe) and Zinc (Zn) 5
B2.3 Radioisotope Measurements and Sedimentation Rates 5
B2.4 Total Organic Carbon and Nitrogen 7
B2.5 Total Phosphorus 7
B2.6 Stable Isotopes of Carbon and Nitrogen 7
B2.7 Diatoms 7

C
Results and Discussion 8
C1 Sediment Properties and Sediment Accumulation 8
C1.1 Sediment Properties 8
C1.2 Accretion and Sediment Accumulation Rates 9
C1.3 Radionuclide Inventories and Focusing Factors 11
C2 Nutrients/Eutrophication 13
C2.1 Sediment Total Carbon, Total Nitrogen and Total Phosphorus 13
C2.2 Stable Isotopes of Carbon and Nitrogen 15
C2.3 Diatom Analysis and Assemblages 17

C3 Sediment Bound Contaminants 21
C3.1 Polycyclic Aromatic Hydrocarbons 22
C3.2 Polychlorinated Biphenyls 28
C3.3 Total DDX and Chlordane 33
C3.4 Polybrominated Diphenylethers (PBDEs) 36
C3.5 Dioxins and Furans 38
C3.6 Iron and Zinc 40

TABLE OF CONTENTS (cont)

Page

D
Summary and Conclusions.....45

E
Acknowledgments.....48

F
References.....49

G
Tables.....61

H
Figures.....80

I
Appendices.....118

Appendix I: Data Tables and QA Documentation.....I

LIST OF TABLES

Table 1: Core Locations and collection dates 62
Table 2: Bulk sediment properties and radioisotope data for core BW 63
Table 3: Bulk sediment properties and radioisotope data for core CM 64
Table 4: Bulk sediment properties and radioisotope data for core LSP 65
Table 5: Bulk sediment properties and radioisotope data for core DM 66
Table 6: Summary data for radioisotope analysis and dating 67
Table 7: Concentrations of various parameters for core BW 68
Table 8: Concentrations of various parameters for core CM 70
Table 9: Concentrations of various parameters for core DM 72
Table 10: Concentrations of various parameters for core LSP 74
Table 11: Concentrations of various parameters for core WS 75
Table 12: List of PAH compounds for analysis 76
Table 13: Diatom metrics for core BW 77
Table 14: Diatom metrics for core CM 78
Table 15: Diatom metrics for core DM 79

LIST OF FIGURES

Figure 1: Study area and core locations 81
Figure 2: Tripod/pulley system at Dravo Marsh 82
Figure 3: Geochronology for core BW 83
Figure 4: Geochronology for core CM 83
Figure 5: Geochronology for core DM 84
Figure 6: Geochronology for core LSP 84
Figure 7: Sediment organic carbon, C/N and sediment phosphorus distribution with depth 85
Figure 8: Depth distribution of the isotopic composition sediment N ($\delta^{15}N$) and C ($\delta^{13}C$) 87
Figure 9: Distribution of diatom indicator species with depth 88
Figure 10: Diatom metrics 91
Figure 11: Relationship between total sediment N and diatom metrics 92
Figure 12: Relationship between total sediment P and diatom metrics 93
Figure 13: Concentrations of total sediment nitrogen (TN) and the nitrogen isotopic composition of TN ($\delta^{15}N$-TN) from 1860 to 2003 94
Figure 14: Concentrations of total sediment phosphorus (TP) and the carbon isotopic composition of total carbon ($\delta^{13}C$-TC) from 1860 to 2003 95
Figure 15: The relationship between total sediment P (TSP) and the carbon isotopic composition of organic matter ($\delta^{13}C$-TC) in Brandywine Creek, Churchmans Marsh and Dravo Marsh 96
Figure 16: Diatom metric for eutrophentic species from 1860 to 2003 97
Figure 17: Depth distribution of total PAHs and the LMW to tPAHs ratio with depth 98
Figure 18: Comparison of benzo[a]pyrene to benzo[e]pyrene 99
Figure 19: Indicator ratios of benzo[a]pyrene to benzo[e]pyrene and fluoranthene to pyrene 100
Figure 20: Concentrations of tPAHs from 1900 to 2003 101
Figure 21: Distribution of tPCBs with depth 102
Figure 22: Distribution of tPCBs and the LMW to tPCBs ratio with depth 103
Figure 23: Distribution of tDDX (DDT+DDD+DDE all forms) and total chlordanes with depth 105
Figure 24: Concentrations of tPCBs from 1900 to 2003 106
Figure 25: Concentrations of tDDXs from 1900 to 2003 107
Figure 26: Distribution of total chlordanes (all forms) with depth 108
Figure 27: Concentrations of total chlordanes from 1900 to 2003 109
Figure 28: Distribution of tPBDEs with depth 110
Figure 29: Concentrations of tPBDEs from 1860-2003 111
Figure 30: Distribution of dioxins and furans with depth 112
Figure 31: Concentrations of total dioxins and furans from 1900 to 2003 113
Figure 32: Concentrations of TEQ for dioxins and furans from 1860-2003 114
Figure 33: Distribution of sediment Fe and Zn with depth 115
Figure 34: Zn enrichment factor (EF) with depth 116
Figure 35: Concentrations of Zn and the EF from 1860-2003 117

Executive Summary

This study involved the chemical analysis of five sediment cores taken from the tidal Christina River Basin and lower Shellpot Creek in northern New Castle County, DE. Of the five cores, four were dated using ^{210}Pb and ^{137}Cs radiometric methods, with three (Churchmans Marsh (CM), Dravo Marsh (DM), and the tidal Brandywine (BW)) providing sufficient temporal coverage (> 50 yrs) for detailed chemical analysis. *The main objective was to evaluate historical trends in organic chemical contaminants (e.g., polychlorinated biphenyls, pesticides, dioxins/furans, polybrominated diphenylethers and polycyclic aromatic hydrocarbons), selected trace metals (e.g., iron and zinc) and nutrients (i.e., sediment phosphorus and nitrogen).* An additional objective was to evaluate if a historical record of eutrophication could be derived from algae analysis (i.e., diatom species in the cores) along with other indicators of potential ecosystem change (e.g., stable isotopes of carbon (δ^{13}C-OM) and nitrogen, (δ^{15}N-TN)).

The range and average sediment accumulation rates (^{137}Cs) inferred from the ^{137}Cs and ^{210}Pb data are similar to other areas within the Delaware Estuary and range from 0.57 to 1.9 cm/yr. There was good agreement between the ^{137}Cs rates and those for the constant accumulation model for ^{210}Pb.

With regard to contaminants, a major finding that emerged from this study is the historic accumulation of zinc in the system, as clearly displayed in the Churchmans Marsh (CM) core. Concentrations of Zn showed a broad peak over background levels starting at or shortly after the turn of the century and persisting to the early to mid-1970s. Using the amount of iron (Fe) within the sediment and referencing the data to bottom concentrations of Zn (and Fe), the sediments of Churchmans Marsh had been up to 40 times above background levels. Current Zn enrichment in Churchmans Marsh is still approximately 5 to 10 times above background. In the other core locations, surface sections are not substantially enriched above background with zinc enrichment factors ranging only from 1 to 2.3. Major sources of historic zinc loading to the tidal river included a National Vulcanized Fiber (NVF) facility on the Red Clay Creek (Yorklyn, DE) and a NVF facility on White Clay Creek (Newark, DE) and a pigment plant located in Newport (DE) along the tidal Christina River. Both NVF facilities ceased operation and have either been remediated (NVF Newark) or continue to be remediated (NVF Yorklyn). The pigment plant and adjacent areas impacted by releases from the plant are designated as a Federal Superfund site. Remedial actions have been taken at the site, in part to address the zinc issue. The coring

analysis clearly shows that the combined loading from these 3 facilities was much higher in the past and that remedial actions taken over the years have yielded substantially lower concentrations of Zn in the sediments of the tidal Christina River.

The other key finding of this study is that concentrations of organic contaminants are lower today, overall, than they were in the past, with some exceptions. Chlorinated organic compounds such as tchlordane, tDDX and dioxins/furans all show a sharp maximum at similar depths (corresponding to the 1960s and 1970s), followed by a decreasing trend towards the surface. Total PCBs also shows higher concentrations at depth with decreasing concentrations towards the surface, with the exception of the Dravo Marsh core where tPCB concentrations at the surface remain elevated (ca. 240 ng/g dw). The DM finding may reflect lingering inputs from local sources and/or the redistribution of previously deposited contamination following major earth works projects in or near the marsh.

Interestingly, the PCB congener composition in both the CM and DM cores showed a shift from mid to higher molecular weight compounds to lower molecular weight compounds from the upper sections (more recent) to the lower sections (longer ago). The opposite was true for the BW core. The high proportion of deca PCB (H10) in the CM and DM cores is unusual and appears to reflect releases from the same pigment plant in Newport that was also responsible for at least part of the zinc contamination. The use of congener-specific PCB methods (rather than typical Aroclor methods) allowed us to identify and characterize the deca PCB signature.

Total dioxins (PCDD) and furans (PCDF) concentrations ranged from <2 to 157 ng/g dw and <1 to 13 ng/g dw, respectively, with distinct distributions with depth and time. The individual congeners were used to calculate the toxic equivalents (TEQs) using published toxic equivalency factors (TEF). The TEQs ranged from <0.01 to 0.45 ng/g dw, generally similar or lower to surface sediments collected in 2007. Highest concentrations of PCDD, PCDF and TEQ were found in the Churchmans Marsh core.

In the three cores analyzed for polybrominated diphenyl esters (PBDEs), tPBDEs were only present in the upper sections with undetectable concentrations below approximately 20 cm (<1980s). The predominant congener is PBE 209 in the upper sections with BDE153 and BDE99 found at depth.

Total PAHs showed a distinct concentration peak in the 1940s, in the CM core, while a bimodal distribution was observed in the DM core and possibly the BW core. The peak of tPAHs

in the CM core maybe related to historic inputs of hydrocarbons from another Federal Superfund site near Newport (Koppers) that used creosote to treat telephone poles and other lumber. Other sources related to urban development including a major shipbuilding complex and a coal gasification facility are also potential historic sources to the area, particularly the DM. Data were compared to indicators of combustion sources, such as coal tar based parking lot sealant, using specific ratios of individual PAHs. Only a limited number of samples were consistent with such a fingerprint and thus this type of sealant does not appear to be a major source to the tidal Christina River.

Lastly, analysis of the diatom assemblages and metrics indicate a shift toward more eutrophic species starting in the late 1940-1950s. There was a strong positive relationship between the eutrophic diatom metric and the concentration of nitrogen and phosphorus in Churchmans and Dravo marshes. This, along with the increases in total sediment N, total sediment P and sediment nitrogen isotopic compositions (δ^{15}N-TN), indicates that increase loadings of nutrients have resulted in a diatom shift in the river.

Overall, this study documents the chemical analysis of three cores taken in the tidal Christina River and tidal Brandywine Creek. Changes were observed in contaminant levels across time that reflect usage globally and most often locally. Contaminant levels appear to be declining when viewed on a longer-term, decadal time scale. However, the concentrations of several contaminants (e.g., PCBs and zinc) remain relatively elevated in this system.

A) Introduction

A1: *Background*

Trace metals and organic contaminants in water are derived from many sources. Natural sources of metals include the weathering products of soils which are then transported in the dissolved or particulate phases. Anthropogenic sources of metals and organic contaminants are introduced to the water via atmospheric deposition, industrial discharges (e.g., mining, metal processing, manufacturing), municipal discharges (waste water treatment), and stormwater runoff of contaminated parcels. Due to the particle-reactive nature of most trace metals and organic compounds, sediments are potential repositories for contaminants and, under certain conditions, can be used to provide a historical record of pollution (Simpson et al., 1983; Orson et al., 1990; 1992; Valette-Silver, 1993; Hornberger et al., 1999; Cooper and Brush, 1993; Church et al., 2006; Velinsky et al., 2007; and others). With minimal diagenetic remobilization, biological mixing, and hydraulic processes, the sediment column can reflect the chronological deposition/inputs of most contaminants. Sediment cores are extremely useful in determining if various pollution control actions were/are effective in reducing contaminant loadings, as well as providing a time frame for system response (Smol, 2008). Hence, coring data are important to determine whether environmental conditions are improving with time and at what rate. The rate information is especially important for modeling programs in which forecasts are developed by extending past trajectories.

A2: *Objectives of Study*

It is the objective of this study to collect sediment cores from the tidal freshwater region of the Christina River and Shellpot Creek (near Wilmington, DE), and determine the chronology of chemical contaminant deposition, nutrient loadings and related ecological response. To meet this objective, we obtained and analyzed the chemical characteristics of sediment cores from depositional areas within the targeted waters. This study aimed to quantify and illustrate the magnitude and extent of sediment contamination in the lower tidal portion of the Christina Watershed and Shellpot Creek and provide insight into the temporal nature of that contamination. It also sought to understand how the trophic status of the system has changed over decadal time scales.

A3: *Study Area*

The Christina River Basin occupies 1480 km^2 in Delaware, Pennsylvania and Maryland, and includes four major watersheds—Brandywine Creek, Red Clay Creek, White Clay Creek, and the Christina River. The Christina River Basin is a rapidly suburbanizing watershed which is characteristic of a typical mid-Atlantic watershed. Land uses in the watershed are approximately 33% for urban/suburban, forested/open space, and agriculture (DNREC, 2007). Percent impervious levels in developed watersheds exceed 10 to 15%, which are thought to represent maximum thresholds needed to protect stream habitat and fisheries (Klein et al., 1979; Roy et al., 2003). Existing water quality problems are derived from wastewater discharges, agricultural runoff, Superfund sites, and runoff from new development. Approximately 40 stream segments listed as impaired in the EPA's 303(d) list have resulted in fish consumption advisories along reaches of the Brandywine Creek, Red Clay Creek, and Christina River.

The river contains many sources of chemical contaminants and has three federal Superfund sites located within the lower tidal river (Koppers Wood, Dupont Chemical, and Halby Chemical), numerous state-lead waste sites, and is listed on Delaware's 303(d) list of impaired waters (DNREC, 2007). Two major tributaries to the Christina, the Red Clay Creek and the White Clay Creek, are listed as impaired due to elevated zinc concentrations. Both of these tributaries have implemented efforts (i.e., total maximum daily loads [TMDL]) to reduce inputs of Zn to the water (DNREC 1996; 1999a,b,c). In addition, the EPA and DNREC in 2001 implemented a TMDL for excess nutrient inputs to the river (high and low flow conditions). Additional TMDL for the Christina Basin, including those for PCBs and other contaminants, are scheduled to be completed in 2010 and beyond.

The Shellpot Creek Watershed, a tributary to the Delaware River Estuary, is located in New Castle County, DE and flows through parts of Wilmington, DE. The creek once flowed into the lower tidal Brandywine but has been diverted directly into the Delaware Estuary. The watershed drains approximately 9,000 acres of mostly developed lands (90% of the watershed area).The impaired segment of Shellpot Creek begins at its headwaters and terminates at its mouth which is its confluence with the Delaware River. The watershed has completed TMDLs for excess nutrients and bacteria (DNREC, 2005). The creek is also currently listed on Delaware's 303(d) list for impairments due to chlordane and PCBs in fish. TMDLs to address those impairments are scheduled for the future.

Current PCB loading rates from Delaware Hazardous Substance Cleanup Act (HSCA) sites via overland flow and subsurface discharge to the tidal Christina Basin have been estimated by Brightfields, Inc. (2009); however, a historical perspective of contaminant inputs and mass loading rates have not been estimated. This project helps to fill that gap.

Cores were obtained in the tidal portion of the tidal Christina River (**Figure 1**). Locations include sites in Churchman Marsh (CM), Brandywine River (BW), Lower Shellpot Creek (LSP), and Walnut Street Bridge in downtown Wilmington, DE (WSB), and Dravo Marsh (DM) also called Old Wilmington Marsh. Salinities in this area are very low and marsh plant diversity indicates a tidal freshwater system. However, during drought conditions the BW and DM sites can occasionally experience salinities of 2 to 4 psu while upstream CM can experience lower salinities of between 1 and 2 psu.

B) Field and Laboratory Methods

B1: *Field Sampling*

Sediment cores were collected in 2007/2008 by staff from The Academy of Natural Sciences and University of Delaware at locations in the tidal river (**Figure 1; Table 1**). Overall, 10 cores were obtained from these sites but not all of them provided good sediment chronologies (based on ^{210}Pb and ^{137}Cs) and as such were not analyzed for various chemical parameters. This report discusses only the cores (i.e., 5 of the 10) on which chemical analyses (e.g., PCBs, PAHs, organic carbon, etc) were accomplished. Of these five cores, three (CM, BR, and DM) had sufficient temporal resolution and are discussed in detail, while the other two cores (LSP and WSB) are presented in a limited manner.

Cores were mainly collected on the marsh surface during mid to low tide. The cores obtained slightly downstream of the Walnut Street Bridge were collected during low tide, but water was present at the sediment surface. Core locations were from the interior of the marsh, away from any obvious disturbances (e.g., creek banks and ditching). At each site two cores were obtained, one for chemical analysis and the other for stratigraphic descriptions of each site. Push-piston cores of approximately 1 to 1.5 m in length were retrieved by a tripod/pulley system (**Figure 2**). The cores were taken to the laboratory and sectioned into specific intervals (e.g., 2 cm). Samples were stored in pre-cleaned jars at -10°C at either Academy or UDEL facilities.

Chain-of custody procedures were followed from the time of collection, shipping and until the analyses were completed.

B2: *Laboratory Methods*

Organic contaminant clean-techniques were used throughout and are well published (Ashley and Baker, 1999; others) and are similar to those used by EPA and NOAA (U.S. EPA, 1987; NOAA, 1993; Wade et al., 1994). All materials coming in contact with the samples were either glass or metal that was cleaned of any contaminants prior to use. Sample ID forms were used and each sample was given a unique laboratory number for sample tracking.

Sediments were analyzed for the following parameters at laboratories operated by the Academy of Natural Sciences (Patrick Center): carbon, nitrogen and phosphorus, PAHs (41+ compounds), total PCBs (100+ congeners), selected pesticides including DDTs and chlordane, and stable isotopes of carbon and nitrogen. In addition, specific sections were analyzed for diatoms via sample digestion, mounting and glass slide light microscopy. Sediments for radioisotope analysis (^{210}Pb and ^{137}Cs) were analyzed at University of Delaware (Center for Earth, Oceans and Environment). Below are brief descriptions of each chemical, biological, or physical method.

B2.1: Organic Contaminants: PAHs, Polychlorinated Biphenyls, Organochlorine Pesticides, and Dioxins and Furans

Prior to organic contaminant analyses, samples were kept frozen at -20°C. Standard operating procedures for the extraction, clean-up and quantification of organic contaminants in sediments are summarized in their respective operating procedure. Briefly, sediment samples were extracted with dichloromethane for 24 h using a Soxhlet apparatus. PAHs were quantified using a capillary gas chromatograph coupled with a mass spectrometer in the electron impact mode after a clean-up procedure employing liquid-solid chromatography with alumina as the stationary phase (Ashley and Baker, 1999). After PAH determination, samples were further cleaned using liquid-solid chromatography with florisil as the stationary phase. Congener-specific PCBs and OCPs (spell this out) were analyzed using a gas chromatograph equipped with a ^{63}Ni electron capture detector (Ashley and Baker, 1999; Kucklick et al., 1996). Twenty-eight singly or coeluting PBDE (BDE 17, 25, 28+33, 30 47, 49, 66, 71, 75, 85+155, 99, 100, 116, 119, 138, 153, 154, 156, 181, 183, 190, 191, 203, 205, 206, 209; Accustandard, 95–99% purity) were quantified at Duke University using a gas chromatography (GC) with a mass spectrometer (MS) operated in negative chemical ionization mode (NCI). Add brief description of dioxin and furan analysis performed by GERG.

B2.2: Sediment Iron (Fe) and Zinc (Zn)

Core sediment (0.500 g) was placed into pre-cleaned Teflon tubes for the MARS microwave digestion system. Approximately 10 ml of concentrated nitric acid (trace metal grade) was slowly added and the sample was allowed to cool and evaporate gases. The tubes were capped tightly and microwaved using EPA SOP 3051. The slurry was mixed and allow to settle for one week in which an aliquot was taken and diluted (100 ml) with ultra clean DDW. The extract was analyzed using a flame Varian AAS linked to a desktop computer. A five-point calibration curve was used to calculate concentrations and samples were diluted if absorbance was greater than 0.750. Concentrations are reported in dry wt and it should be noted that concentrations are not total (i.e., mineral matrix) but strong acid digestion.

B2.3: Radioisotope Measurements and Sedimentation Rates

In the laboratory, sediment cores were extruded vertically and sectioned in 2-cm intervals for analysis. Sediment bulk density (ρ_d) and loss-on-ignition (LOI) measurements were made for each core section to aid interpretation of the downcore radionuclide and chemical data. Dry-bulk density was calculated from porosity (ϕ) using representative values of interstitial fluid density (ρ_d) and mineral density (ρ_m) according to:

$$\rho_d = (1-\phi)\rho_m \tag{1}$$

where ρ_m=2.65 g/cm^3. Porosity was computed gravimetrically from water content (W_c) and using an assumed pore water density of ρ_f=1.0 g/cm^3:

$$\phi = \left(\frac{W_c \rho_m}{W_c \rho_m + (1-W_c)\rho_f} \right) \tag{2}$$

where $W_c = W_{wet} - W_{dry} / W_{wet}$. Dry sediment weight was determined by drying the sectioned wet sediment in a convection oven at 100°C for 24 h. The dry sediment was then ground to a fine powder for LOI determination and radionuclide analysis.

LOI measurements were used to quantify the relative proportion of organogenic (combustible) and minerogenic (residual ash) materials in the sediments. Following the method of Heiri et al. (2001), a 4-gram quantity of sample power was combusted at 550°C in a muffle furnace for 4 h. LOI was computed as follows:

$$LOI = \frac{W_{dry} - W_{ash}}{W_{dry}} \cdot 100\% \tag{3}$$

where W_{dry} is the weight of sample previously dried at 100°C, and W_{ash} is the weight of the residual ash.

To develop sediment chronologies and determine accretion rates for the sediment column, measurements of ^{210}Pb ($t_{1/2}$=22.3 years) and ^{137}Cs ($t_{1/2}$=30.1 years) were made by gamma spectroscopy of the 46.5 and 661.6 keV photopeaks, respectively (Cutshall et al., 1983; Wallbrink et al., 2002). Powder samples were placed in a 60 ml plastic jar and counted for 24-48 h on a Canberra Model 2020 low-energy Germanium detector (LEGe). The radionuclide concentration (activity) of excess ^{210}Pb was determined by subtracting the activity of its parent nuclide ^{214}Bi (609.3 keV) from the total activity. Detector efficiencies were determined from counts of NIST Standard Reference Material 4357 (Inn et al., 2001). The counting geometry of the core samples was kept identical to that of the NIST standard such that a self-absorption

correction for ^{210}Pb was not necessary. Confidence limits reported with radioisotope data are the propagated one-sigma background, calibration, and counting errors.

Three approaches were used to reconstruct the accumulation history of marsh deposits. Two of these methods are based on downcore profiles of ^{210}Pb activity, and the third uses the depth distribution of ^{137}Cs activity. The first approach, the constant activity model (CA), assumes that the specific activity of ^{210}Pb (dpm/g) deposited remains constant through time. In other words, variations in mineral sedimentation rate do not affect the initial concentration of ^{210}Pb. At steady state, excess ^{210}Pb decreases exponentially with depth in the sediment column following:

$$A = A_o \, exp\left(-\lambda z/S\right) \tag{4}$$

where A is the excess activity of ^{210}Pb at depth z, A_o is the initial activity of excess ^{210}Pb, λ is the decay constant for ^{210}Pb (0.3114 years), and S is the vertical accretion rate. The slope of the regression line of ln$A$ versus z is proportional to the accretion rate with dimensions length/time. In this method the age of a sediment interval is derived from a single value of S averaged over the ^{210}Pb profile. The corresponding mass accumulation rate, with the dimensions mass/area/time, is determined by plotting A as a function of cumulative mass, the depth-integrated product of ρ_d and z.

The second method, the constant flux model (CF), relates time and accretion rate to the inventory of excess ^{210}Pb by assuming that the flux of ^{210}Pb to the sediments (rather than A_o concentration) is constant. Sediment age and ^{210}Pb are related as:

$$I = I_o \, exp\left(-\lambda t\right) \tag{5}$$

where I is the inventory of excess ^{210}Pb below depth z (dpm/cm^2), I_o is the total inventory of excess ^{210}Pb in the sediment column, and t is the sediment age at depth z. Radionuclide inventories of excess ^{210}Pb (and ^{137}Cs) are computed as:

$$I_o = \sum_i \rho_{di} x_i A_i \tag{6}$$

where ρ_d is the dry-bulk density, x is the sediment thickness, A is the radionuclide activity, and the i operator indicates the ith depth interval. In the CF model, sediment accretion rates are computed by dividing the length of the dated sediment column by the corresponding age in years.

The third chronological method is based on the first occurrence of ^{137}Cs in the sediment column as an absolute indicator of ca. 1954, the year of ^{137}Cs introduction to the global atmosphere by nuclear weapons testing (Ritchie and McHenry, 1990). The depth of ^{137}Cs penetration divided by the interval between ca. 1954 and the year of core collection is used to compute an average accretion rate. The corresponding mass accumulation rate is determined by plotting ^{137}Cs activity against cumulative mass. The advantage of ^{137}Cs chronology over ^{210}Pb dating methods is that it more closely approximates the absolute age of sediments deposited after ca. 1954.

Both the CA and CF ^{210}Pb models have been widely used to develop sediment chronologies for tidal marsh deposits, but they are based on different assumptions that are not met in all types of depositional environments. The CF model assumes that 1) all ^{210}Pb deposited is derived from direct atmospheric deposition, and 2) variations in A_o are due to changes in the minerogenic sediment accumulation rate S as opposed to changes in ^{210}Pb supply (Appleby and Oldfield, 1978). In other words, a change in S through time will be met by a corresponding change in A_o in accordance with Equation 5. This model was originally developed for lake systems and thus is most appropriate for depositional environments that sequester ^{210}Pb mostly (if not exclusively) through direct atmospheric deposition. Although tidal marshes are exposed to the atmosphere

most of the time, tidal flooding brings particle-bound ^{210}Pb from coastal waters that can increase A_o above that supplied by the atmospheric flux. For this study we computed sediment accretion and accumulation rates using both ^{210}Pb models but place more weight on the CA approach, because the assumptions are less restrictive regarding ^{210}Pb sources.

The following conditions are implicit in all ^{210}Pb and ^{137}Cs dating methods: 1) mixing by burrowing organism has not enhanced particle burial; 2) the modeled radionuclide is chemically immobile; and 3) the sedimentary record is complete and not punctuated by non-depositional or erosional episodes. As elaborated later, these assumptions appear to have been met in this study for cores CM, DM, and BR.

B2.4: Total Organic Carbon and Total Nitrogen

Total organic carbon and total nitrogen were measured using a CE Flash Elemental Analyzer following the guidelines in EPA 440.0, manufacturer instructions and ANSP-PC SOP. Samples were pre-treated with acid to remove inorganic carbon.

B2.5: Total Phosphorus

Total sediment phosphorus was determined using a dry oxidation method modified from Aspila et al. (1976) and Ruttenberg (1992). Solubilized inorganic phosphorus was measured with standard phosphate procedures using an Alpkem Rapid Flow Analyzer. Standard reference material (spinach leaves) and procedural blanks were analyzed periodically during this study. All concentrations were reported on a dry weight basis.

B2.6: Stable Isotopes of Carbon and Nitrogen

The stable isotopic composition of sediments was analyzed using a Finnigan Delta XL coupled to an NA2500 Elemental Analyzer (EA-IRMS). Samples were run in duplicate or triplicate with the results reported in the standard δ (‰) notation: $\delta X = (R_{sample}/R_{standard}) - 1) \times 1000$; where X is either ^{13}C or ^{15}N and R is either $^{13}C/^{12}C$ or $^{15}N/^{14}N$. The $\delta^{15}N$ standard was air ($\delta^{15}N = 0$), and for $\delta^{13}C$ the standard is the Vienna PeeDee Belemite (VPDB) limestone that has been assigned a value of 0.0 ‰. Analytical accuracy was based on the standardization of the UHP N_2 and CO_2 used for continuous flow-IRMS with IAEA N-1 and N-2 for nitrogen and IAEA sucrose for carbon, respectively. An in-house calibrated sediment standard was analyzed every tenth sample. Generally, precision based on replicate sample analysis was better than 0.2‰ for carbon and 0.6‰ for nitrogen.

B2.7: Diatoms

Core sediment was collected (≈1g) and the organic component was oxidized with 70% nitric acid while heated in a CEM microwave (165ºC) for 1.5 h. Diatoms were settled and supernatant was decanted until it reached a neutral pH. A measured amount of digested sample was dripped onto a microscope coverslip and dried. Coverslips were then mounted onto slides using a high refractive index mounting media (Naphrax™). Diatoms were counted and identified using a Zeiss Axioskop with DIC optics. Three hundred valves were counted on 1000x magnification. Identifications were made using the extensive diatom library at ANSP. Several diatom community metrics were calculated based on species autecological preferences based on van Dam et al. (1994). Metrics were calculated using the Phyco-Aide program developed at ANSP.

C) Results and Discussion

C1: *Sediment Bulk Properties and Sediment Accumulation*

The activity of ^{210}Pb and ^{137}Cs (reported as disintegrations per minute per gram of sediment; dpm/g) with depth can be used to determine the sedimentation rate and historical record of contaminants in sediments (Simpson et al., 1983; Orson et al., 1990; 1992; Valette-Silver, 1993; Appleby, 2001; Smol, 2002; Ridgway and Shimmield, 2002; Sommerfield, 2006). This information can be used for the construction of sediment budgets (Schubel and Hirschberg, 1977; Brush et al., 1982; Officer et al., 1984) and to understand chemical contaminant accumulation in aquatic environments (Owens and Cornwell, 1995; Cornwell et al., 1996; Latimer and Quinn, 1996; Van Metre and Callender, 1997; Church et al., 2006; Velinsky et al., 2007). Also, dated sediment cores can provide information as to the changes in loadings of contaminants over time (e.g., Rippey and Anderson, 1996; Gevo et al., 1997; Santschi et al., 2001). Such information is especially useful in tracking the effectiveness of various management actions designed to reduce inputs to specific areas (Owens and Cornwell, 1995; Zhang et al., 1993). However, there are many variables that can affect the usefulness of ^{210}Pb and ^{137}Cs dating in a given area (Appleby and Oldfield, 1978; Crusius and Anderson, 1991; Appleby, 2001). These include mixing of the sediment by benthic organisms (i.e., burrowing organisms), physical mixing from dredging and storm events, post-depositional movement of contaminants and of the ^{210}Pb or ^{137}Cs, and additional inputs of ^{210}Pb from sources in the urban landscape (i.e., urban sediment focusing). The cores obtained in this study provided excellent chronologies of sediment deposition and accumulation. For historical analysis, the sediment accumulation rate derived from the ^{137}Cs distribution was used to produce an age-depth relationship. This, along with the ^{210}Pb results, provides linear rates from approximately 1920-1930 to the present. For dates prior to the 1920-1930s we assume linear rates to the bottom of the cores. While this is useful for this analysis, we are less confident in the dating at the bottom of the cores due to effects associated with compaction, non-linear sedimentation rates, and other factors (Neubauer et al., 2002; Sommerfield, 2006).

C1.1: Sediment Properties

All of the cored deposits consisted of clayey silt with variable quantities of living and dead plant material. Only at the base of core SP-2 was there a noticeable down-core change in

sediment type, from silt to sand. Dry-bulk densities ranged from 0.17 to 1.2 g/cm^3 overall and increased with depth downcore in all cases (**Figures 3-6; Tables 2-5**). This depth increase is consistent with burial compaction of the sediment column due to expulsion of porewater. Only in the lowermost intervals of core LSP-2 did bulk density vary with grain size on account of changes in mineral density (silt to sand).

The amount of organic material in the cores ranged from 7 to 40%, values representative for marsh deposits in general (**Figures 3-6; Tables 2-5**). LOI decreased with depth in all cases, and cores BW-2 and DM-2 displayed a profile that varied inversely with dry-bulk density. This suggests that depth variations in sediment bulk density are partly due to the concentration of organogenic material, at least at sites BW-2 and DM-2. In summary, with the exception of the base of core SP-2, the physical properties data suggest no major changes in sediment type that could bias interpretations of chemical and radionuclide profiles.

C1.2: Accretion and Sediment Accumulation Rates

Brandywine Marsh core BW-2 displayed ^{137}Cs activities that increased up core from the depth of first occurrence at 36-38 cm to a broad peak between 20 and 30 cm, above which activities decreased to near-zero at the core top **(Figure 3; Table 2)**. The overall shape of the profile is consistent with the source function for the mid-Atlantic region (Olsen et al., 1981), but the broad activity maximum is ambiguous regarding the date of peak fallout (e.g., 1963-1964). At this site, accretion and mass accumulation rate calculated from the basal depth of ^{137}Cs activity are 0.75 cm/yr and 0.26 g/cm^2/yr, respectively.

Excess ^{210}Pb profiles for BW-2 exhibited a monotonic decrease in the log of the activity downcore, indicative of steady-state sediment accumulation and radioactive decay **(Figure 3).** Accretion rates determined using the CA and CF ^{210}Pb models were 0.80 and 1.0 cm/yr, respectively, and the corresponding mass accumulation rate was 0.40 g/cm^2/yr. At this site there was good agreement among radionuclide dating methods, suggesting that sediment accumulation has been more-or-less invariant over the period of interest.

Churchmans Marsh core CM-1 exhibited ^{137}Cs and ^{210}Pb distributions that were somewhat similar to those observed for the BW-2 core (**Figure 4; Table 3**). The ^{137}Cs activities increased up core from the depth of first occurrence at 28-30 cm to a broad maximum centered at 20-22 cm, and then decreased to lower, but detectable, activities at the core top. Accretion rates based

on ^{137}Cs and excess ^{210}Pb (CF model) were 0.60 and 0.51 cm/yr, respectively, with corresponding mass accumulation rates of 0.28 and 0.25 g/cm^2/yr. Accretion and accumulation rates could not be determined using the CA model because the excess ^{210}Pb profile did not exhibit a monotonic decrease in activity consistent with steady-state sediment accumulation.

Dravo Marsh core DM-2 had a first occurrence of ^{137}Cs at 40 cm, maximum activity at approximately 18-20 cm, and decreasing activities to the core top (**Figure 5; Table 4**). Accretion and mass accumulation rates derived using ^{137}Cs data were 0.79 cm/y and 0.19 g/cm^2/yr, respectively. Similarly, accretion rates based on the CA and CF ^{210}Pb models were 5.6 and 6.7 mm/yr, respectively, with a corresponding mass accumulation rate of 0.19 g/cm^2/yr. Overall, agreement of ^{137}Cs and ^{210}Pb chronological methods was good at this site.

The Shellpot Creek core did not provide steady-state profiles of ^{137}Cs or ^{210}Pb, precluding computation of ages and accumulation rate using the CA and CF models (**Figure 6; Table 5**). The first occurrence of ^{137}Cs activity was present near the bottom of the core at 96-98 cm, above which there was a broad maximum centered around 70-80 cm. Hence, the entire sediment column must have accumulated after ca. 1954. Based on the depth of ^{137}Cs penetration, accretion and mass accumulation rates are 1.9 cm/yr and 0.60 g/cm^2/yr, respectively. Although the CF ^{210}Pb model yielded an identical accretion rate of 1.9 cm/yr, the sediment inventory of excess ^{210}Pb inventory suggests that most of the ^{210}Pb deposited at this site is not derived from direct atmospheric deposition (see Section C2).

One of the requirements of the constant flux for ^{210}Pb (CF) model is that the initial activity at the surface should be lower with sites of higher sediment accumulation rates. Despite a three-fold difference in sediment accumulation rate among coring sites, there was no relationship between A_o (initial activity) and S (vertical accretion rate) as would be predicted by the CF model. For example, A_o (taken as the 0-2 cm depth interval; **Tables 2-5**), was not lower at sites with a higher sediment accumulation rate. While this result does not completely invalidate the CF ^{210}Pb model, it reveals that this approach may not be the best choice for tidal marsh environments.

An important observation with relevance to chemical contaminant history in the Christina River system is presence of measurable ^{137}Cs activity at the tops of all cores. Given that the global atmospheric flux of ^{137}Cs has been negligible since the early 1980s, this pattern implies that previously deposited ^{137}Cs has been redistributed in the system. Wash-in of soil-bound ^{137}Cs

from the watershed and (or) erosion of subtidal deposits can account for redeposition of ^{137}Cs in river-estuaries. Additionally, bioturbation can rework ^{137}Cs from depth, but the shapes of the ^{210}Pb and ^{137}Cs profiles determined for this study are not suggestive of intense biological mixing. To the extent that ^{137}Cs is an analog for particle-reactive contaminants, its depositional trend suggests that historical pollutants may be undergoing similar processes of reworking and redistribution in the Christina River system.

Table 6 provides the summary information and models for the radioisotopes for the Christina cores. Accretion rates, based on ^{137}Cs, ranged from 0.57 cm/yr at Churchman's Marsh to almost 2 cm/yr at Shellpot Creek. However the data at Shellpot Creek suggest extensive reworking so this rate should be considered tentative, but it does indicate higher accretion than at the other locations. These rates are well within the range of accretion throughout the tidal Delaware Estuary (Sommerfield and Velinsky, unpublished data). At 14 sites in the estuary spanning tidal fresh to marine the range of accretion rates is 0.3 to 1.3 cm/yr with an average of 0.50 ± 0.4 cm/yr (n=32 cores).

In summary, cores BW-2, CM-1, and DM-2 yielded reliable accretion rates with good agreement between ^{137}Cs and ^{210}Pb chronological methods. Because ^{137}Cs was present in the greater extent of the cores, ^{137}Cs-derived accretion rates, using peak concentration interval depth presented in **Tables 2-6,** were used to convert sediment depths to ages for the contaminant and nutrient-eutrophication histories. Dates corresponding to depth intervals within the individual cores appear in **Tables 2-6**. These estimates are a key output of this project and allow us to place the contaminant and nutrient/eutrophication data into historic context.

C1.3: Radionuclide Inventories and Focusing Factors

Sediment inventories of excess ^{210}Pb and ^{137}Cs were computed to compare the relative amount of radionuclide deposited among the four coring sites (CM, DM, BW, and LSP). Because ^{210}Pb and ^{137}Cs have particle-adsorption characteristics not unlike trace metals and some organic contaminants, the sediment inventory of a radionuclide compared to a reference value provides information about contaminant transport pathways and burial in aquatic systems. Reference inventories of 28 dpm/cm^2 for ^{210}Pb and 21 dpm/cm^2 for ^{137}Cs are known from direct measurements of radionuclide atmospheric deposition in the U.S. mid-Atlantic region (Olsen et

al. 1985; Graustien and Turekian, 1986). These reference values represent the total amount of radionuclide that could be buried at a site if supplied by atmospheric deposition alone.

The focusing factor is the ratio of the measured and reference radionuclide inventory. Focusing is the process by which fine-grained materials migrate towards more depositional areas and provide higher inventories that that predicted by reference inventories. To account for this migration, a focusing factor was calculated by comparing the actual ^{210}Pb inventory to the expected ^{210}Pb inventory. A focusing factor greater than unity implies that radionuclide activity has been preferentially transported or "focused" from one location to another by a combination of hydrodynamic flow and sedimentary processes. Conversely, a focusing factor less than unity imply that the atmospheric flux is not sequestered locally perhaps on account of sediment erosion and redistribution. In the case of ^{210}Pb, tidal flooding of a brackish or saline marsh can supply ^{210}Pb in addition to that derived by atmospheric deposition because coastal and estuarine waters usually contain ^{210}Pb activity from non-atmospheric sources. This is not the case in a tidal freshwater system, where all of the ^{210}Pb is atmospherically supplied and focusing occurs through lateral transport of particle-bound ^{210}Pb. ^{137}Cs can be focused in a similar manner as ^{210}Pb, although ^{137}Cs is less particle reactive than ^{210}Pb and tends to desorb from sedimentary particles in brackish and saline waters. Consequently, sediment inventories of ^{137}Cs in freshwater systems tend to be higher than those in estuaries and coastal waters. This must be taken into account when interpreting ^{137}Cs focusing factors for sites that span a wide range of salinities. While our locations can experience low salinities during extreme droughts, it is generally considered a tidal freshwater system as noted by plant communities.

Radionuclide inventories and focusing factors for the four coring sites (CM, DM, BW, and LSP) are presented in **Tables 2-6**. The Brandywine River site (BW-2) had the lowest excess ^{210}Pb inventory and the highest ^{137}Cs inventory among the sites sampled. This result was to be expected given the generally freshwater setting of the site. The ^{210}Pb focusing factor of unity indicates that the sediment column has been accretionary for the period of interest, and that atmospheric deposition is the probable source of radionuclide. In contrast, the ^{137}Cs focusing factor of 2.3 implies a non-atmospheric source of radionuclide, which is difficult to reconcile in light of the ^{210}Pb results.

The Churchman Marsh site (CM-1) had the second highest ^{210}Pb inventory and the lowest ^{137}Cs inventory among the sites. The ^{210}Pb focusing factor of 2.8 suggests that non-

atmospherically derived radionuclide is deposited at this site, perhaps supplied by tidal waters. The ^{137}Cs focusing factor of 0.2 is consistent with loss of particle-bound activity by desorption prior to deposition. The Shellpot Creek site (LSP-2) had the highest ^{210}Pb inventory, several times that of the others, and a ^{137}Cs inventory that was second only to site BW-2. The ^{210}Pb focusing factor of 11.4 suggests influx of radionuclide from tidal estuarine waters, but the ^{137}Cs focusing factor of near-unity is not supportive of an estuarine source. Another possibility is that soil-bound ^{210}Pb and ^{137}Cs eroded from the surrounding landscape and focused at the site. This interpretation is consistent with the site's rapid rate of sediment accumulation (1.9 cm/yr), which most likely results from localized sediment trapping caused by the tidal gate barrier immediately adjacent to the coring site. The Dravo Marsh site (DM-2) had radioisotope inventories and focusing factors within the range of values measured at the other sites.

The focusing factors make clear that the four depositional sites (CM, DM, BW, and LSP) have sequestered ^{210}Pb or ^{137}Cs inventory at levels above that which can be accounted for by atmospheric flux alone. This result confirms that most of the minerogenic material buried at these sites is allochthonous (i.e., transported to the location from elsewhere), and implies that atmospherically sourced, particle-reactive contaminants in the Christina River system will exhibit focusing patterns that depend not only on broad scale atmospheric delivery but also on more regional and local transport processes (e.g., tidal flow and sediment transport). All of the coring sites, although within the Atlantic Coastal Plain, are immediately down gradient from the Piedmont physiographic province. Particles eroded from the Piedmont are transported downstream and later deposited on the Coastal Plain. Contaminants associated with these particles, plus contaminants originating from local sources within the Coastal Plain, and contaminants delivered from tidal exchange, ultimately combine to yield observed profiles in the cores. An important is that the all of the coring sites, while depositional, are subject to both small and large scale processes (i.e., within the tidal waters and from the watershed) that influence radioisotope and contaminant profiles.

C2: Nutrients/Eutrophication

C2.1: Sediment Total Carbon, Total Nitrogen and Total Phosphorus

Sediment total carbon (TC) concentrations for the BW-2, CM-1, and DM-2 cores ranged between <1.0 and 19.8% on a dry weight basis (dw) with an average of 5.5 ± 7.7% TC (±

standard deviation; **Table**s **-11; Figure 7a,b**). Similarly, total nitrogen ranged from 0.1 to 1.2% N with an overall average of 0.40%; while total sediment phosphorus (TSP) ranged from 0.04 to 0.27% TP with an overall average of 0.10%. In the lower Shellpot Creek (LSP) and Walnut Street (WS) cores %TC and %TN averaged slightly lower; 4.3% and 0.29% respectively while TP averaged slightly higher at 0.14% TP.

The three cores, CM, DM, and BW, exhibited different total carbon, nitrogen and phosphorus profiles with depth (**Figure 7a**). In the CM core, TC increased from 1.2% to approximately 7.6% near the surface while in the DM core concentrations increased from 1.0% to 18% near the surface. In the DM core there were two subsurface maxima, one centered at ~ 40 cm (8% OC) and the other centered at ~10 cm of 20% OC. Concentration in the BW core increased only slightly from the bottom (2.2% OC) to the surface (3.8% OC), with a broad subsurface maxima between 20 and 40 cm. Total sediment P increased substantially towards the surface in the CM core (0.06 to 0.18% P) and to a lesser extent in the DM core. In the DW there was no difference between the top and bottom sections in TP concentrations but there was higher concentrations centered around 13 cm of 0.27% P. For the LSP and WS cores, only 5 or 6 sections were analyzed for each. Therefore only limited information is derived from the depth distribution (**Figure 7b**). In the LSP core there was an increase towards the surface of TC and TP while in the WS core concentrations are similar from top to bottom.

The carbon to nitrogen ratio (C/N; atomic units) can be used as a tracer of the source of organic matter to a location and potential diagenetic changes that could occur during burial (Jasper and Gagosian, 1990; Meyers, 1994; Prahl et al., 1994). Diagenesis is any chemical, physical, or biological change undergone by sediment after its initial deposition (Berner, 1980). For example, terrestrial material (e.g., trees) are rich in cellulose (i.e., higher C) compared to algae or marsh plants that have less structural material and are higher in proteins (i.e., higher N). Typical marine plants have C to N ratios of ~ 4-10 while terrestrial material can have C to N values > 15-20. Diagenesis of recent sediments tends to increase the C to N ratio due to preferential remineralization and release of nitrogen compounds; however re-incorporation of bacterially derived N can increase the C to N ratio over time (Fogel et al., 1989; Benner et al; 1991). In the CM core (**Figure 7a**), the C/N ratio changed only slightly with depth and averaged 12.3 ± 1.2, while in the DM core, the C/N ratio increased from 10-13 near the bottom of the core to approximately 18-20 near the surface. In the Brandywine core (BW) the C to N

was more variable (range = 7 to 22), but showed a maxima in the same depth range as the C and N concentrations. In the LSP and WS cores (**Figure 7b**), the C/N ratio were fairly constant (~18) from top to bottom although there were less intervals analyzed. In general the sediments in the cores reflect a dominance of terrestrial sources of organic matter compared to algal sources. Interestingly, the CM core exhibited slightly lower C/N ratios compared to the downstream locations. It would be expected that the ratio may decrease going downstream towards the Delaware Bay where the ratio would be lower (Cifuentes et al., 1988). The change with depth in the DM core, increasing towards the surface along with the increase in OC, might suggest a change in the source of organic matter to this site.

C2.2: Stable Isotopes of Carbon and Nitrogen

Organic carbon and nitrogen isotopic ratios are useful to distinguish between marine and continental plant sources of sedimentary organic matter, processing and cycling of nutrients and in some instances the level of system-wide productivity (Fry, 2006 and others). Most photosynthetic plants incorporate carbon into organic matter using the C3 Calvin pathway, which biochemically discriminates against ^{13}C to produce a $\delta^{13}C$ shift of about -20‰ to -30‰ from the isotope ratio of the inorganic carbon source. C4 plants (e.g., corn, *Spartina*) incorporate CO_2 using a different system (PEP) that discriminates against ^{13}C to produce a $\delta^{13}C$ shift of about -8‰ to -15‰ from the isotope ratio of the inorganic carbon source. Organic matter produced from atmospheric CO_2 ($\delta^{13}C \sim -7$‰) by land plants using the C3 pathway consequently has an average $\delta^{13}C$ (PDB) value of about -27‰ (O'Leary, 1988). The source of inorganic carbon for marine algae (C3 plants) is dissolved bicarbonate, which has a $\delta^{13}C$ value of about 0‰. Marine organic matter consequently typically has $\delta^{13}C$ values between -20‰ and -22‰. The isotopic difference between organic carbon produced by C3 land plants and marine algae has been used to trace the delivery and distribution of organic matter to sediments in estuarine and coastal areas (Cifuentes et al., 1989; Fogel et al. 1992, and many others).

Carbon isotope ratios can be affected by photosynthetic dynamics and by postdepositional diagenesis (Dean et al., 1986; Fogel et al., 1992; Canuel et al., 1995; Zimmerman and Canuel, 2002) and consequently must be interpreted cautiously. A big factor that can impact $\delta^{13}C$ values of plant material is the availability of CO_2 and rate of production during photosynthesis and the possibility of selective diagenesis of organic matter fractions that are isotopically heavy or light.

While the change in $\delta^{13}C$ appears to be small (<2‰) during recent diagenesis (Hayes et al., 1989; Meyers, 1994), shifts due to the availability and rate of production, due to nutrient enrichment or limitation and other factors, can have a large impact on the resultant $\delta^{13}C$ values of deposited organic matter (Fogel et al., 1992; Schelske and Hodell, 1995; Church et al., 2006).

Differences exist between the natural abundances of stable nitrogen isotopes ($\delta^{15}N$, $^{15}N/^{14}N$) in dissolved and particulate matter from terrestrial, estuarine, marine, and anthropogenic sources. Terrestrial occurring soil nitrogen can have a wide range of values, but in general range from -1 to +4‰) similar to atmospheric nitrogen (0‰). Nitrogen isotopic compositions from marine sources tend to be slightly enriched in the heaver isotope (^{15}N) and are very dependent on the source of dissolved nitrogen and its $\delta^{15}N$, and processing in the system (e.g., ammonification, nitrification, denitrification, etc) at the time of formation. A dominant process in many aquatic environments (and groundwater) is denitrification (Cline and Kaplan, 1975). Denitrification is a microbially facilitated process of dissimilatory nitrate reduction that ultimately produces molecular nitrogen (N_2) through a series of intermediate gaseous nitrogen oxide products. This microbial process uses dissolved nitrate during oxidation of organic matter and as nitrate is consumed there is an enrichment of residual nitrate in the system. Algal/plant production and its $\delta^{15}N$ from nitrate would reflect the balance between processes and inputs. There are many points in which nitrogen can be fractionated and its isotopic composition altered. For example, wastewater from treatment facilities have been shown to increase the $\delta^{15}N$ of various fish species (Lake et al., 2001) due to the selective removal of the light isotope (^{14}N) nitrogen during treatment. Anthropogenic nitrogen was substantially enriched in watersheds with greater amount of urbanization and wastewater inputs and the nitrogen was shown to be incorporated into the aquatic food web (McCelland et al., 1997)

The isotopic compositions of sediment C and N exhibited interesting changes within each core (**Fig. 8**). In Churchmans Marsh (CM-1) and Dravo Marsh (DM-1), the $\delta^{15}N$ was lowest in the bottom sections (approx. 4-5‰), increasing towards the surface (up to ~ 8‰). The Brandywine Creek core exhibited little change in $\delta^{15}N$ with depth in the core (5.0±0.4‰ (n=15). The carbon isotopic composition of the sediment ranged from -29 to -23‰ ($\delta^{13}C$ average of -26‰). The $\delta^{13}C$ generally decreased towards the surface from approximately -25‰ near the

bottom of CM-1 and DM-1 to about -28.5‰ at the surface. The $\delta^{13}C$ in the BW core exhibited little change with depth and averaged -24.7 ± 1.2‰ (n=15).

C2.3: Diatom Analysis and Assemblages

Diatoms are microscopic, photosynthetic algae that contain yellow-brown chloroplasts and therefore are also referred to as golden algae. Comprising one of the most common types of phytoplankton, they are found in a diverse range of environments from freshwater to saline oceanic waters. Based upon their shape, diatoms are differentiated between by forms that are centric, i.e. circular, and pennate, i.e. having bilateral disposition of morphological characteristics. They exhibit three main living modes in the environment: 1) planktonic, 2) benthic (i.e., living on or in the bed sediment) and 3) epiphytic.

Diatoms are one of the most powerful water quality indicators; they colonize virtually every aquatic microhabitat and many diatom species have very strict ecological requirements, with well-defined optima and tolerances for environmental variables such as lake pH, nutrient concentration, water salinity and transparency. However, some centric species live in oligotrophic conditions, some benthics in productive environments; what truly works for ecosystem analysis, is the composition of species. Because of their strong relationships to environmental conditions, diatoms are used to derive inference models for such environmental factors. The inference models are developed using calibration sets of both diatoms and measured environmental variables for specific geographic regions. These calibration sets require a large number of sampling sites that maximize the gradient length covered by the variable of interest (e.g., phosphorus concentration, pH, etc.). This is necessary to produce robust quantitative models with high predictive power. These models can then be used to infer the environmental parameter of interest when instrumental measurements are not available and have been successfully used to reconstruct reference conditions and assess the impact of anthropogenic activities on aquatic systems.

Diatom assemblages have been shown to be an important indicator of nutrient concentration within freshwater and marine environments. Due to the fact the diatoms respond quickly and directly to nutrients, they have been used for many years as indicators of nutrient changes in aquatic systems (Potapova et al., 2004; Potapova and Charles, 2007; Ponader et al., 2008). In this study we take a first approach using metrics calculations based on models developed by van

Dam et al. (1994). While this data set is mostly based on freshwater species it does contain some marine diatoms. It provides a first approach to obtain ecological information as a dataset for both diatoms and water characteristics is not available for the Delaware Estuary.

Samples from 41 sections were analyzed for diatom composition from the 3 Christina cores (i.e., BW, CM and DM). At least 500 valves were counted for each sample and over 250 taxa (**Appendix I**) were identified from the samples allowing a robust analysis for nutrient and ecological conditions. The distribution of key diatom species in each of the cores is presented in **Figure 9a,b,c** and below is a brief description of the species distribution for each core:

<u>Dravo Marsh.</u> From the bottom of the core to approximately 25 cm (~1974), brackish and marine diatom species are dominant (*Cyclotella striata, Actinocyclus normanii, Raphoneis amphiceros*, etc.). This type of assemblage is replaced by an assemblage with high nutrient indicator freshwater benthics, such as *Navicula gregaria, N. recens, and N. germanii*. From about 12 cm (~1990) to the surface, planktonic species *Cyclotella meneghiniana* and *C.* cf. *distinguenda* are increasing in abundance while marine species are very rare during this time interval.

<u>Brandywine Creek</u>. Between the bottom of the core to approximately 36-38 cm (~1960), brackish-marine species (e.g., *Cyclotella striata, Delphineis minutum, Actinocyclus normanii*) are dominant. Above this interval they are replaced by eutrophic freshwater species, such as *Fragilaria vaucheriae, Nitzschia amphibia,* and the planktonic *Cyclotella meneghiniana*. Between 24-26 cm (~1975) and 14-16 cm (1987), a short, more marine flora is present that occurred before 1954 but this time in co-occurrence with more abundant freshwater species (e.g., *Aulacoseira granulata, Nitzschia palea, Eunotia tenella*). Above 14-16 cm, species indicating high nutrient levels such as *Nitzschia frustulum, Navicula salinarum, N. gregaria,* and *Cyclotella atomus,* are dominant.

<u>Churchmans Marsh</u>. This core displays a more complex dynamic with brackish-marine species from the bottom of the core to the 24-26 cm interval (~1965), however there were also intervals with more abundant *Cyclotella striata* and *Raphoneis amphiceros*. Above 42-44 cm (~1935), some freshwater eutrophic species also display increases, such as *Nitzschia brevissima* and *Fragilaria vaucheriae*. Above 24-26 cm (~1965), marine–brackish species *Actinocyclus normanii*, *Fallacia pygmaea*, *Cyclotella striata* increase in abundance in co-occurrence with high nutrient freshwater species *Cyclotella meneghiniana, Nitzschia brevissima*, and *Navicula gregaria*. The top of the core displays highly abundant *Cyclotella atomus and Diadesmis contenta*, indicating lower water levels.

To place the Christina Basin diatom data into broader context, various metrics were first calculated using salinity, pH, nitrogen uptake metabolism, and the trophic state from different data sets (van Dam et al., 1994; USGS NAQWA, EPA's National Lake Assessment (NLA)). The samples collected in the tidal Christina span a range of marine brackish to freshwater, making detailed analysis complex. These data sets used for ecological condition analysis are

mainly derived from freshwater systems from rivers and streams in the U.S. or an eastern United States NAWQA-derived subset (NAWQA and NAWQA East), or from more than 1500 lakes sampled within the NLA. All of these metrics have strengths and weaknesses due to the inclusion or omission of species detected in each of the cores. Because most of marine or brackish species present in the Christina River are not occurring or are very rare within the NAWQA and NLA data sets, metrics calculations were based mostly upon the freshwater species occurring in these cores. These were based primarily on the van Dam et al. (1994) summary and synthesis of ecological characteristics of taxa observed in Western Europe, and generally found to have wide geographic application. The van Dam et al. (1994) autecological values for many taxa have been revised to be more relevant for the U.S., and are contained in a data compilation developed for the USGS NAWQA program by Porter (2008) and Porter et al. (2008). To allow a comparison between the current study in the tidal Christina River and the previous study of the tidal Saint Jones River (Velinsky et al., 2007), the data set and metrics by van Dam et al. (1994) will be the focus of this discussion.

The diatom community composition based on the van Dam et al. (1994) metrics show an increase in the proportion of eutrophentic species (i.e., high nutrient species) starting between 30 and 40 cm towards the surface of the core (**Figure 10; Tables 12-14**). Below this depth range, the proportion of mesotrophentic species increases slightly. Interestingly, oligotrophentic species were only randomly detected throughout each of the cores.

To evaluate how nutrient conditions, as reflected by total sediment N and P, impacted the diatom species and metrics in each core, N and P were plotted against the metric for eutrophic species (**Figures 11-12**). For the Brandywine Creek core, there was no relationship between N or P and the diatom metric. In the Dravo Marsh and Churchmans Marsh cores, there was a good relationship between sediment N and P and the diatom metric. The r^2 for N for both cores averaged 0.77 while for P the r^2 averaged 0.51.

Historical Analysis: Concentrations of total sediment N and P exhibited interesting trends within each core over time (**Figures 13-14).** In CM, total N increased from approximately 0.3 to 0.79% starting in the last 1950s. Similarly, in DM, concentrations of TN increased from approximately 0.2 to 1.2% starting in the early 1960s. In the BW, sediment TN increased slightly over time, from 0.19±0.04% before 1960 to an average of 0.35±0.09% after 1963. It is possible that

sediment remineralization processes, with the remobilization of bound N to dissolved N, is occurring after burial in the sediment (Burdige, 2006). This would decrease the sediment levels of TN with time, and could result in an increase in the C to N ratio as N is preferentially remineralized. The changes in C/N with depth (and time) in these cores is not apparent (**Figure 7a; Tables 7-11**). In addition, the stable isotopic composition of the sediment N (δ^{15}N-TN) increases to varying degrees in both cores (**Figure 13**). The increase starts in the mid-1950s in CM and in the mid-1960s in DM, both increasing from about 4-6‰ to approximately 8‰ at the surface. This suggests that there was an increase in loadings to these marshes and that the source(s) of N may have changed over time. Leavitt et al. (2006), Ulseth and Hershey (2005) and Velinsky (unpublished data) show that higher δ^{15}N of the nitrogen is associated with higher inputs from urban sources. Bratton et al. (2003) showed similar trends in deep cores from the Chesapeake Bay. Lastly, this is a similar trend observed in a Woodbury Creek (NJ) marsh (Church et al., 2006). Therefore, the increase in N concentrations, along with near constant C to N ratios, coupled with an increase in δ^{15}N-TN, indicate that N loadings have increased over time and appear to continue to increase.

Schelske and Hodell (1991; 1995) and Perga and Gerdeaux (2004) have shown a relationship between the concentration of P in the sediments or water and the isotopic composition of carbon (δ^{13}C-TC) in the sediments or in fish scales over time. The fish scales were an integrator of the top of the pelagic food web (i.e., phytoplankton). In brief, it is proposed that as P levels increase, primary productivity increases to a point at which there is reduced isotopic fractionation during enzymatic uptake of dissolved CO_2. This reduced fractionation would result in higher isotopic compositions of organic matter (i.e., more ^{13}C enriched) and would suggest that P was helping to control aquatic productivity. Recently, Church et al. (2006) showed a similar trend and relationship in a sediment core from Woodbury Creek, NJ.

In CM there is a gradual increase in TP concentrations starting in the early part of the last century with peak concentrations in 1980 (**Figure 14**). Concentrations decreased afterwards then increased again at the surface. In the BW core, there was a peak in concentration in 1990 while the DM core exhibited a small peak in the 1950s and then increasing concentrations from the 1980s to the present. This time-concentration profile may reflect P usage, especially in detergents (Litke, 1999; Church et al., 2006) as well as other sources such as fertilizers and agricultural runoff, although there is no clear distribution. As with nitrogen, phosphorus can

undergo substantial diagenetic processing related to the carbon, iron and sulfur cycle (Burdige, 2006). These factors make it difficult to accurately interpret the P distributions.

Figure 15 shows the distribution of total sediment P and the isotopic composition of organic matter from the three primary cores (CM, DM, and BW). The BW core shows no relationship while the CM core data indicates a relationship of increasing P with decreasing sediment $\delta^{13}C$. In the DM core, there appears to be two relationships, one at low TSP (increasing P, increasing $\delta^{13}C$) and from 0.06% to 0.10% of increasing P and decreasing $\delta^{13}C$. It is unclear at this point what is causing these relationships (or what they are telling us) but it is possible that changes in the source of organic matter to the marshes (i.e., terrestrial-upland material versus *in situ*-local production) may have changed over time. In both CM and DM sites, the $\delta^{13}C$ decreased (became more negative) since the 1930s (**Figure 15**), which may be an indicator of the development and land use changes in the watershed.

The diatom metrics used to assess eutrophication for each core were plotted against time in **Figure 16**. It appears that starting in late 1950s to early 1960s, the proportion of species that are indicators of high nutrient conditions increased substantially in the DM and CM cores. The increase in the metric corresponded to an increase in N and P sediment concentrations (see above), except for the Brandywine site.

Preliminary analysis of the diatom assemblages and metrics indicate a shift toward more eutrophic species starting in the late 1940-1950s. The proportion of mesotrophic and especially oligotrophic diatom indicators was low throughout the cores. There was a strong positive relationship between the eutrophic diatom metric and the concentration of nitrogen and phosphorus in Churchmans and Dravo marshes. This, along with the increases in total sediment N, total sediment P and sediment nitrogen isotopic compositions ($\delta^{15}N$-TN), indicates that increase loadings of nutrients have resulted in a diatom shift in the river.

C3: <u>Sediment Bound Contaminants</u>

Selected sections from each core were analyzed for a suite of sediment bound contaminants including polycyclic aromatic hydrocarbons (PAHs), polychlorinated biphenyls (PCBs), and specific organo-chlorine pesticides (e.g., DDXs, chlordanes, etc). Three cores were also analyzed for a suite of polybrominated diphenyl ethers (PBDEs). Lastly, core sections were analyzed for strong acid leachable concentrations of zinc (Zn) and iron (Fe).

C3.1: Polycyclic Aromatic Hydrocarbons

Polycyclic aromatic hydrocarbons (PAHs) are a large group of organic chemicals with two or more fused aromatic rings. They have a relatively low solubility in water and have a range in lipophilicity and, in general, adhere to organic particles in water and air. Specific PAH compounds can be carcinogenic and mutagenic to various aquatic organisms at different life stages. PAHs are formed mainly as a result of pyrolytic (combustion) processes, especially during the incomplete combustion of organic materials during industrial and human activities; e.g., processing of coal and oil, vehicle traffic, combustion of oil and gas, and the combustion of refuse. There are a few hundred PAH compounds with a few naturally occurring such as perylene, however most are from anthropogenic sources (e.g., benzo[a]pyrene). Sources to estuarine environments, such as the tidal Christina River, include sewage and industrial discharges, oil spills, bulkheading with creosote wood products, combustion of fossil fuels, and treatment of parking lots with sealcoat. Atmospheric deposition is also a significant source of PAHs to the environment but in the urbanized Christina watershed is most likely not the dominant source.

The sources and nature of hydrocarbon geochemistry can be revealed by the distribution of the individual compounds that comprise saturated (SHC) and aromatic hydrocarbons (PAH) (Farrington, 1980; Hites et al., 1980; Wakeham et al., 1980; Boehm and Farrington, 1984; Boehm, 1984; Pruell and Quinn, 1985). Within the aromatic hydrocarbons, the various alkyl-substituted naphthalenes (i.e., C_1, C_2, C_3) have not been found in organisms and are thought to be derived from petroleum contamination. PAHs can also help discriminate between combustion sources of hydrocarbons and those derived by the direct discharge of oil. Oil contains a greater percentage of alkyl-substituted compounds in the naphthalene, phenanthrene-anthracene, and chrysene series. Refined petroleum products would have a greater abundance of lower than higher molecular weight compounds. The partial combustion of oil reduces the amount of alkyl-substituted compounds leaving the parent structure in greater abundance (Youngblood and Blumer, 1975). Some of the general differences between biogenic and petroleum sources of hydrocarbons are summarized below. These differences will be exploited in the following discussions in evaluating the source of hydrocarbon contamination to the sediments of the various study areas.

General Characteristics of Biogenic and Petroleum Hydrocarbons*.

Natural Biogenic Hydrocarbons

- Narrow range of molecular weight distribution of SHC and PAH (if present), UCM is either low or absent. Odd- to even-numbered alkane ratio is > 1.
- Terrestrial plant material indicated by an alkane distribution from nC_{23} to nC_{34}, centered around nC_{29} or nC_{31}.
- Aquatic organisms have a predominance of nC_{13} to nC_{21} alkanes with greater amounts of odd-numbered compounds.

Fossil Fuel or Petroleum Hydrocarbons

- Wider range in molecular weight distribution of both SHC and PAH, UCM is present in large amounts compared to alkanes and PAHs.
- Odd- to even-numbered alkane ratio = 1.
- Several homologous series with adjacent members in approximately the same concentrations.
- Natural source sources of PAH indicated by less complex distribution with compounds related to structure of precursors (i.e., perylene and retene).
- Direct discharge of oil is indicated by PAHs (e.g., naphthalene, phenanthrene-anthracene, and chrysene series) contains many alkyl-substituted species (i.e., C_1, C_2 and C_3). Greater abundance of lower molecular weight PAHs.
- Combustion products have a greater abundance of un-substituted parent compounds, with homologs which decrease in abundance as the degree of alkyl substitution increases.
- UCM present in greater proportion than resolved peaks.

* Taken from Youngblood and Blumer, 1975; Farrington, 1980; Hites et al., 1980; Wakeham et al., 1980; Boehm and Farrington, 1984; Boehm, 1984; Pruell and Quinn, 1985; Pierce et al., 1986. (SHC – saturated aliphatic hydrocarbons, UCM – unresolved complex mixture; PAH – polycyclic aromatic hydrocarbons)

Low versus high molecular weight PAHs ratios (i.e., LMW and HMW PAHs) are indicative of the input sources of hydrocarbons (Farrington 1980; Boehm and Farrington 1984). Low molecular weight PAHs are defined as 2 to 3 benzene ring compounds, including naphthalenes, anthracenes, phenanthrenes, and dibenzothiophenes. High molecular weight PAHs, with 4 to 5 benzene rings, include compounds such as fluoranthenes, chrysenes, benzo[a]pyrene and dibenz[ah]anthracene. A predominance of LMW over HMW PAHs indicates an oil source of hydrocarbons (Farrington 1980; Boehm and Farrington 1984). Due to weathering and degradation processes, with time LMW PAHs would decrease in abundance relative to HMW PAHs. Also, the combustion of petroleum yields PAHs with more HMW compounds.

Polycyclic aromatic hydrocarbons (PAHs) were detected in all samples analyzed. PAHs comprised 34 individual compounds ranging from the low molecular weight compounds such as naphthalene and phenanthrene (2- and 3-rings) to high molecular weight compounds with 4- and 5- rings, including pyrene and dibenz[a,h]anthracene. Total PAHs (methyl-substituted and unsubstituted forms) ranged from 0.25 to 26.8 μg/g dw among all cores (**Tables 7-11; Appendix I**) with some differences in the distribution with depth (**Figure 17**). The concentrations in the

tidal Christina River were similar to other urban environments such as the tidal Anacostia-Potomac rivers and Baltimore Harbor (Wade et al., 1994; Ashley and Baker, 1999; Riedel et al., 2007), and were lower than those found in the Saint Jones River, Delaware (Velinsky et al., 2007).

Concentrations in CM-1 (Table 8 and Figure 17) were low near the surface (1.68 μg/g dw) increasing to a maximum concentration of 26.8 μg/g dw at 36-38 cm (corresponding to 1945) with the lowest concentrations (<0.5 μg/g dw) near the bottom (pre-1900). In the Dravo Marsh core (DM-2), PAH concentrations were similar overall to the CM core, but the DM core did not exhibit a single strong peak at depth like the CM core. Rather, the DM core showed two smaller peaks. One maxima (8.1 μg/g dw) was at 12-14 cm (circa. 1990) and a deeper maxima (6.5 μg/g dw) was centered around 36-38 cm (circa. 1958). Dual peaks were also seen in the DM core for PCBs about these same dates (see next section). The general rise up to the earlier PAH peak in the DM core appears to have begun as early as 1905. Concentrations near the bottom of the DM core, which date back prior to 1900, ranged from 0.25 to 0.34 μg/g dw, making these pre- turn of the century values consistent with those seen at the bottom of the CM core. The PAH concentrations in these deep sections of the CM and DM cores reflect PAH concentrations that existed just prior to rapid industrial expansion.

The Brandywine Creek core (BW-2) was shorter in length than the other cores and was similar in concentration to the DM core concentrations overall. Further, the PAH concentration at the surface of the BW core (1.68 μg/g dw) were similar to the other two cores at the surface (~ 2-2.7 μg/g dw). Slightly higher concentrations (8.0 to 9.0 μg/g dw) were seen in the BW core between 20 and 30 cm (~1979 to ~1968). Total PAH concentrations near the bottom of BW-2 (between 46 and 52 cm, corresponding to 1944 to 1939) were similar to surface concentrations.

PAH concentrations in the WS core showed little variability from the top of the core to the bottom of the core (Table 11 and Figure 17). The mean and standard deviation among the six intervals analyzed within that core were 9.9 and 1 μg/g dw, respectively. Although we were not able to successfully radiodate this core, it is clear that there is substantial PAH contamination in the sediment deposit from which this core was collected. Similarly, there appears to be considerable PAH contamination in the LSP core (Table 10 and Figure 17), although the vertical profile is not well defined. The mean PAH and standard deviation among five samples collected

from this core were 9.1 and 7.5 μg/g dw, respectively. The maximum PAH concentration in this core was 19.5 μg/g dw, which very roughly corresponds to 1970.

The general increase in PAH in the DM core that began shortly after the turn of the century and continued until ~1958, followed by a 10- to 15-year drop, may be associated with the rise and fall of the shipbuilding industry immediately downstream from the Dravo Marsh (Thompson and O'Byrne, 1999). In addition, the PAH pattern in the DM core may also have been influenced by releases from the nearby Wilmington Coal Gasification Plant, which contaminated nearby surface and subsurface soils and groundwater (DNREC, 2004). It is unclear why the DM core shows a more recent increase from ~1955 to ~1990, followed by a drop. One possible explanation is extensive redistribution of previously contaminated soils and sediments during major roadwork projects (e.g., I-95 and SR-141) or other land disturbing activities in and near DM.

With regard to the CM core, the extremely sharp rise and equally fast fall centered on 1945 suggests there may have been a significant release or spill of petroleum into the tidal Christina about that time. The fact that a significant proportion of PAH mass was lower molecular weight material (Figure 17) tends to support that hypothesis. The idea that lower molecular weights PAHs are often associated with petroleum rather than combustion sources is discussed in more detail below.

As noted earlier, 34 individual compounds were summed to calculate the total PAH (tPAH) fraction. These compounds ranged from 2-ring compounds such as naphthalene to 5-ring aromatic compounds such as di-benzo[a,h]anthracene (**Table 12; Appendix I**). Also included within the 34 individual PAHs are 6 methyl-substituted forms including methylnaphthalene, methylfluorene, and methylphenanthrene. Both the distribution of parent PAHs and methyl-substituted PAHs can be used to help determine the sources of hydrocarbons to the tidal river (i.e., combustion or petrogenic sources). For instance, the phenanthrene to anthracene ratio can be used to help distinguish between combustion (pyrogenic) versus direct oil (petrogenic) sources in aquatic systems since undegraded oil has a very high ratio (50) compared to combustion sources (ca. 0.3; Wakeham et al., 1980; Wade et al., 1994; O'Malley et al., 1994 and 1996; Neff et al., 2005). In CM-1, the phenanthrene to anthracene ratio ranged from 0.1 to 19 (excluding one duplicate value of 176) which are characteristic and typical of many urban environments having a preponderance of combustion sources (Gschwend and Hites, 1981;

Hoffman et al., 1984; Van Metre et al., 2000; Velinsky et al., 2008). The highest ratios were near the surface (19 at 8-10 cm) suggesting more of a petrogenic source to this horizon; interestingly this did not correspond to the peak concentration of tPAHs (**Figure 17**).

The ratio of low molecular weight PAHs to total parent PAHs (LMW:tPAHp); **Figure 17; Tables 7-12, Appendix I**) is also an indicator of petrogenic versus combustion sources. In CM-1, the baseline ratio ranged from approximately 0.1 to 0.2 with peak ratios (0.4 to 0.7) centered on the peak in tPAH concentrations (36-38 cm). This suggests that the sharp peak in PAH concentrations at 36-38 cm (circa. 1945) is more petrogenic in nature and may have resulted from a spill near this site as noted above.

For core BW-2, the phenanthrene to anthracene ratio varied considerably with depth and ranged from <1 to 280. While the highest ratio was observed near the surface, generally higher ratios were found below 25 cm indicating somewhat greater petrogenic sources in the past. High ratios of phenanthrene to anthracene with occasionally low ratios of fluoranthene to pyrene near 0.38 suggests the presence of diesel fuel in at least some of the BW samples (Neff et al., 2005). However, LMW to tPAHp ratios were low at depth (<0.3) more suggestive of a primary combustion source in the distant past. Highest LMW to tPAHp ratios were observed near the subsurface concentration maxima near 20-22 cm (**Figure 17**). It is unclear why these two indicators did not correspond to each other but the ratio of LMW to tPAHp may be more sensitive since it integrates a broader range of compounds. However, it is possible that variable sources of PAHs (various fuel oils, coal based compounds, etc) could have different ratios and their relative loadings may have changed over time.

The Dravo Marsh core (DM-2) had both low phenanthrene to anthracene and LMW to tPAHp ratios from the surface to the bottom of the core. The ratios ranged from 0.2 to 2 and 0.1 to 0.2, indicating that this site was dominated by more combustion-related sources than the other locations. As noted previously, a coal gasification plant operated immediately downstream of the DM coring site for decades (DNREC, 2004), possibly helping to explain the strong pyrogenic signal in the DM-2 core.

Recently, Mahler et al. (2005) and Van Metre et al. (2009) proposed that the ratios of benzo[a]pyrene to benzo[e]pyrene and fluoranthene to pyrene be used as an indicator of coal-based sealcoat used for parking lots. They illustrated that in many locations these ratios suggested that coal-based sealcoat is a dominant source of urban PAHs to various waterways

(Mahler et al., 2005; Van Metre et al., 2006, 2009). Figure 18, taken from Van Metre et al. (2009), illustrates the potential urban sources of PAHs from *in situ* samples from various locations. The ratio of these pair of compounds in stream/lake samples compared to coal-based seal coat suggests that this material is a major source in urban areas. For this study, we plotted only the top part of the core, i.e., the more recent sediment sections, to help determine source functions in the Christina watershed (**Figure 19**). The average ratios for benzo[a]pyrene to benzo[e]pyrene and fluoranthene to pyrene are 0.90±0.53 and 0.99±0.19, respectively, suggesting that coal-based seal coat material is not a major source to the sediments in this area.

Overall, there are both pyrogenic and petrogenic sources of PAHs to the sub-surface sediments of the tidal Christina basin. Sources of PAHs related to urban areas include tire wear; crankcase oil; bus, train and car soot and exhaust; old coal gasification plants; petroleum spills and releases; and possibly seal-coat material (Wakeham et al., 1980; O'Malley et al., 1994; Van Metre et al., 2009). In addition, in core CM-1 and, to a lesser extent, BW-2, there also appears to be an input of petrogenic hydrocarbons dominated by low molecular weight compounds such as phenanthrene, anthracene, and fluoranthene as well as a number of methyl-substituted compounds like 2-methylphenanthrene, 2-methylanthracene, 1-methylanthracene, 1-methylphenanthrene, 9-methylanthracene and 4,5-methylenephenanthrene. These lower molecular weight PAHs are generally more toxic than their higher molecular weight counterparts (Neff et al., 2005; Di Toro and McGrath, 2000).

Van Metre et al. (2000) showed that in cores from different urban environments a shift from uncombusted to more combusted sources of PAHs with decreasing depth (and time). We did not observe this general trend in the Christina but did see a change in sources at specific layers and time.

Historical Analysis: Total PAH concentrations in CM were highest in the mid-1940s (26 μg/g dw) decreasing to lower levels by 1950 and remaining nearly constant since the 1960s (1.4 to 2.5 μg/g dw) to the present (**Figure 20**). Concentrations in core DM showed a bimodal distribution with time with high concentrations around 1955 (6.5 μg/g dw) and in the 1990s (8.1 μg/g dw). After this date, concentrations decreased to 3 μg/g dw at the surface. At BW, the chronology only goes back to the late 1930s and exhibits a bimodal peak from the late 1960s to late 1970s after which concentrations decreased to somewhat lower levels (2-4 μg/g dw).

It is difficult to determine the exact source(s) of PAHs to these cores, but the general development and urbanization/industrialization of the area is the most likely general contributor (Wakeham et al., 1980; Gschwend and Hites, 1981; Wade et al., 1994; O´Malley et al., 1994; 1996; Mahler et al., 2005; Van Metre et al., 2000; 2009). In the CM core, the significant peak in concentration in the 1940s is also when the LMW/tPAHs (**Figure 17**) increased to 0.65 (fraction) suggesting a more distinct petroleum input at this time. The other cores (with the occasional exception in the BW core) generally show a low ratio (0.2 to 0.4) of LMW/tPAH, thus indicating more of a combustion source overall. However, near the CM site, at the confluence of the White Clay Creek and Christina River, was the 130-ha Koppers Company Facilities that operated a wood preserving facility from 1922 to 1971. The facility pressure treated wood with creosote (and some pentachlorophenol). The peak in PAH concentration in the mid-1940s at CM appears to be primarily a signature of this operation. Finally, in the recent sections of all cores, specific PAH ratios (Mahler et al., 2005; Van Metre et al., 2009) indicate asphalt seal-coat as a potential source to the river but this does not appear to be a dominant source as suggested by Van Metre et al. (2009) as in other riverine systems.

C3.2: Polychlorinated Biphenyls

Polychlorinated biphenyls (PCBs) were mainly produced by the Monsanto Corporation from 1930 to 1977 and it is estimated that 5.4×10^8 kg has been produced within the United States (Kennish, 1992). They are or have been used as electrical insulators in many transformers, fire retardant, and additives to oils and paints. There are 209 congeners (or compounds) of PCBs based on the position and number of chorines on the biphenyl structure. As a result, the physical and chemical properties of this group of congeners vary greatly in the environment (ATSDR, 2000). Persistence of PCBs in aquatic sediments is due to their slow rate of degradation and vaporization, low water solubility, and partitioning to particles and organic carbon. Bacteria degrade PCB, with the rate dependent on the position and degree of chlorination of the biphenyl ring and in many cases the absolute concentration present in the sediments (Kennish, 1992 and others). Current sources to this area are thought to be from contaminated sites, runoff from old landfills and accidental spills (e.g., transformer fluids). Recently, Greene (2009a,b) characterized PCB concentrations in water, sediment, and biota of the tidal Christina River at three sites near the coring sites described in this study (Newport, Walnut Street and

Brandywine). This study along with previous studies in the Christina watershed (e.g., DNREC, 2005) will be used to compare data from the current study.

For the present study, total polychlorinated biphenyls (tPCBs) were calculated as the sum of approximately 110 primary congeners (compounds) that were quantified either individually or as coeluters with multiple (2 or 3) congeners (**Tables 7-11; Appendix I**). Among the three marsh cores (CM-1, DM-2, and BW-2), concentrations of tPCBs ranged from 2.2 ng/g dw (near the method detection limit of ≈1.2 ng/g dw; calculated as the mean plus three times the SD of the blanks) to approximately 2107 ng/g dw with an overall median concentration of 122 ng/g dw (**Tables 7-11; Figure 21)**. The Churchmans Marsh core had the maximum concentration (2107 ng/g dw). The peak in the Brandywine core was 685 ng/g dw and that in the Dravo Marsh core was 436 ng/g dw. The surface concentrations in these three cores ranged from 45 to 238 ng/g dw, which is generally consistent with the range observed by Greene (2009a) for surface sediment samples collected in 2007 in the tidal Christina Basin. The peak surface concentration (238 ng/g dw) was observed in the Dravo Marsh core.

The onset of elevated PCB concentrations in the CM core occurred at 42-44 cm, which, based on age dating, corresponds to approximately 1935. This correlates well with the first commercial production of PCBs in the U.S. (1929). Detections of PCBs in the CM core prior to that time are attributed to sediment reworking and possibly downcore diffusion. A sharp peak in PCB in the CM core occurs at 28-30 cm, which translates to approximately 1959. This is roughly a decade prior to the 1970 peak in U.S. production, suggesting that local usage did not perfectly track overall U.S. production. After the CM peak in 1959, PCB concentrations in the CM core steadily decreased to the surface.

The BW core also exhibited a clear onset at depth, peak, and then decline in PCB concentration towards the surface. The onset in that core occurred at 32-34 cm (circa. 1963), and the peak occurred at 14-16 cm (circa. 1987). These dates are significantly later than those seen in the CM core, suggesting different loading histories.

The PCB profile in the DM core is more complex than the CM and BW cores. The DM core exhibits a bimodal distribution in PCB concentration, showing two separate peaks. The onset of the first peak occurred at 48-50 cm (circa. 1942), with the actual peak seen at 36-38 cm (circa. 1958). These dates track the CM core fairly well. After 1958, the PCB concentration in the DM core fell and remained below 50 ng/g dw for at least a decade. Then, concentrations began to

increase again in the late 1970s, rising to a second peak at 10-12 cm (circa. 1992) that was similar in magnitude to the first peak. PCB concentrations in the DM core have fallen somewhat since 1992 but surface concentrations remain high relative to the surface concentrations in the CM and BW cores.

Total PCB concentrations in lower Shellpot Creek (LSP) core ranged from 303 to 3460 ng/g dw and from 76 to 236 ng/g dw in the Walnut Street Bridge boat slip core. The highest concentrations in LSP were observed at 70-72 cm depth interval, which corresponds approximately to 1970. As noted previously, radiodating of the LSP core was not ideal, and so a date of 1970 is only a rough approximation of when the peak PCB concentration in this core occurred. Radiodating of the Walnut Street boat slip core was even more problematic, primarily because this location is subject to non-steady runoff and heavy shoaling. It is interesting to note however, that PCB concentrations in this core did not vary greatly along its length, which represents nearly 100 cm (or roughly 3 ft) of accumulated material. Although the area from which this core was collected may be small in terms of surface area, it appears to contain a significant inventory of PCB mass. Additional testing would be needed to quantify that mass. The other interesting feature of the Walnut Street core is that the surface concentration (197 ng/g dw) is quite similar to the surface concentration of the Dravo Marsh core (238 ng/g dw). These 2 cores are located within a mile and a half of each other, helping to explain the similarity.

To provide additional insights into the PCB core profiles, the 110 congeners determined in the study (excluding the monochlorinated congeners 1 and 3) were grouped into homolog groups (from 1 to 10) based on the number of chlorine atoms substituted on the biphenyl ring (e.g., homolog group H5 contains measured congeners with 5 chlorines; **Appendix I**). In addition, the homologs were summarized into low molecular weight congeners (LMW; i.e., H1 to H5) and high molecular weight congeners (HMW; i.e., H6 to H10). Important in this analysis is the assessment of blank levels given an MDL for tPCBs of approximately 1.2 ng/g dw. It is important to note that at low concentrations (those approaching values of 10 times the MDL, 10 ng/g dw, or lower) which are characteristic of lower portions of cores, congener profiles become less reliable as an accurate representation of true congeneric PCB patterns. However, for completeness, those low concentration profiles have been included in the following analysis.

For simplicity, the ratio of the LMW PCBs to the total PCBs along the CM, DM, BW, LSP and WSC cores are presented in **Figure 22a,b**. The changes in the LMW to tPCB ratio along

with homolog patterns reveal consistent changes with depth in the cores. In the CM and DM cores, the LMW to tPCB ratio was approximately 0.3 to 0.4 in the upper 30 cm or so decreasing from 0.2 at 35-40 cm to 0.1 between by 56 cm in the CM core and to 0.16 by 42 cm in the DM core. In the BW core, the ratio is more variable in the surface 30 cm ranging from 0.47 at the surface to 0.53 at 12-14 cm, and then decreasing to a minimum of 0.34 at 32-34 cm. Below this depth concentrations are near the detection limit and, as such, the ratio increases substantially. The ratio appeared not to change relative to the peak in concentrations in the CM and DM cores, however, the peak concentration in the BW core at 14-16 cm (circa. 1987) is also where there was a slight increase in the ratio (0.53), suggesting a change in source at this depth. In the LSP and WSC cores, higher molecular weight congeners dominate all sections with a LMW:TPCBs ratio of ~0.2.

To further illustrate the compositional change in each core with depth, the homolog patterns for selected sections are presented in the lower graphs in **Figure 22a** for CM, DM and BW. In the surface sections of CM and DM, the homolog patterns are similar, with a dominance of H4 to H6 with lesser, but still significant amounts of H7 to H10). In contrast, in the BW surface sections, the PCB distribution is dominated by H4 through H8 with very little H9 and H10. In the middle sections of the CM and DM profiles, the congener pattern shifts to homologs of higher molecular weight (H8 to H10), potentially suggesting a common historic source influencing both of these cores. Only in the deepest sections of the CM and DM cores does the strong H8 to H10 signal disappear. The BW PCB homolog distribution with depth does not show the higher molecular weight homologs (H8 to H10). Rather, the deeper sections of the BW core show slightly lower molecular weight homolog groups. Finally, in the lower Shellpot Creek and Walnut Street cores, while fewer sections were analyzed, differences are evident (**Figure 22b).** The homolog pattern in the LSP is dominated by H6 and H7 congeners throughout the core (n=5), while the WS core contains higher levels of lower molecular weight congeners in the H4 to H6 homolog groups.

Returning to the issue of high molecular weight homologs in CM and DM, it is noted that a high percentage of H8 to H10 is somewhat unusual and inconsistent with homolog patterns known to exist in commercial PCB Aroclor mixtures (Rushneck et al., 2004). **Figure 23** isolates the concentration of deca PCB (H10) in the three cores (CM, DM, and BW). Concentrations range from near detection level (<0.1 ng/g dw) up to a maximum of 167 ng/g dw. The highest

values were found in the CM core, followed by intermediate values in the DM core, and finally low levels in the BW core. The peak in the CM core occurred in the intervals 28 to 38 cm, corresponding to 1960, while the peak in the DM core occurred at 12 to 22 cm, corresponding to 1985. Interestingly in the DM core there was a deeper maximum of 49 ng/g dw for PCB 209 at 36-38 cm which corresponds to 1960. Surface concentrations of deca PCB were 13, 35, and 1.5 ng/g dw in the CM, DM, and BW, respectively.

Greene (2009a) also reported unusually high percentages of deca PCB (H10) in surface sediment samples collected from the tidal Christina River. Based on the work of Baker et al. (2004) and EPA administrative records, Greene (2009a) attributed the strong deca PCB in the sediments of the tidal Christina River to inadvertent formation of deca PCB during the production of titanium dioxide at a nearby factory in Edge Moor, DE. Superfund administrative records indicate that dust slurries produced at the Edge Moor factory were later handled at a pigments plant in Newport, DE. Those dust slurries are thought to have contained deca PCB. The handling of those materials at the Newport pigment plant along with the discovery of high levels of deca PCB in the nearby CM core provides a linkage between the Edge Moor factory, the Newport pigment plant, and deca PCB contamination in the tidal Christina River. The fact that a strong deca PCB signal was also found in the DM core indicates that at least some of the source material was transported and smeared downstream in the Christina.

Historical Analysis: Concentrations of tPCBs in all cores started to increase after 1930 with highest values after the 1950s through to the present (**Figure 24**). Total PCB concentrations in CM were highest in the late 1950s (2100 ng/g dw), decreasing to 90 ng/g dw by 2006 (**Figure 24**). In DM, there was also a peak in the late 1950s (~400 ng/g dw) and a more recent peak at 1992 of 440 ng/g dw), following the same general bimodal behavior as PAHs (see above). Surface and near surface concentrations of PCBs in DM remained elevated ranging from 240 to 360 ng/g dw. The tidal Brandywine Creek core (BW) concentration-date distribution reflects a source or sources of PCBs that increased in the 1960s with peak inputs in the 1980s up to 1990 (**Figure 25**). Total PCB concentrations were highest around 1988 at 660 ng/g dw, after which concentrations decreased substantially to <50 ng/g dw by 2001. This distribution indicates that one or more dominate sources on the Brandywine were discharging PCBs well after pollution controls (mid to late 1970s) were in place to limit PCB discharges.

The distribution of tPCBs with time in each of the cores appears to reflect sources within each tidal river and the geographic location of each site may act to trap the source(s) upstream or near that site (**Figures 1 and 24**). On initial review, the DM site appears to have two separate primary sources over time that result in the bimodal concentration distribution with time. An alternative explanation is that the more recent peak may reflect significant redistribution of previously deposited PCB contamination as could happen during major earth works projects. As such, the deeper peak in the DM profile may be reflective of the source to the CM while the upper peak more reflective of local disturbance of previously sequestered contamination.

The tidal Christina Basin (and its non-tidal watershed) contains present-day contaminated substance sites that can contribute PCBs (and other chemical contaminants) to the water and sediments (DNREC, 2007; Brightfields, Inc., 2009). Brightfields, Inc. (2009) estimated PCB loads from current waste sites to the tidal Christina River and Brandywine Creek via overland flow of contaminated soils and via groundwater discharge. Mass loads for individual sites ranged from <0.1 g/yr to over 24 kg/yr, with the AMTRAK Former Refueling Facility having the largest estimated load. While there is some uncertainty with these estimates, they do show substantial current inputs to the tidal river that can impact sediment quality and fish species in the area. Our data do show however that past inputs were higher and that controls implemented in the 1970s to the present have lowered the overall input.

C3.3: Total DDX and Chlordane

DDT and its breakdown products (2,4'+ 4,4' forms of DDT (1,1'-(2,2,2-trichloroethylidene)bis[4-chlorobenzene]; DDE (1,1'-(2,2,2-trichloroethenylidene)bis[4-chlorobenzene]) and DDD (1,1'-(2,2-dichloroethylidene)bis[4-chlorobenzene]) were used for insect controls starting in the mid-1940s. DDT was banned in 1972 and has been found to have an approximate environmental half-life of 10 to 20 years (NOAA, 1989; Woodwell et al., 1971). While it was banned nearly 30 years ago, parent DDT is still detectable (and in substantial concentrations) in the sedimentary material collected from various locations in the Delaware and Chesapeake bays (Wade et al., 1994; Greene 2009b). Greene (2009b) summarized total DDT and other contaminants in surface water, sediment, and biota samples collected throughout the tidal and non-tidal Christina Basin in Delaware. Peak DDT concentrations in the water were detected

in the Red Clay Creek at a station near the PA-DE line. The peak chlordane concentration in the water was detected in Little Mill Creek at Maryland Avenue in Wilmington

Chlordane is a multi-component mixture of polychloro-methanoindenes (e.g., oxy-, γ-, and α-chlordane, heptachlor, heptachlor epoxide and cis+trans-nonachlor). Technical grade chlordane contains more than 140 components of which only 120 compounds can be resolved by current analytical techniques. Alpha (α)-chlordane, gamma (γ)-chlordane, heptachlor and trans-nonachlor are the dominant constituents (Dearth and Hites, 1991), and are used to control termites and ants. Because of the toxicity, potential carcinogenicity and environmental persistence of these components and/or metabolites, (e.g., heptachlor, heptachlor epoxide and oxychlordane), the use of chlordane is under federal regulations. The use of chlordane was halted in 1988 after a phased reduction in use since approximately 1975. The half-life of chlordane is similar to that of DDT (i.e., approximately 10 to 20 years), and therefore its persistence is to be expected for many years. However, while the large scale use of chlordane decreased in the late 1980s, it was not fully phased out and was still used in the area.

The parent and breakdown products of DDT and chlordane were detectable in most sediment layers, especially in the upper, more fine-grained sections of each core (**Tables 7-11; Appendix I**). Concentrations of these two pesticides were generally low to moderate overall with occasionally high concentrations at specific intervals in the cores. Total DDX (all forms; tDDX) ranged from <1 to approximately 369 ng/g dw (median of 18 ng/g dw), while total chlordanes ranged from <1 to 151 ng/g dw (median of 2.9 ng/g dw). The highest concentrations of both pesticides were detected in the BW core. Surface concentrations of DDX were 9.3, 29.1, and 8.2 ng/g dw at the CM, DM, and BW coring sites, respectively. Surface concentrations of chlordane were 2.8, 9.7, and 2.5 ng/g dw at the CM, DM, and BW coring sites, respectively. Surface DDX and chlordane concentrations in the DM and BW cores are generally within a factor of 2 of concentration reported by Greene (2009b) for surface sediments collected in 2007 from the lower tidal Christina River and the tidal Brandywine. Surface DDX and chlordane concentrations in the core tops from CM are roughly 5 times higher than the surface concentrations reported by Greene (2009b) for a station in the tidal Christina River just downstream of CM. The differences are far less when the respective datasets are normalized to organic carbon content.

The distribution with depth of both groups of pesticides was similar to each other and in many ways followed the tPCB profiles (**Figures 22 and 26**). In the Churchman Marsh (CM)

core, concentrations were at the detection limits at depth with peak concentrations at 32-34 cm (circa. 1952) for both pesticides, decreasing towards the surface. The Dravo Marsh (DM) core, similar to tPCBs, exhibited a bimodal distribution with higher concentrations at the 36-38 cm (circa. 1958) and 10-12 cm (circa. 1992) intervals, while in Brandywine Creek (BW) concentrations of both pesticides exhibited sharp peaks at approximately similar intervals (1979 to 1982).

The lower Shellpot Creek (LSP) core (n=5) exhibited highest tDDX concentrations at the surface (75 ng/g dw) with decreasing concentrations with depth, while the Walnut Street (WS) core had slightly higher concentrations in the upper 50 cm (20 ± 7 ng/g dw) with lower concentrations at depth (> 66 cm of 11 to 17 ng/g dw). The distribution of total chlordane for both cores is similar. Highest concentrations of total chlordane were observed in the Shellpot Creek core (151 ng/g dw) decreasing with depth and only slightly higher concentrations in the upper 50 cm (3.3 to 8.3 ng/g dw) compared to the bottom two sections (3.1 to 5.7 ng/g dw).

Historical Analysis: Similar temporal distributions of tChl were observed as tDDX in all three cores (**Figures 25 and 27**) and were similar to the trends in tPCBs. In CM, highest concentrations of tDDX (117 ng/g dw) and tChl (6.6 ng/g dw) were observed in the mid-1950s, compared to the mid-1960s for tPCBs (**Figure 24**). In DM there was a bimodal distribution of both pesticide groups with higher concentrations in the early 1960s and again mid-1990s. As described earlier, this may be due to redistribution of previously deposited sediments during land disturbance activities. The peak in tChl concentrations in the mid-1990s was substantially higher than the deeper peak suggesting additional sources during this time period. In the Brandywine (BW), concentrations of tDDX were highest in the mid-1980s, decreasing with time, while the peak in tChl was in the late-1970s. It is not clear why the two distributions are shifted, but the most likely reason is the use history for each class of pesticides and specifically the use/disposal history in this area (i.e., which could be different from other locations). It is unclear why there was a significant increase in tDDX in 1980s in the Brandywine given the use of DDX was limited after 1972. It is possible that some reworking of the sediments in the basin could have released some buried material that contained elevated levels of DDX.

C3.4: Polybrominated Diphenylethers (PBDEs)

Polybrominated diphenylethers (PBDEs) are members of a broader class of brominated chemicals used as flame retardants. There are 209 congeners, or varieties of the basic chemical type, of PBDEs with a wide range in hydrophobic nature (log Kow 7 to 10) and low water solubility. Penta- and octa-BDE mixtures were banned in 2004 in Europe and California after 30 years of use, while deca-BDE is still used today. Hites (2004) concluded that PBDE use in the U.S. differed from use in Europe and other developed countries in that North America used more deca- and penta-BDE formulations. Dominant PBDE congeners in many areas are BDE-47 (tetra PBDE) and BDE-209 (deca-PBDE). BDE-209 is the single most widely produced and used PBDE congener, while BDE-99 and BDE-47 are the predominant congeners detected in the biosphere. Commercial penta-BDE was used mainly in polyurethane foam (mattresses and padding beneath carpets and furniture). Commercial octa-BDE was predominantly used in casings for electronic products (computers, monitors, plastics). Commercial octa-BDE, and deca-BDE mixtures were also used in nylon, textiles, and adhesives. Today, commercial deca-BDE is used primarily in TV casings. Reductive debromination of BDE-209 could potentially produce BDE-99 and BDE-47 as well as other PBDE congeners. PBDEs degrade faster than PCBs with water and sediment half lives of 0.5 to 1.5, respectively (Wania and Dugani, 2003) depending on the congener and media (air, water or sediment). The degradation of many PBDEs leads to lower brominated PBDEs which may be more toxic but there is a debate as to whether BDE-209 degrades significantly over time. In this study we analyzed for 26 PBDE congeners ranging from BDE-30 to the high molecular weight congener, BDE-209.

The three cores analyzed for PBDEs exhibited similar distributions with depth except that in the Brandywine Creek core, concentrations were 10 times higher at peak concentration (**Table 7, Figure 28**). In the Churchmans Marsh, Brandywine Creek and Dravo Marsh cores, tPBDEs concentrations ranged from near the detection limit of 0.5 ng/g dw to 17 ng/g dw (CM), 120 ng/g dw (BW) and 33 ng/g dw (DM), respectively (**Table 6, Figure 28**). Concentrations in the CM core were near the detection limit at depth (32-38 cm, corresponding to ca. 1945) increasing to a maximum concentration of 17 ng/g dw at 16-18 cm (circa. 1980), then decreasing towards the surface to approximately 10 ng/g dw. In the BW core, tPBDE concentrations were above the detection limit at 12-14 cm (ca. 1980s) increasing to peak concentrations (120 ng/g dw) at 8-10 cm (ca. 1996), decreasing to 53 ng/g dw at the surface. Lastly, tPBDEs concentrations started in

the 16-18 cm (ca. 1986) and exhibited peak concentrations of 33 ng/g dw nearer the surface (4-6 cm; ca. 2002).

The dominant BDE congener was 209 accounting for 5 to 100% of the tPBDEs for all cores; especially in the top sections of the cores (**Figure 29**). At depths greater than 28 cm there were substantial amounts of BDE 99 and to a greater extent BDE 153. For example, in the BW core, BDE 153 accounted for 24-63% of the tPBDEs in the lower sections while BDE accounted for >90% in the upper 10 cm. BDE47 accounted for, at most, 11% of the tPBDEs and this was seen in the bottom sections of DM and CM. A similar distribution and change was noted in the Clyde Estuary by Vane et al. (2009) and slightly different by Song et al. (2004). It appears that over time and burial BDE-209 is slowly degraded to lower brominated congeners; however, changing sources of the lower brominated compounds over time cannot be discounted. Near surface dominance by BDE-209 may also be reflective of current high use of this formulation in comparison to the recently phased-out penta and octa technical mixtures.

Historical Analysis: PBDE production in the United States started in the early 1970s with peak production in the 1990s (Hardy, 2002). The use of the various PBDE formulations has most likely changed over the years as different products and usages develop or are discontinued. Onset and peak concentrations varies across the three sites, reflecting variable time inputs and potentially sediment reworking and remobilization. **Figure 29** presents the time-concentration distribution for total PBDEs. Onset of PBDEs was in the late 1960s/1970s in the CM and DM core and in the mid-1980s in the BW core. Detectable concentrations were observed in the sediment in the early 1970s, quickly after production in the U.S. commenced and may be due to sediment mixing or possibly atmospheric deposition. Peak concentrations were similar in the DM and BW cores (~1980s) while somewhat earlier in the CM core (**Figure 29**). There was a change in the composition of PBDEs with BDE209 the dominant congener in the surface sediments. This could be due to source change, degradation of less brominated compounds, or a function of the method and detection limits. It is possible that at the lower concentrations, the recovery of the higher molecular weight congeners is reduced. This would result in lesser amounts of BDE209 at lower concentrations.

C3.5: Dioxins and Furans

Dioxin and furans are a family of organic chemical compounds that share a similar chemical structure (i.e., tetra to octa-chlorodibenzo-p-dioxin [PCDDs] or –furan [PCDFs]). Due to their hydrophobic nature and resistance to degradation, these chemicals, like other hydrophobic organic chemicals, can accumulate in the fatty tissue of animals (e.g., fish and humans). PCDDs include 75 individual compounds while PCDFs include 135 different compounds, with only 7 PCDD and 10 PCDF compounds exhibiting substantial toxic effects. The most studied and potentially toxic form of PCDD is 2,3,7,8-TCDD (i.e., tetra- chlorodibenzo-p-dioxin).

Dioxin and furans are formed by burning chlorine-based chemical compounds with hydrocarbons. The major source of dioxin in the environment comes from waste-burning incinerators (such as municipal solid waste, sewage sludge, medical waste, and hazardous wastes), the burning of various fuels and material (such as coal, wood, petroleum products, and cement kilns), and poorly or uncontrolled combustion sources like forest fires and building fires (U.S. EPA, 2005 update). Dioxin pollution is also affiliated with paper mills which use chlorine bleaching in their process and with the production of polyvinyl chloride (PVC) plastics and with the production of certain chlorinated chemicals (like many pesticides). Dioxins and furans could be formed naturally with evidence of heavier homologues of PCDDs (Alcock and Jones, 1996). However, anthropogenic sources are much higher than background sources. Sources of these compounds are thought to have started to increase in the environment around 1930s to 1940s, with a sharp rise starting in the early 1950s and decreasing concentrations starting in the mid 1980s (Alcock and Jones, 1996). Recently, the U.S. EPA has drafted a plan (which is under public comment) to initiate clean up and remediation goals for CERCLA and RCRA sites (EPA, 2009; draft).

As part of this study, PCDD and PCDF compounds were determined in sediment sections from five cores (CM, DM, BW, LSP, and WS). Compounds included tetra to octa-PCDFs and PCDDs (**Appendix I**). The discussion below will center on the total concentrations along with 2,3,7,8-TCDD and 2,3,7,8-TCDD toxicity equivalents (as explained below).

Among the five cores, total dioxins and furans ranged from 1.2 to 157 ng/g dw and 0.01 to 127 ng/g dw, respectively (**Figure 30; Tables 7-11).** Other than the two samples in CM (32-34 and 36-38 cm, corresponding to the period 1952 to 1945; **Figure 30**), all sediment samples were <20 ng/g dw for tPCDD and <5 ng/g dw for tPCDFs.

In general, the peak in tPCDD concentration at 32-34 cm (circa. 1952) in the CM core and the more diffuse peaks in DM (36-38cm, circa.1958)) and BW (12-16 cm interval, circa.1990) cores coincided with peaks in other organic contaminants. However, in some cases the peaks in tPCDD or tPCDF concentrations were slightly offset from tPCBs, tDDX, and tChlordane peak concentrations by one interval higher or lower. There was no trend in the Shellpot Creek or Walnut Street cores in dioxins or furans. Concentrations of the more toxic dioxin, 2,3,7,8-TCDD, were detected in only seven sediment intervals in all of the cores (**Tables 7-11**). Detectable concentrations ranged from 0.3 to 5.1 pg/g dw with an average concentration of 0.22 pg/g dw. The highest concentration (5.1 pg/g dw) and most in one core (n= 5) were found at the BW site, however there was no concentration trend with depth and detection appeared random.

Toxic Equivalents (TEQs) were calculated by multiplying the concentration of each 2,3,7,8-substituted dioxin and furan compound by their associated human and mammalian toxicity equivalent factor (TEF) and then adding the resulting partial sums. Dioxin-like PCB congeners were not included in these TEQ calculations. Human and mammalian TEFs for dioxins and furans were taken from the World Health Organization (WHO, 2005), as fully described in Van den Berg et al. (2006). For the TEQ calculation, non-detected compounds were set equal to zero (0). The TEQs in the Christina Basin sediment cores ranged from <1.2 to 444 pg/g dw with an overall average of 34 pg/g dw. The TEQ concentrations in the core tops were as follows: 19.9, 32.9, 21.8, 13.9, and 5.5 pg/g dw for cores CM, DM, BW, WS, and LSP, respectively. These values are similar to values reported by Greene (2009b) for surface sediment samples collected from these same waters in 2007. For most core sections, except BW, the TEQ was dominated by hepta-, octa- and tetra-PCDD congeners and to a lesser extent an even mixture of PCDF congeners. This is also consistent with results reported by Greene (2009b) for surface sediment samples. In the BW core, penta- and hexa-PCDF congeners were highest followed by hepta- and octa-PCDD congeners, thereby providing a different TEQ mix than seen in the other cores and suggesting different sourcing. The vertical profiles of TEQs in the CM and DM cores strongly track their associated PCB profiles. In the BW core, however, the TEQ peak appeared to precede the PCB peak.

Historical Analysis: Total dioxins (tPCDD) and total furans (tPCDF) with time are presented in **Figure 31**. Total dioxins and furans in CM peak in concentration (158 and 12 ng/g dw

respectively) in the early 1950s and decrease to near constant levels until the present. The peak tPCDD in the CM core (158 ng/g dw) is much greater than the peak in the DM core (~17.5 ng/g dw) and the BW core (~12.5 ng/g). There are multiple peaks in tPCDD concentrations in the DM core and tfurans appear to mirror the same pattern over time, although muted. Interestingly, in the Brandywine Creek core, peak concentrations of the tPCDD are found in 1990, while there is a broad maximum in tPCDFs in the 1960s to 1980. The historical pattern of TEQ generally follows both the tPCDD and tPCDF time-concentration distribution except in the Brandywine Creek core (**Figure 32**). While tPCDD concentrations peak around 1990, the TEQ concentration is highest in the mid to late 1970s, similar to tPCDFs. This is due to the contribution to the total TEQ from the various furan congeners is highest during this time period.

C3.6: Sediment Iron and Zinc

The Delaware Department of Natural Resources and Environmental Control had a particular interest in the vertical distribution of iron (Fe) and zinc (Zn) in sediment cores collected from the targeted waterways. Sediment levels of iron (Fe) and zinc (Zn) were determined using a strong acid digestion and are not "total" concentrations (i.e., does not include the clay lattice metals). However, this method would obtain the majority of the metals associated with the particles. Among the five cores (CM, DM, BW, LSP, and WS), sediment Fe ranged from 5388 to 45700 μg/g dw (0.53 to 4.5 wt %), while sediment Zn ranged from 71 to 9800 μg/g dw. Iron concentrations were variable with depth in each core (**Figure 33; Tables 7-11**). The average Fe concentration in the BW and CM core were the same with similar variations (3.5 ± 0.5%). The LSP core exhibited slightly lower Fe concentration but was more variable (2.8 ± 1.9%). The Fe concentrations in the DM core were substantially lower than the BW and CM cores (average = 1.2%) with a peak concentration of 3.0% at 8-10 cm (circa. 1995). It is unclear why Fe concentrations in the DM core were a third lower than the other cores.

Zinc concentrations showed much greater variation with depth in the BW, CM, and DM cores (**Figure 34; Tables 7-11**). Concentrations in the BW core were low at depth increasing to their highest levels of 780 μg/g dw at 20-22 cm (circa. 1979), then decreasing towards the surface (490 μg/g dw). Substantially higher Zn concentrations were measured in the CM core. At depth (pre-1900), concentrations were lowest (~ 140 μg/g dw), increasing to 9800 μg/g dw at 36-38 cm (circa. 1945), than decreasing towards the surface to 720 μg/g dw. The Zn distribution

in the DM core exhibited the bimodal distribution as seen for some organic contaminants. There is a deeper peak of 1230 μg/g dw at 36-38 cm (circa. 1958) and a peak of 1000 μg/g dw at 8-10 cm (circa. 1995). Zn concentrations in the DM core were lower than the CM values and were similar to the BW concentrations.

Normalization of the sediment to a reference element not associated with anthropogenic influences is one approach to determining the degree of sediment contamination (Daskalakis and O'Connor, 1995). Elements such as Al (Windom et al., 1989; Schropp et al., 1990), lithium (Li) (Loring et al., 1990) and Fe (Trefrey and Presely, 1976; Sinex and Helz, 1981; Helz et al., 1985; Velinsky et al., 1994; Velinsky et al., 1997) have been used in the past. For this study, Fe was chosen as a normalizing element because: 1) it is the fourth most abundant metal in the earth with a crustal average of 3.5% (Wedepohl, 1971); 2) in most cases anthropogenic sources are small compared to the amount of Fe naturally present; and 3) the ratios of most metals to Fe are fairly constant in the Earths crust. The major caveat in using Fe as a normalizing element, instead of Al or Li, is that Fe undergoes many diagenetic reactions in anoxic/oxic sediments. These reactions include dissolution and precipitation of Fe oxides and Fe-sulfur minerals (i.e., pyrite). However, in the previous studies by Velinsky et al. (1994; 1997) in tidal river sediments, the potential changes in speciation and mobility did not significantly affect the total concentration of sedimentary iron with depth or location. Therefore, Fe was used as normalizing agent for this study.

A useful tool in expressing the degree to which sediment is influenced by anthropogenic sources of trace metals is the enrichment factor (EF) (Trefrey and Presely, 1976; Sinex and Helz, 1981; Helz et al., 1985; Windom et al., 1989; Velinsky et al., 1994; 1997). When normalizing to Fe, the enrichment factor is defined as: $EF = (X/Fe)_{sediment} / (X/Fe)_{unimpacted\ sediment}$, where X/Fe is the ratio of the trace metal (X) to the amount of Fe in the sample. In using the EF, a comparison to a sediment that is unimpacted by anthropogenic sources is necessary [$(X/Fe)_{unimpacted}$] (i.e., critical in this analysis is the choice of metal to Fe ratio for unimpacted sediments). Enrichment factors of 1 indicate no enrichment, while EFs greater than 1 indicate anthropogenic sources of metals to the sediments. While this approach is useful, it may not account for natural variations in sediment types of different geological regions. One way to account for this variability is to derive a ratio from "unimpacted" sediments in the general area of interest (Windom et al., 1989; Schropp et al., 1990). However, in the present study, most samples have the potential to be

impacted above natural levels, except possibly at depth in the cores. Therefore, data from the bottom of the cores, as described below, were used to derive 'natural' or least impacted concentrations of Fe and Zn in the general area.

The Zn to Fe ratios for the bottom section of the three cores (BW, CM, and DM) were 0.011, 0.004, and 0.007, with an average of 0.007. A ratio of 0.007 is somewhat higher than a mean of 0.002 reported by Wedepohl (1968) for river sediments but is quite similar to values seen in other tidal river sediments (Velinsky et al., 1994). A value of 0.007 also has the added advantage of being specific to the tidal Christina Basin. The degree to which sediments in the study area are enriched in trace metals from anthropogenic sources varies from metal to metal and depends on a number of factors, including: 1) choice of $(X/Fe)_{unimpacted}$; 2) biogeochemistry and redox behavior of the metal; and 3) sources and loading history of metals to the study area. Despite these considerations, the present calculation reveals some interesting trends with depth.

Figure 19 presents the EF distribution for the DM, BW and CM cores. The EF for all core samples ranged from 0.5 to 41 with an overall average of 4 (unitless). Given the variations in the $(X/Fe)_{unimpacted}$ value, an EF of <1 to ~2 indicate samples that are at or near background. The BW core shows no enrichment for Zn. In the CM core, there was substantial enrichment of Zn above background with values up to 41 times higher at 42-44cm (~1935). Above and below this broad peak the EF is near background levels. DM sediments were above background from approximately 50 cm (~1925) to the surface with the peak EF at 42-44 cm and above this interval, the EF ranged from 5 to 12 suggesting a continuing source to this location. A more in-depth discussion of zinc enrichment within the CM and DM cores will be presented below.

One of the most noteworthy observations apparent from the present study is the historical rise and fall of zinc concentrations in the sediments at the CM coring site. The onset of zinc enrichment in the CM core appears to have occurred around or shortly after 1900 (**Table 8**). Sediment concentrations of Zn were highest in that core from approximately 1910 to 1950 with a peak of nearly 10,000 ug/g dw and an average of 8850 ± 920 ug/g dw (n=5) during that period (**Table 8 and Figures 33 and 35**). Zinc concentrations at the other coring sites (DM and BW) were substantially lower (**Tables 7 and 9, plus Figures 33 and 35**). Dravo Marsh (DM) concentrations were highest between 1950 and 1958 with a secondary peak in the mid-1990s, while in the BW core, peak concentrations occurred around ~1970 to 1980. As indicated by the EF (see above), changes in Zn concentrations in the BW core were controlled by Fe with little or

no anthropogenic enrichment of Zn, while there was substantial enrichment of Zn in the CM core (up to 40 times above background) in the 1930s. Concentrations of sediment Zn in the DM core started to show enrichment in the late 1930s with highest EF (20) in the mid-1940s and decreasing over time to approximately 5 to 10 in the current century.

Historical Analysis: Primary sources of zinc enrichment over time to Churchmans Marsh and downstream to Dravo Marsh include the now defunct NVF facility located along the Red Clay Creek in Yorklyn, DE (DNREC, 1999a); a similar NVF facility that formerly operated along the White Clay Creek in Newark, DE (DNREC, 1999b); and a pigment plant located in Newport that became a federal Superfund site (U.S. EPA, 1993). All three of these sources began manufacturing operations right around 1900. The NVF Newark plant closed in 1990, while the NVF Yorklyn plant closed in 2009. Both of the NVF facilities used zinc chloride in the manufacture of vulcanized paper products. The Newport pigment plant manufactured Lithopone, a zinc and barium-based paint pigment, up until 1952. Zinc loading from the NVF Yorklyn plant entered the Red Clay Creek and travelled downstream until it combined with the White Clay Creek, which carried the additional zinc load from the NVF Newark plant. The combined load emptied into the tidal Christina River just downstream of Churchmans Marsh (just upstream of Newport, DE). Additional zinc then entered the Christina River as a result of poor waste handling at the Newport pigment plant. The combined zinc loading from these three primary sources produced inordinately high concentrations of zinc (~10,000 μg/g dw) at depth in the CM core and moderately high (~1,250 μg/g dw) concentrations downstream at the DM coring site.

The sediment profiles in CM, and to a lesser extent, DM, clearly show significant inputs of Zn shortly after these three facilities commenced operation along with an associated improvement once controls began to be put in place or processes were changed. Concentrations in the bottom of the CM and DM cores ranged from 71 to 139 μg/g dw (average = 106 ± 33 μg/g dw), only slightly above concentrations found upstream of the NVF Yorklyn facility on the Red Clay Creek (range of 39 to 107 μg/g dw; average = 73 ± 22 μg/g dw; n = 7; DNREC, 1999). Concentrations of Zn in the mid sections of the cores were significantly enriched in Zn, especially in the CM core (**Figure 35**). The core results clearly show that control procedures from the 1960s to the present have resulted in a reduction of Zn inputs to the river

The NVF Yorklyn facility is under active remediation to remove the remaining inventory of zinc from the groundwater beneath the site (DNREC, 2008). The NVF Newark facility has been remediated to address the zinc contamination there (DNREC, 1999c) and an extensive cleanup was implemented at the DuPont Newport site. One component of the DuPont Newport cleanup included dredging approximately 11,000 cubic yards of sediment from the tidal Christina River in the vicinity of Newport in 1999, due in part to elevated concentrations of zinc in the sediments (NRC, 2007). The coring analysis clearly shows that the closing of these facilities and the extensive cleanup action taken have yielded substantially lower concentrations of Zn in the sediments of the tidal Christina River.

D) Summary and Conclusions

This study involved the chemical analysis of five sediment cores taken from the tidal Christina River Basin and lower Shellpot Creek in northern New Castle County, DE. Of the five cores, four were dated using ^{210}Pb and ^{137}Cs radiometric methods, with three (Churchmans Marsh (CM), Dravo Marsh (DM), and the tidal Brandywine (BW)) providing sufficient temporal coverage (> 50 yrs) for detailed chemical analysis. The main objective was to evaluate historical trends in organic chemical contaminants (e.g., polychlorinated biphenyls, pesticides, dioxins/furans, polybrominated diphenylethers and polycyclic aromatic hydrocarbons), selected trace metals (e.g., iron and zinc) and nutrients (i.e., sediment phosphorus and nitrogen). An additional objective was to evaluate if a historical record of eutrophication could be derived from algae analysis (i.e., diatom species in the cores) along with other indicators of potential ecosystem change (e.g., stable isotopes of carbon ($\delta^{13}C$-OM) and nitrogen, ($\delta^{15}N$-TN)).

The range and average sediment accumulation rates (^{137}Cs) inferred from the ^{210}Pb and ^{137}Cs data are similar to other areas within the Delaware Estuary and range from 0.57 to 1.9 cm/yr. Attempts to core and determine age-depth relationships in other locations (i.e., an embayment near Walnut Street) yielded inconclusive dating results. There was good agreement between the ^{137}Cs rates and those for the constant accumulation model for ^{210}Pb.

With regard to contaminants, a major finding that emerged from this study is the historic accumulation of zinc in the system, as clearly displayed in the Churchmans Marsh (CM) core. Concentrations of Zn showed a broad peak over background levels starting at or shortly after the turn of the century and persisting to the early to mid-1970s. Using the amount of iron (Fe) within the sediment and referencing the data to bottom concentrations of Zn (and Fe), the sediments of Churchmans Marsh had been up to 40 times above background levels. Current Zn enrichment in Churchmans Marsh is still approximately 5 to 10 times above background. In the other core locations, surface sections are not substantially enriched above background with zinc enrichment factors ranging only from 1 to 2.3. Major sources of historic zinc loading to the system included two National Vulcanization Facilities (NVF), one on the Red Clay Creek and one on the White Clay Creek, and a pigments plant in Newport. All three of these sources have been remediated and discharges are more formally regulated.

The other key finding of this study is that concentrations of organic contaminants are lower today, overall, than they were in the past, with some exceptions. Chlorinated organic compounds

such as tchlordane, tDDX and dioxins/furans all show a sharp maximum at similar depths (corresponding to the 1960s and 1970s), followed by a decreasing trend towards the surface. Total PCBs also shows higher concentrations at depth with decreasing concentrations towards the surface, with the exception of the Dravo Marsh core where tPCB concentrations at the surface remain elevated (ca. 200 ng/g dw). The Dravo Marsh core exhibits a bimodal distribution in PCB concentration, showing two separate peaks. The onset of the first peak occurred at 48-50 cm (circa. 1942), with the actual peak seen at 36-38 cm (circa. 1958). These dates track the Churchman Marsh core fairly well. After 1958, PCB concentrations in the Dravo Marsh core fell and remained below 50 ng/g dw for at least a decade. At this time, concentrations began to increase again in the late 1970s, rising to a second peak at 10-12 cm (circa. 1992) that was similar in magnitude to the first peak. PCB concentrations in the Dravo Marsh core have fallen somewhat since 1992 but surface concentrations remain high relative to the surface concentrations in the CM and BW cores. The Dravo Marsh finding may reflect lingering inputs from local sources and/or the redistribution of previously deposited contamination following major earth works projects in or near the marsh.

Interestingly, the PCB congener composition in both the Churchmans Marsh and Dravo Marsh cores showed a shift from mid to higher molecular weight compounds to lower molecular weight compounds from the upper sections (more recent) to the lower sections (longer ago). The opposite was true for the BW core. The high proportion of deca PCB (H10) in the Churchmans Marsh and Dravo Marsh cores is unusual and appears to reflect releases from the same pigment plant in Newport that was also responsible for at least part of the zinc contamination. The use of congener-specific PCB methods (rather than typical Aroclor methods) allowed us identify and characterize the deca PCB signature.

Total dioxins (PCDD) and furans (PCDF) concentrations ranged from <2 to 157 ng/g dw and <1 to 13 ng/g dw, respectively with distinct distributions with depth and time. The individual congeners were used to calculate the toxic equivalents (TEQs) using published toxic equivalency factors (TEF). The TEQs ranged from <0.01 to 0.45 ng/g dw. Highest concentrations of PCDD, PCDF and TEQ were found in the Churchmans Marsh core.

In all cores (n=3), tPBDEs are only present in the upper sections with undetectable concentrations below approximately 20cm (<1980s). The predominant congener is PBE 209 in the upper sections with BDE153 and BDE99 found at depth.

Total PAHs showed a distinct concentration peak in the 1940s, in the CM core, while a bimodal distribution was observed in the DM core and possibly the BW core. The peak of tPAHs in the CM core maybe related to historic inputs of hydrocarbons from a creosote facility near the site. Other sources related to urban development, including a major shipbuilding complex and a coal gasification plant, are also potential historic sources to the area, particularly the DM. Data were compared to indicators of combustion sources such as coal tar based parking lot sealant using specific ratios of individual PAHs. Only a limited number of samples were consistent with such a fingerprint and thus this type of sealant does not appear to be a major source to the tidal Christina River.

Lastly, analysis of the diatom assemblages and metrics indicate a shift toward more eutrophic species starting in the late 1940-1950s. There was a strong positive relationship between the eutrophic diatom metric and the concentration of nitrogen and phosphorus in Churchmans and Dravo marshes. This, along with the increases in total sediment N, total sediment P and sediment nitrogen isotopic compositions (δ^{15}N-TN), indicates that increase loadings of nutrients have resulted in a diatom shift in the river.

Overall, this study documents the chemical analysis of three cores taken in the tidal Christina River and tidal Brandywine Creek. Changes were observed in contaminant levels across time that reflect usage globally and most often locally. Overall, contaminant levels appear to be declining when viewed on a longer term, decadal time scale. However, the concentrations of several contaminants (e.g., PCBs and zinc) remain relatively elevated in this system.

E) Acknowledgments

We would like to thank Susanne Molaski (UDEL), Don Charles, Paul Kiry, Paula Zelanko, Mike Schafer, and Linda Zaoudeh for laboratory assistance and data interpretation. Dr. Mihalea Enache did diatom counts, calculated diatom metrics and provided assistance with report preparation. We appreciate the help of Dr. Heather Stapleton (Duke University) for assistance in analyzing a subset of the samples for PBDEs. Dr. Jeff Ashley (Philadelphia University) provided analytical advice and support throughout this project. Roger Thomas assisted in field and Robin Davis provided assistance with final report preparation and review. Financial, field and editorial support was graciously provided by Dr. Richard Greene (DNREC; Watershed Assessment Branch).

F) References

Alcock, R. E. and K.C. Jones. 1996. Dioxins in the Environment: A Review of Trend Data. *Environ. Sci. Technol.* 30: 3133-3143.

Appleby, P.G. 2001. Chronostratigraphic techniques in recent sediments: Chapter 9. In: W.M. Last and J.P. Smol (eds). *Tracking Environmental Change Using Lake Sediments Volume 1: Basin Analysis, Coring, and Chronological Techniques*. Kluwer Academic Publishers, Dordrecht, The Netherlands.

Appleby P.G and F. Oldfield. 1978. The calculation of lead-210 dates assuming a constant rate of supply of unsupported ^{210}Pb to the sediment. *Catena* 5: 1-8.

Ashley, J.T.F. and J.E. Baker. 1999. Hydrophobic organic contaminants in surficial sediments of Baltimore Harbor: Inventories and sources. *Environ. Toxicol. Chem.* 18: 838–849.

Aspila,K.I, H. Aspila, A. Agemian and S.Y. Chau. 1976. A semi-automated method for the determination of inorganic and total phosphate in sediments. *Analyst* 101: 187-197.

ATSDR. 2000. *Toxicological Profile for Polychlorinated Biphenyls* (Update). Agency for Toxic Substances and Disease Registry, Atlanta, GA.

Baker, J.E., M. Toaspern, D. Liebert, and F. Ko. 2004. Decachlorobiphenyl: Using a Non-Aroclor PCB as a Tracer of Estuarine Processes. Society of Environmental Toxicology and Chemistry Poster Session. Portland, OR.

Berner, R. 1980. *Early Diagenesis: A Theoretical Approach.* Princeton University Press, 241 pp.

Benner, R., M. L. Fogel, and E. K. Sprague. 1991. Diagenesis of belowground biomass of *Spartina alterniflora* in salt-marsh sediments. *Limnol. Oceanogr***.** 36: 1358-1374.

Boehm, P.D. 1984. Aspects of the saturated hydrocarbon geochemistry of recent sediments in the Georges Bank region. *Org. Geochem***.**, 7: 11-23.

Boehm, P.D. and J.W. Farrington. 1984. Aspects of the aromatic hydrocarbon geochemistry of recent sediments in the Georges Bank region. *Environ. Sci. Tech.,* 18: 840-845.

Bratton, J.F., S.M. Coleman and R.R. Seal, II. 2003. Eutrophication and carbon sources in Chesapeake Bay over the last 2700 yr.: Human impacts in context. *Geochim. Cosmochim. Acta.* 67: 3385-3402.

Brightfields Inc. 2009. *PCB Mass Loading from Hazardous Substance Release Sites to Surface Waters of the Christina River Basin* (DNREC Contract No. #06-374-MS-A). Prepared for: Site Investigation & Restoration Branch, Division of Air and Waste Management, and Watershed Assessment Branch, Division of Water Resources; Department of Natural Resources Environmental Control; State of Delaware (File# 0985.26.51).

Brush, G.S., E.A. Martin, R.S. DeFries, and C.A. Rice 1982. Comparisons of ^{210}Pb and pollen methods for determining rates of estuarine sediment accumulation. *Quaternary Research.* 18: 196-217.

Burdige, D.J. 2006. *Geochemistry of Marine Sediments*. Princeton University Press. 630 pp.

Canuel, E.A., J.E. Cloern, D.B. Ringelberg, J.B. Guckert and G.H. Rau. 1995. Molecular and isotopic tracers used to examine sources of organic matter and its incorporation into the food webs of San Francisco Bay. *Limnol. Oceanogr*. 40: 67-81

Church, T.M., C. Sommerfield, D.J. Velinsky, D. Point, C. Benoit, D. Amouroux, D. Plaa and O. Donard. 2006. Marsh sediments as records of sedimentation, eutrophication and metal pollution in the urban Delaware Estuary. *Marine Chemistry* 102(1-2):72-95.

Cifuentes, L.A., J.H. Sharp and M.L. Fogel. 1988. Stable carbon and nitrogen isotope biogeochemistry of the Delaware estuary. *Limnol. Oceanogr*. 33: 1102-1115.

Cline, J.D. and I.R. Kaplan 1975. Isotopic fractionation of dissolved nitrate during denitrification in the eastern tropical North Pacific Ocean. *Mar. Chem*. 3: 271-299

Cooper, S. R. and G.S. Brush. 1993. A 2,500-year history of anoxia and eutrophication in Chesapeake Bay *Estuaries* 16: 617-626.

Cornwell J.C., J.C. Stevenson, D.J. Conley and M. Owens. 1996. A sediment chronology of Chesapeake Bay eutrophication. *Estuaries* 19:488-499.

Crusius, J. and R.F. Anderson. 1991. Core compression and surficial sediment loss of lake sediments of high porosity caused by gravity coring. *Limnol. Oceanogr.* 36:1021-1031.

Cutshall, N.H., I.L Larsen and C.R. Olsen. 1983. Direct analysis of ^{210}Pb in sediment samples: Self-absorption corrections. *Nuclear Instruments and Methods in Physics Research*, 206: 309-312.

Daskalakis, K.D. and T.P. O'Connor. 1995. Normalization and elemental sediment contamination in the coastal United States. Environ. Sci. Technol. 29: 470 477.

Dean, W.E., Arthur, M.A., and Claypool, G.E., 1986. Depletion of ^{13}C in Cretaceous marine organic matter: source, diagenetic, or environmental signal? *Mar. Geol*., 70:119-157.

Dearth, M.A. and R.A. Hites. 1991. Complete analysis of technical chlordane using negative ionization mass spectrometry. Environ. Sci. Technol. 25: 245-254.

Delaware Department of Natural Resources and Environmental Control (DNREC). 2008. Amended Total Maximum Daily Load (TMDL) for Zinc in the Red Clay Creek Technical Background and Basis Document (September 15, 2008), State of Delaware Department of

Natural Resources and Environmental Control Division of Water Resources, Watershed Assessment Section, Dover, DE.

Delaware Department of Natural Resources and Environmental Control (DNREC). 2007. Christina Basin Pollution Control Strategy. Department of Natural Resources and Environmental Control, Dover, Delaware.

Delaware Department of Natural Resources and Environmental Control (DNREC). 2005. Sediment Quality Assessment for the Tidal Christina River Basin, Volume 1 Report of Findings. Department of Natural Resources and Environmental Control 715 Grantham Lane, New Castle, Delaware.

Delaware Department of Natural Resources and Environmental Control (DNREC). 2004. Final Plan of Remedial Action, Wilmington Coal Gas Site – Northern Parcel/OU-01. State of Delaware Department of Natural Resources and Environmental Control Site Investigation and Restoration Branch, New Castle, DE.

Delaware Department of Natural Resources and Environmental Control (DNREC). 1999a. Total Maximum Daily Load (TMDL) for Zinc in the Red Clay Creek, New Castle County, DE. Technical Background and Basis Document (August 1, 1999), State of Delaware Department of Natural Resources and Environmental Control Division of Water Resources, Watershed Assessment Section, Dover, DE.

Delaware Department of Natural Resources and Environmental Control (DNREC). 1999b. Total Maximum Daily Load (TMDL) for Zinc in the White Clay Creek, New Castle County, DE. Technical Background and Basis Document (August 1, 1999), State of Delaware Department of Natural Resources and Environmental Control Division of Water Resources, Watershed Assessment Section, Dover, DE.

Delaware Department of Natural Resources and Environmental Control (DNREC). 1999c. Response to Public Comments RE: Proposed Total Max. Daily Loads for Zinc in the Red Clay Creek, DE. Department of Natural Resources and Environmental Control Division of Water Resources, Watershed Assessment Section, Dover, DE.

Delaware Department of Natural Resources and Environmental Control (DNREC). 1996. Final Determination State of Delaware 1996 Clean Water Act Section 303(d) List of Waters Needing TMDLs and Supporting Rationale. Delaware Department of Natural Resources and Environmental Control, Division of Water Resources, Dover, DE.

Di Toro, D.M. and J.A. McGrath. 2000. Technical basis for narcotic chemicals and polcyclic aromatic hydrocarbon criteria. II. Mixtures and sediments. *Environ. Tox. Chem.* 19(8): 1971-1982.

Farrington, J.W. 1980. An overview of the biogeochemistry of fossil fuel hydrocarbons in the marine environment. In*: Petroleum in the Marine Environment*, Eds.: L. Petrakis and F.T. Weiss, Advances in Chemistry Series 185, American Chemical Society, Washington, D.C., pp. 1-22.

Fogel, M.L., L.A. Cifuentes, D.J. Velinsky and J.H. Sharp. 1992. The relationship of carbon availability in estuarine phytoplankton to isotopic composition. *Marine Ecol. Prog. Ser*. 82: 291-300.

Fogel, M.L., E.K. Sprague, A.P. Gize and R.W. Frey. 1989. Diagenesis of organic matter in Georgia salt marshes. *Estuarine, Coastal Shelf Sci*., 28: 211-230.

Fry, B. 2006. *Stable Isotope Ecology*. Springer Science+Business Media, LLC, New York.

Gevo, B., J. Hamilton-Taylor, C. Murdoch, K.C. Jones, M. Kelly and B.J. Tabner. 1997. Depositional time trends and remobilization of PCBs in lake sediments. *Environ. Sci. Technol*. 31: 3274-3280.

Graustein, W.C. and K.K. Turekian. 1986. ^{210}Pb and ^{137}Cs in air and soils measure the rate and vertical distribution of aerosol scavenging. *J. Geophys. Res*., 91: 14,355-14,366.

Greene, R.W. 2009a. *The Chemical, Physical and Biological Fate of Polychlorinated Biphenyls in the Tidal Christina Basin*. A dissertation submitted to the Faculty of the University of Delaware in partial fulfillment of the requirements for the degree of Doctor of Philosophy in Civil Engineering: 359 pp.

Greene, R.W. 2009b. Persistent, Bioaccumulative, and Toxic (PBT) Pollutants in Surface Water, Sediment, and Biota of the Christina Basin and Shellpot Creek Watershed, DE. A presentation summarizing the results of fall 2007 sampling. Delaware Department of Natural Resources and Environmental Control, Watershed Assessment Section, Dover, DE.

Gschwend, P.M.and R.A. Hites 1981. Fluxes of PAHs to marine and lacustrine sediments in the NE United States. *Geochim. Cosmochim. Acta*. 45: 2359-2367.

Hardy, M.L. 2002. A comparison of the properties of the major commercial PBDPO/PBDE product to those of major PBB and PCB products. *Chemosphere* 46: 717-728.

Hayes, J.M, Popp, B.N., Takigiku, R., and Johnson, M.W., 1989. An isotopic study of biogeochemical relationships between carbonates and organic carbon in the Greenhorn Formation. *Geochim. Cosmochim. Acta*, 53:2961-2972.

Heiri, O., A.F. Lotter and G.Lemcke. 2001. Loss on ignition as a method for estimating organic and carbonate content in sediments: reproducibility and comparability of results. *Journal of Paleolimnology*. 25: 101-110.

Helz, G.R., S.A. Sinex, K.L. Ferri, and M. Nichols. 1985. Processes controlling Fe, Mn, and Zn in sediments of Northern Chesapeake Bay. *Estuar. Coast. Shelf Sci*. 21: 1-16.

Hites, R.A. 2004. Polybrominated diphenyl ethers in the environment and in people: A meta-analysis of concentrations. *Environ Science Technol.* 38 (4): 945-956.

Hites, R.A., R.E. Laflamme, J.G. Windsor, J.W. Farrington, and W.G. Deuser 1980. Polycyclic aromatic hydrocarbons in an anoxic sediment core from the Pettaquamscutt River (Rhode Island, USA). *Geochim. Cosmochim. Acta***.**, 44: 873-878.

Hoffman, E.J., G.L. Mills, J.S. Latimer and J.G. Quinn. 1984. Urban runoff as a source of polycyclic aromatic hydrocarbons to coastal waters. *Environ. Sci. Technol*. 18: 580-586.

Hornberger, M.L., S.N. Luoma, A.Green, C. Fuller, and R. Anima. 1999. Historical trends of metals in the sediments of San Francisco Bay, California. *Marine Chemistry.* 64:39-55.

Inn, K.G.W. 2001. The NIST natural-matrix radionuclide standard reference material program for ocean studies. *Journal of Radioanalytical and Nuclear Chemistry.* 241: 227-231.

Jasper, J.P. and R.B. Gagosian. 1990. The sources and deposition of organic matter in the Late Quaternary Pigmy Basin, Gulf of Mexico. *Geochim. Cosmochim. Acta.* 54: 1117-1132.

Kennish, M.J. 1992. *Ecology of Estuaries: Anthropogenic Effects*. Ed: M.J. Kennish, CRC Press, Inc. Boca Raton, FL., 494 pp.

Klein, R.D. 1979. Urbanization and stream water quality impairment. *Water Resources Bulletin.* 15: 948-963.

Kucklick, J.R., H.R. Harvey, P.H. Ostrom, N.E. Ostrom and J.E. Baker. 1996. Organochlorine dynamics in the pelagic food web of Lake Baikal. *Environ. Toxicol. Chem.* 15: 1388-1400.

Lake, J.L., R.A. McKinney, F.A. Osterman, R.J. Pruell, J. Kiddon, S.A. Ryba and A.D. Libby. 2001. Stable nitrogen isotopes as indicators of anthropogenic activities in small freshwater systems. *Can. J. Fish. Aquatic Sci*. 58: 870-878.

Latimer, J.S. and J.G. Quinn. 1996. Historical trends and current inputs of HOCs in an urban estuary: The sedimentary record. *Environ. Sci. Technol.* 30: 623-633.

Leavitt, P.R., C.S. Brock, C. Ebel and A. Patoine. 2006. Landscape-scale effects of urban nitrogen on a chain of freshwater lakes in central North America. *Limnol. Oceanogr*. 51(5): 2262–2277.

Litke, D.W. 1999. *Review of Phosphorus Control Measures in the United States and Their Effects on Water Quality*. U.S. Geological Survey, Water Sources Investigations Report 99-4007, National Water Quality Assessment Program, Denver, CO.

Loring, D.H. 1990. Lithium - a new approach for the granulometric normalization of trace metal data. *Mar. Chem*. 29: 155-168.

McClelland, J.W., I. Valiela and R.H. Michener. 1997. Nitrogen-stable isotope signatures in estuarine food webs: A record of increasing urbanization in coastal watershed. *Limnol. Oceangr*. 42: 930-937.

Mahler, B.J., P.C. Van Metre, T.J. Bashara, J.T. Wilson and D.A. Johns. 2005. Parking lot sealcoat: An unrecognized source of urban Polycyclic Aromatic Hydrocarbons. *Environ. Sci. Technol.* 39(15): 5560-5566.

Meyers, P.A., 1994. Preservation of elemental and isotopic source identification of sedimentary organic matter. *Chem. Geol.* 144: 289-302.

National Oceanic and Atmospheric Administration (NOAA). 1993. *National Status and Trends Program. Sampling and Analytical Methods of the National Status and Trends Program, National Benthic Surveillance and Mussel Watch Project 1984-1992*, Volume III Comprehensive Description of Elemental Analytical Methods. NOAA Tech. Mem. NOS ORCA 71, National Ocean Service, Silver Spring, MD.

National Oceanic and Atmospheric Administration (NOAA). 1989. A summary of data on tissue contamination from the first three years (1986-1988) of the Mussel Watch project. *NOAA Tech. Mem. NOS OMA 49*, Rockville, MD.

National Research Council (NRC). 2007. *Sediment Dredging at Superfund Megasites Assessing the Effectiveness*. National Research Council of the National Academies, The national Academies Press, Washington, D.C.

Neff, J.M., S.A. Stout and D.G. Gunster. 2005. Ecological risk assessment of polycyclic aromatic hydrocarbons in sediments: Identifying sources and ecological hazard. *Integr. Environ. Assess. Manag.* 1(1): 22-33.

Neubauer, I.C. Anderson, J.A. Constantine and S.A. Kuehl. 2002. Sediment deposition and accretion in a mid-Atlantic (U.S.A.) tidal freshwater marsh. *Estuarine, Coastal, and Shelf Science*. 54: 713-727.

Officer, C.B., D.R. Lynch, G.H. Setlock and G.R. Helz.1984. Recent sedimentation rates in Chesapeake Bay. In: Kennedy, V.S. (ed.). *The Estuary as a Filter*. Academic Press, New York, pp 131-157.

O'Leary, M.H., 1988. Carbon isotopes in photosynthesis. *Bioscience,* 38:328-336.

Olsen, C.R., I.L. Larsen, P.D. Lowry, N.H. Cutshall, J.F. Todd and G.T.F. Wong. 1985. Atmospheric fluxes and marsh-soil inventories of ^{7}Be and ^{210}Pb. *Journal of Geophysical Research –Atmospheres.* 90: 10487-10495.

Olsen, C.R., H.J. Simpson, T.H. Peng, R.F. Bopp and R.M. Trier. 1981. Sediment mixing and accumulation effects on radionuclide depth profiles in Hudson estuary sediments. *Journal of Geophysical Research*. 86: 11020-11028.

O´Malley, V.P., T.A. Abrajano and J.Hellou. 1996. Stable carbon isotopic apportionment of individual polycyclic aromatic hydrocarbons in St. John's harbour, Newfoundland. *Environ. Sci. Technol.* 30: 634-639.

O'Malley, V.P., T.A. Abrajano and J. Hellou. 1994. Determination of $^{13}C/^{12}C$ ratios of individual PAH from environmental samples: Can PAH sources be source apportioned? *Org. Geochem*. 21: 809-815.

Orson, R.A., R.L. Simpson and R.E. Good. 1992. A mechanism for accumulation and retention of heavy metals in tidal freshwater marshes of the upper Delaware River Estuary. *Estuar. Coast. Shelf Sci.* 34: 171-186.

Orson, R.A., R.L. Simpson and R.E. Good. 1990. Rates of sediment accumulation in a tidal freshwater marsh. *J. Sed. Petrology*. 60: 859-869.

Owens, M. and J.C. Cornwell. 1995. Sedimentary evidence for decreased heavy metal inputs to the Chesapeake Bay. *Ambio* 24: 24-27.

Perga, M.E. and D. Gerdeaux. 2004. Changes in the $^{\delta 13}C$ of pelagic food webs: The influence of lake area and trophic status on the isotopic signature of whitefish (*Coregonus lavaretus*). *Can. J. Fish. Aquat. Sci.* 61(8): 1485–1492.

Pierce, R.H., R.C. Brown, E.S. Van Vleet, and R.M. Joyce. 1986. Hydrocarbon contamination from coastal development. In: *Organic Marine Chemistry*. Ed: M.L. Sohn, ACS Symposium Series 305, pp. 229-246.

Ponader, K.C., D.F. Charles, T.J. Belton and D.M. Winter. 2008. Total phosphorus inference models and indices for coastal plain streams based on benthic diatom assemblages from artificial substrates. *Hydrobiologia* 610: 139-152.

Porter, S.D. 2008. *Algal attributes: An autecological classification of algal taxa collected by the National Water-Quality Assessment Program*: U.S. Geological Survey Data Series 329, 18 p.

Porter, S.D., D.K. Mueller, N.E. Spahr, M.D. Munn and N.M. Dubrovsky. 2008. Efficacy of algal metrics for assessing nutrient and organic enrichment in flowing waters: *Freshwater Biology.* 53: 1036-1054.

Potapova, M. and D.F. Charles. 2007. Diatom metrics for monitoring eutrophication in rivers of the United States. *Ecological Indicators.* 7: 48-70.

Potapova, M., D.F. Charles, K.C. Ponader and D.M. Winter. 2004. Quantifying species indicator values for trophic diatom indices: a comparison of approaches. *Hydrobiologia.* 517: 25-41.

Prahl, F.G., J.R. Ertel, M.A. Goni, M.A. Sparrow and B. Eversmeyer. 1994. Terrestrial organic carbon contributions to sediments on the Washington margin. *Geochim. Cosmochim. Acta.* 58:3035-3048.

Pruell, R.J. and J.G. Quinn. 1985. Geochemistry of organic contaminants in Narragansett Bay sediments. *Estuar. Coast. Shelf Sci*., 21: 295-312.

Ridgeway, J. and G. Shimmield. 2002. Estuaries as repositories of historical contamination and their impact on shelf seas. *Estuar. Coast. Shelf Sci*. 55: 903-928.

Riedel, G.R., D.J. Velinsky, J.T.F. Ashley and J.Cornwell. 2010. River sediment investigation near Poplar Point in the tidal Anacostia River, Washington, DC. *Aquatic Geochemistry.* (under revision).

Rippey, B. and H. J. Anderson. 1996. Reconstruction of lake P loadings and dynamics using sedimentary record. *Environ. Sci. Technol*. 30: 1786-1789.

Ritchie, J.C. and McHenry, R.J. 1990. Application of radioactive fallout Cesium-137 for measuring soil erosion and sediment accumulation rates and patterns: A review. *Journal of Environmental Quality.* 19: 215-233.

Roy, AH., A.D. Rosemond, M.J. Paul, D.S. Leigh, and J.B. Wallace. 2003. Stream macroinvertebrate response to catchment urbanization (Georgia, U.S.A.). *Freshwater Biology* 48: 329-346.

Rushneck, D.R, A. Bekuveau et al. 2004. Concentrations of dioxin-like PCB congeners in unweathered Aroclors by HRGC/HRMS using EPA Method 1668A. *Chemosphere* 54: 79-97.

Ruttenberg, K.C. 1992. Development of a sequential extraction method for different forms of phosphorus in marine sediments. *Limnol. Oceanogr*. 37: 1460-1482.

Santschi, P.H., B.J. Presley, T.L. Wade, B. Garcia-Romero and M. Baskaran. 2001. Historical contamination of PAHs, PCBs, DDTs, and heavy metals in Mississippi River Delta, Galveston Bay and Tampa Bay sediment cores. *Mar. Environ. Res.* 52: 51-79.

Schelske, C.L. and D.A. Hodell. 1995. Using carbon isotopes of bulk sedimentary organic matter to reconstruct the history of nutrient loading and eutrophication in Lake Erie. *Limnol. Oceanogr*. 40: 918-929.

Schelske, C.L. and D.A. Hodell. 1991. Recent changes in productivity and climate of Lake Ontario detected by isotopic analysis of sediments. *Limnol. Oceanogr*. 36: 961-975.

Schropp, S.J., F.G. Lewis, H.L. Windom, J.D. Ryan, F.D. Calder and L.C. Burney. 1990. Interpretation of metal concentrations in estuarine sediments of Florida using aluminum as a reference element. *Estuaries.* 13: 227-235.

Schubel, J. R. and D. J. Hirschberg. 1977. ^{210}Pb determined sedimentation rate, and accumulation of metals in sediments at a station in Chesapeake Bay. *Chesapeake Sci.* 18: 379-382.

Simpson, R.L., R.E. Good, R. Walker and B.R. Frasco. 1983. The role of Delaware River freshwater tidal wetlands in the retention of nutrients and heavy metals. *J. Environ. Qual*. 12: 41-48.

Sinex, S.A. and G.R. Helz. 1981. Regional geochemistry of trace elements in Chesapeake Bay sediments. *Environ. Geol*. 3: 315-323.

Smol J.P. 2008. *Pollution of Lakes and Rivers: A Paleoenvironmental Perspective*- 2nd edition. Blackwell Publishing, Oxford.

Smol, J.P. 2002. *Pollution of Lakes and Rivers: A Paleoenvironmetal Perspective*. Arnold Press and Oxford University Press, NY.

Sommerfield, C.K. 2006. On sediment accumulation rates and stratigraphic completeness: Lessons from Holocene ocean margins. *Continental Shelf Research*. 26:2225-2240.

Song, W., J.C. Ford, L. An, W.J. Buckleya and K.J. Rockne. 2004. Polybrominated diphenyl ethers in sediments of the Great Lakes. 1. Lake Superior. *Environ. Sci. Tech*. 38(12): 3286-3293.

Thompson, P.M. and S. O'Byrne. 1999. *Images of America Wilmington's Waterfront*. Arcadia Publishing, Charleston, SC.

Trefry, J.H. and B.J. Presley. 1976. Heavy metal transport from the Mississippi River to the Gulf of Mexico. In: *Marine Pollution Transfer*, Eds.: H.L. Windom and R.A. Duce, Heath and Co., Lexington, pp. 39-75.

Ulseth, A.J. and A.E. Hershey. 2005. Natural abundances of stable isotopes trace anthropogenic N and C in an urban stream. *JNABS*: 24(2): 270-289.

United States Environmental Protection Agency (U.S. EPA). 2010. Current Site Information, Diamond State Salvage (accessed online at http://www.epa.gov/reg3hwmd/npl/DE0000122218.htm). U.S. Environmental Protection Agency, Region 3, Philadelphia, PA.

United States Environmental Protection Agency (U.S. EPA). 2009. Draft Recommended Interim Preliminary Remediation Goals for Dioxin in Soil at CERCLA and RCRA Sites. U.S. Environmental Protection Agency, Office of Superfund Remediation and Technology Innovation, Washington, D.C (December, 2009).

United States Environmental Protection Agency (U.S. EPA). 1993. EPA Superfund Record of Decision: E.I. Du Pont de Nemours & Co., Inc. (Newport Pigment Plant Landfill) EPA ID: DED980555122 OU 01 Newport, DE 09/29/1993 (EPA/ROD/R03-93/170). U.S. Environmental Protection Agency, Region 3, Philadelphia, PA.

United States Environmental Protection Agency (U.S. EPA). 1987. Guidance for Sampling of and Analyzing for Organic Contaminants in Sediments. Office of Water Regulations and Standards, Criteria and Standards Division, Washington, D.C.

Valette-Silver , N.J. 1993. The use of sediment cores to reconstruct historical trends in contamination of estuarine and coastal sediments. *Estuaries.* 16: 577-588.

van Dam, H., A. Mertens, and J. Sinkeldam. 1994. A coded checklist and ecological indicator values of freshwater diatoms from The Netherlands. *Neth. J. Aquat. Ecol*. 28: 117–133.

Van den Berg, M., et al. 2006. The 2005 World Health Organization Reevaluation of Human and Mammalian Toxic Equivalency Factors for Dioxins and Dioxin-Like Compounds. *Toxicol. Sci.* 93(2): 223-241.

Van Metre, P.C., B.J. Mahler and J.T. Wilson. 2009. PAHs underfoot: Contaminated dust from coal-tar sealcoated pavement is widespread in the United States. *Environ. Sci. Technol*.: 43(1): 20-25.

Van Metre, P, BJ Mahler, M Scoggins and PA Hamilton. 2006. Parking lot sealcoat: A major source of polycyclic aromatic hydrocarbons (PAHs) in rrban and suburban environments. US Geological Survey and the City of Austin, Fact Sheet 2005–3147.

Van Metre, P.C., B.J. Mahler and E.T. Furlong. 2000. Urban sprawl leaves its PAH signature. *Environ. Sci. Technol*. 34: 4064-4070.

Van Metre, P.C. and Callender, E. 1997. Identifying water-quality trends from ^{210}Pb using dated sediment cores from White Rock Lake Reservoir, Dallas, Texas. *Journal of Paleolimnology.* 17: 239-249.

Vane, C.H., Y.J. Ma, S.J Chen, and B.X. Mai. 2009. Increasing polybrominated diphenyl ether (PBDE) contamination in sediment cores from the inner Clyde Estuary, UK. Environ. *Geochem. Health*. Online edition (04 April 2009).

Velinsky, D.J., G.F. Riedel and J.T.F. Ashley. 2008. Assessment of Water Quality of the Tidal Potomac River in Washington DC: Trace Metals and Organic Contaminants. Final Report (04g-05-WQD03 (WP04)). District of Columbia, Department of the Environment, Washington, DC. (PCER Report: 08-3).

Velinsky, D.J., J.T.F. Ashley and G.R.Riedel. 2007. *Sediment Contaminants in the upper Tidal Potomac River; Washington, DC: Spatial and Temporal Trends.* Final Report submitted to Department of the Environment, District of Columbia. Patrick Center for Environmental Research, The Academy of Natural Sciences.

Velinsky, D.J., T.L. Wade, B. Gammisch and J. Cornwell. 1997. *Sediment Deposition and Inventory of Chemical Contaminants in the Tidal Anacostia River, Washington, D.C.* ICPRB Report #97-2. Interstate Commission on the Potomac River Basin, Rockville, MD.

Velinsky, D.J., T.L. Wade, C. Schlekat and B.J. Presley. 1994. Tidal river sediments in the Washington, D.C. area. I. Distribution and sources of trace metals. *Estuaries.* 17: 305-320.

Wade, T.L., D.J. Velinsky, E. Reinharz and C.E. Schlekat. 1994. Tidal river sediments in the Washington, D.C. area. II. Distribution and sources of chlorinated and non-chlorinated aromatic hydrocarbons. *Estuaries*. 17: 321-333.

Wakeham S.G., C. Schaffner and W. Giger. 1980. Polycyclic aromatic hydrocarbons in recent lake sediments—II. Compounds derived from biogenic precursors during early diagenesis. *Geochim Cosmochim Acta.* 44: 415–429.

Wallbrink, P.J., D.E. Walling and Q. He. 2002. Radionuclide measurement using HPGe gamma spectrometry. In: F. Zapata (Editor), *Handbook for the Assessment of Soil Erosion and Sedimentation Using Environmental Radionuclides*. Kluwer Academic Publishers, Dordrecht, pp. 67-96.

Wania, F. and C.B. Dugani. 2003. Assessing the long-range transport potential of polybrominated diphenyl ethers: a comparison of four multimedia models. *Environmental Toxicology and Chemistry.* 22: 1252–1261.

Wedepohl, K.H. 1971. *Geochemistry*. Holt, Rinehart and Winston, Inc., NY. (Translated from Geochemie, 1967).

Wedepohl, K.H. 1968. Chemical fractionation in the sedimentary environment, in Ahrens, L.H., ed., *Origin and Distribution of the Elements*: Oxford, England, Pergamon Press, pp. 999-1016.

Windom, H.L., S.J. Schropp, F.D. Calder and others. 1989. Natural trace metal concentrations in estuarine and coastal marine sediments of the southeastern United States. *Environ. Sci. Technol.,* 23: 314-320.

Woodwell, G.M., P.P. Craig and H.A. Johnson. 1971. DDT in the biosphere: Where does it go? *Science.* 174: 1101-1107.

Youngblood, W.W. and M. Blumer. 1975. Polycyclic aromatic hydrocarbons in the environment: homologous series in soils and recent marine sediments. *Geochim. Cosmochim. Acta*, 39: 1303-1314.

Zhang, X., E.R. Christensen and M.F. Gin. 1993. Polycyclic aromatic hydrocarbons in dated sediments from Green Bay and Lake Michigan. *Estuaries.* 16: 638-652.

Zimmerman, A.R. and E.A. Canuel. 2002. Sediment geochemical records eutrophication in the mesohaline Chesapeake Bay. *Limnol. Oceanogr*. 47: 1084-1093.

Tables

Table 1. Core locations and collection dates.

Name	Abbreviation	Date	Lat (N)	Long (W)	Depth of Core (cm)	Location
Brandywine River	BW-1	12/3/2007	39° 44.189'	75° 31.546'	36	Embayment
Churchman Marsh	CM-1A	3/25/2008	39° 42.021'	75° 37.810'	82	Marsh
Lower Shellpot Creek	LSP-2	4/15/2008	39° 44.320'	75° 30.597'	102	Marsh
Walnut Street	WS-2A	4/22/2008	39° 44.067'	75° 33.040'	98	Sub-tidal embayment
Dravo Marsh	DM-2	6/22/2008	39° 43.217'	75° 33.722'	106	Marsh

Table 2. Bulk sediment properties and radioisotope data for BW.

Chem ID	Interval	Water Content (%)	Dry Bulk Density (g/cm^3)	Accumulated Mass (g/cm^2)	LOI (%)	Total ^{210}Pb (dpm/g)	Excess ^{210}Pb (dpm/g)	^{137}Cs (dpm/g)	z (cm)	Age Model
9994	0-2	52.20	0.68	1.36	9.33	4.49	1.85	0.22	1	2006
9996	4-6	46.67	0.80	2.96	9.80	3.03	1.16	0.19	5	2000
9998	8-10	50.44	0.72	4.39	9.60	4.20	1.56	0.51	9	1995
10000	12-14	52.49	0.67	5.74	13.30	3.44	1.28	0.96	13	1990
10001	16-18	51.64	0.69	7.13	11.36	3.51	1.02	0.90	17	1984
10004	20-22	49.62	0.73	8.59	13.51	4.15	1.46	4.34	21	1979
10006	24-26	46.95	0.79	10.18	11.39	3.26	0.76	4.07	25	1974
10008	28-30	46.61	0.80	11.78	11.72	2.96	0.70	3.87	29	1968
10010	32-34	40.41	0.95	13.67	10.56	2.31	0.16	1.04	33	1963
10012	36-38	33.73	1.13	15.93	7.23	1.86	0.00	0.00	37	1958
10014	40-42	35.04	1.09	18.11	7.39	2.64	0.36	0.00	41	1952
10016	44-46	35.00	1.09	20.29	7.06	1.68	0.00	0.00	45	1947
10018	48-50	35.04	1.09	22.48	7.78	1.67	0.00	0.00	49	1942
10019	50-52	36.05	1.06	24.60	12.60	2.00	0.38	0.03	51	1939

Table 3. Bulk sediment properties and radioisotope data for CM.

Chem ID	Interval	Water Content (%)	Dry Bulk Density (g/cm^3)	Accumulated Mass (g/cm^2)	LOI (%)	Total ^{210}Pb (dpm/g)	Excess ^{210}Pb (dpm/g)	^{137}Cs (dpm/g)	z (cm)	Age Model
0219	0-2	73.19	0.32	0.64	19.61	9.83	7.60	0.19	1	2005
0221	4-6	72.32	0.33	1.31	18.11	10.65	7.79	0.33	5	1999
0223	8-10	64.79	0.45	2.21	15.27	9.22	6.74	0.34	9	1992
0225	12-14	63.93	0.47	3.14	14.95	6.73	4.55	0.24	13	1985
0227	16-18	63.61	0.47	4.09	15.56	7.01	4.69	0.33	17	1979
0229	20-22	66.55	0.42	4.93	16.98	7.17	4.86	0.50	21	1972
0231	24-26	61.80	0.50	5.93	15.56	6.02	3.93	0.48	25	1965
0233	28-30	49.59	0.73	7.40	11.83	3.88	0.98	0.12	29	1959
0235	32-34	46.65	0.80	9.00	11.80	3.81	0.22	0.00	33	1952
0237	36-38	45.94	0.81	10.63	11.35	3.76	0.63	0.00	37	1945
0239	40-42	45.33	0.83	12.29	11.20	2.61	0.25	0.00	41	1939
0241	44-46	43.45	0.87	14.03	10.46	3.44	0.73	0.00	45	1932
0243	48-50	44.96	0.84	15.71	9.84	3.40	0.09	0.00	49	1925
0245	52-54	42.80	0.89	17.48	10.05	3.08	0.63	0.00	53	1919
0247	56-58	43.31	0.88	19.24	9.43	2.96	0.44	0.00	57	1912
0249	60-62	45.31	0.83	20.90	9.76	2.72	0.33	0.00	61	1909
0251	64-66	41.55	0.92	22.73	8.56	2.76	0.45	0.00	65	1899
0253	68-70	35.53	1.08	24.89	7.40	2.74	0.39	0.00	69	1892
0255	72-74	32.40	1.17	27.22	6.63	2.29	0.04	0.00	73	1878

Table 4. Bulk sediment properties and radioisotope data for LSP.

Chem ID	Interval	Water Content (%)	Dry Bulk Density (g/cm^3)	Accumulated Mass (g/cm^2)	LOI (%)	Total ^{210}Pb (dpm/g)	Excess ^{210}Pb (dpm/g)	^{137}Cs (dpm/g)	z (cm)	Age Model
0429	0-2	70.82	0.36	0.71	20.85	14.79	12.29	0.26	1	2006
0431	4-6	64.01	0.46	1.64	17.61	12.36	10.48	0.33	5	2004
0433	8-10	56.92	0.59	2.82	13.77	14.20	12.15	0.30	9	2002
0435	12-14	63.29	0.48	3.77	18.98	12.47	10.27	0.24	13	2000
0437	16-18	68.21	0.40	4.56	24.48	14.35	12.29	0.22	17	1998
0439	20-22	57.70	0.57	5.71	17.32	14.94	12.19	0.41	21	1996
0441	24-26	55.23	0.62	6.95	16.22	15.31	12.75	0.38	25	1994
0443	28-30	53.68	0.65	8.25	16.68	13.06	10.28	0.38	29	1992
0445	32-34	57.31	0.58	9.42	16.94	11.23	9.31	0.32	33	1990
0447	36-38	63.85	0.47	10.35	17.64	8.79	6.89	0.21	37	1988
0449	40-42	60.96	0.52	11.38	15.49	9.46	7.19	0.20	41	1985
0451	44-46	58.98	0.55	12.48	16.09	8.76	6.71	0.15	45	1983
0453	48-50	67.22	0.41	13.31	24.07	7.51	5.48	0.16	49	1981
0454	50-52	69.16	0.38	14.07	23.33	8.07	5.53	0.22	51	1980
0455	52-54	68.54	0.39	14.85	27.87	7.10	5.67	0.08	53	1979
0457	56-58	71.32	0.35	15.55	33.96	5.18	4.26	0.16	57	1977
0459	60-62	60.15	0.53	16.61	12.36	5.41	2.74	0.52	61	1975
0461	64-66	61.59	0.50	17.62	14.17	5.48	2.90	0.41	65	1973
0463	68-70	60.26	0.53	18.68	12.34	4.19	1.47	0.58	69	1971
0465	72-74	64.75	0.45	19.58	13.90	5.20	2.37	0.59	73	1969
0467	76-78	53.45	0.66	20.89	9.66	4.86	2.71	0.63	77	1966
0469	80-82	55.68	0.61	22.12	11.26	5.11	2.93	0.42	81	1964
0471	84-86	38.72	0.99	24.10	6.09	2.32	0.82	0.18	85	1962
0473	88-90	32.50	1.16	26.43	4.61	1.59	0.29	0.14	89	1960
0475	92-94	30.26	1.23	28.89	3.83	1.99	0.11	0.10	93	1958
0477	96-98	52.58	0.67	30.24	14.02	5.30	2.60	0.37	97	1956
0479	100-102	40.45	0.95	32.13	5.50	2.39	0.33	0.08	101	1954

Table 5. Bulk sediment properties and radioisotope data for DM.

Chem ID	Interval	Water Content (%)	Dry Bulk Density (g/cm^3)	Accumulated Mass (g/cm^2)	LOI (%)	Total ^{210}Pb (dpm/g)	Excess ^{210}Pb (dpm/g)	^{137}Cs (dpm/g)	z (cm)	Age Model
1055	0-2	82.46	0.20	0.39	36.30	10.23	8.78	0.28	1	2006
1057	4-6	79.77	0.23	0.86	32.10	9.25	7.82	0.20	5	2000
1059	8-10	84.76	0.17	1.19	38.91	6.64	5.00	0.27	9	1995
1061	12-14	77.86	0.26	1.71	29.13	5.54	3.62	0.35	13	1990
1063	16-18	69.70	0.37	2.45	21.97	4.98	2.83	0.61	17	1984
1065	20-22	58.08	0.57	3.59	14.03	4.82	2.35	0.54	21	1979
1067	24-26	47.26	0.79	5.16	10.35	2.88	0.15	0.24	25	1974
1069	28-30	48.51	0.76	6.67	10.990	4.24	1.31	0.23	29	1968
1071	32-34	53.22	0.66	7.99	13.589	4.35	1.55	0.27	33	1963
1073	36-38	64.18	0.46	8.92	20.541	4.62	2.33	0.12	37	1958
1075	40-42	54.81	0.63	10.17	15.278	4.11	1.28	0.00	41	1952
1077	44-46	45.53	0.82	11.82	10.678	3.19	0.42	0.00	45	1947
1079	48-50	40.37	0.95	13.72	8.204	2.64	0.00	0.00	49	1942
1081	52-54	37.36	1.03	15.77	7.017	2.30	0.00	0.00	53	1935
1083	56-58	33.92	1.12	18.02	5.744	2.10	0.02	0.00	57	1931
1085	60-62	32.99	1.15	20.32	5.053	2.48	0.00	0.00	61	1927
1087	64-66	37.69	1.02	22.35	6.186	2.21	0.08	0.00	65	1920
1089	68-70	37.95	1.01	24.38	6.863	2.95	0.30	0.00	69	1915

Table 6. Summary data for radioisotope analysis and dating.

		Radioisotope Inventory		Sedimentation Rate			Mass Accumulation Rate		Depositional Flux	Focusing Factor	
Location	**Core**	xsPb-210	Cs-137	xsPb-210 CA	xsPb-210 CF	Cs-137	xsPb-210	Cs-137	xsPb-210	xsPb-210	Cs-137
		dpm/cm^2	dpm/cm^2	cm/yr	cm/yr	cm/yr	g/cm^2-yr	g/cm^2-yr	dpm/cm^2-yr		
Brandywine River	BW-2	28.00	49.00	0.64	0.96	0.66	0.25	0.28	0.53	0.90	2.30
Churchmans Marsh	CM-1	66.00	4.00	0.63	1.00	0.57	0.17	0.15	0.95	2.10	0.20
Shellpot Creek	SP-2	399.00	18.00	1.30	2.10	1.90	0.37	0.60	7.50	12.50	0.90
Dravo Marsh	DM-2	82.00	5.00	NA	0.73	0.74	0.29	0.19	0.85	2.60	0.30

xs – excess; CA – Constant activity model; CF – Constant flux model (modified to match Cs-137 input function)
Depositional flux – based on steady-state atmospheric fluxes of xsPb-210 (32 dpm/cm^2-yr) and Cs-137 (21 dpm/cm^2-yr)

Table 7. Concentrations of various parameters for Core BW.

CHEM ID	Interval cm	Mid-Point cm	Solids %	Age Model yr	$\delta^{13}C$ per mil	$\delta^{15}N$ per mil	TC %	TN %	C/N Atomic
9994	0-2	1	47.3	2006	-26.48	5.37	3.82	0.31	14.50
9996	4-6	5	46.5	2000	-26.57	5.34	4.17	0.29	16.67
9998	8-10	9	49.2	1995	-25.94	4.95	3.96	0.29	15.82
10000	12-14	13	48.1	1990	-23.82	5.36	3.79	0.32	13.84
10001	14-16	15	49.9	1987	-23.54	5.20	3.85	0.34	13.15
10003	18-20	19	51.0	1982	-23.40	5.19	3.93	0.32	14.53
10004	20-22	21	49.6	1979	-26.34	3.94	6.79	0.44	17.91
10006	24-26	25	51.3	1974	-25.63	4.87	5.80	0.31	21.59
10008	28-30	29	52.9	1968	-25.57	4.83	7.02	0.48	16.98
10010	32-34	33	55.6	1963	-25.17	5.05	6.32	0.39	18.74
10012	36-38	37	68.4	1958	-24.11	4.33	2.03	0.16	14.89
10013	38-40	39	67.5	1955	-23.69	4.80	2.14	0.17	14.52
10015	42-44	43	66.1	1950	-23.63	4.94	1.60	0.15	12.20
10017	46-48	47	67.1	1944	-23.53	4.82	1.70	0.26	7.74
10019	50-52	51	64.0	1939	-23.65	5.50	2.22	0.20	13.03

Table 7 (continued). Concentrations of various parameters for Core BW.

CHEM ID	TSP	Fe	Zn	tPAHs	T PCBs	tDDXs	tChlordanes	tDioxins	tFurans	2,3,7,8 TCDD-TEQ	tPBDEs
	%	µg/g dw	µg/g dw	µg/g dw	ng/g dw	ng/g dw	ng/g dw	pg/g dw	pg/g dw	pg/g dw	ng/g dw
9994	0.084	29412	486	1.97	44.64	8.17	2.48	6992	621	21.8	52.8
9996	0.087	34804	471	4.30	45.05	9.50	2.00	5327	551	16.2	48.5
9998	0.087	37237	485	1.03	70.96	13.01	2.77	8507	554	21.4	120.1
10000	0.269	41667	337	2.10	636.80	308.12	7.10	12628	1562	46.2	0.69
10001	0.191	37255	376	2.16	685.04	288.74	6.80	11580	1414	41.7	1.16
10003	0.158	29412	518	2.70	617.66	369.03	6.82	9077	1730	44.8	0.92
10004	0.090	40196	784	8.95	431.11	69.16	51.10	7123	2849	93.0	NA
10006	0.105	40686	769	5.20	120.06	39.66	7.73	6702	2705	68.5	NA
10008	0.122	38725	706	8.01	118.79	63.16	3.40	7055	2868	75.3	1.49
10010	0.121	25490	565	5.01	77.85	41.42	1.53	6668	2239	37.6	1.37
10012	0.085	29796	461	3.40	4.63	1.63	0.44	6927	117	9.5	NA
10013	0.103	31580	392	3.67	3.63	6.59	0.34	7070	116	8.9	NA
10015	0.075	32680	431	2.52	5.79	5.79	0.22	4417	128	6.5	0.85
10017	0.083	35294	486	2.04	2.19	3.60	0.25	6519	233	10.1	NA
10019	0.095	33296	296	2.97	2.95	5.09	0.29	6716	61	8.9	1.14

Concentrations on a dry weight basis. Total PAHs is the sum of 39 individual compounds, total PCBs is the sum of 110 congeners, total DDX is the sum of o,p+pp forms of DDD, DDE, and DDT, and total chlordane is the sum of alpha+gamma chlordane, heptachlor, heptachlor epoxide, oxychlordane, nonachlor and nonachlor epoxide (See Appendix I).

Table 8. Concentrations of various parameters for Core CM.

CHEM ID	Interval cm	Mid-Point cm	Solids %	Age Model yr	$\delta^{13}C$ per mil	$\delta^{15}N$ per mil	TC %	TN %	C/N Atomic
0219	0-2	1	28.3	2005	-28.14	8.08	7.52	0.79	11.09
0221	4-6	5	26.1	1999	-28.11	7.30	7.73	0.75	12.00
0223	8-10	9	33.8	1992	-27.77	6.95	5.71	0.55	12.05
0225	12-14	13	36.8	1985	-27.73	6.60	5.39	0.50	12.64
0227	16-18	17	32.7	1979	-27.42	6.39	6.34	0.60	12.38
0229	20-22	21	44.1	1972	-27.19	5.49	4.93	0.42	13.84
0231	24-26	25	53.2	1965	-26.75	4.71	3.44	0.30	13.26
0233	28-30	29	54.1	1959	-26.93	4.17	3.52	0.31	13.14
0235	32-34	33	54.0	1952	-26.28	4.35	3.66	0.32	13.51
0237	36-38	37	54.5	1945	-25.95	4.13	3.52	0.34	12.05
0240	42-44	43	55.5	1935	-26.00	4.75	3.02	0.26	13.47
0243	48-50	49	57.7	1925	-24.40	4.58	2.65	0.23	13.28
0247	56-58	57	56.1	1912	-25.74	4.08	2.88	0.26	12.84
0251	64-66	65	60.0	1899	-25.47	4.24	1.99	0.20	11.76
0255	72-74	73	66.5	1885	-25.63	4.73	1.73	0.19	10.40
0259	80-82	81	70.1	1872	-24.66	4.79	1.17	0.15	9.07

Table 8 (continued). Concentrations of various parameters for Core CM.

CHEM ID	TSP	Fe	Zn	tPAHs	T PCBs	tDDXs	tChlordanes	tDioxins	tFurans	2,3,7,8 TCDD-TEQ	tPBDEs
	%	µg/g dw	µg/g dw	µg/g dw	ng/g dw	ng/g dw	ng/g dw	pg/g dw	pg/g dw	pg/g dw	ng/g dw
0219	0.180	45656	723	1.68	90.28	9.31	2.79	13306	523	19.9	10.34
0221	NA	37255	973	2.24	157.91	15.91	3.53	13163	525	30.7	12.09
0223	NA	33996	984	1.41	125.85	10.38	1.36	14876	691	30.3	9.72
0225	0.182	35743	980	1.43	189.18	11.98	1.91	18228	838	40.8	10.92
0227	0.170	35351	1086	1.71	339.36	20.54	3.31	18999	754	42.7	17.12
0229	0.125	33824	3817	2.00	487.00	26.39	2.24	10923	616	29.9	3.69
0231	0.101	26471	4078	2.50	781.53	39.82	2.31	11945	606	22.6	1.02
0233	0.106	29223	4374	6.00	2106.59	108.23	4.60	10541	1315	24.5	0.80
0235	0.113	32843	8314	6.83	1809.13	117.59	6.60	157727	12695	444.6	0.34
0237	0.119	36765	9804	26.79	980.36	62.99	4.66	29775	3183	102.5	0.41
0240	0.106	30702	9482	3.18	328.06	20.55	1.49	13028	1562	19.5	NA
0243	0.105	39706	7529	0.90	66.76	3.18	0.38	11904	683	20.3	NA
0247	0.089	37255	9098	1.39	152.68	6.06	0.60	15189	1352	32.5	NA
0251	0.066	30392	4078	2.10	144.25	3.39	0.42	13756	1903	15.2	NA
0255	0.055	33333	149	0.46	4.09	0.68	0.10	18161	54	10.9	NA
0259	0.060	35083	131	0.44	2.83	0.84	0.07	13160	19	7.5	NA

Concentrations on a dry weight basis. NA- Not analyzed. Total PAHs is the sum of 39 individual compounds, total PCBs is the sum of 110 congeners, total DDX is the sum of o,p+pp forms of DDD, DDE, and DDT, and total chlordane is the sum of alpha+gamma chlordane, heptachlor, heptachlor epoxide, oxychlordane, nonachlor and nonachlor epoxide (See Appendix I).

Table 9. Concentrations of various parameters for Core DM.

CHEM ID	Interval	Mid-Point	Solids	Age Model	$\delta^{13}C$	$\delta^{15}N$	TC	TN	C/N
	cm	cm	%	yr	per mil	per mil	%	%	Atomic
1055	0-2	1	15.5	2006	-28.59	7.76	18.19	1.17	18.14
1057	4-6	5	18.6	2000	-28.51	7.80	14.53	0.93	18.20
1058	6-8	7	26.6	1998	-28.01	7.61	10.64	0.68	18.13
1059	8-10	9	14.0	1995	-28.21	7.86	19.77	1.15	20.11
1060	10-12	11	13.8	1992	-28.29	7.36	18.88	1.04	21.13
1061	12-14	13	16.9	1990	-28.26	7.37	17.54	1.01	20.17
1063	16-18	17	32.3	1984	-27.69	7.14	8.77	0.55	18.53
1065	20-22	21	51.0	1979	-27.28	6.22	5.14	0.30	20.18
1067	24-26	25	57.5	1974	-26.91	6.16	4.18	0.26	18.82
1069	28-30	29	54.0	1968	-26.87	6.75	4.86	0.30	19.03
1071	32-34	33	57.6	1963	-26.48	6.56	3.61	0.23	18.10
1073	36-38	37	37.6	1958	-27.07	6.54	8.34	0.50	19.35
1076	42-44	43	44.7	1950	-26.78	7.91	6.49	0.42	17.99
1079	48-50	49	58.7	1942	-25.90	6.83	3.08	0.23	15.85
1083	56-58	57	64.9	1931	-24.51	4.78	1.47	0.13	13.58
1087	64-66	65	62.0	1920	-24.51	4.45	1.69	0.15	12.84
1095	80-82	81	64.3	1905	-25.21	5.77	1.65	0.13	14.67
1102	94-96	95	62.0	1888	-25.28	5.36	1.33	0.14	10.89
1106	102-104	103	61.5	1878	-24.60	5.90	1.04	0.12	10.15

Table 9 (continued). Concentrations of various parameters for Core DM.

CHEM ID	TSP	Fe	Zn	tPAHs	T PCBs	tDDXs	tChlordanes	tDioxins	tFurans	2,3,7,8 TCDD-TEQ	tPBDEs
	%	µg/g dw	µg/g dw	µg/g dw	ng/g dw	ng/g dw	ng/g dw	pg/g dw	pg/g dw	pg/g dw	ng/g dw
1055	0.098	12504	538	2.70	238.49	29.07	9.69	9244	1117	32.9	17.07
1057	0.092	9056	647	1.93	278.19	30.22	9.65	7806	975	33.9	32.64
1058	0.082	18166	742	4.17	239.94	23.45	5.40	16594	2100	69.9	NA
1059	0.087	29762	1045	2.95	356.71	41.19	13.11	10023	1279	32.1	12.47
1060	0.083	20427	777	4.84	436.01	50.41	13.82	6638	769	26.4	15.01
1061	0.082	12276	811	8.05	325.98	33.85	10.93	4429	572	13.8	16.02
1063	0.073	9013	818	5.46	364.52	39.88	9.26	5701	779	24.3	2.42
1065	0.045	7782	594	3.86	180.97	28.13	3.94	5084	1394	27.7	1.51
1067	0.040	5388	299	2.83	45.05	6.87	0.79	3188	778	16.9	NA
1069	0.046	8631	610	2.80	35.87	4.84	0.44	2033	552	12.2	0.29
1071	0.043	10058	678	4.34	48.61	6.74	0.71	2102	608	20.0	0.56
1073	0.090	11043	1230	6.52	394.89	68.54	3.53	11880	4808	93.9	0.46
1076	0.071	6186	1059	5.46	102.14	11.12	1.41	2577	1707	31.0	NA
1079	0.051	6443	319	3.84	19.17	1.39	0.42	9517	2900	33.6	NA
1083	0.058	9497	149	0.97	3.70	0.71	0.14	1438	53	2.6	NA
1087	0.049	14220	175	3.58	2.58	0.71	0.13	1475	244	5.2	0.60
1095	0.054	8185	71	0.79	2.39	0.49	0.12	6085	12	7.5	NA
1102	0.067	17779	84	0.25	2.22	0.47	0.10	1175	11	1.2	NA
1106	0.050	11249	95	0.34	2.82	0.86	0.10	1819	13	2.4	NA

Concentrations on a dry weight basis. TBC - to be completed. Total PAHs is the sum of 39 individual compounds, total PCBs is the sum of 110 congeners, total DDX is the sum of o,p+pp forms of DDD, DDE, and DDT, and total chlordane is the sum of alpha+gamma chlordane, heptachlor, heptachlor epoxide, oxychlordane, nonachlor and nonachlor epoxide (See Appendix I).

Table 10. Concentrations of various parameters for Core LSP.

CHEM ID	Interval	Mid-Point	Solids	Age Model	$\delta^{13}C$	$\delta^{15}N$	TC	TN	C/N
	cm	cm	%	yr	per mil	per mil	%	%	Atomic
0429	0-2	1	27.6	NC	-27.81	3.95	9.10	0.56	19.08
0432	6-8	7	41.1	NC	-28.09	3.33	5.62	0.35	18.54
0464	70-72	71	34.9	NC	-22.25	2.69	4.56	0.25	21.25
0478	98-100	99	58.1	NC	-23.64	4.05	2.00	0.13	17.99
0479	100-102	101	59.5	NC	-23.56	3.45	1.84	0.12	18.29

CHEM ID	TSP	Fe	Zn	tPAHs	T PCBs	tDDXs	tChlordanes	tDioxins	tFurans	2,3,7,8 TCDD-TEQ	tPBDEs
	%	µg/g dw	µg/g dw	µg/g dw	ng/g dw	ng/g dw	ng/g dw	pg/g dw	pg/g dw	pg/g dw	ng/g dw
0429	0.137	19998	350	13.35	673.0	75.32	150.8	5322	223	5.5	NA
0432	0.127	13127	216	8.41	615.9	40.86	82.4	7684	316	7.7	NA
0464	0.180	60668	412	19.45	3456.3	53.67	52.9	7214	744	11.3	NA
0478	0.083	24466	214	2.26	474.8	19.44	13.3	3042	599	5.1	NA
0479	0.065	21275	168	1.78	303.1	16.25	9.0	2950	379	4.2	NA

Concentrations on a dry weight basis. NA – Not analyzed. Total PAHs is the sum of 39 individual compounds, total PCBs is the sum of 110 congeners, total DDX is the sum of o,p+pp forms of DDD, DDE, and DDT, and total chlordane is the sum of alpha+gamma chlordane, heptachlor, heptachlor epoxide, oxychlordane, nonachlor and nonachlor epoxide (See Appendix I).

Table 11. Concentrations of various parameters for Core WS.

CHEM ID	Interval	Mid-Point	Solids	Age Model	$\delta^{13}C$	$\delta^{15}N$	TC	TN	C/N
	cm	cm	%	yr	per mil	per mil	%	%	Atomic
0480	0-2	1	32.4	NC	-25.81	5.02	4.42	0.34	14.94
0483	6-8	7	37.2	NC	-25.83	4.78	4.25	0.28	17.68
0491	22-24	23	42.0	NC	-25.43	4.97	4.02	0.31	15.01
0504	48-50	49	44.6	NC	-25.94	4.53	3.80	0.28	15.95
0513	66-68	67	41.0	NC	-25.80	4.80	4.37	0.30	16.88
0527	94-96	95	44.8	NC	-25.09	5.67	3.73	0.31	13.91

CHEM ID	TSP	Fe	Zn	tPAHs	T PCBs	tDDXs	tChlordanes	tDioxins	tFurans	2,3,7,8 TCDD-TEQ	tPBDEs
	%	µg/g dw	µg/g dw	µg/g dw	ng/g dw	ng/g dw	ng/g dw	pg/g dw	pg/g dw	pg/g dw	ng/g dw
0480	0.174	48519	367	10.00	197.0	25.91	8.15	14339	1331	13.9	NA
0483	0.140	45526	876	9.58	171.4	25.62	7.26	9174	937	12.8	NA
0491	0.157	48905	881	10.50	76.0	10.64	3.39	8963	954	12.0	NA
0504	0.132	52173	974	11.10	236.4	24.56	8.33	4912	409	5.7	NA
0513	0.166	55448	1130	8.14	120.1	10.83	3.06	13321	2552	39.3	NA
0527	0.157	47092	1139	10.24	199.3	16.93	5.67	12049	2061	41.5	NA

Concentrations on a dry weight basis. NA – Not analyzed. Total PAHs is the sum of 39 individual compounds, total PCBs is the sum of 110 congeners, total DDX is the sum of o,p+pp forms of DDD, DDE, and DDT, and total chlordane is the sum of alpha+gamma chlordane, heptachlor, heptachlor epoxide, oxychlordane, nonachlor and nonachlor epoxide (See Appendix I).

Table 12. List of compounds in Figure 17.

PAH Compound	Cmpd #
Naphthalene	1
biphenyl	2
Acenaphthylene	3
Acenaphthene	4
Fluorene	5
Dibenzothiophene	6
Phenanthrene	7
Anthracene	8
Fluoranthene	9
BenzoAfluorene	10
BenzoBfluorene	11
Pyrene	12
Cyclopenta[cd]pyrene	13
Chrysene + Triphenylene	14
Naphthacene	15
Benzo[b]fluoranthene	16
Benzo[k]fluoranthene	17
Benzo[e]pyrene	18
Benzo[a]pyrene	19
Perylene	20
Indeno[1,2,3-cd]pyrene	21
Dibenzo[a,h+a,c]anthracene	22
Benzo[g,h,i]perylene	23
Coronene	24

Table 13. Diatom Metrics determined from species identification: Brandywine Creek Core.

Core ID/ Depth Interval (cm)	Mid-Depth (cm)	Year	Eutrophentic	Meso/ eurotrophentic	Mesotrophentic	Oligotrophentic
BW2 0-2 cm	1	2006	53.57	18.65	5.36	0.00
BW2 4-6 cm	5	2000	52.17	20.16	4.74	0.00
BW2 8-10 cm	9	1995	58.02	13.07	13.47	0.00
BW2 12-14 cm	13	1990	25.94	0.40	17.43	1.39
BW2 14-16 cm	15	1987	45.56	7.69	3.94	2.96
BW2 18-20 cm	19	1982	39.48	3.37	6.15	10.32
BW2 20-22 cm	21	1979	46.61	2.79	6.18	0.00
BW2 24-26 cm	25	1974	53.58	4.26	5.22	0.77
BW2 28-30 cm	29	1968	58.22	6.53	4.55	0.20
BW2 32-34 cm	33	1963	32.29	5.06	3.84	0.35
BW2 36-38 cm	37	1958	25.75	4.99	1.40	0.20
BW2 38-40 cm	39	1955	34.40	2.00	4.60	0.00
BW2 42-44 cm	43	1950	26.53	1.78	2.18	0.40
BW2 46-48 cm	47	1944	27.17	1.52	1.96	0.43
BW2 50-52 cm	51	1939	30.54	5.39	2.59	0.40

Metrics based on van Dam et al. (1994)

Table 14. Diatom Metrics determined from species identification: Churchmans Marsh Core.

Core ID/ Depth Interval (cm)	Mid-Depth (cm)	Year	Eutrophentic	Meso/ eurotrophentic	Mesotrophentic	Oligotrophentic	Oligo/ mesotrophentic
CM1 0-2 cm	1	2005	76.61	4.29	0.97	0.00	76.61
CM1 4-6 cm	5	1999	81.46	2.96	0.59	0.20	81.46
CM1 8-10 cm	9	1992	71.40	6.06	1.14	0.00	71.40
CM1 12-14 cm	13	1985	71.54	2.17	0.99	0.00	71.54
CM1 16-18 cm	17	1979	74.16	2.78	0.00	0.00	74.16
CM1 20-22 cm	21	1972	63.00	3.80	3.00	0.00	63.00
CM! 24-26 cm	25	1965	57.60	6.80	1.20	0.40	57.60
CM1 28-30 cm	29	1959	42.63	10.61	3.34	1.18	42.63
CM1 32-34 cm	33	1952	45.87	7.87	1.57	0.20	45.87
CM1 36-38 cm	37	1945	27.63	8.75	2.58	0.00	27.63
CM1 42-44 cm	43	1935	33.67	7.77	2.19	0.00	33.67
CM1 48-50 cm	49	1925	39.80	8.20	4.20	0.40	39.80
CM1 56-58 cm	57	1912	35.23	7.24	0.78	0.20	35.23
CM1 64-66 cm	65	1899	40.08	9.13	2.38	0.40	40.08
CM1 72-74 cm	73	1885	32.03	3.92	0.87	0.00	32.03
CM1 80-82 cm	81	1872	35.57	4.25	0.22	1.57	35.57

Metrics based on van Dam et al. (1994)

Table 15. Diatom Metrics determined from species identification: Dravo Marsh Core.

Core ID/ Depth Interval (cm)	Mid-Depth (cm)	Year	Eutrophentic	Meso/ eurotrophentic	Mesotrophentic	Oligotrophentic	Oligo/ mesotrophentic
DM2 0-2 cm	1	2006	64.66	7.57	4.47	0.19	64.66
DM2 4-6 cm	5	2000	71.79	3.55	2.37	0.00	71.79
DM 8-10 cm	9	1995	67.13	6.53	4.36	0.20	67.13
DM2 12-14 cm	13	1990	69.41	3.73	4.31	0.78	69.41
DM2 16-18 cm	17	1984	55.45	3.96	1.78	0.40	55.45
DM2 20-22 cm	21	1979	58.27	3.54	3.94	0.20	58.27
DM2 24-26 cm	25	1974	46.22	4.78	0.80	0.20	46.22
DM2 32-34 cm	33	1963	35.39	5.37	0.99	0.20	35.39
DM2 42-44 cm	43	1950	36.67	6.67	1.57	1.57	36.67
DM2 56-58 cm	57	1931	33.27	4.47	2.14	0.58	33.27
DM2 64-66 cm	65	1920	40.59	4.16	2.18	0.20	40.59
DM2 80-82 cm	81	1905	25.84	4.57	5.96	0.00	25.84

Metrics based on van Dam et al. (1994)

Figures

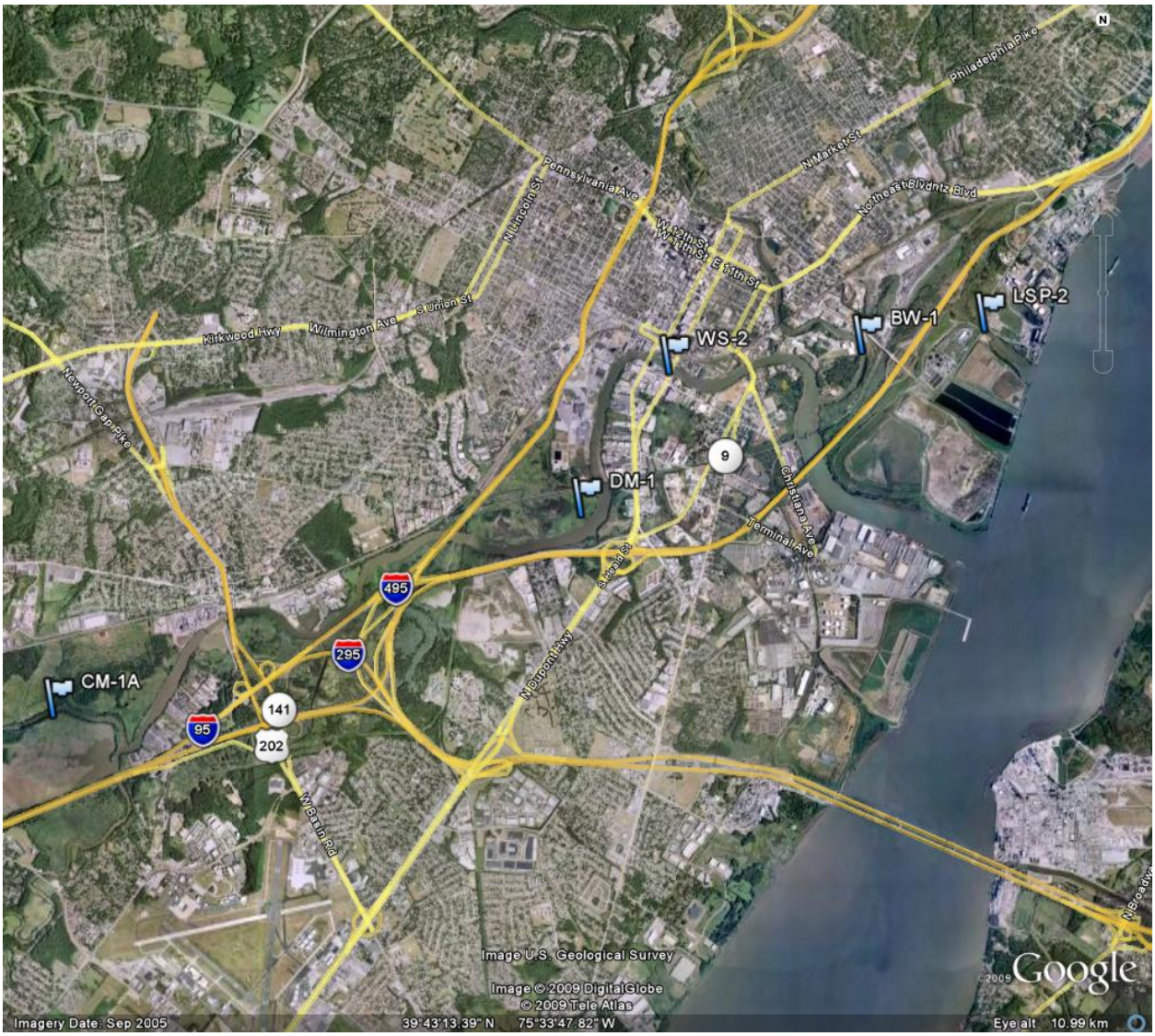

Figure 1. Coring locations within the tidal Christina River system. Key: CM – Churchmans Marsh, DM – Dravo Marsh (Old Wilmington Marsh), WS - Walnut Street embayment, BW-Brandywine wetland, and LSP – Lower Shellpot.

Figure 2. Tripod and pulley system used to retrieve push-piston cores at Dravo Marsh within the tidal Christina River system.

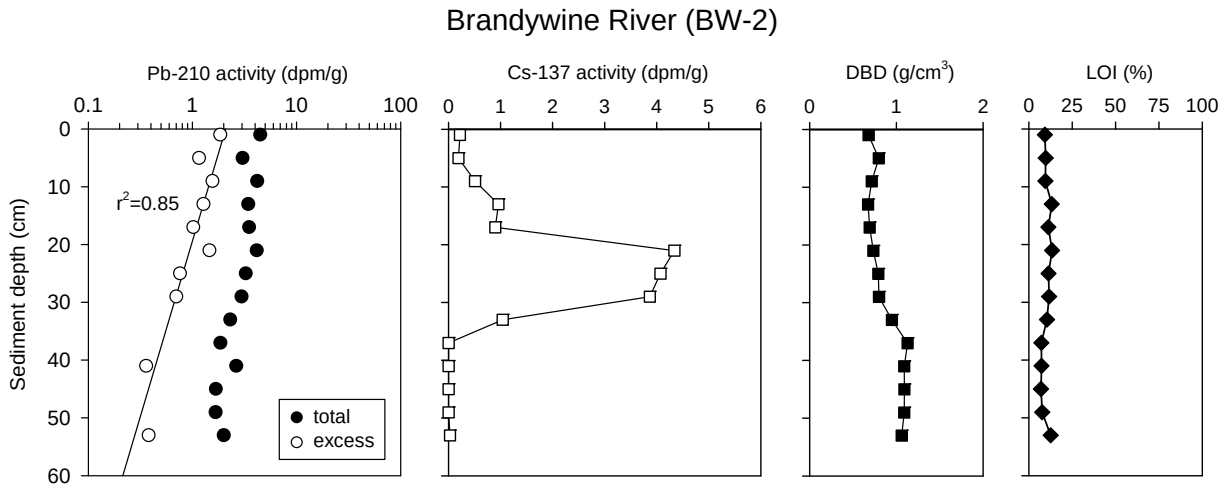

Figure 3. Geochronology for the Brandywine Creek marsh using excess ^{210}Pb and transient fallout ^{137}Cs. The radionuclides give comparable sedimentation rates of 0.80 (constant activity model) and 0.10 cm/yr, respectively. The first occurrence of ^{137}Cs at 36-38 cm is assumed concordant with ca. 1954.

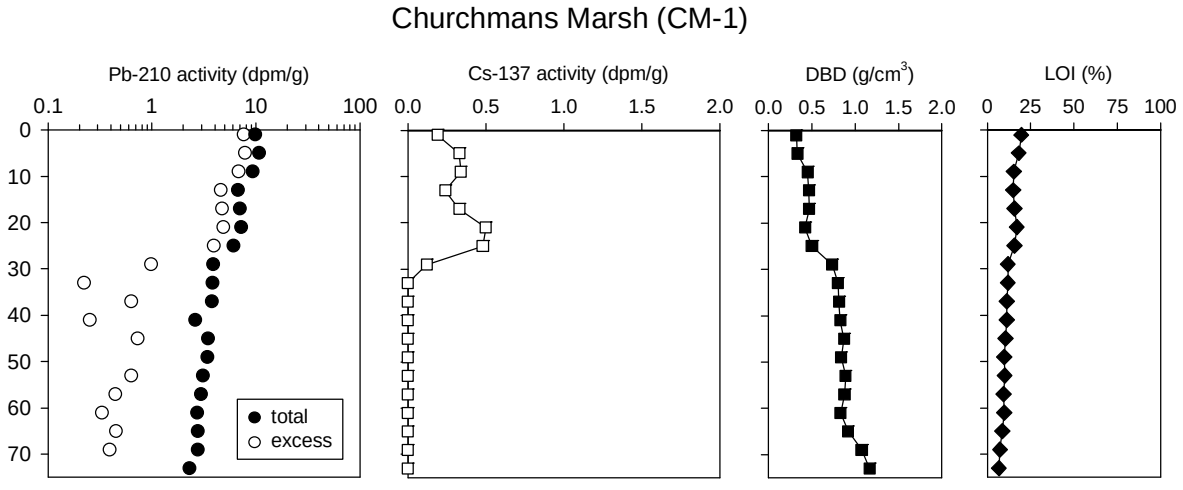

Figure 4. Geochronology for the Churchmans Marsh using excess ^{210}Pb and transient fallout ^{137}Cs. The radionuclides give comparable sedimentation rates of 0.51 (constant flux model) and 0.60 cm/yr, respectively. The first occurrence of ^{137}Cs at 32-34 cm is assumed concordant with ca. 1954.

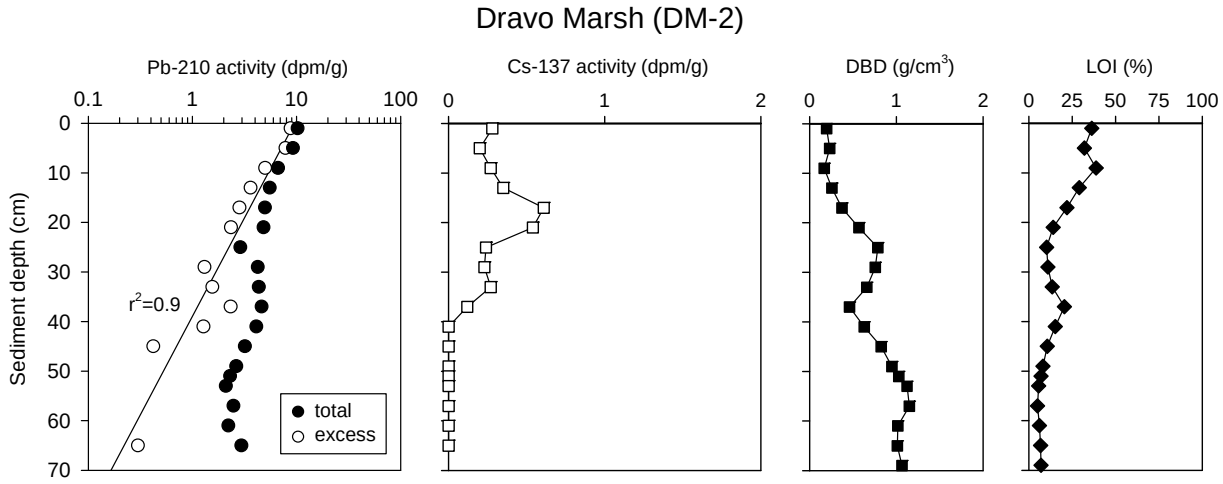

Figure 5. Geochronology for the Dravo Marsh using excess ^{210}Pb and transient fallout ^{137}Cs. The radionuclides give comparable sedimentation rates of 0.56 (constant activity model) and 0.79 cm/yr, respectively. The first occurrence of ^{137}Cs at 38-40 cm is assumed concordant with ca. 1954.

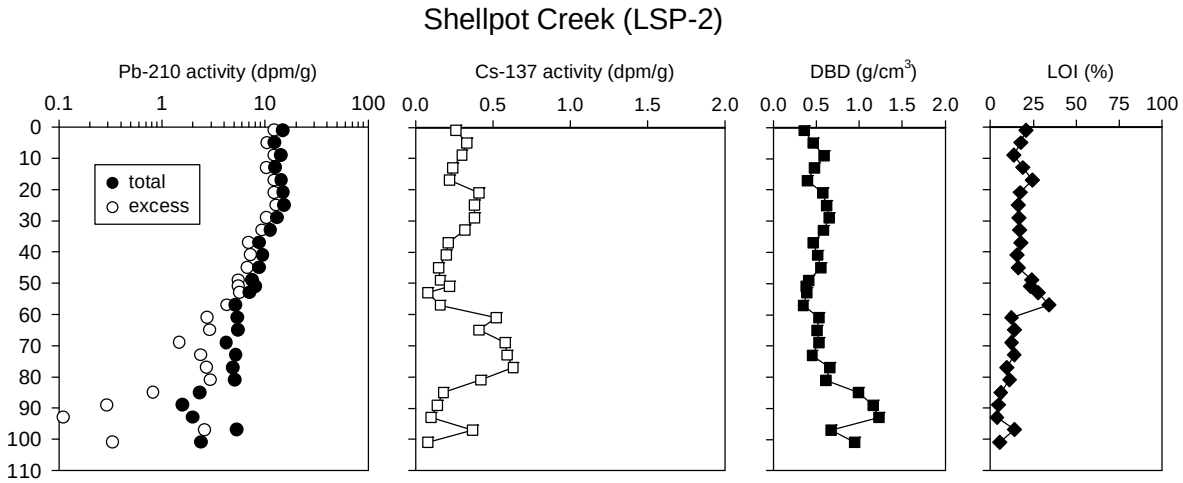

Figure 6. . Geochronology for the Shellpot Creek using excess ^{210}Pb and transient fallout ^{137}Cs. The radionuclides give identical sedimentation rates of 0.19 cm/yr using the constant flux model for ^{210}Pb. The first occurrence of ^{137}Cs at 100-102 cm is assumed concordant with ca. 1954.

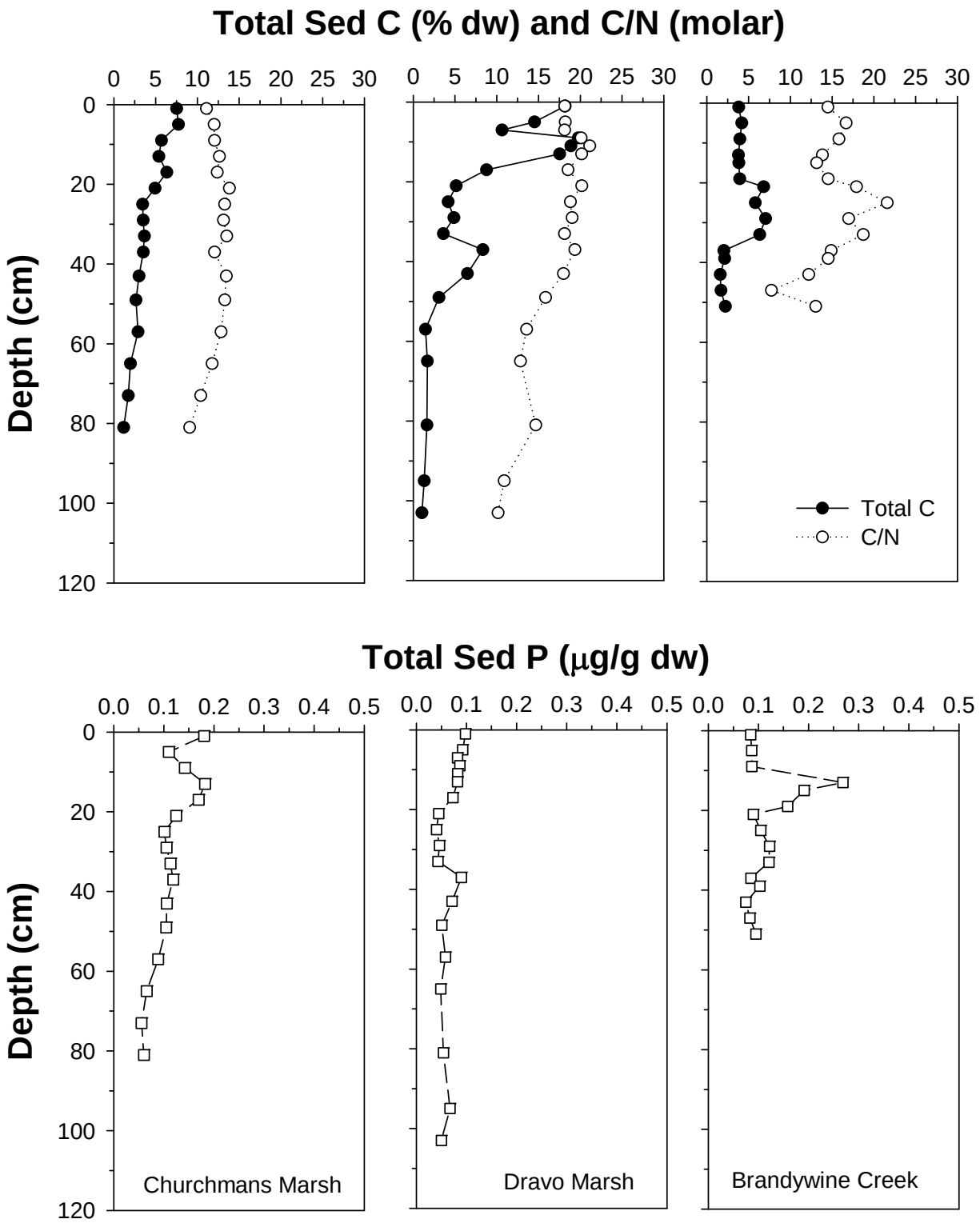

Figure 7a. Sediment organic carbon, C/N and sediment phosphorus distribution with depth for Churchmans, Dravo and Brandywine marshes.

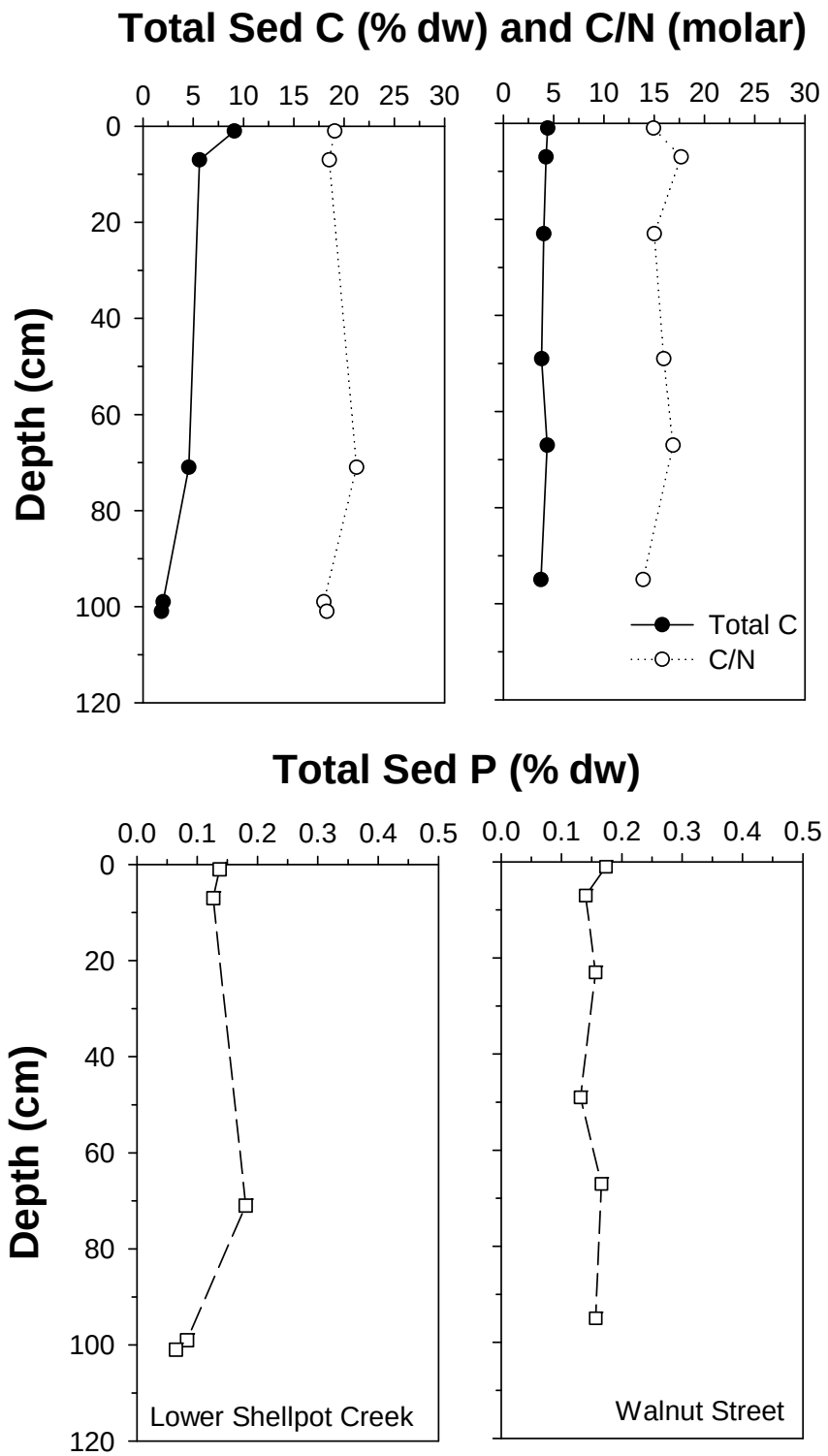

Figure 7b. Sediment organic carbon, C/N and sediment phosphorus distribution with depth for the cores from lower Shellpot Creek and Walnut Street Bridge.

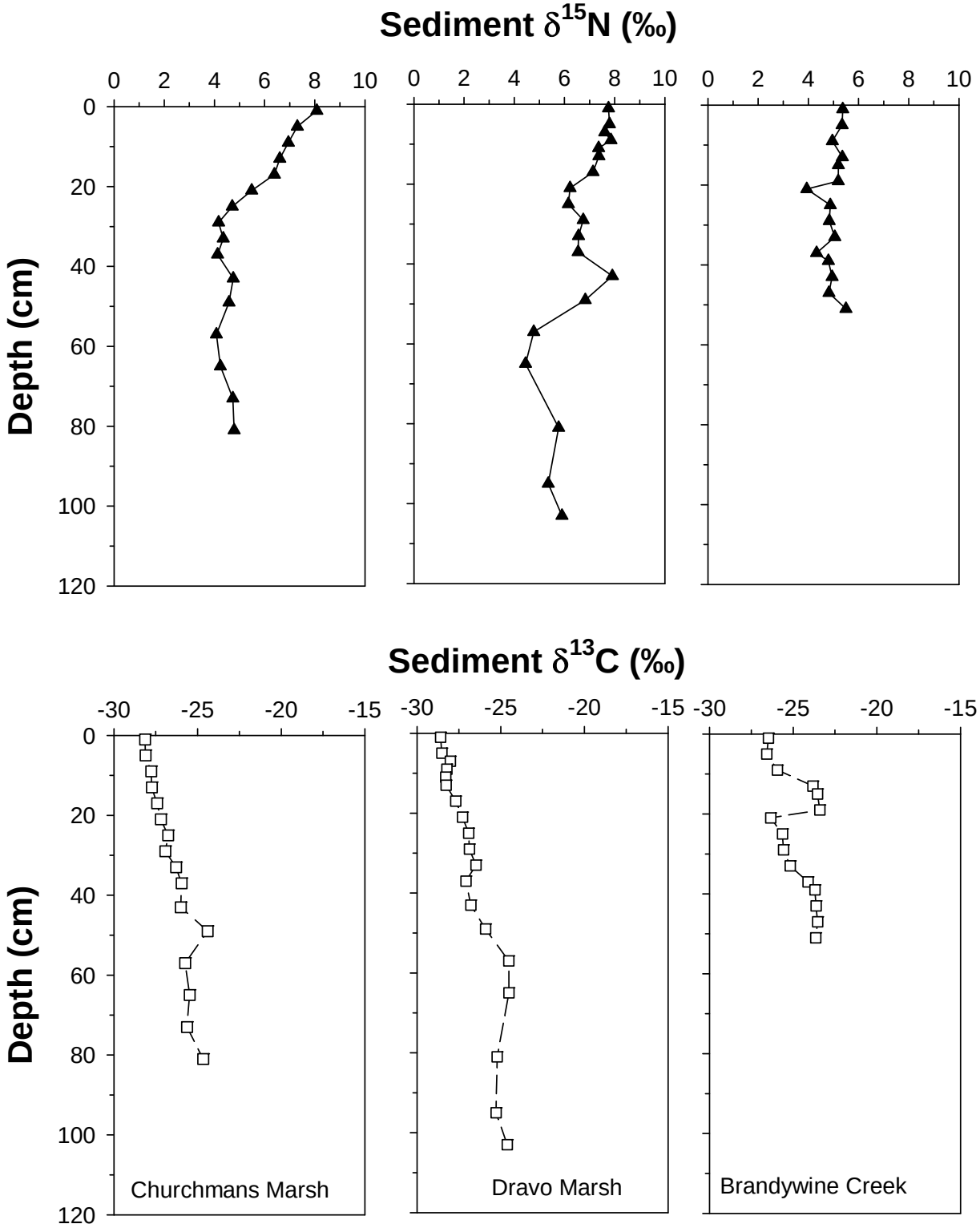

Figure 8. Depth distribution of the isotopic composition sediment N ($\delta^{15}N$) and C ($\delta^{13}C$).

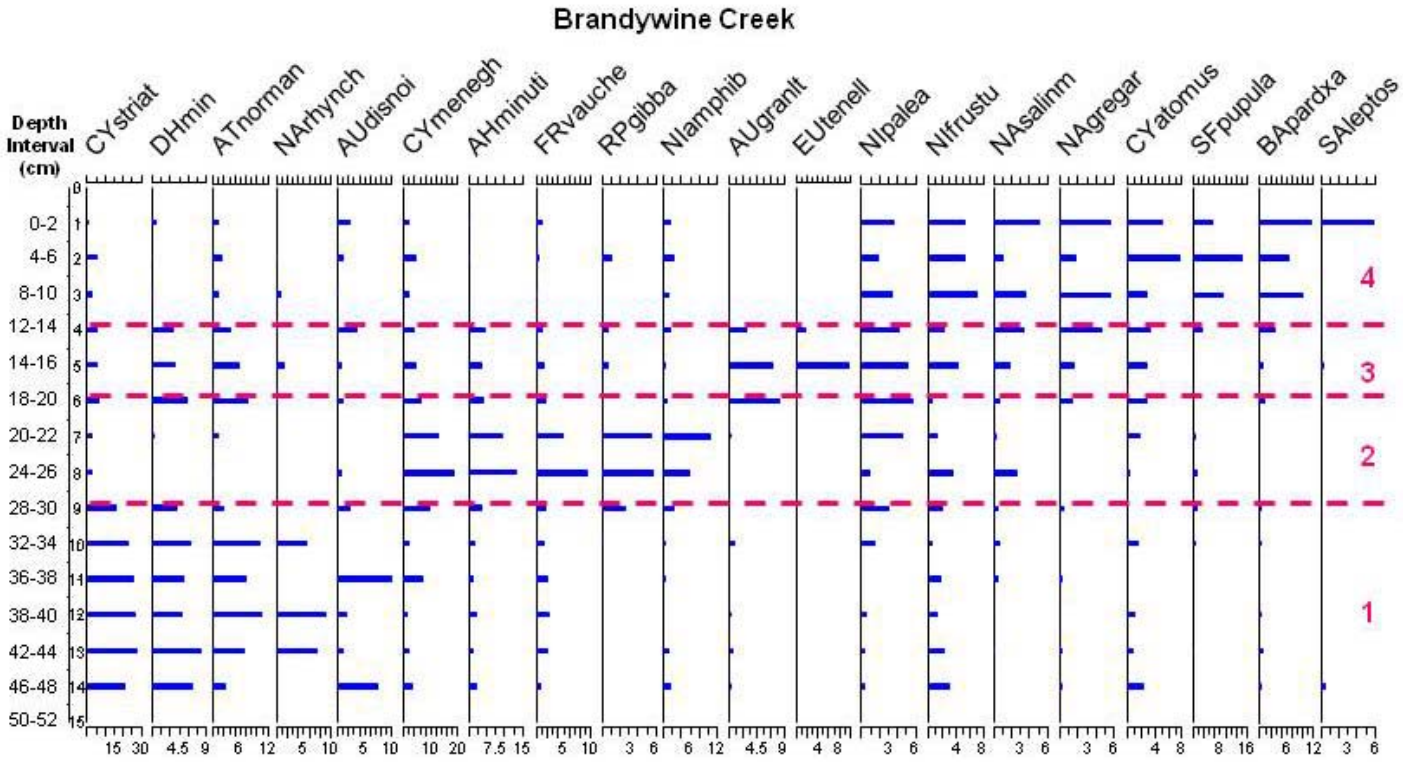

Figure 9a. Distribution of various diatom indicator species with depth in the Brandywine Creek Core.

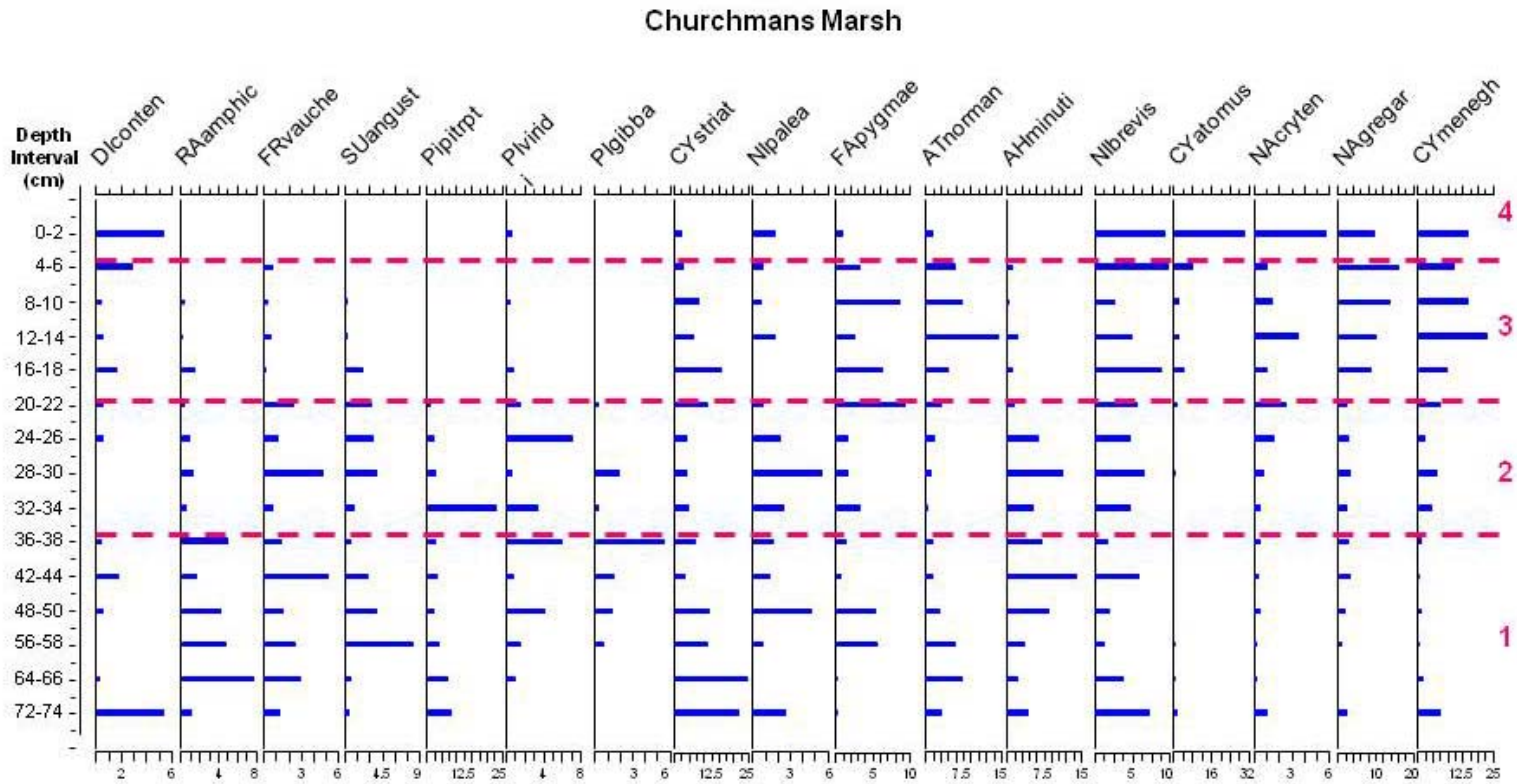

Figure 9b. Distribution of various diatom indicator species with depth in the Churchmans Marsh core.

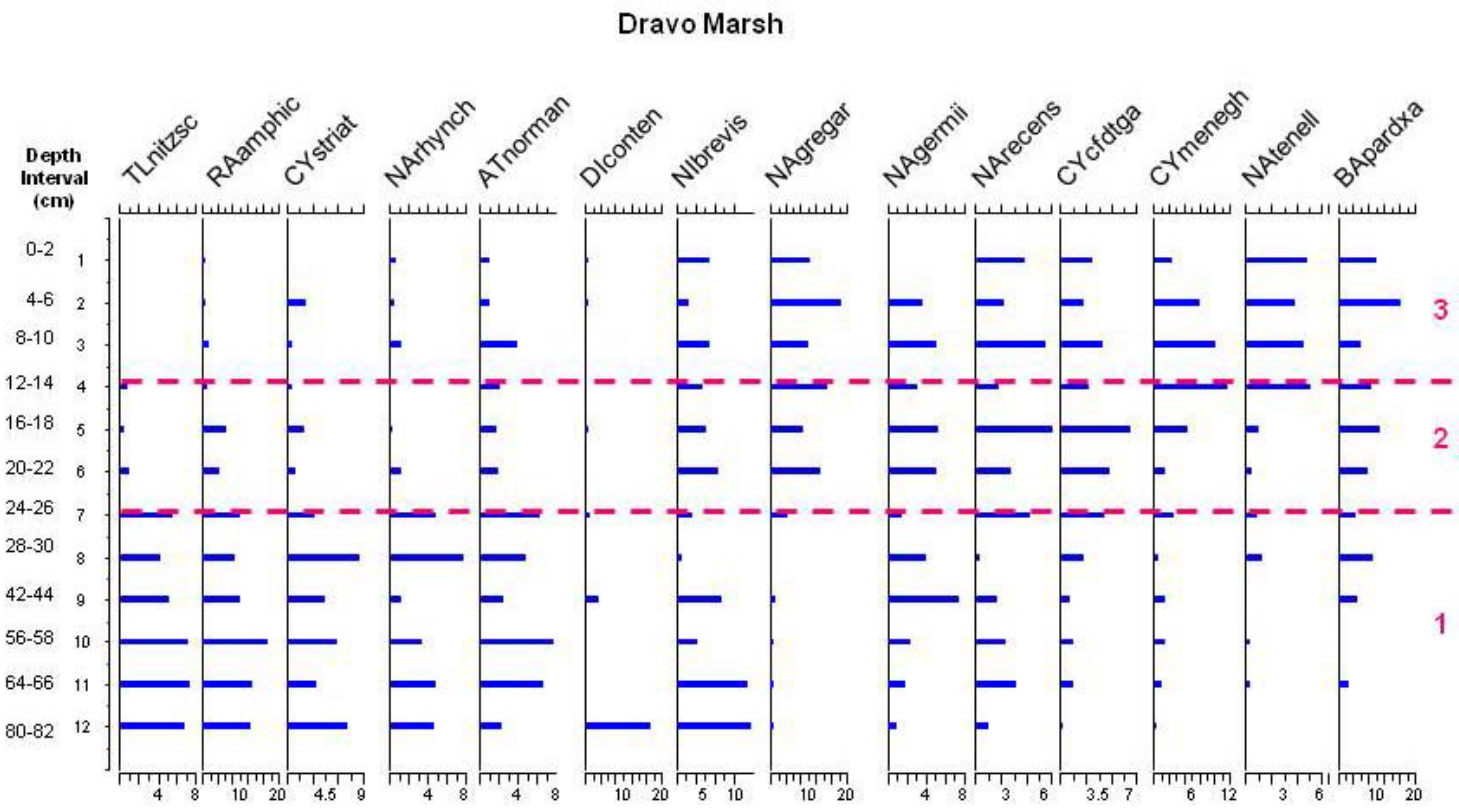

Figure 9c. Distribution of various diatom indicator species with depth in the Dravo Marsh core.

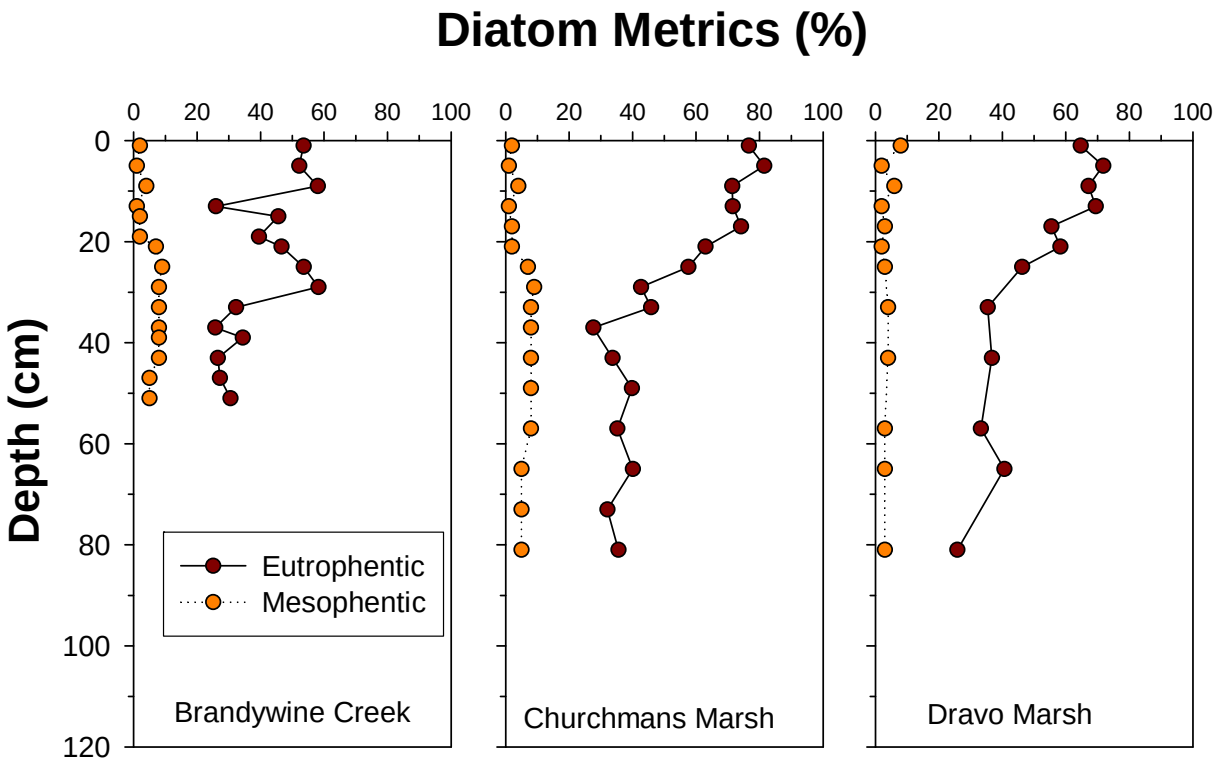

Figure 10. Diatom metrics for the cores of the tidal Christina River using the van Dam et al. (1994).

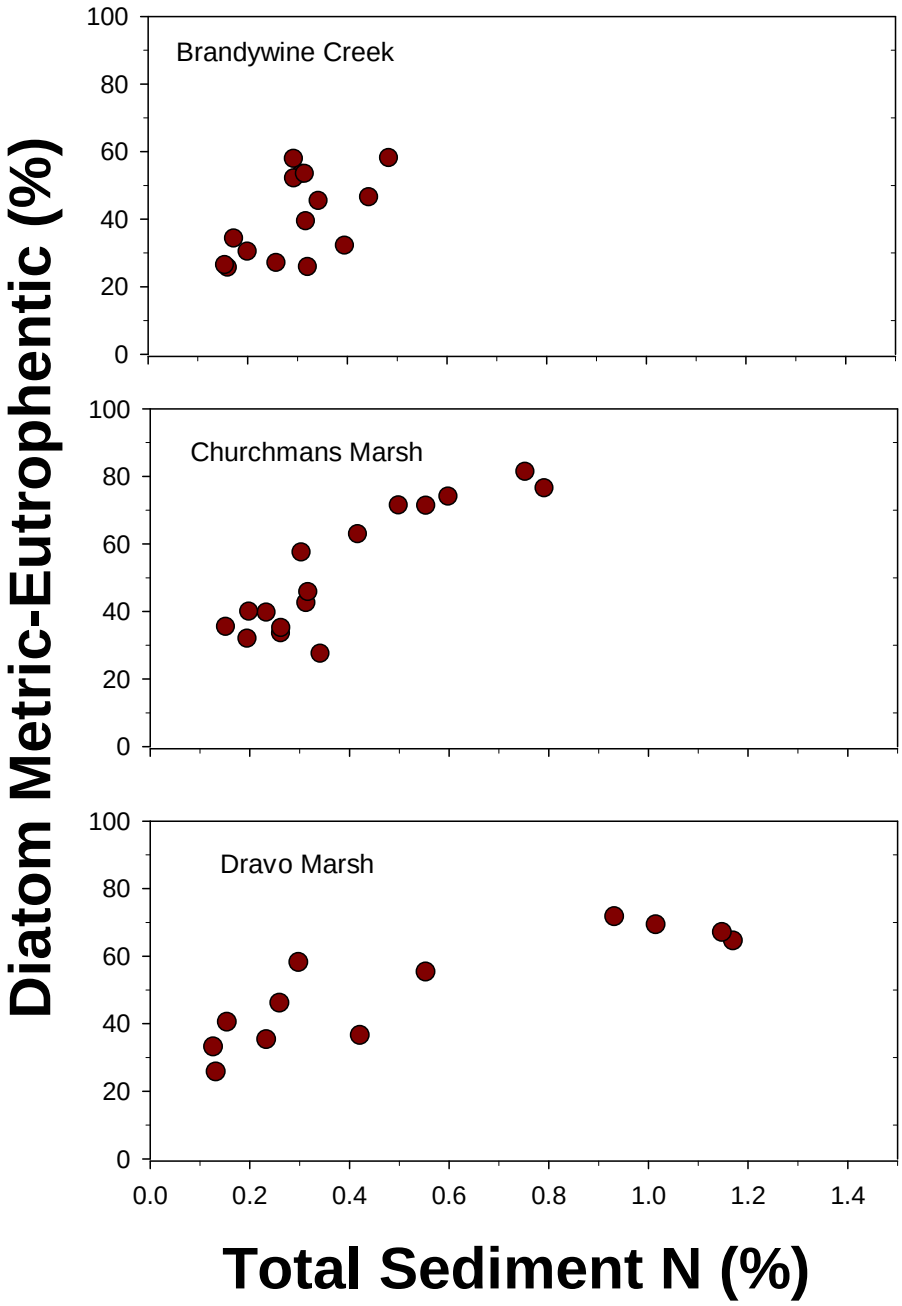

Figure 11. Relationship between total sediment N and the diatom metric for eutrophentic species in each core.

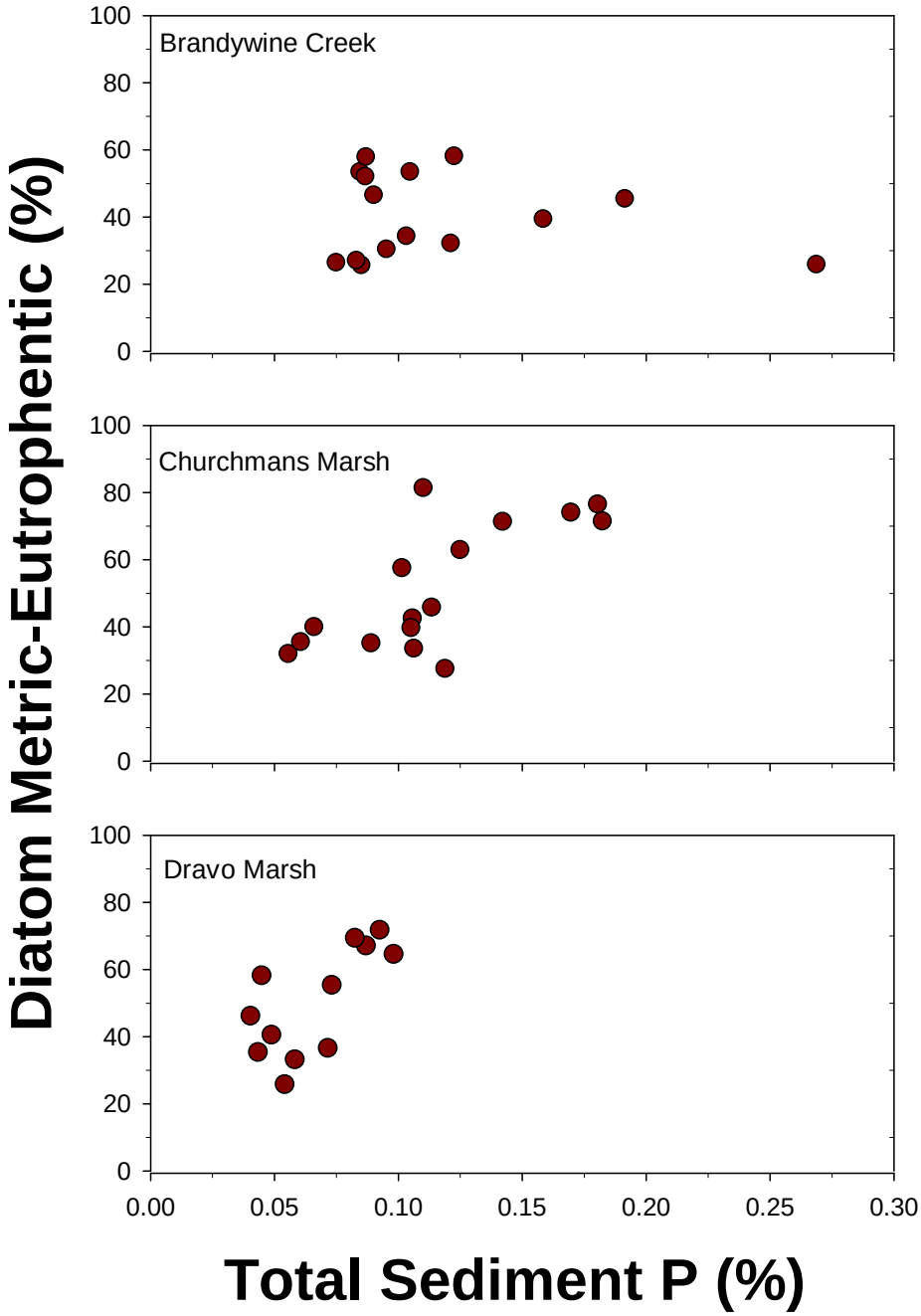

Figure 12. Relationship between total sediment P and the diatom metric for eutrophentic species in each core.

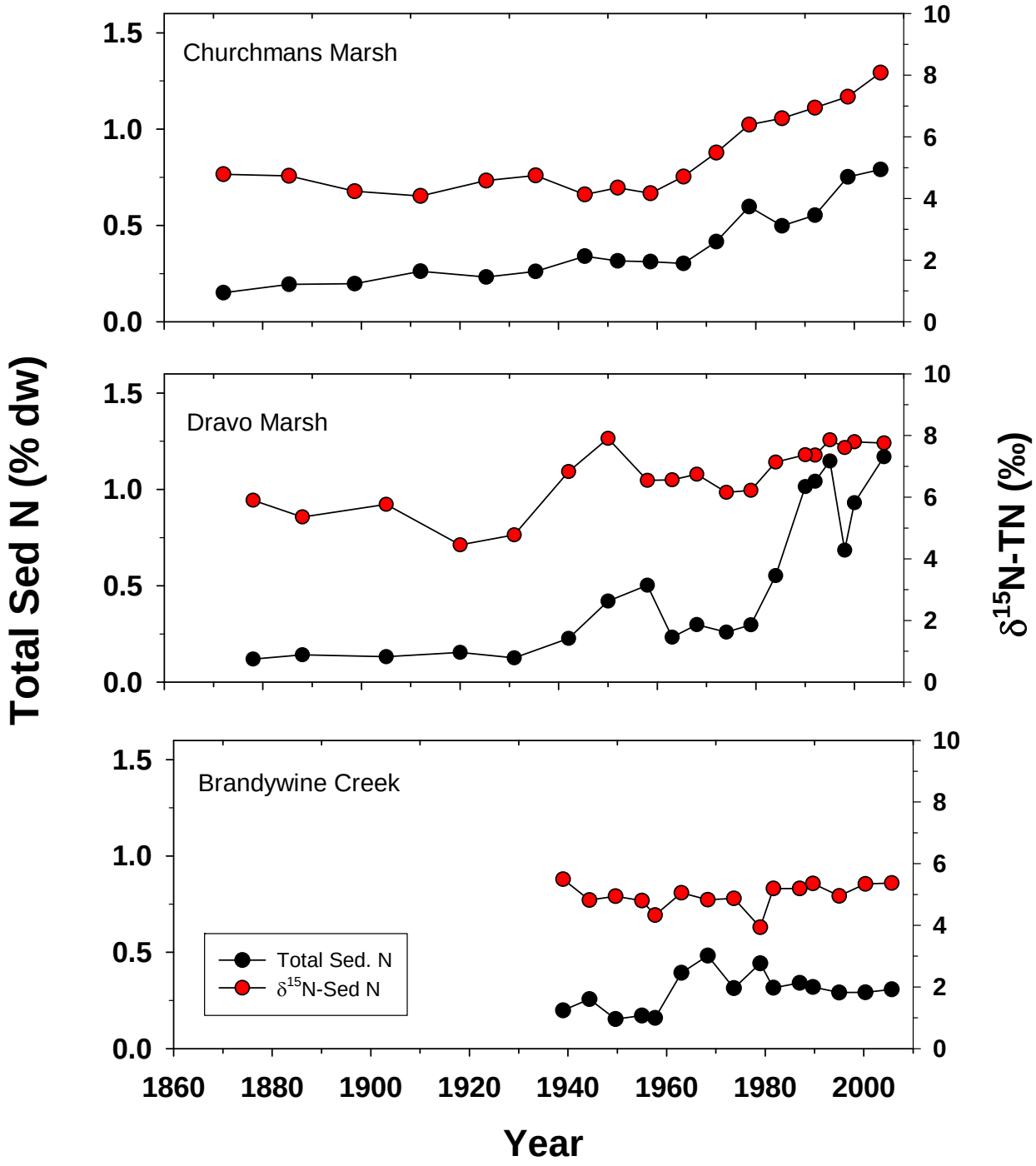

Figure 13. Concentrations of total sediment nitrogen (TN) and the nitrogen isotopic composition of TN (δ^{15}N-TN) from 1860 to 2003.

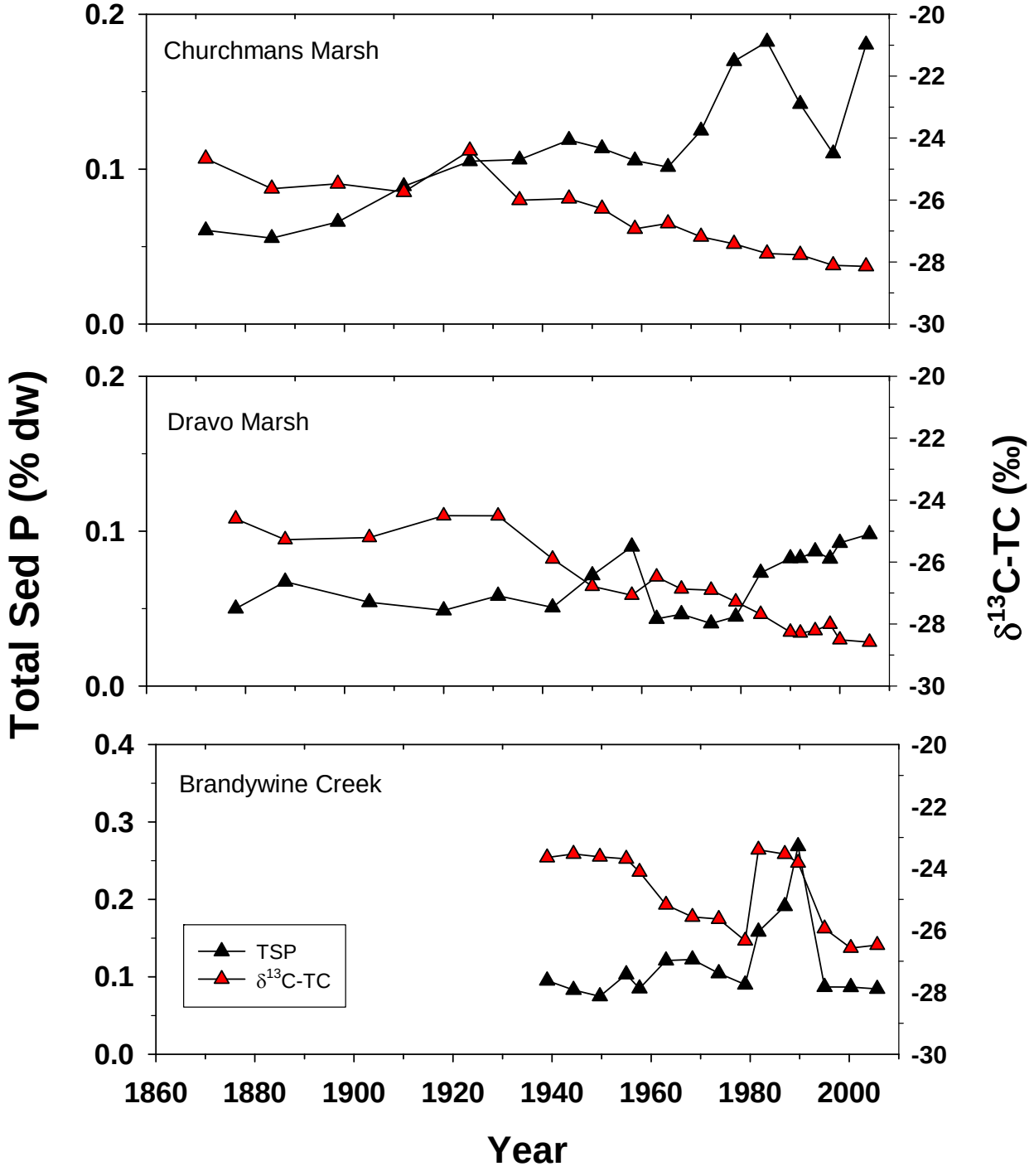

Figure 14. Concentrations of total sediment phosphorus (TSP) and the carbon isotopic composition of total carbon (δ^{13}C-TC) from 1860 to 2003.

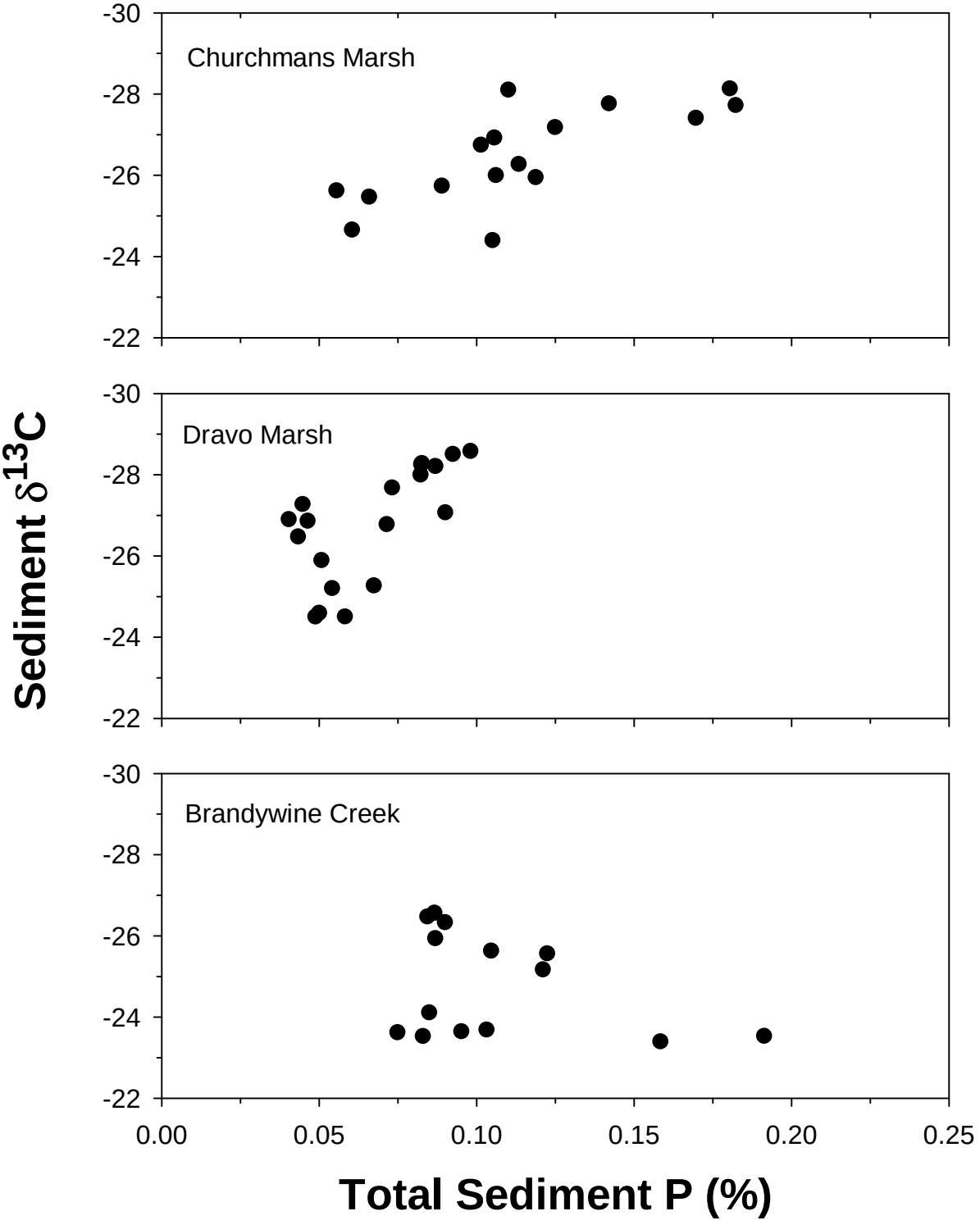

Figure 15. The relationship between total sediment P (TSP) and the carbon isotopic composition of organic matter (δ^{13}C-TC) in Brandywine Creek, Churchmans Marsh, and Dravo Marsh.

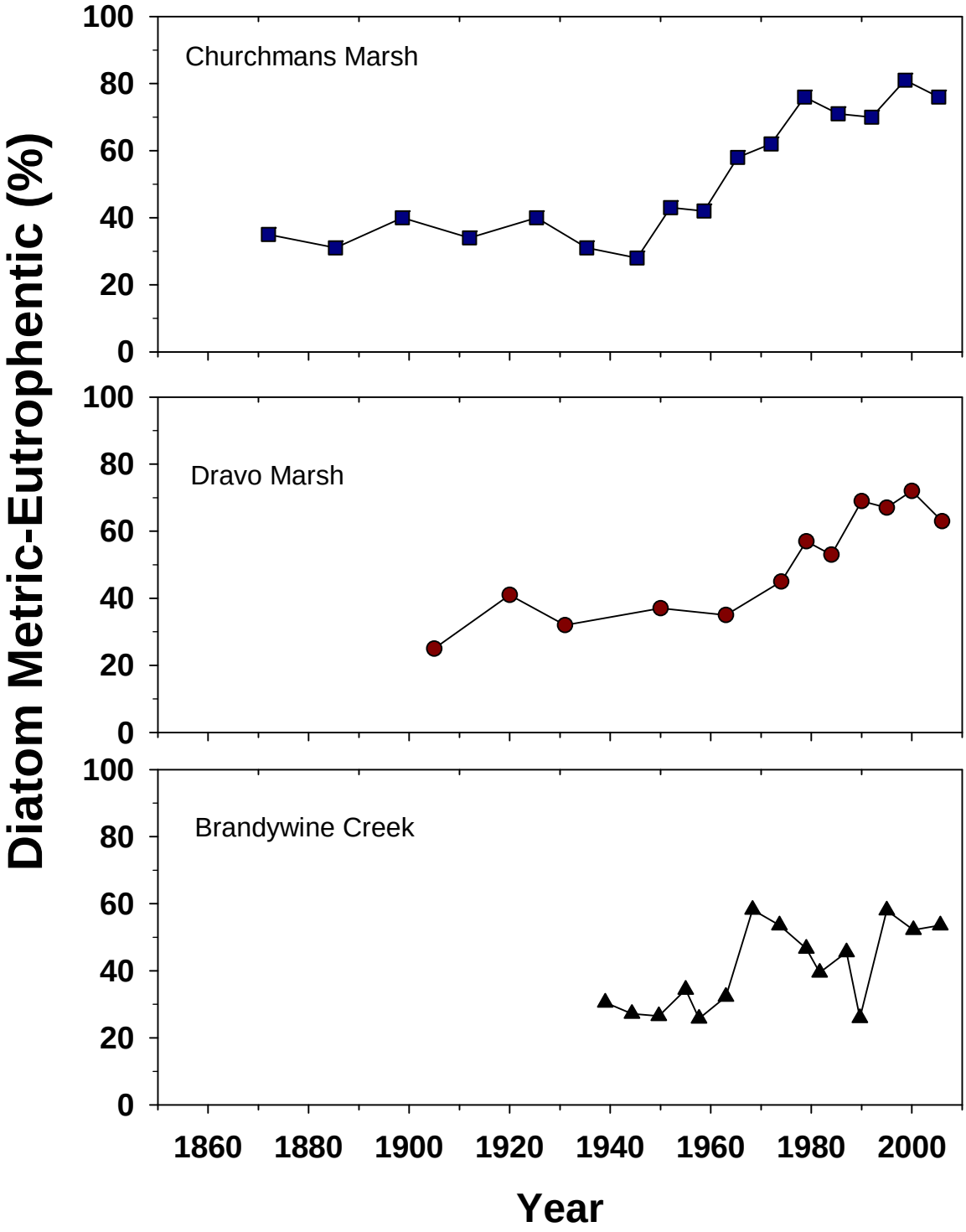

Figure 16. Diatom metric for eutrophentic species from 1860 to 2003.

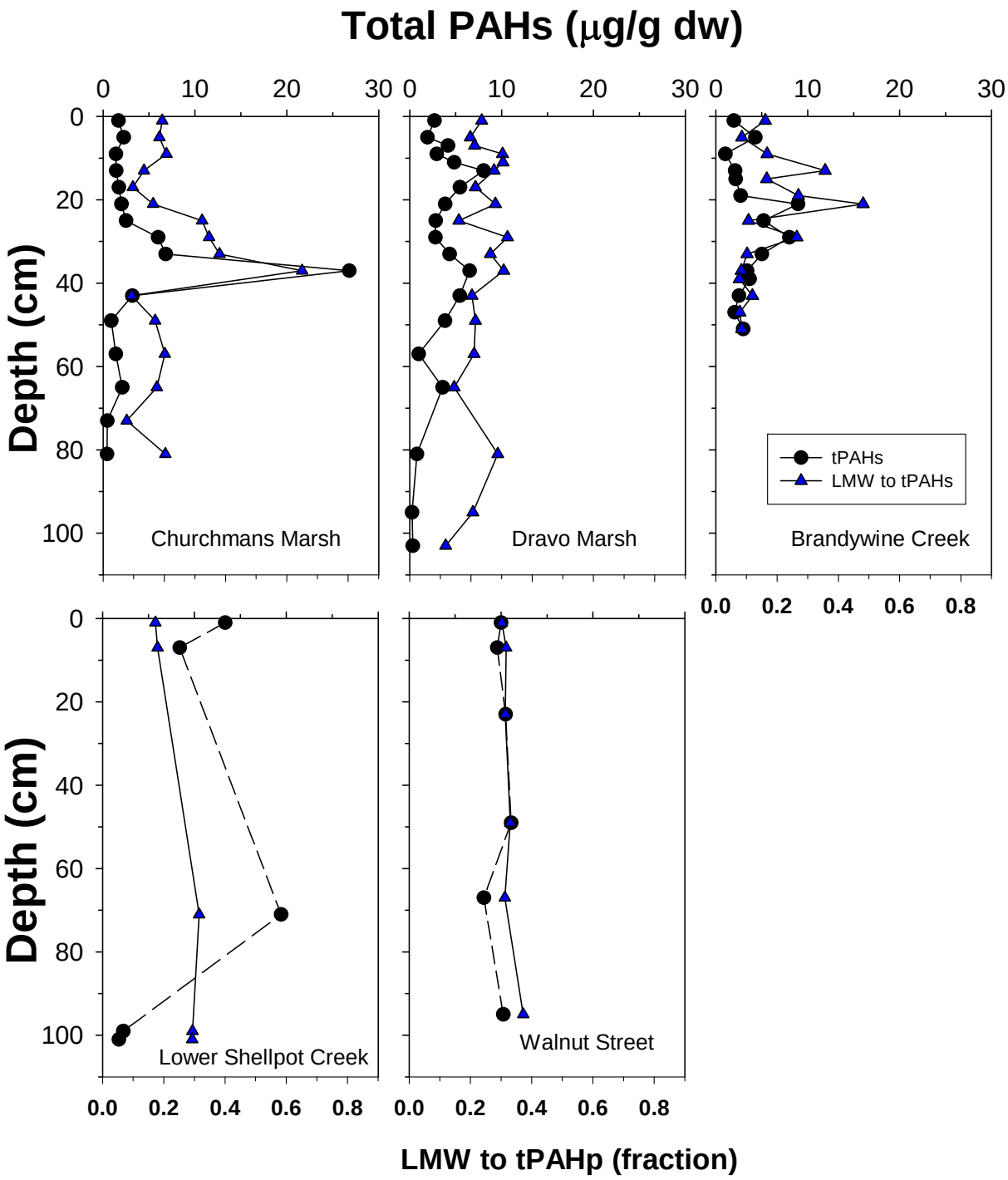

Figure 17. Depth distribution of total polycyclic aromatic hydrocarbons (tPAHs) and the low molecular weight (LMW) to tPAHs in the sediments of the tidal Christina River and Brandywine Creek.

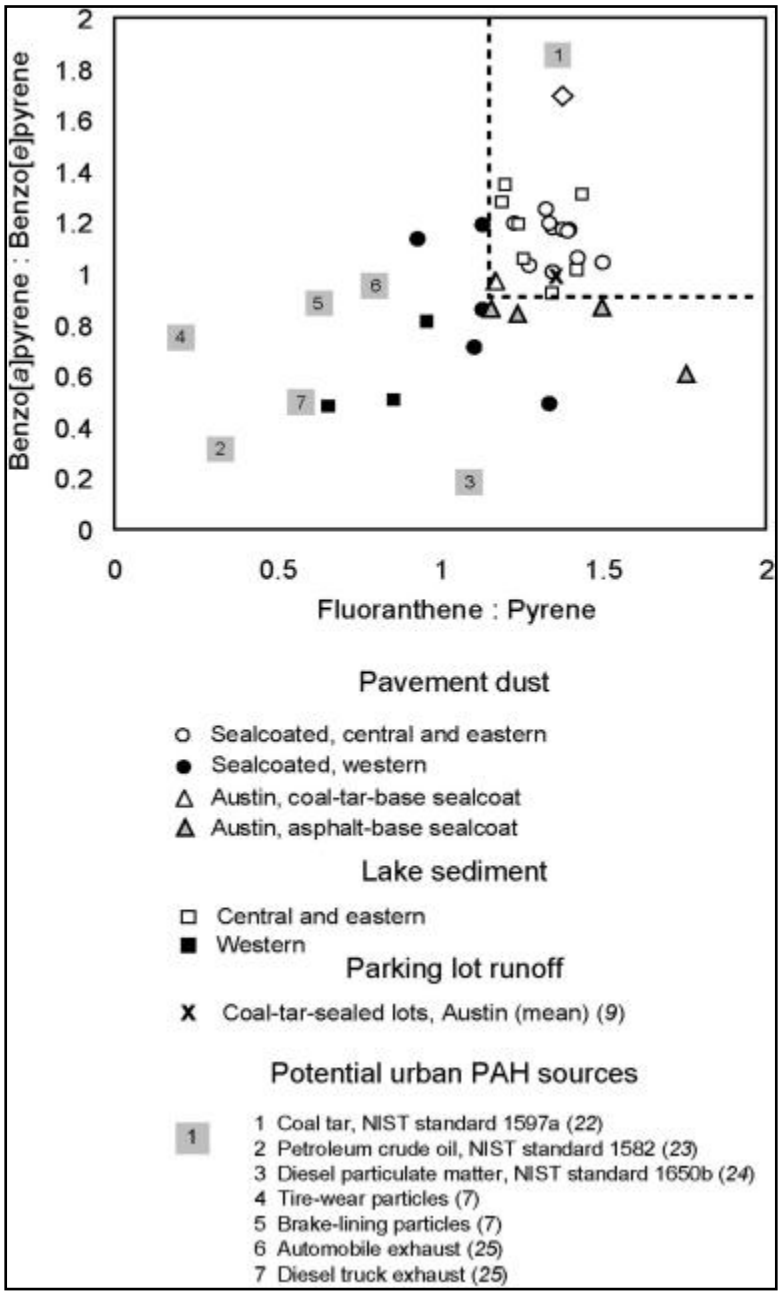

Figure 18. Adapted from Van Metre et al (2009). Comparison of source-indicator ratios of benzo[a]pyrene to benzo[e]pyrene and fluoranthene to pyrene in dust samples, lake samples and seal-coat samples from central and eastern cities (USA). Dashed line indicates approximate separation between samples from central and eastern cities and those from western cities.

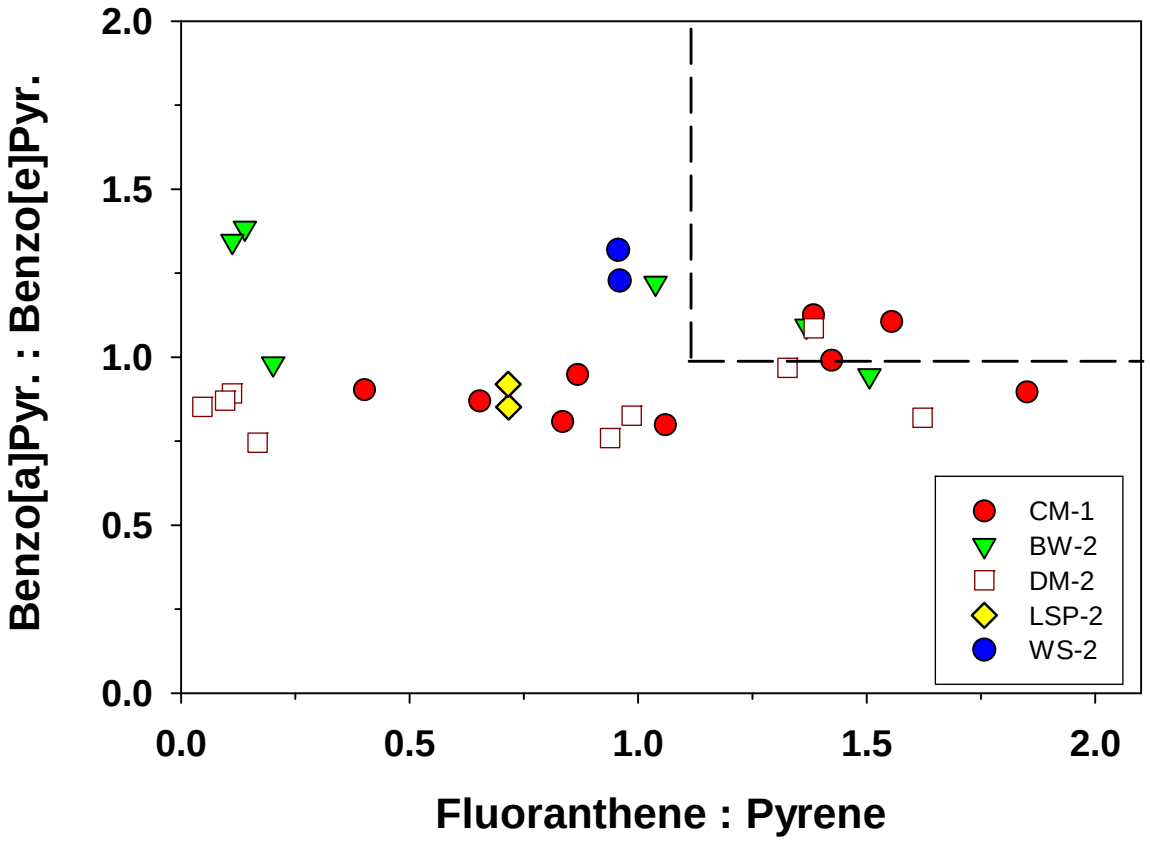

Figure 19. Indicator ratios of benzo[a]pyrene to benzo[e]pyrene and fluoranthene to pyrene in the top sections of all sediment samples collected in the tidal Christina and Brandywine watersheds. The dotted box is related to the area in the van Metre et al. (2009) that suggests high coal tar sealants for parking lots.

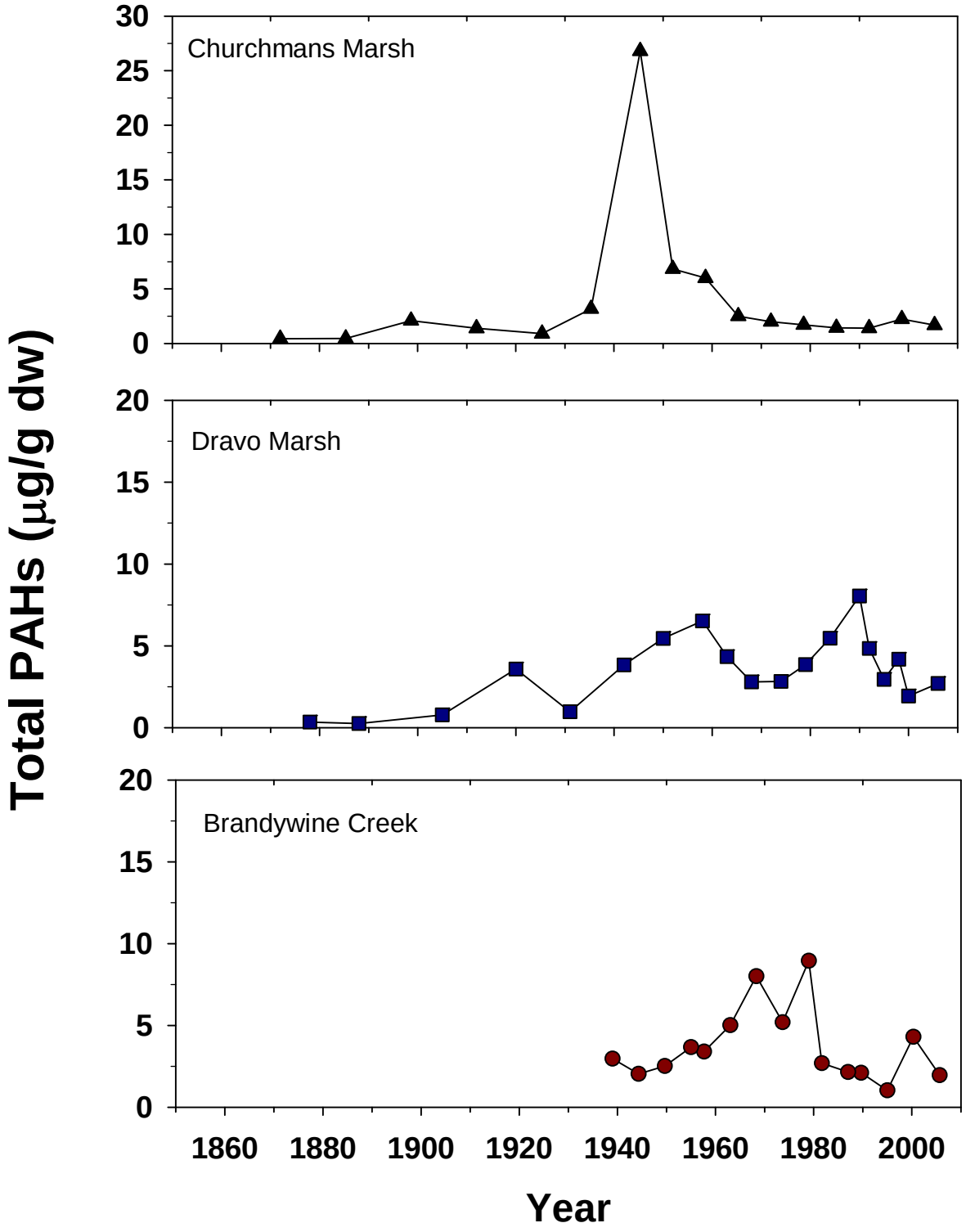

Figure 20. Concentrations of tPAHs from 1860 to 2003 (Note scale change).

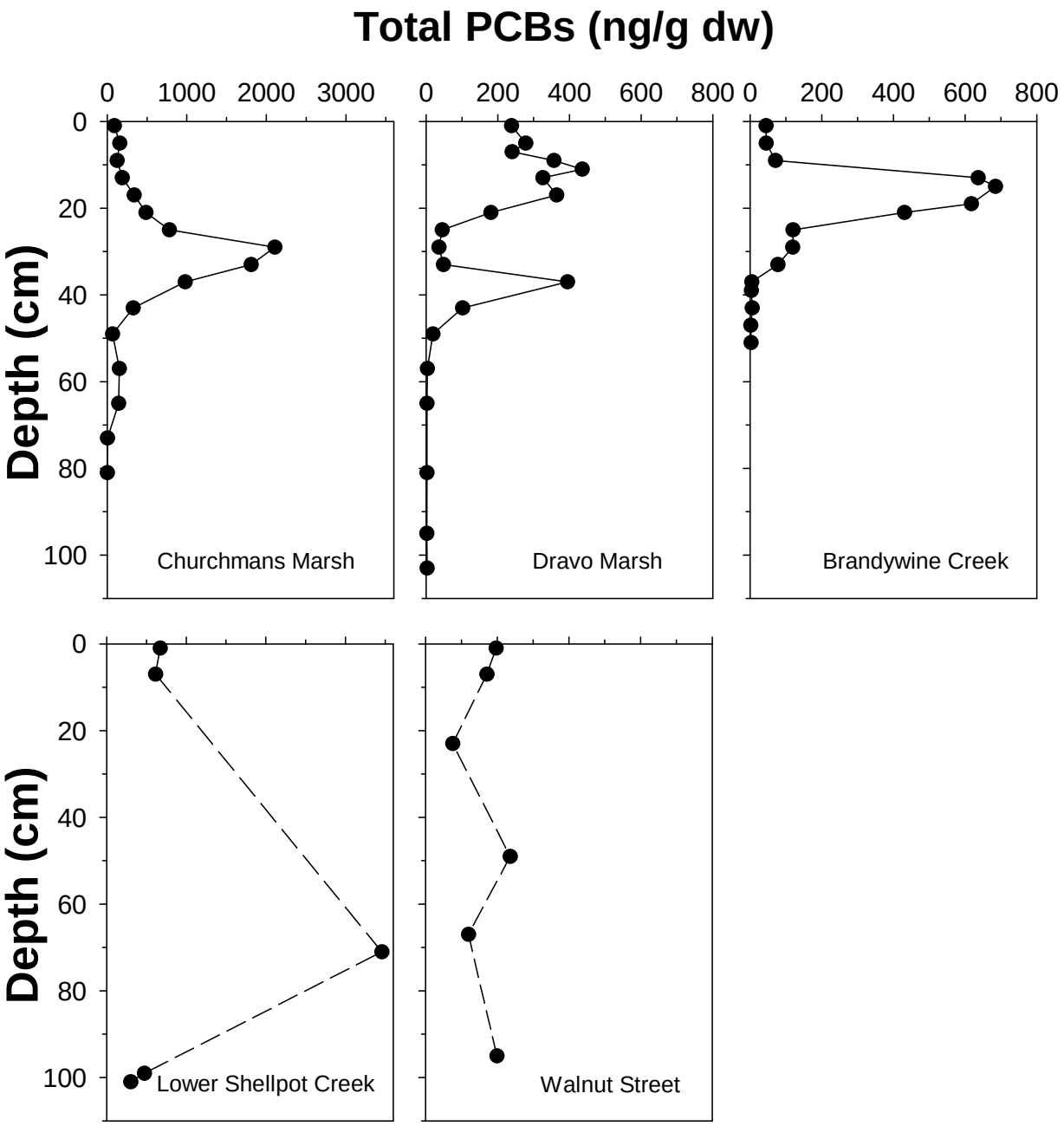

Figure 21. Depth distribution of total PCBs in the five cores in the tidal Christina River and Brandywine Creek.

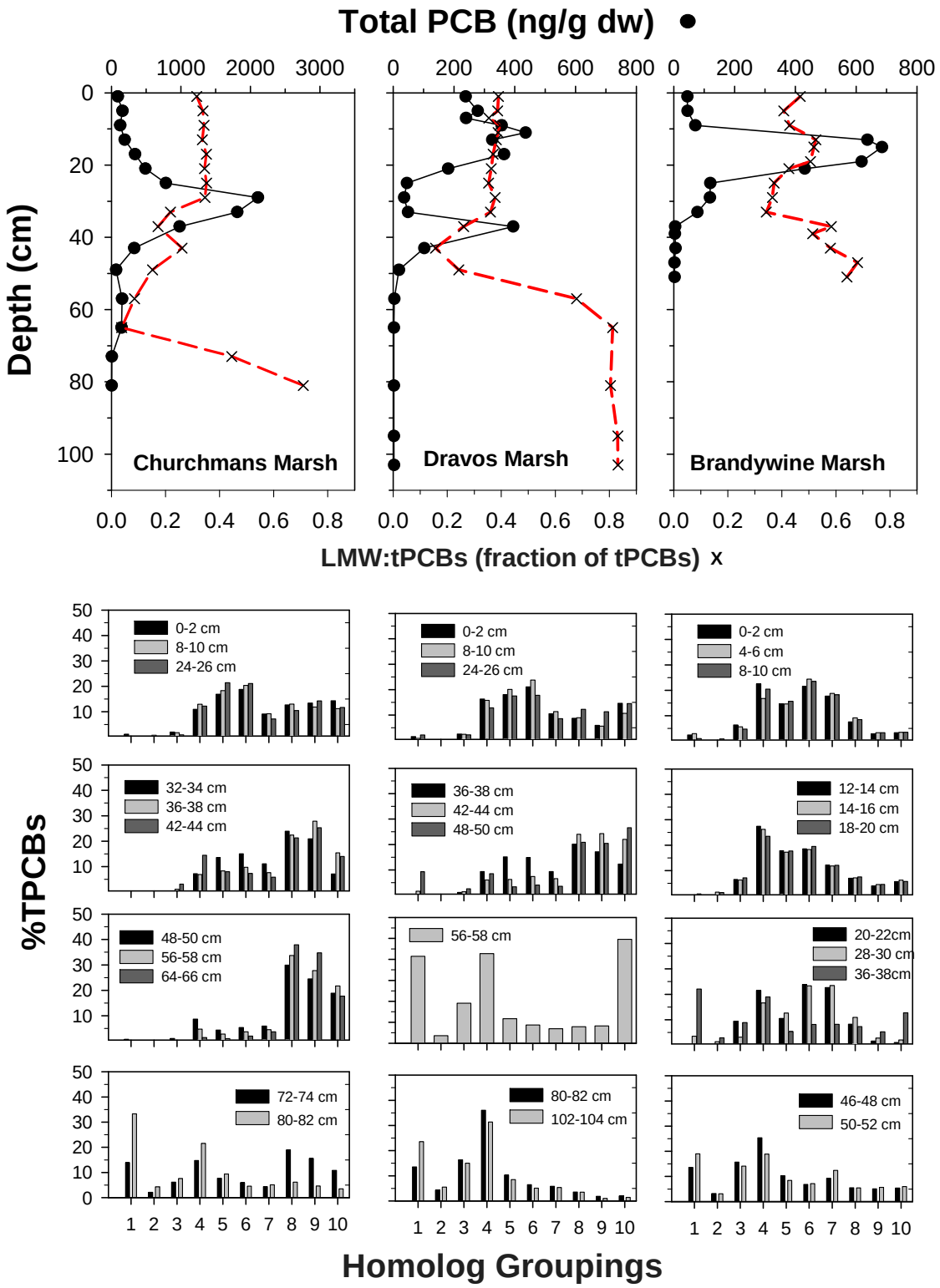

Figure 22a. Depth distribution of total PCBs, LMW to tPCBs ratio and selected homolog distributions with depth.

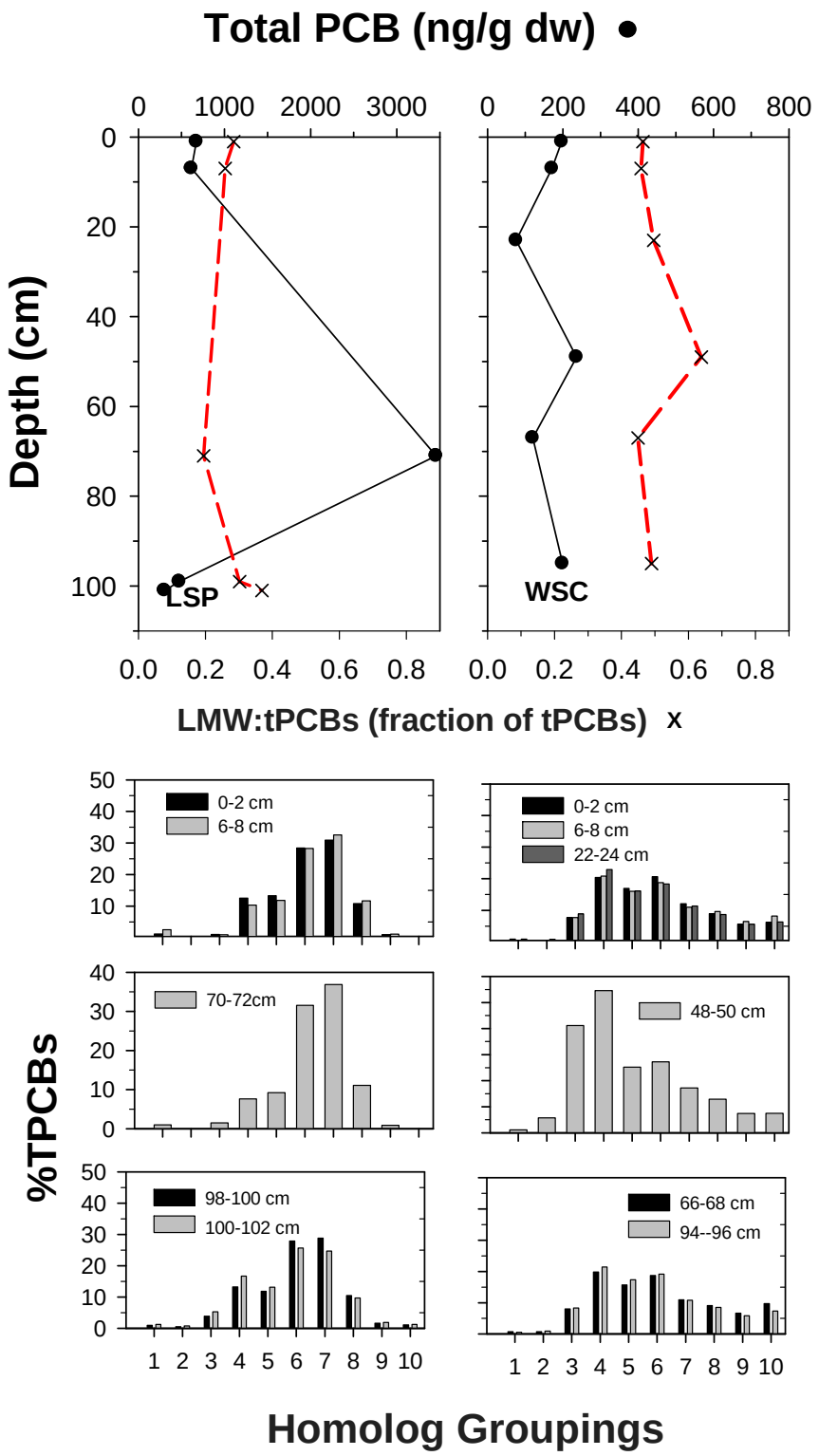

Figure 22b. Depth distribution of total PCBs, LMW to tPCBs ratio and selected homolog distributions with depth

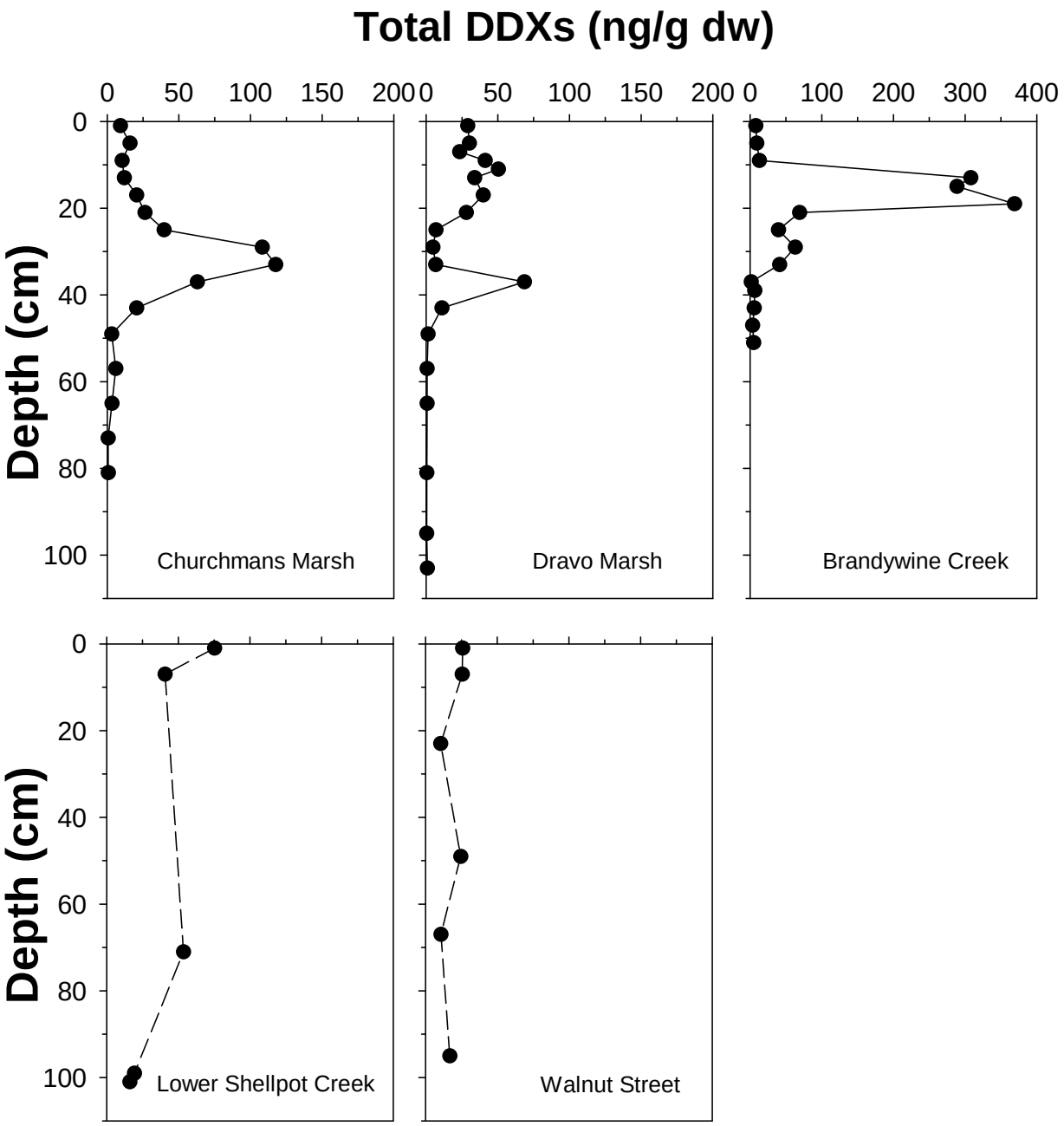

Figure 23. Total DDX (DDT+DDD+DDE all forms) with depth in the tidal Christina River and Brandywine Creek.

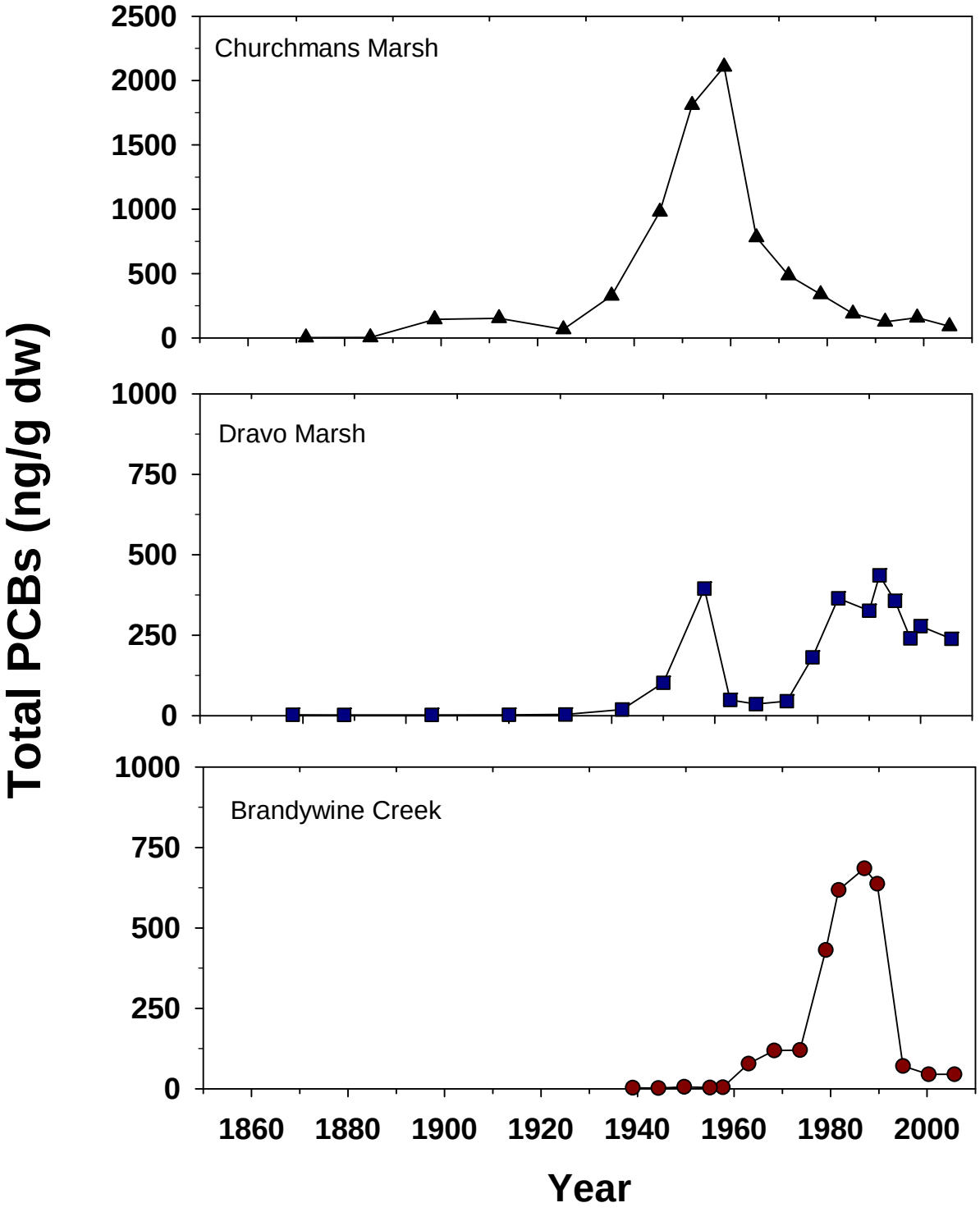

Figure 24. Concentrations of tPCBs from 1860 to 2003 (Note scale change).

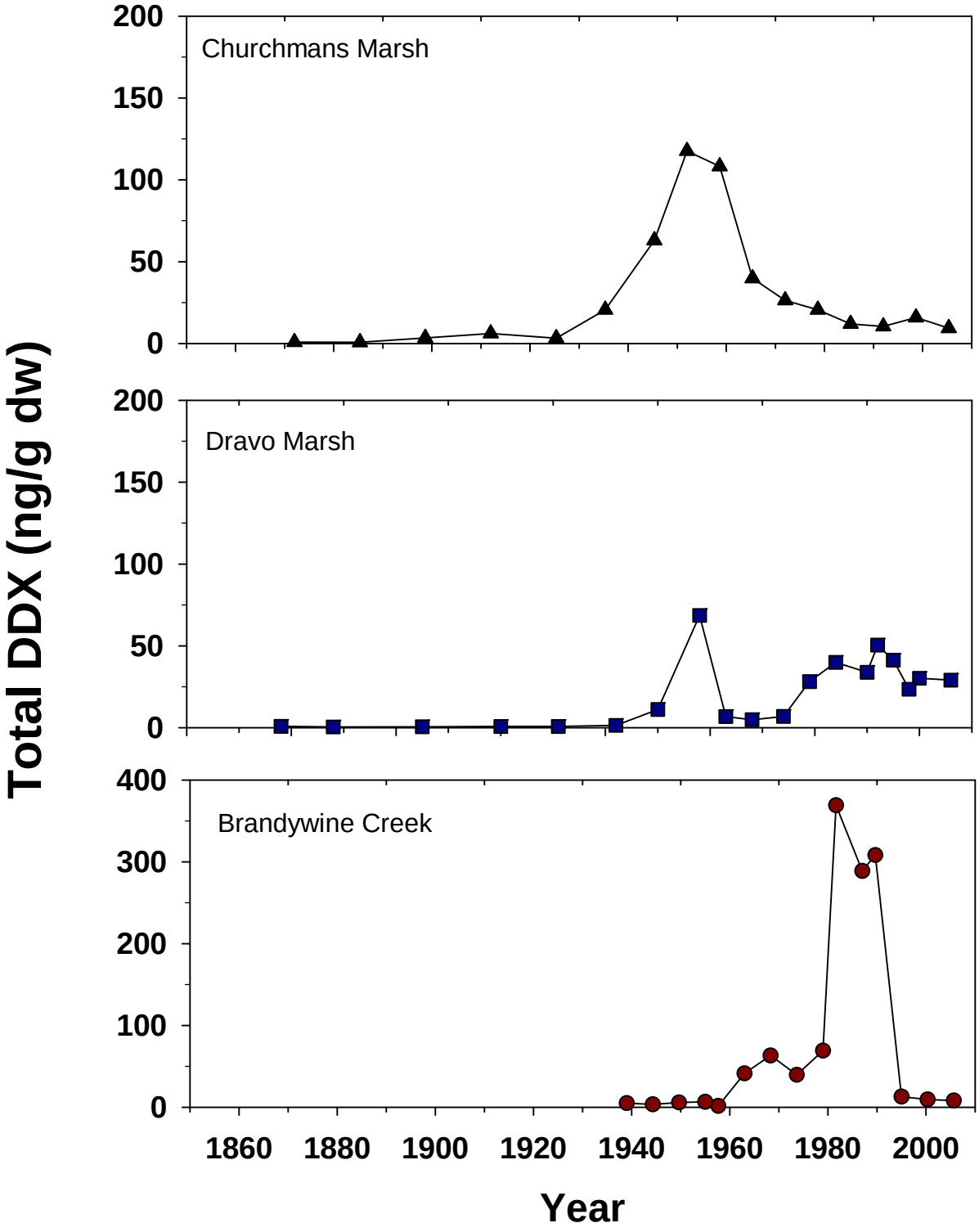

Figure 25. Concentrations of tDDXs from 1860 to 2003 (Note scale change).

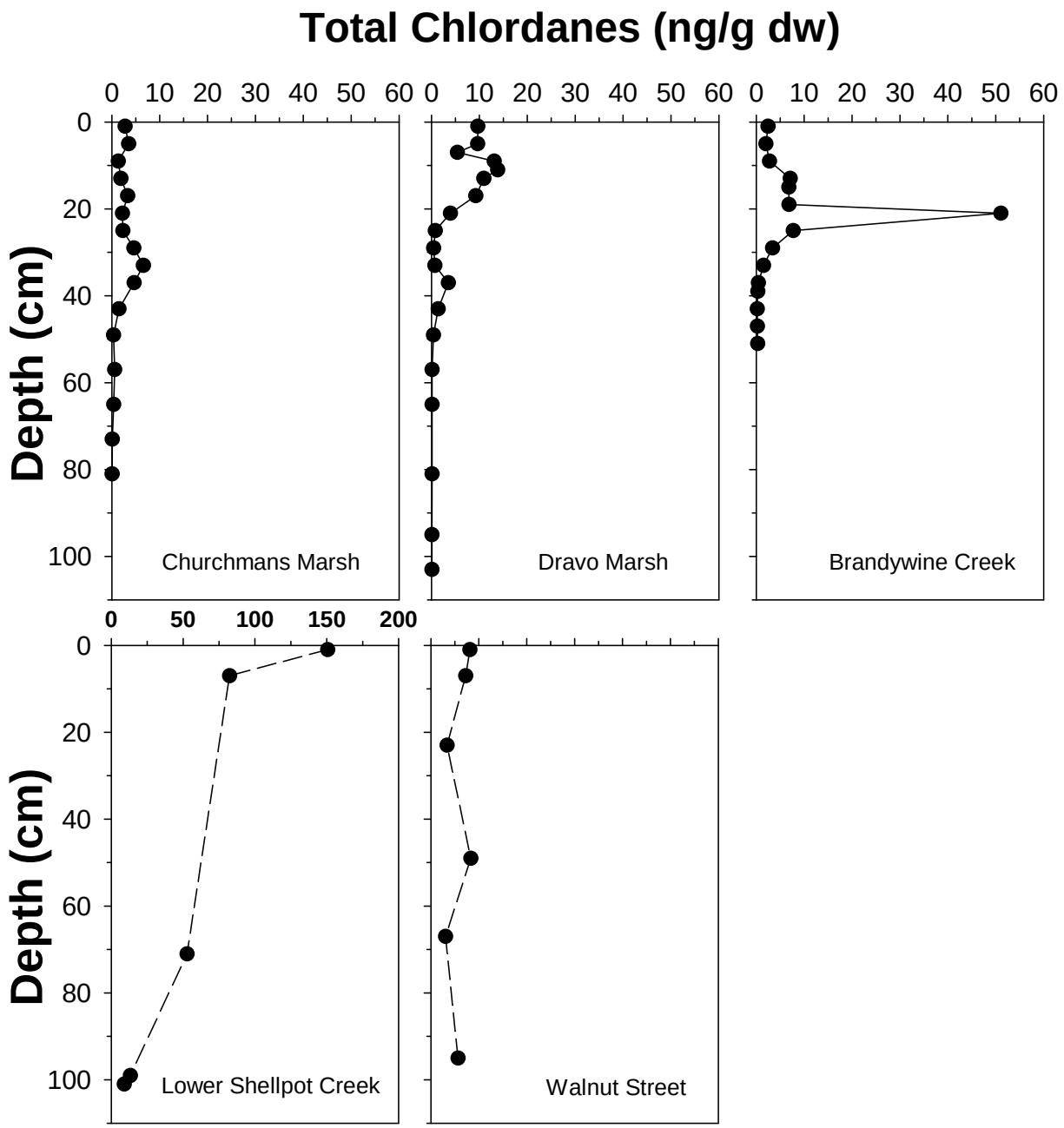

Figure 26. Total chlordane with depth in the tidal Christina River and Brandywine Creek.

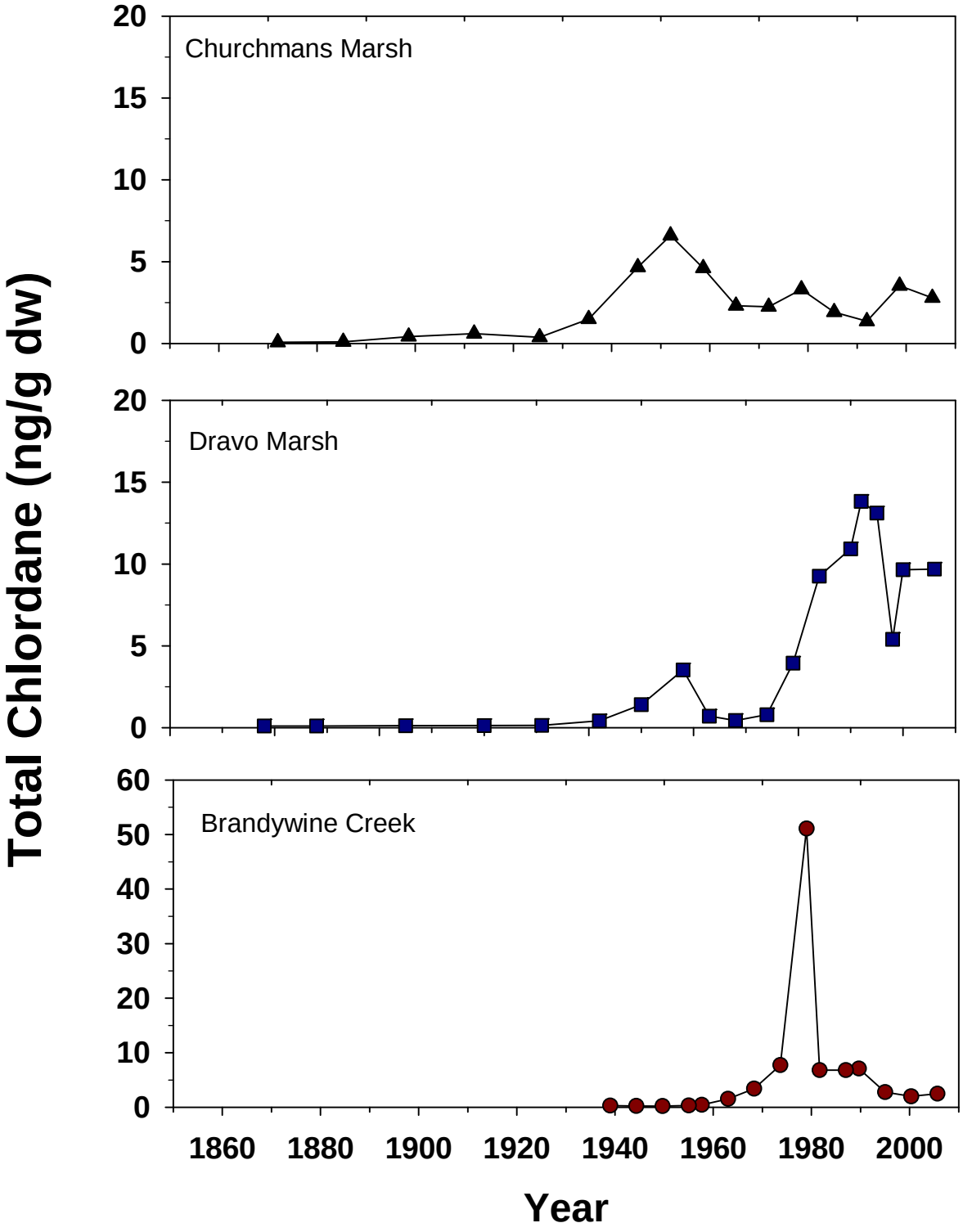

Figure 27. Concentrations of total chlordane from 1860 to 2003 (Note scale change).

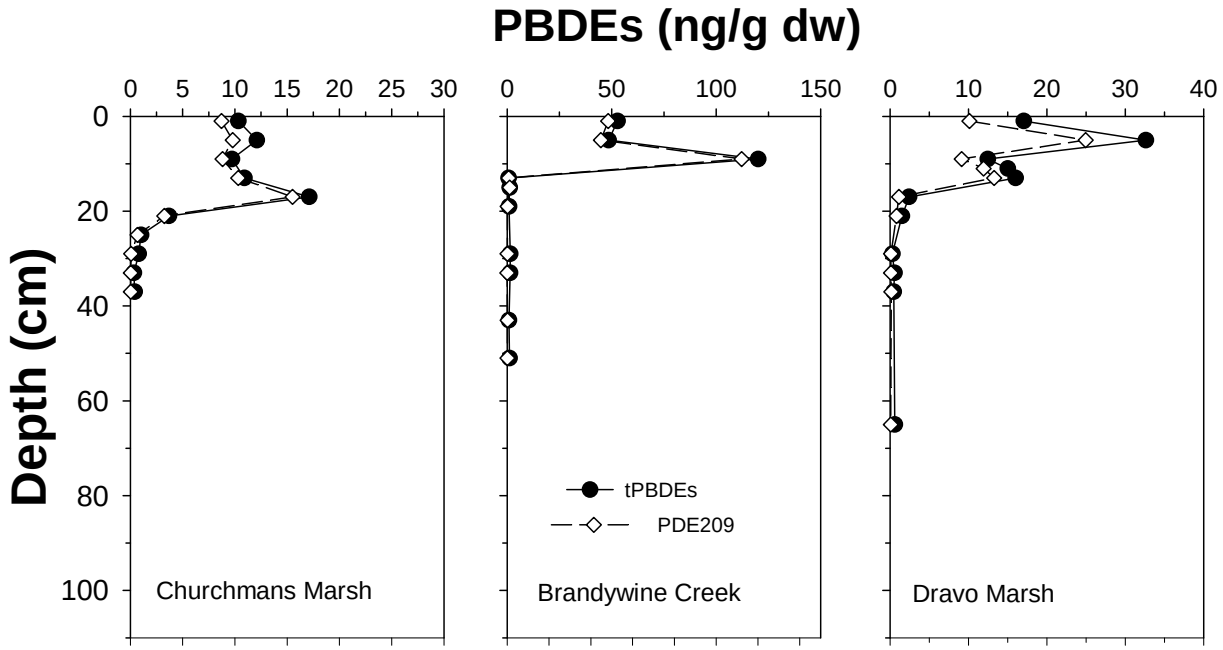

Figure 28. Total PBDEs and the deca congener BDE-209 with depth in the tidal Christina River and Brandywine Creek.

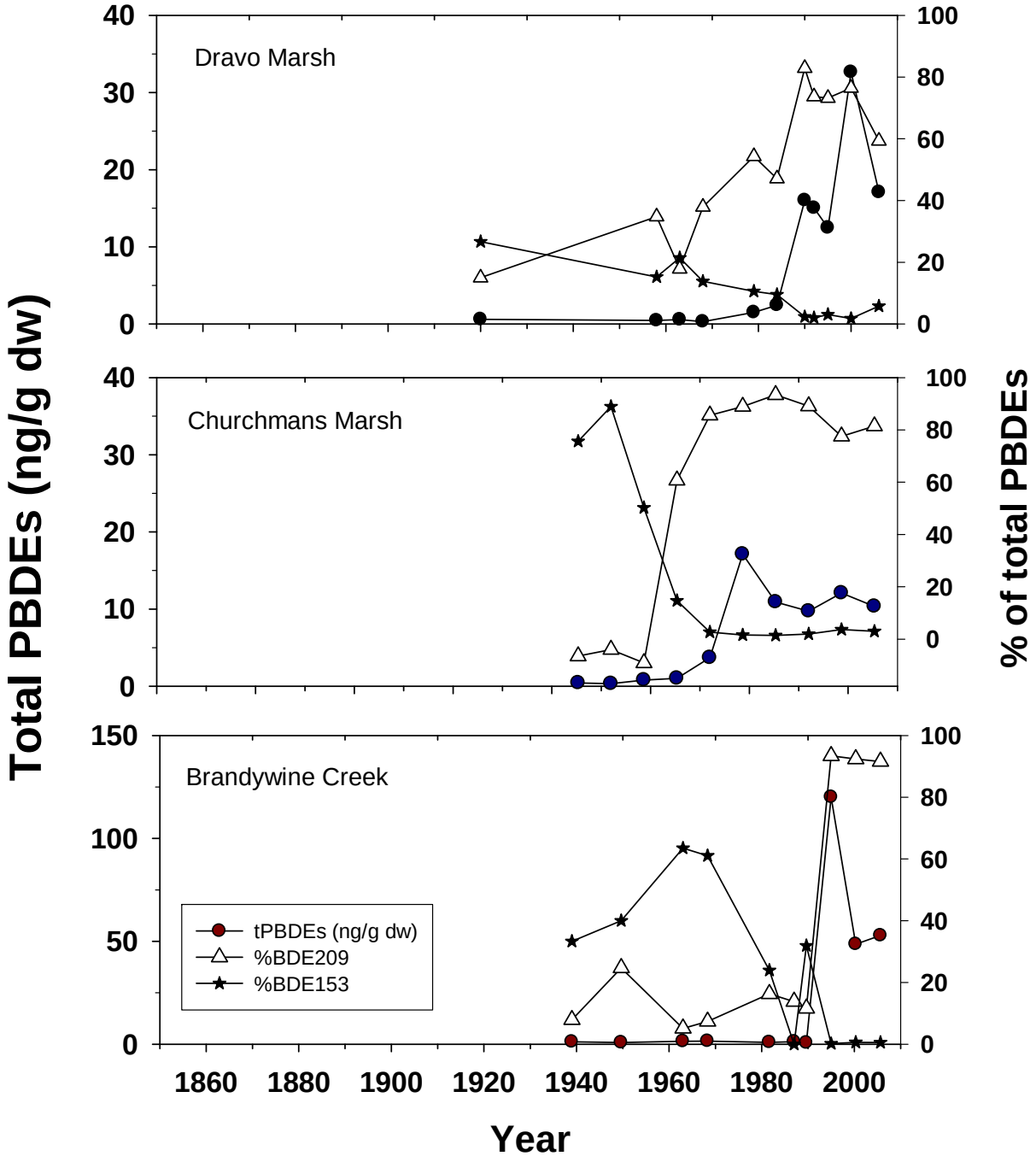

Figure 29. Concentrations of tPBDEs from 1860 to 2003. The circle is for tPBDEs, the triangle is for the percentage of BDE209 and the star is the percentage of BDE 153.

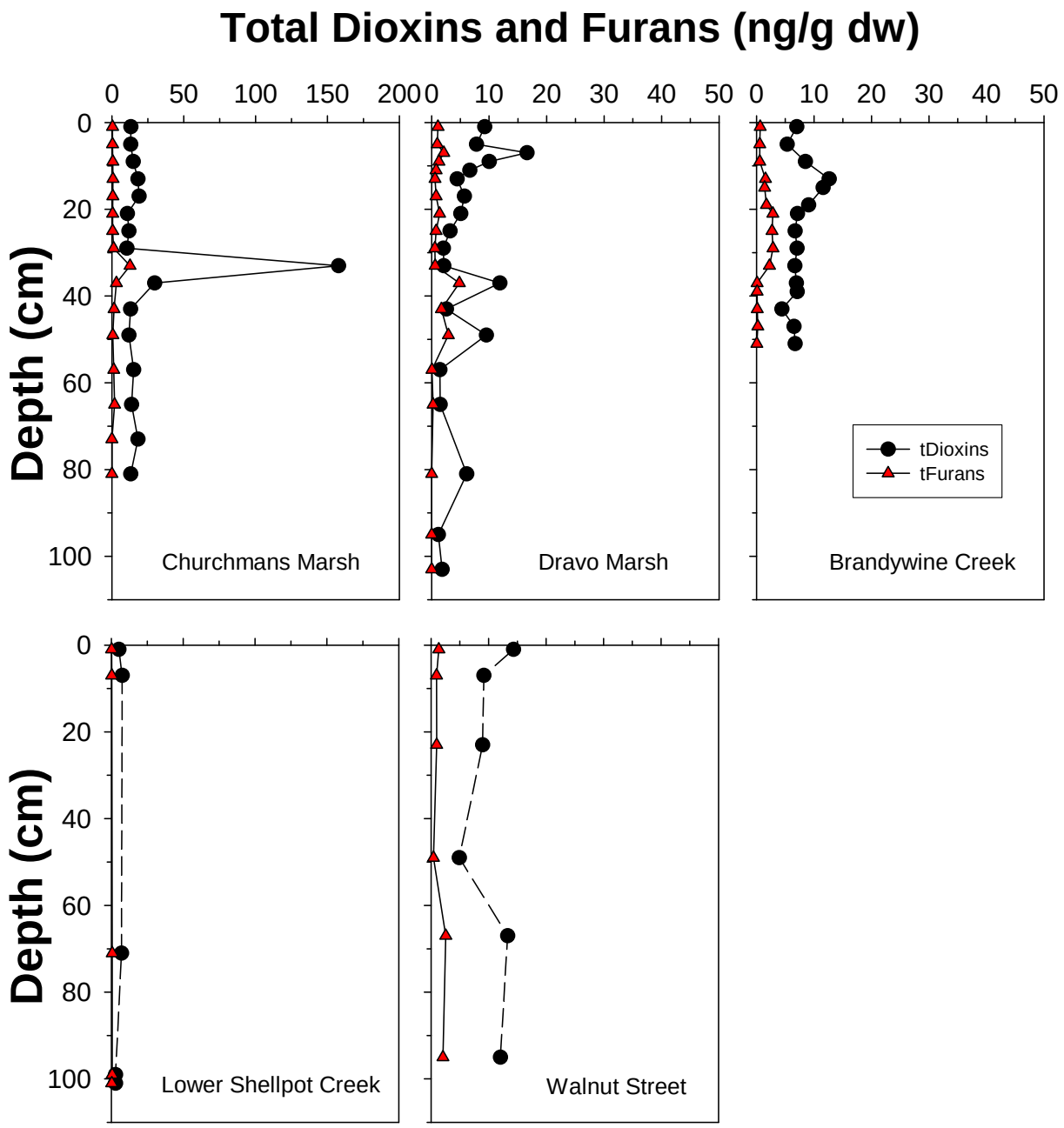

Figure 30. Total dioxins (tPCDD) and furans (tPCDF) with depth in the tidal Christina River and Brandywine Creek.

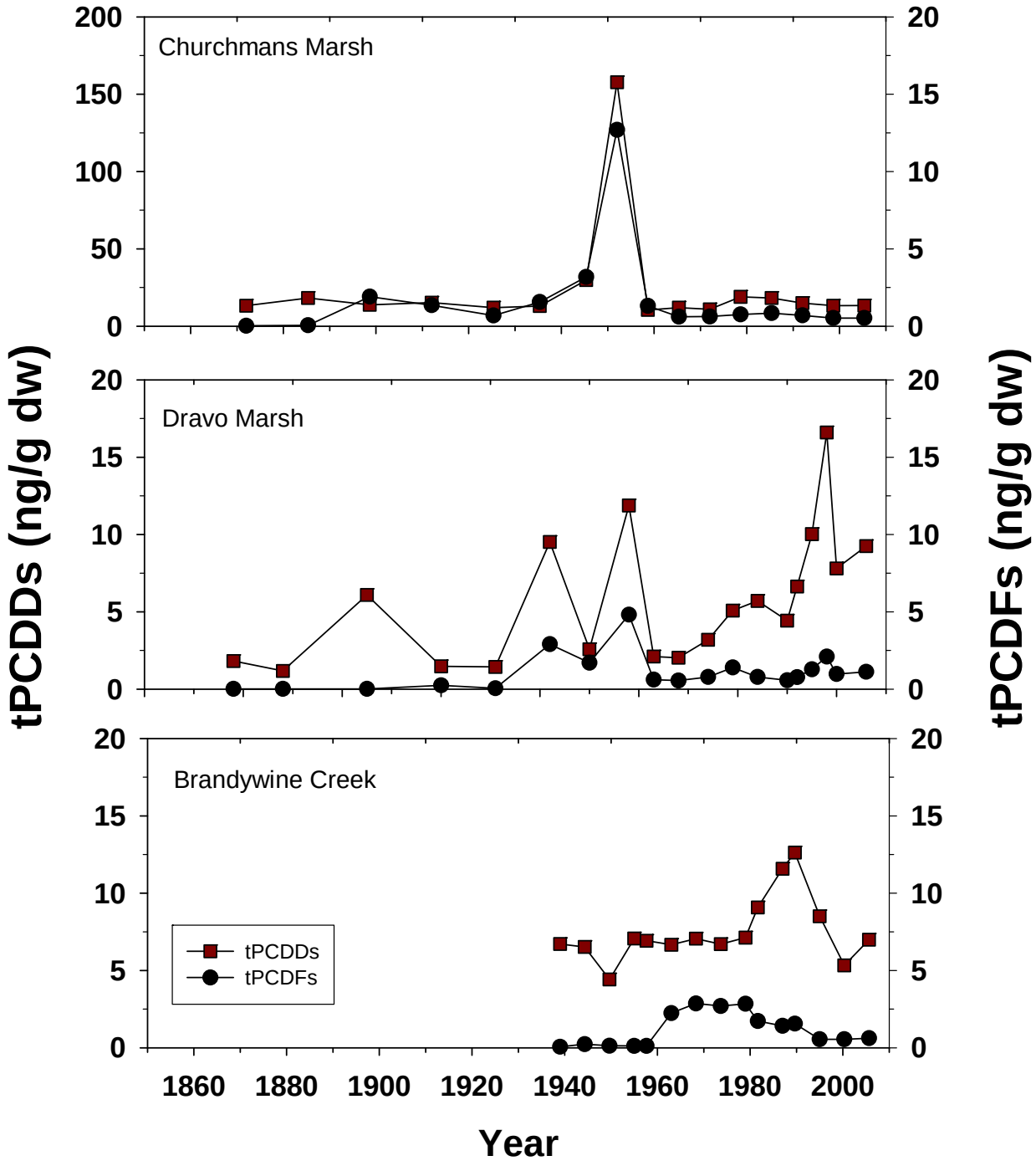

Figure 31. Concentrations of total dioxins and total furans from 1860 to 2003 (Note scale changes).

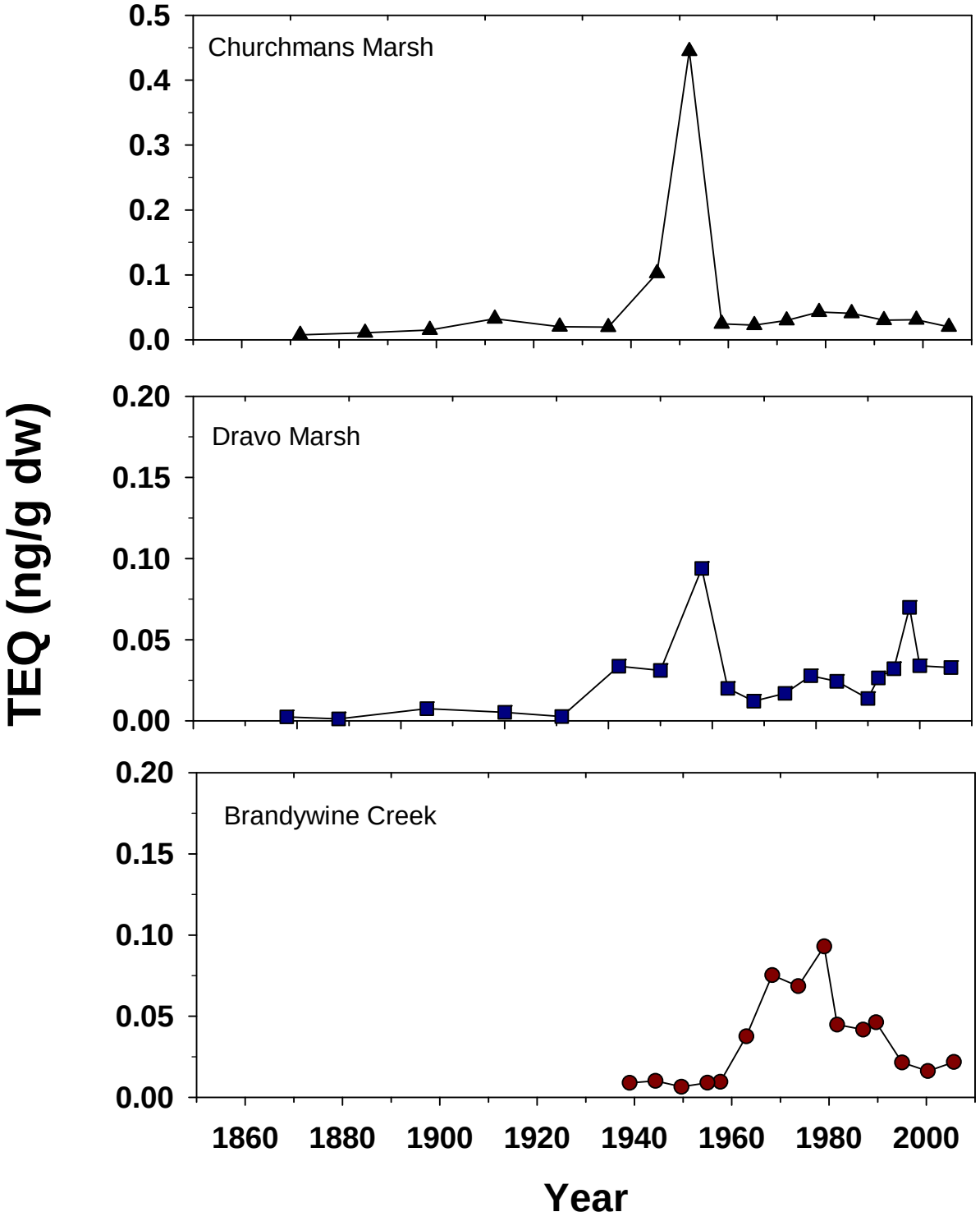

Figure 32. Concentrations of TEQ for dioxins and furans from 1860 to 2003 (Note scale changes).

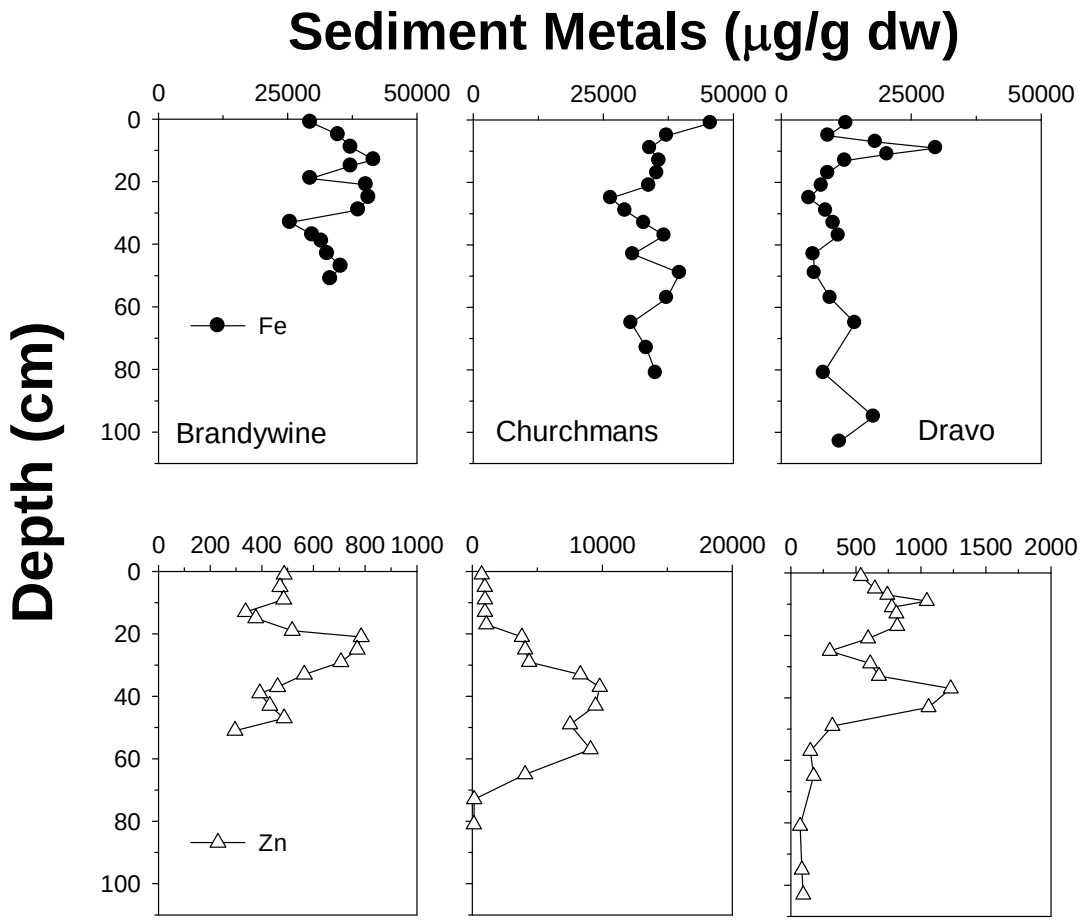

Figure 33. Depth distribution of sediment iron (Fe) and zinc (Zn) in the tidal Brandywine Creek, Churchmans Marsh and Dravo Marsh (Note scale changes).

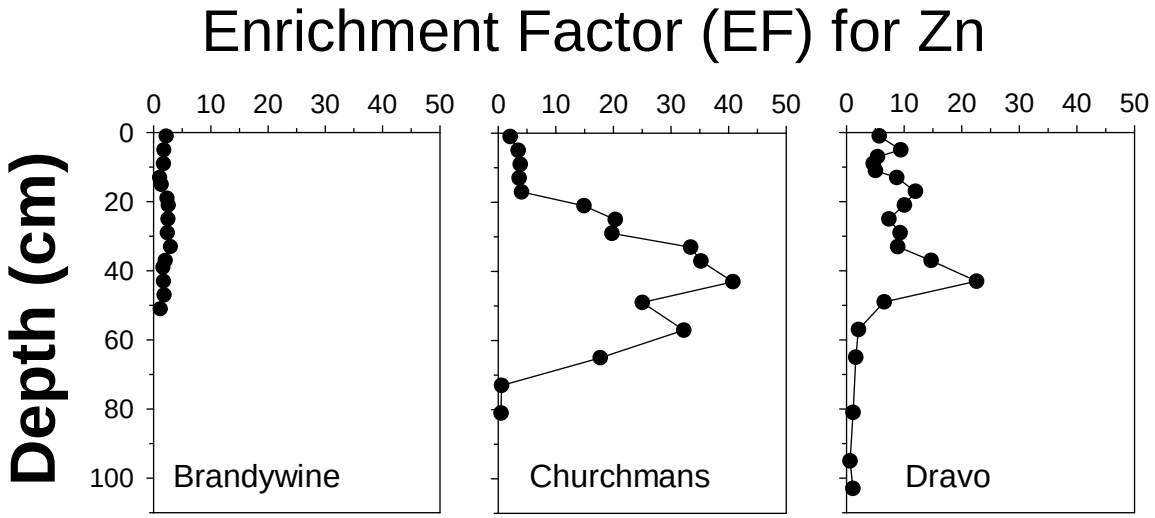

Figure 34. Depth distribution of the Zn enrichment factor (EF) in the tidal Brandywine Creek, Churchmans Marsh and Dravo Marsh.

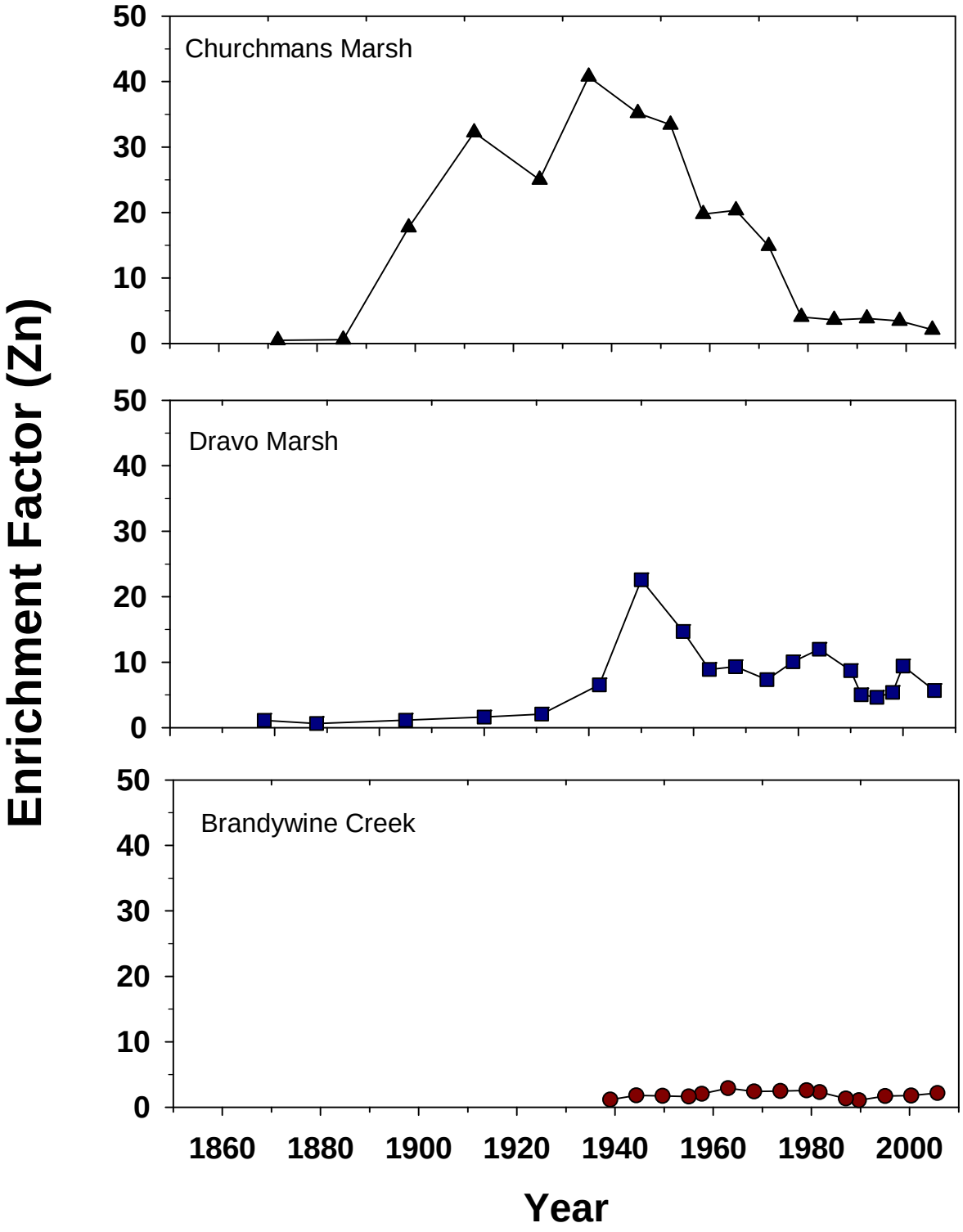

Figure 35. The time distribution of sediment concentrations of zinc (Zn) and the enrichment factor (EF) from 1860 to 2003.

Appendices

Excel File with Data and QA
(Separate Disk; electronic files)

FINAL REPORT

to

Dr. Richard Greene
Delaware Department of Natural Resources and Environmental Control
Division of Water Resources
Watershed Assessment Branch
820 Silver Lake Blvd., Suite 220
Dover, DE 19904-2464

Vertical Profiles of Radioisotopes, Contaminants, Nutrients and Diatoms in Sediment Cores from the Tidal Christina River Basin: A Historical Analysis

PCER Report No. 09-02

By
Drs. David Velinsky, Christopher Sommerfield[1] and Don Charles
Patrick Center for Environmental Research
The Academy of Natural Sciences
Philadelphia, PA 19103

[1]University of Delaware
College of Earth, Ocean and Environment
Lewes, DE

April 16, 2010

FINAL REPORT

to

Dr. Richard Greene
Delaware Department of Natural Resources and Environmental Control
Division of Water Resources
Watershed Assessment Branch
820 Silver Lake Blvd., Suite 220
Dover, DE 19904-2464

Vertical Profiles of Radioisotopes, Contaminants, Nutrients and Diatoms in Sediment Cores from the Tidal Christina River Basin: A Historical Analysis

PCER Report No. 09-02

By
Drs. David Velinsky, Christopher Sommerfield[1] and Don Charles
Patrick Center for Environmental Research
The Academy of Natural Sciences
Philadelphia, PA 19103

[1]University of Delaware
College of Earth, Ocean and Environment
Lewes, DE

April 16, 2010

TABLE OF CONTENTS

Page

List of Tables iii
List of Figures iv
Executive Summary v

A
Introduction **1**
A1 Background 1
A2 Objectives of Study 1
A3 Study Area 2

B
Field and Laboratory Methods 3
B1 Field Sampling 3
B2 Laboratory Methods 4
B2.1 Organic Contaminants 4
B2.2 Iron (Fe) and Zinc (Zn) 5
B2.3 Radioisotope Measurements and Sedimentation Rates 5
B2.4 Total Organic Carbon and Nitrogen 7
B2.5 Total Phosphorus 7
B2.6 Stable Isotopes of Carbon and Nitrogen 7
B2.7 Diatoms 7

C
Results and Discussion 8
C1 Sediment Properties and Sediment Accumulation 8
C1.1 Sediment Properties 8
C1.2 Accretion and Sediment Accumulation Rates 9
C1.3 Radionuclide Inventories and Focusing Factors 11
C2 Nutrients/Eutrophication 13
C2.1 Sediment Total Carbon, Total Nitrogen and Total Phosphorus 13
C2.2 Stable Isotopes of Carbon and Nitrogen 15
C2.3 Diatom Analysis and Assemblages 17

C3 Sediment Bound Contaminants 21
C3.1 Polycyclic Aromatic Hydrocarbons 22
C3.2 Polychlorinated Biphenyls 28
C3.3 Total DDX and Chlordane 33
C3.4 Polybrominated Diphenylethers (PBDEs) 36
C3.5 Dioxins and Furans 38
C3.6 Iron and Zinc 40

TABLE OF CONTENTS (cont)

Page

D
Summary and Conclusions.....45

E
Acknowledgments.....48

F
References.....49

G
Tables.....61

H
Figures.....80

I
Appendices.....118

Appendix I: Data Tables and QA Documentation.....I

LIST OF TABLES

Table 1: Core Locations and collection dates 62
Table 2: Bulk sediment properties and radioisotope data for core BW 63
Table 3: Bulk sediment properties and radioisotope data for core CM 64
Table 4: Bulk sediment properties and radioisotope data for core LSP 65
Table 5: Bulk sediment properties and radioisotope data for core DM 66
Table 6: Summary data for radioisotope analysis and dating 67
Table 7: Concentrations of various parameters for core BW 68
Table 8: Concentrations of various parameters for core CM 70
Table 9: Concentrations of various parameters for core DM 72
Table 10: Concentrations of various parameters for core LSP 74
Table 11: Concentrations of various parameters for core WS 75
Table 12: List of PAH compounds for analysis 76
Table 13: Diatom metrics for core BW 77
Table 14: Diatom metrics for core CM 78
Table 15: Diatom metrics for core DM 79

LIST OF FIGURES

Figure 1: Study area and core locations 81
Figure 2: Tripod/pulley system at Dravo Marsh 82
Figure 3: Geochronology for core BW 83
Figure 4: Geochronology for core CM 83
Figure 5: Geochronology for core DM 84
Figure 6: Geochronology for core LSP 84
Figure 7: Sediment organic carbon, C/N and sediment phosphorus distribution with depth 85
Figure 8: Depth distribution of the isotopic composition sediment N ($\delta^{15}N$) and C ($\delta^{13}C$) 87
Figure 9: Distribution of diatom indicator species with depth 88
Figure 10: Diatom metrics 91
Figure 11: Relationship between total sediment N and diatom metrics 92
Figure 12: Relationship between total sediment P and diatom metrics 93
Figure 13: Concentrations of total sediment nitrogen (TN) and the nitrogen isotopic composition of TN ($\delta^{15}N$-TN) from 1860 to 2003 94
Figure 14: Concentrations of total sediment phosphorus (TP) and the carbon isotopic composition of total carbon ($\delta^{13}C$-TC) from 1860 to 2003 95
Figure 15: The relationship between total sediment P (TSP) and the carbon isotopic composition of organic matter ($\delta^{13}C$-TC) in Brandywine Creek, Churchmans Marsh and Dravo Marsh 96
Figure 16: Diatom metric for eutrophentic species from 1860 to 2003 97
Figure 17: Depth distribution of total PAHs and the LMW to tPAHs ratio with depth 98
Figure 18: Comparison of benzo[a]pyrene to benzo[e]pyrene 99
Figure 19: Indicator ratios of benzo[a]pyrene to benzo[e]pyrene and fluoranthene to pyrene 100
Figure 20: Concentrations of tPAHs from 1900 to 2003 101
Figure 21: Distribution of tPCBs with depth 102
Figure 22: Distribution of tPCBs and the LMW to tPCBs ratio with depth 103
Figure 23: Distribution of tDDX (DDT+DDD+DDE all forms) and total chlordanes with depth 105
Figure 24: Concentrations of tPCBs from 1900 to 2003 106
Figure 25: Concentrations of tDDXs from 1900 to 2003 107
Figure 26: Distribution of total chlordanes (all forms) with depth 108
Figure 27: Concentrations of total chlordanes from 1900 to 2003 109
Figure 28: Distribution of tPBDEs with depth 110
Figure 29: Concentrations of tPBDEs from 1860-2003 111
Figure 30: Distribution of dioxins and furans with depth 112
Figure 31: Concentrations of total dioxins and furans from 1900 to 2003 113
Figure 32: Concentrations of TEQ for dioxins and furans from 1860-2003 114
Figure 33: Distribution of sediment Fe and Zn with depth 115
Figure 34: Zn enrichment factor (EF) with depth 116
Figure 35: Concentrations of Zn and the EF from 1860-2003 117

Executive Summary

This study involved the chemical analysis of five sediment cores taken from the tidal Christina River Basin and lower Shellpot Creek in northern New Castle County, DE. Of the five cores, four were dated using ^{210}Pb and ^{137}Cs radiometric methods, with three (Churchmans Marsh (CM), Dravo Marsh (DM), and the tidal Brandywine (BW)) providing sufficient temporal coverage (> 50 yrs) for detailed chemical analysis. *The main objective was to evaluate historical trends in organic chemical contaminants (e.g., polychlorinated biphenyls, pesticides, dioxins/furans, polybrominated diphenylethers and polycyclic aromatic hydrocarbons), selected trace metals (e.g., iron and zinc) and nutrients (i.e., sediment phosphorus and nitrogen).* An additional objective was to evaluate if a historical record of eutrophication could be derived from algae analysis (i.e., diatom species in the cores) along with other indicators of potential ecosystem change (e.g., stable isotopes of carbon (δ^{13}C-OM) and nitrogen, (δ^{15}N-TN)).

The range and average sediment accumulation rates (^{137}Cs) inferred from the ^{137}Cs and ^{210}Pb data are similar to other areas within the Delaware Estuary and range from 0.57 to 1.9 cm/yr. There was good agreement between the ^{137}Cs rates and those for the constant accumulation model for ^{210}Pb.

With regard to contaminants, a major finding that emerged from this study is the historic accumulation of zinc in the system, as clearly displayed in the Churchmans Marsh (CM) core. Concentrations of Zn showed a broad peak over background levels starting at or shortly after the turn of the century and persisting to the early to mid-1970s. Using the amount of iron (Fe) within the sediment and referencing the data to bottom concentrations of Zn (and Fe), the sediments of Churchmans Marsh had been up to 40 times above background levels. Current Zn enrichment in Churchmans Marsh is still approximately 5 to 10 times above background. In the other core locations, surface sections are not substantially enriched above background with zinc enrichment factors ranging only from 1 to 2.3. Major sources of historic zinc loading to the tidal river included a National Vulcanized Fiber (NVF) facility on the Red Clay Creek (Yorklyn, DE) and a NVF facility on White Clay Creek (Newark, DE) and a pigment plant located in Newport (DE) along the tidal Christina River. Both NVF facilities ceased operation and have either been remediated (NVF Newark) or continue to be remediated (NVF Yorklyn). The pigment plant and adjacent areas impacted by releases from the plant are designated as a Federal Superfund site. Remedial actions have been taken at the site, in part to address the zinc issue. The coring

analysis clearly shows that the combined loading from these 3 facilities was much higher in the past and that remedial actions taken over the years have yielded substantially lower concentrations of Zn in the sediments of the tidal Christina River.

The other key finding of this study is that concentrations of organic contaminants are lower today, overall, than they were in the past, with some exceptions. Chlorinated organic compounds such as tchlordane, tDDX and dioxins/furans all show a sharp maximum at similar depths (corresponding to the 1960s and 1970s), followed by a decreasing trend towards the surface. Total PCBs also shows higher concentrations at depth with decreasing concentrations towards the surface, with the exception of the Dravo Marsh core where tPCB concentrations at the surface remain elevated (ca. 240 ng/g dw). The DM finding may reflect lingering inputs from local sources and/or the redistribution of previously deposited contamination following major earth works projects in or near the marsh.

Interestingly, the PCB congener composition in both the CM and DM cores showed a shift from mid to higher molecular weight compounds to lower molecular weight compounds from the upper sections (more recent) to the lower sections (longer ago). The opposite was true for the BW core. The high proportion of deca PCB (H10) in the CM and DM cores is unusual and appears to reflect releases from the same pigment plant in Newport that was also responsible for at least part of the zinc contamination. The use of congener-specific PCB methods (rather than typical Aroclor methods) allowed us to identify and characterize the deca PCB signature.

Total dioxins (PCDD) and furans (PCDF) concentrations ranged from <2 to 157 ng/g dw and <1 to 13 ng/g dw, respectively, with distinct distributions with depth and time. The individual congeners were used to calculate the toxic equivalents (TEQs) using published toxic equivalency factors (TEF). The TEQs ranged from <0.01 to 0.45 ng/g dw, generally similar or lower to surface sediments collected in 2007. Highest concentrations of PCDD, PCDF and TEQ were found in the Churchmans Marsh core.

In the three cores analyzed for polybrominated diphenyl esters (PBDEs), tPBDEs were only present in the upper sections with undetectable concentrations below approximately 20 cm (<1980s). The predominant congener is PBE 209 in the upper sections with BDE153 and BDE99 found at depth.

Total PAHs showed a distinct concentration peak in the 1940s, in the CM core, while a bimodal distribution was observed in the DM core and possibly the BW core. The peak of tPAHs

in the CM core maybe related to historic inputs of hydrocarbons from another Federal Superfund site near Newport (Koppers) that used creosote to treat telephone poles and other lumber. Other sources related to urban development including a major shipbuilding complex and a coal gasification facility are also potential historic sources to the area, particularly the DM. Data were compared to indicators of combustion sources, such as coal tar based parking lot sealant, using specific ratios of individual PAHs. Only a limited number of samples were consistent with such a fingerprint and thus this type of sealant does not appear to be a major source to the tidal Christina River.

Lastly, analysis of the diatom assemblages and metrics indicate a shift toward more eutrophic species starting in the late 1940-1950s. There was a strong positive relationship between the eutrophic diatom metric and the concentration of nitrogen and phosphorus in Churchmans and Dravo marshes. This, along with the increases in total sediment N, total sediment P and sediment nitrogen isotopic compositions (δ^{15}N-TN), indicates that increase loadings of nutrients have resulted in a diatom shift in the river.

Overall, this study documents the chemical analysis of three cores taken in the tidal Christina River and tidal Brandywine Creek. Changes were observed in contaminant levels across time that reflect usage globally and most often locally. Contaminant levels appear to be declining when viewed on a longer-term, decadal time scale. However, the concentrations of several contaminants (e.g., PCBs and zinc) remain relatively elevated in this system.

A) Introduction

A1: *Background*

Trace metals and organic contaminants in water are derived from many sources. Natural sources of metals include the weathering products of soils which are then transported in the dissolved or particulate phases. Anthropogenic sources of metals and organic contaminants are introduced to the water via atmospheric deposition, industrial discharges (e.g., mining, metal processing, manufacturing), municipal discharges (waste water treatment), and stormwater runoff of contaminated parcels. Due to the particle-reactive nature of most trace metals and organic compounds, sediments are potential repositories for contaminants and, under certain conditions, can be used to provide a historical record of pollution (Simpson et al., 1983; Orson et al., 1990; 1992; Valette-Silver, 1993; Hornberger et al., 1999; Cooper and Brush, 1993; Church et al., 2006; Velinsky et al., 2007; and others). With minimal diagenetic remobilization, biological mixing, and hydraulic processes, the sediment column can reflect the chronological deposition/inputs of most contaminants. Sediment cores are extremely useful in determining if various pollution control actions were/are effective in reducing contaminant loadings, as well as providing a time frame for system response (Smol, 2008). Hence, coring data are important to determine whether environmental conditions are improving with time and at what rate. The rate information is especially important for modeling programs in which forecasts are developed by extending past trajectories.

A2: *Objectives of Study*

It is the objective of this study to collect sediment cores from the tidal freshwater region of the Christina River and Shellpot Creek (near Wilmington, DE), and determine the chronology of chemical contaminant deposition, nutrient loadings and related ecological response. To meet this objective, we obtained and analyzed the chemical characteristics of sediment cores from depositional areas within the targeted waters. This study aimed to quantify and illustrate the magnitude and extent of sediment contamination in the lower tidal portion of the Christina Watershed and Shellpot Creek and provide insight into the temporal nature of that contamination. It also sought to understand how the trophic status of the system has changed over decadal time scales.

A3: *Study Area*

The Christina River Basin occupies 1480 km^2 in Delaware, Pennsylvania and Maryland, and includes four major watersheds—Brandywine Creek, Red Clay Creek, White Clay Creek, and the Christina River. The Christina River Basin is a rapidly suburbanizing watershed which is characteristic of a typical mid-Atlantic watershed. Land uses in the watershed are approximately 33% for urban/suburban, forested/open space, and agriculture (DNREC, 2007). Percent impervious levels in developed watersheds exceed 10 to 15%, which are thought to represent maximum thresholds needed to protect stream habitat and fisheries (Klein et al., 1979; Roy et al., 2003). Existing water quality problems are derived from wastewater discharges, agricultural runoff, Superfund sites, and runoff from new development. Approximately 40 stream segments listed as impaired in the EPA's 303(d) list have resulted in fish consumption advisories along reaches of the Brandywine Creek, Red Clay Creek, and Christina River.

The river contains many sources of chemical contaminants and has three federal Superfund sites located within the lower tidal river (Koppers Wood, Dupont Chemical, and Halby Chemical), numerous state-lead waste sites, and is listed on Delaware's 303(d) list of impaired waters (DNREC, 2007). Two major tributaries to the Christina, the Red Clay Creek and the White Clay Creek, are listed as impaired due to elevated zinc concentrations. Both of these tributaries have implemented efforts (i.e., total maximum daily loads [TMDL]) to reduce inputs of Zn to the water (DNREC 1996; 1999a,b,c). In addition, the EPA and DNREC in 2001 implemented a TMDL for excess nutrient inputs to the river (high and low flow conditions). Additional TMDL for the Christina Basin, including those for PCBs and other contaminants, are scheduled to be completed in 2010 and beyond.

The Shellpot Creek Watershed, a tributary to the Delaware River Estuary, is located in New Castle County, DE and flows through parts of Wilmington, DE. The creek once flowed into the lower tidal Brandywine but has been diverted directly into the Delaware Estuary. The watershed drains approximately 9,000 acres of mostly developed lands (90% of the watershed area).The impaired segment of Shellpot Creek begins at its headwaters and terminates at its mouth which is its confluence with the Delaware River. The watershed has completed TMDLs for excess nutrients and bacteria (DNREC, 2005). The creek is also currently listed on Delaware's 303(d) list for impairments due to chlordane and PCBs in fish. TMDLs to address those impairments are scheduled for the future.

Current PCB loading rates from Delaware Hazardous Substance Cleanup Act (HSCA) sites via overland flow and subsurface discharge to the tidal Christina Basin have been estimated by Brightfields, Inc. (2009); however, a historical perspective of contaminant inputs and mass loading rates have not been estimated. This project helps to fill that gap.

Cores were obtained in the tidal portion of the tidal Christina River (**Figure 1**). Locations include sites in Churchman Marsh (CM), Brandywine River (BW), Lower Shellpot Creek (LSP), and Walnut Street Bridge in downtown Wilmington, DE (WSB), and Dravo Marsh (DM) also called Old Wilmington Marsh. Salinities in this area are very low and marsh plant diversity indicates a tidal freshwater system. However, during drought conditions the BW and DM sites can occasionally experience salinities of 2 to 4 psu while upstream CM can experience lower salinities of between 1 and 2 psu.

B) Field and Laboratory Methods

B1: *Field Sampling*

Sediment cores were collected in 2007/2008 by staff from The Academy of Natural Sciences and University of Delaware at locations in the tidal river (**Figure 1; Table 1**). Overall, 10 cores were obtained from these sites but not all of them provided good sediment chronologies (based on ^{210}Pb and ^{137}Cs) and as such were not analyzed for various chemical parameters. This report discusses only the cores (i.e., 5 of the 10) on which chemical analyses (e.g., PCBs, PAHs, organic carbon, etc) were accomplished. Of these five cores, three (CM, BR, and DM) had sufficient temporal resolution and are discussed in detail, while the other two cores (LSP and WSB) are presented in a limited manner.

Cores were mainly collected on the marsh surface during mid to low tide. The cores obtained slightly downstream of the Walnut Street Bridge were collected during low tide, but water was present at the sediment surface. Core locations were from the interior of the marsh, away from any obvious disturbances (e.g., creek banks and ditching). At each site two cores were obtained, one for chemical analysis and the other for stratigraphic descriptions of each site. Push-piston cores of approximately 1 to 1.5 m in length were retrieved by a tripod/pulley system (**Figure 2**). The cores were taken to the laboratory and sectioned into specific intervals (e.g., 2 cm). Samples were stored in pre-cleaned jars at -10°C at either Academy or UDEL facilities.

Chain-of custody procedures were followed from the time of collection, shipping and until the analyses were completed.

B2: *Laboratory Methods*

Organic contaminant clean-techniques were used throughout and are well published (Ashley and Baker, 1999; others) and are similar to those used by EPA and NOAA (U.S. EPA, 1987; NOAA, 1993; Wade et al., 1994). All materials coming in contact with the samples were either glass or metal that was cleaned of any contaminants prior to use. Sample ID forms were used and each sample was given a unique laboratory number for sample tracking.

Sediments were analyzed for the following parameters at laboratories operated by the Academy of Natural Sciences (Patrick Center): carbon, nitrogen and phosphorus, PAHs (41+ compounds), total PCBs (100+ congeners), selected pesticides including DDTs and chlordane, and stable isotopes of carbon and nitrogen. In addition, specific sections were analyzed for diatoms via sample digestion, mounting and glass slide light microscopy. Sediments for radioisotope analysis (^{210}Pb and ^{137}Cs) were analyzed at University of Delaware (Center for Earth, Oceans and Environment). Below are brief descriptions of each chemical, biological, or physical method.

B2.1: Organic Contaminants: PAHs, Polychlorinated Biphenyls, Organochlorine Pesticides, and Dioxins and Furans

Prior to organic contaminant analyses, samples were kept frozen at -20°C. Standard operating procedures for the extraction, clean-up and quantification of organic contaminants in sediments are summarized in their respective operating procedure. Briefly, sediment samples were extracted with dichloromethane for 24 h using a Soxhlet apparatus. PAHs were quantified using a capillary gas chromatograph coupled with a mass spectrometer in the electron impact mode after a clean-up procedure employing liquid-solid chromatography with alumina as the stationary phase (Ashley and Baker, 1999). After PAH determination, samples were further cleaned using liquid-solid chromatography with florisil as the stationary phase. Congener-specific PCBs and OCPs (spell this out) were analyzed using a gas chromatograph equipped with a ^{63}Ni electron capture detector (Ashley and Baker, 1999; Kucklick et al., 1996). Twenty-eight singly or coeluting PBDE (BDE 17, 25, 28+33, 30 47, 49, 66, 71, 75, 85+155, 99, 100, 116, 119, 138, 153, 154, 156, 181, 183, 190, 191, 203, 205, 206, 209; Accustandard, 95–99% purity) were quantified at Duke University using a gas chromatography (GC) with a mass spectrometer (MS) operated in negative chemical ionization mode (NCI). Add brief description of dioxin and furan analysis performed by GERG.

B2.2: Sediment Iron (Fe) and Zinc (Zn)

Core sediment (0.500 g) was placed into pre-cleaned Teflon tubes for the MARS microwave digestion system. Approximately 10 ml of concentrated nitric acid (trace metal grade) was slowly added and the sample was allowed to cool and evaporate gases. The tubes were capped tightly and microwaved using EPA SOP 3051. The slurry was mixed and allow to settle for one week in which an aliquot was taken and diluted (100 ml) with ultra clean DDW. The extract was analyzed using a flame Varian AAS linked to a desktop computer. A five-point calibration curve was used to calculate concentrations and samples were diluted if absorbance was greater than 0.750. Concentrations are reported in dry wt and it should be noted that concentrations are not total (i.e., mineral matrix) but strong acid digestion.

B2.3: Radioisotope Measurements and Sedimentation Rates

In the laboratory, sediment cores were extruded vertically and sectioned in 2-cm intervals for analysis. Sediment bulk density (ρ_d) and loss-on-ignition (LOI) measurements were made for each core section to aid interpretation of the downcore radionuclide and chemical data. Dry-bulk density was calculated from porosity (ϕ) using representative values of interstitial fluid density (ρ_d) and mineral density (ρ_m) according to:

$$\rho_d = (1-\phi)\rho_m \tag{1}$$

where ρ_m=2.65 g/cm^3. Porosity was computed gravimetrically from water content (W_c) and using an assumed pore water density of ρ_f=1.0 g/cm^3:

$$\phi = \left(\frac{W_c \rho_m}{W_c \rho_m + (1-W_c)\rho_f} \right) \tag{2}$$

where $W_c = W_{wet} - W_{dry} / W_{wet}$. Dry sediment weight was determined by drying the sectioned wet sediment in a convection oven at 100°C for 24 h. The dry sediment was then ground to a fine powder for LOI determination and radionuclide analysis.

LOI measurements were used to quantify the relative proportion of organogenic (combustible) and minerogenic (residual ash) materials in the sediments. Following the method of Heiri et al. (2001), a 4-gram quantity of sample power was combusted at 550°C in a muffle furnace for 4 h. LOI was computed as follows:

$$LOI = \frac{W_{dry} - W_{ash}}{W_{dry}} \cdot 100\% \tag{3}$$

where W_{dry} is the weight of sample previously dried at 100°C, and W_{ash} is the weight of the residual ash.

To develop sediment chronologies and determine accretion rates for the sediment column, measurements of ^{210}Pb ($t_{1/2}$=22.3 years) and ^{137}Cs ($t_{1/2}$=30.1 years) were made by gamma spectroscopy of the 46.5 and 661.6 keV photopeaks, respectively (Cutshall et al., 1983; Wallbrink et al., 2002). Powder samples were placed in a 60 ml plastic jar and counted for 24-48 h on a Canberra Model 2020 low-energy Germanium detector (LEGe). The radionuclide concentration (activity) of excess ^{210}Pb was determined by subtracting the activity of its parent nuclide ^{214}Bi (609.3 keV) from the total activity. Detector efficiencies were determined from counts of NIST Standard Reference Material 4357 (Inn et al., 2001). The counting geometry of the core samples was kept identical to that of the NIST standard such that a self-absorption

correction for ^{210}Pb was not necessary. Confidence limits reported with radioisotope data are the propagated one-sigma background, calibration, and counting errors.

Three approaches were used to reconstruct the accumulation history of marsh deposits. Two of these methods are based on downcore profiles of ^{210}Pb activity, and the third uses the depth distribution of ^{137}Cs activity. The first approach, the constant activity model (CA), assumes that the specific activity of ^{210}Pb (dpm/g) deposited remains constant through time. In other words, variations in mineral sedimentation rate do not affect the initial concentration of ^{210}Pb. At steady state, excess ^{210}Pb decreases exponentially with depth in the sediment column following:

$$A = A_o \, exp\left(-\lambda z/S\right) \tag{4}$$

where A is the excess activity of ^{210}Pb at depth z, A_o is the initial activity of excess ^{210}Pb, λ is the decay constant for ^{210}Pb (0.3114 years), and S is the vertical accretion rate. The slope of the regression line of ln$A$ versus z is proportional to the accretion rate with dimensions length/time. In this method the age of a sediment interval is derived from a single value of S averaged over the ^{210}Pb profile. The corresponding mass accumulation rate, with the dimensions mass/area/time, is determined by plotting A as a function of cumulative mass, the depth-integrated product of ρ_d and z.

The second method, the constant flux model (CF), relates time and accretion rate to the inventory of excess ^{210}Pb by assuming that the flux of ^{210}Pb to the sediments (rather than A_o concentration) is constant. Sediment age and ^{210}Pb are related as:

$$I = I_o \, exp\left(-\lambda t\right) \tag{5}$$

where I is the inventory of excess ^{210}Pb below depth z (dpm/cm^2), I_o is the total inventory of excess ^{210}Pb in the sediment column, and t is the sediment age at depth z. Radionuclide inventories of excess ^{210}Pb (and ^{137}Cs) are computed as:

$$I_o = \sum_i \rho_{di} x_i A_i \tag{6}$$

where ρ_d is the dry-bulk density, x is the sediment thickness, A is the radionuclide activity, and the i operator indicates the ith depth interval. In the CF model, sediment accretion rates are computed by dividing the length of the dated sediment column by the corresponding age in years.

The third chronological method is based on the first occurrence of ^{137}Cs in the sediment column as an absolute indicator of ca. 1954, the year of ^{137}Cs introduction to the global atmosphere by nuclear weapons testing (Ritchie and McHenry, 1990). The depth of ^{137}Cs penetration divided by the interval between ca. 1954 and the year of core collection is used to compute an average accretion rate. The corresponding mass accumulation rate is determined by plotting ^{137}Cs activity against cumulative mass. The advantage of ^{137}Cs chronology over ^{210}Pb dating methods is that it more closely approximates the absolute age of sediments deposited after ca. 1954.

Both the CA and CF ^{210}Pb models have been widely used to develop sediment chronologies for tidal marsh deposits, but they are based on different assumptions that are not met in all types of depositional environments. The CF model assumes that 1) all ^{210}Pb deposited is derived from direct atmospheric deposition, and 2) variations in A_o are due to changes in the minerogenic sediment accumulation rate S as opposed to changes in ^{210}Pb supply (Appleby and Oldfield, 1978). In other words, a change in S through time will be met by a corresponding change in A_o in accordance with Equation 5. This model was originally developed for lake systems and thus is most appropriate for depositional environments that sequester ^{210}Pb mostly (if not exclusively) through direct atmospheric deposition. Although tidal marshes are exposed to the atmosphere

most of the time, tidal flooding brings particle-bound ^{210}Pb from coastal waters that can increase A_o above that supplied by the atmospheric flux. For this study we computed sediment accretion and accumulation rates using both ^{210}Pb models but place more weight on the CA approach, because the assumptions are less restrictive regarding ^{210}Pb sources.

The following conditions are implicit in all ^{210}Pb and ^{137}Cs dating methods: 1) mixing by burrowing organism has not enhanced particle burial; 2) the modeled radionuclide is chemically immobile; and 3) the sedimentary record is complete and not punctuated by non-depositional or erosional episodes. As elaborated later, these assumptions appear to have been met in this study for cores CM, DM, and BR.

B2.4: Total Organic Carbon and Total Nitrogen

Total organic carbon and total nitrogen were measured using a CE Flash Elemental Analyzer following the guidelines in EPA 440.0, manufacturer instructions and ANSP-PC SOP. Samples were pre-treated with acid to remove inorganic carbon.

B2.5: Total Phosphorus

Total sediment phosphorus was determined using a dry oxidation method modified from Aspila et al. (1976) and Ruttenberg (1992). Solubilized inorganic phosphorus was measured with standard phosphate procedures using an Alpkem Rapid Flow Analyzer. Standard reference material (spinach leaves) and procedural blanks were analyzed periodically during this study. All concentrations were reported on a dry weight basis.

B2.6: Stable Isotopes of Carbon and Nitrogen

The stable isotopic composition of sediments was analyzed using a Finnigan Delta XL coupled to an NA2500 Elemental Analyzer (EA-IRMS). Samples were run in duplicate or triplicate with the results reported in the standard δ (‰) notation: $\delta X = (R_{sample}/R_{standard}) - 1) \times 1000$; where X is either ^{13}C or ^{15}N and R is either $^{13}C/^{12}C$ or $^{15}N/^{14}N$. The $\delta^{15}N$ standard was air ($\delta^{15}N = 0$), and for $\delta^{13}C$ the standard is the Vienna PeeDee Belemite (VPDB) limestone that has been assigned a value of 0.0 ‰. Analytical accuracy was based on the standardization of the UHP N_2 and CO_2 used for continuous flow-IRMS with IAEA N-1 and N-2 for nitrogen and IAEA sucrose for carbon, respectively. An in-house calibrated sediment standard was analyzed every tenth sample. Generally, precision based on replicate sample analysis was better than 0.2‰ for carbon and 0.6‰ for nitrogen.

B2.7: Diatoms

Core sediment was collected (≈1g) and the organic component was oxidized with 70% nitric acid while heated in a CEM microwave (165ºC) for 1.5 h. Diatoms were settled and supernatant was decanted until it reached a neutral pH. A measured amount of digested sample was dripped onto a microscope coverslip and dried. Coverslips were then mounted onto slides using a high refractive index mounting media (Naphrax™). Diatoms were counted and identified using a Zeiss Axioskop with DIC optics. Three hundred valves were counted on 1000x magnification. Identifications were made using the extensive diatom library at ANSP. Several diatom community metrics were calculated based on species autecological preferences based on van Dam et al. (1994). Metrics were calculated using the Phyco-Aide program developed at ANSP.

C) Results and Discussion

C1: *Sediment Bulk Properties and Sediment Accumulation*

The activity of ^{210}Pb and ^{137}Cs (reported as disintegrations per minute per gram of sediment; dpm/g) with depth can be used to determine the sedimentation rate and historical record of contaminants in sediments (Simpson et al., 1983; Orson et al., 1990; 1992; Valette-Silver, 1993; Appleby, 2001; Smol, 2002; Ridgway and Shimmield, 2002; Sommerfield, 2006). This information can be used for the construction of sediment budgets (Schubel and Hirschberg, 1977; Brush et al., 1982; Officer et al., 1984) and to understand chemical contaminant accumulation in aquatic environments (Owens and Cornwell, 1995; Cornwell et al., 1996; Latimer and Quinn, 1996; Van Metre and Callender, 1997; Church et al., 2006; Velinsky et al., 2007). Also, dated sediment cores can provide information as to the changes in loadings of contaminants over time (e.g., Rippey and Anderson, 1996; Gevo et al., 1997; Santschi et al., 2001). Such information is especially useful in tracking the effectiveness of various management actions designed to reduce inputs to specific areas (Owens and Cornwell, 1995; Zhang et al., 1993). However, there are many variables that can affect the usefulness of ^{210}Pb and ^{137}Cs dating in a given area (Appleby and Oldfield, 1978; Crusius and Anderson, 1991; Appleby, 2001). These include mixing of the sediment by benthic organisms (i.e., burrowing organisms), physical mixing from dredging and storm events, post-depositional movement of contaminants and of the ^{210}Pb or ^{137}Cs, and additional inputs of ^{210}Pb from sources in the urban landscape (i.e., urban sediment focusing). The cores obtained in this study provided excellent chronologies of sediment deposition and accumulation. For historical analysis, the sediment accumulation rate derived from the ^{137}Cs distribution was used to produce an age-depth relationship. This, along with the ^{210}Pb results, provides linear rates from approximately 1920-1930 to the present. For dates prior to the 1920-1930s we assume linear rates to the bottom of the cores. While this is useful for this analysis, we are less confident in the dating at the bottom of the cores due to effects associated with compaction, non-linear sedimentation rates, and other factors (Neubauer et al., 2002; Sommerfield, 2006).

C1.1: Sediment Properties

All of the cored deposits consisted of clayey silt with variable quantities of living and dead plant material. Only at the base of core SP-2 was there a noticeable down-core change in

sediment type, from silt to sand. Dry-bulk densities ranged from 0.17 to 1.2 g/cm^3 overall and increased with depth downcore in all cases (**Figures 3-6; Tables 2-5**). This depth increase is consistent with burial compaction of the sediment column due to expulsion of porewater. Only in the lowermost intervals of core LSP-2 did bulk density vary with grain size on account of changes in mineral density (silt to sand).

The amount of organic material in the cores ranged from 7 to 40%, values representative for marsh deposits in general (**Figures 3-6; Tables 2-5**). LOI decreased with depth in all cases, and cores BW-2 and DM-2 displayed a profile that varied inversely with dry-bulk density. This suggests that depth variations in sediment bulk density are partly due to the concentration of organogenic material, at least at sites BW-2 and DM-2. In summary, with the exception of the base of core SP-2, the physical properties data suggest no major changes in sediment type that could bias interpretations of chemical and radionuclide profiles.

C1.2: Accretion and Sediment Accumulation Rates

Brandywine Marsh core BW-2 displayed ^{137}Cs activities that increased up core from the depth of first occurrence at 36-38 cm to a broad peak between 20 and 30 cm, above which activities decreased to near-zero at the core top **(Figure 3; Table 2)**. The overall shape of the profile is consistent with the source function for the mid-Atlantic region (Olsen et al., 1981), but the broad activity maximum is ambiguous regarding the date of peak fallout (e.g., 1963-1964). At this site, accretion and mass accumulation rate calculated from the basal depth of ^{137}Cs activity are 0.75 cm/yr and 0.26 g/cm^2/yr, respectively.

Excess ^{210}Pb profiles for BW-2 exhibited a monotonic decrease in the log of the activity downcore, indicative of steady-state sediment accumulation and radioactive decay **(Figure 3).** Accretion rates determined using the CA and CF ^{210}Pb models were 0.80 and 1.0 cm/yr, respectively, and the corresponding mass accumulation rate was 0.40 g/cm^2/yr. At this site there was good agreement among radionuclide dating methods, suggesting that sediment accumulation has been more-or-less invariant over the period of interest.

Churchmans Marsh core CM-1 exhibited ^{137}Cs and ^{210}Pb distributions that were somewhat similar to those observed for the BW-2 core (**Figure 4; Table 3**). The ^{137}Cs activities increased up core from the depth of first occurrence at 28-30 cm to a broad maximum centered at 20-22 cm, and then decreased to lower, but detectable, activities at the core top. Accretion rates based

on ^{137}Cs and excess ^{210}Pb (CF model) were 0.60 and 0.51 cm/yr, respectively, with corresponding mass accumulation rates of 0.28 and 0.25 g/cm^2/yr. Accretion and accumulation rates could not be determined using the CA model because the excess ^{210}Pb profile did not exhibit a monotonic decrease in activity consistent with steady-state sediment accumulation.

Dravo Marsh core DM-2 had a first occurrence of ^{137}Cs at 40 cm, maximum activity at approximately 18-20 cm, and decreasing activities to the core top (**Figure 5; Table 4**). Accretion and mass accumulation rates derived using ^{137}Cs data were 0.79 cm/y and 0.19 g/cm^2/yr, respectively. Similarly, accretion rates based on the CA and CF ^{210}Pb models were 5.6 and 6.7 mm/yr, respectively, with a corresponding mass accumulation rate of 0.19 g/cm^2/yr. Overall, agreement of ^{137}Cs and ^{210}Pb chronological methods was good at this site.

The Shellpot Creek core did not provide steady-state profiles of ^{137}Cs or ^{210}Pb, precluding computation of ages and accumulation rate using the CA and CF models (**Figure 6; Table 5**). The first occurrence of ^{137}Cs activity was present near the bottom of the core at 96-98 cm, above which there was a broad maximum centered around 70-80 cm. Hence, the entire sediment column must have accumulated after ca. 1954. Based on the depth of ^{137}Cs penetration, accretion and mass accumulation rates are 1.9 cm/yr and 0.60 g/cm^2/yr, respectively. Although the CF ^{210}Pb model yielded an identical accretion rate of 1.9 cm/yr, the sediment inventory of excess ^{210}Pb inventory suggests that most of the ^{210}Pb deposited at this site is not derived from direct atmospheric deposition (see Section C2).

One of the requirements of the constant flux for ^{210}Pb (CF) model is that the initial activity at the surface should be lower with sites of higher sediment accumulation rates. Despite a three-fold difference in sediment accumulation rate among coring sites, there was no relationship between A_o (initial activity) and S (vertical accretion rate) as would be predicted by the CF model. For example, A_o (taken as the 0-2 cm depth interval; **Tables 2-5**), was not lower at sites with a higher sediment accumulation rate. While this result does not completely invalidate the CF ^{210}Pb model, it reveals that this approach may not be the best choice for tidal marsh environments.

An important observation with relevance to chemical contaminant history in the Christina River system is presence of measurable ^{137}Cs activity at the tops of all cores. Given that the global atmospheric flux of ^{137}Cs has been negligible since the early 1980s, this pattern implies that previously deposited ^{137}Cs has been redistributed in the system. Wash-in of soil-bound ^{137}Cs

from the watershed and (or) erosion of subtidal deposits can account for redeposition of ^{137}Cs in river-estuaries. Additionally, bioturbation can rework ^{137}Cs from depth, but the shapes of the ^{210}Pb and ^{137}Cs profiles determined for this study are not suggestive of intense biological mixing. To the extent that ^{137}Cs is an analog for particle-reactive contaminants, its depositional trend suggests that historical pollutants may be undergoing similar processes of reworking and redistribution in the Christina River system.

Table 6 provides the summary information and models for the radioisotopes for the Christina cores. Accretion rates, based on ^{137}Cs, ranged from 0.57 cm/yr at Churchman's Marsh to almost 2 cm/yr at Shellpot Creek. However the data at Shellpot Creek suggest extensive reworking so this rate should be considered tentative, but it does indicate higher accretion than at the other locations. These rates are well within the range of accretion throughout the tidal Delaware Estuary (Sommerfield and Velinsky, unpublished data). At 14 sites in the estuary spanning tidal fresh to marine the range of accretion rates is 0.3 to 1.3 cm/yr with an average of 0.50 ± 0.4 cm/yr (n=32 cores).

In summary, cores BW-2, CM-1, and DM-2 yielded reliable accretion rates with good agreement between ^{137}Cs and ^{210}Pb chronological methods. Because ^{137}Cs was present in the greater extent of the cores, ^{137}Cs-derived accretion rates, using peak concentration interval depth presented in **Tables 2-6,** were used to convert sediment depths to ages for the contaminant and nutrient-eutrophication histories. Dates corresponding to depth intervals within the individual cores appear in **Tables 2-6**. These estimates are a key output of this project and allow us to place the contaminant and nutrient/eutrophication data into historic context.

C1.3: Radionuclide Inventories and Focusing Factors

Sediment inventories of excess ^{210}Pb and ^{137}Cs were computed to compare the relative amount of radionuclide deposited among the four coring sites (CM, DM, BW, and LSP). Because ^{210}Pb and ^{137}Cs have particle-adsorption characteristics not unlike trace metals and some organic contaminants, the sediment inventory of a radionuclide compared to a reference value provides information about contaminant transport pathways and burial in aquatic systems. Reference inventories of 28 dpm/cm^2 for ^{210}Pb and 21 dpm/cm^2 for ^{137}Cs are known from direct measurements of radionuclide atmospheric deposition in the U.S. mid-Atlantic region (Olsen et

al. 1985; Graustien and Turekian, 1986). These reference values represent the total amount of radionuclide that could be buried at a site if supplied by atmospheric deposition alone.

The focusing factor is the ratio of the measured and reference radionuclide inventory. Focusing is the process by which fine-grained materials migrate towards more depositional areas and provide higher inventories that that predicted by reference inventories. To account for this migration, a focusing factor was calculated by comparing the actual ^{210}Pb inventory to the expected ^{210}Pb inventory. A focusing factor greater than unity implies that radionuclide activity has been preferentially transported or "focused" from one location to another by a combination of hydrodynamic flow and sedimentary processes. Conversely, a focusing factor less than unity imply that the atmospheric flux is not sequestered locally perhaps on account of sediment erosion and redistribution. In the case of ^{210}Pb, tidal flooding of a brackish or saline marsh can supply ^{210}Pb in addition to that derived by atmospheric deposition because coastal and estuarine waters usually contain ^{210}Pb activity from non-atmospheric sources. This is not the case in a tidal freshwater system, where all of the ^{210}Pb is atmospherically supplied and focusing occurs through lateral transport of particle-bound ^{210}Pb. ^{137}Cs can be focused in a similar manner as ^{210}Pb, although ^{137}Cs is less particle reactive than ^{210}Pb and tends to desorb from sedimentary particles in brackish and saline waters. Consequently, sediment inventories of ^{137}Cs in freshwater systems tend to be higher than those in estuaries and coastal waters. This must be taken into account when interpreting ^{137}Cs focusing factors for sites that span a wide range of salinities. While our locations can experience low salinities during extreme droughts, it is generally considered a tidal freshwater system as noted by plant communities.

Radionuclide inventories and focusing factors for the four coring sites (CM, DM, BW, and LSP) are presented in **Tables 2-6**. The Brandywine River site (BW-2) had the lowest excess ^{210}Pb inventory and the highest ^{137}Cs inventory among the sites sampled. This result was to be expected given the generally freshwater setting of the site. The ^{210}Pb focusing factor of unity indicates that the sediment column has been accretionary for the period of interest, and that atmospheric deposition is the probable source of radionuclide. In contrast, the ^{137}Cs focusing factor of 2.3 implies a non-atmospheric source of radionuclide, which is difficult to reconcile in light of the ^{210}Pb results.

The Churchman Marsh site (CM-1) had the second highest ^{210}Pb inventory and the lowest ^{137}Cs inventory among the sites. The ^{210}Pb focusing factor of 2.8 suggests that non-

atmospherically derived radionuclide is deposited at this site, perhaps supplied by tidal waters. The ^{137}Cs focusing factor of 0.2 is consistent with loss of particle-bound activity by desorption prior to deposition. The Shellpot Creek site (LSP-2) had the highest ^{210}Pb inventory, several times that of the others, and a ^{137}Cs inventory that was second only to site BW-2. The ^{210}Pb focusing factor of 11.4 suggests influx of radionuclide from tidal estuarine waters, but the ^{137}Cs focusing factor of near-unity is not supportive of an estuarine source. Another possibility is that soil-bound ^{210}Pb and ^{137}Cs eroded from the surrounding landscape and focused at the site. This interpretation is consistent with the site's rapid rate of sediment accumulation (1.9 cm/yr), which most likely results from localized sediment trapping caused by the tidal gate barrier immediately adjacent to the coring site. The Dravo Marsh site (DM-2) had radioisotope inventories and focusing factors within the range of values measured at the other sites.

The focusing factors make clear that the four depositional sites (CM, DM, BW, and LSP) have sequestered ^{210}Pb or ^{137}Cs inventory at levels above that which can be accounted for by atmospheric flux alone. This result confirms that most of the minerogenic material buried at these sites is allochthonous (i.e., transported to the location from elsewhere), and implies that atmospherically sourced, particle-reactive contaminants in the Christina River system will exhibit focusing patterns that depend not only on broad scale atmospheric delivery but also on more regional and local transport processes (e.g., tidal flow and sediment transport). All of the coring sites, although within the Atlantic Coastal Plain, are immediately down gradient from the Piedmont physiographic province. Particles eroded from the Piedmont are transported downstream and later deposited on the Coastal Plain. Contaminants associated with these particles, plus contaminants originating from local sources within the Coastal Plain, and contaminants delivered from tidal exchange, ultimately combine to yield observed profiles in the cores. An important is that the all of the coring sites, while depositional, are subject to both small and large scale processes (i.e., within the tidal waters and from the watershed) that influence radioisotope and contaminant profiles.

C2: Nutrients/Eutrophication

C2.1: Sediment Total Carbon, Total Nitrogen and Total Phosphorus

Sediment total carbon (TC) concentrations for the BW-2, CM-1, and DM-2 cores ranged between <1.0 and 19.8% on a dry weight basis (dw) with an average of 5.5 ± 7.7% TC (±

standard deviation; **Table**s **-11; Figure 7a,b**). Similarly, total nitrogen ranged from 0.1 to 1.2% N with an overall average of 0.40%; while total sediment phosphorus (TSP) ranged from 0.04 to 0.27% TP with an overall average of 0.10%. In the lower Shellpot Creek (LSP) and Walnut Street (WS) cores %TC and %TN averaged slightly lower; 4.3% and 0.29% respectively while TP averaged slightly higher at 0.14% TP.

The three cores, CM, DM, and BW, exhibited different total carbon, nitrogen and phosphorus profiles with depth (**Figure 7a**). In the CM core, TC increased from 1.2% to approximately 7.6% near the surface while in the DM core concentrations increased from 1.0% to 18% near the surface. In the DM core there were two subsurface maxima, one centered at ~ 40 cm (8% OC) and the other centered at ~10 cm of 20% OC. Concentration in the BW core increased only slightly from the bottom (2.2% OC) to the surface (3.8% OC), with a broad subsurface maxima between 20 and 40 cm. Total sediment P increased substantially towards the surface in the CM core (0.06 to 0.18% P) and to a lesser extent in the DM core. In the DW there was no difference between the top and bottom sections in TP concentrations but there was higher concentrations centered around 13 cm of 0.27% P. For the LSP and WS cores, only 5 or 6 sections were analyzed for each. Therefore only limited information is derived from the depth distribution (**Figure 7b**). In the LSP core there was an increase towards the surface of TC and TP while in the WS core concentrations are similar from top to bottom.

The carbon to nitrogen ratio (C/N; atomic units) can be used as a tracer of the source of organic matter to a location and potential diagenetic changes that could occur during burial (Jasper and Gagosian, 1990; Meyers, 1994; Prahl et al., 1994). Diagenesis is any chemical, physical, or biological change undergone by sediment after its initial deposition (Berner, 1980). For example, terrestrial material (e.g., trees) are rich in cellulose (i.e., higher C) compared to algae or marsh plants that have less structural material and are higher in proteins (i.e., higher N). Typical marine plants have C to N ratios of ~ 4-10 while terrestrial material can have C to N values > 15-20. Diagenesis of recent sediments tends to increase the C to N ratio due to preferential remineralization and release of nitrogen compounds; however re-incorporation of bacterially derived N can increase the C to N ratio over time (Fogel et al., 1989; Benner et al; 1991). In the CM core (**Figure 7a**), the C/N ratio changed only slightly with depth and averaged 12.3 ± 1.2, while in the DM core, the C/N ratio increased from 10-13 near the bottom of the core to approximately 18-20 near the surface. In the Brandywine core (BW) the C to N

was more variable (range = 7 to 22), but showed a maxima in the same depth range as the C and N concentrations. In the LSP and WS cores (**Figure 7b**), the C/N ratio were fairly constant (~18) from top to bottom although there were less intervals analyzed. In general the sediments in the cores reflect a dominance of terrestrial sources of organic matter compared to algal sources. Interestingly, the CM core exhibited slightly lower C/N ratios compared to the downstream locations. It would be expected that the ratio may decrease going downstream towards the Delaware Bay where the ratio would be lower (Cifuentes et al., 1988). The change with depth in the DM core, increasing towards the surface along with the increase in OC, might suggest a change in the source of organic matter to this site.

C2.2: Stable Isotopes of Carbon and Nitrogen

Organic carbon and nitrogen isotopic ratios are useful to distinguish between marine and continental plant sources of sedimentary organic matter, processing and cycling of nutrients and in some instances the level of system-wide productivity (Fry, 2006 and others). Most photosynthetic plants incorporate carbon into organic matter using the C3 Calvin pathway, which biochemically discriminates against ^{13}C to produce a $\delta^{13}C$ shift of about -20‰ to -30‰ from the isotope ratio of the inorganic carbon source. C4 plants (e.g., corn, *Spartina*) incorporate CO_2 using a different system (PEP) that discriminates against ^{13}C to produce a $\delta^{13}C$ shift of about -8‰ to -15‰ from the isotope ratio of the inorganic carbon source. Organic matter produced from atmospheric CO_2 ($\delta^{13}C \sim -7$‰) by land plants using the C3 pathway consequently has an average $\delta^{13}C$ (PDB) value of about -27‰ (O'Leary, 1988). The source of inorganic carbon for marine algae (C3 plants) is dissolved bicarbonate, which has a $\delta^{13}C$ value of about 0‰. Marine organic matter consequently typically has $\delta^{13}C$ values between -20‰ and -22‰. The isotopic difference between organic carbon produced by C3 land plants and marine algae has been used to trace the delivery and distribution of organic matter to sediments in estuarine and coastal areas (Cifuentes et al., 1989; Fogel et al. 1992, and many others).

Carbon isotope ratios can be affected by photosynthetic dynamics and by postdepositional diagenesis (Dean et al., 1986; Fogel et al., 1992; Canuel et al., 1995; Zimmerman and Canuel, 2002) and consequently must be interpreted cautiously. A big factor that can impact $\delta^{13}C$ values of plant material is the availability of CO_2 and rate of production during photosynthesis and the possibility of selective diagenesis of organic matter fractions that are isotopically heavy or light.

While the change in $\delta^{13}C$ appears to be small (<2‰) during recent diagenesis (Hayes et al., 1989; Meyers, 1994), shifts due to the availability and rate of production, due to nutrient enrichment or limitation and other factors, can have a large impact on the resultant $\delta^{13}C$ values of deposited organic matter (Fogel et al., 1992; Schelske and Hodell, 1995; Church et al., 2006).

Differences exist between the natural abundances of stable nitrogen isotopes ($\delta^{15}N$, $^{15}N/^{14}N$) in dissolved and particulate matter from terrestrial, estuarine, marine, and anthropogenic sources. Terrestrial occurring soil nitrogen can have a wide range of values, but in general range from -1 to +4‰) similar to atmospheric nitrogen (0‰). Nitrogen isotopic compositions from marine sources tend to be slightly enriched in the heaver isotope (^{15}N) and are very dependent on the source of dissolved nitrogen and its $\delta^{15}N$, and processing in the system (e.g., ammonification, nitrification, denitrification, etc) at the time of formation. A dominant process in many aquatic environments (and groundwater) is denitrification (Cline and Kaplan, 1975). Denitrification is a microbially facilitated process of dissimilatory nitrate reduction that ultimately produces molecular nitrogen (N_2) through a series of intermediate gaseous nitrogen oxide products. This microbial process uses dissolved nitrate during oxidation of organic matter and as nitrate is consumed there is an enrichment of residual nitrate in the system. Algal/plant production and its $\delta^{15}N$ from nitrate would reflect the balance between processes and inputs. There are many points in which nitrogen can be fractionated and its isotopic composition altered. For example, wastewater from treatment facilities have been shown to increase the $\delta^{15}N$ of various fish species (Lake et al., 2001) due to the selective removal of the light isotope (^{14}N) nitrogen during treatment. Anthropogenic nitrogen was substantially enriched in watersheds with greater amount of urbanization and wastewater inputs and the nitrogen was shown to be incorporated into the aquatic food web (McCelland et al., 1997)

The isotopic compositions of sediment C and N exhibited interesting changes within each core (**Fig. 8**). In Churchmans Marsh (CM-1) and Dravo Marsh (DM-1), the $\delta^{15}N$ was lowest in the bottom sections (approx. 4-5‰), increasing towards the surface (up to ~ 8‰). The Brandywine Creek core exhibited little change in $\delta^{15}N$ with depth in the core (5.0±0.4‰ (n=15). The carbon isotopic composition of the sediment ranged from -29 to -23‰ ($\delta^{13}C$ average of -26‰). The $\delta^{13}C$ generally decreased towards the surface from approximately -25‰ near the

bottom of CM-1 and DM-1 to about -28.5‰ at the surface. The $\delta^{13}C$ in the BW core exhibited little change with depth and averaged -24.7 ± 1.2‰ (n=15).

C2.3: Diatom Analysis and Assemblages

Diatoms are microscopic, photosynthetic algae that contain yellow-brown chloroplasts and therefore are also referred to as golden algae. Comprising one of the most common types of phytoplankton, they are found in a diverse range of environments from freshwater to saline oceanic waters. Based upon their shape, diatoms are differentiated between by forms that are centric, i.e. circular, and pennate, i.e. having bilateral disposition of morphological characteristics. They exhibit three main living modes in the environment: 1) planktonic, 2) benthic (i.e., living on or in the bed sediment) and 3) epiphytic.

Diatoms are one of the most powerful water quality indicators; they colonize virtually every aquatic microhabitat and many diatom species have very strict ecological requirements, with well-defined optima and tolerances for environmental variables such as lake pH, nutrient concentration, water salinity and transparency. However, some centric species live in oligotrophic conditions, some benthics in productive environments; what truly works for ecosystem analysis, is the composition of species. Because of their strong relationships to environmental conditions, diatoms are used to derive inference models for such environmental factors. The inference models are developed using calibration sets of both diatoms and measured environmental variables for specific geographic regions. These calibration sets require a large number of sampling sites that maximize the gradient length covered by the variable of interest (e.g., phosphorus concentration, pH, etc.). This is necessary to produce robust quantitative models with high predictive power. These models can then be used to infer the environmental parameter of interest when instrumental measurements are not available and have been successfully used to reconstruct reference conditions and assess the impact of anthropogenic activities on aquatic systems.

Diatom assemblages have been shown to be an important indicator of nutrient concentration within freshwater and marine environments. Due to the fact the diatoms respond quickly and directly to nutrients, they have been used for many years as indicators of nutrient changes in aquatic systems (Potapova et al., 2004; Potapova and Charles, 2007; Ponader et al., 2008). In this study we take a first approach using metrics calculations based on models developed by van

Dam et al. (1994). While this data set is mostly based on freshwater species it does contain some marine diatoms. It provides a first approach to obtain ecological information as a dataset for both diatoms and water characteristics is not available for the Delaware Estuary.

Samples from 41 sections were analyzed for diatom composition from the 3 Christina cores (i.e., BW, CM and DM). At least 500 valves were counted for each sample and over 250 taxa (**Appendix I**) were identified from the samples allowing a robust analysis for nutrient and ecological conditions. The distribution of key diatom species in each of the cores is presented in **Figure 9a,b,c** and below is a brief description of the species distribution for each core:

<u>Dravo Marsh.</u> From the bottom of the core to approximately 25 cm (~1974), brackish and marine diatom species are dominant (*Cyclotella striata, Actinocyclus normanii, Raphoneis amphiceros*, etc.). This type of assemblage is replaced by an assemblage with high nutrient indicator freshwater benthics, such as *Navicula gregaria, N. recens, and N. germanii*. From about 12 cm (~1990) to the surface, planktonic species *Cyclotella meneghiniana* and *C.* cf. *distinguenda* are increasing in abundance while marine species are very rare during this time interval.

<u>Brandywine Creek</u>. Between the bottom of the core to approximately 36-38 cm (~1960), brackish-marine species (e.g., *Cyclotella striata, Delphineis minutum, Actinocyclus normanii*) are dominant. Above this interval they are replaced by eutrophic freshwater species, such as *Fragilaria vaucheriae, Nitzschia amphibia,* and the planktonic *Cyclotella meneghiniana*. Between 24-26 cm (~1975) and 14-16 cm (1987), a short, more marine flora is present that occurred before 1954 but this time in co-occurrence with more abundant freshwater species (e.g., *Aulacoseira granulata, Nitzschia palea, Eunotia tenella*). Above 14-16 cm, species indicating high nutrient levels such as *Nitzschia frustulum, Navicula salinarum, N. gregaria,* and *Cyclotella atomus,* are dominant.

<u>Churchmans Marsh</u>. This core displays a more complex dynamic with brackish-marine species from the bottom of the core to the 24-26 cm interval (~1965), however there were also intervals with more abundant *Cyclotella striata* and *Raphoneis amphiceros*. Above 42-44 cm (~1935), some freshwater eutrophic species also display increases, such as *Nitzschia brevissima* and *Fragilaria vaucheriae*. Above 24-26 cm (~1965), marine–brackish species *Actinocyclus normanii*, *Fallacia pygmaea*, *Cyclotella striata* increase in abundance in co-occurrence with high nutrient freshwater species *Cyclotella meneghiniana, Nitzschia brevissima*, and *Navicula gregaria*. The top of the core displays highly abundant *Cyclotella atomus and Diadesmis contenta*, indicating lower water levels.

To place the Christina Basin diatom data into broader context, various metrics were first calculated using salinity, pH, nitrogen uptake metabolism, and the trophic state from different data sets (van Dam et al., 1994; USGS NAQWA, EPA's National Lake Assessment (NLA)). The samples collected in the tidal Christina span a range of marine brackish to freshwater, making detailed analysis complex. These data sets used for ecological condition analysis are

mainly derived from freshwater systems from rivers and streams in the U.S. or an eastern United States NAWQA-derived subset (NAWQA and NAWQA East), or from more than 1500 lakes sampled within the NLA. All of these metrics have strengths and weaknesses due to the inclusion or omission of species detected in each of the cores. Because most of marine or brackish species present in the Christina River are not occurring or are very rare within the NAWQA and NLA data sets, metrics calculations were based mostly upon the freshwater species occurring in these cores. These were based primarily on the van Dam et al. (1994) summary and synthesis of ecological characteristics of taxa observed in Western Europe, and generally found to have wide geographic application. The van Dam et al. (1994) autecological values for many taxa have been revised to be more relevant for the U.S., and are contained in a data compilation developed for the USGS NAWQA program by Porter (2008) and Porter et al. (2008). To allow a comparison between the current study in the tidal Christina River and the previous study of the tidal Saint Jones River (Velinsky et al., 2007), the data set and metrics by van Dam et al. (1994) will be the focus of this discussion.

The diatom community composition based on the van Dam et al. (1994) metrics show an increase in the proportion of eutrophentic species (i.e., high nutrient species) starting between 30 and 40 cm towards the surface of the core (**Figure 10; Tables 12-14**). Below this depth range, the proportion of mesotrophentic species increases slightly. Interestingly, oligotrophentic species were only randomly detected throughout each of the cores.

To evaluate how nutrient conditions, as reflected by total sediment N and P, impacted the diatom species and metrics in each core, N and P were plotted against the metric for eutrophic species (**Figures 11-12**). For the Brandywine Creek core, there was no relationship between N or P and the diatom metric. In the Dravo Marsh and Churchmans Marsh cores, there was a good relationship between sediment N and P and the diatom metric. The r^2 for N for both cores averaged 0.77 while for P the r^2 averaged 0.51.

Historical Analysis: Concentrations of total sediment N and P exhibited interesting trends within each core over time (**Figures 13-14).** In CM, total N increased from approximately 0.3 to 0.79% starting in the last 1950s. Similarly, in DM, concentrations of TN increased from approximately 0.2 to 1.2% starting in the early 1960s. In the BW, sediment TN increased slightly over time, from 0.19±0.04% before 1960 to an average of 0.35±0.09% after 1963. It is possible that

sediment remineralization processes, with the remobilization of bound N to dissolved N, is occurring after burial in the sediment (Burdige, 2006). This would decrease the sediment levels of TN with time, and could result in an increase in the C to N ratio as N is preferentially remineralized. The changes in C/N with depth (and time) in these cores is not apparent (**Figure 7a; Tables 7-11**). In addition, the stable isotopic composition of the sediment N (δ^{15}N-TN) increases to varying degrees in both cores (**Figure 13**). The increase starts in the mid-1950s in CM and in the mid-1960s in DM, both increasing from about 4-6‰ to approximately 8‰ at the surface. This suggests that there was an increase in loadings to these marshes and that the source(s) of N may have changed over time. Leavitt et al. (2006), Ulseth and Hershey (2005) and Velinsky (unpublished data) show that higher δ^{15}N of the nitrogen is associated with higher inputs from urban sources. Bratton et al. (2003) showed similar trends in deep cores from the Chesapeake Bay. Lastly, this is a similar trend observed in a Woodbury Creek (NJ) marsh (Church et al., 2006). Therefore, the increase in N concentrations, along with near constant C to N ratios, coupled with an increase in δ^{15}N-TN, indicate that N loadings have increased over time and appear to continue to increase.

Schelske and Hodell (1991; 1995) and Perga and Gerdeaux (2004) have shown a relationship between the concentration of P in the sediments or water and the isotopic composition of carbon (δ^{13}C-TC) in the sediments or in fish scales over time. The fish scales were an integrator of the top of the pelagic food web (i.e., phytoplankton). In brief, it is proposed that as P levels increase, primary productivity increases to a point at which there is reduced isotopic fractionation during enzymatic uptake of dissolved CO_2. This reduced fractionation would result in higher isotopic compositions of organic matter (i.e., more ^{13}C enriched) and would suggest that P was helping to control aquatic productivity. Recently, Church et al. (2006) showed a similar trend and relationship in a sediment core from Woodbury Creek, NJ.

In CM there is a gradual increase in TP concentrations starting in the early part of the last century with peak concentrations in 1980 (**Figure 14**). Concentrations decreased afterwards then increased again at the surface. In the BW core, there was a peak in concentration in 1990 while the DM core exhibited a small peak in the 1950s and then increasing concentrations from the 1980s to the present. This time-concentration profile may reflect P usage, especially in detergents (Litke, 1999; Church et al., 2006) as well as other sources such as fertilizers and agricultural runoff, although there is no clear distribution. As with nitrogen, phosphorus can

undergo substantial diagenetic processing related to the carbon, iron and sulfur cycle (Burdige, 2006). These factors make it difficult to accurately interpret the P distributions.

Figure 15 shows the distribution of total sediment P and the isotopic composition of organic matter from the three primary cores (CM, DM, and BW). The BW core shows no relationship while the CM core data indicates a relationship of increasing P with decreasing sediment $\delta^{13}C$. In the DM core, there appears to be two relationships, one at low TSP (increasing P, increasing $\delta^{13}C$) and from 0.06% to 0.10% of increasing P and decreasing $\delta^{13}C$. It is unclear at this point what is causing these relationships (or what they are telling us) but it is possible that changes in the source of organic matter to the marshes (i.e., terrestrial-upland material versus *in situ*-local production) may have changed over time. In both CM and DM sites, the $\delta^{13}C$ decreased (became more negative) since the 1930s (**Figure 15**), which may be an indicator of the development and land use changes in the watershed.

The diatom metrics used to assess eutrophication for each core were plotted against time in **Figure 16**. It appears that starting in late 1950s to early 1960s, the proportion of species that are indicators of high nutrient conditions increased substantially in the DM and CM cores. The increase in the metric corresponded to an increase in N and P sediment concentrations (see above), except for the Brandywine site.

Preliminary analysis of the diatom assemblages and metrics indicate a shift toward more eutrophic species starting in the late 1940-1950s. The proportion of mesotrophic and especially oligotrophic diatom indicators was low throughout the cores. There was a strong positive relationship between the eutrophic diatom metric and the concentration of nitrogen and phosphorus in Churchmans and Dravo marshes. This, along with the increases in total sediment N, total sediment P and sediment nitrogen isotopic compositions ($\delta^{15}N$-TN), indicates that increase loadings of nutrients have resulted in a diatom shift in the river.

C3: <u>Sediment Bound Contaminants</u>

Selected sections from each core were analyzed for a suite of sediment bound contaminants including polycyclic aromatic hydrocarbons (PAHs), polychlorinated biphenyls (PCBs), and specific organo-chlorine pesticides (e.g., DDXs, chlordanes, etc). Three cores were also analyzed for a suite of polybrominated diphenyl ethers (PBDEs). Lastly, core sections were analyzed for strong acid leachable concentrations of zinc (Zn) and iron (Fe).

C3.1: Polycyclic Aromatic Hydrocarbons

Polycyclic aromatic hydrocarbons (PAHs) are a large group of organic chemicals with two or more fused aromatic rings. They have a relatively low solubility in water and have a range in lipophilicity and, in general, adhere to organic particles in water and air. Specific PAH compounds can be carcinogenic and mutagenic to various aquatic organisms at different life stages. PAHs are formed mainly as a result of pyrolytic (combustion) processes, especially during the incomplete combustion of organic materials during industrial and human activities; e.g., processing of coal and oil, vehicle traffic, combustion of oil and gas, and the combustion of refuse. There are a few hundred PAH compounds with a few naturally occurring such as perylene, however most are from anthropogenic sources (e.g., benzo[a]pyrene). Sources to estuarine environments, such as the tidal Christina River, include sewage and industrial discharges, oil spills, bulkheading with creosote wood products, combustion of fossil fuels, and treatment of parking lots with sealcoat. Atmospheric deposition is also a significant source of PAHs to the environment but in the urbanized Christina watershed is most likely not the dominant source.

The sources and nature of hydrocarbon geochemistry can be revealed by the distribution of the individual compounds that comprise saturated (SHC) and aromatic hydrocarbons (PAH) (Farrington, 1980; Hites et al., 1980; Wakeham et al., 1980; Boehm and Farrington, 1984; Boehm, 1984; Pruell and Quinn, 1985). Within the aromatic hydrocarbons, the various alkyl-substituted naphthalenes (i.e., C_1, C_2, C_3) have not been found in organisms and are thought to be derived from petroleum contamination. PAHs can also help discriminate between combustion sources of hydrocarbons and those derived by the direct discharge of oil. Oil contains a greater percentage of alkyl-substituted compounds in the naphthalene, phenanthrene-anthracene, and chrysene series. Refined petroleum products would have a greater abundance of lower than higher molecular weight compounds. The partial combustion of oil reduces the amount of alkyl-substituted compounds leaving the parent structure in greater abundance (Youngblood and Blumer, 1975). Some of the general differences between biogenic and petroleum sources of hydrocarbons are summarized below. These differences will be exploited in the following discussions in evaluating the source of hydrocarbon contamination to the sediments of the various study areas.

General Characteristics of Biogenic and Petroleum Hydrocarbons*.

Natural Biogenic Hydrocarbons

- Narrow range of molecular weight distribution of SHC and PAH (if present), UCM is either low or absent. Odd- to even-numbered alkane ratio is > 1.
- Terrestrial plant material indicated by an alkane distribution from nC_{23} to nC_{34}, centered around nC_{29} or nC_{31}.
- Aquatic organisms have a predominance of nC_{13} to nC_{21} alkanes with greater amounts of odd-numbered compounds.

Fossil Fuel or Petroleum Hydrocarbons

- Wider range in molecular weight distribution of both SHC and PAH, UCM is present in large amounts compared to alkanes and PAHs.
- Odd- to even-numbered alkane ratio = 1.
- Several homologous series with adjacent members in approximately the same concentrations.
- Natural source sources of PAH indicated by less complex distribution with compounds related to structure of precursors (i.e., perylene and retene).
- Direct discharge of oil is indicated by PAHs (e.g., naphthalene, phenanthrene-anthracene, and chrysene series) contains many alkyl-substituted species (i.e., C_1, C_2 and C_3). Greater abundance of lower molecular weight PAHs.
- Combustion products have a greater abundance of un-substituted parent compounds, with homologs which decrease in abundance as the degree of alkyl substitution increases.
- UCM present in greater proportion than resolved peaks.

* Taken from Youngblood and Blumer, 1975; Farrington, 1980; Hites et al., 1980; Wakeham et al., 1980; Boehm and Farrington, 1984; Boehm, 1984; Pruell and Quinn, 1985; Pierce et al., 1986. (SHC – saturated aliphatic hydrocarbons, UCM – unresolved complex mixture; PAH – polycyclic aromatic hydrocarbons)

Low versus high molecular weight PAHs ratios (i.e., LMW and HMW PAHs) are indicative of the input sources of hydrocarbons (Farrington 1980; Boehm and Farrington 1984). Low molecular weight PAHs are defined as 2 to 3 benzene ring compounds, including naphthalenes, anthracenes, phenanthrenes, and dibenzothiophenes. High molecular weight PAHs, with 4 to 5 benzene rings, include compounds such as fluoranthenes, chrysenes, benzo[a]pyrene and dibenz[ah]anthracene. A predominance of LMW over HMW PAHs indicates an oil source of hydrocarbons (Farrington 1980; Boehm and Farrington 1984). Due to weathering and degradation processes, with time LMW PAHs would decrease in abundance relative to HMW PAHs. Also, the combustion of petroleum yields PAHs with more HMW compounds.

Polycyclic aromatic hydrocarbons (PAHs) were detected in all samples analyzed. PAHs comprised 34 individual compounds ranging from the low molecular weight compounds such as naphthalene and phenanthrene (2- and 3-rings) to high molecular weight compounds with 4- and 5- rings, including pyrene and dibenz[a,h]anthracene. Total PAHs (methyl-substituted and unsubstituted forms) ranged from 0.25 to 26.8 μg/g dw among all cores (**Tables 7-11; Appendix I**) with some differences in the distribution with depth (**Figure 17**). The concentrations in the

tidal Christina River were similar to other urban environments such as the tidal Anacostia-Potomac rivers and Baltimore Harbor (Wade et al., 1994; Ashley and Baker, 1999; Riedel et al., 2007), and were lower than those found in the Saint Jones River, Delaware (Velinsky et al., 2007).

Concentrations in CM-1 (Table 8 and Figure 17) were low near the surface (1.68 μg/g dw) increasing to a maximum concentration of 26.8 μg/g dw at 36-38 cm (corresponding to 1945) with the lowest concentrations (<0.5 μg/g dw) near the bottom (pre-1900). In the Dravo Marsh core (DM-2), PAH concentrations were similar overall to the CM core, but the DM core did not exhibit a single strong peak at depth like the CM core. Rather, the DM core showed two smaller peaks. One maxima (8.1 μg/g dw) was at 12-14 cm (circa. 1990) and a deeper maxima (6.5 μg/g dw) was centered around 36-38 cm (circa. 1958). Dual peaks were also seen in the DM core for PCBs about these same dates (see next section). The general rise up to the earlier PAH peak in the DM core appears to have begun as early as 1905. Concentrations near the bottom of the DM core, which date back prior to 1900, ranged from 0.25 to 0.34 μg/g dw, making these pre- turn of the century values consistent with those seen at the bottom of the CM core. The PAH concentrations in these deep sections of the CM and DM cores reflect PAH concentrations that existed just prior to rapid industrial expansion.

The Brandywine Creek core (BW-2) was shorter in length than the other cores and was similar in concentration to the DM core concentrations overall. Further, the PAH concentration at the surface of the BW core (1.68 μg/g dw) were similar to the other two cores at the surface (~ 2-2.7 μg/g dw). Slightly higher concentrations (8.0 to 9.0 μg/g dw) were seen in the BW core between 20 and 30 cm (~1979 to ~1968). Total PAH concentrations near the bottom of BW-2 (between 46 and 52 cm, corresponding to 1944 to 1939) were similar to surface concentrations.

PAH concentrations in the WS core showed little variability from the top of the core to the bottom of the core (Table 11 and Figure 17). The mean and standard deviation among the six intervals analyzed within that core were 9.9 and 1 μg/g dw, respectively. Although we were not able to successfully radiodate this core, it is clear that there is substantial PAH contamination in the sediment deposit from which this core was collected. Similarly, there appears to be considerable PAH contamination in the LSP core (Table 10 and Figure 17), although the vertical profile is not well defined. The mean PAH and standard deviation among five samples collected

from this core were 9.1 and 7.5 μg/g dw, respectively. The maximum PAH concentration in this core was 19.5 μg/g dw, which very roughly corresponds to 1970.

The general increase in PAH in the DM core that began shortly after the turn of the century and continued until ~1958, followed by a 10- to 15-year drop, may be associated with the rise and fall of the shipbuilding industry immediately downstream from the Dravo Marsh (Thompson and O'Byrne, 1999). In addition, the PAH pattern in the DM core may also have been influenced by releases from the nearby Wilmington Coal Gasification Plant, which contaminated nearby surface and subsurface soils and groundwater (DNREC, 2004). It is unclear why the DM core shows a more recent increase from ~1955 to ~1990, followed by a drop. One possible explanation is extensive redistribution of previously contaminated soils and sediments during major roadwork projects (e.g., I-95 and SR-141) or other land disturbing activities in and near DM.

With regard to the CM core, the extremely sharp rise and equally fast fall centered on 1945 suggests there may have been a significant release or spill of petroleum into the tidal Christina about that time. The fact that a significant proportion of PAH mass was lower molecular weight material (Figure 17) tends to support that hypothesis. The idea that lower molecular weights PAHs are often associated with petroleum rather than combustion sources is discussed in more detail below.

As noted earlier, 34 individual compounds were summed to calculate the total PAH (tPAH) fraction. These compounds ranged from 2-ring compounds such as naphthalene to 5-ring aromatic compounds such as di-benzo[a,h]anthracene (**Table 12; Appendix I**). Also included within the 34 individual PAHs are 6 methyl-substituted forms including methylnaphthalene, methylfluorene, and methylphenanthrene. Both the distribution of parent PAHs and methyl-substituted PAHs can be used to help determine the sources of hydrocarbons to the tidal river (i.e., combustion or petrogenic sources). For instance, the phenanthrene to anthracene ratio can be used to help distinguish between combustion (pyrogenic) versus direct oil (petrogenic) sources in aquatic systems since undegraded oil has a very high ratio (50) compared to combustion sources (ca. 0.3; Wakeham et al., 1980; Wade et al., 1994; O'Malley et al., 1994 and 1996; Neff et al., 2005). In CM-1, the phenanthrene to anthracene ratio ranged from 0.1 to 19 (excluding one duplicate value of 176) which are characteristic and typical of many urban environments having a preponderance of combustion sources (Gschwend and Hites, 1981;

Hoffman et al., 1984; Van Metre et al., 2000; Velinsky et al., 2008). The highest ratios were near the surface (19 at 8-10 cm) suggesting more of a petrogenic source to this horizon; interestingly this did not correspond to the peak concentration of tPAHs (**Figure 17**).

The ratio of low molecular weight PAHs to total parent PAHs (LMW:tPAHp); **Figure 17; Tables 7-12, Appendix I**) is also an indicator of petrogenic versus combustion sources. In CM-1, the baseline ratio ranged from approximately 0.1 to 0.2 with peak ratios (0.4 to 0.7) centered on the peak in tPAH concentrations (36-38 cm). This suggests that the sharp peak in PAH concentrations at 36-38 cm (circa. 1945) is more petrogenic in nature and may have resulted from a spill near this site as noted above.

For core BW-2, the phenanthrene to anthracene ratio varied considerably with depth and ranged from <1 to 280. While the highest ratio was observed near the surface, generally higher ratios were found below 25 cm indicating somewhat greater petrogenic sources in the past. High ratios of phenanthrene to anthracene with occasionally low ratios of fluoranthene to pyrene near 0.38 suggests the presence of diesel fuel in at least some of the BW samples (Neff et al., 2005). However, LMW to tPAHp ratios were low at depth (<0.3) more suggestive of a primary combustion source in the distant past. Highest LMW to tPAHp ratios were observed near the subsurface concentration maxima near 20-22 cm (**Figure 17**). It is unclear why these two indicators did not correspond to each other but the ratio of LMW to tPAHp may be more sensitive since it integrates a broader range of compounds. However, it is possible that variable sources of PAHs (various fuel oils, coal based compounds, etc) could have different ratios and their relative loadings may have changed over time.

The Dravo Marsh core (DM-2) had both low phenanthrene to anthracene and LMW to tPAHp ratios from the surface to the bottom of the core. The ratios ranged from 0.2 to 2 and 0.1 to 0.2, indicating that this site was dominated by more combustion-related sources than the other locations. As noted previously, a coal gasification plant operated immediately downstream of the DM coring site for decades (DNREC, 2004), possibly helping to explain the strong pyrogenic signal in the DM-2 core.

Recently, Mahler et al. (2005) and Van Metre et al. (2009) proposed that the ratios of benzo[a]pyrene to benzo[e]pyrene and fluoranthene to pyrene be used as an indicator of coal-based sealcoat used for parking lots. They illustrated that in many locations these ratios suggested that coal-based sealcoat is a dominant source of urban PAHs to various waterways

(Mahler et al., 2005; Van Metre et al., 2006, 2009). Figure 18, taken from Van Metre et al. (2009), illustrates the potential urban sources of PAHs from *in situ* samples from various locations. The ratio of these pair of compounds in stream/lake samples compared to coal-based seal coat suggests that this material is a major source in urban areas. For this study, we plotted only the top part of the core, i.e., the more recent sediment sections, to help determine source functions in the Christina watershed (**Figure 19**). The average ratios for benzo[a]pyrene to benzo[e]pyrene and fluoranthene to pyrene are 0.90±0.53 and 0.99±0.19, respectively, suggesting that coal-based seal coat material is not a major source to the sediments in this area.

Overall, there are both pyrogenic and petrogenic sources of PAHs to the sub-surface sediments of the tidal Christina basin. Sources of PAHs related to urban areas include tire wear; crankcase oil; bus, train and car soot and exhaust; old coal gasification plants; petroleum spills and releases; and possibly seal-coat material (Wakeham et al., 1980; O'Malley et al., 1994; Van Metre et al., 2009). In addition, in core CM-1 and, to a lesser extent, BW-2, there also appears to be an input of petrogenic hydrocarbons dominated by low molecular weight compounds such as phenanthrene, anthracene, and fluoranthene as well as a number of methyl-substituted compounds like 2-methylphenanthrene, 2-methylanthracene, 1-methylanthracene, 1-methylphenanthrene, 9-methylanthracene and 4,5-methylenephenanthrene. These lower molecular weight PAHs are generally more toxic than their higher molecular weight counterparts (Neff et al., 2005; Di Toro and McGrath, 2000).

Van Metre et al. (2000) showed that in cores from different urban environments a shift from uncombusted to more combusted sources of PAHs with decreasing depth (and time). We did not observe this general trend in the Christina but did see a change in sources at specific layers and time.

Historical Analysis: Total PAH concentrations in CM were highest in the mid-1940s (26 μg/g dw) decreasing to lower levels by 1950 and remaining nearly constant since the 1960s (1.4 to 2.5 μg/g dw) to the present (**Figure 20**). Concentrations in core DM showed a bimodal distribution with time with high concentrations around 1955 (6.5 μg/g dw) and in the 1990s (8.1 μg/g dw). After this date, concentrations decreased to 3 μg/g dw at the surface. At BW, the chronology only goes back to the late 1930s and exhibits a bimodal peak from the late 1960s to late 1970s after which concentrations decreased to somewhat lower levels (2-4 μg/g dw).

It is difficult to determine the exact source(s) of PAHs to these cores, but the general development and urbanization/industrialization of the area is the most likely general contributor (Wakeham et al., 1980; Gschwend and Hites, 1981; Wade et al., 1994; O´Malley et al., 1994; 1996; Mahler et al., 2005; Van Metre et al., 2000; 2009). In the CM core, the significant peak in concentration in the 1940s is also when the LMW/tPAHs (**Figure 17**) increased to 0.65 (fraction) suggesting a more distinct petroleum input at this time. The other cores (with the occasional exception in the BW core) generally show a low ratio (0.2 to 0.4) of LMW/tPAH, thus indicating more of a combustion source overall. However, near the CM site, at the confluence of the White Clay Creek and Christina River, was the 130-ha Koppers Company Facilities that operated a wood preserving facility from 1922 to 1971. The facility pressure treated wood with creosote (and some pentachlorophenol). The peak in PAH concentration in the mid-1940s at CM appears to be primarily a signature of this operation. Finally, in the recent sections of all cores, specific PAH ratios (Mahler et al., 2005; Van Metre et al., 2009) indicate asphalt seal-coat as a potential source to the river but this does not appear to be a dominant source as suggested by Van Metre et al. (2009) as in other riverine systems.

C3.2: Polychlorinated Biphenyls

Polychlorinated biphenyls (PCBs) were mainly produced by the Monsanto Corporation from 1930 to 1977 and it is estimated that 5.4×10^8 kg has been produced within the United States (Kennish, 1992). They are or have been used as electrical insulators in many transformers, fire retardant, and additives to oils and paints. There are 209 congeners (or compounds) of PCBs based on the position and number of chorines on the biphenyl structure. As a result, the physical and chemical properties of this group of congeners vary greatly in the environment (ATSDR, 2000). Persistence of PCBs in aquatic sediments is due to their slow rate of degradation and vaporization, low water solubility, and partitioning to particles and organic carbon. Bacteria degrade PCB, with the rate dependent on the position and degree of chlorination of the biphenyl ring and in many cases the absolute concentration present in the sediments (Kennish, 1992 and others). Current sources to this area are thought to be from contaminated sites, runoff from old landfills and accidental spills (e.g., transformer fluids). Recently, Greene (2009a,b) characterized PCB concentrations in water, sediment, and biota of the tidal Christina River at three sites near the coring sites described in this study (Newport, Walnut Street and

Brandywine). This study along with previous studies in the Christina watershed (e.g., DNREC, 2005) will be used to compare data from the current study.

For the present study, total polychlorinated biphenyls (tPCBs) were calculated as the sum of approximately 110 primary congeners (compounds) that were quantified either individually or as coeluters with multiple (2 or 3) congeners (**Tables 7-11; Appendix I**). Among the three marsh cores (CM-1, DM-2, and BW-2), concentrations of tPCBs ranged from 2.2 ng/g dw (near the method detection limit of ≈1.2 ng/g dw; calculated as the mean plus three times the SD of the blanks) to approximately 2107 ng/g dw with an overall median concentration of 122 ng/g dw (**Tables 7-11; Figure 21)**. The Churchmans Marsh core had the maximum concentration (2107 ng/g dw). The peak in the Brandywine core was 685 ng/g dw and that in the Dravo Marsh core was 436 ng/g dw. The surface concentrations in these three cores ranged from 45 to 238 ng/g dw, which is generally consistent with the range observed by Greene (2009a) for surface sediment samples collected in 2007 in the tidal Christina Basin. The peak surface concentration (238 ng/g dw) was observed in the Dravo Marsh core.

The onset of elevated PCB concentrations in the CM core occurred at 42-44 cm, which, based on age dating, corresponds to approximately 1935. This correlates well with the first commercial production of PCBs in the U.S. (1929). Detections of PCBs in the CM core prior to that time are attributed to sediment reworking and possibly downcore diffusion. A sharp peak in PCB in the CM core occurs at 28-30 cm, which translates to approximately 1959. This is roughly a decade prior to the 1970 peak in U.S. production, suggesting that local usage did not perfectly track overall U.S. production. After the CM peak in 1959, PCB concentrations in the CM core steadily decreased to the surface.

The BW core also exhibited a clear onset at depth, peak, and then decline in PCB concentration towards the surface. The onset in that core occurred at 32-34 cm (circa. 1963), and the peak occurred at 14-16 cm (circa. 1987). These dates are significantly later than those seen in the CM core, suggesting different loading histories.

The PCB profile in the DM core is more complex than the CM and BW cores. The DM core exhibits a bimodal distribution in PCB concentration, showing two separate peaks. The onset of the first peak occurred at 48-50 cm (circa. 1942), with the actual peak seen at 36-38 cm (circa. 1958). These dates track the CM core fairly well. After 1958, the PCB concentration in the DM core fell and remained below 50 ng/g dw for at least a decade. Then, concentrations began to

increase again in the late 1970s, rising to a second peak at 10-12 cm (circa. 1992) that was similar in magnitude to the first peak. PCB concentrations in the DM core have fallen somewhat since 1992 but surface concentrations remain high relative to the surface concentrations in the CM and BW cores.

Total PCB concentrations in lower Shellpot Creek (LSP) core ranged from 303 to 3460 ng/g dw and from 76 to 236 ng/g dw in the Walnut Street Bridge boat slip core. The highest concentrations in LSP were observed at 70-72 cm depth interval, which corresponds approximately to 1970. As noted previously, radiodating of the LSP core was not ideal, and so a date of 1970 is only a rough approximation of when the peak PCB concentration in this core occurred. Radiodating of the Walnut Street boat slip core was even more problematic, primarily because this location is subject to non-steady runoff and heavy shoaling. It is interesting to note however, that PCB concentrations in this core did not vary greatly along its length, which represents nearly 100 cm (or roughly 3 ft) of accumulated material. Although the area from which this core was collected may be small in terms of surface area, it appears to contain a significant inventory of PCB mass. Additional testing would be needed to quantify that mass. The other interesting feature of the Walnut Street core is that the surface concentration (197 ng/g dw) is quite similar to the surface concentration of the Dravo Marsh core (238 ng/g dw). These 2 cores are located within a mile and a half of each other, helping to explain the similarity.

To provide additional insights into the PCB core profiles, the 110 congeners determined in the study (excluding the monochlorinated congeners 1 and 3) were grouped into homolog groups (from 1 to 10) based on the number of chlorine atoms substituted on the biphenyl ring (e.g., homolog group H5 contains measured congeners with 5 chlorines; **Appendix I**). In addition, the homologs were summarized into low molecular weight congeners (LMW; i.e., H1 to H5) and high molecular weight congeners (HMW; i.e., H6 to H10). Important in this analysis is the assessment of blank levels given an MDL for tPCBs of approximately 1.2 ng/g dw. It is important to note that at low concentrations (those approaching values of 10 times the MDL, 10 ng/g dw, or lower) which are characteristic of lower portions of cores, congener profiles become less reliable as an accurate representation of true congeneric PCB patterns. However, for completeness, those low concentration profiles have been included in the following analysis.

For simplicity, the ratio of the LMW PCBs to the total PCBs along the CM, DM, BW, LSP and WSC cores are presented in **Figure 22a,b**. The changes in the LMW to tPCB ratio along

with homolog patterns reveal consistent changes with depth in the cores. In the CM and DM cores, the LMW to tPCB ratio was approximately 0.3 to 0.4 in the upper 30 cm or so decreasing from 0.2 at 35-40 cm to 0.1 between by 56 cm in the CM core and to 0.16 by 42 cm in the DM core. In the BW core, the ratio is more variable in the surface 30 cm ranging from 0.47 at the surface to 0.53 at 12-14 cm, and then decreasing to a minimum of 0.34 at 32-34 cm. Below this depth concentrations are near the detection limit and, as such, the ratio increases substantially. The ratio appeared not to change relative to the peak in concentrations in the CM and DM cores, however, the peak concentration in the BW core at 14-16 cm (circa. 1987) is also where there was a slight increase in the ratio (0.53), suggesting a change in source at this depth. In the LSP and WSC cores, higher molecular weight congeners dominate all sections with a LMW:TPCBs ratio of ~0.2.

To further illustrate the compositional change in each core with depth, the homolog patterns for selected sections are presented in the lower graphs in **Figure 22a** for CM, DM and BW. In the surface sections of CM and DM, the homolog patterns are similar, with a dominance of H4 to H6 with lesser, but still significant amounts of H7 to H10). In contrast, in the BW surface sections, the PCB distribution is dominated by H4 through H8 with very little H9 and H10. In the middle sections of the CM and DM profiles, the congener pattern shifts to homologs of higher molecular weight (H8 to H10), potentially suggesting a common historic source influencing both of these cores. Only in the deepest sections of the CM and DM cores does the strong H8 to H10 signal disappear. The BW PCB homolog distribution with depth does not show the higher molecular weight homologs (H8 to H10). Rather, the deeper sections of the BW core show slightly lower molecular weight homolog groups. Finally, in the lower Shellpot Creek and Walnut Street cores, while fewer sections were analyzed, differences are evident (**Figure 22b).** The homolog pattern in the LSP is dominated by H6 and H7 congeners throughout the core (n=5), while the WS core contains higher levels of lower molecular weight congeners in the H4 to H6 homolog groups.

Returning to the issue of high molecular weight homologs in CM and DM, it is noted that a high percentage of H8 to H10 is somewhat unusual and inconsistent with homolog patterns known to exist in commercial PCB Aroclor mixtures (Rushneck et al., 2004). **Figure 23** isolates the concentration of deca PCB (H10) in the three cores (CM, DM, and BW). Concentrations range from near detection level (<0.1 ng/g dw) up to a maximum of 167 ng/g dw. The highest

values were found in the CM core, followed by intermediate values in the DM core, and finally low levels in the BW core. The peak in the CM core occurred in the intervals 28 to 38 cm, corresponding to 1960, while the peak in the DM core occurred at 12 to 22 cm, corresponding to 1985. Interestingly in the DM core there was a deeper maximum of 49 ng/g dw for PCB 209 at 36-38 cm which corresponds to 1960. Surface concentrations of deca PCB were 13, 35, and 1.5 ng/g dw in the CM, DM, and BW, respectively.

Greene (2009a) also reported unusually high percentages of deca PCB (H10) in surface sediment samples collected from the tidal Christina River. Based on the work of Baker et al. (2004) and EPA administrative records, Greene (2009a) attributed the strong deca PCB in the sediments of the tidal Christina River to inadvertent formation of deca PCB during the production of titanium dioxide at a nearby factory in Edge Moor, DE. Superfund administrative records indicate that dust slurries produced at the Edge Moor factory were later handled at a pigments plant in Newport, DE. Those dust slurries are thought to have contained deca PCB. The handling of those materials at the Newport pigment plant along with the discovery of high levels of deca PCB in the nearby CM core provides a linkage between the Edge Moor factory, the Newport pigment plant, and deca PCB contamination in the tidal Christina River. The fact that a strong deca PCB signal was also found in the DM core indicates that at least some of the source material was transported and smeared downstream in the Christina.

Historical Analysis: Concentrations of tPCBs in all cores started to increase after 1930 with highest values after the 1950s through to the present (**Figure 24**). Total PCB concentrations in CM were highest in the late 1950s (2100 ng/g dw), decreasing to 90 ng/g dw by 2006 (**Figure 24**). In DM, there was also a peak in the late 1950s (~400 ng/g dw) and a more recent peak at 1992 of 440 ng/g dw), following the same general bimodal behavior as PAHs (see above). Surface and near surface concentrations of PCBs in DM remained elevated ranging from 240 to 360 ng/g dw. The tidal Brandywine Creek core (BW) concentration-date distribution reflects a source or sources of PCBs that increased in the 1960s with peak inputs in the 1980s up to 1990 (**Figure 25**). Total PCB concentrations were highest around 1988 at 660 ng/g dw, after which concentrations decreased substantially to <50 ng/g dw by 2001. This distribution indicates that one or more dominate sources on the Brandywine were discharging PCBs well after pollution controls (mid to late 1970s) were in place to limit PCB discharges.

The distribution of tPCBs with time in each of the cores appears to reflect sources within each tidal river and the geographic location of each site may act to trap the source(s) upstream or near that site (**Figures 1 and 24**). On initial review, the DM site appears to have two separate primary sources over time that result in the bimodal concentration distribution with time. An alternative explanation is that the more recent peak may reflect significant redistribution of previously deposited PCB contamination as could happen during major earth works projects. As such, the deeper peak in the DM profile may be reflective of the source to the CM while the upper peak more reflective of local disturbance of previously sequestered contamination.

The tidal Christina Basin (and its non-tidal watershed) contains present-day contaminated substance sites that can contribute PCBs (and other chemical contaminants) to the water and sediments (DNREC, 2007; Brightfields, Inc., 2009). Brightfields, Inc. (2009) estimated PCB loads from current waste sites to the tidal Christina River and Brandywine Creek via overland flow of contaminated soils and via groundwater discharge. Mass loads for individual sites ranged from <0.1 g/yr to over 24 kg/yr, with the AMTRAK Former Refueling Facility having the largest estimated load. While there is some uncertainty with these estimates, they do show substantial current inputs to the tidal river that can impact sediment quality and fish species in the area. Our data do show however that past inputs were higher and that controls implemented in the 1970s to the present have lowered the overall input.

C3.3: Total DDX and Chlordane

DDT and its breakdown products (2,4'+ 4,4' forms of DDT (1,1'-(2,2,2-trichloroethylidene)bis[4-chlorobenzene]; DDE (1,1'-(2,2,2-trichloroethenylidene)bis[4-chlorobenzene]) and DDD (1,1'-(2,2-dichloroethylidene)bis[4-chlorobenzene]) were used for insect controls starting in the mid-1940s. DDT was banned in 1972 and has been found to have an approximate environmental half-life of 10 to 20 years (NOAA, 1989; Woodwell et al., 1971). While it was banned nearly 30 years ago, parent DDT is still detectable (and in substantial concentrations) in the sedimentary material collected from various locations in the Delaware and Chesapeake bays (Wade et al., 1994; Greene 2009b). Greene (2009b) summarized total DDT and other contaminants in surface water, sediment, and biota samples collected throughout the tidal and non-tidal Christina Basin in Delaware. Peak DDT concentrations in the water were detected

in the Red Clay Creek at a station near the PA-DE line. The peak chlordane concentration in the water was detected in Little Mill Creek at Maryland Avenue in Wilmington

Chlordane is a multi-component mixture of polychloro-methanoindenes (e.g., oxy-, γ-, and α-chlordane, heptachlor, heptachlor epoxide and cis+trans-nonachlor). Technical grade chlordane contains more than 140 components of which only 120 compounds can be resolved by current analytical techniques. Alpha (α)-chlordane, gamma (γ)-chlordane, heptachlor and trans-nonachlor are the dominant constituents (Dearth and Hites, 1991), and are used to control termites and ants. Because of the toxicity, potential carcinogenicity and environmental persistence of these components and/or metabolites, (e.g., heptachlor, heptachlor epoxide and oxychlordane), the use of chlordane is under federal regulations. The use of chlordane was halted in 1988 after a phased reduction in use since approximately 1975. The half-life of chlordane is similar to that of DDT (i.e., approximately 10 to 20 years), and therefore its persistence is to be expected for many years. However, while the large scale use of chlordane decreased in the late 1980s, it was not fully phased out and was still used in the area.

The parent and breakdown products of DDT and chlordane were detectable in most sediment layers, especially in the upper, more fine-grained sections of each core (**Tables 7-11; Appendix I**). Concentrations of these two pesticides were generally low to moderate overall with occasionally high concentrations at specific intervals in the cores. Total DDX (all forms; tDDX) ranged from <1 to approximately 369 ng/g dw (median of 18 ng/g dw), while total chlordanes ranged from <1 to 151 ng/g dw (median of 2.9 ng/g dw). The highest concentrations of both pesticides were detected in the BW core. Surface concentrations of DDX were 9.3, 29.1, and 8.2 ng/g dw at the CM, DM, and BW coring sites, respectively. Surface concentrations of chlordane were 2.8, 9.7, and 2.5 ng/g dw at the CM, DM, and BW coring sites, respectively. Surface DDX and chlordane concentrations in the DM and BW cores are generally within a factor of 2 of concentration reported by Greene (2009b) for surface sediments collected in 2007 from the lower tidal Christina River and the tidal Brandywine. Surface DDX and chlordane concentrations in the core tops from CM are roughly 5 times higher than the surface concentrations reported by Greene (2009b) for a station in the tidal Christina River just downstream of CM. The differences are far less when the respective datasets are normalized to organic carbon content.

The distribution with depth of both groups of pesticides was similar to each other and in many ways followed the tPCB profiles (**Figures 22 and 26**). In the Churchman Marsh (CM)

core, concentrations were at the detection limits at depth with peak concentrations at 32-34 cm (circa. 1952) for both pesticides, decreasing towards the surface. The Dravo Marsh (DM) core, similar to tPCBs, exhibited a bimodal distribution with higher concentrations at the 36-38 cm (circa. 1958) and 10-12 cm (circa. 1992) intervals, while in Brandywine Creek (BW) concentrations of both pesticides exhibited sharp peaks at approximately similar intervals (1979 to 1982).

The lower Shellpot Creek (LSP) core (n=5) exhibited highest tDDX concentrations at the surface (75 ng/g dw) with decreasing concentrations with depth, while the Walnut Street (WS) core had slightly higher concentrations in the upper 50 cm (20 ± 7 ng/g dw) with lower concentrations at depth (> 66 cm of 11 to 17 ng/g dw). The distribution of total chlordane for both cores is similar. Highest concentrations of total chlordane were observed in the Shellpot Creek core (151 ng/g dw) decreasing with depth and only slightly higher concentrations in the upper 50 cm (3.3 to 8.3 ng/g dw) compared to the bottom two sections (3.1 to 5.7 ng/g dw).

Historical Analysis: Similar temporal distributions of tChl were observed as tDDX in all three cores (**Figures 25 and 27**) and were similar to the trends in tPCBs. In CM, highest concentrations of tDDX (117 ng/g dw) and tChl (6.6 ng/g dw) were observed in the mid-1950s, compared to the mid-1960s for tPCBs (**Figure 24**). In DM there was a bimodal distribution of both pesticide groups with higher concentrations in the early 1960s and again mid-1990s. As described earlier, this may be due to redistribution of previously deposited sediments during land disturbance activities. The peak in tChl concentrations in the mid-1990s was substantially higher than the deeper peak suggesting additional sources during this time period. In the Brandywine (BW), concentrations of tDDX were highest in the mid-1980s, decreasing with time, while the peak in tChl was in the late-1970s. It is not clear why the two distributions are shifted, but the most likely reason is the use history for each class of pesticides and specifically the use/disposal history in this area (i.e., which could be different from other locations). It is unclear why there was a significant increase in tDDX in 1980s in the Brandywine given the use of DDX was limited after 1972. It is possible that some reworking of the sediments in the basin could have released some buried material that contained elevated levels of DDX.

C3.4: Polybrominated Diphenylethers (PBDEs)

Polybrominated diphenylethers (PBDEs) are members of a broader class of brominated chemicals used as flame retardants. There are 209 congeners, or varieties of the basic chemical type, of PBDEs with a wide range in hydrophobic nature (log Kow 7 to 10) and low water solubility. Penta- and octa-BDE mixtures were banned in 2004 in Europe and California after 30 years of use, while deca-BDE is still used today. Hites (2004) concluded that PBDE use in the U.S. differed from use in Europe and other developed countries in that North America used more deca- and penta-BDE formulations. Dominant PBDE congeners in many areas are BDE-47 (tetra PBDE) and BDE-209 (deca-PBDE). BDE-209 is the single most widely produced and used PBDE congener, while BDE-99 and BDE-47 are the predominant congeners detected in the biosphere. Commercial penta-BDE was used mainly in polyurethane foam (mattresses and padding beneath carpets and furniture). Commercial octa-BDE was predominantly used in casings for electronic products (computers, monitors, plastics). Commercial octa-BDE, and deca-BDE mixtures were also used in nylon, textiles, and adhesives. Today, commercial deca-BDE is used primarily in TV casings. Reductive debromination of BDE-209 could potentially produce BDE-99 and BDE-47 as well as other PBDE congeners. PBDEs degrade faster than PCBs with water and sediment half lives of 0.5 to 1.5, respectively (Wania and Dugani, 2003) depending on the congener and media (air, water or sediment). The degradation of many PBDEs leads to lower brominated PBDEs which may be more toxic but there is a debate as to whether BDE-209 degrades significantly over time. In this study we analyzed for 26 PBDE congeners ranging from BDE-30 to the high molecular weight congener, BDE-209.

The three cores analyzed for PBDEs exhibited similar distributions with depth except that in the Brandywine Creek core, concentrations were 10 times higher at peak concentration (**Table 7, Figure 28**). In the Churchmans Marsh, Brandywine Creek and Dravo Marsh cores, tPBDEs concentrations ranged from near the detection limit of 0.5 ng/g dw to 17 ng/g dw (CM), 120 ng/g dw (BW) and 33 ng/g dw (DM), respectively (**Table 6, Figure 28**). Concentrations in the CM core were near the detection limit at depth (32-38 cm, corresponding to ca. 1945) increasing to a maximum concentration of 17 ng/g dw at 16-18 cm (circa. 1980), then decreasing towards the surface to approximately 10 ng/g dw. In the BW core, tPBDE concentrations were above the detection limit at 12-14 cm (ca. 1980s) increasing to peak concentrations (120 ng/g dw) at 8-10 cm (ca. 1996), decreasing to 53 ng/g dw at the surface. Lastly, tPBDEs concentrations started in

the 16-18 cm (ca. 1986) and exhibited peak concentrations of 33 ng/g dw nearer the surface (4-6 cm; ca. 2002).

The dominant BDE congener was 209 accounting for 5 to 100% of the tPBDEs for all cores; especially in the top sections of the cores (**Figure 29**). At depths greater than 28 cm there were substantial amounts of BDE 99 and to a greater extent BDE 153. For example, in the BW core, BDE 153 accounted for 24-63% of the tPBDEs in the lower sections while BDE accounted for >90% in the upper 10 cm. BDE47 accounted for, at most, 11% of the tPBDEs and this was seen in the bottom sections of DM and CM. A similar distribution and change was noted in the Clyde Estuary by Vane et al. (2009) and slightly different by Song et al. (2004). It appears that over time and burial BDE-209 is slowly degraded to lower brominated congeners; however, changing sources of the lower brominated compounds over time cannot be discounted. Near surface dominance by BDE-209 may also be reflective of current high use of this formulation in comparison to the recently phased-out penta and octa technical mixtures.

Historical Analysis: PBDE production in the United States started in the early 1970s with peak production in the 1990s (Hardy, 2002). The use of the various PBDE formulations has most likely changed over the years as different products and usages develop or are discontinued. Onset and peak concentrations varies across the three sites, reflecting variable time inputs and potentially sediment reworking and remobilization. **Figure 29** presents the time-concentration distribution for total PBDEs. Onset of PBDEs was in the late 1960s/1970s in the CM and DM core and in the mid-1980s in the BW core. Detectable concentrations were observed in the sediment in the early 1970s, quickly after production in the U.S. commenced and may be due to sediment mixing or possibly atmospheric deposition. Peak concentrations were similar in the DM and BW cores (~1980s) while somewhat earlier in the CM core (**Figure 29**). There was a change in the composition of PBDEs with BDE209 the dominant congener in the surface sediments. This could be due to source change, degradation of less brominated compounds, or a function of the method and detection limits. It is possible that at the lower concentrations, the recovery of the higher molecular weight congeners is reduced. This would result in lesser amounts of BDE209 at lower concentrations.

C3.5: Dioxins and Furans

Dioxin and furans are a family of organic chemical compounds that share a similar chemical structure (i.e., tetra to octa-chlorodibenzo-p-dioxin [PCDDs] or –furan [PCDFs]). Due to their hydrophobic nature and resistance to degradation, these chemicals, like other hydrophobic organic chemicals, can accumulate in the fatty tissue of animals (e.g., fish and humans). PCDDs include 75 individual compounds while PCDFs include 135 different compounds, with only 7 PCDD and 10 PCDF compounds exhibiting substantial toxic effects. The most studied and potentially toxic form of PCDD is 2,3,7,8-TCDD (i.e., tetra- chlorodibenzo-p-dioxin).

Dioxin and furans are formed by burning chlorine-based chemical compounds with hydrocarbons. The major source of dioxin in the environment comes from waste-burning incinerators (such as municipal solid waste, sewage sludge, medical waste, and hazardous wastes), the burning of various fuels and material (such as coal, wood, petroleum products, and cement kilns), and poorly or uncontrolled combustion sources like forest fires and building fires (U.S. EPA, 2005 update). Dioxin pollution is also affiliated with paper mills which use chlorine bleaching in their process and with the production of polyvinyl chloride (PVC) plastics and with the production of certain chlorinated chemicals (like many pesticides). Dioxins and furans could be formed naturally with evidence of heavier homologues of PCDDs (Alcock and Jones, 1996). However, anthropogenic sources are much higher than background sources. Sources of these compounds are thought to have started to increase in the environment around 1930s to 1940s, with a sharp rise starting in the early 1950s and decreasing concentrations starting in the mid 1980s (Alcock and Jones, 1996). Recently, the U.S. EPA has drafted a plan (which is under public comment) to initiate clean up and remediation goals for CERCLA and RCRA sites (EPA, 2009; draft).

As part of this study, PCDD and PCDF compounds were determined in sediment sections from five cores (CM, DM, BW, LSP, and WS). Compounds included tetra to octa-PCDFs and PCDDs (**Appendix I**). The discussion below will center on the total concentrations along with 2,3,7,8-TCDD and 2,3,7,8-TCDD toxicity equivalents (as explained below).

Among the five cores, total dioxins and furans ranged from 1.2 to 157 ng/g dw and 0.01 to 127 ng/g dw, respectively (**Figure 30; Tables 7-11).** Other than the two samples in CM (32-34 and 36-38 cm, corresponding to the period 1952 to 1945; **Figure 30**), all sediment samples were <20 ng/g dw for tPCDD and <5 ng/g dw for tPCDFs.

In general, the peak in tPCDD concentration at 32-34 cm (circa. 1952) in the CM core and the more diffuse peaks in DM (36-38cm, circa.1958)) and BW (12-16 cm interval, circa.1990) cores coincided with peaks in other organic contaminants. However, in some cases the peaks in tPCDD or tPCDF concentrations were slightly offset from tPCBs, tDDX, and tChlordane peak concentrations by one interval higher or lower. There was no trend in the Shellpot Creek or Walnut Street cores in dioxins or furans. Concentrations of the more toxic dioxin, 2,3,7,8-TCDD, were detected in only seven sediment intervals in all of the cores (**Tables 7-11**). Detectable concentrations ranged from 0.3 to 5.1 pg/g dw with an average concentration of 0.22 pg/g dw. The highest concentration (5.1 pg/g dw) and most in one core (n= 5) were found at the BW site, however there was no concentration trend with depth and detection appeared random.

Toxic Equivalents (TEQs) were calculated by multiplying the concentration of each 2,3,7,8-substituted dioxin and furan compound by their associated human and mammalian toxicity equivalent factor (TEF) and then adding the resulting partial sums. Dioxin-like PCB congeners were not included in these TEQ calculations. Human and mammalian TEFs for dioxins and furans were taken from the World Health Organization (WHO, 2005), as fully described in Van den Berg et al. (2006). For the TEQ calculation, non-detected compounds were set equal to zero (0). The TEQs in the Christina Basin sediment cores ranged from <1.2 to 444 pg/g dw with an overall average of 34 pg/g dw. The TEQ concentrations in the core tops were as follows: 19.9, 32.9, 21.8, 13.9, and 5.5 pg/g dw for cores CM, DM, BW, WS, and LSP, respectively. These values are similar to values reported by Greene (2009b) for surface sediment samples collected from these same waters in 2007. For most core sections, except BW, the TEQ was dominated by hepta-, octa- and tetra-PCDD congeners and to a lesser extent an even mixture of PCDF congeners. This is also consistent with results reported by Greene (2009b) for surface sediment samples. In the BW core, penta- and hexa-PCDF congeners were highest followed by hepta- and octa-PCDD congeners, thereby providing a different TEQ mix than seen in the other cores and suggesting different sourcing. The vertical profiles of TEQs in the CM and DM cores strongly track their associated PCB profiles. In the BW core, however, the TEQ peak appeared to precede the PCB peak.

Historical Analysis: Total dioxins (tPCDD) and total furans (tPCDF) with time are presented in **Figure 31**. Total dioxins and furans in CM peak in concentration (158 and 12 ng/g dw

respectively) in the early 1950s and decrease to near constant levels until the present. The peak tPCDD in the CM core (158 ng/g dw) is much greater than the peak in the DM core (~17.5 ng/g dw) and the BW core (~12.5 ng/g). There are multiple peaks in tPCDD concentrations in the DM core and tfurans appear to mirror the same pattern over time, although muted. Interestingly, in the Brandywine Creek core, peak concentrations of the tPCDD are found in 1990, while there is a broad maximum in tPCDFs in the 1960s to 1980. The historical pattern of TEQ generally follows both the tPCDD and tPCDF time-concentration distribution except in the Brandywine Creek core (**Figure 32**). While tPCDD concentrations peak around 1990, the TEQ concentration is highest in the mid to late 1970s, similar to tPCDFs. This is due to the contribution to the total TEQ from the various furan congeners is highest during this time period.

C3.6: Sediment Iron and Zinc

The Delaware Department of Natural Resources and Environmental Control had a particular interest in the vertical distribution of iron (Fe) and zinc (Zn) in sediment cores collected from the targeted waterways. Sediment levels of iron (Fe) and zinc (Zn) were determined using a strong acid digestion and are not "total" concentrations (i.e., does not include the clay lattice metals). However, this method would obtain the majority of the metals associated with the particles. Among the five cores (CM, DM, BW, LSP, and WS), sediment Fe ranged from 5388 to 45700 μg/g dw (0.53 to 4.5 wt %), while sediment Zn ranged from 71 to 9800 μg/g dw. Iron concentrations were variable with depth in each core (**Figure 33; Tables 7-11**). The average Fe concentration in the BW and CM core were the same with similar variations (3.5 ± 0.5%). The LSP core exhibited slightly lower Fe concentration but was more variable (2.8 ± 1.9%). The Fe concentrations in the DM core were substantially lower than the BW and CM cores (average = 1.2%) with a peak concentration of 3.0% at 8-10 cm (circa. 1995). It is unclear why Fe concentrations in the DM core were a third lower than the other cores.

Zinc concentrations showed much greater variation with depth in the BW, CM, and DM cores (**Figure 34; Tables 7-11**). Concentrations in the BW core were low at depth increasing to their highest levels of 780 μg/g dw at 20-22 cm (circa. 1979), then decreasing towards the surface (490 μg/g dw). Substantially higher Zn concentrations were measured in the CM core. At depth (pre-1900), concentrations were lowest (~ 140 μg/g dw), increasing to 9800 μg/g dw at 36-38 cm (circa. 1945), than decreasing towards the surface to 720 μg/g dw. The Zn distribution

in the DM core exhibited the bimodal distribution as seen for some organic contaminants. There is a deeper peak of 1230 μg/g dw at 36-38 cm (circa. 1958) and a peak of 1000 μg/g dw at 8-10 cm (circa. 1995). Zn concentrations in the DM core were lower than the CM values and were similar to the BW concentrations.

Normalization of the sediment to a reference element not associated with anthropogenic influences is one approach to determining the degree of sediment contamination (Daskalakis and O'Connor, 1995). Elements such as Al (Windom et al., 1989; Schropp et al., 1990), lithium (Li) (Loring et al., 1990) and Fe (Trefrey and Presely, 1976; Sinex and Helz, 1981; Helz et al., 1985; Velinsky et al., 1994; Velinsky et al., 1997) have been used in the past. For this study, Fe was chosen as a normalizing element because: 1) it is the fourth most abundant metal in the earth with a crustal average of 3.5% (Wedepohl, 1971); 2) in most cases anthropogenic sources are small compared to the amount of Fe naturally present; and 3) the ratios of most metals to Fe are fairly constant in the Earths crust. The major caveat in using Fe as a normalizing element, instead of Al or Li, is that Fe undergoes many diagenetic reactions in anoxic/oxic sediments. These reactions include dissolution and precipitation of Fe oxides and Fe-sulfur minerals (i.e., pyrite). However, in the previous studies by Velinsky et al. (1994; 1997) in tidal river sediments, the potential changes in speciation and mobility did not significantly affect the total concentration of sedimentary iron with depth or location. Therefore, Fe was used as normalizing agent for this study.

A useful tool in expressing the degree to which sediment is influenced by anthropogenic sources of trace metals is the enrichment factor (EF) (Trefrey and Presely, 1976; Sinex and Helz, 1981; Helz et al., 1985; Windom et al., 1989; Velinsky et al., 1994; 1997). When normalizing to Fe, the enrichment factor is defined as: $EF = (X/Fe)_{sediment} / (X/Fe)_{unimpacted\ sediment}$, where X/Fe is the ratio of the trace metal (X) to the amount of Fe in the sample. In using the EF, a comparison to a sediment that is unimpacted by anthropogenic sources is necessary [$(X/Fe)_{unimpacted}$] (i.e., critical in this analysis is the choice of metal to Fe ratio for unimpacted sediments). Enrichment factors of 1 indicate no enrichment, while EFs greater than 1 indicate anthropogenic sources of metals to the sediments. While this approach is useful, it may not account for natural variations in sediment types of different geological regions. One way to account for this variability is to derive a ratio from "unimpacted" sediments in the general area of interest (Windom et al., 1989; Schropp et al., 1990). However, in the present study, most samples have the potential to be

impacted above natural levels, except possibly at depth in the cores. Therefore, data from the bottom of the cores, as described below, were used to derive 'natural' or least impacted concentrations of Fe and Zn in the general area.

The Zn to Fe ratios for the bottom section of the three cores (BW, CM, and DM) were 0.011, 0.004, and 0.007, with an average of 0.007. A ratio of 0.007 is somewhat higher than a mean of 0.002 reported by Wedepohl (1968) for river sediments but is quite similar to values seen in other tidal river sediments (Velinsky et al., 1994). A value of 0.007 also has the added advantage of being specific to the tidal Christina Basin. The degree to which sediments in the study area are enriched in trace metals from anthropogenic sources varies from metal to metal and depends on a number of factors, including: 1) choice of $(X/Fe)_{unimpacted}$; 2) biogeochemistry and redox behavior of the metal; and 3) sources and loading history of metals to the study area. Despite these considerations, the present calculation reveals some interesting trends with depth.

Figure 19 presents the EF distribution for the DM, BW and CM cores. The EF for all core samples ranged from 0.5 to 41 with an overall average of 4 (unitless). Given the variations in the $(X/Fe)_{unimpacted}$ value, an EF of <1 to ~2 indicate samples that are at or near background. The BW core shows no enrichment for Zn. In the CM core, there was substantial enrichment of Zn above background with values up to 41 times higher at 42-44cm (~1935). Above and below this broad peak the EF is near background levels. DM sediments were above background from approximately 50 cm (~1925) to the surface with the peak EF at 42-44 cm and above this interval, the EF ranged from 5 to 12 suggesting a continuing source to this location. A more in-depth discussion of zinc enrichment within the CM and DM cores will be presented below.

One of the most noteworthy observations apparent from the present study is the historical rise and fall of zinc concentrations in the sediments at the CM coring site. The onset of zinc enrichment in the CM core appears to have occurred around or shortly after 1900 (**Table 8**). Sediment concentrations of Zn were highest in that core from approximately 1910 to 1950 with a peak of nearly 10,000 ug/g dw and an average of 8850 ± 920 ug/g dw (n=5) during that period (**Table 8 and Figures 33 and 35**). Zinc concentrations at the other coring sites (DM and BW) were substantially lower (**Tables 7 and 9, plus Figures 33 and 35**). Dravo Marsh (DM) concentrations were highest between 1950 and 1958 with a secondary peak in the mid-1990s, while in the BW core, peak concentrations occurred around ~1970 to 1980. As indicated by the EF (see above), changes in Zn concentrations in the BW core were controlled by Fe with little or

no anthropogenic enrichment of Zn, while there was substantial enrichment of Zn in the CM core (up to 40 times above background) in the 1930s. Concentrations of sediment Zn in the DM core started to show enrichment in the late 1930s with highest EF (20) in the mid-1940s and decreasing over time to approximately 5 to 10 in the current century.

Historical Analysis: Primary sources of zinc enrichment over time to Churchmans Marsh and downstream to Dravo Marsh include the now defunct NVF facility located along the Red Clay Creek in Yorklyn, DE (DNREC, 1999a); a similar NVF facility that formerly operated along the White Clay Creek in Newark, DE (DNREC, 1999b); and a pigment plant located in Newport that became a federal Superfund site (U.S. EPA, 1993). All three of these sources began manufacturing operations right around 1900. The NVF Newark plant closed in 1990, while the NVF Yorklyn plant closed in 2009. Both of the NVF facilities used zinc chloride in the manufacture of vulcanized paper products. The Newport pigment plant manufactured Lithopone, a zinc and barium-based paint pigment, up until 1952. Zinc loading from the NVF Yorklyn plant entered the Red Clay Creek and travelled downstream until it combined with the White Clay Creek, which carried the additional zinc load from the NVF Newark plant. The combined load emptied into the tidal Christina River just downstream of Churchmans Marsh (just upstream of Newport, DE). Additional zinc then entered the Christina River as a result of poor waste handling at the Newport pigment plant. The combined zinc loading from these three primary sources produced inordinately high concentrations of zinc (~10,000 μg/g dw) at depth in the CM core and moderately high (~1,250 μg/g dw) concentrations downstream at the DM coring site.

The sediment profiles in CM, and to a lesser extent, DM, clearly show significant inputs of Zn shortly after these three facilities commenced operation along with an associated improvement once controls began to be put in place or processes were changed. Concentrations in the bottom of the CM and DM cores ranged from 71 to 139 μg/g dw (average = 106 ± 33 μg/g dw), only slightly above concentrations found upstream of the NVF Yorklyn facility on the Red Clay Creek (range of 39 to 107 μg/g dw; average = 73 ± 22 μg/g dw; n = 7; DNREC, 1999). Concentrations of Zn in the mid sections of the cores were significantly enriched in Zn, especially in the CM core (**Figure 35**). The core results clearly show that control procedures from the 1960s to the present have resulted in a reduction of Zn inputs to the river

The NVF Yorklyn facility is under active remediation to remove the remaining inventory of zinc from the groundwater beneath the site (DNREC, 2008). The NVF Newark facility has been remediated to address the zinc contamination there (DNREC, 1999c) and an extensive cleanup was implemented at the DuPont Newport site. One component of the DuPont Newport cleanup included dredging approximately 11,000 cubic yards of sediment from the tidal Christina River in the vicinity of Newport in 1999, due in part to elevated concentrations of zinc in the sediments (NRC, 2007). The coring analysis clearly shows that the closing of these facilities and the extensive cleanup action taken have yielded substantially lower concentrations of Zn in the sediments of the tidal Christina River.

D) Summary and Conclusions

This study involved the chemical analysis of five sediment cores taken from the tidal Christina River Basin and lower Shellpot Creek in northern New Castle County, DE. Of the five cores, four were dated using ^{210}Pb and ^{137}Cs radiometric methods, with three (Churchmans Marsh (CM), Dravo Marsh (DM), and the tidal Brandywine (BW)) providing sufficient temporal coverage (> 50 yrs) for detailed chemical analysis. The main objective was to evaluate historical trends in organic chemical contaminants (e.g., polychlorinated biphenyls, pesticides, dioxins/furans, polybrominated diphenylethers and polycyclic aromatic hydrocarbons), selected trace metals (e.g., iron and zinc) and nutrients (i.e., sediment phosphorus and nitrogen). An additional objective was to evaluate if a historical record of eutrophication could be derived from algae analysis (i.e., diatom species in the cores) along with other indicators of potential ecosystem change (e.g., stable isotopes of carbon ($\delta^{13}C$-OM) and nitrogen, ($\delta^{15}N$-TN)).

The range and average sediment accumulation rates (^{137}Cs) inferred from the ^{210}Pb and ^{137}Cs data are similar to other areas within the Delaware Estuary and range from 0.57 to 1.9 cm/yr. Attempts to core and determine age-depth relationships in other locations (i.e., an embayment near Walnut Street) yielded inconclusive dating results. There was good agreement between the ^{137}Cs rates and those for the constant accumulation model for ^{210}Pb.

With regard to contaminants, a major finding that emerged from this study is the historic accumulation of zinc in the system, as clearly displayed in the Churchmans Marsh (CM) core. Concentrations of Zn showed a broad peak over background levels starting at or shortly after the turn of the century and persisting to the early to mid-1970s. Using the amount of iron (Fe) within the sediment and referencing the data to bottom concentrations of Zn (and Fe), the sediments of Churchmans Marsh had been up to 40 times above background levels. Current Zn enrichment in Churchmans Marsh is still approximately 5 to 10 times above background. In the other core locations, surface sections are not substantially enriched above background with zinc enrichment factors ranging only from 1 to 2.3. Major sources of historic zinc loading to the system included two National Vulcanization Facilities (NVF), one on the Red Clay Creek and one on the White Clay Creek, and a pigments plant in Newport. All three of these sources have been remediated and discharges are more formally regulated.

The other key finding of this study is that concentrations of organic contaminants are lower today, overall, than they were in the past, with some exceptions. Chlorinated organic compounds

such as tchlordane, tDDX and dioxins/furans all show a sharp maximum at similar depths (corresponding to the 1960s and 1970s), followed by a decreasing trend towards the surface. Total PCBs also shows higher concentrations at depth with decreasing concentrations towards the surface, with the exception of the Dravo Marsh core where tPCB concentrations at the surface remain elevated (ca. 200 ng/g dw). The Dravo Marsh core exhibits a bimodal distribution in PCB concentration, showing two separate peaks. The onset of the first peak occurred at 48-50 cm (circa. 1942), with the actual peak seen at 36-38 cm (circa. 1958). These dates track the Churchman Marsh core fairly well. After 1958, PCB concentrations in the Dravo Marsh core fell and remained below 50 ng/g dw for at least a decade. At this time, concentrations began to increase again in the late 1970s, rising to a second peak at 10-12 cm (circa. 1992) that was similar in magnitude to the first peak. PCB concentrations in the Dravo Marsh core have fallen somewhat since 1992 but surface concentrations remain high relative to the surface concentrations in the CM and BW cores. The Dravo Marsh finding may reflect lingering inputs from local sources and/or the redistribution of previously deposited contamination following major earth works projects in or near the marsh.

Interestingly, the PCB congener composition in both the Churchmans Marsh and Dravo Marsh cores showed a shift from mid to higher molecular weight compounds to lower molecular weight compounds from the upper sections (more recent) to the lower sections (longer ago). The opposite was true for the BW core. The high proportion of deca PCB (H10) in the Churchmans Marsh and Dravo Marsh cores is unusual and appears to reflect releases from the same pigment plant in Newport that was also responsible for at least part of the zinc contamination. The use of congener-specific PCB methods (rather than typical Aroclor methods) allowed us identify and characterize the deca PCB signature.

Total dioxins (PCDD) and furans (PCDF) concentrations ranged from <2 to 157 ng/g dw and <1 to 13 ng/g dw, respectively with distinct distributions with depth and time. The individual congeners were used to calculate the toxic equivalents (TEQs) using published toxic equivalency factors (TEF). The TEQs ranged from <0.01 to 0.45 ng/g dw. Highest concentrations of PCDD, PCDF and TEQ were found in the Churchmans Marsh core.

In all cores (n=3), tPBDEs are only present in the upper sections with undetectable concentrations below approximately 20cm (<1980s). The predominant congener is PBE 209 in the upper sections with BDE153 and BDE99 found at depth.

Total PAHs showed a distinct concentration peak in the 1940s, in the CM core, while a bimodal distribution was observed in the DM core and possibly the BW core. The peak of tPAHs in the CM core maybe related to historic inputs of hydrocarbons from a creosote facility near the site. Other sources related to urban development, including a major shipbuilding complex and a coal gasification plant, are also potential historic sources to the area, particularly the DM. Data were compared to indicators of combustion sources such as coal tar based parking lot sealant using specific ratios of individual PAHs. Only a limited number of samples were consistent with such a fingerprint and thus this type of sealant does not appear to be a major source to the tidal Christina River.

Lastly, analysis of the diatom assemblages and metrics indicate a shift toward more eutrophic species starting in the late 1940-1950s. There was a strong positive relationship between the eutrophic diatom metric and the concentration of nitrogen and phosphorus in Churchmans and Dravo marshes. This, along with the increases in total sediment N, total sediment P and sediment nitrogen isotopic compositions (δ^{15}N-TN), indicates that increase loadings of nutrients have resulted in a diatom shift in the river.

Overall, this study documents the chemical analysis of three cores taken in the tidal Christina River and tidal Brandywine Creek. Changes were observed in contaminant levels across time that reflect usage globally and most often locally. Overall, contaminant levels appear to be declining when viewed on a longer term, decadal time scale. However, the concentrations of several contaminants (e.g., PCBs and zinc) remain relatively elevated in this system.

E) Acknowledgments

We would like to thank Susanne Molaski (UDEL), Don Charles, Paul Kiry, Paula Zelanko, Mike Schafer, and Linda Zaoudeh for laboratory assistance and data interpretation. Dr. Mihalea Enache did diatom counts, calculated diatom metrics and provided assistance with report preparation. We appreciate the help of Dr. Heather Stapleton (Duke University) for assistance in analyzing a subset of the samples for PBDEs. Dr. Jeff Ashley (Philadelphia University) provided analytical advice and support throughout this project. Roger Thomas assisted in field and Robin Davis provided assistance with final report preparation and review. Financial, field and editorial support was graciously provided by Dr. Richard Greene (DNREC; Watershed Assessment Branch).

F) References

Alcock, R. E. and K.C. Jones. 1996. Dioxins in the Environment: A Review of Trend Data. *Environ. Sci. Technol.* 30: 3133-3143.

Appleby, P.G. 2001. Chronostratigraphic techniques in recent sediments: Chapter 9. In: W.M. Last and J.P. Smol (eds). *Tracking Environmental Change Using Lake Sediments Volume 1: Basin Analysis, Coring, and Chronological Techniques*. Kluwer Academic Publishers, Dordrecht, The Netherlands.

Appleby P.G and F. Oldfield. 1978. The calculation of lead-210 dates assuming a constant rate of supply of unsupported ^{210}Pb to the sediment. *Catena* 5: 1-8.

Ashley, J.T.F. and J.E. Baker. 1999. Hydrophobic organic contaminants in surficial sediments of Baltimore Harbor: Inventories and sources. *Environ. Toxicol. Chem.* 18: 838–849.

Aspila,K.I, H. Aspila, A. Agemian and S.Y. Chau. 1976. A semi-automated method for the determination of inorganic and total phosphate in sediments. *Analyst* 101: 187-197.

ATSDR. 2000. *Toxicological Profile for Polychlorinated Biphenyls* (Update). Agency for Toxic Substances and Disease Registry, Atlanta, GA.

Baker, J.E., M. Toaspern, D. Liebert, and F. Ko. 2004. Decachlorobiphenyl: Using a Non-Aroclor PCB as a Tracer of Estuarine Processes. Society of Environmental Toxicology and Chemistry Poster Session. Portland, OR.

Berner, R. 1980. *Early Diagenesis: A Theoretical Approach.* Princeton University Press, 241 pp.

Benner, R., M. L. Fogel, and E. K. Sprague. 1991. Diagenesis of belowground biomass of *Spartina alterniflora* in salt-marsh sediments. *Limnol. Oceanogr***.** 36: 1358-1374.

Boehm, P.D. 1984. Aspects of the saturated hydrocarbon geochemistry of recent sediments in the Georges Bank region. *Org. Geochem***.**, 7: 11-23.

Boehm, P.D. and J.W. Farrington. 1984. Aspects of the aromatic hydrocarbon geochemistry of recent sediments in the Georges Bank region. *Environ. Sci. Tech.,* 18: 840-845.

Bratton, J.F., S.M. Coleman and R.R. Seal, II. 2003. Eutrophication and carbon sources in Chesapeake Bay over the last 2700 yr.: Human impacts in context. *Geochim. Cosmochim. Acta.* 67: 3385-3402.

Brightfields Inc. 2009. *PCB Mass Loading from Hazardous Substance Release Sites to Surface Waters of the Christina River Basin* (DNREC Contract No. #06-374-MS-A). Prepared for: Site Investigation & Restoration Branch, Division of Air and Waste Management, and Watershed Assessment Branch, Division of Water Resources; Department of Natural Resources Environmental Control; State of Delaware (File# 0985.26.51).

Brush, G.S., E.A. Martin, R.S. DeFries, and C.A. Rice 1982. Comparisons of ^{210}Pb and pollen methods for determining rates of estuarine sediment accumulation. *Quaternary Research.* 18: 196-217.

Burdige, D.J. 2006. *Geochemistry of Marine Sediments*. Princeton University Press. 630 pp.

Canuel, E.A., J.E. Cloern, D.B. Ringelberg, J.B. Guckert and G.H. Rau. 1995. Molecular and isotopic tracers used to examine sources of organic matter and its incorporation into the food webs of San Francisco Bay. *Limnol. Oceanogr*. 40: 67-81

Church, T.M., C. Sommerfield, D.J. Velinsky, D. Point, C. Benoit, D. Amouroux, D. Plaa and O. Donard. 2006. Marsh sediments as records of sedimentation, eutrophication and metal pollution in the urban Delaware Estuary. *Marine Chemistry* 102(1-2):72-95.

Cifuentes, L.A., J.H. Sharp and M.L. Fogel. 1988. Stable carbon and nitrogen isotope biogeochemistry of the Delaware estuary. *Limnol. Oceanogr*. 33: 1102-1115.

Cline, J.D. and I.R. Kaplan 1975. Isotopic fractionation of dissolved nitrate during denitrification in the eastern tropical North Pacific Ocean. *Mar. Chem*. 3: 271-299

Cooper, S. R. and G.S. Brush. 1993. A 2,500-year history of anoxia and eutrophication in Chesapeake Bay *Estuaries* 16: 617-626.

Cornwell J.C., J.C. Stevenson, D.J. Conley and M. Owens. 1996. A sediment chronology of Chesapeake Bay eutrophication. *Estuaries* 19:488-499.

Crusius, J. and R.F. Anderson. 1991. Core compression and surficial sediment loss of lake sediments of high porosity caused by gravity coring. *Limnol. Oceanogr.* 36:1021-1031.

Cutshall, N.H., I.L Larsen and C.R. Olsen. 1983. Direct analysis of ^{210}Pb in sediment samples: Self-absorption corrections. *Nuclear Instruments and Methods in Physics Research*, 206: 309-312.

Daskalakis, K.D. and T.P. O'Connor. 1995. Normalization and elemental sediment contamination in the coastal United States. Environ. Sci. Technol. 29: 470 477.

Dean, W.E., Arthur, M.A., and Claypool, G.E., 1986. Depletion of ^{13}C in Cretaceous marine organic matter: source, diagenetic, or environmental signal? *Mar. Geol*., 70:119-157.

Dearth, M.A. and R.A. Hites. 1991. Complete analysis of technical chlordane using negative ionization mass spectrometry. Environ. Sci. Technol. 25: 245-254.

Delaware Department of Natural Resources and Environmental Control (DNREC). 2008. Amended Total Maximum Daily Load (TMDL) for Zinc in the Red Clay Creek Technical Background and Basis Document (September 15, 2008), State of Delaware Department of

Natural Resources and Environmental Control Division of Water Resources, Watershed Assessment Section, Dover, DE.

Delaware Department of Natural Resources and Environmental Control (DNREC). 2007. Christina Basin Pollution Control Strategy. Department of Natural Resources and Environmental Control, Dover, Delaware.

Delaware Department of Natural Resources and Environmental Control (DNREC). 2005. Sediment Quality Assessment for the Tidal Christina River Basin, Volume 1 Report of Findings. Department of Natural Resources and Environmental Control 715 Grantham Lane, New Castle, Delaware.

Delaware Department of Natural Resources and Environmental Control (DNREC). 2004. Final Plan of Remedial Action, Wilmington Coal Gas Site – Northern Parcel/OU-01. State of Delaware Department of Natural Resources and Environmental Control Site Investigation and Restoration Branch, New Castle, DE.

Delaware Department of Natural Resources and Environmental Control (DNREC). 1999a. Total Maximum Daily Load (TMDL) for Zinc in the Red Clay Creek, New Castle County, DE. Technical Background and Basis Document (August 1, 1999), State of Delaware Department of Natural Resources and Environmental Control Division of Water Resources, Watershed Assessment Section, Dover, DE.

Delaware Department of Natural Resources and Environmental Control (DNREC). 1999b. Total Maximum Daily Load (TMDL) for Zinc in the White Clay Creek, New Castle County, DE. Technical Background and Basis Document (August 1, 1999), State of Delaware Department of Natural Resources and Environmental Control Division of Water Resources, Watershed Assessment Section, Dover, DE.

Delaware Department of Natural Resources and Environmental Control (DNREC). 1999c. Response to Public Comments RE: Proposed Total Max. Daily Loads for Zinc in the Red Clay Creek, DE. Department of Natural Resources and Environmental Control Division of Water Resources, Watershed Assessment Section, Dover, DE.

Delaware Department of Natural Resources and Environmental Control (DNREC). 1996. Final Determination State of Delaware 1996 Clean Water Act Section 303(d) List of Waters Needing TMDLs and Supporting Rationale. Delaware Department of Natural Resources and Environmental Control, Division of Water Resources, Dover, DE.

Di Toro, D.M. and J.A. McGrath. 2000. Technical basis for narcotic chemicals and polcyclic aromatic hydrocarbon criteria. II. Mixtures and sediments. *Environ. Tox. Chem.* 19(8): 1971-1982.

Farrington, J.W. 1980. An overview of the biogeochemistry of fossil fuel hydrocarbons in the marine environment. In*: Petroleum in the Marine Environment*, Eds.: L. Petrakis and F.T. Weiss, Advances in Chemistry Series 185, American Chemical Society, Washington, D.C., pp. 1-22.

Fogel, M.L., L.A. Cifuentes, D.J. Velinsky and J.H. Sharp. 1992. The relationship of carbon availability in estuarine phytoplankton to isotopic composition. *Marine Ecol. Prog. Ser*. 82: 291-300.

Fogel, M.L., E.K. Sprague, A.P. Gize and R.W. Frey. 1989. Diagenesis of organic matter in Georgia salt marshes. *Estuarine, Coastal Shelf Sci*., 28: 211-230.

Fry, B. 2006. *Stable Isotope Ecology*. Springer Science+Business Media, LLC, New York.

Gevo, B., J. Hamilton-Taylor, C. Murdoch, K.C. Jones, M. Kelly and B.J. Tabner. 1997. Depositional time trends and remobilization of PCBs in lake sediments. *Environ. Sci. Technol*. 31: 3274-3280.

Graustein, W.C. and K.K. Turekian. 1986. ^{210}Pb and ^{137}Cs in air and soils measure the rate and vertical distribution of aerosol scavenging. *J. Geophys. Res*., 91: 14,355-14,366.

Greene, R.W. 2009a. *The Chemical, Physical and Biological Fate of Polychlorinated Biphenyls in the Tidal Christina Basin*. A dissertation submitted to the Faculty of the University of Delaware in partial fulfillment of the requirements for the degree of Doctor of Philosophy in Civil Engineering: 359 pp.

Greene, R.W. 2009b. Persistent, Bioaccumulative, and Toxic (PBT) Pollutants in Surface Water, Sediment, and Biota of the Christina Basin and Shellpot Creek Watershed, DE. A presentation summarizing the results of fall 2007 sampling. Delaware Department of Natural Resources and Environmental Control, Watershed Assessment Section, Dover, DE.

Gschwend, P.M.and R.A. Hites 1981. Fluxes of PAHs to marine and lacustrine sediments in the NE United States. *Geochim. Cosmochim. Acta*. 45: 2359-2367.

Hardy, M.L. 2002. A comparison of the properties of the major commercial PBDPO/PBDE product to those of major PBB and PCB products. *Chemosphere* 46: 717-728.

Hayes, J.M, Popp, B.N., Takigiku, R., and Johnson, M.W., 1989. An isotopic study of biogeochemical relationships between carbonates and organic carbon in the Greenhorn Formation. *Geochim. Cosmochim. Acta*, 53:2961-2972.

Heiri, O., A.F. Lotter and G.Lemcke. 2001. Loss on ignition as a method for estimating organic and carbonate content in sediments: reproducibility and comparability of results. *Journal of Paleolimnology*. 25: 101-110.

Helz, G.R., S.A. Sinex, K.L. Ferri, and M. Nichols. 1985. Processes controlling Fe, Mn, and Zn in sediments of Northern Chesapeake Bay. *Estuar. Coast. Shelf Sci*. 21: 1-16.

Hites, R.A. 2004. Polybrominated diphenyl ethers in the environment and in people: A meta-analysis of concentrations. *Environ Science Technol.* 38 (4): 945-956.

Hites, R.A., R.E. Laflamme, J.G. Windsor, J.W. Farrington, and W.G. Deuser 1980. Polycyclic aromatic hydrocarbons in an anoxic sediment core from the Pettaquamscutt River (Rhode Island, USA). *Geochim. Cosmochim. Acta***.**, 44: 873-878.

Hoffman, E.J., G.L. Mills, J.S. Latimer and J.G. Quinn. 1984. Urban runoff as a source of polycyclic aromatic hydrocarbons to coastal waters. *Environ. Sci. Technol*. 18: 580-586.

Hornberger, M.L., S.N. Luoma, A.Green, C. Fuller, and R. Anima. 1999. Historical trends of metals in the sediments of San Francisco Bay, California. *Marine Chemistry.* 64:39-55.

Inn, K.G.W. 2001. The NIST natural-matrix radionuclide standard reference material program for ocean studies. *Journal of Radioanalytical and Nuclear Chemistry.* 241: 227-231.

Jasper, J.P. and R.B. Gagosian. 1990. The sources and deposition of organic matter in the Late Quaternary Pigmy Basin, Gulf of Mexico. *Geochim. Cosmochim. Acta.* 54: 1117-1132.

Kennish, M.J. 1992. *Ecology of Estuaries: Anthropogenic Effects*. Ed: M.J. Kennish, CRC Press, Inc. Boca Raton, FL., 494 pp.

Klein, R.D. 1979. Urbanization and stream water quality impairment. *Water Resources Bulletin.* 15: 948-963.

Kucklick, J.R., H.R. Harvey, P.H. Ostrom, N.E. Ostrom and J.E. Baker. 1996. Organochlorine dynamics in the pelagic food web of Lake Baikal. *Environ. Toxicol. Chem.* 15: 1388-1400.

Lake, J.L., R.A. McKinney, F.A. Osterman, R.J. Pruell, J. Kiddon, S.A. Ryba and A.D. Libby. 2001. Stable nitrogen isotopes as indicators of anthropogenic activities in small freshwater systems. *Can. J. Fish. Aquatic Sci*. 58: 870-878.

Latimer, J.S. and J.G. Quinn. 1996. Historical trends and current inputs of HOCs in an urban estuary: The sedimentary record. *Environ. Sci. Technol.* 30: 623-633.

Leavitt, P.R., C.S. Brock, C. Ebel and A. Patoine. 2006. Landscape-scale effects of urban nitrogen on a chain of freshwater lakes in central North America. *Limnol. Oceanogr*. 51(5): 2262–2277.

Litke, D.W. 1999. *Review of Phosphorus Control Measures in the United States and Their Effects on Water Quality*. U.S. Geological Survey, Water Sources Investigations Report 99-4007, National Water Quality Assessment Program, Denver, CO.

Loring, D.H. 1990. Lithium - a new approach for the granulometric normalization of trace metal data. *Mar. Chem*. 29: 155-168.

McClelland, J.W., I. Valiela and R.H. Michener. 1997. Nitrogen-stable isotope signatures in estuarine food webs: A record of increasing urbanization in coastal watershed. *Limnol. Oceangr*. 42: 930-937.

Mahler, B.J., P.C. Van Metre, T.J. Bashara, J.T. Wilson and D.A. Johns. 2005. Parking lot sealcoat: An unrecognized source of urban Polycyclic Aromatic Hydrocarbons. *Environ. Sci. Technol.* 39(15): 5560-5566.

Meyers, P.A., 1994. Preservation of elemental and isotopic source identification of sedimentary organic matter. *Chem. Geol.* 144: 289-302.

National Oceanic and Atmospheric Administration (NOAA). 1993. *National Status and Trends Program. Sampling and Analytical Methods of the National Status and Trends Program, National Benthic Surveillance and Mussel Watch Project 1984-1992*, Volume III Comprehensive Description of Elemental Analytical Methods. NOAA Tech. Mem. NOS ORCA 71, National Ocean Service, Silver Spring, MD.

National Oceanic and Atmospheric Administration (NOAA). 1989. A summary of data on tissue contamination from the first three years (1986-1988) of the Mussel Watch project. *NOAA Tech. Mem. NOS OMA 49*, Rockville, MD.

National Research Council (NRC). 2007. *Sediment Dredging at Superfund Megasites Assessing the Effectiveness*. National Research Council of the National Academies, The national Academies Press, Washington, D.C.

Neff, J.M., S.A. Stout and D.G. Gunster. 2005. Ecological risk assessment of polycyclic aromatic hydrocarbons in sediments: Identifying sources and ecological hazard. *Integr. Environ. Assess. Manag.* 1(1): 22-33.

Neubauer, I.C. Anderson, J.A. Constantine and S.A. Kuehl. 2002. Sediment deposition and accretion in a mid-Atlantic (U.S.A.) tidal freshwater marsh. *Estuarine, Coastal, and Shelf Science*. 54: 713-727.

Officer, C.B., D.R. Lynch, G.H. Setlock and G.R. Helz.1984. Recent sedimentation rates in Chesapeake Bay. In: Kennedy, V.S. (ed.). *The Estuary as a Filter*. Academic Press, New York, pp 131-157.

O'Leary, M.H., 1988. Carbon isotopes in photosynthesis. *Bioscience,* 38:328-336.

Olsen, C.R., I.L. Larsen, P.D. Lowry, N.H. Cutshall, J.F. Todd and G.T.F. Wong. 1985. Atmospheric fluxes and marsh-soil inventories of ^{7}Be and ^{210}Pb. *Journal of Geophysical Research –Atmospheres.* 90: 10487-10495.

Olsen, C.R., H.J. Simpson, T.H. Peng, R.F. Bopp and R.M. Trier. 1981. Sediment mixing and accumulation effects on radionuclide depth profiles in Hudson estuary sediments. *Journal of Geophysical Research*. 86: 11020-11028.

O´Malley, V.P., T.A. Abrajano and J.Hellou. 1996. Stable carbon isotopic apportionment of individual polycyclic aromatic hydrocarbons in St. John's harbour, Newfoundland. *Environ. Sci. Technol.* 30: 634-639.

O'Malley, V.P., T.A. Abrajano and J. Hellou. 1994. Determination of $^{13}C/^{12}C$ ratios of individual PAH from environmental samples: Can PAH sources be source apportioned? *Org. Geochem*. 21: 809-815.

Orson, R.A., R.L. Simpson and R.E. Good. 1992. A mechanism for accumulation and retention of heavy metals in tidal freshwater marshes of the upper Delaware River Estuary. *Estuar. Coast. Shelf Sci.* 34: 171-186.

Orson, R.A., R.L. Simpson and R.E. Good. 1990. Rates of sediment accumulation in a tidal freshwater marsh. *J. Sed. Petrology*. 60: 859-869.

Owens, M. and J.C. Cornwell. 1995. Sedimentary evidence for decreased heavy metal inputs to the Chesapeake Bay. *Ambio* 24: 24-27.

Perga, M.E. and D. Gerdeaux. 2004. Changes in the $^{\delta 13}C$ of pelagic food webs: The influence of lake area and trophic status on the isotopic signature of whitefish (*Coregonus lavaretus*). *Can. J. Fish. Aquat. Sci.* 61(8): 1485–1492.

Pierce, R.H., R.C. Brown, E.S. Van Vleet, and R.M. Joyce. 1986. Hydrocarbon contamination from coastal development. In: *Organic Marine Chemistry*. Ed: M.L. Sohn, ACS Symposium Series 305, pp. 229-246.

Ponader, K.C., D.F. Charles, T.J. Belton and D.M. Winter. 2008. Total phosphorus inference models and indices for coastal plain streams based on benthic diatom assemblages from artificial substrates. *Hydrobiologia* 610: 139-152.

Porter, S.D. 2008. *Algal attributes: An autecological classification of algal taxa collected by the National Water-Quality Assessment Program*: U.S. Geological Survey Data Series 329, 18 p.

Porter, S.D., D.K. Mueller, N.E. Spahr, M.D. Munn and N.M. Dubrovsky. 2008. Efficacy of algal metrics for assessing nutrient and organic enrichment in flowing waters: *Freshwater Biology.* 53: 1036-1054.

Potapova, M. and D.F. Charles. 2007. Diatom metrics for monitoring eutrophication in rivers of the United States. *Ecological Indicators.* 7: 48-70.

Potapova, M., D.F. Charles, K.C. Ponader and D.M. Winter. 2004. Quantifying species indicator values for trophic diatom indices: a comparison of approaches. *Hydrobiologia.* 517: 25-41.

Prahl, F.G., J.R. Ertel, M.A. Goni, M.A. Sparrow and B. Eversmeyer. 1994. Terrestrial organic carbon contributions to sediments on the Washington margin. *Geochim. Cosmochim. Acta.* 58:3035-3048.

Pruell, R.J. and J.G. Quinn. 1985. Geochemistry of organic contaminants in Narragansett Bay sediments. *Estuar. Coast. Shelf Sci*., 21: 295-312.

Ridgeway, J. and G. Shimmield. 2002. Estuaries as repositories of historical contamination and their impact on shelf seas. *Estuar. Coast. Shelf Sci*. 55: 903-928.

Riedel, G.R., D.J. Velinsky, J.T.F. Ashley and J.Cornwell. 2010. River sediment investigation near Poplar Point in the tidal Anacostia River, Washington, DC. *Aquatic Geochemistry.* (under revision).

Rippey, B. and H. J. Anderson. 1996. Reconstruction of lake P loadings and dynamics using sedimentary record. *Environ. Sci. Technol*. 30: 1786-1789.

Ritchie, J.C. and McHenry, R.J. 1990. Application of radioactive fallout Cesium-137 for measuring soil erosion and sediment accumulation rates and patterns: A review. *Journal of Environmental Quality.* 19: 215-233.

Roy, AH., A.D. Rosemond, M.J. Paul, D.S. Leigh, and J.B. Wallace. 2003. Stream macroinvertebrate response to catchment urbanization (Georgia, U.S.A.). *Freshwater Biology* 48: 329-346.

Rushneck, D.R, A. Bekuveau et al. 2004. Concentrations of dioxin-like PCB congeners in unweathered Aroclors by HRGC/HRMS using EPA Method 1668A. *Chemosphere* 54: 79-97.

Ruttenberg, K.C. 1992. Development of a sequential extraction method for different forms of phosphorus in marine sediments. *Limnol. Oceanogr*. 37: 1460-1482.

Santschi, P.H., B.J. Presley, T.L. Wade, B. Garcia-Romero and M. Baskaran. 2001. Historical contamination of PAHs, PCBs, DDTs, and heavy metals in Mississippi River Delta, Galveston Bay and Tampa Bay sediment cores. *Mar. Environ. Res.* 52: 51-79.

Schelske, C.L. and D.A. Hodell. 1995. Using carbon isotopes of bulk sedimentary organic matter to reconstruct the history of nutrient loading and eutrophication in Lake Erie. *Limnol. Oceanogr*. 40: 918-929.

Schelske, C.L. and D.A. Hodell. 1991. Recent changes in productivity and climate of Lake Ontario detected by isotopic analysis of sediments. *Limnol. Oceanogr*. 36: 961-975.

Schropp, S.J., F.G. Lewis, H.L. Windom, J.D. Ryan, F.D. Calder and L.C. Burney. 1990. Interpretation of metal concentrations in estuarine sediments of Florida using aluminum as a reference element. *Estuaries.* 13: 227-235.

Schubel, J. R. and D. J. Hirschberg. 1977. ^{210}Pb determined sedimentation rate, and accumulation of metals in sediments at a station in Chesapeake Bay. *Chesapeake Sci.* 18: 379-382.

Simpson, R.L., R.E. Good, R. Walker and B.R. Frasco. 1983. The role of Delaware River freshwater tidal wetlands in the retention of nutrients and heavy metals. *J. Environ. Qual*. 12: 41-48.

Sinex, S.A. and G.R. Helz. 1981. Regional geochemistry of trace elements in Chesapeake Bay sediments. *Environ. Geol*. 3: 315-323.

Smol J.P. 2008. *Pollution of Lakes and Rivers: A Paleoenvironmental Perspective*- 2nd edition. Blackwell Publishing, Oxford.

Smol, J.P. 2002. *Pollution of Lakes and Rivers: A Paleoenvironmetal Perspective*. Arnold Press and Oxford University Press, NY.

Sommerfield, C.K. 2006. On sediment accumulation rates and stratigraphic completeness: Lessons from Holocene ocean margins. *Continental Shelf Research*. 26:2225-2240.

Song, W., J.C. Ford, L. An, W.J. Buckleya and K.J. Rockne. 2004. Polybrominated diphenyl ethers in sediments of the Great Lakes. 1. Lake Superior. *Environ. Sci. Tech*. 38(12): 3286-3293.

Thompson, P.M. and S. O'Byrne. 1999. *Images of America Wilmington's Waterfront*. Arcadia Publishing, Charleston, SC.

Trefry, J.H. and B.J. Presley. 1976. Heavy metal transport from the Mississippi River to the Gulf of Mexico. In: *Marine Pollution Transfer*, Eds.: H.L. Windom and R.A. Duce, Heath and Co., Lexington, pp. 39-75.

Ulseth, A.J. and A.E. Hershey. 2005. Natural abundances of stable isotopes trace anthropogenic N and C in an urban stream. *JNABS*: 24(2): 270-289.

United States Environmental Protection Agency (U.S. EPA). 2010. Current Site Information, Diamond State Salvage (accessed online at http://www.epa.gov/reg3hwmd/npl/DE0000122218.htm). U.S. Environmental Protection Agency, Region 3, Philadelphia, PA.

United States Environmental Protection Agency (U.S. EPA). 2009. Draft Recommended Interim Preliminary Remediation Goals for Dioxin in Soil at CERCLA and RCRA Sites. U.S. Environmental Protection Agency, Office of Superfund Remediation and Technology Innovation, Washington, D.C (December, 2009).

United States Environmental Protection Agency (U.S. EPA). 1993. EPA Superfund Record of Decision: E.I. Du Pont de Nemours & Co., Inc. (Newport Pigment Plant Landfill) EPA ID: DED980555122 OU 01 Newport, DE 09/29/1993 (EPA/ROD/R03-93/170). U.S. Environmental Protection Agency, Region 3, Philadelphia, PA.

United States Environmental Protection Agency (U.S. EPA). 1987. Guidance for Sampling of and Analyzing for Organic Contaminants in Sediments. Office of Water Regulations and Standards, Criteria and Standards Division, Washington, D.C.

Valette-Silver , N.J. 1993. The use of sediment cores to reconstruct historical trends in contamination of estuarine and coastal sediments. *Estuaries.* 16: 577-588.

van Dam, H., A. Mertens, and J. Sinkeldam. 1994. A coded checklist and ecological indicator values of freshwater diatoms from The Netherlands. *Neth. J. Aquat. Ecol*. 28: 117–133.

Van den Berg, M., et al. 2006. The 2005 World Health Organization Reevaluation of Human and Mammalian Toxic Equivalency Factors for Dioxins and Dioxin-Like Compounds. *Toxicol. Sci.* 93(2): 223-241.

Van Metre, P.C., B.J. Mahler and J.T. Wilson. 2009. PAHs underfoot: Contaminated dust from coal-tar sealcoated pavement is widespread in the United States. *Environ. Sci. Technol*.: 43(1): 20-25.

Van Metre, P, BJ Mahler, M Scoggins and PA Hamilton. 2006. Parking lot sealcoat: A major source of polycyclic aromatic hydrocarbons (PAHs) in rrban and suburban environments. US Geological Survey and the City of Austin, Fact Sheet 2005–3147.

Van Metre, P.C., B.J. Mahler and E.T. Furlong. 2000. Urban sprawl leaves its PAH signature. *Environ. Sci. Technol*. 34: 4064-4070.

Van Metre, P.C. and Callender, E. 1997. Identifying water-quality trends from ^{210}Pb using dated sediment cores from White Rock Lake Reservoir, Dallas, Texas. *Journal of Paleolimnology.* 17: 239-249.

Vane, C.H., Y.J. Ma, S.J Chen, and B.X. Mai. 2009. Increasing polybrominated diphenyl ether (PBDE) contamination in sediment cores from the inner Clyde Estuary, UK. Environ. *Geochem. Health*. Online edition (04 April 2009).

Velinsky, D.J., G.F. Riedel and J.T.F. Ashley. 2008. Assessment of Water Quality of the Tidal Potomac River in Washington DC: Trace Metals and Organic Contaminants. Final Report (04g-05-WQD03 (WP04)). District of Columbia, Department of the Environment, Washington, DC. (PCER Report: 08-3).

Velinsky, D.J., J.T.F. Ashley and G.R.Riedel. 2007. *Sediment Contaminants in the upper Tidal Potomac River; Washington, DC: Spatial and Temporal Trends.* Final Report submitted to Department of the Environment, District of Columbia. Patrick Center for Environmental Research, The Academy of Natural Sciences.

Velinsky, D.J., T.L. Wade, B. Gammisch and J. Cornwell. 1997. *Sediment Deposition and Inventory of Chemical Contaminants in the Tidal Anacostia River, Washington, D.C.* ICPRB Report #97-2. Interstate Commission on the Potomac River Basin, Rockville, MD.

Velinsky, D.J., T.L. Wade, C. Schlekat and B.J. Presley. 1994. Tidal river sediments in the Washington, D.C. area. I. Distribution and sources of trace metals. *Estuaries.* 17: 305-320.

Wade, T.L., D.J. Velinsky, E. Reinharz and C.E. Schlekat. 1994. Tidal river sediments in the Washington, D.C. area. II. Distribution and sources of chlorinated and non-chlorinated aromatic hydrocarbons. *Estuaries*. 17: 321-333.

Wakeham S.G., C. Schaffner and W. Giger. 1980. Polycyclic aromatic hydrocarbons in recent lake sediments—II. Compounds derived from biogenic precursors during early diagenesis. *Geochim Cosmochim Acta.* 44: 415–429.

Wallbrink, P.J., D.E. Walling and Q. He. 2002. Radionuclide measurement using HPGe gamma spectrometry. In: F. Zapata (Editor), *Handbook for the Assessment of Soil Erosion and Sedimentation Using Environmental Radionuclides*. Kluwer Academic Publishers, Dordrecht, pp. 67-96.

Wania, F. and C.B. Dugani. 2003. Assessing the long-range transport potential of polybrominated diphenyl ethers: a comparison of four multimedia models. *Environmental Toxicology and Chemistry.* 22: 1252–1261.

Wedepohl, K.H. 1971. *Geochemistry*. Holt, Rinehart and Winston, Inc., NY. (Translated from Geochemie, 1967).

Wedepohl, K.H. 1968. Chemical fractionation in the sedimentary environment, in Ahrens, L.H., ed., *Origin and Distribution of the Elements*: Oxford, England, Pergamon Press, pp. 999-1016.

Windom, H.L., S.J. Schropp, F.D. Calder and others. 1989. Natural trace metal concentrations in estuarine and coastal marine sediments of the southeastern United States. *Environ. Sci. Technol.,* 23: 314-320.

Woodwell, G.M., P.P. Craig and H.A. Johnson. 1971. DDT in the biosphere: Where does it go? *Science.* 174: 1101-1107.

Youngblood, W.W. and M. Blumer. 1975. Polycyclic aromatic hydrocarbons in the environment: homologous series in soils and recent marine sediments. *Geochim. Cosmochim. Acta*, 39: 1303-1314.

Zhang, X., E.R. Christensen and M.F. Gin. 1993. Polycyclic aromatic hydrocarbons in dated sediments from Green Bay and Lake Michigan. *Estuaries.* 16: 638-652.

Zimmerman, A.R. and E.A. Canuel. 2002. Sediment geochemical records eutrophication in the mesohaline Chesapeake Bay. *Limnol. Oceanogr*. 47: 1084-1093.

Tables

Table 1. Core locations and collection dates.

Name	Abbreviation	Date	Lat (N)	Long (W)	Depth of Core (cm)	Location
Brandywine River	BW-1	12/3/2007	39° 44.189'	75° 31.546'	36	Embayment
Churchman Marsh	CM-1A	3/25/2008	39° 42.021'	75° 37.810'	82	Marsh
Lower Shellpot Creek	LSP-2	4/15/2008	39° 44.320'	75° 30.597'	102	Marsh
Walnut Street	WS-2A	4/22/2008	39° 44.067'	75° 33.040'	98	Sub-tidal embayment
Dravo Marsh	DM-2	6/22/2008	39° 43.217'	75° 33.722'	106	Marsh

Table 2. Bulk sediment properties and radioisotope data for BW.

Chem ID	Interval	Water Content (%)	Dry Bulk Density (g/cm^3)	Accumulated Mass (g/cm^2)	LOI (%)	Total ^{210}Pb (dpm/g)	Excess ^{210}Pb (dpm/g)	^{137}Cs (dpm/g)	z (cm)	Age Model
9994	0-2	52.20	0.68	1.36	9.33	4.49	1.85	0.22	1	2006
9996	4-6	46.67	0.80	2.96	9.80	3.03	1.16	0.19	5	2000
9998	8-10	50.44	0.72	4.39	9.60	4.20	1.56	0.51	9	1995
10000	12-14	52.49	0.67	5.74	13.30	3.44	1.28	0.96	13	1990
10001	16-18	51.64	0.69	7.13	11.36	3.51	1.02	0.90	17	1984
10004	20-22	49.62	0.73	8.59	13.51	4.15	1.46	4.34	21	1979
10006	24-26	46.95	0.79	10.18	11.39	3.26	0.76	4.07	25	1974
10008	28-30	46.61	0.80	11.78	11.72	2.96	0.70	3.87	29	1968
10010	32-34	40.41	0.95	13.67	10.56	2.31	0.16	1.04	33	1963
10012	36-38	33.73	1.13	15.93	7.23	1.86	0.00	0.00	37	1958
10014	40-42	35.04	1.09	18.11	7.39	2.64	0.36	0.00	41	1952
10016	44-46	35.00	1.09	20.29	7.06	1.68	0.00	0.00	45	1947
10018	48-50	35.04	1.09	22.48	7.78	1.67	0.00	0.00	49	1942
10019	50-52	36.05	1.06	24.60	12.60	2.00	0.38	0.03	51	1939

Table 3. Bulk sediment properties and radioisotope data for CM.

Chem ID	Interval	Water Content (%)	Dry Bulk Density (g/cm^3)	Accumulated Mass (g/cm^2)	LOI (%)	Total ^{210}Pb (dpm/g)	Excess ^{210}Pb (dpm/g)	^{137}Cs (dpm/g)	z (cm)	Age Model
0219	0-2	73.19	0.32	0.64	19.61	9.83	7.60	0.19	1	2005
0221	4-6	72.32	0.33	1.31	18.11	10.65	7.79	0.33	5	1999
0223	8-10	64.79	0.45	2.21	15.27	9.22	6.74	0.34	9	1992
0225	12-14	63.93	0.47	3.14	14.95	6.73	4.55	0.24	13	1985
0227	16-18	63.61	0.47	4.09	15.56	7.01	4.69	0.33	17	1979
0229	20-22	66.55	0.42	4.93	16.98	7.17	4.86	0.50	21	1972
0231	24-26	61.80	0.50	5.93	15.56	6.02	3.93	0.48	25	1965
0233	28-30	49.59	0.73	7.40	11.83	3.88	0.98	0.12	29	1959
0235	32-34	46.65	0.80	9.00	11.80	3.81	0.22	0.00	33	1952
0237	36-38	45.94	0.81	10.63	11.35	3.76	0.63	0.00	37	1945
0239	40-42	45.33	0.83	12.29	11.20	2.61	0.25	0.00	41	1939
0241	44-46	43.45	0.87	14.03	10.46	3.44	0.73	0.00	45	1932
0243	48-50	44.96	0.84	15.71	9.84	3.40	0.09	0.00	49	1925
0245	52-54	42.80	0.89	17.48	10.05	3.08	0.63	0.00	53	1919
0247	56-58	43.31	0.88	19.24	9.43	2.96	0.44	0.00	57	1912
0249	60-62	45.31	0.83	20.90	9.76	2.72	0.33	0.00	61	1909
0251	64-66	41.55	0.92	22.73	8.56	2.76	0.45	0.00	65	1899
0253	68-70	35.53	1.08	24.89	7.40	2.74	0.39	0.00	69	1892
0255	72-74	32.40	1.17	27.22	6.63	2.29	0.04	0.00	73	1878

Table 4. Bulk sediment properties and radioisotope data for LSP.

Chem ID	Interval	Water Content (%)	Dry Bulk Density (g/cm^3)	Accumulated Mass (g/cm^2)	LOI (%)	Total ^{210}Pb (dpm/g)	Excess ^{210}Pb (dpm/g)	^{137}Cs (dpm/g)	z (cm)	Age Model
0429	0-2	70.82	0.36	0.71	20.85	14.79	12.29	0.26	1	2006
0431	4-6	64.01	0.46	1.64	17.61	12.36	10.48	0.33	5	2004
0433	8-10	56.92	0.59	2.82	13.77	14.20	12.15	0.30	9	2002
0435	12-14	63.29	0.48	3.77	18.98	12.47	10.27	0.24	13	2000
0437	16-18	68.21	0.40	4.56	24.48	14.35	12.29	0.22	17	1998
0439	20-22	57.70	0.57	5.71	17.32	14.94	12.19	0.41	21	1996
0441	24-26	55.23	0.62	6.95	16.22	15.31	12.75	0.38	25	1994
0443	28-30	53.68	0.65	8.25	16.68	13.06	10.28	0.38	29	1992
0445	32-34	57.31	0.58	9.42	16.94	11.23	9.31	0.32	33	1990
0447	36-38	63.85	0.47	10.35	17.64	8.79	6.89	0.21	37	1988
0449	40-42	60.96	0.52	11.38	15.49	9.46	7.19	0.20	41	1985
0451	44-46	58.98	0.55	12.48	16.09	8.76	6.71	0.15	45	1983
0453	48-50	67.22	0.41	13.31	24.07	7.51	5.48	0.16	49	1981
0454	50-52	69.16	0.38	14.07	23.33	8.07	5.53	0.22	51	1980
0455	52-54	68.54	0.39	14.85	27.87	7.10	5.67	0.08	53	1979
0457	56-58	71.32	0.35	15.55	33.96	5.18	4.26	0.16	57	1977
0459	60-62	60.15	0.53	16.61	12.36	5.41	2.74	0.52	61	1975
0461	64-66	61.59	0.50	17.62	14.17	5.48	2.90	0.41	65	1973
0463	68-70	60.26	0.53	18.68	12.34	4.19	1.47	0.58	69	1971
0465	72-74	64.75	0.45	19.58	13.90	5.20	2.37	0.59	73	1969
0467	76-78	53.45	0.66	20.89	9.66	4.86	2.71	0.63	77	1966
0469	80-82	55.68	0.61	22.12	11.26	5.11	2.93	0.42	81	1964
0471	84-86	38.72	0.99	24.10	6.09	2.32	0.82	0.18	85	1962
0473	88-90	32.50	1.16	26.43	4.61	1.59	0.29	0.14	89	1960
0475	92-94	30.26	1.23	28.89	3.83	1.99	0.11	0.10	93	1958
0477	96-98	52.58	0.67	30.24	14.02	5.30	2.60	0.37	97	1956
0479	100-102	40.45	0.95	32.13	5.50	2.39	0.33	0.08	101	1954

Table 5. Bulk sediment properties and radioisotope data for DM.

Chem ID	Interval	Water Content (%)	Dry Bulk Density (g/cm^3)	Accumulated Mass (g/cm^2)	LOI (%)	Total ^{210}Pb (dpm/g)	Excess ^{210}Pb (dpm/g)	^{137}Cs (dpm/g)	z (cm)	Age Model
1055	0-2	82.46	0.20	0.39	36.30	10.23	8.78	0.28	1	2006
1057	4-6	79.77	0.23	0.86	32.10	9.25	7.82	0.20	5	2000
1059	8-10	84.76	0.17	1.19	38.91	6.64	5.00	0.27	9	1995
1061	12-14	77.86	0.26	1.71	29.13	5.54	3.62	0.35	13	1990
1063	16-18	69.70	0.37	2.45	21.97	4.98	2.83	0.61	17	1984
1065	20-22	58.08	0.57	3.59	14.03	4.82	2.35	0.54	21	1979
1067	24-26	47.26	0.79	5.16	10.35	2.88	0.15	0.24	25	1974
1069	28-30	48.51	0.76	6.67	10.990	4.24	1.31	0.23	29	1968
1071	32-34	53.22	0.66	7.99	13.589	4.35	1.55	0.27	33	1963
1073	36-38	64.18	0.46	8.92	20.541	4.62	2.33	0.12	37	1958
1075	40-42	54.81	0.63	10.17	15.278	4.11	1.28	0.00	41	1952
1077	44-46	45.53	0.82	11.82	10.678	3.19	0.42	0.00	45	1947
1079	48-50	40.37	0.95	13.72	8.204	2.64	0.00	0.00	49	1942
1081	52-54	37.36	1.03	15.77	7.017	2.30	0.00	0.00	53	1935
1083	56-58	33.92	1.12	18.02	5.744	2.10	0.02	0.00	57	1931
1085	60-62	32.99	1.15	20.32	5.053	2.48	0.00	0.00	61	1927
1087	64-66	37.69	1.02	22.35	6.186	2.21	0.08	0.00	65	1920
1089	68-70	37.95	1.01	24.38	6.863	2.95	0.30	0.00	69	1915

Table 6. Summary data for radioisotope analysis and dating.

		Radioisotope Inventory		Sedimentation Rate			Mass Accumulation Rate		Depositional Flux	Focusing Factor	
Location	**Core**	xsPb-210	Cs-137	xsPb-210 CA	xsPb-210 CF	Cs-137	xsPb-210	Cs-137	xsPb-210	xsPb-210	Cs-137
		dpm/cm^2	dpm/cm^2	cm/yr	cm/yr	cm/yr	g/cm^2-yr	g/cm^2-yr	dpm/cm^2-yr		
Brandywine River	BW-2	28.00	49.00	0.64	0.96	0.66	0.25	0.28	0.53	0.90	2.30
Churchmans Marsh	CM-1	66.00	4.00	0.63	1.00	0.57	0.17	0.15	0.95	2.10	0.20
Shellpot Creek	SP-2	399.00	18.00	1.30	2.10	1.90	0.37	0.60	7.50	12.50	0.90
Dravo Marsh	DM-2	82.00	5.00	NA	0.73	0.74	0.29	0.19	0.85	2.60	0.30

xs – excess; CA – Constant activity model; CF – Constant flux model (modified to match Cs-137 input function)
Depositional flux – based on steady-state atmospheric fluxes of xsPb-210 (32 dpm/cm^2-yr) and Cs-137 (21 dpm/cm^2-yr)

Table 7. Concentrations of various parameters for Core BW.

CHEM ID	Interval cm	Mid-Point cm	Solids %	Age Model yr	$\delta^{13}C$ per mil	$\delta^{15}N$ per mil	TC %	TN %	C/N Atomic
9994	0-2	1	47.3	2006	-26.48	5.37	3.82	0.31	14.50
9996	4-6	5	46.5	2000	-26.57	5.34	4.17	0.29	16.67
9998	8-10	9	49.2	1995	-25.94	4.95	3.96	0.29	15.82
10000	12-14	13	48.1	1990	-23.82	5.36	3.79	0.32	13.84
10001	14-16	15	49.9	1987	-23.54	5.20	3.85	0.34	13.15
10003	18-20	19	51.0	1982	-23.40	5.19	3.93	0.32	14.53
10004	20-22	21	49.6	1979	-26.34	3.94	6.79	0.44	17.91
10006	24-26	25	51.3	1974	-25.63	4.87	5.80	0.31	21.59
10008	28-30	29	52.9	1968	-25.57	4.83	7.02	0.48	16.98
10010	32-34	33	55.6	1963	-25.17	5.05	6.32	0.39	18.74
10012	36-38	37	68.4	1958	-24.11	4.33	2.03	0.16	14.89
10013	38-40	39	67.5	1955	-23.69	4.80	2.14	0.17	14.52
10015	42-44	43	66.1	1950	-23.63	4.94	1.60	0.15	12.20
10017	46-48	47	67.1	1944	-23.53	4.82	1.70	0.26	7.74
10019	50-52	51	64.0	1939	-23.65	5.50	2.22	0.20	13.03

Table 7 (continued). Concentrations of various parameters for Core BW.

CHEM ID	TSP	Fe	Zn	tPAHs	T PCBs	tDDXs	tChlordanes	tDioxins	tFurans	2,3,7,8 TCDD-TEQ	tPBDEs
	%	µg/g dw	µg/g dw	µg/g dw	ng/g dw	ng/g dw	ng/g dw	pg/g dw	pg/g dw	pg/g dw	ng/g dw
9994	0.084	29412	486	1.97	44.64	8.17	2.48	6992	621	21.8	52.8
9996	0.087	34804	471	4.30	45.05	9.50	2.00	5327	551	16.2	48.5
9998	0.087	37237	485	1.03	70.96	13.01	2.77	8507	554	21.4	120.1
10000	0.269	41667	337	2.10	636.80	308.12	7.10	12628	1562	46.2	0.69
10001	0.191	37255	376	2.16	685.04	288.74	6.80	11580	1414	41.7	1.16
10003	0.158	29412	518	2.70	617.66	369.03	6.82	9077	1730	44.8	0.92
10004	0.090	40196	784	8.95	431.11	69.16	51.10	7123	2849	93.0	NA
10006	0.105	40686	769	5.20	120.06	39.66	7.73	6702	2705	68.5	NA
10008	0.122	38725	706	8.01	118.79	63.16	3.40	7055	2868	75.3	1.49
10010	0.121	25490	565	5.01	77.85	41.42	1.53	6668	2239	37.6	1.37
10012	0.085	29796	461	3.40	4.63	1.63	0.44	6927	117	9.5	NA
10013	0.103	31580	392	3.67	3.63	6.59	0.34	7070	116	8.9	NA
10015	0.075	32680	431	2.52	5.79	5.79	0.22	4417	128	6.5	0.85
10017	0.083	35294	486	2.04	2.19	3.60	0.25	6519	233	10.1	NA
10019	0.095	33296	296	2.97	2.95	5.09	0.29	6716	61	8.9	1.14

Concentrations on a dry weight basis. Total PAHs is the sum of 39 individual compounds, total PCBs is the sum of 110 congeners, total DDX is the sum of o,p+pp forms of DDD, DDE, and DDT, and total chlordane is the sum of alpha+gamma chlordane, heptachlor, heptachlor epoxide, oxychlordane, nonachlor and nonachlor epoxide (See Appendix I).

Table 8. Concentrations of various parameters for Core CM.

CHEM ID	Interval cm	Mid-Point cm	Solids %	Age Model yr	$\delta^{13}C$ per mil	$\delta^{15}N$ per mil	TC %	TN %	C/N Atomic
0219	0-2	1	28.3	2005	-28.14	8.08	7.52	0.79	11.09
0221	4-6	5	26.1	1999	-28.11	7.30	7.73	0.75	12.00
0223	8-10	9	33.8	1992	-27.77	6.95	5.71	0.55	12.05
0225	12-14	13	36.8	1985	-27.73	6.60	5.39	0.50	12.64
0227	16-18	17	32.7	1979	-27.42	6.39	6.34	0.60	12.38
0229	20-22	21	44.1	1972	-27.19	5.49	4.93	0.42	13.84
0231	24-26	25	53.2	1965	-26.75	4.71	3.44	0.30	13.26
0233	28-30	29	54.1	1959	-26.93	4.17	3.52	0.31	13.14
0235	32-34	33	54.0	1952	-26.28	4.35	3.66	0.32	13.51
0237	36-38	37	54.5	1945	-25.95	4.13	3.52	0.34	12.05
0240	42-44	43	55.5	1935	-26.00	4.75	3.02	0.26	13.47
0243	48-50	49	57.7	1925	-24.40	4.58	2.65	0.23	13.28
0247	56-58	57	56.1	1912	-25.74	4.08	2.88	0.26	12.84
0251	64-66	65	60.0	1899	-25.47	4.24	1.99	0.20	11.76
0255	72-74	73	66.5	1885	-25.63	4.73	1.73	0.19	10.40
0259	80-82	81	70.1	1872	-24.66	4.79	1.17	0.15	9.07

Table 8 (continued). Concentrations of various parameters for Core CM.

CHEM ID	TSP	Fe	Zn	tPAHs	T PCBs	tDDXs	tChlordanes	tDioxins	tFurans	2,3,7,8 TCDD-TEQ	tPBDEs
	%	µg/g dw	µg/g dw	µg/g dw	ng/g dw	ng/g dw	ng/g dw	pg/g dw	pg/g dw	pg/g dw	ng/g dw
0219	0.180	45656	723	1.68	90.28	9.31	2.79	13306	523	19.9	10.34
0221	NA	37255	973	2.24	157.91	15.91	3.53	13163	525	30.7	12.09
0223	NA	33996	984	1.41	125.85	10.38	1.36	14876	691	30.3	9.72
0225	0.182	35743	980	1.43	189.18	11.98	1.91	18228	838	40.8	10.92
0227	0.170	35351	1086	1.71	339.36	20.54	3.31	18999	754	42.7	17.12
0229	0.125	33824	3817	2.00	487.00	26.39	2.24	10923	616	29.9	3.69
0231	0.101	26471	4078	2.50	781.53	39.82	2.31	11945	606	22.6	1.02
0233	0.106	29223	4374	6.00	2106.59	108.23	4.60	10541	1315	24.5	0.80
0235	0.113	32843	8314	6.83	1809.13	117.59	6.60	157727	12695	444.6	0.34
0237	0.119	36765	9804	26.79	980.36	62.99	4.66	29775	3183	102.5	0.41
0240	0.106	30702	9482	3.18	328.06	20.55	1.49	13028	1562	19.5	NA
0243	0.105	39706	7529	0.90	66.76	3.18	0.38	11904	683	20.3	NA
0247	0.089	37255	9098	1.39	152.68	6.06	0.60	15189	1352	32.5	NA
0251	0.066	30392	4078	2.10	144.25	3.39	0.42	13756	1903	15.2	NA
0255	0.055	33333	149	0.46	4.09	0.68	0.10	18161	54	10.9	NA
0259	0.060	35083	131	0.44	2.83	0.84	0.07	13160	19	7.5	NA

Concentrations on a dry weight basis. NA- Not analyzed. Total PAHs is the sum of 39 individual compounds, total PCBs is the sum of 110 congeners, total DDX is the sum of o,p+pp forms of DDD, DDE, and DDT, and total chlordane is the sum of alpha+gamma chlordane, heptachlor, heptachlor epoxide, oxychlordane, nonachlor and nonachlor epoxide (See Appendix I).

Table 9. Concentrations of various parameters for Core DM.

CHEM ID	Interval	Mid-Point	Solids	Age Model	$\delta^{13}C$	$\delta^{15}N$	TC	TN	C/N
	cm	cm	%	yr	per mil	per mil	%	%	Atomic
1055	0-2	1	15.5	2006	-28.59	7.76	18.19	1.17	18.14
1057	4-6	5	18.6	2000	-28.51	7.80	14.53	0.93	18.20
1058	6-8	7	26.6	1998	-28.01	7.61	10.64	0.68	18.13
1059	8-10	9	14.0	1995	-28.21	7.86	19.77	1.15	20.11
1060	10-12	11	13.8	1992	-28.29	7.36	18.88	1.04	21.13
1061	12-14	13	16.9	1990	-28.26	7.37	17.54	1.01	20.17
1063	16-18	17	32.3	1984	-27.69	7.14	8.77	0.55	18.53
1065	20-22	21	51.0	1979	-27.28	6.22	5.14	0.30	20.18
1067	24-26	25	57.5	1974	-26.91	6.16	4.18	0.26	18.82
1069	28-30	29	54.0	1968	-26.87	6.75	4.86	0.30	19.03
1071	32-34	33	57.6	1963	-26.48	6.56	3.61	0.23	18.10
1073	36-38	37	37.6	1958	-27.07	6.54	8.34	0.50	19.35
1076	42-44	43	44.7	1950	-26.78	7.91	6.49	0.42	17.99
1079	48-50	49	58.7	1942	-25.90	6.83	3.08	0.23	15.85
1083	56-58	57	64.9	1931	-24.51	4.78	1.47	0.13	13.58
1087	64-66	65	62.0	1920	-24.51	4.45	1.69	0.15	12.84
1095	80-82	81	64.3	1905	-25.21	5.77	1.65	0.13	14.67
1102	94-96	95	62.0	1888	-25.28	5.36	1.33	0.14	10.89
1106	102-104	103	61.5	1878	-24.60	5.90	1.04	0.12	10.15

Table 9 (continued). Concentrations of various parameters for Core DM.

CHEM ID	TSP	Fe	Zn	tPAHs	T PCBs	tDDXs	tChlordanes	tDioxins	tFurans	2,3,7,8 TCDD-TEQ	tPBDEs
	%	µg/g dw	µg/g dw	µg/g dw	ng/g dw	ng/g dw	ng/g dw	pg/g dw	pg/g dw	pg/g dw	ng/g dw
1055	0.098	12504	538	2.70	238.49	29.07	9.69	9244	1117	32.9	17.07
1057	0.092	9056	647	1.93	278.19	30.22	9.65	7806	975	33.9	32.64
1058	0.082	18166	742	4.17	239.94	23.45	5.40	16594	2100	69.9	NA
1059	0.087	29762	1045	2.95	356.71	41.19	13.11	10023	1279	32.1	12.47
1060	0.083	20427	777	4.84	436.01	50.41	13.82	6638	769	26.4	15.01
1061	0.082	12276	811	8.05	325.98	33.85	10.93	4429	572	13.8	16.02
1063	0.073	9013	818	5.46	364.52	39.88	9.26	5701	779	24.3	2.42
1065	0.045	7782	594	3.86	180.97	28.13	3.94	5084	1394	27.7	1.51
1067	0.040	5388	299	2.83	45.05	6.87	0.79	3188	778	16.9	NA
1069	0.046	8631	610	2.80	35.87	4.84	0.44	2033	552	12.2	0.29
1071	0.043	10058	678	4.34	48.61	6.74	0.71	2102	608	20.0	0.56
1073	0.090	11043	1230	6.52	394.89	68.54	3.53	11880	4808	93.9	0.46
1076	0.071	6186	1059	5.46	102.14	11.12	1.41	2577	1707	31.0	NA
1079	0.051	6443	319	3.84	19.17	1.39	0.42	9517	2900	33.6	NA
1083	0.058	9497	149	0.97	3.70	0.71	0.14	1438	53	2.6	NA
1087	0.049	14220	175	3.58	2.58	0.71	0.13	1475	244	5.2	0.60
1095	0.054	8185	71	0.79	2.39	0.49	0.12	6085	12	7.5	NA
1102	0.067	17779	84	0.25	2.22	0.47	0.10	1175	11	1.2	NA
1106	0.050	11249	95	0.34	2.82	0.86	0.10	1819	13	2.4	NA

Concentrations on a dry weight basis. TBC - to be completed. Total PAHs is the sum of 39 individual compounds, total PCBs is the sum of 110 congeners, total DDX is the sum of o,p+pp forms of DDD, DDE, and DDT, and total chlordane is the sum of alpha+gamma chlordane, heptachlor, heptachlor epoxide, oxychlordane, nonachlor and nonachlor epoxide (See Appendix I).

Table 10. Concentrations of various parameters for Core LSP.

CHEM ID	Interval	Mid-Point	Solids	Age Model	$\delta^{13}C$	$\delta^{15}N$	TC	TN	C/N
	cm	cm	%	yr	per mil	per mil	%	%	Atomic
0429	0-2	1	27.6	NC	-27.81	3.95	9.10	0.56	19.08
0432	6-8	7	41.1	NC	-28.09	3.33	5.62	0.35	18.54
0464	70-72	71	34.9	NC	-22.25	2.69	4.56	0.25	21.25
0478	98-100	99	58.1	NC	-23.64	4.05	2.00	0.13	17.99
0479	100-102	101	59.5	NC	-23.56	3.45	1.84	0.12	18.29

CHEM ID	TSP	Fe	Zn	tPAHs	T PCBs	tDDXs	tChlordanes	tDioxins	tFurans	2,3,7,8 TCDD-TEQ	tPBDEs
	%	µg/g dw	µg/g dw	µg/g dw	ng/g dw	ng/g dw	ng/g dw	pg/g dw	pg/g dw	pg/g dw	ng/g dw
0429	0.137	19998	350	13.35	673.0	75.32	150.8	5322	223	5.5	NA
0432	0.127	13127	216	8.41	615.9	40.86	82.4	7684	316	7.7	NA
0464	0.180	60668	412	19.45	3456.3	53.67	52.9	7214	744	11.3	NA
0478	0.083	24466	214	2.26	474.8	19.44	13.3	3042	599	5.1	NA
0479	0.065	21275	168	1.78	303.1	16.25	9.0	2950	379	4.2	NA

Concentrations on a dry weight basis. NA – Not analyzed. Total PAHs is the sum of 39 individual compounds, total PCBs is the sum of 110 congeners, total DDX is the sum of o,p+pp forms of DDD, DDE, and DDT, and total chlordane is the sum of alpha+gamma chlordane, heptachlor, heptachlor epoxide, oxychlordane, nonachlor and nonachlor epoxide (See Appendix I).

Table 11. Concentrations of various parameters for Core WS.

CHEM ID	Interval	Mid-Point	Solids	Age Model	$\delta^{13}C$	$\delta^{15}N$	TC	TN	C/N
	cm	cm	%	yr	per mil	per mil	%	%	Atomic
0480	0-2	1	32.4	NC	-25.81	5.02	4.42	0.34	14.94
0483	6-8	7	37.2	NC	-25.83	4.78	4.25	0.28	17.68
0491	22-24	23	42.0	NC	-25.43	4.97	4.02	0.31	15.01
0504	48-50	49	44.6	NC	-25.94	4.53	3.80	0.28	15.95
0513	66-68	67	41.0	NC	-25.80	4.80	4.37	0.30	16.88
0527	94-96	95	44.8	NC	-25.09	5.67	3.73	0.31	13.91

CHEM ID	TSP	Fe	Zn	tPAHs	T PCBs	tDDXs	tChlordanes	tDioxins	tFurans	2,3,7,8 TCDD-TEQ	tPBDEs
	%	µg/g dw	µg/g dw	µg/g dw	ng/g dw	ng/g dw	ng/g dw	pg/g dw	pg/g dw	pg/g dw	ng/g dw
0480	0.174	48519	367	10.00	197.0	25.91	8.15	14339	1331	13.9	NA
0483	0.140	45526	876	9.58	171.4	25.62	7.26	9174	937	12.8	NA
0491	0.157	48905	881	10.50	76.0	10.64	3.39	8963	954	12.0	NA
0504	0.132	52173	974	11.10	236.4	24.56	8.33	4912	409	5.7	NA
0513	0.166	55448	1130	8.14	120.1	10.83	3.06	13321	2552	39.3	NA
0527	0.157	47092	1139	10.24	199.3	16.93	5.67	12049	2061	41.5	NA

Concentrations on a dry weight basis. NA – Not analyzed. Total PAHs is the sum of 39 individual compounds, total PCBs is the sum of 110 congeners, total DDX is the sum of o,p+pp forms of DDD, DDE, and DDT, and total chlordane is the sum of alpha+gamma chlordane, heptachlor, heptachlor epoxide, oxychlordane, nonachlor and nonachlor epoxide (See Appendix I).

Table 12. List of compounds in Figure 17.

PAH Compound	Cmpd #
Naphthalene	1
biphenyl	2
Acenaphthylene	3
Acenaphthene	4
Fluorene	5
Dibenzothiophene	6
Phenanthrene	7
Anthracene	8
Fluoranthene	9
BenzoAfluorene	10
BenzoBfluorene	11
Pyrene	12
Cyclopenta[cd]pyrene	13
Chrysene + Triphenylene	14
Naphthacene	15
Benzo[b]fluoranthene	16
Benzo[k]fluoranthene	17
Benzo[e]pyrene	18
Benzo[a]pyrene	19
Perylene	20
Indeno[1,2,3-cd]pyrene	21
Dibenzo[a,h+a,c]anthracene	22
Benzo[g,h,i]perylene	23
Coronene	24

Table 13. Diatom Metrics determined from species identification: Brandywine Creek Core.

Core ID/ Depth Interval (cm)	Mid-Depth (cm)	Year	Eutrophentic	Meso/ eurotrophentic	Mesotrophentic	Oligotrophentic
BW2 0-2 cm	1	2006	53.57	18.65	5.36	0.00
BW2 4-6 cm	5	2000	52.17	20.16	4.74	0.00
BW2 8-10 cm	9	1995	58.02	13.07	13.47	0.00
BW2 12-14 cm	13	1990	25.94	0.40	17.43	1.39
BW2 14-16 cm	15	1987	45.56	7.69	3.94	2.96
BW2 18-20 cm	19	1982	39.48	3.37	6.15	10.32
BW2 20-22 cm	21	1979	46.61	2.79	6.18	0.00
BW2 24-26 cm	25	1974	53.58	4.26	5.22	0.77
BW2 28-30 cm	29	1968	58.22	6.53	4.55	0.20
BW2 32-34 cm	33	1963	32.29	5.06	3.84	0.35
BW2 36-38 cm	37	1958	25.75	4.99	1.40	0.20
BW2 38-40 cm	39	1955	34.40	2.00	4.60	0.00
BW2 42-44 cm	43	1950	26.53	1.78	2.18	0.40
BW2 46-48 cm	47	1944	27.17	1.52	1.96	0.43
BW2 50-52 cm	51	1939	30.54	5.39	2.59	0.40

Metrics based on van Dam et al. (1994)

Table 14. Diatom Metrics determined from species identification: Churchmans Marsh Core.

Core ID/ Depth Interval (cm)	Mid-Depth (cm)	Year	Eutrophentic	Meso/ eurotrophentic	Mesotrophentic	Oligotrophentic	Oligo/ mesotrophentic
CM1 0-2 cm	1	2005	76.61	4.29	0.97	0.00	76.61
CM1 4-6 cm	5	1999	81.46	2.96	0.59	0.20	81.46
CM1 8-10 cm	9	1992	71.40	6.06	1.14	0.00	71.40
CM1 12-14 cm	13	1985	71.54	2.17	0.99	0.00	71.54
CM1 16-18 cm	17	1979	74.16	2.78	0.00	0.00	74.16
CM1 20-22 cm	21	1972	63.00	3.80	3.00	0.00	63.00
CM! 24-26 cm	25	1965	57.60	6.80	1.20	0.40	57.60
CM1 28-30 cm	29	1959	42.63	10.61	3.34	1.18	42.63
CM1 32-34 cm	33	1952	45.87	7.87	1.57	0.20	45.87
CM1 36-38 cm	37	1945	27.63	8.75	2.58	0.00	27.63
CM1 42-44 cm	43	1935	33.67	7.77	2.19	0.00	33.67
CM1 48-50 cm	49	1925	39.80	8.20	4.20	0.40	39.80
CM1 56-58 cm	57	1912	35.23	7.24	0.78	0.20	35.23
CM1 64-66 cm	65	1899	40.08	9.13	2.38	0.40	40.08
CM1 72-74 cm	73	1885	32.03	3.92	0.87	0.00	32.03
CM1 80-82 cm	81	1872	35.57	4.25	0.22	1.57	35.57

Metrics based on van Dam et al. (1994)

Table 15. Diatom Metrics determined from species identification: Dravo Marsh Core.

Core ID/ Depth Interval (cm)	Mid-Depth (cm)	Year	Eutrophentic	Meso/ eurotrophentic	Mesotrophentic	Oligotrophentic	Oligo/ mesotrophentic
DM2 0-2 cm	1	2006	64.66	7.57	4.47	0.19	64.66
DM2 4-6 cm	5	2000	71.79	3.55	2.37	0.00	71.79
DM 8-10 cm	9	1995	67.13	6.53	4.36	0.20	67.13
DM2 12-14 cm	13	1990	69.41	3.73	4.31	0.78	69.41
DM2 16-18 cm	17	1984	55.45	3.96	1.78	0.40	55.45
DM2 20-22 cm	21	1979	58.27	3.54	3.94	0.20	58.27
DM2 24-26 cm	25	1974	46.22	4.78	0.80	0.20	46.22
DM2 32-34 cm	33	1963	35.39	5.37	0.99	0.20	35.39
DM2 42-44 cm	43	1950	36.67	6.67	1.57	1.57	36.67
DM2 56-58 cm	57	1931	33.27	4.47	2.14	0.58	33.27
DM2 64-66 cm	65	1920	40.59	4.16	2.18	0.20	40.59
DM2 80-82 cm	81	1905	25.84	4.57	5.96	0.00	25.84

Metrics based on van Dam et al. (1994)

Figures

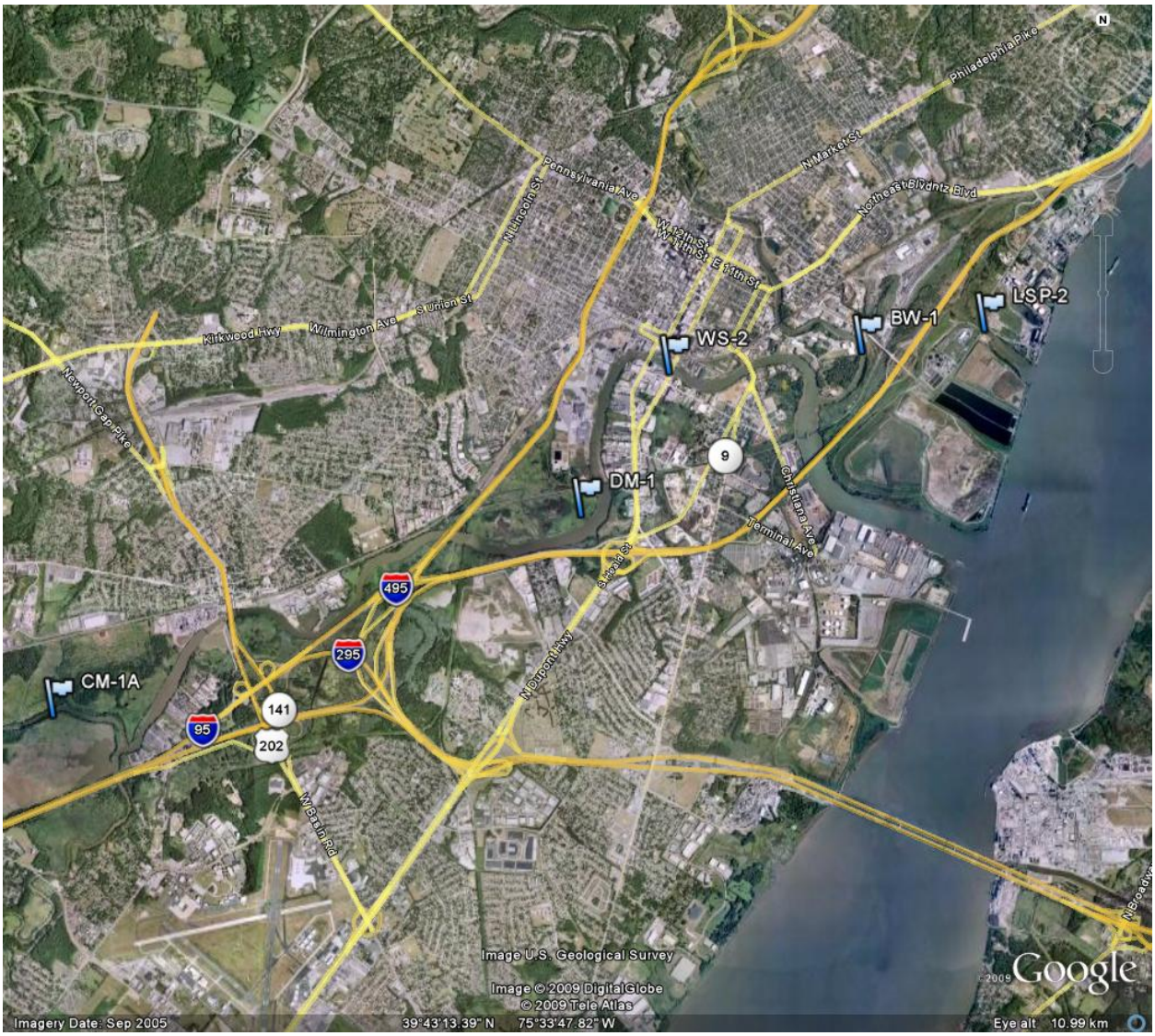

Figure 1. Coring locations within the tidal Christina River system. Key: CM – Churchmans Marsh, DM – Dravo Marsh (Old Wilmington Marsh), WS - Walnut Street embayment, BW-Brandywine wetland, and LSP – Lower Shellpot.

Figure 2. Tripod and pulley system used to retrieve push-piston cores at Dravo Marsh within the tidal Christina River system.

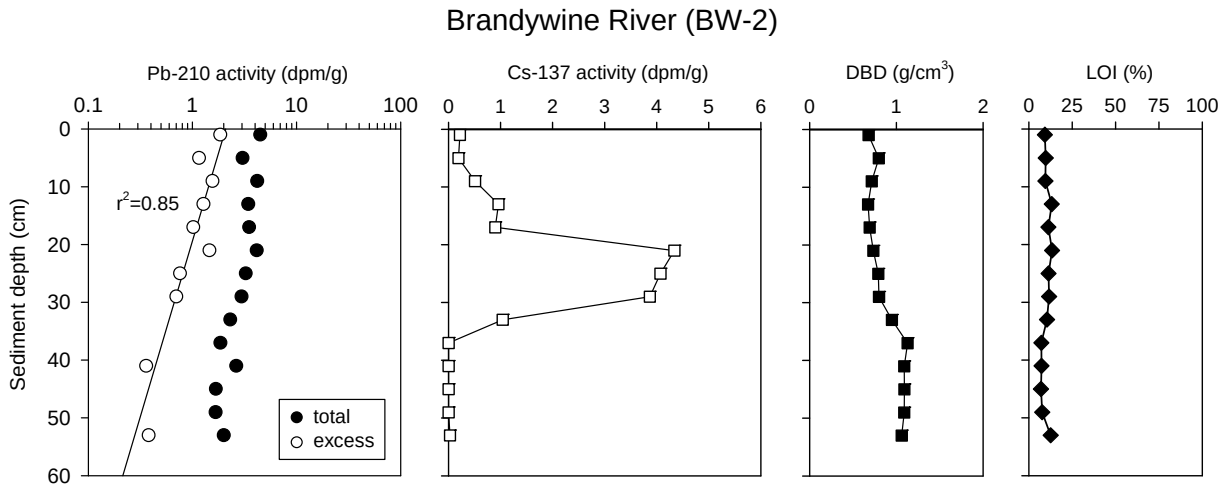

Figure 3. Geochronology for the Brandywine Creek marsh using excess ^{210}Pb and transient fallout ^{137}Cs. The radionuclides give comparable sedimentation rates of 0.80 (constant activity model) and 0.10 cm/yr, respectively. The first occurrence of ^{137}Cs at 36-38 cm is assumed concordant with ca. 1954.

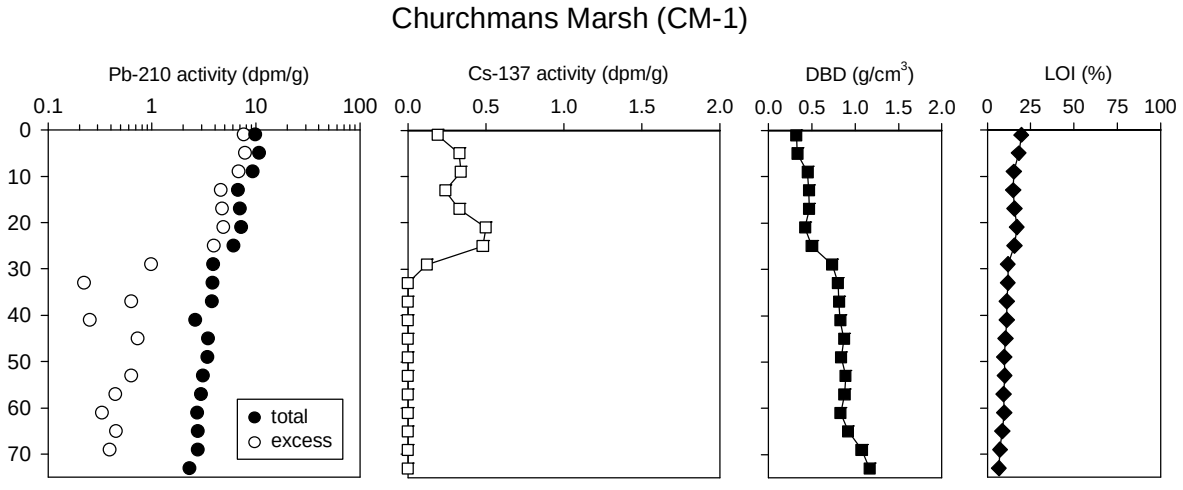

Figure 4. Geochronology for the Churchmans Marsh using excess ^{210}Pb and transient fallout ^{137}Cs. The radionuclides give comparable sedimentation rates of 0.51 (constant flux model) and 0.60 cm/yr, respectively. The first occurrence of ^{137}Cs at 32-34 cm is assumed concordant with ca. 1954.

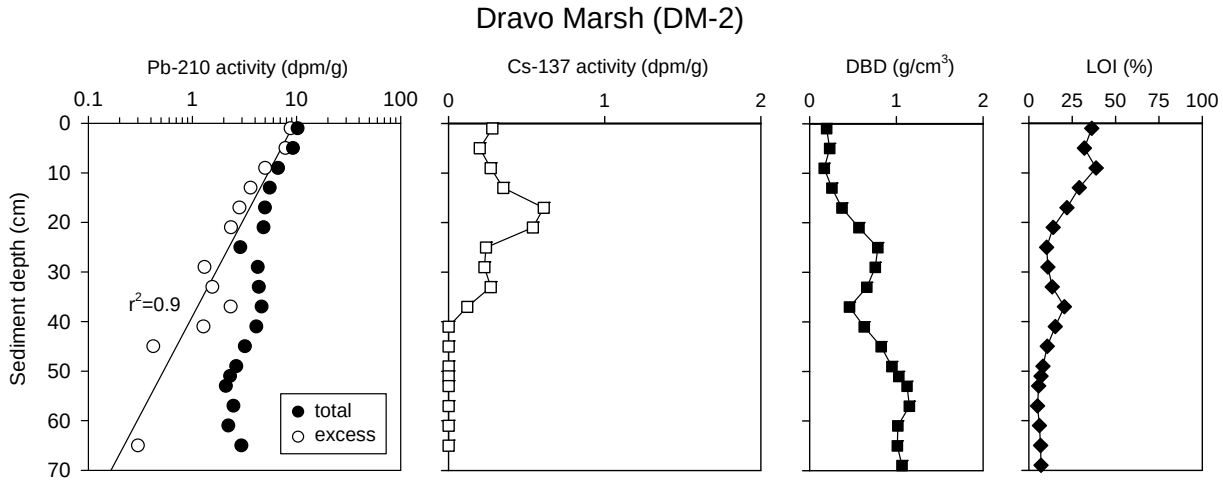

Figure 5. Geochronology for the Dravo Marsh using excess ^{210}Pb and transient fallout ^{137}Cs. The radionuclides give comparable sedimentation rates of 0.56 (constant activity model) and 0.79 cm/yr, respectively. The first occurrence of ^{137}Cs at 38-40 cm is assumed concordant with ca. 1954.

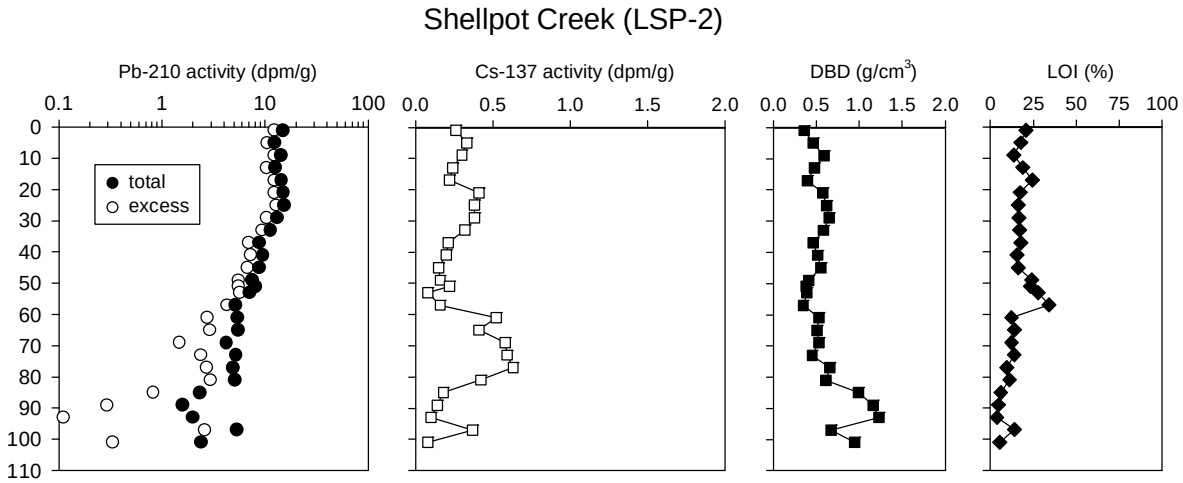

Figure 6. . Geochronology for the Shellpot Creek using excess ^{210}Pb and transient fallout ^{137}Cs. The radionuclides give identical sedimentation rates of 0.19 cm/yr using the constant flux model for ^{210}Pb. The first occurrence of ^{137}Cs at 100-102 cm is assumed concordant with ca. 1954.

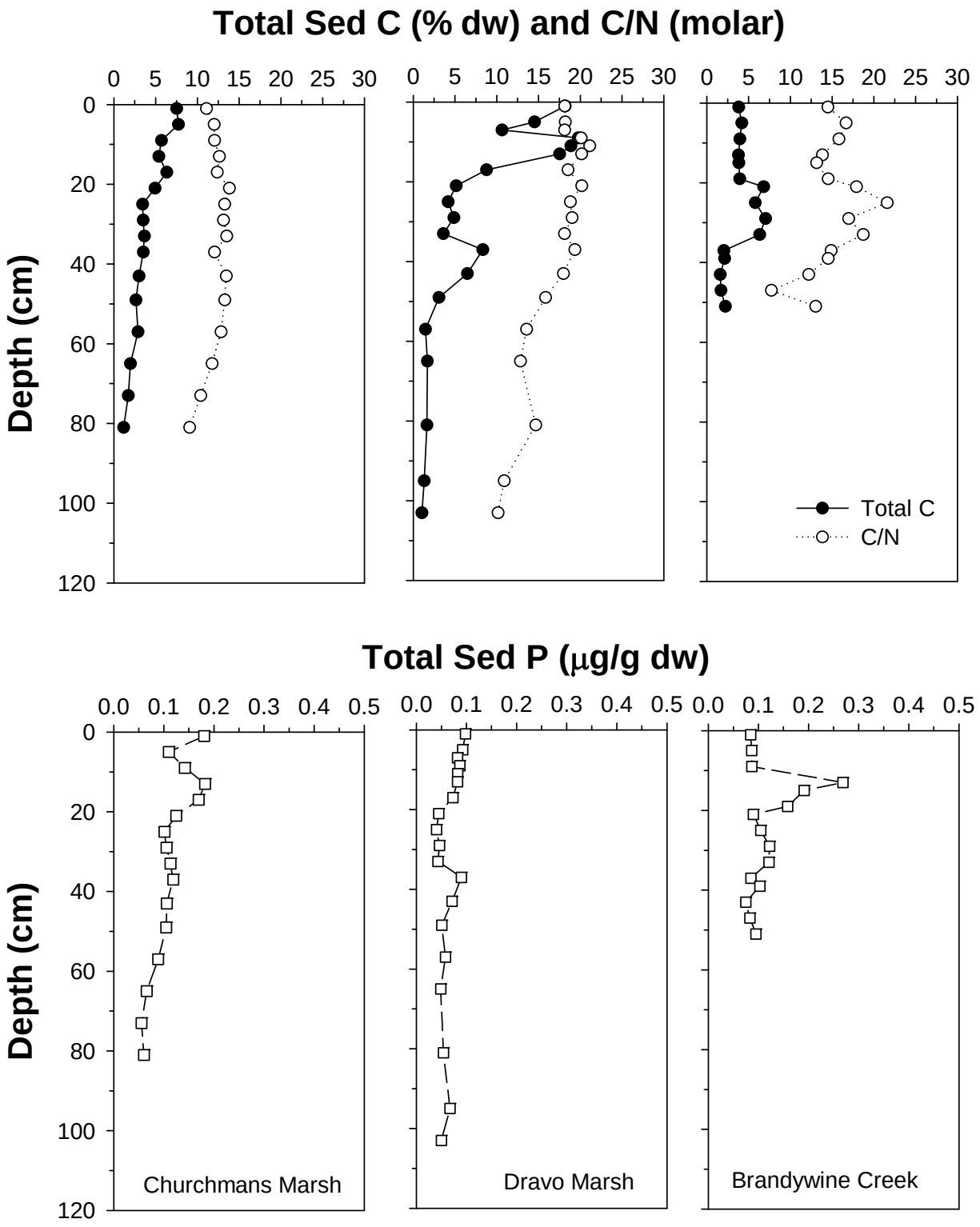

Figure 7a. Sediment organic carbon, C/N and sediment phosphorus distribution with depth for Churchmans, Dravo and Brandywine marshes.

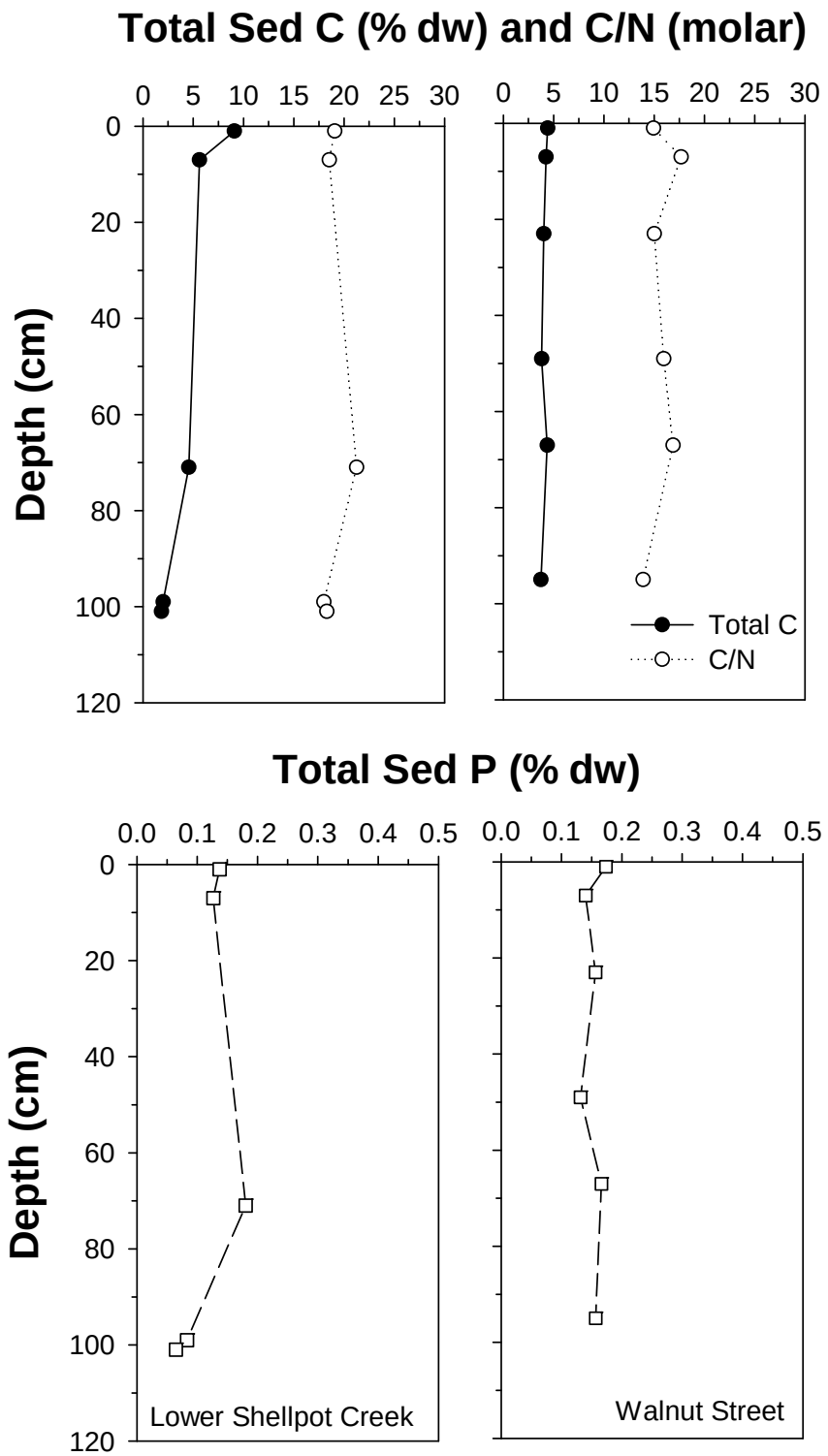

Figure 7b. Sediment organic carbon, C/N and sediment phosphorus distribution with depth for the cores from lower Shellpot Creek and Walnut Street Bridge.

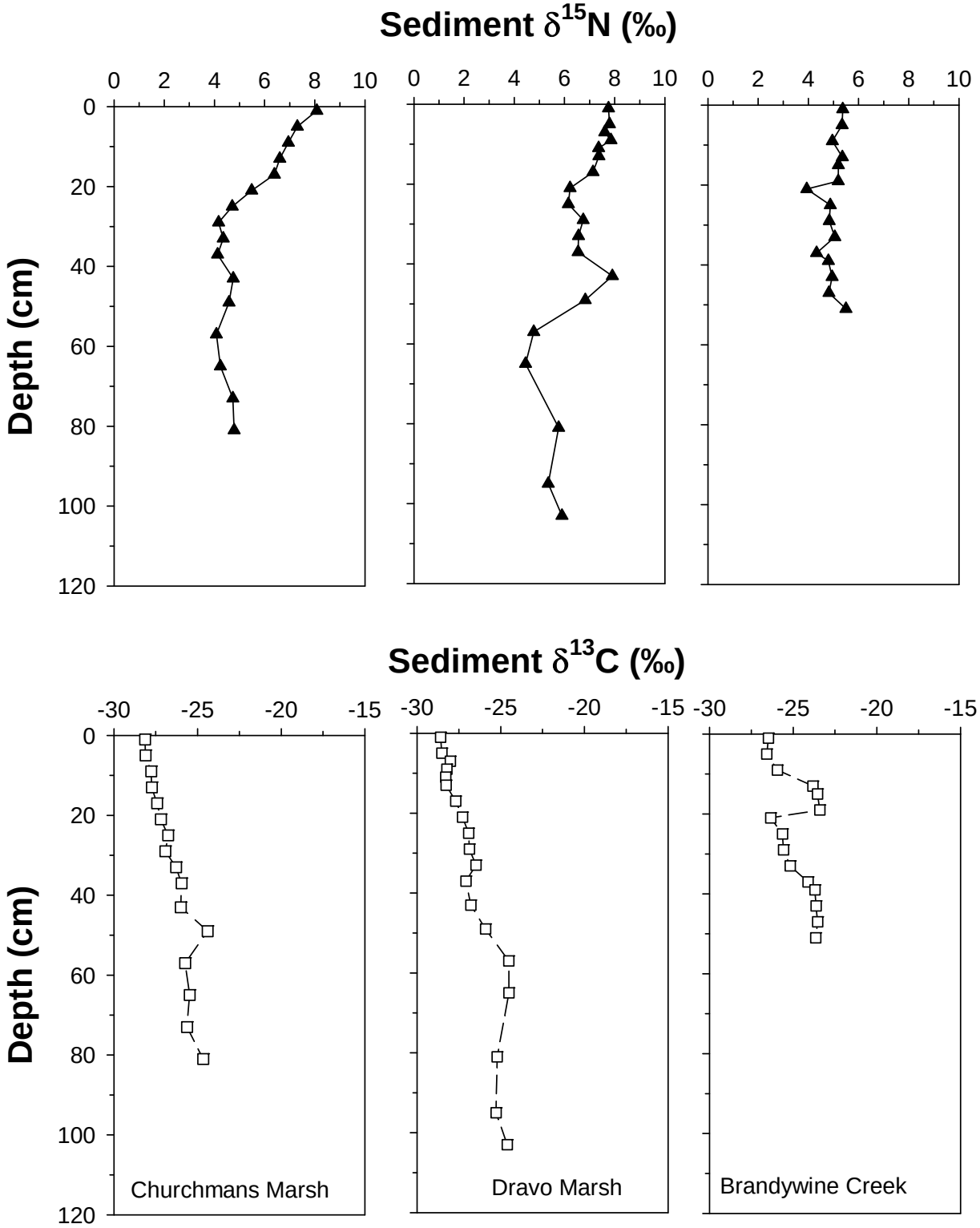

Figure 8. Depth distribution of the isotopic composition sediment N ($\delta^{15}N$) and C ($\delta^{13}C$).

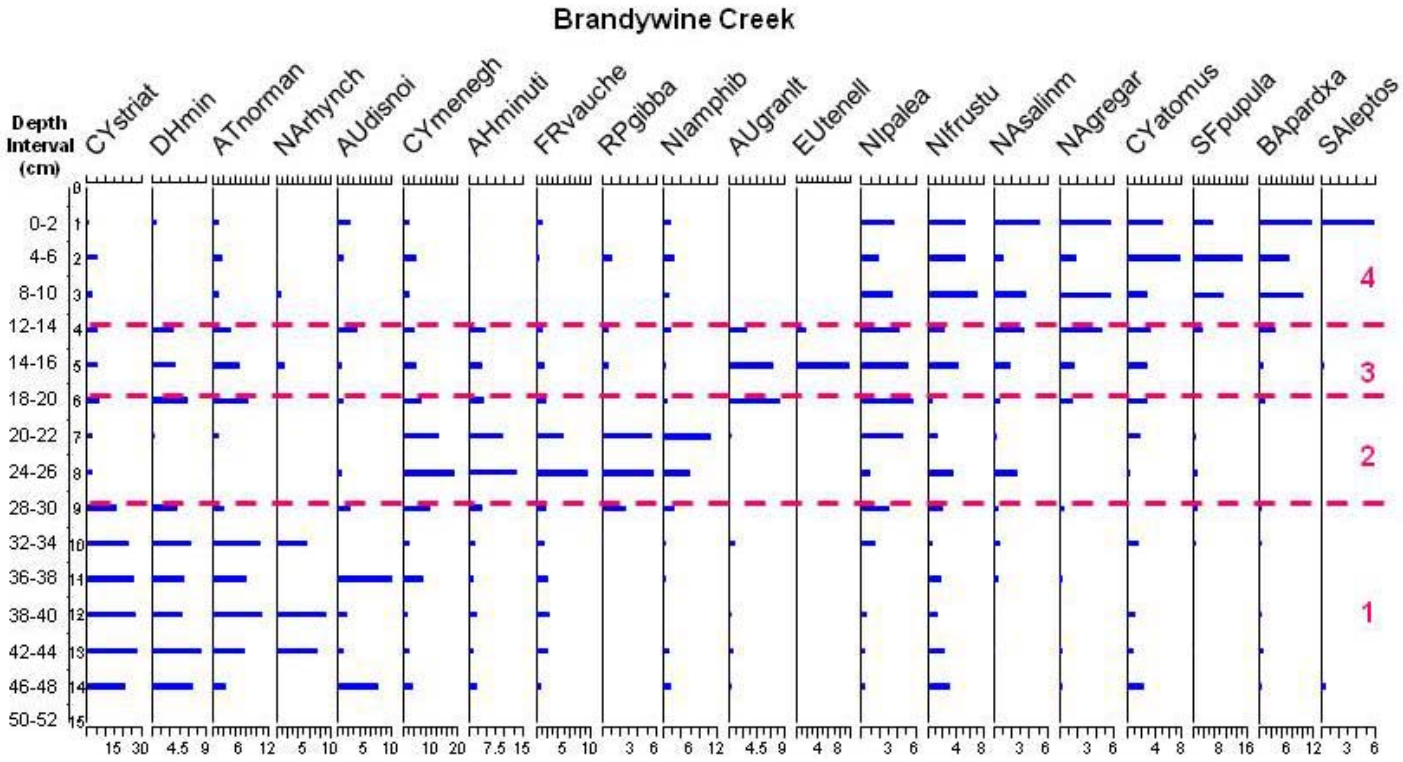

Figure 9a. Distribution of various diatom indicator species with depth in the Brandywine Creek Core.

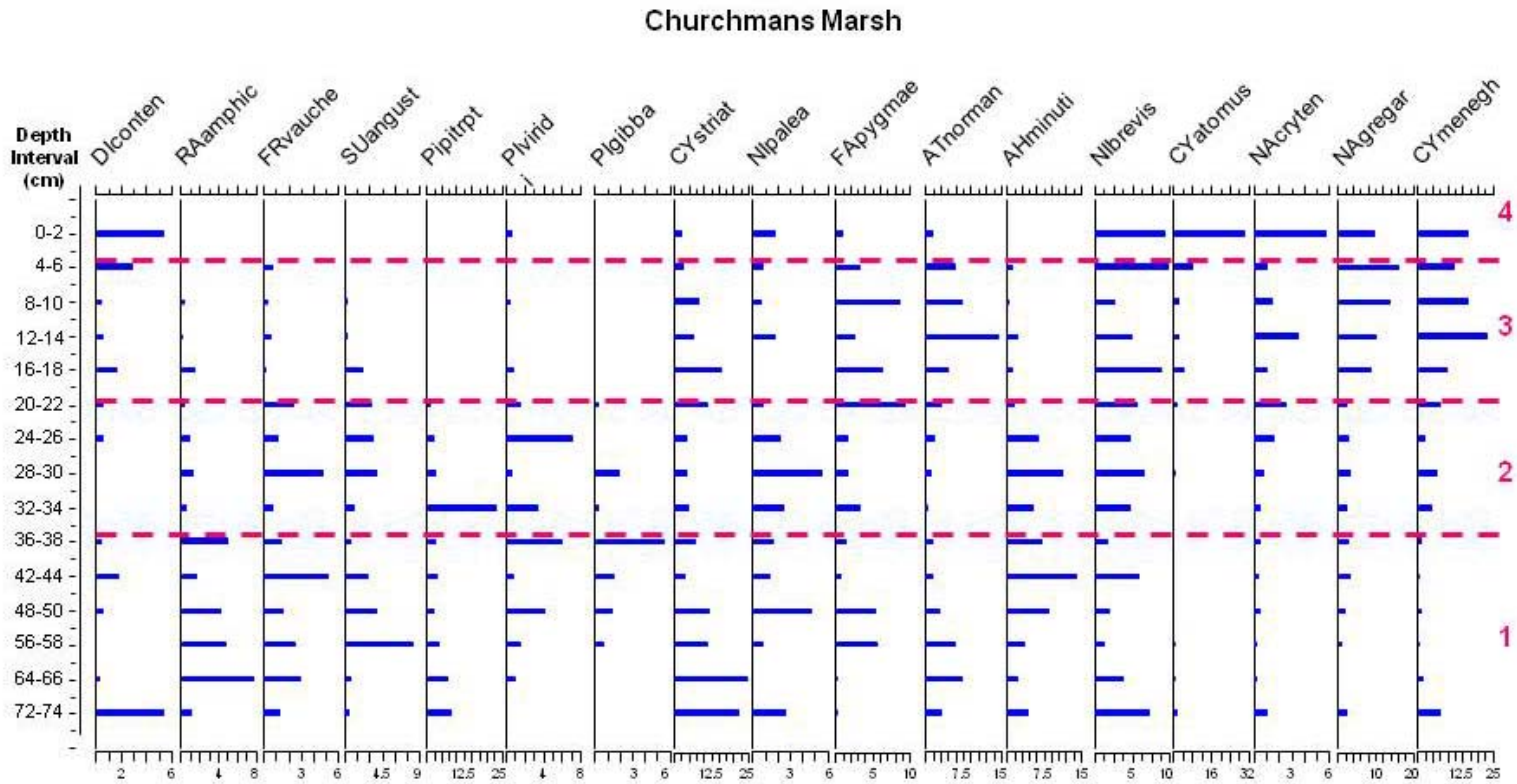

Figure 9b. Distribution of various diatom indicator species with depth in the Churchmans Marsh core.

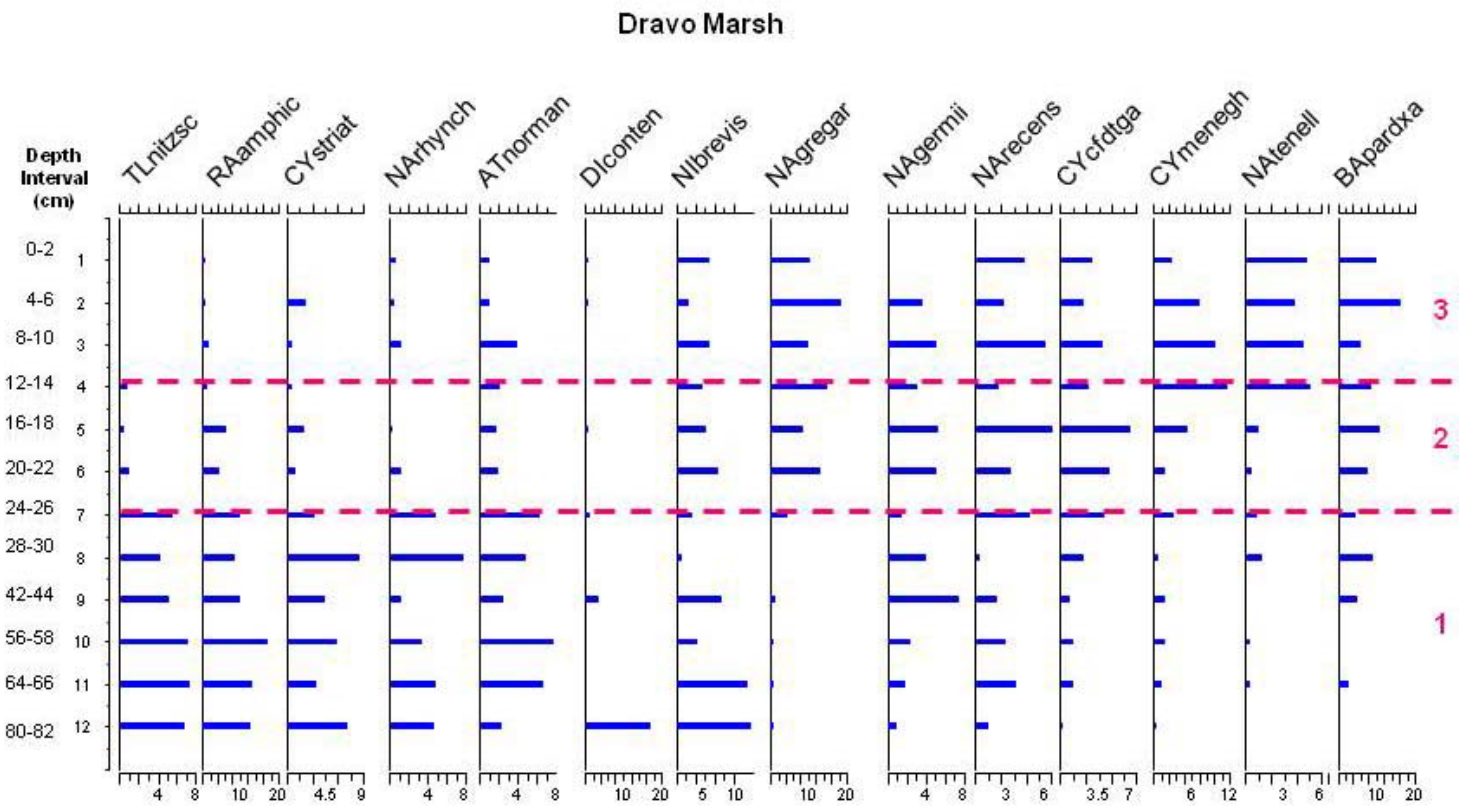

Figure 9c. Distribution of various diatom indicator species with depth in the Dravo Marsh core.

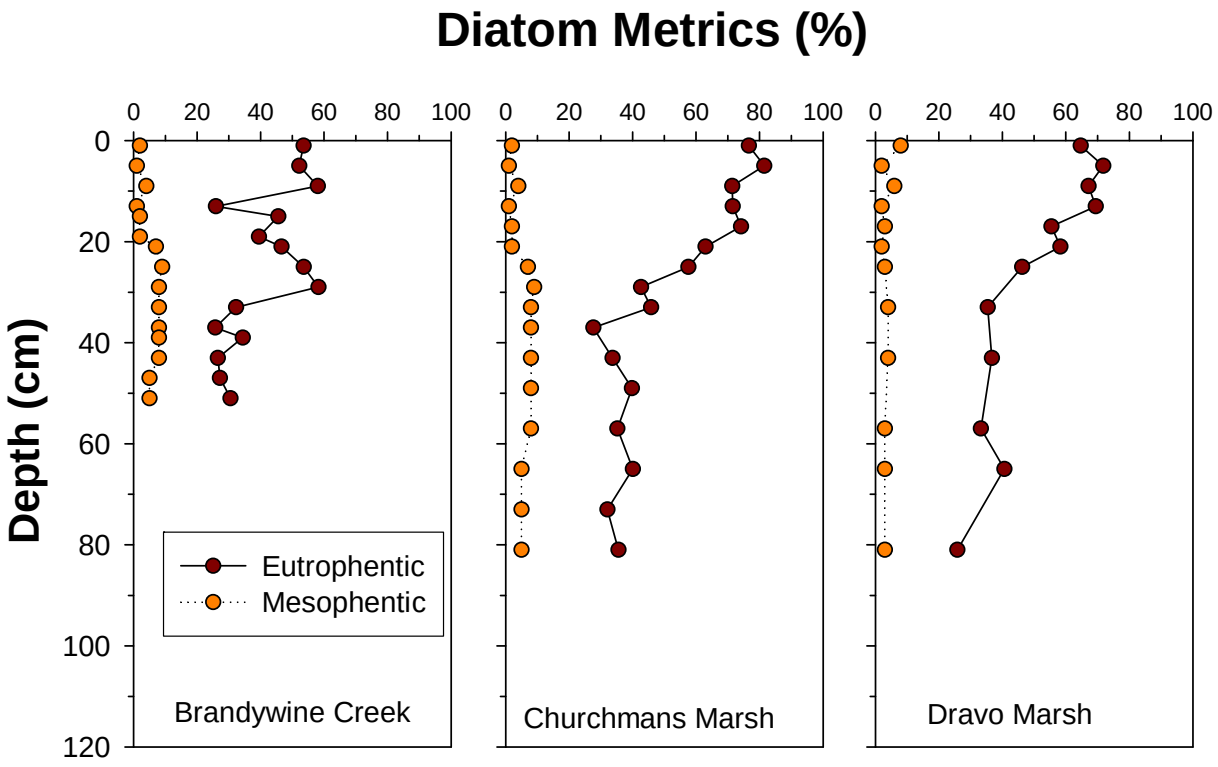

Figure 10. Diatom metrics for the cores of the tidal Christina River using the van Dam et al. (1994).

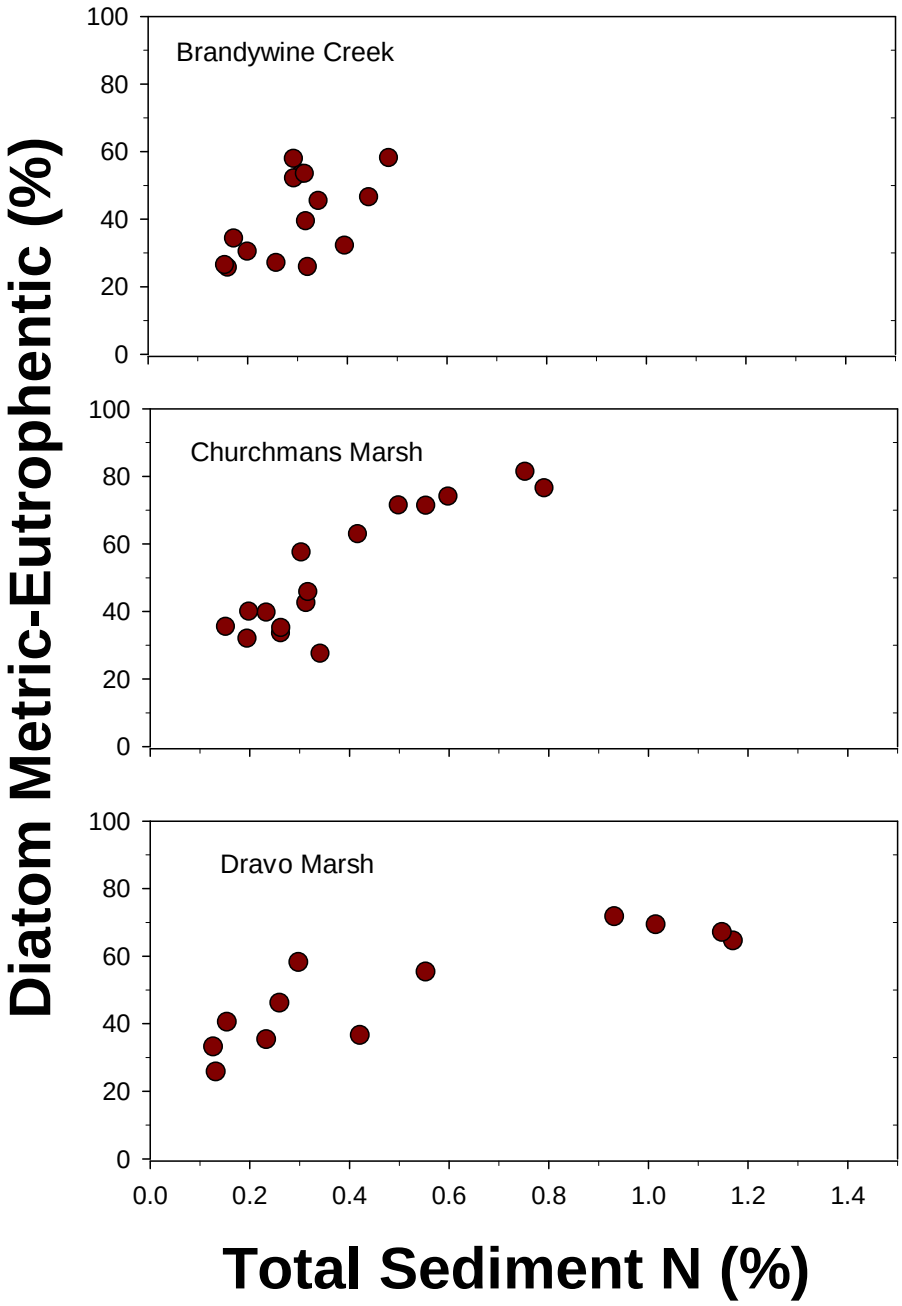

Figure 11. Relationship between total sediment N and the diatom metric for eutrophentic species in each core.

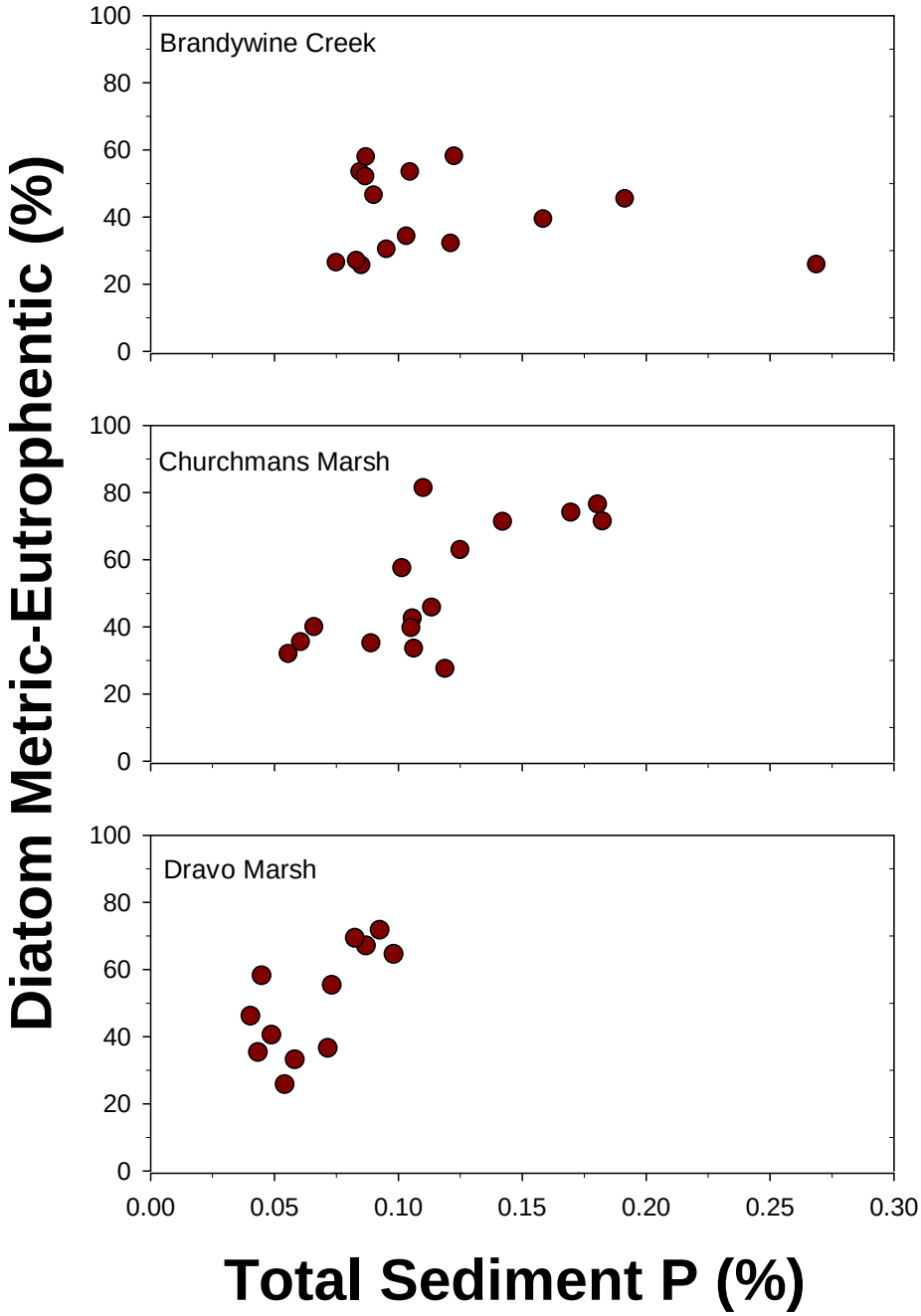

Figure 12. Relationship between total sediment P and the diatom metric for eutrophentic species in each core.

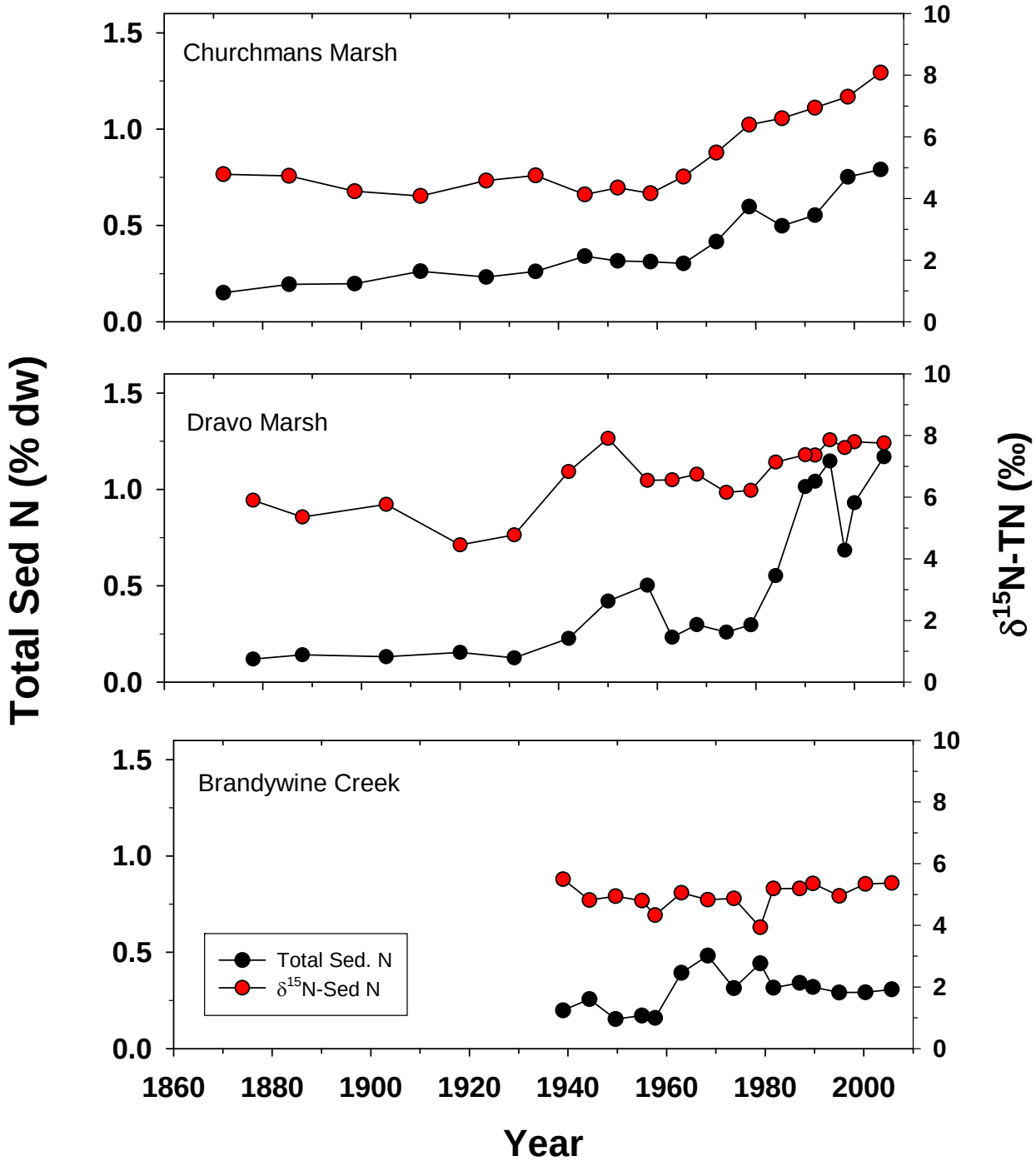

Figure 13. Concentrations of total sediment nitrogen (TN) and the nitrogen isotopic composition of TN (δ^{15}N-TN) from 1860 to 2003.

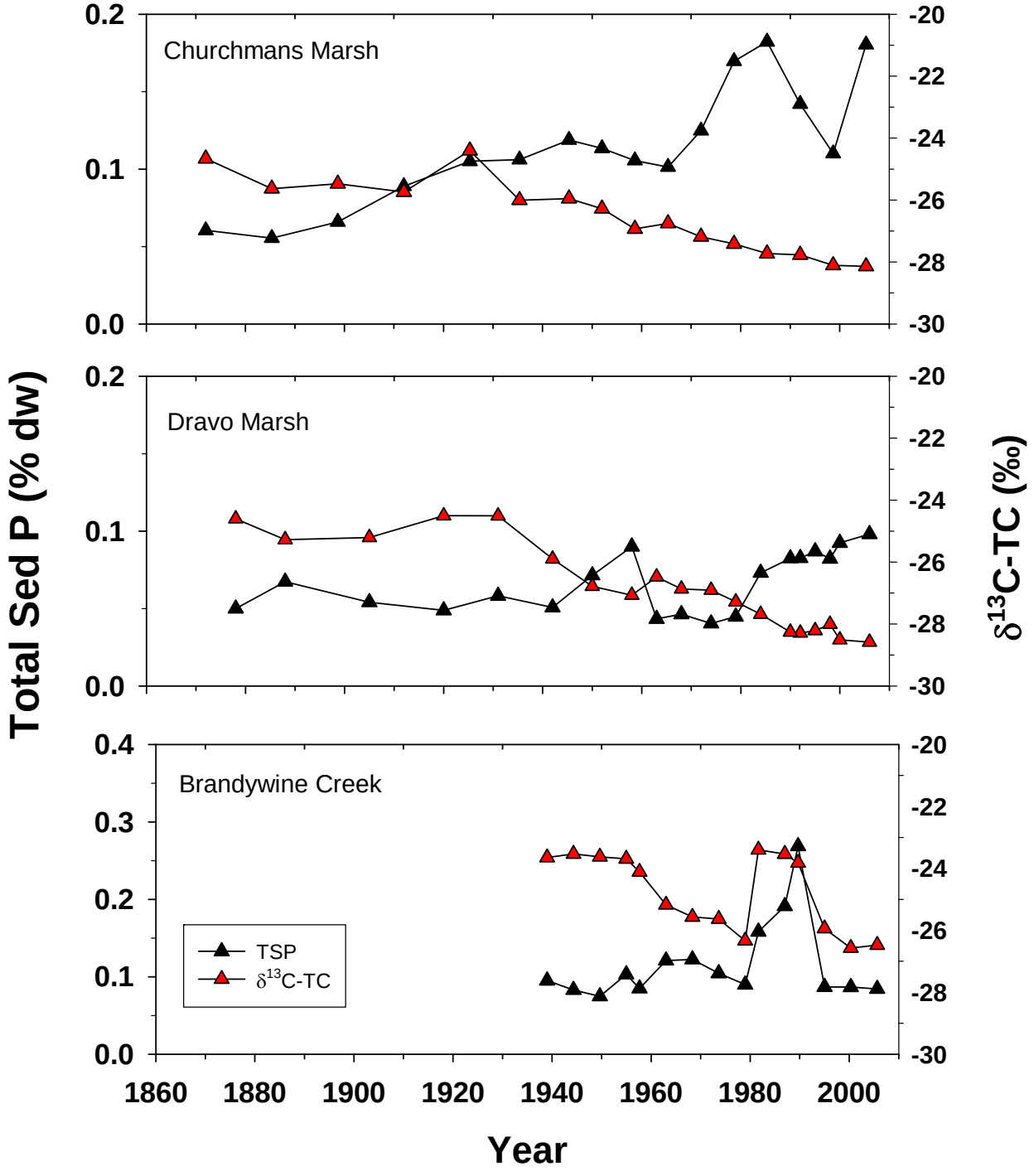

Figure 14. Concentrations of total sediment phosphorus (TSP) and the carbon isotopic composition of total carbon (δ^{13}C-TC) from 1860 to 2003.

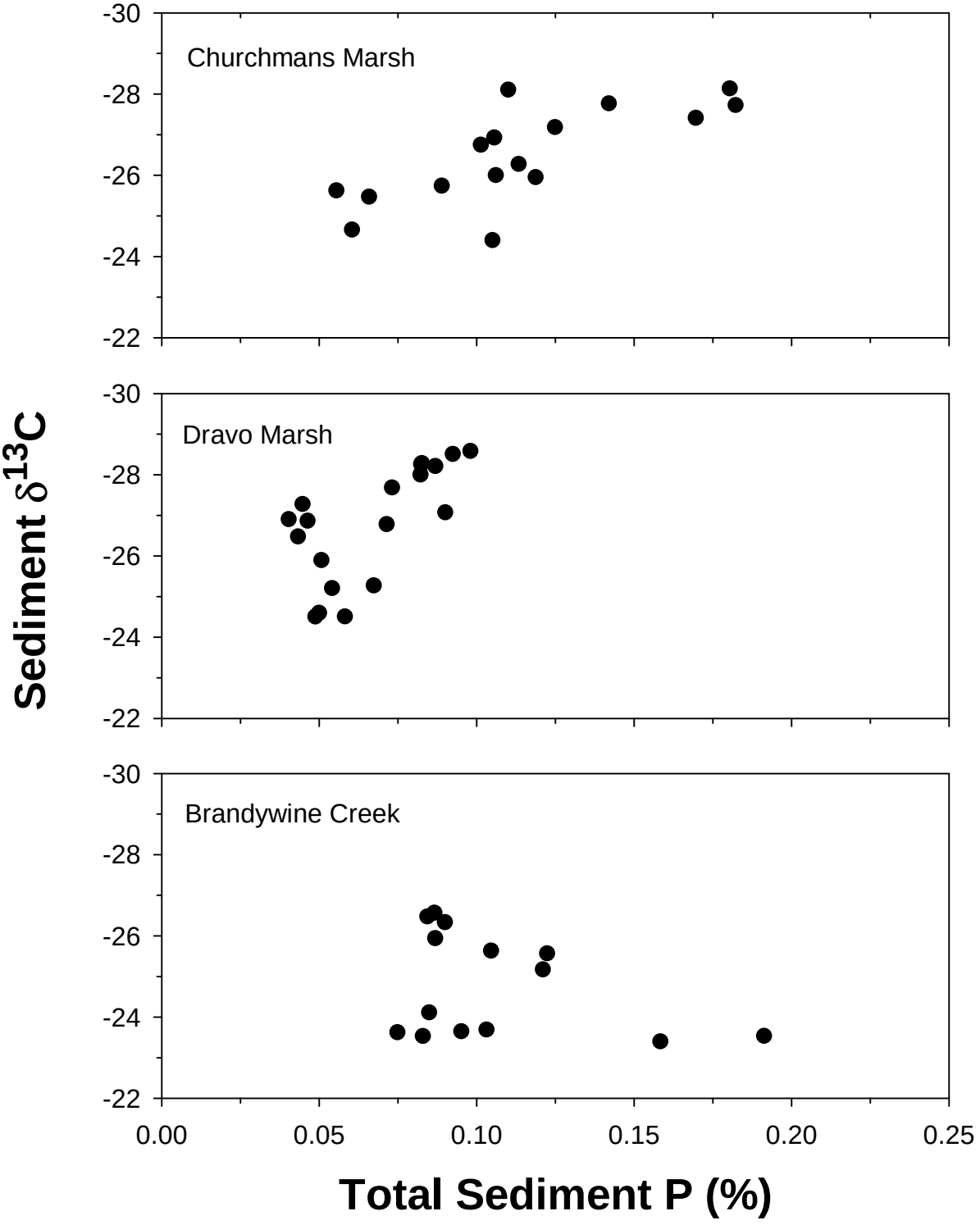

Figure 15. The relationship between total sediment P (TSP) and the carbon isotopic composition of organic matter (δ^{13}C-TC) in Brandywine Creek, Churchmans Marsh, and Dravo Marsh.

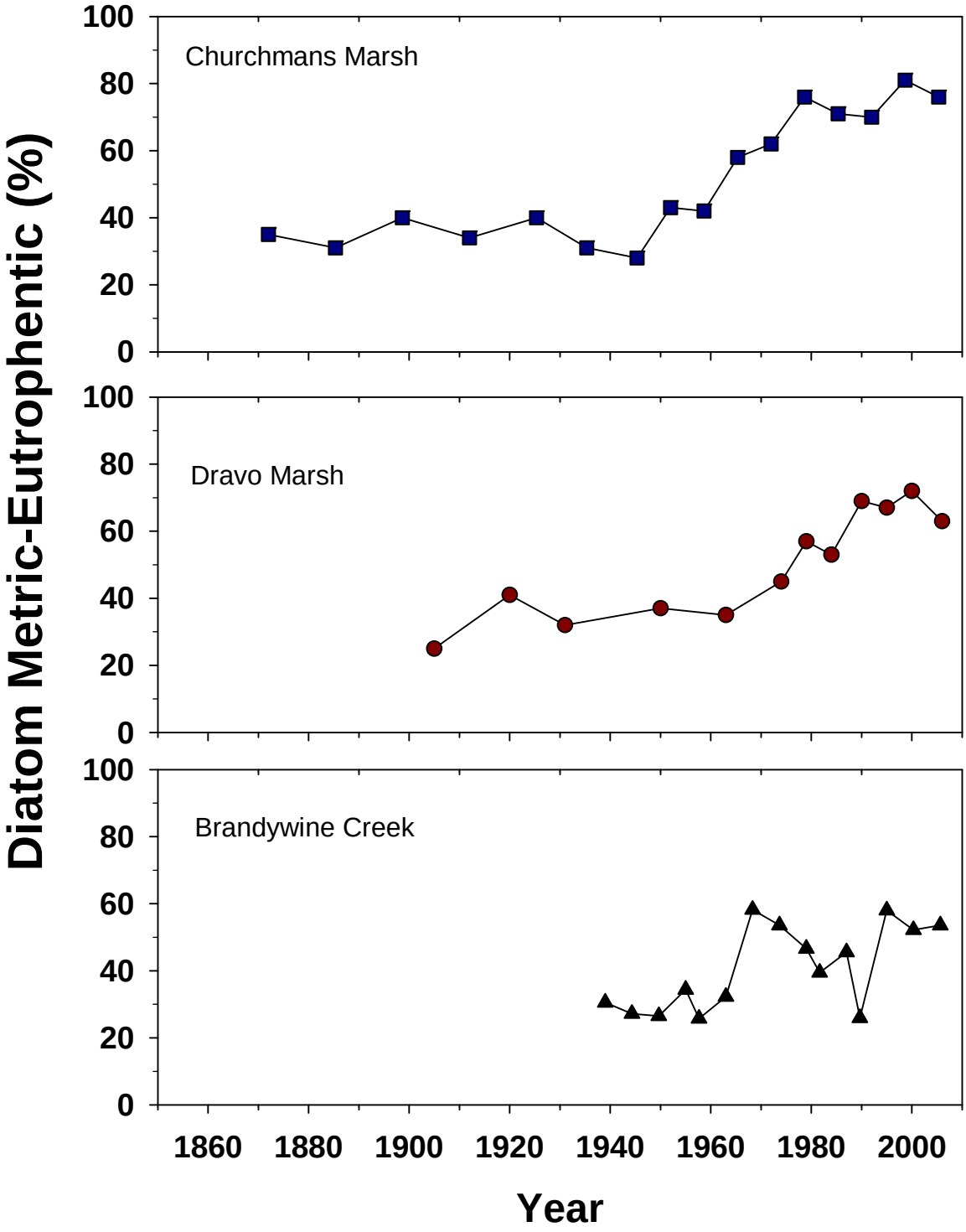

Figure 16. Diatom metric for eutrophentic species from 1860 to 2003.

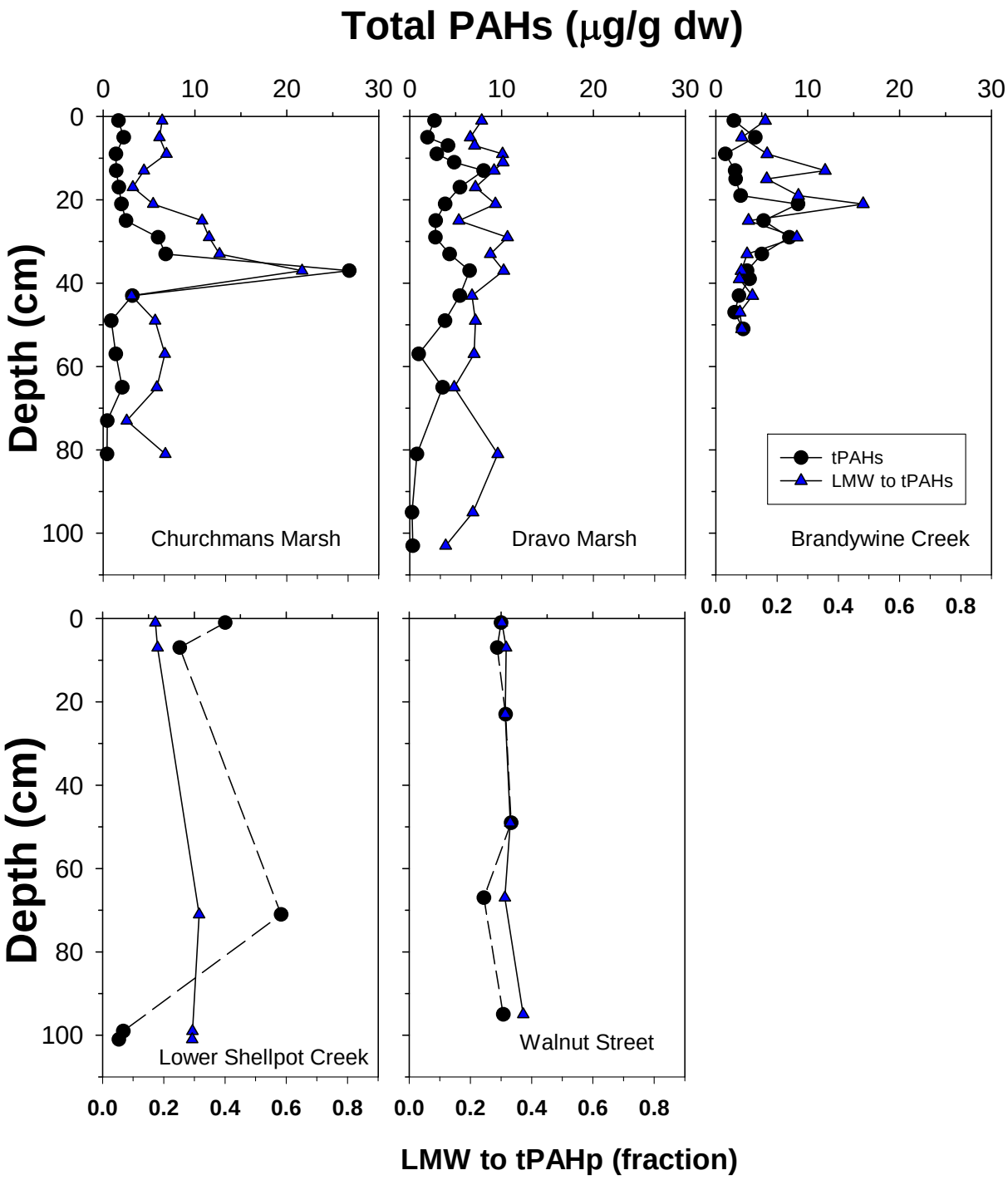

Figure 17. Depth distribution of total polycyclic aromatic hydrocarbons (tPAHs) and the low molecular weight (LMW) to tPAHs in the sediments of the tidal Christina River and Brandywine Creek.

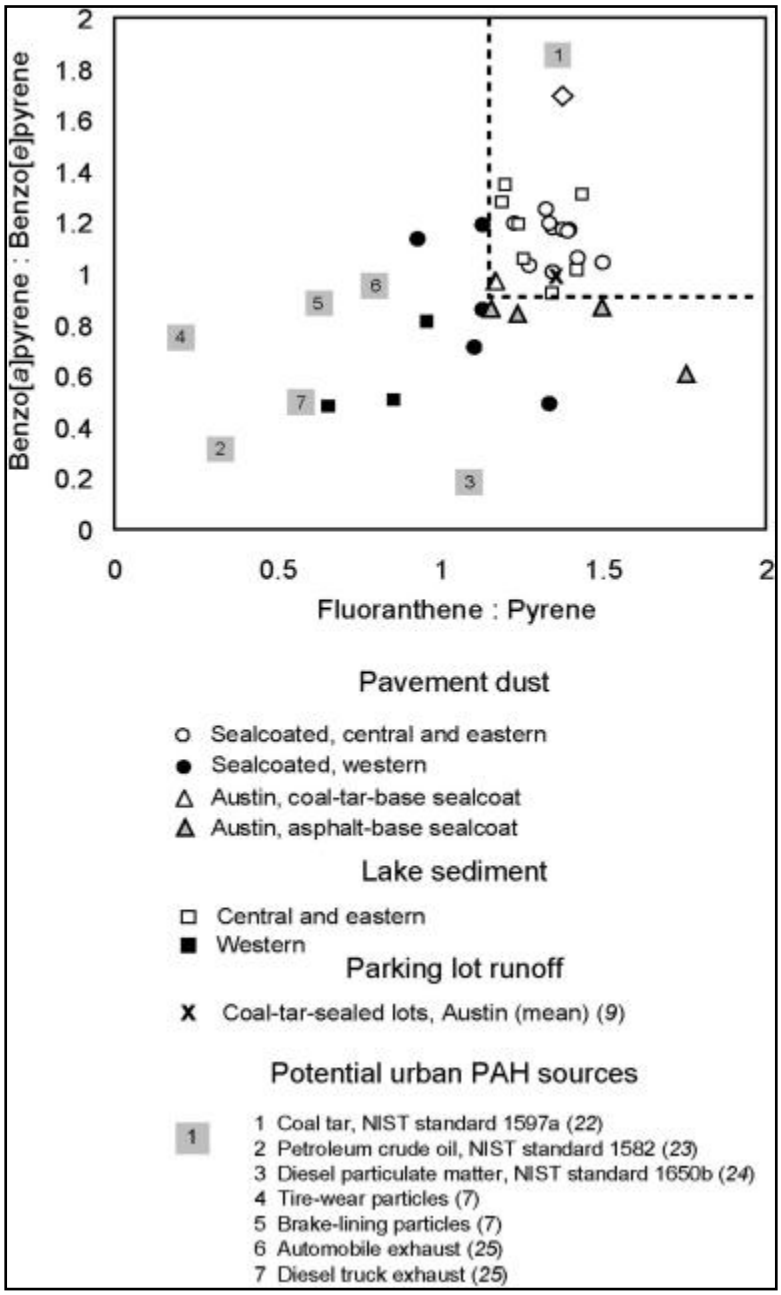

Figure 18. Adapted from Van Metre et al (2009). Comparison of source-indicator ratios of benzo[a]pyrene to benzo[e]pyrene and fluoranthene to pyrene in dust samples, lake samples and seal-coat samples from central and eastern cities (USA). Dashed line indicates approximate separation between samples from central and eastern cities and those from western cities.

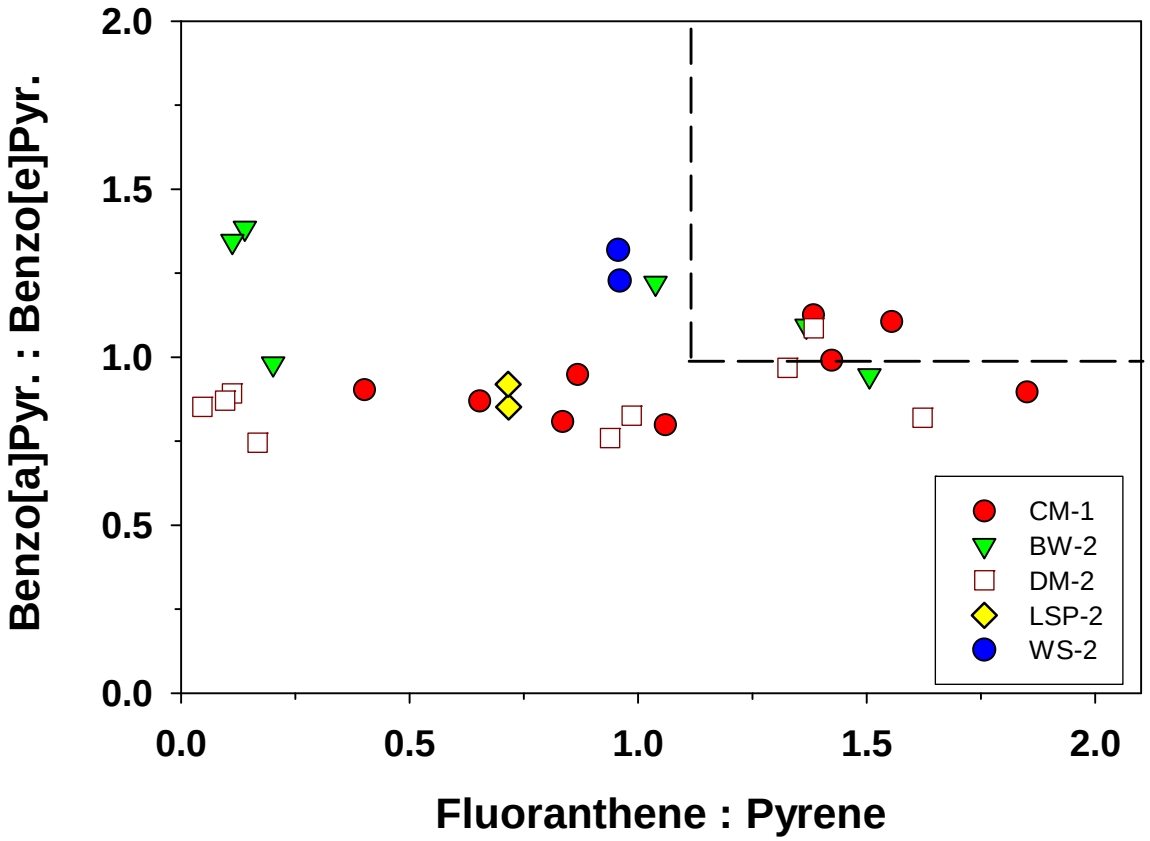

Figure 19. Indicator ratios of benzo[a]pyrene to benzo[e]pyrene and fluoranthene to pyrene in the top sections of all sediment samples collected in the tidal Christina and Brandywine watersheds. The dotted box is related to the area in the van Metre et al. (2009) that suggests high coal tar sealants for parking lots.

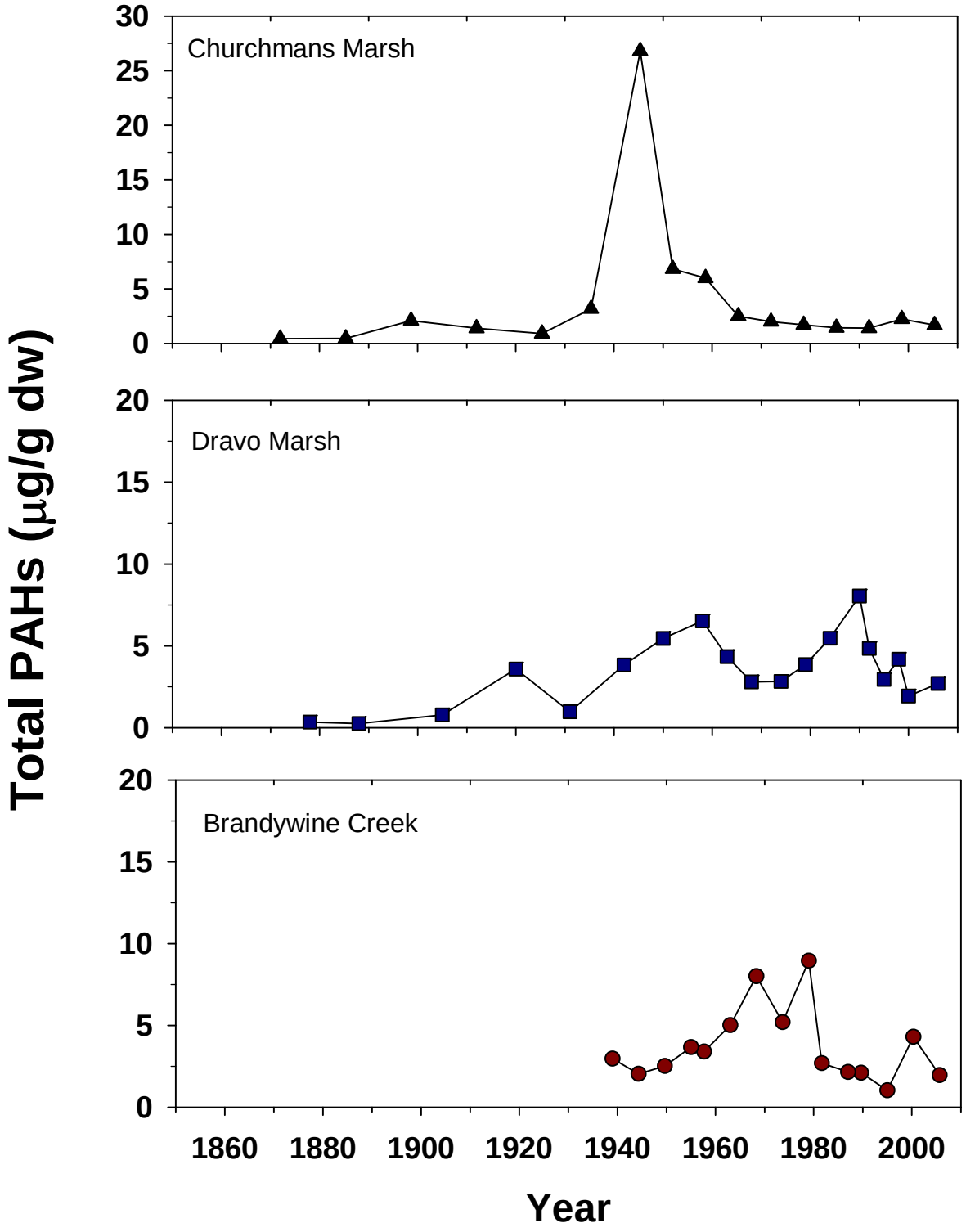

Figure 20. Concentrations of tPAHs from 1860 to 2003 (Note scale change).

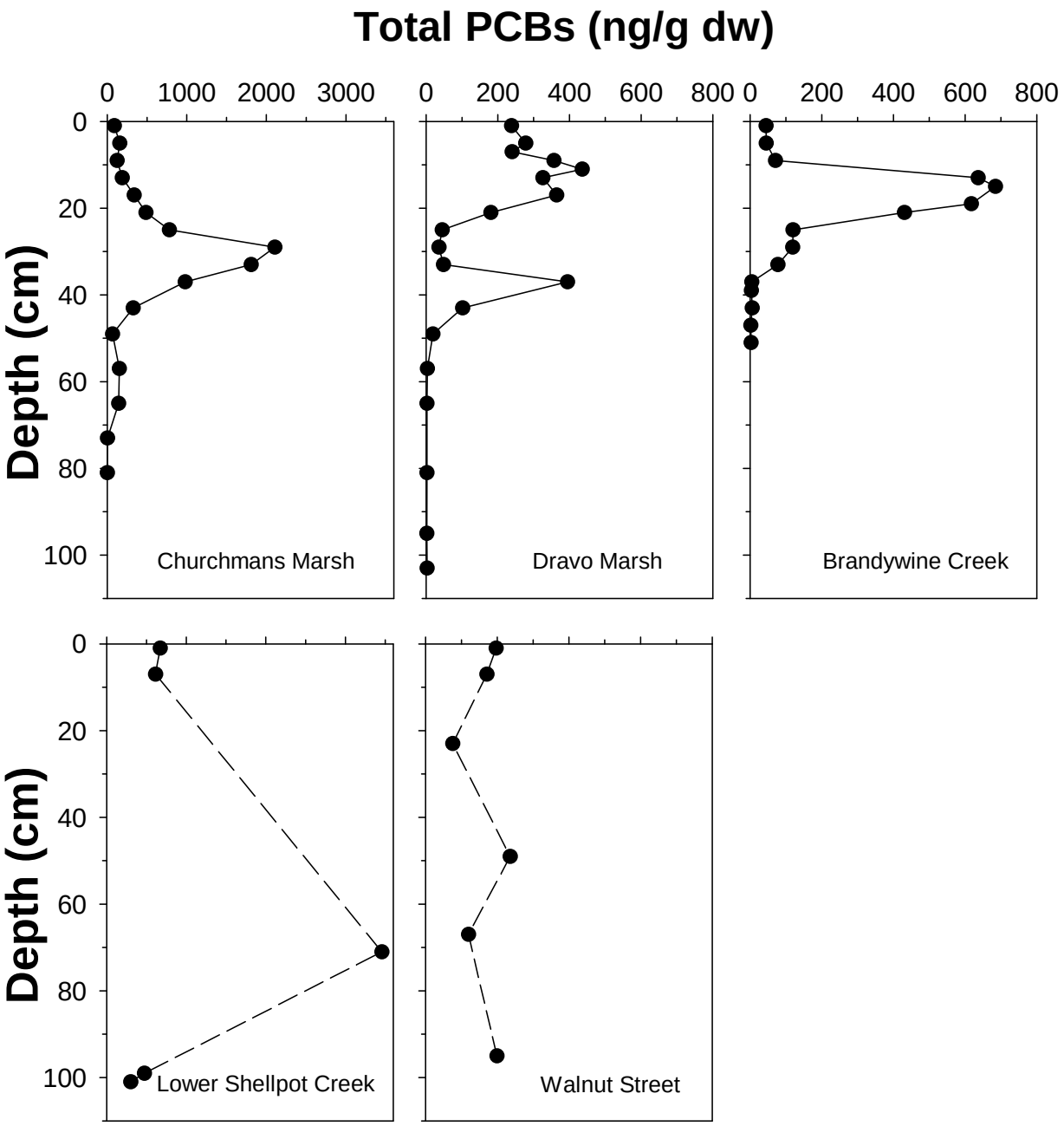

Figure 21. Depth distribution of total PCBs in the five cores in the tidal Christina River and Brandywine Creek.

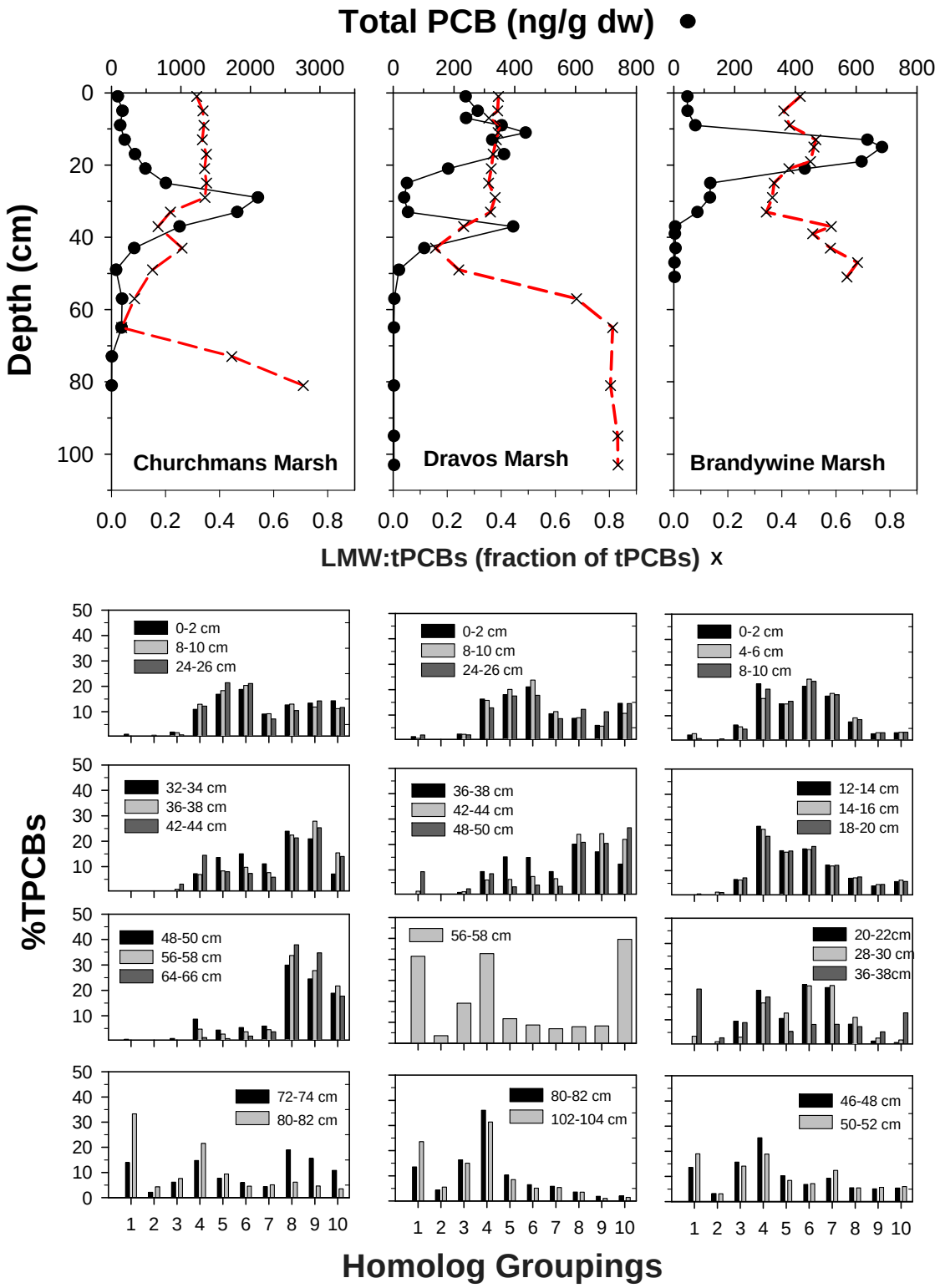

Figure 22a. Depth distribution of total PCBs, LMW to tPCBs ratio and selected homolog distributions with depth.

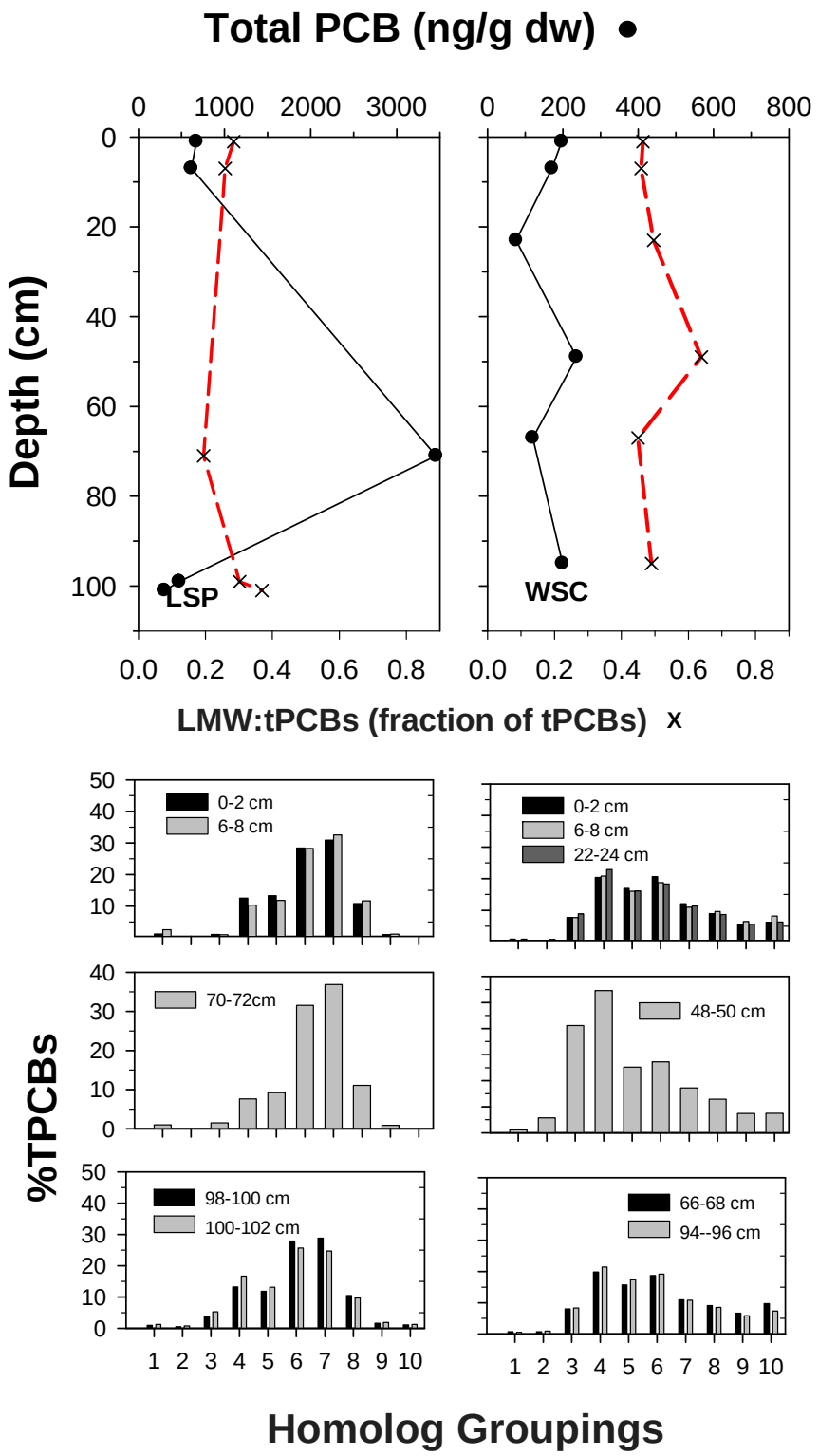

Figure 22b. Depth distribution of total PCBs, LMW to tPCBs ratio and selected homolog distributions with depth

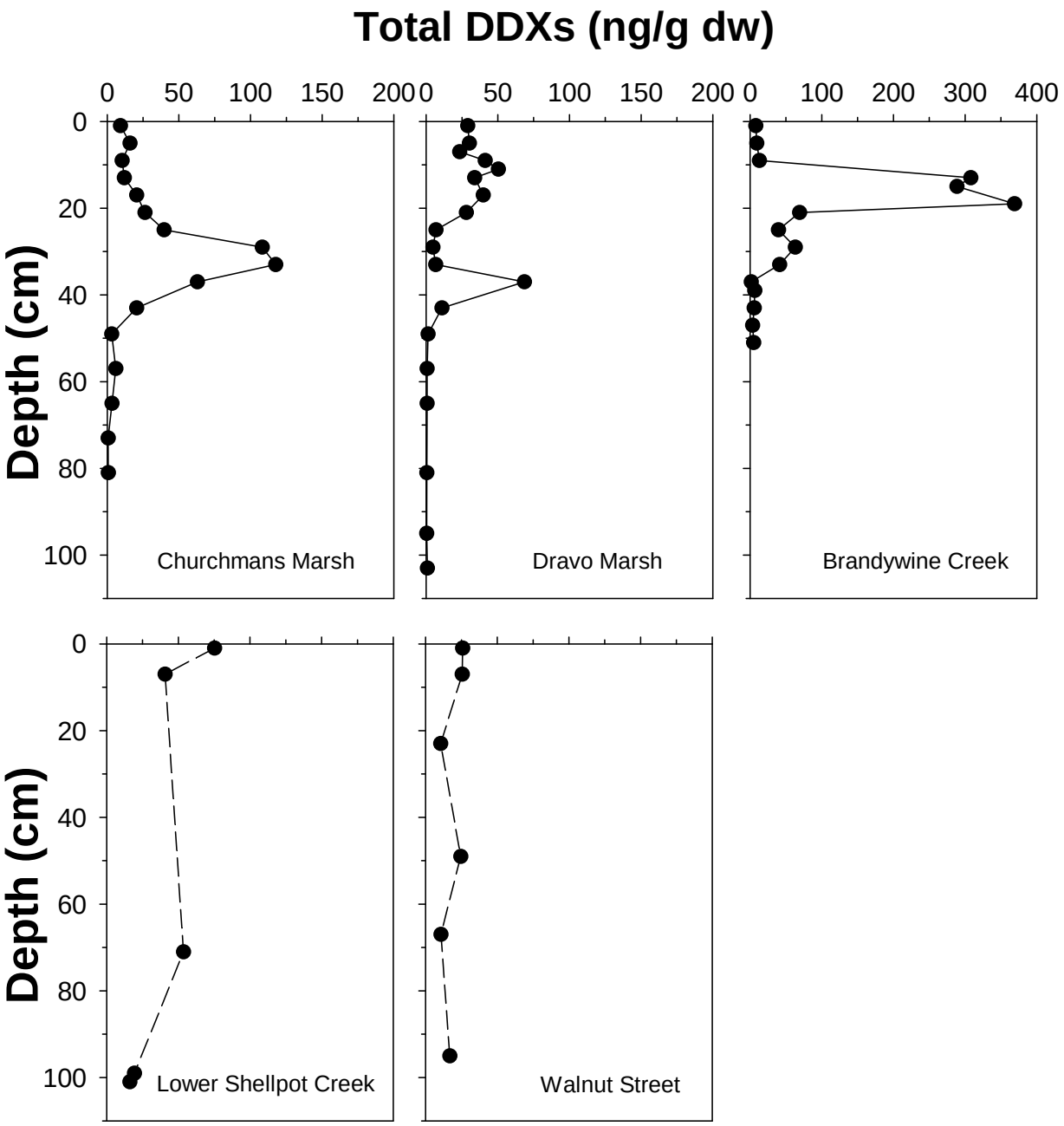

Figure 23. Total DDX (DDT+DDD+DDE all forms) with depth in the tidal Christina River and Brandywine Creek.

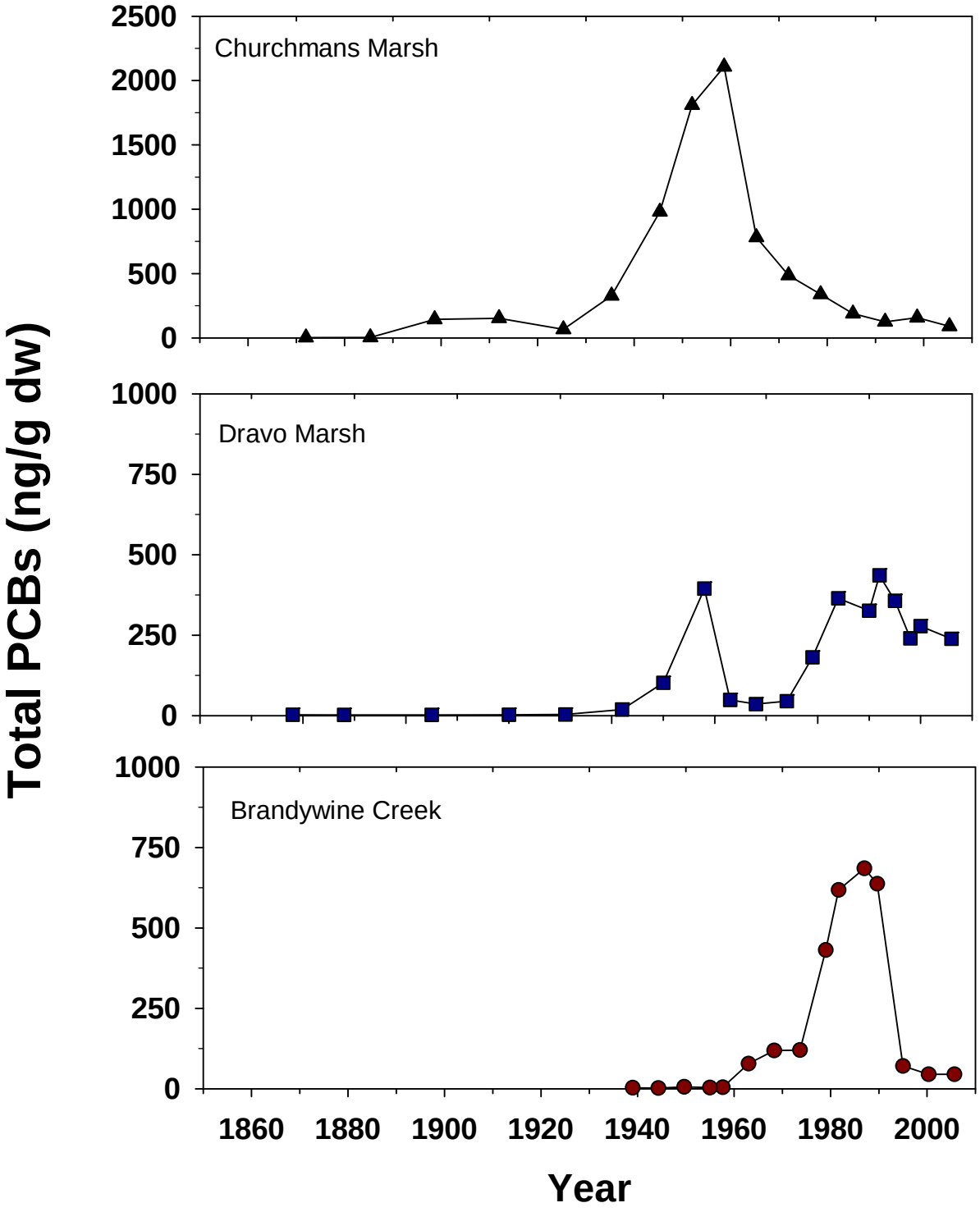

Figure 24. Concentrations of tPCBs from 1860 to 2003 (Note scale change).

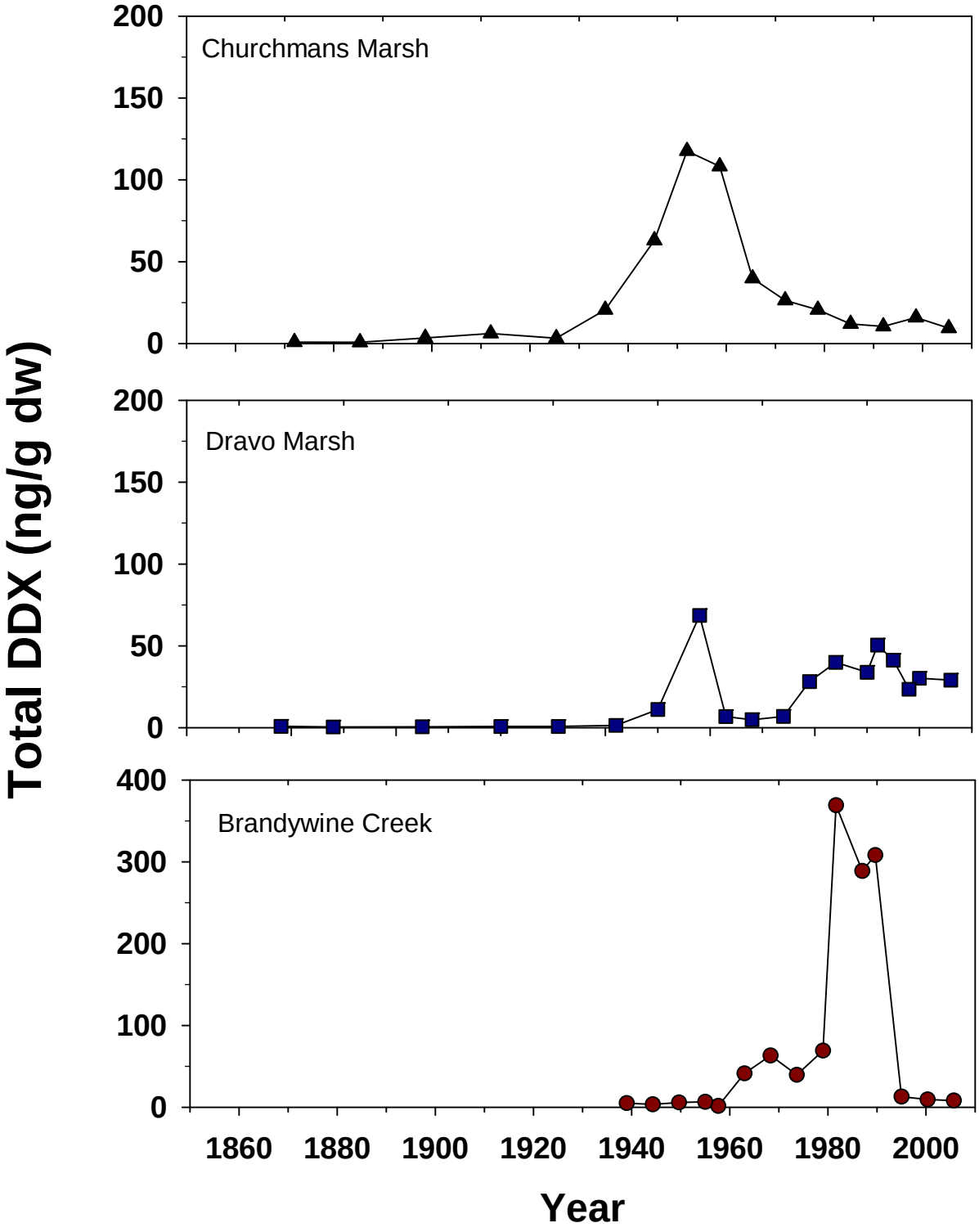

Figure 25. Concentrations of tDDXs from 1860 to 2003 (Note scale change).

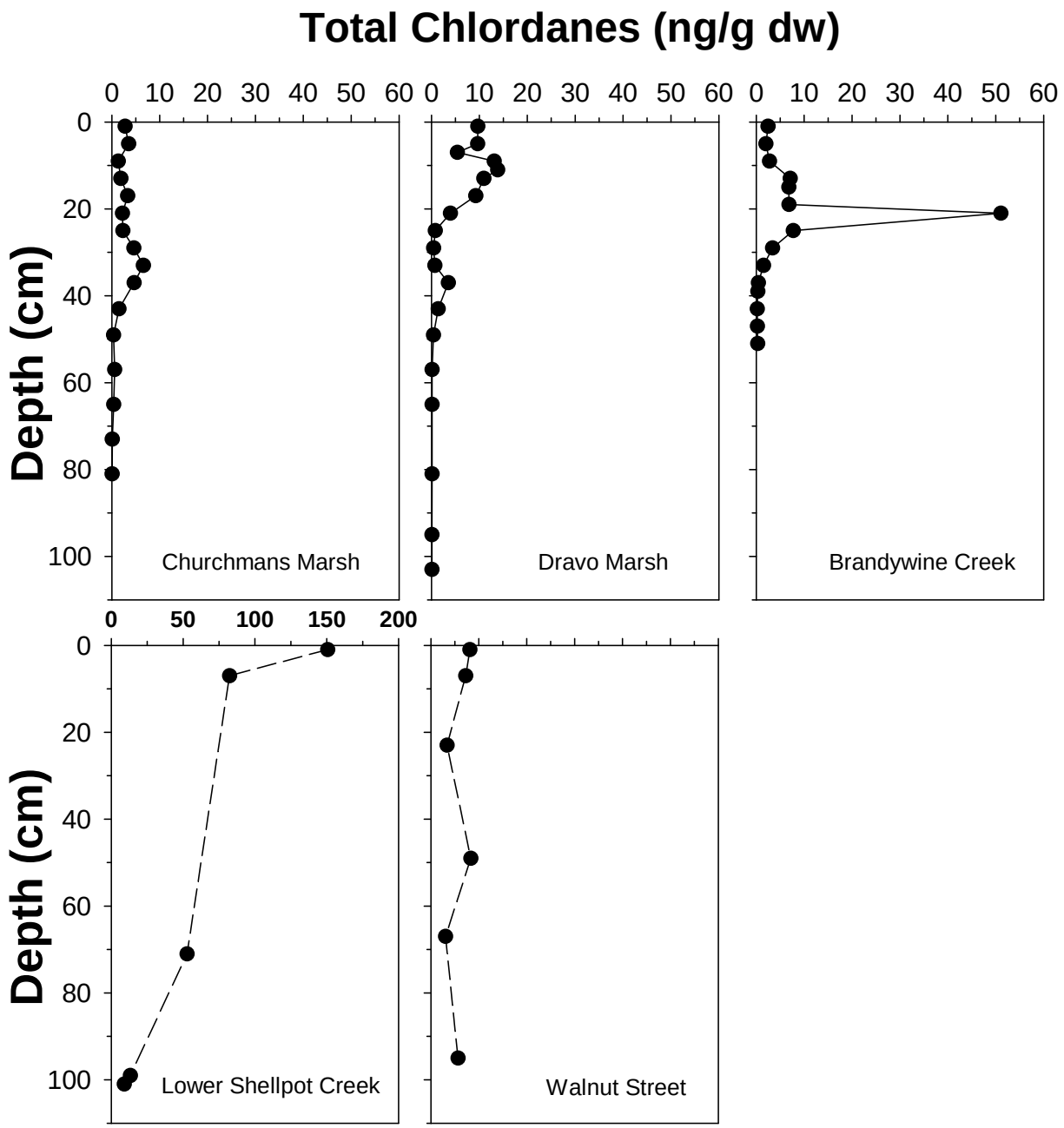

Figure 26. Total chlordane with depth in the tidal Christina River and Brandywine Creek.

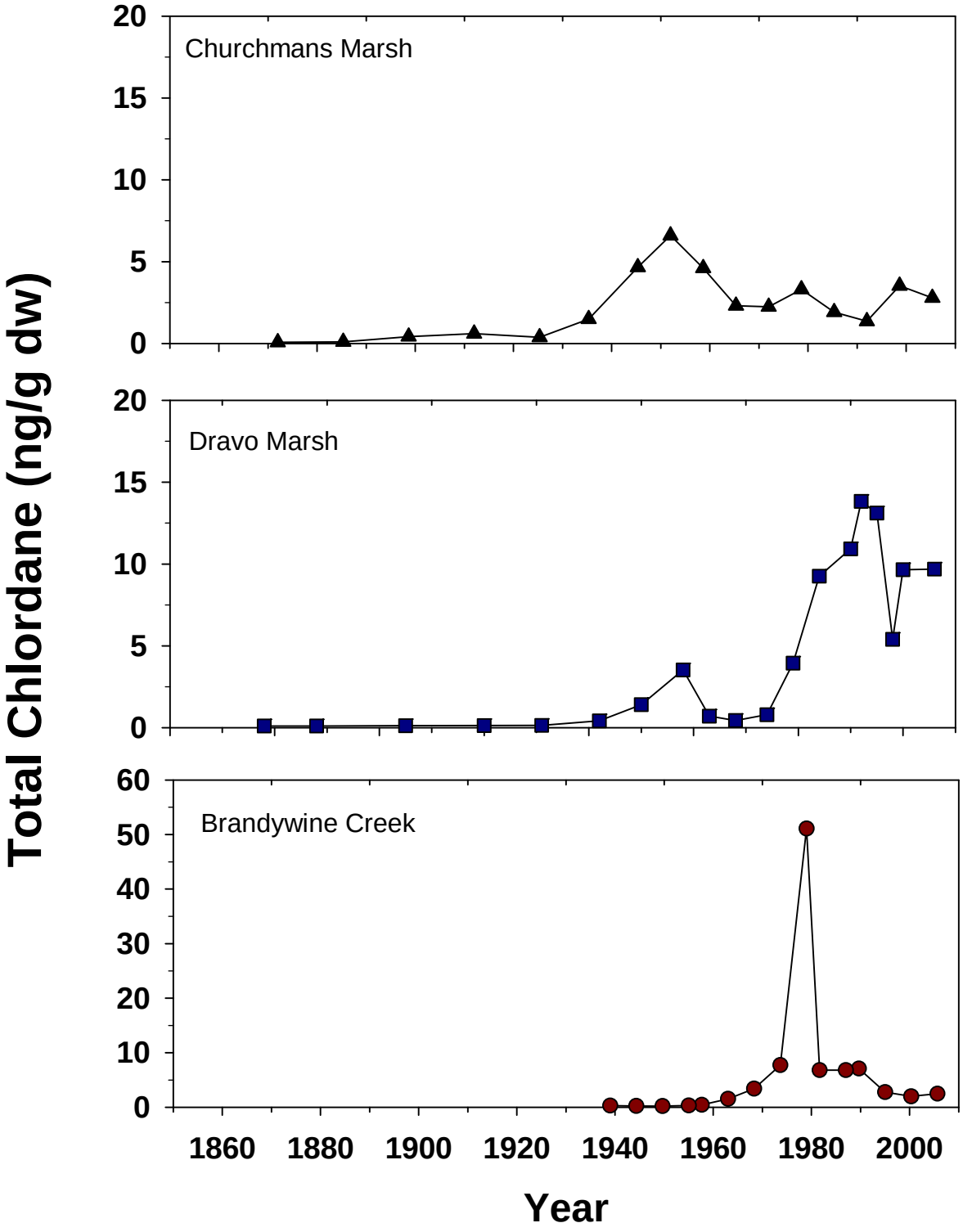

Figure 27. Concentrations of total chlordane from 1860 to 2003 (Note scale change).

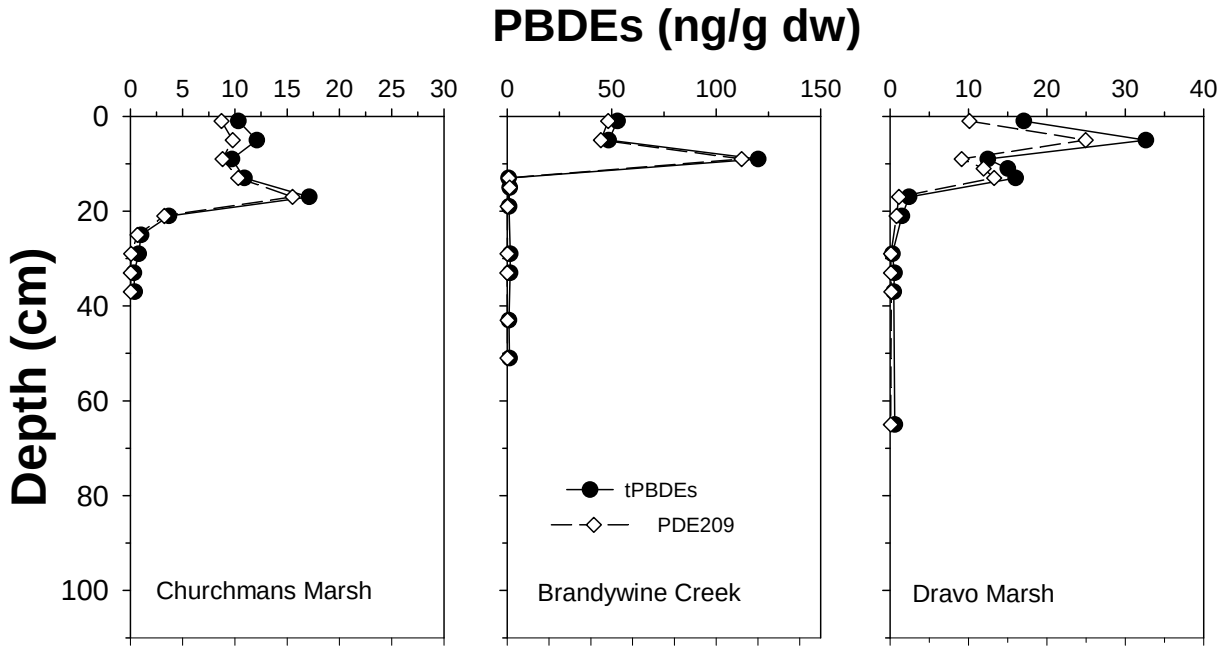

Figure 28. Total PBDEs and the deca congener BDE-209 with depth in the tidal Christina River and Brandywine Creek.

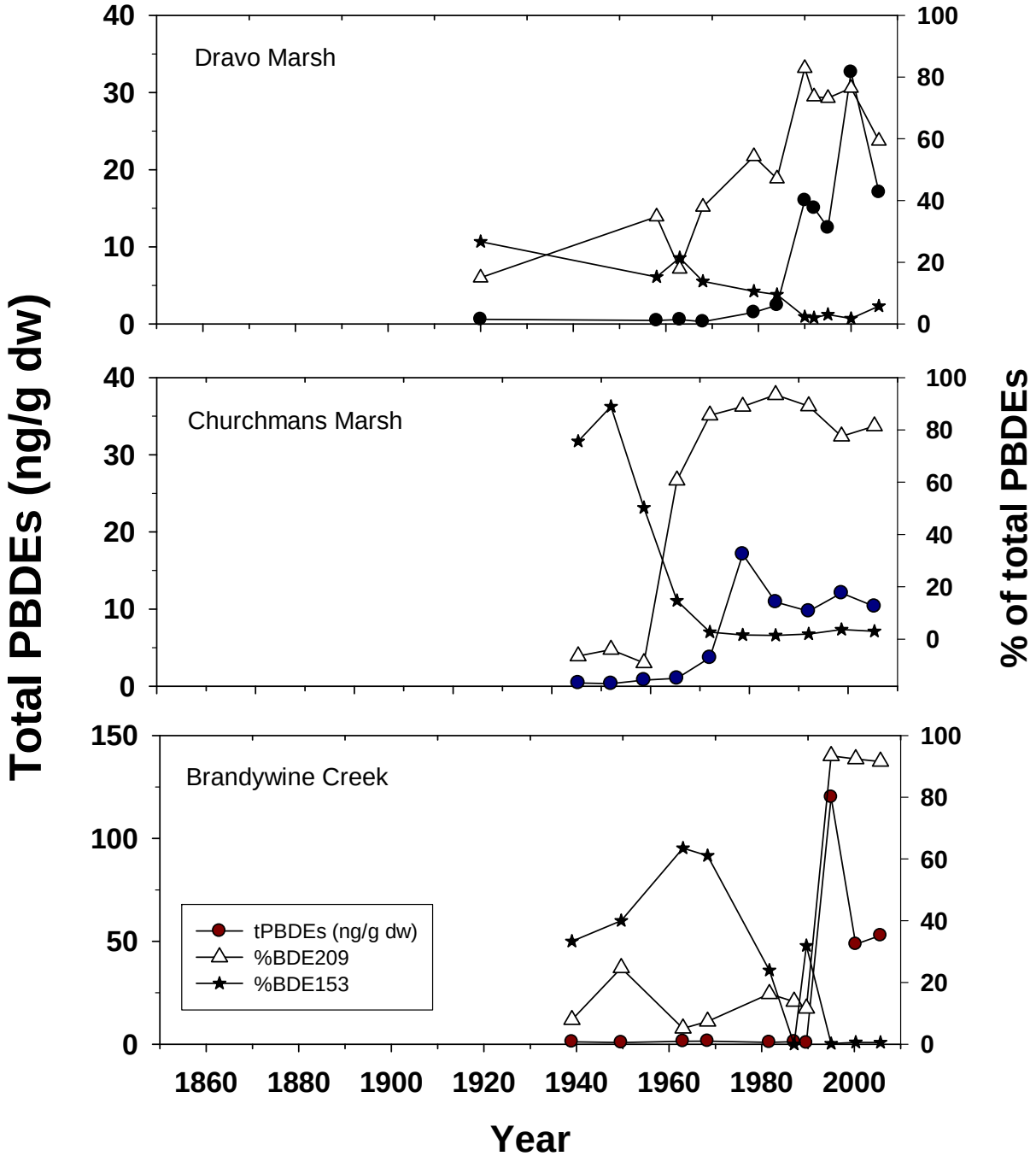

Figure 29. Concentrations of tPBDEs from 1860 to 2003. The circle is for tPBDEs, the triangle is for the percentage of BDE209 and the star is the percentage of BDE 153.

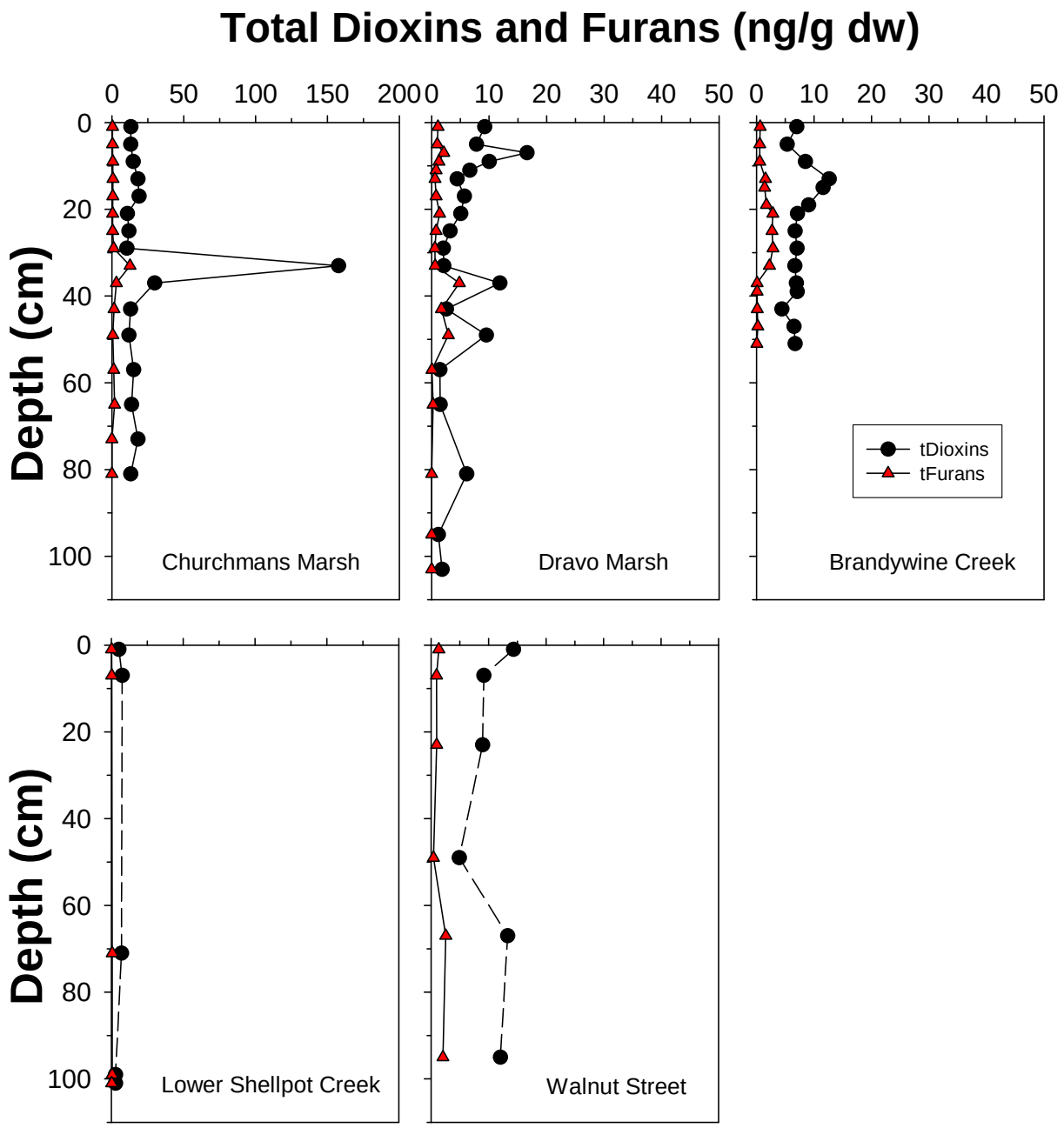

Figure 30. Total dioxins (tPCDD) and furans (tPCDF) with depth in the tidal Christina River and Brandywine Creek.

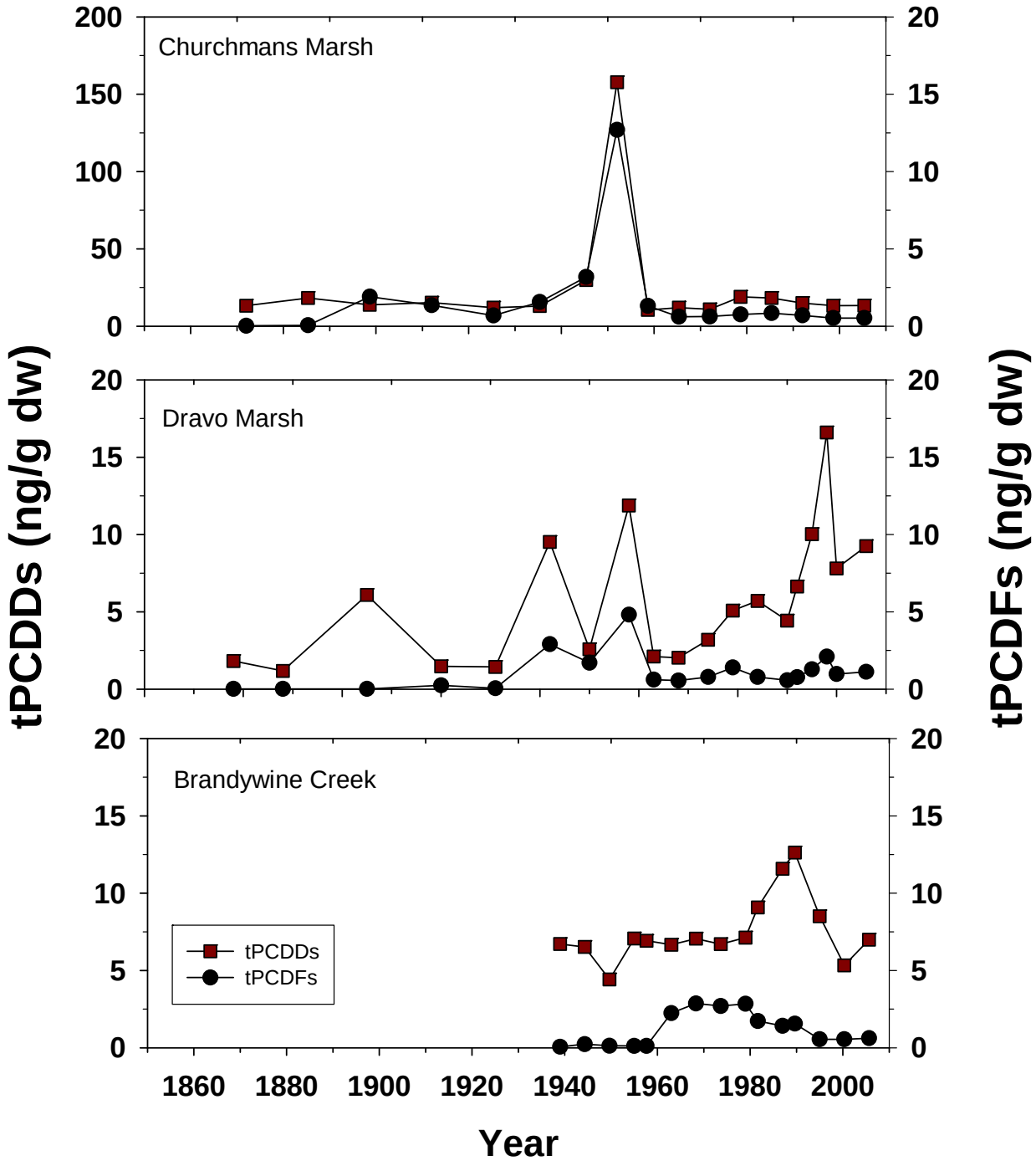

Figure 31. Concentrations of total dioxins and total furans from 1860 to 2003 (Note scale changes).

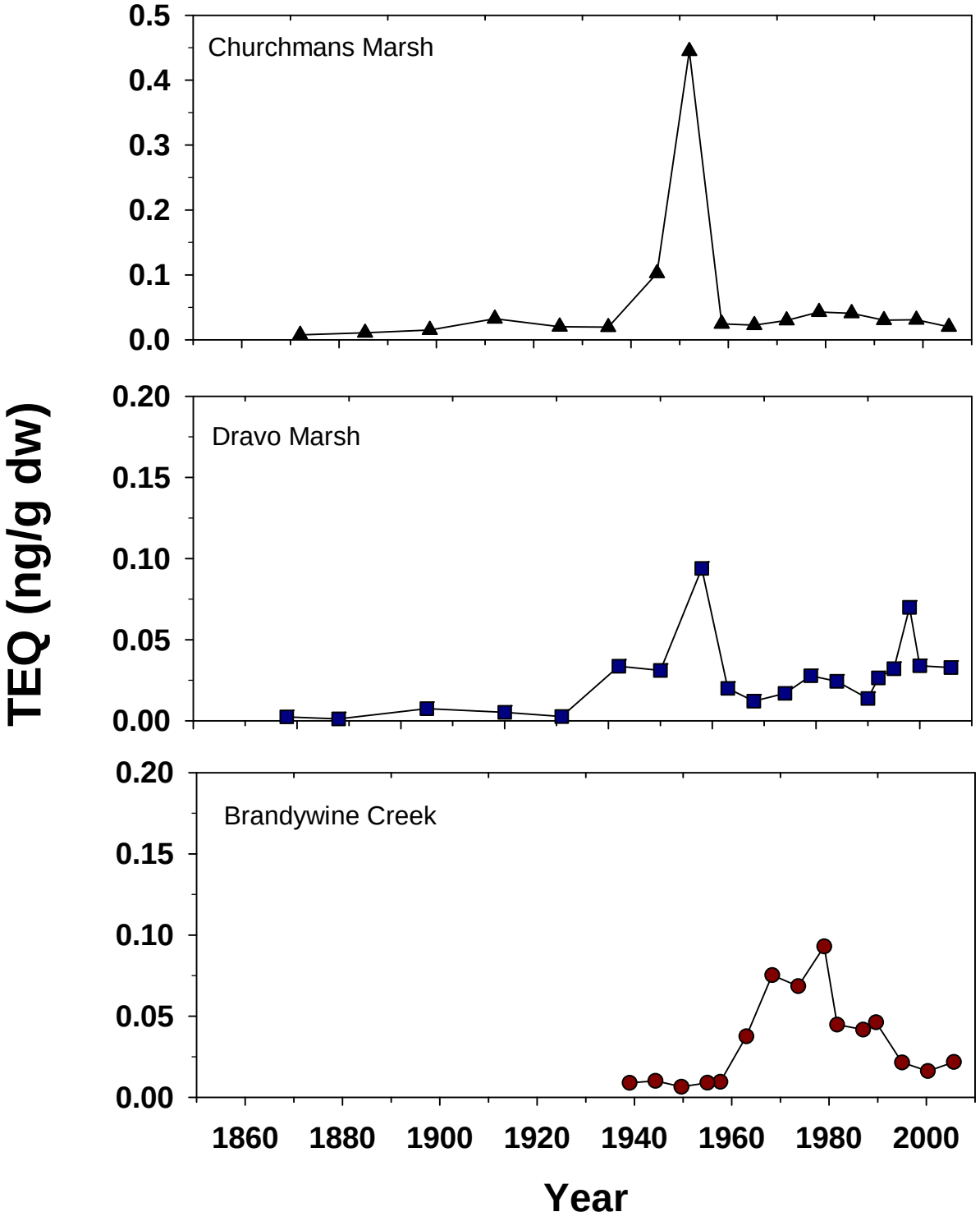

Figure 32. Concentrations of TEQ for dioxins and furans from 1860 to 2003 (Note scale changes).

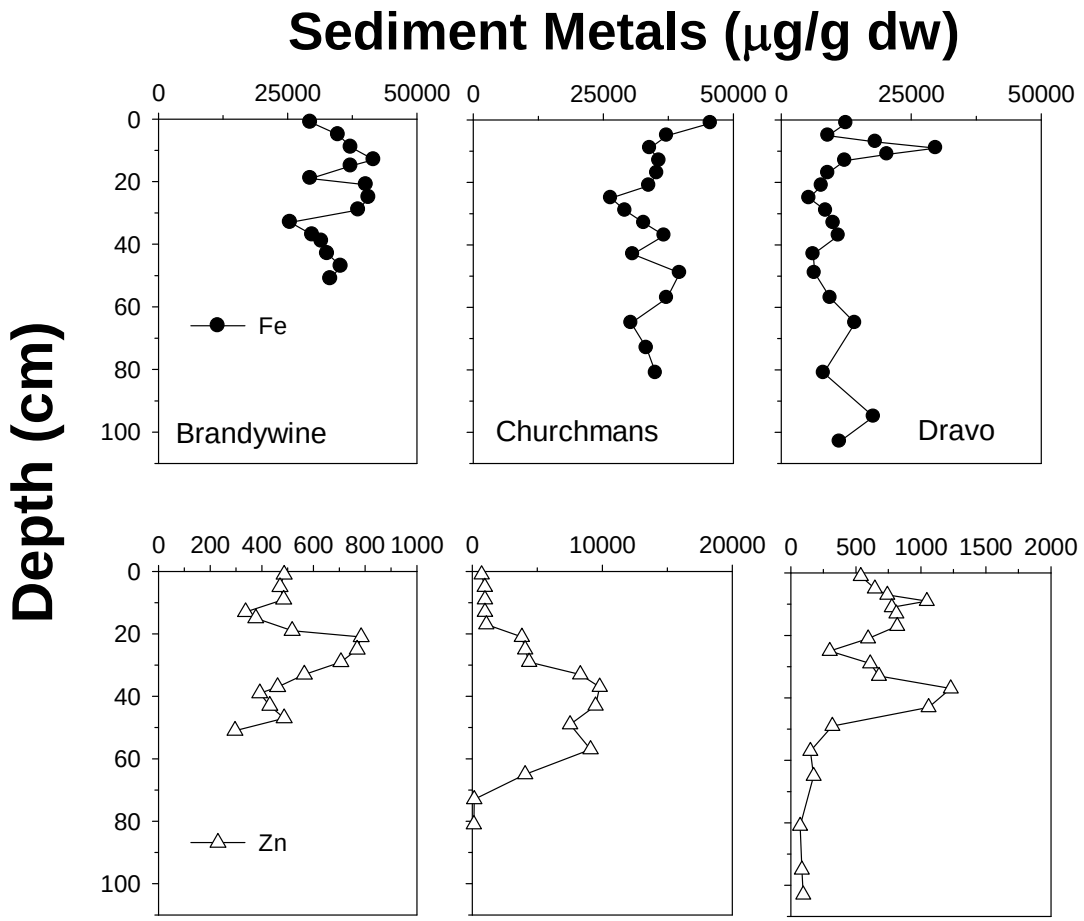

Figure 33. Depth distribution of sediment iron (Fe) and zinc (Zn) in the tidal Brandywine Creek, Churchmans Marsh and Dravo Marsh (Note scale changes).

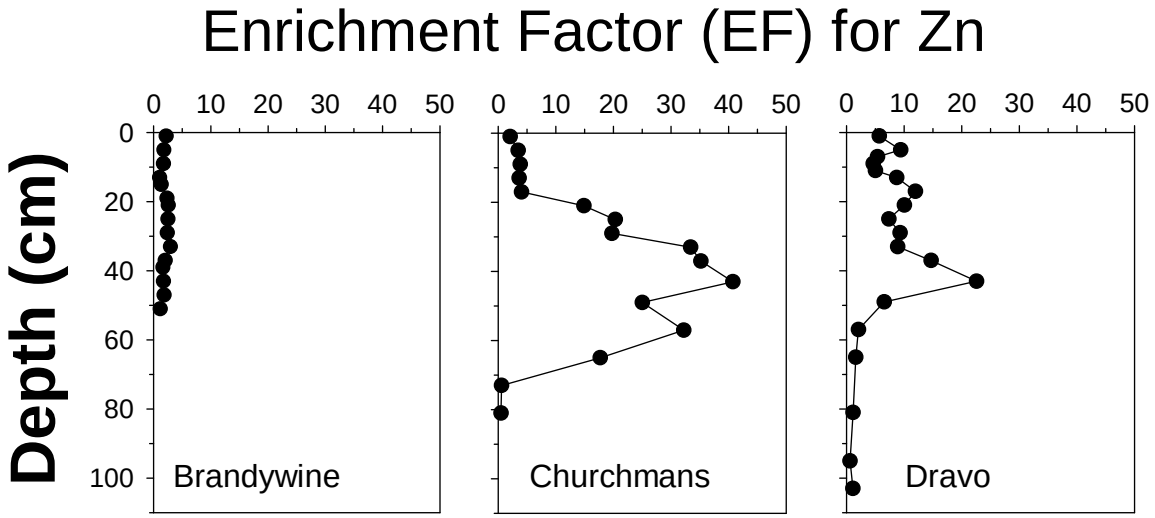

Figure 34. Depth distribution of the Zn enrichment factor (EF) in the tidal Brandywine Creek, Churchmans Marsh and Dravo Marsh.

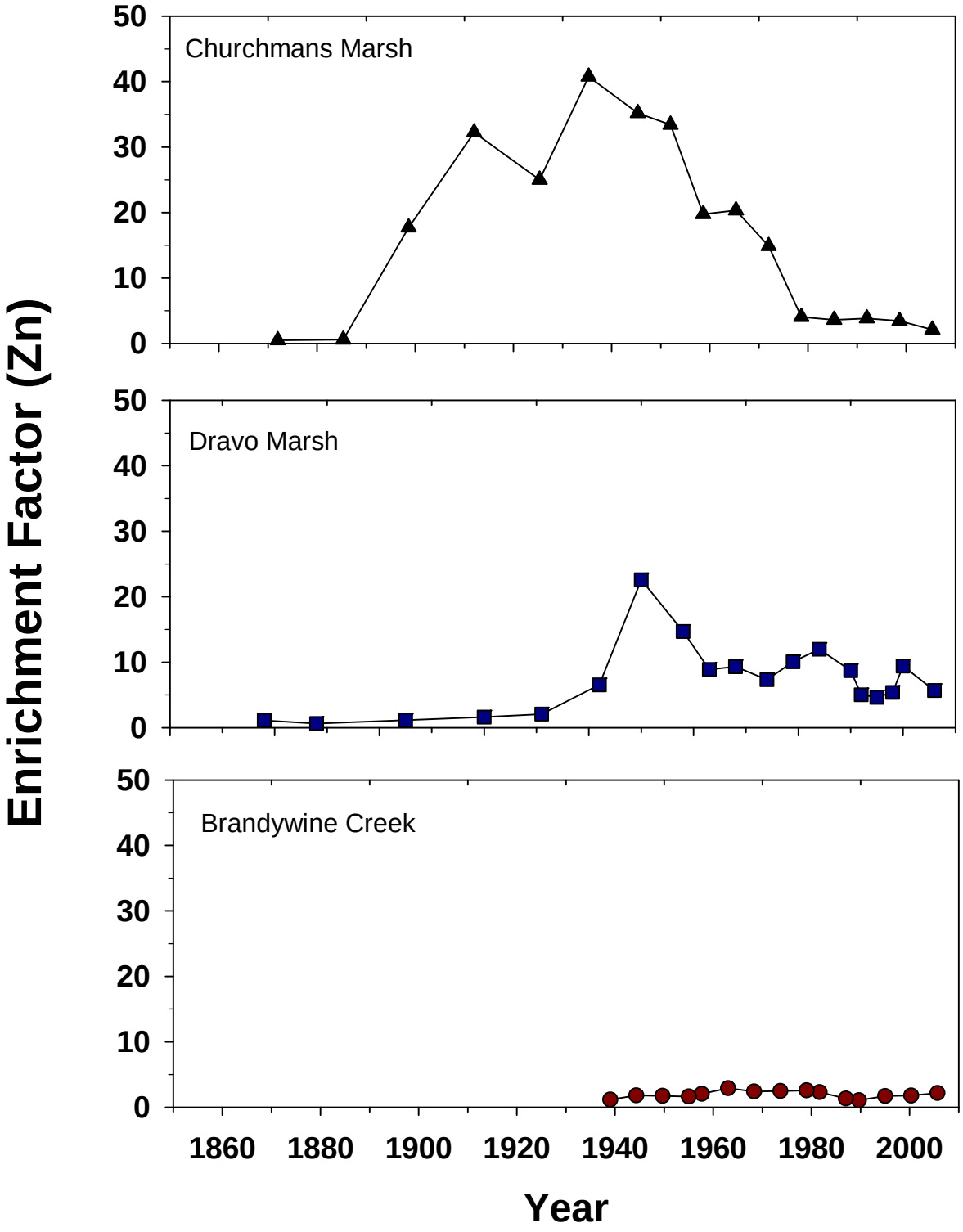

Figure 35. The time distribution of sediment concentrations of zinc (Zn) and the enrichment factor (EF) from 1860 to 2003.

Appendices

Excel File with Data and QA
(Separate Disk; electronic files)

TABLE OF CONTENTS

Page

List of Tables iii
List of Figures iv
Executive Summary v

A
Introduction **1**
A1 Background 1
A2 Objectives of Study 1
A3 Study Area 2

B
Field and Laboratory Methods 3
B1 Field Sampling 3
B2 Laboratory Methods 4
B2.1 Organic Contaminants 4
B2.2 Iron (Fe) and Zinc (Zn) 5
B2.3 Radioisotope Measurements and Sedimentation Rates 5
B2.4 Total Organic Carbon and Nitrogen 7
B2.5 Total Phosphorus 7
B2.6 Stable Isotopes of Carbon and Nitrogen 7
B2.7 Diatoms 7

C
Results and Discussion 8
C1 Sediment Properties and Sediment Accumulation 8
C1.1 Sediment Properties 8
C1.2 Accretion and Sediment Accumulation Rates 9
C1.3 Radionuclide Inventories and Focusing Factors 11
C2 Nutrients/Eutrophication 13
C2.1 Sediment Total Carbon, Total Nitrogen and Total Phosphorus 13
C2.2 Stable Isotopes of Carbon and Nitrogen 15
C2.3 Diatom Analysis and Assemblages 17

C3 Sediment Bound Contaminants 21
C3.1 Polycyclic Aromatic Hydrocarbons 22
C3.2 Polychlorinated Biphenyls 28
C3.3 Total DDX and Chlordane 33
C3.4 Polybrominated Diphenylethers (PBDEs) 36
C3.5 Dioxins and Furans 38
C3.6 Iron and Zinc 40

TABLE OF CONTENTS (cont)

Page

D
Summary and Conclusions.....45

E
Acknowledgments.....48

F
References.....49

G
Tables.....61

H
Figures.....80

I
Appendices.....118

Appendix I: Data Tables and QA Documentation.....I

LIST OF TABLES

Table 1: Core Locations and collection dates 62
Table 2: Bulk sediment properties and radioisotope data for core BW 63
Table 3: Bulk sediment properties and radioisotope data for core CM 64
Table 4: Bulk sediment properties and radioisotope data for core LSP 65
Table 5: Bulk sediment properties and radioisotope data for core DM 66
Table 6: Summary data for radioisotope analysis and dating 67
Table 7: Concentrations of various parameters for core BW 68
Table 8: Concentrations of various parameters for core CM 70
Table 9: Concentrations of various parameters for core DM 72
Table 10: Concentrations of various parameters for core LSP 74
Table 11: Concentrations of various parameters for core WS 75
Table 12: List of PAH compounds for analysis 76
Table 13: Diatom metrics for core BW 77
Table 14: Diatom metrics for core CM 78
Table 15: Diatom metrics for core DM 79

LIST OF FIGURES

Figure 1: Study area and core locations 81
Figure 2: Tripod/pulley system at Dravo Marsh 82
Figure 3: Geochronology for core BW 83
Figure 4: Geochronology for core CM 83
Figure 5: Geochronology for core DM 84
Figure 6: Geochronology for core LSP 84
Figure 7: Sediment organic carbon, C/N and sediment phosphorus distribution with depth 85
Figure 8: Depth distribution of the isotopic composition sediment N ($\delta^{15}N$) and C ($\delta^{13}C$) 87
Figure 9: Distribution of diatom indicator species with depth 88
Figure 10: Diatom metrics 91
Figure 11: Relationship between total sediment N and diatom metrics 92
Figure 12: Relationship between total sediment P and diatom metrics 93
Figure 13: Concentrations of total sediment nitrogen (TN) and the nitrogen isotopic composition of TN ($\delta^{15}N$-TN) from 1860 to 2003 94
Figure 14: Concentrations of total sediment phosphorus (TP) and the carbon isotopic composition of total carbon ($\delta^{13}C$-TC) from 1860 to 2003 95
Figure 15: The relationship between total sediment P (TSP) and the carbon isotopic composition of organic matter ($\delta^{13}C$-TC) in Brandywine Creek, Churchmans Marsh and Dravo Marsh 96
Figure 16: Diatom metric for eutrophentic species from 1860 to 2003 97
Figure 17: Depth distribution of total PAHs and the LMW to tPAHs ratio with depth 98
Figure 18: Comparison of benzo[a]pyrene to benzo[e]pyrene 99
Figure 19: Indicator ratios of benzo[a]pyrene to benzo[e]pyrene and fluoranthene to pyrene 100
Figure 20: Concentrations of tPAHs from 1900 to 2003 101
Figure 21: Distribution of tPCBs with depth 102
Figure 22: Distribution of tPCBs and the LMW to tPCBs ratio with depth 103
Figure 23: Distribution of tDDX (DDT+DDD+DDE all forms) and total chlordanes with depth 105
Figure 24: Concentrations of tPCBs from 1900 to 2003 106
Figure 25: Concentrations of tDDXs from 1900 to 2003 107
Figure 26: Distribution of total chlordanes (all forms) with depth 108
Figure 27: Concentrations of total chlordanes from 1900 to 2003 109
Figure 28: Distribution of tPBDEs with depth 110
Figure 29: Concentrations of tPBDEs from 1860-2003 111
Figure 30: Distribution of dioxins and furans with depth 112
Figure 31: Concentrations of total dioxins and furans from 1900 to 2003 113
Figure 32: Concentrations of TEQ for dioxins and furans from 1860-2003 114
Figure 33: Distribution of sediment Fe and Zn with depth 115
Figure 34: Zn enrichment factor (EF) with depth 116
Figure 35: Concentrations of Zn and the EF from 1860-2003 117

Executive Summary

This study involved the chemical analysis of five sediment cores taken from the tidal Christina River Basin and lower Shellpot Creek in northern New Castle County, DE. Of the five cores, four were dated using ^{210}Pb and ^{137}Cs radiometric methods, with three (Churchmans Marsh (CM), Dravo Marsh (DM), and the tidal Brandywine (BW)) providing sufficient temporal coverage (> 50 yrs) for detailed chemical analysis. *The main objective was to evaluate historical trends in organic chemical contaminants (e.g., polychlorinated biphenyls, pesticides, dioxins/furans, polybrominated diphenylethers and polycyclic aromatic hydrocarbons), selected trace metals (e.g., iron and zinc) and nutrients (i.e., sediment phosphorus and nitrogen).* An additional objective was to evaluate if a historical record of eutrophication could be derived from algae analysis (i.e., diatom species in the cores) along with other indicators of potential ecosystem change (e.g., stable isotopes of carbon (δ^{13}C-OM) and nitrogen, (δ^{15}N-TN)).

The range and average sediment accumulation rates (^{137}Cs) inferred from the ^{137}Cs and ^{210}Pb data are similar to other areas within the Delaware Estuary and range from 0.57 to 1.9 cm/yr. There was good agreement between the ^{137}Cs rates and those for the constant accumulation model for ^{210}Pb.

With regard to contaminants, a major finding that emerged from this study is the historic accumulation of zinc in the system, as clearly displayed in the Churchmans Marsh (CM) core. Concentrations of Zn showed a broad peak over background levels starting at or shortly after the turn of the century and persisting to the early to mid-1970s. Using the amount of iron (Fe) within the sediment and referencing the data to bottom concentrations of Zn (and Fe), the sediments of Churchmans Marsh had been up to 40 times above background levels. Current Zn enrichment in Churchmans Marsh is still approximately 5 to 10 times above background. In the other core locations, surface sections are not substantially enriched above background with zinc enrichment factors ranging only from 1 to 2.3. Major sources of historic zinc loading to the tidal river included a National Vulcanized Fiber (NVF) facility on the Red Clay Creek (Yorklyn, DE) and a NVF facility on White Clay Creek (Newark, DE) and a pigment plant located in Newport (DE) along the tidal Christina River. Both NVF facilities ceased operation and have either been remediated (NVF Newark) or continue to be remediated (NVF Yorklyn). The pigment plant and adjacent areas impacted by releases from the plant are designated as a Federal Superfund site. Remedial actions have been taken at the site, in part to address the zinc issue. The coring

analysis clearly shows that the combined loading from these 3 facilities was much higher in the past and that remedial actions taken over the years have yielded substantially lower concentrations of Zn in the sediments of the tidal Christina River.

The other key finding of this study is that concentrations of organic contaminants are lower today, overall, than they were in the past, with some exceptions. Chlorinated organic compounds such as tchlordane, tDDX and dioxins/furans all show a sharp maximum at similar depths (corresponding to the 1960s and 1970s), followed by a decreasing trend towards the surface. Total PCBs also shows higher concentrations at depth with decreasing concentrations towards the surface, with the exception of the Dravo Marsh core where tPCB concentrations at the surface remain elevated (ca. 240 ng/g dw). The DM finding may reflect lingering inputs from local sources and/or the redistribution of previously deposited contamination following major earth works projects in or near the marsh.

Interestingly, the PCB congener composition in both the CM and DM cores showed a shift from mid to higher molecular weight compounds to lower molecular weight compounds from the upper sections (more recent) to the lower sections (longer ago). The opposite was true for the BW core. The high proportion of deca PCB (H10) in the CM and DM cores is unusual and appears to reflect releases from the same pigment plant in Newport that was also responsible for at least part of the zinc contamination. The use of congener-specific PCB methods (rather than typical Aroclor methods) allowed us to identify and characterize the deca PCB signature.

Total dioxins (PCDD) and furans (PCDF) concentrations ranged from <2 to 157 ng/g dw and <1 to 13 ng/g dw, respectively, with distinct distributions with depth and time. The individual congeners were used to calculate the toxic equivalents (TEQs) using published toxic equivalency factors (TEF). The TEQs ranged from <0.01 to 0.45 ng/g dw, generally similar or lower to surface sediments collected in 2007. Highest concentrations of PCDD, PCDF and TEQ were found in the Churchmans Marsh core.

In the three cores analyzed for polybrominated diphenyl esters (PBDEs), tPBDEs were only present in the upper sections with undetectable concentrations below approximately 20 cm (<1980s). The predominant congener is PBE 209 in the upper sections with BDE153 and BDE99 found at depth.

Total PAHs showed a distinct concentration peak in the 1940s, in the CM core, while a bimodal distribution was observed in the DM core and possibly the BW core. The peak of tPAHs

in the CM core maybe related to historic inputs of hydrocarbons from another Federal Superfund site near Newport (Koppers) that used creosote to treat telephone poles and other lumber. Other sources related to urban development including a major shipbuilding complex and a coal gasification facility are also potential historic sources to the area, particularly the DM. Data were compared to indicators of combustion sources, such as coal tar based parking lot sealant, using specific ratios of individual PAHs. Only a limited number of samples were consistent with such a fingerprint and thus this type of sealant does not appear to be a major source to the tidal Christina River.

Lastly, analysis of the diatom assemblages and metrics indicate a shift toward more eutrophic species starting in the late 1940-1950s. There was a strong positive relationship between the eutrophic diatom metric and the concentration of nitrogen and phosphorus in Churchmans and Dravo marshes. This, along with the increases in total sediment N, total sediment P and sediment nitrogen isotopic compositions (δ^{15}N-TN), indicates that increase loadings of nutrients have resulted in a diatom shift in the river.

Overall, this study documents the chemical analysis of three cores taken in the tidal Christina River and tidal Brandywine Creek. Changes were observed in contaminant levels across time that reflect usage globally and most often locally. Contaminant levels appear to be declining when viewed on a longer-term, decadal time scale. However, the concentrations of several contaminants (e.g., PCBs and zinc) remain relatively elevated in this system.

A) Introduction

A1: *Background*

Trace metals and organic contaminants in water are derived from many sources. Natural sources of metals include the weathering products of soils which are then transported in the dissolved or particulate phases. Anthropogenic sources of metals and organic contaminants are introduced to the water via atmospheric deposition, industrial discharges (e.g., mining, metal processing, manufacturing), municipal discharges (waste water treatment), and stormwater runoff of contaminated parcels. Due to the particle-reactive nature of most trace metals and organic compounds, sediments are potential repositories for contaminants and, under certain conditions, can be used to provide a historical record of pollution (Simpson et al., 1983; Orson et al., 1990; 1992; Valette-Silver, 1993; Hornberger et al., 1999; Cooper and Brush, 1993; Church et al., 2006; Velinsky et al., 2007; and others). With minimal diagenetic remobilization, biological mixing, and hydraulic processes, the sediment column can reflect the chronological deposition/inputs of most contaminants. Sediment cores are extremely useful in determining if various pollution control actions were/are effective in reducing contaminant loadings, as well as providing a time frame for system response (Smol, 2008). Hence, coring data are important to determine whether environmental conditions are improving with time and at what rate. The rate information is especially important for modeling programs in which forecasts are developed by extending past trajectories.

A2: *Objectives of Study*

It is the objective of this study to collect sediment cores from the tidal freshwater region of the Christina River and Shellpot Creek (near Wilmington, DE), and determine the chronology of chemical contaminant deposition, nutrient loadings and related ecological response. To meet this objective, we obtained and analyzed the chemical characteristics of sediment cores from depositional areas within the targeted waters. This study aimed to quantify and illustrate the magnitude and extent of sediment contamination in the lower tidal portion of the Christina Watershed and Shellpot Creek and provide insight into the temporal nature of that contamination. It also sought to understand how the trophic status of the system has changed over decadal time scales.

A3: *Study Area*

The Christina River Basin occupies 1480 km^2 in Delaware, Pennsylvania and Maryland, and includes four major watersheds—Brandywine Creek, Red Clay Creek, White Clay Creek, and the Christina River. The Christina River Basin is a rapidly suburbanizing watershed which is characteristic of a typical mid-Atlantic watershed. Land uses in the watershed are approximately 33% for urban/suburban, forested/open space, and agriculture (DNREC, 2007). Percent impervious levels in developed watersheds exceed 10 to 15%, which are thought to represent maximum thresholds needed to protect stream habitat and fisheries (Klein et al., 1979; Roy et al., 2003). Existing water quality problems are derived from wastewater discharges, agricultural runoff, Superfund sites, and runoff from new development. Approximately 40 stream segments listed as impaired in the EPA's 303(d) list have resulted in fish consumption advisories along reaches of the Brandywine Creek, Red Clay Creek, and Christina River.

The river contains many sources of chemical contaminants and has three federal Superfund sites located within the lower tidal river (Koppers Wood, Dupont Chemical, and Halby Chemical), numerous state-lead waste sites, and is listed on Delaware's 303(d) list of impaired waters (DNREC, 2007). Two major tributaries to the Christina, the Red Clay Creek and the White Clay Creek, are listed as impaired due to elevated zinc concentrations. Both of these tributaries have implemented efforts (i.e., total maximum daily loads [TMDL]) to reduce inputs of Zn to the water (DNREC 1996; 1999a,b,c). In addition, the EPA and DNREC in 2001 implemented a TMDL for excess nutrient inputs to the river (high and low flow conditions). Additional TMDL for the Christina Basin, including those for PCBs and other contaminants, are scheduled to be completed in 2010 and beyond.

The Shellpot Creek Watershed, a tributary to the Delaware River Estuary, is located in New Castle County, DE and flows through parts of Wilmington, DE. The creek once flowed into the lower tidal Brandywine but has been diverted directly into the Delaware Estuary. The watershed drains approximately 9,000 acres of mostly developed lands (90% of the watershed area).The impaired segment of Shellpot Creek begins at its headwaters and terminates at its mouth which is its confluence with the Delaware River. The watershed has completed TMDLs for excess nutrients and bacteria (DNREC, 2005). The creek is also currently listed on Delaware's 303(d) list for impairments due to chlordane and PCBs in fish. TMDLs to address those impairments are scheduled for the future.

Current PCB loading rates from Delaware Hazardous Substance Cleanup Act (HSCA) sites via overland flow and subsurface discharge to the tidal Christina Basin have been estimated by Brightfields, Inc. (2009); however, a historical perspective of contaminant inputs and mass loading rates have not been estimated. This project helps to fill that gap.

Cores were obtained in the tidal portion of the tidal Christina River (**Figure 1**). Locations include sites in Churchman Marsh (CM), Brandywine River (BW), Lower Shellpot Creek (LSP), and Walnut Street Bridge in downtown Wilmington, DE (WSB), and Dravo Marsh (DM) also called Old Wilmington Marsh. Salinities in this area are very low and marsh plant diversity indicates a tidal freshwater system. However, during drought conditions the BW and DM sites can occasionally experience salinities of 2 to 4 psu while upstream CM can experience lower salinities of between 1 and 2 psu.

B) Field and Laboratory Methods

B1: *Field Sampling*

Sediment cores were collected in 2007/2008 by staff from The Academy of Natural Sciences and University of Delaware at locations in the tidal river (**Figure 1; Table 1**). Overall, 10 cores were obtained from these sites but not all of them provided good sediment chronologies (based on ^{210}Pb and ^{137}Cs) and as such were not analyzed for various chemical parameters. This report discusses only the cores (i.e., 5 of the 10) on which chemical analyses (e.g., PCBs, PAHs, organic carbon, etc) were accomplished. Of these five cores, three (CM, BR, and DM) had sufficient temporal resolution and are discussed in detail, while the other two cores (LSP and WSB) are presented in a limited manner.

Cores were mainly collected on the marsh surface during mid to low tide. The cores obtained slightly downstream of the Walnut Street Bridge were collected during low tide, but water was present at the sediment surface. Core locations were from the interior of the marsh, away from any obvious disturbances (e.g., creek banks and ditching). At each site two cores were obtained, one for chemical analysis and the other for stratigraphic descriptions of each site. Push-piston cores of approximately 1 to 1.5 m in length were retrieved by a tripod/pulley system (**Figure 2**). The cores were taken to the laboratory and sectioned into specific intervals (e.g., 2 cm). Samples were stored in pre-cleaned jars at -10°C at either Academy or UDEL facilities.

Chain-of custody procedures were followed from the time of collection, shipping and until the analyses were completed.

B2: *Laboratory Methods*

Organic contaminant clean-techniques were used throughout and are well published (Ashley and Baker, 1999; others) and are similar to those used by EPA and NOAA (U.S. EPA, 1987; NOAA, 1993; Wade et al., 1994). All materials coming in contact with the samples were either glass or metal that was cleaned of any contaminants prior to use. Sample ID forms were used and each sample was given a unique laboratory number for sample tracking.

Sediments were analyzed for the following parameters at laboratories operated by the Academy of Natural Sciences (Patrick Center): carbon, nitrogen and phosphorus, PAHs (41+ compounds), total PCBs (100+ congeners), selected pesticides including DDTs and chlordane, and stable isotopes of carbon and nitrogen. In addition, specific sections were analyzed for diatoms via sample digestion, mounting and glass slide light microscopy. Sediments for radioisotope analysis (^{210}Pb and ^{137}Cs) were analyzed at University of Delaware (Center for Earth, Oceans and Environment). Below are brief descriptions of each chemical, biological, or physical method.

B2.1: Organic Contaminants: PAHs, Polychlorinated Biphenyls, Organochlorine Pesticides, and Dioxins and Furans

Prior to organic contaminant analyses, samples were kept frozen at -20°C. Standard operating procedures for the extraction, clean-up and quantification of organic contaminants in sediments are summarized in their respective operating procedure. Briefly, sediment samples were extracted with dichloromethane for 24 h using a Soxhlet apparatus. PAHs were quantified using a capillary gas chromatograph coupled with a mass spectrometer in the electron impact mode after a clean-up procedure employing liquid-solid chromatography with alumina as the stationary phase (Ashley and Baker, 1999). After PAH determination, samples were further cleaned using liquid-solid chromatography with florisil as the stationary phase. Congener-specific PCBs and OCPs (spell this out) were analyzed using a gas chromatograph equipped with a ^{63}Ni electron capture detector (Ashley and Baker, 1999; Kucklick et al., 1996). Twenty-eight singly or coeluting PBDE (BDE 17, 25, 28+33, 30 47, 49, 66, 71, 75, 85+155, 99, 100, 116, 119, 138, 153, 154, 156, 181, 183, 190, 191, 203, 205, 206, 209; Accustandard, 95–99% purity) were quantified at Duke University using a gas chromatography (GC) with a mass spectrometer (MS) operated in negative chemical ionization mode (NCI). Add brief description of dioxin and furan analysis performed by GERG.

B2.2: Sediment Iron (Fe) and Zinc (Zn)

Core sediment (0.500 g) was placed into pre-cleaned Teflon tubes for the MARS microwave digestion system. Approximately 10 ml of concentrated nitric acid (trace metal grade) was slowly added and the sample was allowed to cool and evaporate gases. The tubes were capped tightly and microwaved using EPA SOP 3051. The slurry was mixed and allow to settle for one week in which an aliquot was taken and diluted (100 ml) with ultra clean DDW. The extract was analyzed using a flame Varian AAS linked to a desktop computer. A five-point calibration curve was used to calculate concentrations and samples were diluted if absorbance was greater than 0.750. Concentrations are reported in dry wt and it should be noted that concentrations are not total (i.e., mineral matrix) but strong acid digestion.

B2.3: Radioisotope Measurements and Sedimentation Rates

In the laboratory, sediment cores were extruded vertically and sectioned in 2-cm intervals for analysis. Sediment bulk density (ρ_d) and loss-on-ignition (LOI) measurements were made for each core section to aid interpretation of the downcore radionuclide and chemical data. Dry-bulk density was calculated from porosity (ϕ) using representative values of interstitial fluid density (ρ_d) and mineral density (ρ_m) according to:

$$\rho_d = (1-\phi)\rho_m \tag{1}$$

where ρ_m=2.65 g/cm^3. Porosity was computed gravimetrically from water content (W_c) and using an assumed pore water density of ρ_f=1.0 g/cm^3:

$$\phi = \left(\frac{W_c \rho_m}{W_c \rho_m + (1-W_c)\rho_f} \right) \tag{2}$$

where $W_c = W_{wet} - W_{dry} / W_{wet}$. Dry sediment weight was determined by drying the sectioned wet sediment in a convection oven at 100°C for 24 h. The dry sediment was then ground to a fine powder for LOI determination and radionuclide analysis.

LOI measurements were used to quantify the relative proportion of organogenic (combustible) and minerogenic (residual ash) materials in the sediments. Following the method of Heiri et al. (2001), a 4-gram quantity of sample power was combusted at 550°C in a muffle furnace for 4 h. LOI was computed as follows:

$$LOI = \frac{W_{dry} - W_{ash}}{W_{dry}} \cdot 100\% \tag{3}$$

where W_{dry} is the weight of sample previously dried at 100°C, and W_{ash} is the weight of the residual ash.

To develop sediment chronologies and determine accretion rates for the sediment column, measurements of ^{210}Pb ($t_{1/2}$=22.3 years) and ^{137}Cs ($t_{1/2}$=30.1 years) were made by gamma spectroscopy of the 46.5 and 661.6 keV photopeaks, respectively (Cutshall et al., 1983; Wallbrink et al., 2002). Powder samples were placed in a 60 ml plastic jar and counted for 24-48 h on a Canberra Model 2020 low-energy Germanium detector (LEGe). The radionuclide concentration (activity) of excess ^{210}Pb was determined by subtracting the activity of its parent nuclide ^{214}Bi (609.3 keV) from the total activity. Detector efficiencies were determined from counts of NIST Standard Reference Material 4357 (Inn et al., 2001). The counting geometry of the core samples was kept identical to that of the NIST standard such that a self-absorption

correction for ^{210}Pb was not necessary. Confidence limits reported with radioisotope data are the propagated one-sigma background, calibration, and counting errors.

Three approaches were used to reconstruct the accumulation history of marsh deposits. Two of these methods are based on downcore profiles of ^{210}Pb activity, and the third uses the depth distribution of ^{137}Cs activity. The first approach, the constant activity model (CA), assumes that the specific activity of ^{210}Pb (dpm/g) deposited remains constant through time. In other words, variations in mineral sedimentation rate do not affect the initial concentration of ^{210}Pb. At steady state, excess ^{210}Pb decreases exponentially with depth in the sediment column following:

$$A = A_o \, exp\left(-\lambda z / S\right) \tag{4}$$

where A is the excess activity of ^{210}Pb at depth z, A_o is the initial activity of excess ^{210}Pb, λ is the decay constant for ^{210}Pb (0.0311 years^{-1}), and S is the vertical accretion rate. The slope of the regression line of ln$A$ versus z is proportional to the accretion rate with dimensions length/time. In this method the age of a sediment interval is derived from a single value of S averaged over the ^{210}Pb profile. The corresponding mass accumulation rate, with the dimensions mass/area/time, is determined by plotting A as a function of cumulative mass, the depth-integrated product of ρ_d and z.

The second method, the constant flux model (CF), relates time and accretion rate to the inventory of excess ^{210}Pb by assuming that the flux of ^{210}Pb to the sediments (rather than A_o concentration) is constant. Sediment age and ^{210}Pb are related as:

$$I = I_o \, exp\left(-\lambda t\right) \tag{5}$$

where I is the inventory of excess ^{210}Pb below depth z (dpm/cm^2), I_o is the total inventory of excess ^{210}Pb in the sediment column, and t is the sediment age at depth z. Radionuclide inventories of excess ^{210}Pb (and ^{137}Cs) are computed as:

$$I_o = \sum_i \rho_{di} x_i A_i \tag{6}$$

where ρ_d is the dry-bulk density, x is the sediment thickness, A is the radionuclide activity, and the i operator indicates the ith depth interval. In the CF model, sediment accretion rates are computed by dividing the length of the dated sediment column by the corresponding age in years.

The third chronological method is based on the first occurrence of ^{137}Cs in the sediment column as an absolute indicator of ca. 1954, the year of ^{137}Cs introduction to the global atmosphere by nuclear weapons testing (Ritchie and McHenry, 1990). The depth of ^{137}Cs penetration divided by the interval between ca. 1954 and the year of core collection is used to compute an average accretion rate. The corresponding mass accumulation rate is determined by plotting ^{137}Cs activity against cumulative mass. The advantage of ^{137}Cs chronology over ^{210}Pb dating methods is that it more closely approximates the absolute age of sediments deposited after ca. 1954.

Both the CA and CF ^{210}Pb models have been widely used to develop sediment chronologies for tidal marsh deposits, but they are based on different assumptions that are not met in all types of depositional environments. The CF model assumes that 1) all ^{210}Pb deposited is derived from direct atmospheric deposition, and 2) variations in A_o are due to changes in the minerogenic sediment accumulation rate S as opposed to changes in ^{210}Pb supply (Appleby and Oldfield, 1978). In other words, a change in S through time will be met by a corresponding change in A_o in accordance with Equation 5. This model was originally developed for lake systems and thus is most appropriate for depositional environments that sequester ^{210}Pb mostly (if not exclusively) through direct atmospheric deposition. Although tidal marshes are exposed to the atmosphere

most of the time, tidal flooding brings particle-bound ^{210}Pb from coastal waters that can increase A_o above that supplied by the atmospheric flux. For this study we computed sediment accretion and accumulation rates using both ^{210}Pb models but place more weight on the CA approach, because the assumptions are less restrictive regarding ^{210}Pb sources.

The following conditions are implicit in all ^{210}Pb and ^{137}Cs dating methods: 1) mixing by burrowing organism has not enhanced particle burial; 2) the modeled radionuclide is chemically immobile; and 3) the sedimentary record is complete and not punctuated by non-depositional or erosional episodes. As elaborated later, these assumptions appear to have been met in this study for cores CM, DM, and BR.

B2.4: Total Organic Carbon and Total Nitrogen

Total organic carbon and total nitrogen were measured using a CE Flash Elemental Analyzer following the guidelines in EPA 440.0, manufacturer instructions and ANSP-PC SOP. Samples were pre-treated with acid to remove inorganic carbon.

B2.5: Total Phosphorus

Total sediment phosphorus was determined using a dry oxidation method modified from Aspila et al. (1976) and Ruttenberg (1992). Solubilized inorganic phosphorus was measured with standard phosphate procedures using an Alpkem Rapid Flow Analyzer. Standard reference material (spinach leaves) and procedural blanks were analyzed periodically during this study. All concentrations were reported on a dry weight basis.

B2.6: Stable Isotopes of Carbon and Nitrogen

The stable isotopic composition of sediments was analyzed using a Finnigan Delta XL coupled to an NA2500 Elemental Analyzer (EA-IRMS). Samples were run in duplicate or triplicate with the results reported in the standard δ (‰) notation: $\delta X = (R_{sample}/R_{standard}) - 1) \times 1000$; where X is either ^{13}C or ^{15}N and R is either $^{13}C/^{12}C$ or $^{15}N/^{14}N$. The $\delta^{15}N$ standard was air ($\delta^{15}N = 0$), and for $\delta^{13}C$ the standard is the Vienna PeeDee Belemite (VPDB) limestone that has been assigned a value of 0.0 ‰. Analytical accuracy was based on the standardization of the UHP N_2 and CO_2 used for continuous flow-IRMS with IAEA N-1 and N-2 for nitrogen and IAEA sucrose for carbon, respectively. An in-house calibrated sediment standard was analyzed every tenth sample. Generally, precision based on replicate sample analysis was better than 0.2‰ for carbon and 0.6‰ for nitrogen.

B2.7: Diatoms

Core sediment was collected (≈1g) and the organic component was oxidized with 70% nitric acid while heated in a CEM microwave (165ºC) for 1.5 h. Diatoms were settled and supernatant was decanted until it reached a neutral pH. A measured amount of digested sample was dripped onto a microscope coverslip and dried. Coverslips were then mounted onto slides using a high refractive index mounting media (Naphrax™). Diatoms were counted and identified using a Zeiss Axioskop with DIC optics. Three hundred valves were counted on 1000x magnification. Identifications were made using the extensive diatom library at ANSP. Several diatom community metrics were calculated based on species autecological preferences based on van Dam et al. (1994). Metrics were calculated using the Phyco-Aide program developed at ANSP.

C) Results and Discussion

C1: *Sediment Bulk Properties and Sediment Accumulation*

The activity of ^{210}Pb and ^{137}Cs (reported as disintegrations per minute per gram of sediment; dpm/g) with depth can be used to determine the sedimentation rate and historical record of contaminants in sediments (Simpson et al., 1983; Orson et al., 1990; 1992; Valette-Silver, 1993; Appleby, 2001; Smol, 2002; Ridgway and Shimmield, 2002; Sommerfield, 2006). This information can be used for the construction of sediment budgets (Schubel and Hirschberg, 1977; Brush et al., 1982; Officer et al., 1984) and to understand chemical contaminant accumulation in aquatic environments (Owens and Cornwell, 1995; Cornwell et al., 1996; Latimer and Quinn, 1996; Van Metre and Callender, 1997; Church et al., 2006; Velinsky et al., 2007). Also, dated sediment cores can provide information as to the changes in loadings of contaminants over time (e.g., Rippey and Anderson, 1996; Gevo et al., 1997; Santschi et al., 2001). Such information is especially useful in tracking the effectiveness of various management actions designed to reduce inputs to specific areas (Owens and Cornwell, 1995; Zhang et al., 1993). However, there are many variables that can affect the usefulness of ^{210}Pb and ^{137}Cs dating in a given area (Appleby and Oldfield, 1978; Crusius and Anderson, 1991; Appleby, 2001). These include mixing of the sediment by benthic organisms (i.e., burrowing organisms), physical mixing from dredging and storm events, post-depositional movement of contaminants and of the ^{210}Pb or ^{137}Cs, and additional inputs of ^{210}Pb from sources in the urban landscape (i.e., urban sediment focusing). The cores obtained in this study provided excellent chronologies of sediment deposition and accumulation. For historical analysis, the sediment accumulation rate derived from the ^{137}Cs distribution was used to produce an age-depth relationship. This, along with the ^{210}Pb results, provides linear rates from approximately 1920-1930 to the present. For dates prior to the 1920-1930s we assume linear rates to the bottom of the cores. While this is useful for this analysis, we are less confident in the dating at the bottom of the cores due to effects associated with compaction, non-linear sedimentation rates, and other factors (Neubauer et al., 2002; Sommerfield, 2006).

C1.1: Sediment Properties

All of the cored deposits consisted of clayey silt with variable quantities of living and dead plant material. Only at the base of core SP-2 was there a noticeable down-core change in

sediment type, from silt to sand. Dry-bulk densities ranged from 0.17 to 1.2 g/cm^3 overall and increased with depth downcore in all cases (**Figures 3-6; Tables 2-5**). This depth increase is consistent with burial compaction of the sediment column due to expulsion of porewater. Only in the lowermost intervals of core LSP-2 did bulk density vary with grain size on account of changes in mineral density (silt to sand).

The amount of organic material in the cores ranged from 7 to 40%, values representative for marsh deposits in general (**Figures 3-6; Tables 2-5**). LOI decreased with depth in all cases, and cores BW-2 and DM-2 displayed a profile that varied inversely with dry-bulk density. This suggests that depth variations in sediment bulk density are partly due to the concentration of organogenic material, at least at sites BW-2 and DM-2. In summary, with the exception of the base of core SP-2, the physical properties data suggest no major changes in sediment type that could bias interpretations of chemical and radionuclide profiles.

C1.2: Accretion and Sediment Accumulation Rates

Brandywine Marsh core BW-2 displayed ^{137}Cs activities that increased up core from the depth of first occurrence at 36-38 cm to a broad peak between 20 and 30 cm, above which activities decreased to near-zero at the core top **(Figure 3; Table 2)**. The overall shape of the profile is consistent with the source function for the mid-Atlantic region (Olsen et al., 1981), but the broad activity maximum is ambiguous regarding the date of peak fallout (e.g., 1963-1964). At this site, accretion and mass accumulation rate calculated from the basal depth of ^{137}Cs activity are 0.75 cm/yr and 0.26 g/cm^2/yr, respectively.

Excess ^{210}Pb profiles for BW-2 exhibited a monotonic decrease in the log of the activity downcore, indicative of steady-state sediment accumulation and radioactive decay **(Figure 3).** Accretion rates determined using the CA and CF ^{210}Pb models were 0.80 and 1.0 cm/yr, respectively, and the corresponding mass accumulation rate was 0.40 g/cm^2/yr. At this site there was good agreement among radionuclide dating methods, suggesting that sediment accumulation has been more-or-less invariant over the period of interest.

Churchmans Marsh core CM-1 exhibited ^{137}Cs and ^{210}Pb distributions that were somewhat similar to those observed for the BW-2 core (**Figure 4; Table 3**). The ^{137}Cs activities increased up core from the depth of first occurrence at 28-30 cm to a broad maximum centered at 20-22 cm, and then decreased to lower, but detectable, activities at the core top. Accretion rates based

on ^{137}Cs and excess ^{210}Pb (CF model) were 0.60 and 0.51 cm/yr, respectively, with corresponding mass accumulation rates of 0.28 and 0.25 g/cm^2/yr. Accretion and accumulation rates could not be determined using the CA model because the excess ^{210}Pb profile did not exhibit a monotonic decrease in activity consistent with steady-state sediment accumulation.

Dravo Marsh core DM-2 had a first occurrence of ^{137}Cs at 40 cm, maximum activity at approximately 18-20 cm, and decreasing activities to the core top (**Figure 5; Table 4**). Accretion and mass accumulation rates derived using ^{137}Cs data were 0.79 cm/y and 0.19 g/cm^2/yr, respectively. Similarly, accretion rates based on the CA and CF ^{210}Pb models were 5.6 and 6.7 mm/yr, respectively, with a corresponding mass accumulation rate of 0.19 g/cm^2/yr. Overall, agreement of ^{137}Cs and ^{210}Pb chronological methods was good at this site.

The Shellpot Creek core did not provide steady-state profiles of ^{137}Cs or ^{210}Pb, precluding computation of ages and accumulation rate using the CA and CF models (**Figure 6; Table 5**). The first occurrence of ^{137}Cs activity was present near the bottom of the core at 96-98 cm, above which there was a broad maximum centered around 70-80 cm. Hence, the entire sediment column must have accumulated after ca. 1954. Based on the depth of ^{137}Cs penetration, accretion and mass accumulation rates are 1.9 cm/yr and 0.60 g/cm^2/yr, respectively. Although the CF ^{210}Pb model yielded an identical accretion rate of 1.9 cm/yr, the sediment inventory of excess ^{210}Pb inventory suggests that most of the ^{210}Pb deposited at this site is not derived from direct atmospheric deposition (see Section C2).

One of the requirements of the constant flux for ^{210}Pb (CF) model is that the initial activity at the surface should be lower with sites of higher sediment accumulation rates. Despite a three-fold difference in sediment accumulation rate among coring sites, there was no relationship between A_o (initial activity) and S (vertical accretion rate) as would be predicted by the CF model. For example, A_o (taken as the 0-2 cm depth interval; **Tables 2-5**), was not lower at sites with a higher sediment accumulation rate. While this result does not completely invalidate the CF ^{210}Pb model, it reveals that this approach may not be the best choice for tidal marsh environments.

An important observation with relevance to chemical contaminant history in the Christina River system is presence of measurable ^{137}Cs activity at the tops of all cores. Given that the global atmospheric flux of ^{137}Cs has been negligible since the early 1980s, this pattern implies that previously deposited ^{137}Cs has been redistributed in the system. Wash-in of soil-bound ^{137}Cs

from the watershed and (or) erosion of subtidal deposits can account for redeposition of ^{137}Cs in river-estuaries. Additionally, bioturbation can rework ^{137}Cs from depth, but the shapes of the ^{210}Pb and ^{137}Cs profiles determined for this study are not suggestive of intense biological mixing. To the extent that ^{137}Cs is an analog for particle-reactive contaminants, its depositional trend suggests that historical pollutants may be undergoing similar processes of reworking and redistribution in the Christina River system.

Table 6 provides the summary information and models for the radioisotopes for the Christina cores. Accretion rates, based on ^{137}Cs, ranged from 0.57 cm/yr at Churchman's Marsh to almost 2 cm/yr at Shellpot Creek. However the data at Shellpot Creek suggest extensive reworking so this rate should be considered tentative, but it does indicate higher accretion than at the other locations. These rates are well within the range of accretion throughout the tidal Delaware Estuary (Sommerfield and Velinsky, unpublished data). At 14 sites in the estuary spanning tidal fresh to marine the range of accretion rates is 0.3 to 1.3 cm/yr with an average of 0.50 ± 0.4 cm/yr (n=32 cores).

In summary, cores BW-2, CM-1, and DM-2 yielded reliable accretion rates with good agreement between ^{137}Cs and ^{210}Pb chronological methods. Because ^{137}Cs was present in the greater extent of the cores, ^{137}Cs-derived accretion rates, using peak concentration interval depth presented in **Tables 2-6,** were used to convert sediment depths to ages for the contaminant and nutrient-eutrophication histories. Dates corresponding to depth intervals within the individual cores appear in **Tables 2-6**. These estimates are a key output of this project and allow us to place the contaminant and nutrient/eutrophication data into historic context.

C1.3: Radionuclide Inventories and Focusing Factors

Sediment inventories of excess ^{210}Pb and ^{137}Cs were computed to compare the relative amount of radionuclide deposited among the four coring sites (CM, DM, BW, and LSP). Because ^{210}Pb and ^{137}Cs have particle-adsorption characteristics not unlike trace metals and some organic contaminants, the sediment inventory of a radionuclide compared to a reference value provides information about contaminant transport pathways and burial in aquatic systems. Reference inventories of 28 dpm/cm^2 for ^{210}Pb and 21 dpm/cm^2 for ^{137}Cs are known from direct measurements of radionuclide atmospheric deposition in the U.S. mid-Atlantic region (Olsen et

al. 1985; Graustien and Turekian, 1986). These reference values represent the total amount of radionuclide that could be buried at a site if supplied by atmospheric deposition alone.

The focusing factor is the ratio of the measured and reference radionuclide inventory. Focusing is the process by which fine-grained materials migrate towards more depositional areas and provide higher inventories that that predicted by reference inventories. To account for this migration, a focusing factor was calculated by comparing the actual ^{210}Pb inventory to the expected ^{210}Pb inventory. A focusing factor greater than unity implies that radionuclide activity has been preferentially transported or "focused" from one location to another by a combination of hydrodynamic flow and sedimentary processes. Conversely, a focusing factor less than unity imply that the atmospheric flux is not sequestered locally perhaps on account of sediment erosion and redistribution. In the case of ^{210}Pb, tidal flooding of a brackish or saline marsh can supply ^{210}Pb in addition to that derived by atmospheric deposition because coastal and estuarine waters usually contain ^{210}Pb activity from non-atmospheric sources. This is not the case in a tidal freshwater system, where all of the ^{210}Pb is atmospherically supplied and focusing occurs through lateral transport of particle-bound ^{210}Pb. ^{137}Cs can be focused in a similar manner as ^{210}Pb, although ^{137}Cs is less particle reactive than ^{210}Pb and tends to desorb from sedimentary particles in brackish and saline waters. Consequently, sediment inventories of ^{137}Cs in freshwater systems tend to be higher than those in estuaries and coastal waters. This must be taken into account when interpreting ^{137}Cs focusing factors for sites that span a wide range of salinities. While our locations can experience low salinities during extreme droughts, it is generally considered a tidal freshwater system as noted by plant communities.

Radionuclide inventories and focusing factors for the four coring sites (CM, DM, BW, and LSP) are presented in **Tables 2-6**. The Brandywine River site (BW-2) had the lowest excess ^{210}Pb inventory and the highest ^{137}Cs inventory among the sites sampled. This result was to be expected given the generally freshwater setting of the site. The ^{210}Pb focusing factor of unity indicates that the sediment column has been accretionary for the period of interest, and that atmospheric deposition is the probable source of radionuclide. In contrast, the ^{137}Cs focusing factor of 2.3 implies a non-atmospheric source of radionuclide, which is difficult to reconcile in light of the ^{210}Pb results.

The Churchman Marsh site (CM-1) had the second highest ^{210}Pb inventory and the lowest ^{137}Cs inventory among the sites. The ^{210}Pb focusing factor of 2.8 suggests that non-

atmospherically derived radionuclide is deposited at this site, perhaps supplied by tidal waters. The ^{137}Cs focusing factor of 0.2 is consistent with loss of particle-bound activity by desorption prior to deposition. The Shellpot Creek site (LSP-2) had the highest ^{210}Pb inventory, several times that of the others, and a ^{137}Cs inventory that was second only to site BW-2. The ^{210}Pb focusing factor of 11.4 suggests influx of radionuclide from tidal estuarine waters, but the ^{137}Cs focusing factor of near-unity is not supportive of an estuarine source. Another possibility is that soil-bound ^{210}Pb and ^{137}Cs eroded from the surrounding landscape and focused at the site. This interpretation is consistent with the site's rapid rate of sediment accumulation (1.9 cm/yr), which most likely results from localized sediment trapping caused by the tidal gate barrier immediately adjacent to the coring site. The Dravo Marsh site (DM-2) had radioisotope inventories and focusing factors within the range of values measured at the other sites.

The focusing factors make clear that the four depositional sites (CM, DM, BW, and LSP) have sequestered ^{210}Pb or ^{137}Cs inventory at levels above that which can be accounted for by atmospheric flux alone. This result confirms that most of the minerogenic material buried at these sites is allochthonous (i.e., transported to the location from elsewhere), and implies that atmospherically sourced, particle-reactive contaminants in the Christina River system will exhibit focusing patterns that depend not only on broad scale atmospheric delivery but also on more regional and local transport processes (e.g., tidal flow and sediment transport). All of the coring sites, although within the Atlantic Coastal Plain, are immediately down gradient from the Piedmont physiographic province. Particles eroded from the Piedmont are transported downstream and later deposited on the Coastal Plain. Contaminants associated with these particles, plus contaminants originating from local sources within the Coastal Plain, and contaminants delivered from tidal exchange, ultimately combine to yield observed profiles in the cores. An important is that the all of the coring sites, while depositional, are subject to both small and large scale processes (i.e., within the tidal waters and from the watershed) that influence radioisotope and contaminant profiles.

C2: Nutrients/Eutrophication

C2.1: Sediment Total Carbon, Total Nitrogen and Total Phosphorus

Sediment total carbon (TC) concentrations for the BW-2, CM-1, and DM-2 cores ranged between <1.0 and 19.8% on a dry weight basis (dw) with an average of 5.5 ± 7.7% TC (±

standard deviation; **Table**s **-11; Figure 7a,b**). Similarly, total nitrogen ranged from 0.1 to 1.2% N with an overall average of 0.40%; while total sediment phosphorus (TSP) ranged from 0.04 to 0.27% TP with an overall average of 0.10%. In the lower Shellpot Creek (LSP) and Walnut Street (WS) cores %TC and %TN averaged slightly lower; 4.3% and 0.29% respectively while TP averaged slightly higher at 0.14% TP.

The three cores, CM, DM, and BW, exhibited different total carbon, nitrogen and phosphorus profiles with depth (**Figure 7a**). In the CM core, TC increased from 1.2% to approximately 7.6% near the surface while in the DM core concentrations increased from 1.0% to 18% near the surface. In the DM core there were two subsurface maxima, one centered at ~ 40 cm (8% OC) and the other centered at ~10 cm of 20% OC. Concentration in the BW core increased only slightly from the bottom (2.2% OC) to the surface (3.8% OC), with a broad subsurface maxima between 20 and 40 cm. Total sediment P increased substantially towards the surface in the CM core (0.06 to 0.18% P) and to a lesser extent in the DM core. In the DW there was no difference between the top and bottom sections in TP concentrations but there was higher concentrations centered around 13 cm of 0.27% P. For the LSP and WS cores, only 5 or 6 sections were analyzed for each. Therefore only limited information is derived from the depth distribution (**Figure 7b**). In the LSP core there was an increase towards the surface of TC and TP while in the WS core concentrations are similar from top to bottom.

The carbon to nitrogen ratio (C/N; atomic units) can be used as a tracer of the source of organic matter to a location and potential diagenetic changes that could occur during burial (Jasper and Gagosian, 1990; Meyers, 1994; Prahl et al., 1994). Diagenesis is any chemical, physical, or biological change undergone by sediment after its initial deposition (Berner, 1980). For example, terrestrial material (e.g., trees) are rich in cellulose (i.e., higher C) compared to algae or marsh plants that have less structural material and are higher in proteins (i.e., higher N). Typical marine plants have C to N ratios of ~ 4-10 while terrestrial material can have C to N values > 15-20. Diagenesis of recent sediments tends to increase the C to N ratio due to preferential remineralization and release of nitrogen compounds; however re-incorporation of bacterially derived N can increase the C to N ratio over time (Fogel et al., 1989; Benner et al; 1991). In the CM core (**Figure 7a**), the C/N ratio changed only slightly with depth and averaged 12.3 ± 1.2, while in the DM core, the C/N ratio increased from 10-13 near the bottom of the core to approximately 18-20 near the surface. In the Brandywine core (BW) the C to N

was more variable (range = 7 to 22), but showed a maxima in the same depth range as the C and N concentrations. In the LSP and WS cores (**Figure 7b**), the C/N ratio were fairly constant (~18) from top to bottom although there were less intervals analyzed. In general the sediments in the cores reflect a dominance of terrestrial sources of organic matter compared to algal sources. Interestingly, the CM core exhibited slightly lower C/N ratios compared to the downstream locations. It would be expected that the ratio may decrease going downstream towards the Delaware Bay where the ratio would be lower (Cifuentes et al., 1988). The change with depth in the DM core, increasing towards the surface along with the increase in OC, might suggest a change in the source of organic matter to this site.

C2.2: Stable Isotopes of Carbon and Nitrogen

Organic carbon and nitrogen isotopic ratios are useful to distinguish between marine and continental plant sources of sedimentary organic matter, processing and cycling of nutrients and in some instances the level of system-wide productivity (Fry, 2006 and others). Most photosynthetic plants incorporate carbon into organic matter using the C3 Calvin pathway, which biochemically discriminates against ^{13}C to produce a $\delta^{13}C$ shift of about -20‰ to -30‰ from the isotope ratio of the inorganic carbon source. C4 plants (e.g., corn, *Spartina*) incorporate CO_2 using a different system (PEP) that discriminates against ^{13}C to produce a $\delta^{13}C$ shift of about -8‰ to -15‰ from the isotope ratio of the inorganic carbon source. Organic matter produced from atmospheric CO_2 ($\delta^{13}C \sim -7$‰) by land plants using the C3 pathway consequently has an average $\delta^{13}C$ (PDB) value of about -27‰ (O'Leary, 1988). The source of inorganic carbon for marine algae (C3 plants) is dissolved bicarbonate, which has a $\delta^{13}C$ value of about 0‰. Marine organic matter consequently typically has $\delta^{13}C$ values between -20‰ and -22‰. The isotopic difference between organic carbon produced by C3 land plants and marine algae has been used to trace the delivery and distribution of organic matter to sediments in estuarine and coastal areas (Cifuentes et al., 1989; Fogel et al. 1992, and many others).

Carbon isotope ratios can be affected by photosynthetic dynamics and by postdepositional diagenesis (Dean et al., 1986; Fogel et al., 1992; Canuel et al., 1995; Zimmerman and Canuel, 2002) and consequently must be interpreted cautiously. A big factor that can impact $\delta^{13}C$ values of plant material is the availability of CO_2 and rate of production during photosynthesis and the possibility of selective diagenesis of organic matter fractions that are isotopically heavy or light.

While the change in $\delta^{13}C$ appears to be small (<2‰) during recent diagenesis (Hayes et al., 1989; Meyers, 1994), shifts due to the availability and rate of production, due to nutrient enrichment or limitation and other factors, can have a large impact on the resultant $\delta^{13}C$ values of deposited organic matter (Fogel et al., 1992; Schelske and Hodell, 1995; Church et al., 2006).

Differences exist between the natural abundances of stable nitrogen isotopes ($\delta^{15}N$, $^{15}N/^{14}N$) in dissolved and particulate matter from terrestrial, estuarine, marine, and anthropogenic sources. Terrestrial occurring soil nitrogen can have a wide range of values, but in general range from -1 to +4‰) similar to atmospheric nitrogen (0‰). Nitrogen isotopic compositions from marine sources tend to be slightly enriched in the heaver isotope (^{15}N) and are very dependent on the source of dissolved nitrogen and its $\delta^{15}N$, and processing in the system (e.g., ammonification, nitrification, denitrification, etc) at the time of formation. A dominant process in many aquatic environments (and groundwater) is denitrification (Cline and Kaplan, 1975). Denitrification is a microbially facilitated process of dissimilatory nitrate reduction that ultimately produces molecular nitrogen (N_2) through a series of intermediate gaseous nitrogen oxide products. This microbial process uses dissolved nitrate during oxidation of organic matter and as nitrate is consumed there is an enrichment of residual nitrate in the system. Algal/plant production and its $\delta^{15}N$ from nitrate would reflect the balance between processes and inputs. There are many points in which nitrogen can be fractionated and its isotopic composition altered. For example, wastewater from treatment facilities have been shown to increase the $\delta^{15}N$ of various fish species (Lake et al., 2001) due to the selective removal of the light isotope (^{14}N) nitrogen during treatment. Anthropogenic nitrogen was substantially enriched in watersheds with greater amount of urbanization and wastewater inputs and the nitrogen was shown to be incorporated into the aquatic food web (McCelland et al., 1997)

The isotopic compositions of sediment C and N exhibited interesting changes within each core (**Fig. 8**). In Churchmans Marsh (CM-1) and Dravo Marsh (DM-1), the $\delta^{15}N$ was lowest in the bottom sections (approx. 4-5‰), increasing towards the surface (up to ~ 8‰). The Brandywine Creek core exhibited little change in $\delta^{15}N$ with depth in the core (5.0±0.4‰ (n=15). The carbon isotopic composition of the sediment ranged from -29 to -23‰ ($\delta^{13}C$ average of -26‰). The $\delta^{13}C$ generally decreased towards the surface from approximately -25‰ near the

bottom of CM-1 and DM-1 to about -28.5‰ at the surface. The $\delta^{13}C$ in the BW core exhibited little change with depth and averaged -24.7 ± 1.2‰ (n=15).

C2.3: Diatom Analysis and Assemblages

Diatoms are microscopic, photosynthetic algae that contain yellow-brown chloroplasts and therefore are also referred to as golden algae. Comprising one of the most common types of phytoplankton, they are found in a diverse range of environments from freshwater to saline oceanic waters. Based upon their shape, diatoms are differentiated between by forms that are centric, i.e. circular, and pennate, i.e. having bilateral disposition of morphological characteristics. They exhibit three main living modes in the environment: 1) planktonic, 2) benthic (i.e., living on or in the bed sediment) and 3) epiphytic.

Diatoms are one of the most powerful water quality indicators; they colonize virtually every aquatic microhabitat and many diatom species have very strict ecological requirements, with well-defined optima and tolerances for environmental variables such as lake pH, nutrient concentration, water salinity and transparency. However, some centric species live in oligotrophic conditions, some benthics in productive environments; what truly works for ecosystem analysis, is the composition of species. Because of their strong relationships to environmental conditions, diatoms are used to derive inference models for such environmental factors. The inference models are developed using calibration sets of both diatoms and measured environmental variables for specific geographic regions. These calibration sets require a large number of sampling sites that maximize the gradient length covered by the variable of interest (e.g., phosphorus concentration, pH, etc.). This is necessary to produce robust quantitative models with high predictive power. These models can then be used to infer the environmental parameter of interest when instrumental measurements are not available and have been successfully used to reconstruct reference conditions and assess the impact of anthropogenic activities on aquatic systems.

Diatom assemblages have been shown to be an important indicator of nutrient concentration within freshwater and marine environments. Due to the fact the diatoms respond quickly and directly to nutrients, they have been used for many years as indicators of nutrient changes in aquatic systems (Potapova et al., 2004; Potapova and Charles, 2007; Ponader et al., 2008). In this study we take a first approach using metrics calculations based on models developed by van

Dam et al. (1994). While this data set is mostly based on freshwater species it does contain some marine diatoms. It provides a first approach to obtain ecological information as a dataset for both diatoms and water characteristics is not available for the Delaware Estuary.

Samples from 41 sections were analyzed for diatom composition from the 3 Christina cores (i.e., BW, CM and DM). At least 500 valves were counted for each sample and over 250 taxa (**Appendix I**) were identified from the samples allowing a robust analysis for nutrient and ecological conditions. The distribution of key diatom species in each of the cores is presented in **Figure 9a,b,c** and below is a brief description of the species distribution for each core:

<u>Dravo Marsh.</u> From the bottom of the core to approximately 25 cm (~1974), brackish and marine diatom species are dominant (*Cyclotella striata, Actinocyclus normanii, Raphoneis amphiceros*, etc.). This type of assemblage is replaced by an assemblage with high nutrient indicator freshwater benthics, such as *Navicula gregaria, N. recens, and N. germanii*. From about 12 cm (~1990) to the surface, planktonic species *Cyclotella meneghiniana* and *C.* cf. *distinguenda* are increasing in abundance while marine species are very rare during this time interval.

<u>Brandywine Creek</u>. Between the bottom of the core to approximately 36-38 cm (~1960), brackish-marine species (e.g., *Cyclotella striata, Delphineis minutum, Actinocyclus normanii*) are dominant. Above this interval they are replaced by eutrophic freshwater species, such as *Fragilaria vaucheriae, Nitzschia amphibia,* and the planktonic *Cyclotella meneghiniana*. Between 24-26 cm (~1975) and 14-16 cm (1987), a short, more marine flora is present that occurred before 1954 but this time in co-occurrence with more abundant freshwater species (e.g., *Aulacoseira granulata, Nitzschia palea, Eunotia tenella*). Above 14-16 cm, species indicating high nutrient levels such as *Nitzschia frustulum, Navicula salinarum, N. gregaria,* and *Cyclotella atomus,* are dominant.

<u>Churchmans Marsh</u>. This core displays a more complex dynamic with brackish-marine species from the bottom of the core to the 24-26 cm interval (~1965), however there were also intervals with more abundant *Cyclotella striata* and *Raphoneis amphiceros*. Above 42-44 cm (~1935), some freshwater eutrophic species also display increases, such as *Nitzschia brevissima* and *Fragilaria vaucheriae*. Above 24-26 cm (~1965), marine–brackish species *Actinocyclus normanii*, *Fallacia pygmaea*, *Cyclotella striata* increase in abundance in co-occurrence with high nutrient freshwater species *Cyclotella meneghiniana, Nitzschia brevissima*, and *Navicula gregaria*. The top of the core displays highly abundant *Cyclotella atomus and Diadesmis contenta*, indicating lower water levels.

To place the Christina Basin diatom data into broader context, various metrics were first calculated using salinity, pH, nitrogen uptake metabolism, and the trophic state from different data sets (van Dam et al., 1994; USGS NAQWA, EPA's National Lake Assessment (NLA)). The samples collected in the tidal Christina span a range of marine brackish to freshwater, making detailed analysis complex. These data sets used for ecological condition analysis are

mainly derived from freshwater systems from rivers and streams in the U.S. or an eastern United States NAWQA-derived subset (NAWQA and NAWQA East), or from more than 1500 lakes sampled within the NLA. All of these metrics have strengths and weaknesses due to the inclusion or omission of species detected in each of the cores. Because most of marine or brackish species present in the Christina River are not occurring or are very rare within the NAWQA and NLA data sets, metrics calculations were based mostly upon the freshwater species occurring in these cores. These were based primarily on the van Dam et al. (1994) summary and synthesis of ecological characteristics of taxa observed in Western Europe, and generally found to have wide geographic application. The van Dam et al. (1994) autecological values for many taxa have been revised to be more relevant for the U.S., and are contained in a data compilation developed for the USGS NAWQA program by Porter (2008) and Porter et al. (2008). To allow a comparison between the current study in the tidal Christina River and the previous study of the tidal Saint Jones River (Velinsky et al., 2007), the data set and metrics by van Dam et al. (1994) will be the focus of this discussion.

The diatom community composition based on the van Dam et al. (1994) metrics show an increase in the proportion of eutrophentic species (i.e., high nutrient species) starting between 30 and 40 cm towards the surface of the core (**Figure 10; Tables 12-14**). Below this depth range, the proportion of mesotrophentic species increases slightly. Interestingly, oligotrophentic species were only randomly detected throughout each of the cores.

To evaluate how nutrient conditions, as reflected by total sediment N and P, impacted the diatom species and metrics in each core, N and P were plotted against the metric for eutrophic species (**Figures 11-12**). For the Brandywine Creek core, there was no relationship between N or P and the diatom metric. In the Dravo Marsh and Churchmans Marsh cores, there was a good relationship between sediment N and P and the diatom metric. The r^2 for N for both cores averaged 0.77 while for P the r^2 averaged 0.51.

Historical Analysis: Concentrations of total sediment N and P exhibited interesting trends within each core over time (**Figures 13-14).** In CM, total N increased from approximately 0.3 to 0.79% starting in the last 1950s. Similarly, in DM, concentrations of TN increased from approximately 0.2 to 1.2% starting in the early 1960s. In the BW, sediment TN increased slightly over time, from 0.19±0.04% before 1960 to an average of 0.35±0.09% after 1963. It is possible that

sediment remineralization processes, with the remobilization of bound N to dissolved N, is occurring after burial in the sediment (Burdige, 2006). This would decrease the sediment levels of TN with time, and could result in an increase in the C to N ratio as N is preferentially remineralized. The changes in C/N with depth (and time) in these cores is not apparent (**Figure 7a; Tables 7-11**). In addition, the stable isotopic composition of the sediment N (δ^{15}N-TN) increases to varying degrees in both cores (**Figure 13**). The increase starts in the mid-1950s in CM and in the mid-1960s in DM, both increasing from about 4-6‰ to approximately 8‰ at the surface. This suggests that there was an increase in loadings to these marshes and that the source(s) of N may have changed over time. Leavitt et al. (2006), Ulseth and Hershey (2005) and Velinsky (unpublished data) show that higher δ^{15}N of the nitrogen is associated with higher inputs from urban sources. Bratton et al. (2003) showed similar trends in deep cores from the Chesapeake Bay. Lastly, this is a similar trend observed in a Woodbury Creek (NJ) marsh (Church et al., 2006). Therefore, the increase in N concentrations, along with near constant C to N ratios, coupled with an increase in δ^{15}N-TN, indicate that N loadings have increased over time and appear to continue to increase.

Schelske and Hodell (1991; 1995) and Perga and Gerdeaux (2004) have shown a relationship between the concentration of P in the sediments or water and the isotopic composition of carbon (δ^{13}C-TC) in the sediments or in fish scales over time. The fish scales were an integrator of the top of the pelagic food web (i.e., phytoplankton). In brief, it is proposed that as P levels increase, primary productivity increases to a point at which there is reduced isotopic fractionation during enzymatic uptake of dissolved CO_2. This reduced fractionation would result in higher isotopic compositions of organic matter (i.e., more ^{13}C enriched) and would suggest that P was helping to control aquatic productivity. Recently, Church et al. (2006) showed a similar trend and relationship in a sediment core from Woodbury Creek, NJ.

In CM there is a gradual increase in TP concentrations starting in the early part of the last century with peak concentrations in 1980 (**Figure 14**). Concentrations decreased afterwards then increased again at the surface. In the BW core, there was a peak in concentration in 1990 while the DM core exhibited a small peak in the 1950s and then increasing concentrations from the 1980s to the present. This time-concentration profile may reflect P usage, especially in detergents (Litke, 1999; Church et al., 2006) as well as other sources such as fertilizers and agricultural runoff, although there is no clear distribution. As with nitrogen, phosphorus can

undergo substantial diagenetic processing related to the carbon, iron and sulfur cycle (Burdige, 2006). These factors make it difficult to accurately interpret the P distributions.

Figure 15 shows the distribution of total sediment P and the isotopic composition of organic matter from the three primary cores (CM, DM, and BW). The BW core shows no relationship while the CM core data indicates a relationship of increasing P with decreasing sediment $\delta^{13}C$. In the DM core, there appears to be two relationships, one at low TSP (increasing P, increasing $\delta^{13}C$) and from 0.06% to 0.10% of increasing P and decreasing $\delta^{13}C$. It is unclear at this point what is causing these relationships (or what they are telling us) but it is possible that changes in the source of organic matter to the marshes (i.e., terrestrial-upland material versus *in situ*-local production) may have changed over time. In both CM and DM sites, the $\delta^{13}C$ decreased (became more negative) since the 1930s (**Figure 15**), which may be an indicator of the development and land use changes in the watershed.

The diatom metrics used to assess eutrophication for each core were plotted against time in **Figure 16**. It appears that starting in late 1950s to early 1960s, the proportion of species that are indicators of high nutrient conditions increased substantially in the DM and CM cores. The increase in the metric corresponded to an increase in N and P sediment concentrations (see above), except for the Brandywine site.

Preliminary analysis of the diatom assemblages and metrics indicate a shift toward more eutrophic species starting in the late 1940-1950s. The proportion of mesotrophic and especially oligotrophic diatom indicators was low throughout the cores. There was a strong positive relationship between the eutrophic diatom metric and the concentration of nitrogen and phosphorus in Churchmans and Dravo marshes. This, along with the increases in total sediment N, total sediment P and sediment nitrogen isotopic compositions ($\delta^{15}N$-TN), indicates that increase loadings of nutrients have resulted in a diatom shift in the river.

C3: <u>Sediment Bound Contaminants</u>

Selected sections from each core were analyzed for a suite of sediment bound contaminants including polycyclic aromatic hydrocarbons (PAHs), polychlorinated biphenyls (PCBs), and specific organo-chlorine pesticides (e.g., DDXs, chlordanes, etc). Three cores were also analyzed for a suite of polybrominated diphenyl ethers (PBDEs). Lastly, core sections were analyzed for strong acid leachable concentrations of zinc (Zn) and iron (Fe).

C3.1: Polycyclic Aromatic Hydrocarbons

Polycyclic aromatic hydrocarbons (PAHs) are a large group of organic chemicals with two or more fused aromatic rings. They have a relatively low solubility in water and have a range in lipophilicity and, in general, adhere to organic particles in water and air. Specific PAH compounds can be carcinogenic and mutagenic to various aquatic organisms at different life stages. PAHs are formed mainly as a result of pyrolytic (combustion) processes, especially during the incomplete combustion of organic materials during industrial and human activities; e.g., processing of coal and oil, vehicle traffic, combustion of oil and gas, and the combustion of refuse. There are a few hundred PAH compounds with a few naturally occurring such as perylene, however most are from anthropogenic sources (e.g., benzo[a]pyrene). Sources to estuarine environments, such as the tidal Christina River, include sewage and industrial discharges, oil spills, bulkheading with creosote wood products, combustion of fossil fuels, and treatment of parking lots with sealcoat. Atmospheric deposition is also a significant source of PAHs to the environment but in the urbanized Christina watershed is most likely not the dominant source.

The sources and nature of hydrocarbon geochemistry can be revealed by the distribution of the individual compounds that comprise saturated (SHC) and aromatic hydrocarbons (PAH) (Farrington, 1980; Hites et al., 1980; Wakeham et al., 1980; Boehm and Farrington, 1984; Boehm, 1984; Pruell and Quinn, 1985). Within the aromatic hydrocarbons, the various alkyl-substituted naphthalenes (i.e., C_1, C_2, C_3) have not been found in organisms and are thought to be derived from petroleum contamination. PAHs can also help discriminate between combustion sources of hydrocarbons and those derived by the direct discharge of oil. Oil contains a greater percentage of alkyl-substituted compounds in the naphthalene, phenanthrene-anthracene, and chrysene series. Refined petroleum products would have a greater abundance of lower than higher molecular weight compounds. The partial combustion of oil reduces the amount of alkyl-substituted compounds leaving the parent structure in greater abundance (Youngblood and Blumer, 1975). Some of the general differences between biogenic and petroleum sources of hydrocarbons are summarized below. These differences will be exploited in the following discussions in evaluating the source of hydrocarbon contamination to the sediments of the various study areas.

General Characteristics of Biogenic and Petroleum Hydrocarbons*.

Natural Biogenic Hydrocarbons

- Narrow range of molecular weight distribution of SHC and PAH (if present), UCM is either low or absent. Odd- to even-numbered alkane ratio is > 1.
- Terrestrial plant material indicated by an alkane distribution from nC_{23} to nC_{34}, centered around nC_{29} or nC_{31}.
- Aquatic organisms have a predominance of nC_{13} to nC_{21} alkanes with greater amounts of odd-numbered compounds.

Fossil Fuel or Petroleum Hydrocarbons

- Wider range in molecular weight distribution of both SHC and PAH, UCM is present in large amounts compared to alkanes and PAHs.
- Odd- to even-numbered alkane ratio = 1.
- Several homologous series with adjacent members in approximately the same concentrations.
- Natural source sources of PAH indicated by less complex distribution with compounds related to structure of precursors (i.e., perylene and retene).
- Direct discharge of oil is indicated by PAHs (e.g., naphthalene, phenanthrene-anthracene, and chrysene series) contains many alkyl-substituted species (i.e., C_1, C_2 and C_3). Greater abundance of lower molecular weight PAHs.
- Combustion products have a greater abundance of un-substituted parent compounds, with homologs which decrease in abundance as the degree of alkyl substitution increases.
- UCM present in greater proportion than resolved peaks.

* Taken from Youngblood and Blumer, 1975; Farrington, 1980; Hites et al., 1980; Wakeham et al., 1980; Boehm and Farrington, 1984; Boehm, 1984; Pruell and Quinn, 1985; Pierce et al., 1986. (SHC – saturated aliphatic hydrocarbons, UCM – unresolved complex mixture; PAH – polycyclic aromatic hydrocarbons)

Low versus high molecular weight PAHs ratios (i.e., LMW and HMW PAHs) are indicative of the input sources of hydrocarbons (Farrington 1980; Boehm and Farrington 1984). Low molecular weight PAHs are defined as 2 to 3 benzene ring compounds, including naphthalenes, anthracenes, phenanthrenes, and dibenzothiophenes. High molecular weight PAHs, with 4 to 5 benzene rings, include compounds such as fluoranthenes, chrysenes, benzo[a]pyrene and dibenz[ah]anthracene. A predominance of LMW over HMW PAHs indicates an oil source of hydrocarbons (Farrington 1980; Boehm and Farrington 1984). Due to weathering and degradation processes, with time LMW PAHs would decrease in abundance relative to HMW PAHs. Also, the combustion of petroleum yields PAHs with more HMW compounds.

Polycyclic aromatic hydrocarbons (PAHs) were detected in all samples analyzed. PAHs comprised 34 individual compounds ranging from the low molecular weight compounds such as naphthalene and phenanthrene (2- and 3-rings) to high molecular weight compounds with 4- and 5- rings, including pyrene and dibenz[a,h]anthracene. Total PAHs (methyl-substituted and unsubstituted forms) ranged from 0.25 to 26.8 μg/g dw among all cores (**Tables 7-11; Appendix I**) with some differences in the distribution with depth (**Figure 17**). The concentrations in the

tidal Christina River were similar to other urban environments such as the tidal Anacostia-Potomac rivers and Baltimore Harbor (Wade et al., 1994; Ashley and Baker, 1999; Riedel et al., 2007), and were lower than those found in the Saint Jones River, Delaware (Velinsky et al., 2007).

Concentrations in CM-1 (Table 8 and Figure 17) were low near the surface (1.68 μg/g dw) increasing to a maximum concentration of 26.8 μg/g dw at 36-38 cm (corresponding to 1945) with the lowest concentrations (<0.5 μg/g dw) near the bottom (pre-1900). In the Dravo Marsh core (DM-2), PAH concentrations were similar overall to the CM core, but the DM core did not exhibit a single strong peak at depth like the CM core. Rather, the DM core showed two smaller peaks. One maxima (8.1 μg/g dw) was at 12-14 cm (circa. 1990) and a deeper maxima (6.5 μg/g dw) was centered around 36-38 cm (circa. 1958). Dual peaks were also seen in the DM core for PCBs about these same dates (see next section). The general rise up to the earlier PAH peak in the DM core appears to have begun as early as 1905. Concentrations near the bottom of the DM core, which date back prior to 1900, ranged from 0.25 to 0.34 μg/g dw, making these pre- turn of the century values consistent with those seen at the bottom of the CM core. The PAH concentrations in these deep sections of the CM and DM cores reflect PAH concentrations that existed just prior to rapid industrial expansion.

The Brandywine Creek core (BW-2) was shorter in length than the other cores and was similar in concentration to the DM core concentrations overall. Further, the PAH concentration at the surface of the BW core (1.68 μg/g dw) were similar to the other two cores at the surface (~ 2-2.7 μg/g dw). Slightly higher concentrations (8.0 to 9.0 μg/g dw) were seen in the BW core between 20 and 30 cm (~1979 to ~1968). Total PAH concentrations near the bottom of BW-2 (between 46 and 52 cm, corresponding to 1944 to 1939) were similar to surface concentrations.

PAH concentrations in the WS core showed little variability from the top of the core to the bottom of the core (Table 11 and Figure 17). The mean and standard deviation among the six intervals analyzed within that core were 9.9 and 1 μg/g dw, respectively. Although we were not able to successfully radiodate this core, it is clear that there is substantial PAH contamination in the sediment deposit from which this core was collected. Similarly, there appears to be considerable PAH contamination in the LSP core (Table 10 and Figure 17), although the vertical profile is not well defined. The mean PAH and standard deviation among five samples collected

from this core were 9.1 and 7.5 μg/g dw, respectively. The maximum PAH concentration in this core was 19.5 μg/g dw, which very roughly corresponds to 1970.

The general increase in PAH in the DM core that began shortly after the turn of the century and continued until ~1958, followed by a 10- to 15-year drop, may be associated with the rise and fall of the shipbuilding industry immediately downstream from the Dravo Marsh (Thompson and O'Byrne, 1999). In addition, the PAH pattern in the DM core may also have been influenced by releases from the nearby Wilmington Coal Gasification Plant, which contaminated nearby surface and subsurface soils and groundwater (DNREC, 2004). It is unclear why the DM core shows a more recent increase from ~1955 to ~1990, followed by a drop. One possible explanation is extensive redistribution of previously contaminated soils and sediments during major roadwork projects (e.g., I-95 and SR-141) or other land disturbing activities in and near DM.

With regard to the CM core, the extremely sharp rise and equally fast fall centered on 1945 suggests there may have been a significant release or spill of petroleum into the tidal Christina about that time. The fact that a significant proportion of PAH mass was lower molecular weight material (Figure 17) tends to support that hypothesis. The idea that lower molecular weights PAHs are often associated with petroleum rather than combustion sources is discussed in more detail below.

As noted earlier, 34 individual compounds were summed to calculate the total PAH (tPAH) fraction. These compounds ranged from 2-ring compounds such as naphthalene to 5-ring aromatic compounds such as di-benzo[a,h]anthracene (**Table 12; Appendix I**). Also included within the 34 individual PAHs are 6 methyl-substituted forms including methylnaphthalene, methylfluorene, and methylphenanthrene. Both the distribution of parent PAHs and methyl-substituted PAHs can be used to help determine the sources of hydrocarbons to the tidal river (i.e., combustion or petrogenic sources). For instance, the phenanthrene to anthracene ratio can be used to help distinguish between combustion (pyrogenic) versus direct oil (petrogenic) sources in aquatic systems since undegraded oil has a very high ratio (50) compared to combustion sources (ca. 0.3; Wakeham et al., 1980; Wade et al., 1994; O'Malley et al., 1994 and 1996; Neff et al., 2005). In CM-1, the phenanthrene to anthracene ratio ranged from 0.1 to 19 (excluding one duplicate value of 176) which are characteristic and typical of many urban environments having a preponderance of combustion sources (Gschwend and Hites, 1981;

Hoffman et al., 1984; Van Metre et al., 2000; Velinsky et al., 2008). The highest ratios were near the surface (19 at 8-10 cm) suggesting more of a petrogenic source to this horizon; interestingly this did not correspond to the peak concentration of tPAHs (**Figure 17**).

The ratio of low molecular weight PAHs to total parent PAHs (LMW:tPAHp); **Figure 17; Tables 7-12, Appendix I**) is also an indicator of petrogenic versus combustion sources. In CM-1, the baseline ratio ranged from approximately 0.1 to 0.2 with peak ratios (0.4 to 0.7) centered on the peak in tPAH concentrations (36-38 cm). This suggests that the sharp peak in PAH concentrations at 36-38 cm (circa. 1945) is more petrogenic in nature and may have resulted from a spill near this site as noted above.

For core BW-2, the phenanthrene to anthracene ratio varied considerably with depth and ranged from <1 to 280. While the highest ratio was observed near the surface, generally higher ratios were found below 25 cm indicating somewhat greater petrogenic sources in the past. High ratios of phenanthrene to anthracene with occasionally low ratios of fluoranthene to pyrene near 0.38 suggests the presence of diesel fuel in at least some of the BW samples (Neff et al., 2005). However, LMW to tPAHp ratios were low at depth (<0.3) more suggestive of a primary combustion source in the distant past. Highest LMW to tPAHp ratios were observed near the subsurface concentration maxima near 20-22 cm (**Figure 17**). It is unclear why these two indicators did not correspond to each other but the ratio of LMW to tPAHp may be more sensitive since it integrates a broader range of compounds. However, it is possible that variable sources of PAHs (various fuel oils, coal based compounds, etc) could have different ratios and their relative loadings may have changed over time.

The Dravo Marsh core (DM-2) had both low phenanthrene to anthracene and LMW to tPAHp ratios from the surface to the bottom of the core. The ratios ranged from 0.2 to 2 and 0.1 to 0.2, indicating that this site was dominated by more combustion-related sources than the other locations. As noted previously, a coal gasification plant operated immediately downstream of the DM coring site for decades (DNREC, 2004), possibly helping to explain the strong pyrogenic signal in the DM-2 core.

Recently, Mahler et al. (2005) and Van Metre et al. (2009) proposed that the ratios of benzo[a]pyrene to benzo[e]pyrene and fluoranthene to pyrene be used as an indicator of coal-based sealcoat used for parking lots. They illustrated that in many locations these ratios suggested that coal-based sealcoat is a dominant source of urban PAHs to various waterways

(Mahler et al., 2005; Van Metre et al., 2006, 2009). Figure 18, taken from Van Metre et al. (2009), illustrates the potential urban sources of PAHs from *in situ* samples from various locations. The ratio of these pair of compounds in stream/lake samples compared to coal-based seal coat suggests that this material is a major source in urban areas. For this study, we plotted only the top part of the core, i.e., the more recent sediment sections, to help determine source functions in the Christina watershed (**Figure 19**). The average ratios for benzo[a]pyrene to benzo[e]pyrene and fluoranthene to pyrene are 0.90±0.53 and 0.99±0.19, respectively, suggesting that coal-based seal coat material is not a major source to the sediments in this area.

Overall, there are both pyrogenic and petrogenic sources of PAHs to the sub-surface sediments of the tidal Christina basin. Sources of PAHs related to urban areas include tire wear; crankcase oil; bus, train and car soot and exhaust; old coal gasification plants; petroleum spills and releases; and possibly seal-coat material (Wakeham et al., 1980; O'Malley et al., 1994; Van Metre et al., 2009). In addition, in core CM-1 and, to a lesser extent, BW-2, there also appears to be an input of petrogenic hydrocarbons dominated by low molecular weight compounds such as phenanthrene, anthracene, and fluoranthene as well as a number of methyl-substituted compounds like 2-methylphenanthrene, 2-methylanthracene, 1-methylanthracene, 1-methylphenanthrene, 9-methylanthracene and 4,5-methylenephenanthrene. These lower molecular weight PAHs are generally more toxic than their higher molecular weight counterparts (Neff et al., 2005; Di Toro and McGrath, 2000).

Van Metre et al. (2000) showed that in cores from different urban environments a shift from uncombusted to more combusted sources of PAHs with decreasing depth (and time). We did not observe this general trend in the Christina but did see a change in sources at specific layers and time.

Historical Analysis: Total PAH concentrations in CM were highest in the mid-1940s (26 μg/g dw) decreasing to lower levels by 1950 and remaining nearly constant since the 1960s (1.4 to 2.5 μg/g dw) to the present (**Figure 20**). Concentrations in core DM showed a bimodal distribution with time with high concentrations around 1955 (6.5 μg/g dw) and in the 1990s (8.1 μg/g dw). After this date, concentrations decreased to 3 μg/g dw at the surface. At BW, the chronology only goes back to the late 1930s and exhibits a bimodal peak from the late 1960s to late 1970s after which concentrations decreased to somewhat lower levels (2-4 μg/g dw).

It is difficult to determine the exact source(s) of PAHs to these cores, but the general development and urbanization/industrialization of the area is the most likely general contributor (Wakeham et al., 1980; Gschwend and Hites, 1981; Wade et al., 1994; O´Malley et al., 1994; 1996; Mahler et al., 2005; Van Metre et al., 2000; 2009). In the CM core, the significant peak in concentration in the 1940s is also when the LMW/tPAHs (**Figure 17**) increased to 0.65 (fraction) suggesting a more distinct petroleum input at this time. The other cores (with the occasional exception in the BW core) generally show a low ratio (0.2 to 0.4) of LMW/tPAH, thus indicating more of a combustion source overall. However, near the CM site, at the confluence of the White Clay Creek and Christina River, was the 130-ha Koppers Company Facilities that operated a wood preserving facility from 1922 to 1971. The facility pressure treated wood with creosote (and some pentachlorophenol). The peak in PAH concentration in the mid-1940s at CM appears to be primarily a signature of this operation. Finally, in the recent sections of all cores, specific PAH ratios (Mahler et al., 2005; Van Metre et al., 2009) indicate asphalt seal-coat as a potential source to the river but this does not appear to be a dominant source as suggested by Van Metre et al. (2009) as in other riverine systems.

C3.2: Polychlorinated Biphenyls

Polychlorinated biphenyls (PCBs) were mainly produced by the Monsanto Corporation from 1930 to 1977 and it is estimated that 5.4×10^8 kg has been produced within the United States (Kennish, 1992). They are or have been used as electrical insulators in many transformers, fire retardant, and additives to oils and paints. There are 209 congeners (or compounds) of PCBs based on the position and number of chorines on the biphenyl structure. As a result, the physical and chemical properties of this group of congeners vary greatly in the environment (ATSDR, 2000). Persistence of PCBs in aquatic sediments is due to their slow rate of degradation and vaporization, low water solubility, and partitioning to particles and organic carbon. Bacteria degrade PCB, with the rate dependent on the position and degree of chlorination of the biphenyl ring and in many cases the absolute concentration present in the sediments (Kennish, 1992 and others). Current sources to this area are thought to be from contaminated sites, runoff from old landfills and accidental spills (e.g., transformer fluids). Recently, Greene (2009a,b) characterized PCB concentrations in water, sediment, and biota of the tidal Christina River at three sites near the coring sites described in this study (Newport, Walnut Street and

Brandywine). This study along with previous studies in the Christina watershed (e.g., DNREC, 2005) will be used to compare data from the current study.

For the present study, total polychlorinated biphenyls (tPCBs) were calculated as the sum of approximately 110 primary congeners (compounds) that were quantified either individually or as coeluters with multiple (2 or 3) congeners (**Tables 7-11; Appendix I**). Among the three marsh cores (CM-1, DM-2, and BW-2), concentrations of tPCBs ranged from 2.2 ng/g dw (near the method detection limit of ≈1.2 ng/g dw; calculated as the mean plus three times the SD of the blanks) to approximately 2107 ng/g dw with an overall median concentration of 122 ng/g dw (**Tables 7-11; Figure 21)**. The Churchmans Marsh core had the maximum concentration (2107 ng/g dw). The peak in the Brandywine core was 685 ng/g dw and that in the Dravo Marsh core was 436 ng/g dw. The surface concentrations in these three cores ranged from 45 to 238 ng/g dw, which is generally consistent with the range observed by Greene (2009a) for surface sediment samples collected in 2007 in the tidal Christina Basin. The peak surface concentration (238 ng/g dw) was observed in the Dravo Marsh core.

The onset of elevated PCB concentrations in the CM core occurred at 42-44 cm, which, based on age dating, corresponds to approximately 1935. This correlates well with the first commercial production of PCBs in the U.S. (1929). Detections of PCBs in the CM core prior to that time are attributed to sediment reworking and possibly downcore diffusion. A sharp peak in PCB in the CM core occurs at 28-30 cm, which translates to approximately 1959. This is roughly a decade prior to the 1970 peak in U.S. production, suggesting that local usage did not perfectly track overall U.S. production. After the CM peak in 1959, PCB concentrations in the CM core steadily decreased to the surface.

The BW core also exhibited a clear onset at depth, peak, and then decline in PCB concentration towards the surface. The onset in that core occurred at 32-34 cm (circa. 1963), and the peak occurred at 14-16 cm (circa. 1987). These dates are significantly later than those seen in the CM core, suggesting different loading histories.

The PCB profile in the DM core is more complex than the CM and BW cores. The DM core exhibits a bimodal distribution in PCB concentration, showing two separate peaks. The onset of the first peak occurred at 48-50 cm (circa. 1942), with the actual peak seen at 36-38 cm (circa. 1958). These dates track the CM core fairly well. After 1958, the PCB concentration in the DM core fell and remained below 50 ng/g dw for at least a decade. Then, concentrations began to

increase again in the late 1970s, rising to a second peak at 10-12 cm (circa. 1992) that was similar in magnitude to the first peak. PCB concentrations in the DM core have fallen somewhat since 1992 but surface concentrations remain high relative to the surface concentrations in the CM and BW cores.

Total PCB concentrations in lower Shellpot Creek (LSP) core ranged from 303 to 3460 ng/g dw and from 76 to 236 ng/g dw in the Walnut Street Bridge boat slip core. The highest concentrations in LSP were observed at 70-72 cm depth interval, which corresponds approximately to 1970. As noted previously, radiodating of the LSP core was not ideal, and so a date of 1970 is only a rough approximation of when the peak PCB concentration in this core occurred. Radiodating of the Walnut Street boat slip core was even more problematic, primarily because this location is subject to non-steady runoff and heavy shoaling. It is interesting to note however, that PCB concentrations in this core did not vary greatly along its length, which represents nearly 100 cm (or roughly 3 ft) of accumulated material. Although the area from which this core was collected may be small in terms of surface area, it appears to contain a significant inventory of PCB mass. Additional testing would be needed to quantify that mass. The other interesting feature of the Walnut Street core is that the surface concentration (197 ng/g dw) is quite similar to the surface concentration of the Dravo Marsh core (238 ng/g dw). These 2 cores are located within a mile and a half of each other, helping to explain the similarity.

To provide additional insights into the PCB core profiles, the 110 congeners determined in the study (excluding the monochlorinated congeners 1 and 3) were grouped into homolog groups (from 1 to 10) based on the number of chlorine atoms substituted on the biphenyl ring (e.g., homolog group H5 contains measured congeners with 5 chlorines; **Appendix I**). In addition, the homologs were summarized into low molecular weight congeners (LMW; i.e., H1 to H5) and high molecular weight congeners (HMW; i.e., H6 to H10). Important in this analysis is the assessment of blank levels given an MDL for tPCBs of approximately 1.2 ng/g dw. It is important to note that at low concentrations (those approaching values of 10 times the MDL, 10 ng/g dw, or lower) which are characteristic of lower portions of cores, congener profiles become less reliable as an accurate representation of true congeneric PCB patterns. However, for completeness, those low concentration profiles have been included in the following analysis.

For simplicity, the ratio of the LMW PCBs to the total PCBs along the CM, DM, BW, LSP and WSC cores are presented in **Figure 22a,b**. The changes in the LMW to tPCB ratio along

with homolog patterns reveal consistent changes with depth in the cores. In the CM and DM cores, the LMW to tPCB ratio was approximately 0.3 to 0.4 in the upper 30 cm or so decreasing from 0.2 at 35-40 cm to 0.1 between by 56 cm in the CM core and to 0.16 by 42 cm in the DM core. In the BW core, the ratio is more variable in the surface 30 cm ranging from 0.47 at the surface to 0.53 at 12-14 cm, and then decreasing to a minimum of 0.34 at 32-34 cm. Below this depth concentrations are near the detection limit and, as such, the ratio increases substantially. The ratio appeared not to change relative to the peak in concentrations in the CM and DM cores, however, the peak concentration in the BW core at 14-16 cm (circa. 1987) is also where there was a slight increase in the ratio (0.53), suggesting a change in source at this depth. In the LSP and WSC cores, higher molecular weight congeners dominate all sections with a LMW:TPCBs ratio of ~0.2.

To further illustrate the compositional change in each core with depth, the homolog patterns for selected sections are presented in the lower graphs in **Figure 22a** for CM, DM and BW. In the surface sections of CM and DM, the homolog patterns are similar, with a dominance of H4 to H6 with lesser, but still significant amounts of H7 to H10). In contrast, in the BW surface sections, the PCB distribution is dominated by H4 through H8 with very little H9 and H10. In the middle sections of the CM and DM profiles, the congener pattern shifts to homologs of higher molecular weight (H8 to H10), potentially suggesting a common historic source influencing both of these cores. Only in the deepest sections of the CM and DM cores does the strong H8 to H10 signal disappear. The BW PCB homolog distribution with depth does not show the higher molecular weight homologs (H8 to H10). Rather, the deeper sections of the BW core show slightly lower molecular weight homolog groups. Finally, in the lower Shellpot Creek and Walnut Street cores, while fewer sections were analyzed, differences are evident (**Figure 22b).** The homolog pattern in the LSP is dominated by H6 and H7 congeners throughout the core (n=5), while the WS core contains higher levels of lower molecular weight congeners in the H4 to H6 homolog groups.

Returning to the issue of high molecular weight homologs in CM and DM, it is noted that a high percentage of H8 to H10 is somewhat unusual and inconsistent with homolog patterns known to exist in commercial PCB Aroclor mixtures (Rushneck et al., 2004). **Figure 23** isolates the concentration of deca PCB (H10) in the three cores (CM, DM, and BW). Concentrations range from near detection level (<0.1 ng/g dw) up to a maximum of 167 ng/g dw. The highest

values were found in the CM core, followed by intermediate values in the DM core, and finally low levels in the BW core. The peak in the CM core occurred in the intervals 28 to 38 cm, corresponding to 1960, while the peak in the DM core occurred at 12 to 22 cm, corresponding to 1985. Interestingly in the DM core there was a deeper maximum of 49 ng/g dw for PCB 209 at 36-38 cm which corresponds to 1960. Surface concentrations of deca PCB were 13, 35, and 1.5 ng/g dw in the CM, DM, and BW, respectively.

Greene (2009a) also reported unusually high percentages of deca PCB (H10) in surface sediment samples collected from the tidal Christina River. Based on the work of Baker et al. (2004) and EPA administrative records, Greene (2009a) attributed the strong deca PCB in the sediments of the tidal Christina River to inadvertent formation of deca PCB during the production of titanium dioxide at a nearby factory in Edge Moor, DE. Superfund administrative records indicate that dust slurries produced at the Edge Moor factory were later handled at a pigments plant in Newport, DE. Those dust slurries are thought to have contained deca PCB. The handling of those materials at the Newport pigment plant along with the discovery of high levels of deca PCB in the nearby CM core provides a linkage between the Edge Moor factory, the Newport pigment plant, and deca PCB contamination in the tidal Christina River. The fact that a strong deca PCB signal was also found in the DM core indicates that at least some of the source material was transported and smeared downstream in the Christina.

Historical Analysis: Concentrations of tPCBs in all cores started to increase after 1930 with highest values after the 1950s through to the present (**Figure 24**). Total PCB concentrations in CM were highest in the late 1950s (2100 ng/g dw), decreasing to 90 ng/g dw by 2006 (**Figure 24**). In DM, there was also a peak in the late 1950s (~400 ng/g dw) and a more recent peak at 1992 of 440 ng/g dw), following the same general bimodal behavior as PAHs (see above). Surface and near surface concentrations of PCBs in DM remained elevated ranging from 240 to 360 ng/g dw. The tidal Brandywine Creek core (BW) concentration-date distribution reflects a source or sources of PCBs that increased in the 1960s with peak inputs in the 1980s up to 1990 (**Figure 25**). Total PCB concentrations were highest around 1988 at 660 ng/g dw, after which concentrations decreased substantially to <50 ng/g dw by 2001. This distribution indicates that one or more dominate sources on the Brandywine were discharging PCBs well after pollution controls (mid to late 1970s) were in place to limit PCB discharges.

The distribution of tPCBs with time in each of the cores appears to reflect sources within each tidal river and the geographic location of each site may act to trap the source(s) upstream or near that site (**Figures 1 and 24**). On initial review, the DM site appears to have two separate primary sources over time that result in the bimodal concentration distribution with time. An alternative explanation is that the more recent peak may reflect significant redistribution of previously deposited PCB contamination as could happen during major earth works projects. As such, the deeper peak in the DM profile may be reflective of the source to the CM while the upper peak more reflective of local disturbance of previously sequestered contamination.

The tidal Christina Basin (and its non-tidal watershed) contains present-day contaminated substance sites that can contribute PCBs (and other chemical contaminants) to the water and sediments (DNREC, 2007; Brightfields, Inc., 2009). Brightfields, Inc. (2009) estimated PCB loads from current waste sites to the tidal Christina River and Brandywine Creek via overland flow of contaminated soils and via groundwater discharge. Mass loads for individual sites ranged from <0.1 g/yr to over 24 kg/yr, with the AMTRAK Former Refueling Facility having the largest estimated load. While there is some uncertainty with these estimates, they do show substantial current inputs to the tidal river that can impact sediment quality and fish species in the area. Our data do show however that past inputs were higher and that controls implemented in the 1970s to the present have lowered the overall input.

C3.3: Total DDX and Chlordane

DDT and its breakdown products (2,4'+ 4,4' forms of DDT (1,1'-(2,2,2-trichloroethylidene)bis[4-chlorobenzene]; DDE (1,1'-(2,2,2-trichloroethenylidene)bis[4-chlorobenzene]) and DDD (1,1'-(2,2-dichloroethylidene)bis[4-chlorobenzene]) were used for insect controls starting in the mid-1940s. DDT was banned in 1972 and has been found to have an approximate environmental half-life of 10 to 20 years (NOAA, 1989; Woodwell et al., 1971). While it was banned nearly 30 years ago, parent DDT is still detectable (and in substantial concentrations) in the sedimentary material collected from various locations in the Delaware and Chesapeake bays (Wade et al., 1994; Greene 2009b). Greene (2009b) summarized total DDT and other contaminants in surface water, sediment, and biota samples collected throughout the tidal and non-tidal Christina Basin in Delaware. Peak DDT concentrations in the water were detected

in the Red Clay Creek at a station near the PA-DE line. The peak chlordane concentration in the water was detected in Little Mill Creek at Maryland Avenue in Wilmington

Chlordane is a multi-component mixture of polychloro-methanoindenes (e.g., oxy-, γ-, and α-chlordane, heptachlor, heptachlor epoxide and cis+trans-nonachlor). Technical grade chlordane contains more than 140 components of which only 120 compounds can be resolved by current analytical techniques. Alpha (α)-chlordane, gamma (γ)-chlordane, heptachlor and trans-nonachlor are the dominant constituents (Dearth and Hites, 1991), and are used to control termites and ants. Because of the toxicity, potential carcinogenicity and environmental persistence of these components and/or metabolites, (e.g., heptachlor, heptachlor epoxide and oxychlordane), the use of chlordane is under federal regulations. The use of chlordane was halted in 1988 after a phased reduction in use since approximately 1975. The half-life of chlordane is similar to that of DDT (i.e., approximately 10 to 20 years), and therefore its persistence is to be expected for many years. However, while the large scale use of chlordane decreased in the late 1980s, it was not fully phased out and was still used in the area.

The parent and breakdown products of DDT and chlordane were detectable in most sediment layers, especially in the upper, more fine-grained sections of each core (**Tables 7-11; Appendix I**). Concentrations of these two pesticides were generally low to moderate overall with occasionally high concentrations at specific intervals in the cores. Total DDX (all forms; tDDX) ranged from <1 to approximately 369 ng/g dw (median of 18 ng/g dw), while total chlordanes ranged from <1 to 151 ng/g dw (median of 2.9 ng/g dw). The highest concentrations of both pesticides were detected in the BW core. Surface concentrations of DDX were 9.3, 29.1, and 8.2 ng/g dw at the CM, DM, and BW coring sites, respectively. Surface concentrations of chlordane were 2.8, 9.7, and 2.5 ng/g dw at the CM, DM, and BW coring sites, respectively. Surface DDX and chlordane concentrations in the DM and BW cores are generally within a factor of 2 of concentration reported by Greene (2009b) for surface sediments collected in 2007 from the lower tidal Christina River and the tidal Brandywine. Surface DDX and chlordane concentrations in the core tops from CM are roughly 5 times higher than the surface concentrations reported by Greene (2009b) for a station in the tidal Christina River just downstream of CM. The differences are far less when the respective datasets are normalized to organic carbon content.

The distribution with depth of both groups of pesticides was similar to each other and in many ways followed the tPCB profiles (**Figures 22 and 26**). In the Churchman Marsh (CM)

core, concentrations were at the detection limits at depth with peak concentrations at 32-34 cm (circa. 1952) for both pesticides, decreasing towards the surface. The Dravo Marsh (DM) core, similar to tPCBs, exhibited a bimodal distribution with higher concentrations at the 36-38 cm (circa. 1958) and 10-12 cm (circa. 1992) intervals, while in Brandywine Creek (BW) concentrations of both pesticides exhibited sharp peaks at approximately similar intervals (1979 to 1982).

The lower Shellpot Creek (LSP) core (n=5) exhibited highest tDDX concentrations at the surface (75 ng/g dw) with decreasing concentrations with depth, while the Walnut Street (WS) core had slightly higher concentrations in the upper 50 cm (20 ± 7 ng/g dw) with lower concentrations at depth (> 66 cm of 11 to 17 ng/g dw). The distribution of total chlordane for both cores is similar. Highest concentrations of total chlordane were observed in the Shellpot Creek core (151 ng/g dw) decreasing with depth and only slightly higher concentrations in the upper 50 cm (3.3 to 8.3 ng/g dw) compared to the bottom two sections (3.1 to 5.7 ng/g dw).

Historical Analysis: Similar temporal distributions of tChl were observed as tDDX in all three cores (**Figures 25 and 27**) and were similar to the trends in tPCBs. In CM, highest concentrations of tDDX (117 ng/g dw) and tChl (6.6 ng/g dw) were observed in the mid-1950s, compared to the mid-1960s for tPCBs (**Figure 24**). In DM there was a bimodal distribution of both pesticide groups with higher concentrations in the early 1960s and again mid-1990s. As described earlier, this may be due to redistribution of previously deposited sediments during land disturbance activities. The peak in tChl concentrations in the mid-1990s was substantially higher than the deeper peak suggesting additional sources during this time period. In the Brandywine (BW), concentrations of tDDX were highest in the mid-1980s, decreasing with time, while the peak in tChl was in the late-1970s. It is not clear why the two distributions are shifted, but the most likely reason is the use history for each class of pesticides and specifically the use/disposal history in this area (i.e., which could be different from other locations). It is unclear why there was a significant increase in tDDX in 1980s in the Brandywine given the use of DDX was limited after 1972. It is possible that some reworking of the sediments in the basin could have released some buried material that contained elevated levels of DDX.

C3.4: Polybrominated Diphenylethers (PBDEs)

Polybrominated diphenylethers (PBDEs) are members of a broader class of brominated chemicals used as flame retardants. There are 209 congeners, or varieties of the basic chemical type, of PBDEs with a wide range in hydrophobic nature (log Kow 7 to 10) and low water solubility. Penta- and octa-BDE mixtures were banned in 2004 in Europe and California after 30 years of use, while deca-BDE is still used today. Hites (2004) concluded that PBDE use in the U.S. differed from use in Europe and other developed countries in that North America used more deca- and penta-BDE formulations. Dominant PBDE congeners in many areas are BDE-47 (tetra PBDE) and BDE-209 (deca-PBDE). BDE-209 is the single most widely produced and used PBDE congener, while BDE-99 and BDE-47 are the predominant congeners detected in the biosphere. Commercial penta-BDE was used mainly in polyurethane foam (mattresses and padding beneath carpets and furniture). Commercial octa-BDE was predominantly used in casings for electronic products (computers, monitors, plastics). Commercial octa-BDE, and deca-BDE mixtures were also used in nylon, textiles, and adhesives. Today, commercial deca-BDE is used primarily in TV casings. Reductive debromination of BDE-209 could potentially produce BDE-99 and BDE-47 as well as other PBDE congeners. PBDEs degrade faster than PCBs with water and sediment half lives of 0.5 to 1.5, respectively (Wania and Dugani, 2003) depending on the congener and media (air, water or sediment). The degradation of many PBDEs leads to lower brominated PBDEs which may be more toxic but there is a debate as to whether BDE-209 degrades significantly over time. In this study we analyzed for 26 PBDE congeners ranging from BDE-30 to the high molecular weight congener, BDE-209.

The three cores analyzed for PBDEs exhibited similar distributions with depth except that in the Brandywine Creek core, concentrations were 10 times higher at peak concentration (**Table 7, Figure 28**). In the Churchmans Marsh, Brandywine Creek and Dravo Marsh cores, tPBDEs concentrations ranged from near the detection limit of 0.5 ng/g dw to 17 ng/g dw (CM), 120 ng/g dw (BW) and 33 ng/g dw (DM), respectively (**Table 6, Figure 28**). Concentrations in the CM core were near the detection limit at depth (32-38 cm, corresponding to ca. 1945) increasing to a maximum concentration of 17 ng/g dw at 16-18 cm (circa. 1980), then decreasing towards the surface to approximately 10 ng/g dw. In the BW core, tPBDE concentrations were above the detection limit at 12-14 cm (ca. 1980s) increasing to peak concentrations (120 ng/g dw) at 8-10 cm (ca. 1996), decreasing to 53 ng/g dw at the surface. Lastly, tPBDEs concentrations started in

the 16-18 cm (ca. 1986) and exhibited peak concentrations of 33 ng/g dw nearer the surface (4-6 cm; ca. 2002).

The dominant BDE congener was 209 accounting for 5 to 100% of the tPBDEs for all cores; especially in the top sections of the cores (**Figure 29**). At depths greater than 28 cm there were substantial amounts of BDE 99 and to a greater extent BDE 153. For example, in the BW core, BDE 153 accounted for 24-63% of the tPBDEs in the lower sections while BDE accounted for >90% in the upper 10 cm. BDE47 accounted for, at most, 11% of the tPBDEs and this was seen in the bottom sections of DM and CM. A similar distribution and change was noted in the Clyde Estuary by Vane et al. (2009) and slightly different by Song et al. (2004). It appears that over time and burial BDE-209 is slowly degraded to lower brominated congeners; however, changing sources of the lower brominated compounds over time cannot be discounted. Near surface dominance by BDE-209 may also be reflective of current high use of this formulation in comparison to the recently phased-out penta and octa technical mixtures.

Historical Analysis: PBDE production in the United States started in the early 1970s with peak production in the 1990s (Hardy, 2002). The use of the various PBDE formulations has most likely changed over the years as different products and usages develop or are discontinued. Onset and peak concentrations varies across the three sites, reflecting variable time inputs and potentially sediment reworking and remobilization. **Figure 29** presents the time-concentration distribution for total PBDEs. Onset of PBDEs was in the late 1960s/1970s in the CM and DM core and in the mid-1980s in the BW core. Detectable concentrations were observed in the sediment in the early 1970s, quickly after production in the U.S. commenced and may be due to sediment mixing or possibly atmospheric deposition. Peak concentrations were similar in the DM and BW cores (~1980s) while somewhat earlier in the CM core (**Figure 29**). There was a change in the composition of PBDEs with BDE209 the dominant congener in the surface sediments. This could be due to source change, degradation of less brominated compounds, or a function of the method and detection limits. It is possible that at the lower concentrations, the recovery of the higher molecular weight congeners is reduced. This would result in lesser amounts of BDE209 at lower concentrations.

C3.5: Dioxins and Furans

Dioxin and furans are a family of organic chemical compounds that share a similar chemical structure (i.e., tetra to octa-chlorodibenzo-p-dioxin [PCDDs] or –furan [PCDFs]). Due to their hydrophobic nature and resistance to degradation, these chemicals, like other hydrophobic organic chemicals, can accumulate in the fatty tissue of animals (e.g., fish and humans). PCDDs include 75 individual compounds while PCDFs include 135 different compounds, with only 7 PCDD and 10 PCDF compounds exhibiting substantial toxic effects. The most studied and potentially toxic form of PCDD is 2,3,7,8-TCDD (i.e., tetra- chlorodibenzo-p-dioxin).

Dioxin and furans are formed by burning chlorine-based chemical compounds with hydrocarbons. The major source of dioxin in the environment comes from waste-burning incinerators (such as municipal solid waste, sewage sludge, medical waste, and hazardous wastes), the burning of various fuels and material (such as coal, wood, petroleum products, and cement kilns), and poorly or uncontrolled combustion sources like forest fires and building fires (U.S. EPA, 2005 update). Dioxin pollution is also affiliated with paper mills which use chlorine bleaching in their process and with the production of polyvinyl chloride (PVC) plastics and with the production of certain chlorinated chemicals (like many pesticides). Dioxins and furans could be formed naturally with evidence of heavier homologues of PCDDs (Alcock and Jones, 1996). However, anthropogenic sources are much higher than background sources. Sources of these compounds are thought to have started to increase in the environment around 1930s to 1940s, with a sharp rise starting in the early 1950s and decreasing concentrations starting in the mid 1980s (Alcock and Jones, 1996). Recently, the U.S. EPA has drafted a plan (which is under public comment) to initiate clean up and remediation goals for CERCLA and RCRA sites (EPA, 2009; draft).

As part of this study, PCDD and PCDF compounds were determined in sediment sections from five cores (CM, DM, BW, LSP, and WS). Compounds included tetra to octa-PCDFs and PCDDs (**Appendix I**). The discussion below will center on the total concentrations along with 2,3,7,8-TCDD and 2,3,7,8-TCDD toxicity equivalents (as explained below).

Among the five cores, total dioxins and furans ranged from 1.2 to 157 ng/g dw and 0.01 to 127 ng/g dw, respectively (**Figure 30; Tables 7-11).** Other than the two samples in CM (32-34 and 36-38 cm, corresponding to the period 1952 to 1945; **Figure 30**), all sediment samples were <20 ng/g dw for tPCDD and <5 ng/g dw for tPCDFs.

In general, the peak in tPCDD concentration at 32-34 cm (circa. 1952) in the CM core and the more diffuse peaks in DM (36-38cm, circa.1958)) and BW (12-16 cm interval, circa.1990) cores coincided with peaks in other organic contaminants. However, in some cases the peaks in tPCDD or tPCDF concentrations were slightly offset from tPCBs, tDDX, and tChlordane peak concentrations by one interval higher or lower. There was no trend in the Shellpot Creek or Walnut Street cores in dioxins or furans. Concentrations of the more toxic dioxin, 2,3,7,8-TCDD, were detected in only seven sediment intervals in all of the cores (**Tables 7-11**). Detectable concentrations ranged from 0.3 to 5.1 pg/g dw with an average concentration of 0.22 pg/g dw. The highest concentration (5.1 pg/g dw) and most in one core (n= 5) were found at the BW site, however there was no concentration trend with depth and detection appeared random.

Toxic Equivalents (TEQs) were calculated by multiplying the concentration of each 2,3,7,8-substituted dioxin and furan compound by their associated human and mammalian toxicity equivalent factor (TEF) and then adding the resulting partial sums. Dioxin-like PCB congeners were not included in these TEQ calculations. Human and mammalian TEFs for dioxins and furans were taken from the World Health Organization (WHO, 2005), as fully described in Van den Berg et al. (2006). For the TEQ calculation, non-detected compounds were set equal to zero (0). The TEQs in the Christina Basin sediment cores ranged from <1.2 to 444 pg/g dw with an overall average of 34 pg/g dw. The TEQ concentrations in the core tops were as follows: 19.9, 32.9, 21.8, 13.9, and 5.5 pg/g dw for cores CM, DM, BW, WS, and LSP, respectively. These values are similar to values reported by Greene (2009b) for surface sediment samples collected from these same waters in 2007. For most core sections, except BW, the TEQ was dominated by hepta-, octa- and tetra-PCDD congeners and to a lesser extent an even mixture of PCDF congeners. This is also consistent with results reported by Greene (2009b) for surface sediment samples. In the BW core, penta- and hexa-PCDF congeners were highest followed by hepta- and octa-PCDD congeners, thereby providing a different TEQ mix than seen in the other cores and suggesting different sourcing. The vertical profiles of TEQs in the CM and DM cores strongly track their associated PCB profiles. In the BW core, however, the TEQ peak appeared to precede the PCB peak.

Historical Analysis: Total dioxins (tPCDD) and total furans (tPCDF) with time are presented in **Figure 31**. Total dioxins and furans in CM peak in concentration (158 and 12 ng/g dw

respectively) in the early 1950s and decrease to near constant levels until the present. The peak tPCDD in the CM core (158 ng/g dw) is much greater than the peak in the DM core (~17.5 ng/g dw) and the BW core (~12.5 ng/g). There are multiple peaks in tPCDD concentrations in the DM core and tfurans appear to mirror the same pattern over time, although muted. Interestingly, in the Brandywine Creek core, peak concentrations of the tPCDD are found in 1990, while there is a broad maximum in tPCDFs in the 1960s to 1980. The historical pattern of TEQ generally follows both the tPCDD and tPCDF time-concentration distribution except in the Brandywine Creek core (**Figure 32**). While tPCDD concentrations peak around 1990, the TEQ concentration is highest in the mid to late 1970s, similar to tPCDFs. This is due to the contribution to the total TEQ from the various furan congeners is highest during this time period.

C3.6: Sediment Iron and Zinc

The Delaware Department of Natural Resources and Environmental Control had a particular interest in the vertical distribution of iron (Fe) and zinc (Zn) in sediment cores collected from the targeted waterways. Sediment levels of iron (Fe) and zinc (Zn) were determined using a strong acid digestion and are not "total" concentrations (i.e., does not include the clay lattice metals). However, this method would obtain the majority of the metals associated with the particles. Among the five cores (CM, DM, BW, LSP, and WS), sediment Fe ranged from 5388 to 45700 μg/g dw (0.53 to 4.5 wt %), while sediment Zn ranged from 71 to 9800 μg/g dw. Iron concentrations were variable with depth in each core (**Figure 33; Tables 7-11**). The average Fe concentration in the BW and CM core were the same with similar variations (3.5 ± 0.5%). The LSP core exhibited slightly lower Fe concentration but was more variable (2.8 ± 1.9%). The Fe concentrations in the DM core were substantially lower than the BW and CM cores (average = 1.2%) with a peak concentration of 3.0% at 8-10 cm (circa. 1995). It is unclear why Fe concentrations in the DM core were a third lower than the other cores.

Zinc concentrations showed much greater variation with depth in the BW, CM, and DM cores (**Figure 34; Tables 7-11**). Concentrations in the BW core were low at depth increasing to their highest levels of 780 μg/g dw at 20-22 cm (circa. 1979), then decreasing towards the surface (490 μg/g dw). Substantially higher Zn concentrations were measured in the CM core. At depth (pre-1900), concentrations were lowest (~ 140 μg/g dw), increasing to 9800 μg/g dw at 36-38 cm (circa. 1945), than decreasing towards the surface to 720 μg/g dw. The Zn distribution

in the DM core exhibited the bimodal distribution as seen for some organic contaminants. There is a deeper peak of 1230 μg/g dw at 36-38 cm (circa. 1958) and a peak of 1000 μg/g dw at 8-10 cm (circa. 1995). Zn concentrations in the DM core were lower than the CM values and were similar to the BW concentrations.

Normalization of the sediment to a reference element not associated with anthropogenic influences is one approach to determining the degree of sediment contamination (Daskalakis and O'Connor, 1995). Elements such as Al (Windom et al., 1989; Schropp et al., 1990), lithium (Li) (Loring et al., 1990) and Fe (Trefrey and Presely, 1976; Sinex and Helz, 1981; Helz et al., 1985; Velinsky et al., 1994; Velinsky et al., 1997) have been used in the past. For this study, Fe was chosen as a normalizing element because: 1) it is the fourth most abundant metal in the earth with a crustal average of 3.5% (Wedepohl, 1971); 2) in most cases anthropogenic sources are small compared to the amount of Fe naturally present; and 3) the ratios of most metals to Fe are fairly constant in the Earths crust. The major caveat in using Fe as a normalizing element, instead of Al or Li, is that Fe undergoes many diagenetic reactions in anoxic/oxic sediments. These reactions include dissolution and precipitation of Fe oxides and Fe-sulfur minerals (i.e., pyrite). However, in the previous studies by Velinsky et al. (1994; 1997) in tidal river sediments, the potential changes in speciation and mobility did not significantly affect the total concentration of sedimentary iron with depth or location. Therefore, Fe was used as normalizing agent for this study.

A useful tool in expressing the degree to which sediment is influenced by anthropogenic sources of trace metals is the enrichment factor (EF) (Trefrey and Presely, 1976; Sinex and Helz, 1981; Helz et al., 1985; Windom et al., 1989; Velinsky et al., 1994; 1997). When normalizing to Fe, the enrichment factor is defined as: $EF = (X/Fe)_{sediment} / (X/Fe)_{unimpacted\ sediment}$, where X/Fe is the ratio of the trace metal (X) to the amount of Fe in the sample. In using the EF, a comparison to a sediment that is unimpacted by anthropogenic sources is necessary [$(X/Fe)_{unimpacted}$] (i.e., critical in this analysis is the choice of metal to Fe ratio for unimpacted sediments). Enrichment factors of 1 indicate no enrichment, while EFs greater than 1 indicate anthropogenic sources of metals to the sediments. While this approach is useful, it may not account for natural variations in sediment types of different geological regions. One way to account for this variability is to derive a ratio from "unimpacted" sediments in the general area of interest (Windom et al., 1989; Schropp et al., 1990). However, in the present study, most samples have the potential to be

impacted above natural levels, except possibly at depth in the cores. Therefore, data from the bottom of the cores, as described below, were used to derive 'natural' or least impacted concentrations of Fe and Zn in the general area.

The Zn to Fe ratios for the bottom section of the three cores (BW, CM, and DM) were 0.011, 0.004, and 0.007, with an average of 0.007. A ratio of 0.007 is somewhat higher than a mean of 0.002 reported by Wedepohl (1968) for river sediments but is quite similar to values seen in other tidal river sediments (Velinsky et al., 1994). A value of 0.007 also has the added advantage of being specific to the tidal Christina Basin. The degree to which sediments in the study area are enriched in trace metals from anthropogenic sources varies from metal to metal and depends on a number of factors, including: 1) choice of $(X/Fe)_{unimpacted}$; 2) biogeochemistry and redox behavior of the metal; and 3) sources and loading history of metals to the study area. Despite these considerations, the present calculation reveals some interesting trends with depth.

Figure 19 presents the EF distribution for the DM, BW and CM cores. The EF for all core samples ranged from 0.5 to 41 with an overall average of 4 (unitless). Given the variations in the $(X/Fe)_{unimpacted}$ value, an EF of <1 to ~2 indicate samples that are at or near background. The BW core shows no enrichment for Zn. In the CM core, there was substantial enrichment of Zn above background with values up to 41 times higher at 42-44cm (~1935). Above and below this broad peak the EF is near background levels. DM sediments were above background from approximately 50 cm (~1925) to the surface with the peak EF at 42-44 cm and above this interval, the EF ranged from 5 to 12 suggesting a continuing source to this location. A more in-depth discussion of zinc enrichment within the CM and DM cores will be presented below.

One of the most noteworthy observations apparent from the present study is the historical rise and fall of zinc concentrations in the sediments at the CM coring site. The onset of zinc enrichment in the CM core appears to have occurred around or shortly after 1900 (**Table 8**). Sediment concentrations of Zn were highest in that core from approximately 1910 to 1950 with a peak of nearly 10,000 ug/g dw and an average of 8850 ± 920 ug/g dw (n=5) during that period (**Table 8 and Figures 33 and 35**). Zinc concentrations at the other coring sites (DM and BW) were substantially lower (**Tables 7 and 9, plus Figures 33 and 35**). Dravo Marsh (DM) concentrations were highest between 1950 and 1958 with a secondary peak in the mid-1990s, while in the BW core, peak concentrations occurred around ~1970 to 1980. As indicated by the EF (see above), changes in Zn concentrations in the BW core were controlled by Fe with little or

no anthropogenic enrichment of Zn, while there was substantial enrichment of Zn in the CM core (up to 40 times above background) in the 1930s. Concentrations of sediment Zn in the DM core started to show enrichment in the late 1930s with highest EF (20) in the mid-1940s and decreasing over time to approximately 5 to 10 in the current century.

Historical Analysis: Primary sources of zinc enrichment over time to Churchmans Marsh and downstream to Dravo Marsh include the now defunct NVF facility located along the Red Clay Creek in Yorklyn, DE (DNREC, 1999a); a similar NVF facility that formerly operated along the White Clay Creek in Newark, DE (DNREC, 1999b); and a pigment plant located in Newport that became a federal Superfund site (U.S. EPA, 1993). All three of these sources began manufacturing operations right around 1900. The NVF Newark plant closed in 1990, while the NVF Yorklyn plant closed in 2009. Both of the NVF facilities used zinc chloride in the manufacture of vulcanized paper products. The Newport pigment plant manufactured Lithopone, a zinc and barium-based paint pigment, up until 1952. Zinc loading from the NVF Yorklyn plant entered the Red Clay Creek and travelled downstream until it combined with the White Clay Creek, which carried the additional zinc load from the NVF Newark plant. The combined load emptied into the tidal Christina River just downstream of Churchmans Marsh (just upstream of Newport, DE). Additional zinc then entered the Christina River as a result of poor waste handling at the Newport pigment plant. The combined zinc loading from these three primary sources produced inordinately high concentrations of zinc (~10,000 μg/g dw) at depth in the CM core and moderately high (~1,250 μg/g dw) concentrations downstream at the DM coring site.

The sediment profiles in CM, and to a lesser extent, DM, clearly show significant inputs of Zn shortly after these three facilities commenced operation along with an associated improvement once controls began to be put in place or processes were changed. Concentrations in the bottom of the CM and DM cores ranged from 71 to 139 μg/g dw (average = 106 ± 33 μg/g dw), only slightly above concentrations found upstream of the NVF Yorklyn facility on the Red Clay Creek (range of 39 to 107 μg/g dw; average = 73 ± 22 μg/g dw; n = 7; DNREC, 1999). Concentrations of Zn in the mid sections of the cores were significantly enriched in Zn, especially in the CM core (**Figure 35**). The core results clearly show that control procedures from the 1960s to the present have resulted in a reduction of Zn inputs to the river

The NVF Yorklyn facility is under active remediation to remove the remaining inventory of zinc from the groundwater beneath the site (DNREC, 2008). The NVF Newark facility has been remediated to address the zinc contamination there (DNREC, 1999c) and an extensive cleanup was implemented at the DuPont Newport site. One component of the DuPont Newport cleanup included dredging approximately 11,000 cubic yards of sediment from the tidal Christina River in the vicinity of Newport in 1999, due in part to elevated concentrations of zinc in the sediments (NRC, 2007). The coring analysis clearly shows that the closing of these facilities and the extensive cleanup action taken have yielded substantially lower concentrations of Zn in the sediments of the tidal Christina River.

D) Summary and Conclusions

This study involved the chemical analysis of five sediment cores taken from the tidal Christina River Basin and lower Shellpot Creek in northern New Castle County, DE. Of the five cores, four were dated using ^{210}Pb and ^{137}Cs radiometric methods, with three (Churchmans Marsh (CM), Dravo Marsh (DM), and the tidal Brandywine (BW)) providing sufficient temporal coverage (> 50 yrs) for detailed chemical analysis. The main objective was to evaluate historical trends in organic chemical contaminants (e.g., polychlorinated biphenyls, pesticides, dioxins/furans, polybrominated diphenylethers and polycyclic aromatic hydrocarbons), selected trace metals (e.g., iron and zinc) and nutrients (i.e., sediment phosphorus and nitrogen). An additional objective was to evaluate if a historical record of eutrophication could be derived from algae analysis (i.e., diatom species in the cores) along with other indicators of potential ecosystem change (e.g., stable isotopes of carbon ($\delta^{13}C$-OM) and nitrogen, ($\delta^{15}N$-TN)).

The range and average sediment accumulation rates (^{137}Cs) inferred from the ^{210}Pb and ^{137}Cs data are similar to other areas within the Delaware Estuary and range from 0.57 to 1.9 cm/yr. Attempts to core and determine age-depth relationships in other locations (i.e., an embayment near Walnut Street) yielded inconclusive dating results. There was good agreement between the ^{137}Cs rates and those for the constant accumulation model for ^{210}Pb.

With regard to contaminants, a major finding that emerged from this study is the historic accumulation of zinc in the system, as clearly displayed in the Churchmans Marsh (CM) core. Concentrations of Zn showed a broad peak over background levels starting at or shortly after the turn of the century and persisting to the early to mid-1970s. Using the amount of iron (Fe) within the sediment and referencing the data to bottom concentrations of Zn (and Fe), the sediments of Churchmans Marsh had been up to 40 times above background levels. Current Zn enrichment in Churchmans Marsh is still approximately 5 to 10 times above background. In the other core locations, surface sections are not substantially enriched above background with zinc enrichment factors ranging only from 1 to 2.3. Major sources of historic zinc loading to the system included two National Vulcanization Facilities (NVF), one on the Red Clay Creek and one on the White Clay Creek, and a pigments plant in Newport. All three of these sources have been remediated and discharges are more formally regulated.

The other key finding of this study is that concentrations of organic contaminants are lower today, overall, than they were in the past, with some exceptions. Chlorinated organic compounds

such as tchlordane, tDDX and dioxins/furans all show a sharp maximum at similar depths (corresponding to the 1960s and 1970s), followed by a decreasing trend towards the surface. Total PCBs also shows higher concentrations at depth with decreasing concentrations towards the surface, with the exception of the Dravo Marsh core where tPCB concentrations at the surface remain elevated (ca. 200 ng/g dw). The Dravo Marsh core exhibits a bimodal distribution in PCB concentration, showing two separate peaks. The onset of the first peak occurred at 48-50 cm (circa. 1942), with the actual peak seen at 36-38 cm (circa. 1958). These dates track the Churchman Marsh core fairly well. After 1958, PCB concentrations in the Dravo Marsh core fell and remained below 50 ng/g dw for at least a decade. At this time, concentrations began to increase again in the late 1970s, rising to a second peak at 10-12 cm (circa. 1992) that was similar in magnitude to the first peak. PCB concentrations in the Dravo Marsh core have fallen somewhat since 1992 but surface concentrations remain high relative to the surface concentrations in the CM and BW cores. The Dravo Marsh finding may reflect lingering inputs from local sources and/or the redistribution of previously deposited contamination following major earth works projects in or near the marsh.

Interestingly, the PCB congener composition in both the Churchmans Marsh and Dravo Marsh cores showed a shift from mid to higher molecular weight compounds to lower molecular weight compounds from the upper sections (more recent) to the lower sections (longer ago). The opposite was true for the BW core. The high proportion of deca PCB (H10) in the Churchmans Marsh and Dravo Marsh cores is unusual and appears to reflect releases from the same pigment plant in Newport that was also responsible for at least part of the zinc contamination. The use of congener-specific PCB methods (rather than typical Aroclor methods) allowed us identify and characterize the deca PCB signature.

Total dioxins (PCDD) and furans (PCDF) concentrations ranged from <2 to 157 ng/g dw and <1 to 13 ng/g dw, respectively with distinct distributions with depth and time. The individual congeners were used to calculate the toxic equivalents (TEQs) using published toxic equivalency factors (TEF). The TEQs ranged from <0.01 to 0.45 ng/g dw. Highest concentrations of PCDD, PCDF and TEQ were found in the Churchmans Marsh core.

In all cores (n=3), tPBDEs are only present in the upper sections with undetectable concentrations below approximately 20cm (<1980s). The predominant congener is PBE 209 in the upper sections with BDE153 and BDE99 found at depth.

Total PAHs showed a distinct concentration peak in the 1940s, in the CM core, while a bimodal distribution was observed in the DM core and possibly the BW core. The peak of tPAHs in the CM core maybe related to historic inputs of hydrocarbons from a creosote facility near the site. Other sources related to urban development, including a major shipbuilding complex and a coal gasification plant, are also potential historic sources to the area, particularly the DM. Data were compared to indicators of combustion sources such as coal tar based parking lot sealant using specific ratios of individual PAHs. Only a limited number of samples were consistent with such a fingerprint and thus this type of sealant does not appear to be a major source to the tidal Christina River.

Lastly, analysis of the diatom assemblages and metrics indicate a shift toward more eutrophic species starting in the late 1940-1950s. There was a strong positive relationship between the eutrophic diatom metric and the concentration of nitrogen and phosphorus in Churchmans and Dravo marshes. This, along with the increases in total sediment N, total sediment P and sediment nitrogen isotopic compositions (δ^{15}N-TN), indicates that increase loadings of nutrients have resulted in a diatom shift in the river.

Overall, this study documents the chemical analysis of three cores taken in the tidal Christina River and tidal Brandywine Creek. Changes were observed in contaminant levels across time that reflect usage globally and most often locally. Overall, contaminant levels appear to be declining when viewed on a longer term, decadal time scale. However, the concentrations of several contaminants (e.g., PCBs and zinc) remain relatively elevated in this system.

E) Acknowledgments

We would like to thank Susanne Molaski (UDEL), Don Charles, Paul Kiry, Paula Zelanko, Mike Schafer, and Linda Zaoudeh for laboratory assistance and data interpretation. Dr. Mihalea Enache did diatom counts, calculated diatom metrics and provided assistance with report preparation. We appreciate the help of Dr. Heather Stapleton (Duke University) for assistance in analyzing a subset of the samples for PBDEs. Dr. Jeff Ashley (Philadelphia University) provided analytical advice and support throughout this project. Roger Thomas assisted in field and Robin Davis provided assistance with final report preparation and review. Financial, field and editorial support was graciously provided by Dr. Richard Greene (DNREC; Watershed Assessment Branch).

F) References

Alcock, R. E. and K.C. Jones. 1996. Dioxins in the Environment: A Review of Trend Data. *Environ. Sci. Technol.* 30: 3133-3143.

Appleby, P.G. 2001. Chronostratigraphic techniques in recent sediments: Chapter 9. In: W.M. Last and J.P. Smol (eds). *Tracking Environmental Change Using Lake Sediments Volume 1: Basin Analysis, Coring, and Chronological Techniques*. Kluwer Academic Publishers, Dordrecht, The Netherlands.

Appleby P.G and F. Oldfield. 1978. The calculation of lead-210 dates assuming a constant rate of supply of unsupported ^{210}Pb to the sediment. *Catena* 5: 1-8.

Ashley, J.T.F. and J.E. Baker. 1999. Hydrophobic organic contaminants in surficial sediments of Baltimore Harbor: Inventories and sources. *Environ. Toxicol. Chem.* 18: 838–849.

Aspila,K.I, H. Aspila, A. Agemian and S.Y. Chau. 1976. A semi-automated method for the determination of inorganic and total phosphate in sediments. *Analyst* 101: 187-197.

ATSDR. 2000. *Toxicological Profile for Polychlorinated Biphenyls* (Update). Agency for Toxic Substances and Disease Registry, Atlanta, GA.

Baker, J.E., M. Toaspern, D. Liebert, and F. Ko. 2004. Decachlorobiphenyl: Using a Non-Aroclor PCB as a Tracer of Estuarine Processes. Society of Environmental Toxicology and Chemistry Poster Session. Portland, OR.

Berner, R. 1980. *Early Diagenesis: A Theoretical Approach.* Princeton University Press, 241 pp.

Benner, R., M. L. Fogel, and E. K. Sprague. 1991. Diagenesis of belowground biomass of *Spartina alterniflora* in salt-marsh sediments. *Limnol. Oceanogr***.** 36: 1358-1374.

Boehm, P.D. 1984. Aspects of the saturated hydrocarbon geochemistry of recent sediments in the Georges Bank region. *Org. Geochem***.**, 7: 11-23.

Boehm, P.D. and J.W. Farrington. 1984. Aspects of the aromatic hydrocarbon geochemistry of recent sediments in the Georges Bank region. *Environ. Sci. Tech.,* 18: 840-845.

Bratton, J.F., S.M. Coleman and R.R. Seal, II. 2003. Eutrophication and carbon sources in Chesapeake Bay over the last 2700 yr.: Human impacts in context. *Geochim. Cosmochim. Acta.* 67: 3385-3402.

Brightfields Inc. 2009. *PCB Mass Loading from Hazardous Substance Release Sites to Surface Waters of the Christina River Basin* (DNREC Contract No. #06-374-MS-A). Prepared for: Site Investigation & Restoration Branch, Division of Air and Waste Management, and Watershed Assessment Branch, Division of Water Resources; Department of Natural Resources Environmental Control; State of Delaware (File# 0985.26.51).

Brush, G.S., E.A. Martin, R.S. DeFries, and C.A. Rice 1982. Comparisons of ^{210}Pb and pollen methods for determining rates of estuarine sediment accumulation. *Quaternary Research.* 18: 196-217.

Burdige, D.J. 2006. *Geochemistry of Marine Sediments*. Princeton University Press. 630 pp.

Canuel, E.A., J.E. Cloern, D.B. Ringelberg, J.B. Guckert and G.H. Rau. 1995. Molecular and isotopic tracers used to examine sources of organic matter and its incorporation into the food webs of San Francisco Bay. *Limnol. Oceanogr*. 40: 67-81

Church, T.M., C. Sommerfield, D.J. Velinsky, D. Point, C. Benoit, D. Amouroux, D. Plaa and O. Donard. 2006. Marsh sediments as records of sedimentation, eutrophication and metal pollution in the urban Delaware Estuary. *Marine Chemistry* 102(1-2):72-95.

Cifuentes, L.A., J.H. Sharp and M.L. Fogel. 1988. Stable carbon and nitrogen isotope biogeochemistry of the Delaware estuary. *Limnol. Oceanogr*. 33: 1102-1115.

Cline, J.D. and I.R. Kaplan 1975. Isotopic fractionation of dissolved nitrate during denitrification in the eastern tropical North Pacific Ocean. *Mar. Chem*. 3: 271-299

Cooper, S. R. and G.S. Brush. 1993. A 2,500-year history of anoxia and eutrophication in Chesapeake Bay *Estuaries* 16: 617-626.

Cornwell J.C., J.C. Stevenson, D.J. Conley and M. Owens. 1996. A sediment chronology of Chesapeake Bay eutrophication. *Estuaries* 19:488-499.

Crusius, J. and R.F. Anderson. 1991. Core compression and surficial sediment loss of lake sediments of high porosity caused by gravity coring. *Limnol. Oceanogr.* 36:1021-1031.

Cutshall, N.H., I.L Larsen and C.R. Olsen. 1983. Direct analysis of ^{210}Pb in sediment samples: Self-absorption corrections. *Nuclear Instruments and Methods in Physics Research*, 206: 309-312.

Daskalakis, K.D. and T.P. O'Connor. 1995. Normalization and elemental sediment contamination in the coastal United States. Environ. Sci. Technol. 29: 470 477.

Dean, W.E., Arthur, M.A., and Claypool, G.E., 1986. Depletion of ^{13}C in Cretaceous marine organic matter: source, diagenetic, or environmental signal? *Mar. Geol*., 70:119-157.

Dearth, M.A. and R.A. Hites. 1991. Complete analysis of technical chlordane using negative ionization mass spectrometry. Environ. Sci. Technol. 25: 245-254.

Delaware Department of Natural Resources and Environmental Control (DNREC). 2008. Amended Total Maximum Daily Load (TMDL) for Zinc in the Red Clay Creek Technical Background and Basis Document (September 15, 2008), State of Delaware Department of

Natural Resources and Environmental Control Division of Water Resources, Watershed Assessment Section, Dover, DE.

Delaware Department of Natural Resources and Environmental Control (DNREC). 2007. Christina Basin Pollution Control Strategy. Department of Natural Resources and Environmental Control, Dover, Delaware.

Delaware Department of Natural Resources and Environmental Control (DNREC). 2005. Sediment Quality Assessment for the Tidal Christina River Basin, Volume 1 Report of Findings. Department of Natural Resources and Environmental Control 715 Grantham Lane, New Castle, Delaware.

Delaware Department of Natural Resources and Environmental Control (DNREC). 2004. Final Plan of Remedial Action, Wilmington Coal Gas Site – Northern Parcel/OU-01. State of Delaware Department of Natural Resources and Environmental Control Site Investigation and Restoration Branch, New Castle, DE.

Delaware Department of Natural Resources and Environmental Control (DNREC). 1999a. Total Maximum Daily Load (TMDL) for Zinc in the Red Clay Creek, New Castle County, DE. Technical Background and Basis Document (August 1, 1999), State of Delaware Department of Natural Resources and Environmental Control Division of Water Resources, Watershed Assessment Section, Dover, DE.

Delaware Department of Natural Resources and Environmental Control (DNREC). 1999b. Total Maximum Daily Load (TMDL) for Zinc in the White Clay Creek, New Castle County, DE. Technical Background and Basis Document (August 1, 1999), State of Delaware Department of Natural Resources and Environmental Control Division of Water Resources, Watershed Assessment Section, Dover, DE.

Delaware Department of Natural Resources and Environmental Control (DNREC). 1999c. Response to Public Comments RE: Proposed Total Max. Daily Loads for Zinc in the Red Clay Creek, DE. Department of Natural Resources and Environmental Control Division of Water Resources, Watershed Assessment Section, Dover, DE.

Delaware Department of Natural Resources and Environmental Control (DNREC). 1996. Final Determination State of Delaware 1996 Clean Water Act Section 303(d) List of Waters Needing TMDLs and Supporting Rationale. Delaware Department of Natural Resources and Environmental Control, Division of Water Resources, Dover, DE.

Di Toro, D.M. and J.A. McGrath. 2000. Technical basis for narcotic chemicals and polcyclic aromatic hydrocarbon criteria. II. Mixtures and sediments. *Environ. Tox. Chem.* 19(8): 1971-1982.

Farrington, J.W. 1980. An overview of the biogeochemistry of fossil fuel hydrocarbons in the marine environment. In*: Petroleum in the Marine Environment*, Eds.: L. Petrakis and F.T. Weiss, Advances in Chemistry Series 185, American Chemical Society, Washington, D.C., pp. 1-22.

Fogel, M.L., L.A. Cifuentes, D.J. Velinsky and J.H. Sharp. 1992. The relationship of carbon availability in estuarine phytoplankton to isotopic composition. *Marine Ecol. Prog. Ser*. 82: 291-300.

Fogel, M.L., E.K. Sprague, A.P. Gize and R.W. Frey. 1989. Diagenesis of organic matter in Georgia salt marshes. *Estuarine, Coastal Shelf Sci*., 28: 211-230.

Fry, B. 2006. *Stable Isotope Ecology*. Springer Science+Business Media, LLC, New York.

Gevo, B., J. Hamilton-Taylor, C. Murdoch, K.C. Jones, M. Kelly and B.J. Tabner. 1997. Depositional time trends and remobilization of PCBs in lake sediments. *Environ. Sci. Technol*. 31: 3274-3280.

Graustein, W.C. and K.K. Turekian. 1986. ^{210}Pb and ^{137}Cs in air and soils measure the rate and vertical distribution of aerosol scavenging. *J. Geophys. Res*., 91: 14,355-14,366.

Greene, R.W. 2009a. *The Chemical, Physical and Biological Fate of Polychlorinated Biphenyls in the Tidal Christina Basin*. A dissertation submitted to the Faculty of the University of Delaware in partial fulfillment of the requirements for the degree of Doctor of Philosophy in Civil Engineering: 359 pp.

Greene, R.W. 2009b. Persistent, Bioaccumulative, and Toxic (PBT) Pollutants in Surface Water, Sediment, and Biota of the Christina Basin and Shellpot Creek Watershed, DE. A presentation summarizing the results of fall 2007 sampling. Delaware Department of Natural Resources and Environmental Control, Watershed Assessment Section, Dover, DE.

Gschwend, P.M.and R.A. Hites 1981. Fluxes of PAHs to marine and lacustrine sediments in the NE United States. *Geochim. Cosmochim. Acta*. 45: 2359-2367.

Hardy, M.L. 2002. A comparison of the properties of the major commercial PBDPO/PBDE product to those of major PBB and PCB products. *Chemosphere* 46: 717-728.

Hayes, J.M, Popp, B.N., Takigiku, R., and Johnson, M.W., 1989. An isotopic study of biogeochemical relationships between carbonates and organic carbon in the Greenhorn Formation. *Geochim. Cosmochim. Acta*, 53:2961-2972.

Heiri, O., A.F. Lotter and G.Lemcke. 2001. Loss on ignition as a method for estimating organic and carbonate content in sediments: reproducibility and comparability of results. *Journal of Paleolimnology*. 25: 101-110.

Helz, G.R., S.A. Sinex, K.L. Ferri, and M. Nichols. 1985. Processes controlling Fe, Mn, and Zn in sediments of Northern Chesapeake Bay. *Estuar. Coast. Shelf Sci*. 21: 1-16.

Hites, R.A. 2004. Polybrominated diphenyl ethers in the environment and in people: A meta-analysis of concentrations. *Environ Science Technol.* 38 (4): 945-956.

Hites, R.A., R.E. Laflamme, J.G. Windsor, J.W. Farrington, and W.G. Deuser 1980. Polycyclic aromatic hydrocarbons in an anoxic sediment core from the Pettaquamscutt River (Rhode Island, USA). *Geochim. Cosmochim. Acta***.**, 44: 873-878.

Hoffman, E.J., G.L. Mills, J.S. Latimer and J.G. Quinn. 1984. Urban runoff as a source of polycyclic aromatic hydrocarbons to coastal waters. *Environ. Sci. Technol*. 18: 580-586.

Hornberger, M.L., S.N. Luoma, A.Green, C. Fuller, and R. Anima. 1999. Historical trends of metals in the sediments of San Francisco Bay, California. *Marine Chemistry.* 64:39-55.

Inn, K.G.W. 2001. The NIST natural-matrix radionuclide standard reference material program for ocean studies. *Journal of Radioanalytical and Nuclear Chemistry.* 241: 227-231.

Jasper, J.P. and R.B. Gagosian. 1990. The sources and deposition of organic matter in the Late Quaternary Pigmy Basin, Gulf of Mexico. *Geochim. Cosmochim. Acta.* 54: 1117-1132.

Kennish, M.J. 1992. *Ecology of Estuaries: Anthropogenic Effects*. Ed: M.J. Kennish, CRC Press, Inc. Boca Raton, FL., 494 pp.

Klein, R.D. 1979. Urbanization and stream water quality impairment. *Water Resources Bulletin.* 15: 948-963.

Kucklick, J.R., H.R. Harvey, P.H. Ostrom, N.E. Ostrom and J.E. Baker. 1996. Organochlorine dynamics in the pelagic food web of Lake Baikal. *Environ. Toxicol. Chem.* 15: 1388-1400.

Lake, J.L., R.A. McKinney, F.A. Osterman, R.J. Pruell, J. Kiddon, S.A. Ryba and A.D. Libby. 2001. Stable nitrogen isotopes as indicators of anthropogenic activities in small freshwater systems. *Can. J. Fish. Aquatic Sci*. 58: 870-878.

Latimer, J.S. and J.G. Quinn. 1996. Historical trends and current inputs of HOCs in an urban estuary: The sedimentary record. *Environ. Sci. Technol.* 30: 623-633.

Leavitt, P.R., C.S. Brock, C. Ebel and A. Patoine. 2006. Landscape-scale effects of urban nitrogen on a chain of freshwater lakes in central North America. *Limnol. Oceanogr*. 51(5): 2262–2277.

Litke, D.W. 1999. *Review of Phosphorus Control Measures in the United States and Their Effects on Water Quality*. U.S. Geological Survey, Water Sources Investigations Report 99-4007, National Water Quality Assessment Program, Denver, CO.

Loring, D.H. 1990. Lithium - a new approach for the granulometric normalization of trace metal data. *Mar. Chem*. 29: 155-168.

McClelland, J.W., I. Valiela and R.H. Michener. 1997. Nitrogen-stable isotope signatures in estuarine food webs: A record of increasing urbanization in coastal watershed. *Limnol. Oceangr*. 42: 930-937.

Mahler, B.J., P.C. Van Metre, T.J. Bashara, J.T. Wilson and D.A. Johns. 2005. Parking lot sealcoat: An unrecognized source of urban Polycyclic Aromatic Hydrocarbons. *Environ. Sci. Technol.* 39(15): 5560-5566.

Meyers, P.A., 1994. Preservation of elemental and isotopic source identification of sedimentary organic matter. *Chem. Geol.* 144: 289-302.

National Oceanic and Atmospheric Administration (NOAA). 1993. *National Status and Trends Program. Sampling and Analytical Methods of the National Status and Trends Program, National Benthic Surveillance and Mussel Watch Project 1984-1992*, Volume III Comprehensive Description of Elemental Analytical Methods. NOAA Tech. Mem. NOS ORCA 71, National Ocean Service, Silver Spring, MD.

National Oceanic and Atmospheric Administration (NOAA). 1989. A summary of data on tissue contamination from the first three years (1986-1988) of the Mussel Watch project. *NOAA Tech. Mem. NOS OMA 49*, Rockville, MD.

National Research Council (NRC). 2007. *Sediment Dredging at Superfund Megasites Assessing the Effectiveness*. National Research Council of the National Academies, The national Academies Press, Washington, D.C.

Neff, J.M., S.A. Stout and D.G. Gunster. 2005. Ecological risk assessment of polycyclic aromatic hydrocarbons in sediments: Identifying sources and ecological hazard. *Integr. Environ. Assess. Manag.* 1(1): 22-33.

Neubauer, I.C. Anderson, J.A. Constantine and S.A. Kuehl. 2002. Sediment deposition and accretion in a mid-Atlantic (U.S.A.) tidal freshwater marsh. *Estuarine, Coastal, and Shelf Science*. 54: 713-727.

Officer, C.B., D.R. Lynch, G.H. Setlock and G.R. Helz.1984. Recent sedimentation rates in Chesapeake Bay. In: Kennedy, V.S. (ed.). *The Estuary as a Filter*. Academic Press, New York, pp 131-157.

O'Leary, M.H., 1988. Carbon isotopes in photosynthesis. *Bioscience,* 38:328-336.

Olsen, C.R., I.L. Larsen, P.D. Lowry, N.H. Cutshall, J.F. Todd and G.T.F. Wong. 1985. Atmospheric fluxes and marsh-soil inventories of ^{7}Be and ^{210}Pb. *Journal of Geophysical Research –Atmospheres.* 90: 10487-10495.

Olsen, C.R., H.J. Simpson, T.H. Peng, R.F. Bopp and R.M. Trier. 1981. Sediment mixing and accumulation effects on radionuclide depth profiles in Hudson estuary sediments. *Journal of Geophysical Research*. 86: 11020-11028.

O´Malley, V.P., T.A. Abrajano and J.Hellou. 1996. Stable carbon isotopic apportionment of individual polycyclic aromatic hydrocarbons in St. John's harbour, Newfoundland. *Environ. Sci. Technol.* 30: 634-639.

O'Malley, V.P., T.A. Abrajano and J. Hellou. 1994. Determination of $^{13}C/^{12}C$ ratios of individual PAH from environmental samples: Can PAH sources be source apportioned? *Org. Geochem*. 21: 809-815.

Orson, R.A., R.L. Simpson and R.E. Good. 1992. A mechanism for accumulation and retention of heavy metals in tidal freshwater marshes of the upper Delaware River Estuary. *Estuar. Coast. Shelf Sci.* 34: 171-186.

Orson, R.A., R.L. Simpson and R.E. Good. 1990. Rates of sediment accumulation in a tidal freshwater marsh. *J. Sed. Petrology*. 60: 859-869.

Owens, M. and J.C. Cornwell. 1995. Sedimentary evidence for decreased heavy metal inputs to the Chesapeake Bay. *Ambio* 24: 24-27.

Perga, M.E. and D. Gerdeaux. 2004. Changes in the $^{\delta 13}C$ of pelagic food webs: The influence of lake area and trophic status on the isotopic signature of whitefish (*Coregonus lavaretus*). *Can. J. Fish. Aquat. Sci.* 61(8): 1485–1492.

Pierce, R.H., R.C. Brown, E.S. Van Vleet, and R.M. Joyce. 1986. Hydrocarbon contamination from coastal development. In: *Organic Marine Chemistry*. Ed: M.L. Sohn, ACS Symposium Series 305, pp. 229-246.

Ponader, K.C., D.F. Charles, T.J. Belton and D.M. Winter. 2008. Total phosphorus inference models and indices for coastal plain streams based on benthic diatom assemblages from artificial substrates. *Hydrobiologia* 610: 139-152.

Porter, S.D. 2008. *Algal attributes: An autecological classification of algal taxa collected by the National Water-Quality Assessment Program*: U.S. Geological Survey Data Series 329, 18 p.

Porter, S.D., D.K. Mueller, N.E. Spahr, M.D. Munn and N.M. Dubrovsky. 2008. Efficacy of algal metrics for assessing nutrient and organic enrichment in flowing waters: *Freshwater Biology.* 53: 1036-1054.

Potapova, M. and D.F. Charles. 2007. Diatom metrics for monitoring eutrophication in rivers of the United States. *Ecological Indicators.* 7: 48-70.

Potapova, M., D.F. Charles, K.C. Ponader and D.M. Winter. 2004. Quantifying species indicator values for trophic diatom indices: a comparison of approaches. *Hydrobiologia.* 517: 25-41.

Prahl, F.G., J.R. Ertel, M.A. Goni, M.A. Sparrow and B. Eversmeyer. 1994. Terrestrial organic carbon contributions to sediments on the Washington margin. *Geochim. Cosmochim. Acta.* 58:3035-3048.

Pruell, R.J. and J.G. Quinn. 1985. Geochemistry of organic contaminants in Narragansett Bay sediments. *Estuar. Coast. Shelf Sci*., 21: 295-312.

Ridgeway, J. and G. Shimmield. 2002. Estuaries as repositories of historical contamination and their impact on shelf seas. *Estuar. Coast. Shelf Sci*. 55: 903-928.

Riedel, G.R., D.J. Velinsky, J.T.F. Ashley and J.Cornwell. 2010. River sediment investigation near Poplar Point in the tidal Anacostia River, Washington, DC. *Aquatic Geochemistry.* (under revision).

Rippey, B. and H. J. Anderson. 1996. Reconstruction of lake P loadings and dynamics using sedimentary record. *Environ. Sci. Technol*. 30: 1786-1789.

Ritchie, J.C. and McHenry, R.J. 1990. Application of radioactive fallout Cesium-137 for measuring soil erosion and sediment accumulation rates and patterns: A review. *Journal of Environmental Quality.* 19: 215-233.

Roy, AH., A.D. Rosemond, M.J. Paul, D.S. Leigh, and J.B. Wallace. 2003. Stream macroinvertebrate response to catchment urbanization (Georgia, U.S.A.). *Freshwater Biology* 48: 329-346.

Rushneck, D.R, A. Bekuveau et al. 2004. Concentrations of dioxin-like PCB congeners in unweathered Aroclors by HRGC/HRMS using EPA Method 1668A. *Chemosphere* 54: 79-97.

Ruttenberg, K.C. 1992. Development of a sequential extraction method for different forms of phosphorus in marine sediments. *Limnol. Oceanogr*. 37: 1460-1482.

Santschi, P.H., B.J. Presley, T.L. Wade, B. Garcia-Romero and M. Baskaran. 2001. Historical contamination of PAHs, PCBs, DDTs, and heavy metals in Mississippi River Delta, Galveston Bay and Tampa Bay sediment cores. *Mar. Environ. Res.* 52: 51-79.

Schelske, C.L. and D.A. Hodell. 1995. Using carbon isotopes of bulk sedimentary organic matter to reconstruct the history of nutrient loading and eutrophication in Lake Erie. *Limnol. Oceanogr*. 40: 918-929.

Schelske, C.L. and D.A. Hodell. 1991. Recent changes in productivity and climate of Lake Ontario detected by isotopic analysis of sediments. *Limnol. Oceanogr*. 36: 961-975.

Schropp, S.J., F.G. Lewis, H.L. Windom, J.D. Ryan, F.D. Calder and L.C. Burney. 1990. Interpretation of metal concentrations in estuarine sediments of Florida using aluminum as a reference element. *Estuaries.* 13: 227-235.

Schubel, J. R. and D. J. Hirschberg. 1977. ^{210}Pb determined sedimentation rate, and accumulation of metals in sediments at a station in Chesapeake Bay. *Chesapeake Sci.* 18: 379-382.

Simpson, R.L., R.E. Good, R. Walker and B.R. Frasco. 1983. The role of Delaware River freshwater tidal wetlands in the retention of nutrients and heavy metals. *J. Environ. Qual*. 12: 41-48.

Sinex, S.A. and G.R. Helz. 1981. Regional geochemistry of trace elements in Chesapeake Bay sediments. *Environ. Geol*. 3: 315-323.

Smol J.P. 2008. *Pollution of Lakes and Rivers: A Paleoenvironmental Perspective*- 2nd edition. Blackwell Publishing, Oxford.

Smol, J.P. 2002. *Pollution of Lakes and Rivers: A Paleoenvironmetal Perspective*. Arnold Press and Oxford University Press, NY.

Sommerfield, C.K. 2006. On sediment accumulation rates and stratigraphic completeness: Lessons from Holocene ocean margins. *Continental Shelf Research*. 26:2225-2240.

Song, W., J.C. Ford, L. An, W.J. Buckleya and K.J. Rockne. 2004. Polybrominated diphenyl ethers in sediments of the Great Lakes. 1. Lake Superior. *Environ. Sci. Tech*. 38(12): 3286-3293.

Thompson, P.M. and S. O'Byrne. 1999. *Images of America Wilmington's Waterfront*. Arcadia Publishing, Charleston, SC.

Trefry, J.H. and B.J. Presley. 1976. Heavy metal transport from the Mississippi River to the Gulf of Mexico. In: *Marine Pollution Transfer*, Eds.: H.L. Windom and R.A. Duce, Heath and Co., Lexington, pp. 39-75.

Ulseth, A.J. and A.E. Hershey. 2005. Natural abundances of stable isotopes trace anthropogenic N and C in an urban stream. *JNABS*: 24(2): 270-289.

United States Environmental Protection Agency (U.S. EPA). 2010. Current Site Information, Diamond State Salvage (accessed online at http://www.epa.gov/reg3hwmd/npl/DE0000122218.htm). U.S. Environmental Protection Agency, Region 3, Philadelphia, PA.

United States Environmental Protection Agency (U.S. EPA). 2009. Draft Recommended Interim Preliminary Remediation Goals for Dioxin in Soil at CERCLA and RCRA Sites. U.S. Environmental Protection Agency, Office of Superfund Remediation and Technology Innovation, Washington, D.C (December, 2009).

United States Environmental Protection Agency (U.S. EPA). 1993. EPA Superfund Record of Decision: E.I. Du Pont de Nemours & Co., Inc. (Newport Pigment Plant Landfill) EPA ID: DED980555122 OU 01 Newport, DE 09/29/1993 (EPA/ROD/R03-93/170). U.S. Environmental Protection Agency, Region 3, Philadelphia, PA.

United States Environmental Protection Agency (U.S. EPA). 1987. Guidance for Sampling of and Analyzing for Organic Contaminants in Sediments. Office of Water Regulations and Standards, Criteria and Standards Division, Washington, D.C.

Valette-Silver , N.J. 1993. The use of sediment cores to reconstruct historical trends in contamination of estuarine and coastal sediments. *Estuaries.* 16: 577-588.

van Dam, H., A. Mertens, and J. Sinkeldam. 1994. A coded checklist and ecological indicator values of freshwater diatoms from The Netherlands. *Neth. J. Aquat. Ecol*. 28: 117–133.

Van den Berg, M., et al. 2006. The 2005 World Health Organization Reevaluation of Human and Mammalian Toxic Equivalency Factors for Dioxins and Dioxin-Like Compounds. *Toxicol. Sci.* 93(2): 223-241.

Van Metre, P.C., B.J. Mahler and J.T. Wilson. 2009. PAHs underfoot: Contaminated dust from coal-tar sealcoated pavement is widespread in the United States. *Environ. Sci. Technol*.: 43(1): 20-25.

Van Metre, P, BJ Mahler, M Scoggins and PA Hamilton. 2006. Parking lot sealcoat: A major source of polycyclic aromatic hydrocarbons (PAHs) in rrban and suburban environments. US Geological Survey and the City of Austin, Fact Sheet 2005–3147.

Van Metre, P.C., B.J. Mahler and E.T. Furlong. 2000. Urban sprawl leaves its PAH signature. *Environ. Sci. Technol*. 34: 4064-4070.

Van Metre, P.C. and Callender, E. 1997. Identifying water-quality trends from ^{210}Pb using dated sediment cores from White Rock Lake Reservoir, Dallas, Texas. *Journal of Paleolimnology.* 17: 239-249.

Vane, C.H., Y.J. Ma, S.J Chen, and B.X. Mai. 2009. Increasing polybrominated diphenyl ether (PBDE) contamination in sediment cores from the inner Clyde Estuary, UK. Environ. *Geochem. Health*. Online edition (04 April 2009).

Velinsky, D.J., G.F. Riedel and J.T.F. Ashley. 2008. Assessment of Water Quality of the Tidal Potomac River in Washington DC: Trace Metals and Organic Contaminants. Final Report (04g-05-WQD03 (WP04)). District of Columbia, Department of the Environment, Washington, DC. (PCER Report: 08-3).

Velinsky, D.J., J.T.F. Ashley and G.R.Riedel. 2007. *Sediment Contaminants in the upper Tidal Potomac River; Washington, DC: Spatial and Temporal Trends.* Final Report submitted to Department of the Environment, District of Columbia. Patrick Center for Environmental Research, The Academy of Natural Sciences.

Velinsky, D.J., T.L. Wade, B. Gammisch and J. Cornwell. 1997. *Sediment Deposition and Inventory of Chemical Contaminants in the Tidal Anacostia River, Washington, D.C.* ICPRB Report #97-2. Interstate Commission on the Potomac River Basin, Rockville, MD.

Velinsky, D.J., T.L. Wade, C. Schlekat and B.J. Presley. 1994. Tidal river sediments in the Washington, D.C. area. I. Distribution and sources of trace metals. *Estuaries.* 17: 305-320.

Wade, T.L., D.J. Velinsky, E. Reinharz and C.E. Schlekat. 1994. Tidal river sediments in the Washington, D.C. area. II. Distribution and sources of chlorinated and non-chlorinated aromatic hydrocarbons. *Estuaries*. 17: 321-333.

Wakeham S.G., C. Schaffner and W. Giger. 1980. Polycyclic aromatic hydrocarbons in recent lake sediments—II. Compounds derived from biogenic precursors during early diagenesis. *Geochim Cosmochim Acta.* 44: 415–429.

Wallbrink, P.J., D.E. Walling and Q. He. 2002. Radionuclide measurement using HPGe gamma spectrometry. In: F. Zapata (Editor), *Handbook for the Assessment of Soil Erosion and Sedimentation Using Environmental Radionuclides*. Kluwer Academic Publishers, Dordrecht, pp. 67-96.

Wania, F. and C.B. Dugani. 2003. Assessing the long-range transport potential of polybrominated diphenyl ethers: a comparison of four multimedia models. *Environmental Toxicology and Chemistry.* 22: 1252–1261.

Wedepohl, K.H. 1971. *Geochemistry*. Holt, Rinehart and Winston, Inc., NY. (Translated from Geochemie, 1967).

Wedepohl, K.H. 1968. Chemical fractionation in the sedimentary environment, in Ahrens, L.H., ed., *Origin and Distribution of the Elements*: Oxford, England, Pergamon Press, pp. 999-1016.

Windom, H.L., S.J. Schropp, F.D. Calder and others. 1989. Natural trace metal concentrations in estuarine and coastal marine sediments of the southeastern United States. *Environ. Sci. Technol.,* 23: 314-320.

Woodwell, G.M., P.P. Craig and H.A. Johnson. 1971. DDT in the biosphere: Where does it go? *Science.* 174: 1101-1107.

Youngblood, W.W. and M. Blumer. 1975. Polycyclic aromatic hydrocarbons in the environment: homologous series in soils and recent marine sediments. *Geochim. Cosmochim. Acta*, 39: 1303-1314.

Zhang, X., E.R. Christensen and M.F. Gin. 1993. Polycyclic aromatic hydrocarbons in dated sediments from Green Bay and Lake Michigan. *Estuaries.* 16: 638-652.

Zimmerman, A.R. and E.A. Canuel. 2002. Sediment geochemical records eutrophication in the mesohaline Chesapeake Bay. *Limnol. Oceanogr*. 47: 1084-1093.

Tables

Table 1. Core locations and collection dates.

Name	Abbreviation	Date	Lat (N)	Long (W)	Depth of Core (cm)	Location
Brandywine River	BW-1	12/3/2007	39° 44.189'	75° 31.546'	36	Embayment
Churchman Marsh	CM-1A	3/25/2008	39° 42.021'	75° 37.810'	82	Marsh
Lower Shellpot Creek	LSP-2	4/15/2008	39° 44.320'	75° 30.597'	102	Marsh
Walnut Street	WS-2A	4/22/2008	39° 44.067'	75° 33.040'	98	Sub-tidal embayment
Dravo Marsh	DM-2	6/22/2008	39° 43.217'	75° 33.722'	106	Marsh

Table 2. Bulk sediment properties and radioisotope data for BW.

Chem ID	Interval	Water Content (%)	Dry Bulk Density (g/cm^3)	Accumulated Mass (g/cm^2)	LOI (%)	Total ^{210}Pb (dpm/g)	Excess ^{210}Pb (dpm/g)	^{137}Cs (dpm/g)	z (cm)	Age Model
9994	0-2	52.20	0.68	1.36	9.33	4.49	1.85	0.22	1	2006
9996	4-6	46.67	0.80	2.96	9.80	3.03	1.16	0.19	5	2000
9998	8-10	50.44	0.72	4.39	9.60	4.20	1.56	0.51	9	1995
10000	12-14	52.49	0.67	5.74	13.30	3.44	1.28	0.96	13	1990
10001	16-18	51.64	0.69	7.13	11.36	3.51	1.02	0.90	17	1984
10004	20-22	49.62	0.73	8.59	13.51	4.15	1.46	4.34	21	1979
10006	24-26	46.95	0.79	10.18	11.39	3.26	0.76	4.07	25	1974
10008	28-30	46.61	0.80	11.78	11.72	2.96	0.70	3.87	29	1968
10010	32-34	40.41	0.95	13.67	10.56	2.31	0.16	1.04	33	1963
10012	36-38	33.73	1.13	15.93	7.23	1.86	0.00	0.00	37	1958
10014	40-42	35.04	1.09	18.11	7.39	2.64	0.36	0.00	41	1952
10016	44-46	35.00	1.09	20.29	7.06	1.68	0.00	0.00	45	1947
10018	48-50	35.04	1.09	22.48	7.78	1.67	0.00	0.00	49	1942
10019	50-52	36.05	1.06	24.60	12.60	2.00	0.38	0.03	51	1939

Table 3. Bulk sediment properties and radioisotope data for CM.

Chem ID	Interval	Water Content (%)	Dry Bulk Density (g/cm^3)	Accumulated Mass (g/cm^2)	LOI (%)	Total ^{210}Pb (dpm/g)	Excess ^{210}Pb (dpm/g)	^{137}Cs (dpm/g)	z (cm)	Age Model
0219	0-2	73.19	0.32	0.64	19.61	9.83	7.60	0.19	1	2005
0221	4-6	72.32	0.33	1.31	18.11	10.65	7.79	0.33	5	1999
0223	8-10	64.79	0.45	2.21	15.27	9.22	6.74	0.34	9	1992
0225	12-14	63.93	0.47	3.14	14.95	6.73	4.55	0.24	13	1985
0227	16-18	63.61	0.47	4.09	15.56	7.01	4.69	0.33	17	1979
0229	20-22	66.55	0.42	4.93	16.98	7.17	4.86	0.50	21	1972
0231	24-26	61.80	0.50	5.93	15.56	6.02	3.93	0.48	25	1965
0233	28-30	49.59	0.73	7.40	11.83	3.88	0.98	0.12	29	1959
0235	32-34	46.65	0.80	9.00	11.80	3.81	0.22	0.00	33	1952
0237	36-38	45.94	0.81	10.63	11.35	3.76	0.63	0.00	37	1945
0239	40-42	45.33	0.83	12.29	11.20	2.61	0.25	0.00	41	1939
0241	44-46	43.45	0.87	14.03	10.46	3.44	0.73	0.00	45	1932
0243	48-50	44.96	0.84	15.71	9.84	3.40	0.09	0.00	49	1925
0245	52-54	42.80	0.89	17.48	10.05	3.08	0.63	0.00	53	1919
0247	56-58	43.31	0.88	19.24	9.43	2.96	0.44	0.00	57	1912
0249	60-62	45.31	0.83	20.90	9.76	2.72	0.33	0.00	61	1909
0251	64-66	41.55	0.92	22.73	8.56	2.76	0.45	0.00	65	1899
0253	68-70	35.53	1.08	24.89	7.40	2.74	0.39	0.00	69	1892
0255	72-74	32.40	1.17	27.22	6.63	2.29	0.04	0.00	73	1878

Table 4. Bulk sediment properties and radioisotope data for LSP.

Chem ID	Interval	Water Content (%)	Dry Bulk Density (g/cm^3)	Accumulated Mass (g/cm^2)	LOI (%)	Total ^{210}Pb (dpm/g)	Excess ^{210}Pb (dpm/g)	^{137}Cs (dpm/g)	z (cm)	Age Model
0429	0-2	70.82	0.36	0.71	20.85	14.79	12.29	0.26	1	2006
0431	4-6	64.01	0.46	1.64	17.61	12.36	10.48	0.33	5	2004
0433	8-10	56.92	0.59	2.82	13.77	14.20	12.15	0.30	9	2002
0435	12-14	63.29	0.48	3.77	18.98	12.47	10.27	0.24	13	2000
0437	16-18	68.21	0.40	4.56	24.48	14.35	12.29	0.22	17	1998
0439	20-22	57.70	0.57	5.71	17.32	14.94	12.19	0.41	21	1996
0441	24-26	55.23	0.62	6.95	16.22	15.31	12.75	0.38	25	1994
0443	28-30	53.68	0.65	8.25	16.68	13.06	10.28	0.38	29	1992
0445	32-34	57.31	0.58	9.42	16.94	11.23	9.31	0.32	33	1990
0447	36-38	63.85	0.47	10.35	17.64	8.79	6.89	0.21	37	1988
0449	40-42	60.96	0.52	11.38	15.49	9.46	7.19	0.20	41	1985
0451	44-46	58.98	0.55	12.48	16.09	8.76	6.71	0.15	45	1983
0453	48-50	67.22	0.41	13.31	24.07	7.51	5.48	0.16	49	1981
0454	50-52	69.16	0.38	14.07	23.33	8.07	5.53	0.22	51	1980
0455	52-54	68.54	0.39	14.85	27.87	7.10	5.67	0.08	53	1979
0457	56-58	71.32	0.35	15.55	33.96	5.18	4.26	0.16	57	1977
0459	60-62	60.15	0.53	16.61	12.36	5.41	2.74	0.52	61	1975
0461	64-66	61.59	0.50	17.62	14.17	5.48	2.90	0.41	65	1973
0463	68-70	60.26	0.53	18.68	12.34	4.19	1.47	0.58	69	1971
0465	72-74	64.75	0.45	19.58	13.90	5.20	2.37	0.59	73	1969
0467	76-78	53.45	0.66	20.89	9.66	4.86	2.71	0.63	77	1966
0469	80-82	55.68	0.61	22.12	11.26	5.11	2.93	0.42	81	1964
0471	84-86	38.72	0.99	24.10	6.09	2.32	0.82	0.18	85	1962
0473	88-90	32.50	1.16	26.43	4.61	1.59	0.29	0.14	89	1960
0475	92-94	30.26	1.23	28.89	3.83	1.99	0.11	0.10	93	1958
0477	96-98	52.58	0.67	30.24	14.02	5.30	2.60	0.37	97	1956
0479	100-102	40.45	0.95	32.13	5.50	2.39	0.33	0.08	101	1954

Table 5. Bulk sediment properties and radioisotope data for DM.

Chem ID	Interval	Water Content (%)	Dry Bulk Density (g/cm^3)	Accumulated Mass (g/cm^2)	LOI (%)	Total ^{210}Pb (dpm/g)	Excess ^{210}Pb (dpm/g)	^{137}Cs (dpm/g)	z (cm)	Age Model
1055	0-2	82.46	0.20	0.39	36.30	10.23	8.78	0.28	1	2006
1057	4-6	79.77	0.23	0.86	32.10	9.25	7.82	0.20	5	2000
1059	8-10	84.76	0.17	1.19	38.91	6.64	5.00	0.27	9	1995
1061	12-14	77.86	0.26	1.71	29.13	5.54	3.62	0.35	13	1990
1063	16-18	69.70	0.37	2.45	21.97	4.98	2.83	0.61	17	1984
1065	20-22	58.08	0.57	3.59	14.03	4.82	2.35	0.54	21	1979
1067	24-26	47.26	0.79	5.16	10.35	2.88	0.15	0.24	25	1974
1069	28-30	48.51	0.76	6.67	10.990	4.24	1.31	0.23	29	1968
1071	32-34	53.22	0.66	7.99	13.589	4.35	1.55	0.27	33	1963
1073	36-38	64.18	0.46	8.92	20.541	4.62	2.33	0.12	37	1958
1075	40-42	54.81	0.63	10.17	15.278	4.11	1.28	0.00	41	1952
1077	44-46	45.53	0.82	11.82	10.678	3.19	0.42	0.00	45	1947
1079	48-50	40.37	0.95	13.72	8.204	2.64	0.00	0.00	49	1942
1081	52-54	37.36	1.03	15.77	7.017	2.30	0.00	0.00	53	1935
1083	56-58	33.92	1.12	18.02	5.744	2.10	0.02	0.00	57	1931
1085	60-62	32.99	1.15	20.32	5.053	2.48	0.00	0.00	61	1927
1087	64-66	37.69	1.02	22.35	6.186	2.21	0.08	0.00	65	1920
1089	68-70	37.95	1.01	24.38	6.863	2.95	0.30	0.00	69	1915

Table 6. Summary data for radioisotope analysis and dating.

		Radioisotope Inventory		Sedimentation Rate			Mass Accumulation Rate		Depositional Flux	Focusing Factor	
Location	**Core**	xsPb-210	Cs-137	xsPb-210 CA	xsPb-210 CF	Cs-137	xsPb-210	Cs-137	xsPb-210	xsPb-210	Cs-137
		dpm/cm^2	dpm/cm^2	cm/yr	cm/yr	cm/yr	g/cm^2-yr	g/cm^2-yr	dpm/cm^2-yr		
Brandywine River	BW-2	28.00	49.00	0.64	0.96	0.66	0.25	0.28	0.53	0.90	2.30
Churchmans Marsh	CM-1	66.00	4.00	0.63	1.00	0.57	0.17	0.15	0.95	2.10	0.20
Shellpot Creek	SP-2	399.00	18.00	1.30	2.10	1.90	0.37	0.60	7.50	12.50	0.90
Dravo Marsh	DM-2	82.00	5.00	NA	0.73	0.74	0.29	0.19	0.85	2.60	0.30

xs – excess; CA – Constant activity model; CF – Constant flux model (modified to match Cs-137 input function)
Depositional flux – based on steady-state atmospheric fluxes of xsPb-210 (32 dpm/cm^2-yr) and Cs-137 (21 dpm/cm^2-yr)

Table 7. Concentrations of various parameters for Core BW.

CHEM ID	Interval cm	Mid-Point cm	Solids %	Age Model yr	$\delta^{13}C$ per mil	$\delta^{15}N$ per mil	TC %	TN %	C/N Atomic
9994	0-2	1	47.3	2006	-26.48	5.37	3.82	0.31	14.50
9996	4-6	5	46.5	2000	-26.57	5.34	4.17	0.29	16.67
9998	8-10	9	49.2	1995	-25.94	4.95	3.96	0.29	15.82
10000	12-14	13	48.1	1990	-23.82	5.36	3.79	0.32	13.84
10001	14-16	15	49.9	1987	-23.54	5.20	3.85	0.34	13.15
10003	18-20	19	51.0	1982	-23.40	5.19	3.93	0.32	14.53
10004	20-22	21	49.6	1979	-26.34	3.94	6.79	0.44	17.91
10006	24-26	25	51.3	1974	-25.63	4.87	5.80	0.31	21.59
10008	28-30	29	52.9	1968	-25.57	4.83	7.02	0.48	16.98
10010	32-34	33	55.6	1963	-25.17	5.05	6.32	0.39	18.74
10012	36-38	37	68.4	1958	-24.11	4.33	2.03	0.16	14.89
10013	38-40	39	67.5	1955	-23.69	4.80	2.14	0.17	14.52
10015	42-44	43	66.1	1950	-23.63	4.94	1.60	0.15	12.20
10017	46-48	47	67.1	1944	-23.53	4.82	1.70	0.26	7.74
10019	50-52	51	64.0	1939	-23.65	5.50	2.22	0.20	13.03

Table 7 (continued). Concentrations of various parameters for Core BW.

CHEM ID	TSP	Fe	Zn	tPAHs	T PCBs	tDDXs	tChlordanes	tDioxins	tFurans	2,3,7,8 TCDD-TEQ	tPBDEs
	%	µg/g dw	µg/g dw	µg/g dw	ng/g dw	ng/g dw	ng/g dw	pg/g dw	pg/g dw	pg/g dw	ng/g dw
9994	0.084	29412	486	1.97	44.64	8.17	2.48	6992	621	21.8	52.8
9996	0.087	34804	471	4.30	45.05	9.50	2.00	5327	551	16.2	48.5
9998	0.087	37237	485	1.03	70.96	13.01	2.77	8507	554	21.4	120.1
10000	0.269	41667	337	2.10	636.80	308.12	7.10	12628	1562	46.2	0.69
10001	0.191	37255	376	2.16	685.04	288.74	6.80	11580	1414	41.7	1.16
10003	0.158	29412	518	2.70	617.66	369.03	6.82	9077	1730	44.8	0.92
10004	0.090	40196	784	8.95	431.11	69.16	51.10	7123	2849	93.0	NA
10006	0.105	40686	769	5.20	120.06	39.66	7.73	6702	2705	68.5	NA
10008	0.122	38725	706	8.01	118.79	63.16	3.40	7055	2868	75.3	1.49
10010	0.121	25490	565	5.01	77.85	41.42	1.53	6668	2239	37.6	1.37
10012	0.085	29796	461	3.40	4.63	1.63	0.44	6927	117	9.5	NA
10013	0.103	31580	392	3.67	3.63	6.59	0.34	7070	116	8.9	NA
10015	0.075	32680	431	2.52	5.79	5.79	0.22	4417	128	6.5	0.85
10017	0.083	35294	486	2.04	2.19	3.60	0.25	6519	233	10.1	NA
10019	0.095	33296	296	2.97	2.95	5.09	0.29	6716	61	8.9	1.14

Concentrations on a dry weight basis. Total PAHs is the sum of 39 individual compounds, total PCBs is the sum of 110 congeners, total DDX is the sum of o,p+pp forms of DDD, DDE, and DDT, and total chlordane is the sum of alpha+gamma chlordane, heptachlor, heptachlor epoxide, oxychlordane, nonachlor and nonachlor epoxide (See Appendix I).

Table 8. Concentrations of various parameters for Core CM.

CHEM ID	Interval cm	Mid-Point cm	Solids %	Age Model yr	$\delta^{13}C$ per mil	$\delta^{15}N$ per mil	TC %	TN %	C/N Atomic
0219	0-2	1	28.3	2005	-28.14	8.08	7.52	0.79	11.09
0221	4-6	5	26.1	1999	-28.11	7.30	7.73	0.75	12.00
0223	8-10	9	33.8	1992	-27.77	6.95	5.71	0.55	12.05
0225	12-14	13	36.8	1985	-27.73	6.60	5.39	0.50	12.64
0227	16-18	17	32.7	1979	-27.42	6.39	6.34	0.60	12.38
0229	20-22	21	44.1	1972	-27.19	5.49	4.93	0.42	13.84
0231	24-26	25	53.2	1965	-26.75	4.71	3.44	0.30	13.26
0233	28-30	29	54.1	1959	-26.93	4.17	3.52	0.31	13.14
0235	32-34	33	54.0	1952	-26.28	4.35	3.66	0.32	13.51
0237	36-38	37	54.5	1945	-25.95	4.13	3.52	0.34	12.05
0240	42-44	43	55.5	1935	-26.00	4.75	3.02	0.26	13.47
0243	48-50	49	57.7	1925	-24.40	4.58	2.65	0.23	13.28
0247	56-58	57	56.1	1912	-25.74	4.08	2.88	0.26	12.84
0251	64-66	65	60.0	1899	-25.47	4.24	1.99	0.20	11.76
0255	72-74	73	66.5	1885	-25.63	4.73	1.73	0.19	10.40
0259	80-82	81	70.1	1872	-24.66	4.79	1.17	0.15	9.07

Table 8 (continued). Concentrations of various parameters for Core CM.

CHEM ID	TSP	Fe	Zn	tPAHs	T PCBs	tDDXs	tChlordanes	tDioxins	tFurans	2,3,7,8 TCDD-TEQ	tPBDEs
	%	µg/g dw	µg/g dw	µg/g dw	ng/g dw	ng/g dw	ng/g dw	pg/g dw	pg/g dw	pg/g dw	ng/g dw
0219	0.180	45656	723	1.68	90.28	9.31	2.79	13306	523	19.9	10.34
0221	NA	37255	973	2.24	157.91	15.91	3.53	13163	525	30.7	12.09
0223	NA	33996	984	1.41	125.85	10.38	1.36	14876	691	30.3	9.72
0225	0.182	35743	980	1.43	189.18	11.98	1.91	18228	838	40.8	10.92
0227	0.170	35351	1086	1.71	339.36	20.54	3.31	18999	754	42.7	17.12
0229	0.125	33824	3817	2.00	487.00	26.39	2.24	10923	616	29.9	3.69
0231	0.101	26471	4078	2.50	781.53	39.82	2.31	11945	606	22.6	1.02
0233	0.106	29223	4374	6.00	2106.59	108.23	4.60	10541	1315	24.5	0.80
0235	0.113	32843	8314	6.83	1809.13	117.59	6.60	157727	12695	444.6	0.34
0237	0.119	36765	9804	26.79	980.36	62.99	4.66	29775	3183	102.5	0.41
0240	0.106	30702	9482	3.18	328.06	20.55	1.49	13028	1562	19.5	NA
0243	0.105	39706	7529	0.90	66.76	3.18	0.38	11904	683	20.3	NA
0247	0.089	37255	9098	1.39	152.68	6.06	0.60	15189	1352	32.5	NA
0251	0.066	30392	4078	2.10	144.25	3.39	0.42	13756	1903	15.2	NA
0255	0.055	33333	149	0.46	4.09	0.68	0.10	18161	54	10.9	NA
0259	0.060	35083	131	0.44	2.83	0.84	0.07	13160	19	7.5	NA

Concentrations on a dry weight basis. NA- Not analyzed. Total PAHs is the sum of 39 individual compounds, total PCBs is the sum of 110 congeners, total DDX is the sum of o,p+pp forms of DDD, DDE, and DDT, and total chlordane is the sum of alpha+gamma chlordane, heptachlor, heptachlor epoxide, oxychlordane, nonachlor and nonachlor epoxide (See Appendix I).

Table 9. Concentrations of various parameters for Core DM.

CHEM ID	Interval	Mid-Point	Solids	Age Model	$\delta^{13}C$	$\delta^{15}N$	TC	TN	C/N
	cm	cm	%	yr	per mil	per mil	%	%	Atomic
1055	0-2	1	15.5	2006	-28.59	7.76	18.19	1.17	18.14
1057	4-6	5	18.6	2000	-28.51	7.80	14.53	0.93	18.20
1058	6-8	7	26.6	1998	-28.01	7.61	10.64	0.68	18.13
1059	8-10	9	14.0	1995	-28.21	7.86	19.77	1.15	20.11
1060	10-12	11	13.8	1992	-28.29	7.36	18.88	1.04	21.13
1061	12-14	13	16.9	1990	-28.26	7.37	17.54	1.01	20.17
1063	16-18	17	32.3	1984	-27.69	7.14	8.77	0.55	18.53
1065	20-22	21	51.0	1979	-27.28	6.22	5.14	0.30	20.18
1067	24-26	25	57.5	1974	-26.91	6.16	4.18	0.26	18.82
1069	28-30	29	54.0	1968	-26.87	6.75	4.86	0.30	19.03
1071	32-34	33	57.6	1963	-26.48	6.56	3.61	0.23	18.10
1073	36-38	37	37.6	1958	-27.07	6.54	8.34	0.50	19.35
1076	42-44	43	44.7	1950	-26.78	7.91	6.49	0.42	17.99
1079	48-50	49	58.7	1942	-25.90	6.83	3.08	0.23	15.85
1083	56-58	57	64.9	1931	-24.51	4.78	1.47	0.13	13.58
1087	64-66	65	62.0	1920	-24.51	4.45	1.69	0.15	12.84
1095	80-82	81	64.3	1905	-25.21	5.77	1.65	0.13	14.67
1102	94-96	95	62.0	1888	-25.28	5.36	1.33	0.14	10.89
1106	102-104	103	61.5	1878	-24.60	5.90	1.04	0.12	10.15

Table 9 (continued). Concentrations of various parameters for Core DM.

CHEM ID	TSP	Fe	Zn	tPAHs	T PCBs	tDDXs	tChlordanes	tDioxins	tFurans	2,3,7,8 TCDD-TEQ	tPBDEs
	%	µg/g dw	µg/g dw	µg/g dw	ng/g dw	ng/g dw	ng/g dw	pg/g dw	pg/g dw	pg/g dw	ng/g dw
1055	0.098	12504	538	2.70	238.49	29.07	9.69	9244	1117	32.9	17.07
1057	0.092	9056	647	1.93	278.19	30.22	9.65	7806	975	33.9	32.64
1058	0.082	18166	742	4.17	239.94	23.45	5.40	16594	2100	69.9	NA
1059	0.087	29762	1045	2.95	356.71	41.19	13.11	10023	1279	32.1	12.47
1060	0.083	20427	777	4.84	436.01	50.41	13.82	6638	769	26.4	15.01
1061	0.082	12276	811	8.05	325.98	33.85	10.93	4429	572	13.8	16.02
1063	0.073	9013	818	5.46	364.52	39.88	9.26	5701	779	24.3	2.42
1065	0.045	7782	594	3.86	180.97	28.13	3.94	5084	1394	27.7	1.51
1067	0.040	5388	299	2.83	45.05	6.87	0.79	3188	778	16.9	NA
1069	0.046	8631	610	2.80	35.87	4.84	0.44	2033	552	12.2	0.29
1071	0.043	10058	678	4.34	48.61	6.74	0.71	2102	608	20.0	0.56
1073	0.090	11043	1230	6.52	394.89	68.54	3.53	11880	4808	93.9	0.46
1076	0.071	6186	1059	5.46	102.14	11.12	1.41	2577	1707	31.0	NA
1079	0.051	6443	319	3.84	19.17	1.39	0.42	9517	2900	33.6	NA
1083	0.058	9497	149	0.97	3.70	0.71	0.14	1438	53	2.6	NA
1087	0.049	14220	175	3.58	2.58	0.71	0.13	1475	244	5.2	0.60
1095	0.054	8185	71	0.79	2.39	0.49	0.12	6085	12	7.5	NA
1102	0.067	17779	84	0.25	2.22	0.47	0.10	1175	11	1.2	NA
1106	0.050	11249	95	0.34	2.82	0.86	0.10	1819	13	2.4	NA

Concentrations on a dry weight basis. TBC - to be completed. Total PAHs is the sum of 39 individual compounds, total PCBs is the sum of 110 congeners, total DDX is the sum of o,p+pp forms of DDD, DDE, and DDT, and total chlordane is the sum of alpha+gamma chlordane, heptachlor, heptachlor epoxide, oxychlordane, nonachlor and nonachlor epoxide (See Appendix I).

Table 10. Concentrations of various parameters for Core LSP.

CHEM ID	Interval	Mid-Point	Solids	Age Model	$\delta^{13}C$	$\delta^{15}N$	TC	TN	C/N
	cm	cm	%	yr	per mil	per mil	%	%	Atomic
0429	0-2	1	27.6	NC	-27.81	3.95	9.10	0.56	19.08
0432	6-8	7	41.1	NC	-28.09	3.33	5.62	0.35	18.54
0464	70-72	71	34.9	NC	-22.25	2.69	4.56	0.25	21.25
0478	98-100	99	58.1	NC	-23.64	4.05	2.00	0.13	17.99
0479	100-102	101	59.5	NC	-23.56	3.45	1.84	0.12	18.29

CHEM ID	TSP	Fe	Zn	tPAHs	T PCBs	tDDXs	tChlordanes	tDioxins	tFurans	2,3,7,8 TCDD-TEQ	tPBDEs
	%	µg/g dw	µg/g dw	µg/g dw	ng/g dw	ng/g dw	ng/g dw	pg/g dw	pg/g dw	pg/g dw	ng/g dw
0429	0.137	19998	350	13.35	673.0	75.32	150.8	5322	223	5.5	NA
0432	0.127	13127	216	8.41	615.9	40.86	82.4	7684	316	7.7	NA
0464	0.180	60668	412	19.45	3456.3	53.67	52.9	7214	744	11.3	NA
0478	0.083	24466	214	2.26	474.8	19.44	13.3	3042	599	5.1	NA
0479	0.065	21275	168	1.78	303.1	16.25	9.0	2950	379	4.2	NA

Concentrations on a dry weight basis. NA – Not analyzed. Total PAHs is the sum of 39 individual compounds, total PCBs is the sum of 110 congeners, total DDX is the sum of o,p+pp forms of DDD, DDE, and DDT, and total chlordane is the sum of alpha+gamma chlordane, heptachlor, heptachlor epoxide, oxychlordane, nonachlor and nonachlor epoxide (See Appendix I).

Table 11. Concentrations of various parameters for Core WS.

CHEM ID	Interval	Mid-Point	Solids	Age Model	$\delta^{13}C$	$\delta^{15}N$	TC	TN	C/N
	cm	cm	%	yr	per mil	per mil	%	%	Atomic
0480	0-2	1	32.4	NC	-25.81	5.02	4.42	0.34	14.94
0483	6-8	7	37.2	NC	-25.83	4.78	4.25	0.28	17.68
0491	22-24	23	42.0	NC	-25.43	4.97	4.02	0.31	15.01
0504	48-50	49	44.6	NC	-25.94	4.53	3.80	0.28	15.95
0513	66-68	67	41.0	NC	-25.80	4.80	4.37	0.30	16.88
0527	94-96	95	44.8	NC	-25.09	5.67	3.73	0.31	13.91

CHEM ID	TSP	Fe	Zn	tPAHs	T PCBs	tDDXs	tChlordanes	tDioxins	tFurans	2,3,7,8 TCDD-TEQ	tPBDEs
	%	µg/g dw	µg/g dw	µg/g dw	ng/g dw	ng/g dw	ng/g dw	pg/g dw	pg/g dw	pg/g dw	ng/g dw
0480	0.174	48519	367	10.00	197.0	25.91	8.15	14339	1331	13.9	NA
0483	0.140	45526	876	9.58	171.4	25.62	7.26	9174	937	12.8	NA
0491	0.157	48905	881	10.50	76.0	10.64	3.39	8963	954	12.0	NA
0504	0.132	52173	974	11.10	236.4	24.56	8.33	4912	409	5.7	NA
0513	0.166	55448	1130	8.14	120.1	10.83	3.06	13321	2552	39.3	NA
0527	0.157	47092	1139	10.24	199.3	16.93	5.67	12049	2061	41.5	NA

Concentrations on a dry weight basis. NA – Not analyzed. Total PAHs is the sum of 39 individual compounds, total PCBs is the sum of 110 congeners, total DDX is the sum of o,p+pp forms of DDD, DDE, and DDT, and total chlordane is the sum of alpha+gamma chlordane, heptachlor, heptachlor epoxide, oxychlordane, nonachlor and nonachlor epoxide (See Appendix I).

Table 12. List of compounds in Figure 17.

PAH Compound	Cmpd #
Naphthalene	1
biphenyl	2
Acenaphthylene	3
Acenaphthene	4
Fluorene	5
Dibenzothiophene	6
Phenanthrene	7
Anthracene	8
Fluoranthene	9
BenzoAfluorene	10
BenzoBfluorene	11
Pyrene	12
Cyclopenta[cd]pyrene	13
Chrysene + Triphenylene	14
Naphthacene	15
Benzo[b]fluoranthene	16
Benzo[k]fluoranthene	17
Benzo[e]pyrene	18
Benzo[a]pyrene	19
Perylene	20
Indeno[1,2,3-cd]pyrene	21
Dibenzo[a,h+a,c]anthracene	22
Benzo[g,h,i]perylene	23
Coronene	24

Table 13. Diatom Metrics determined from species identification: Brandywine Creek Core.

Core ID/ Depth Interval (cm)	Mid-Depth (cm)	Year	Eutrophentic	Meso/ eurotrophentic	Mesotrophentic	Oligotrophentic
BW2 0-2 cm	1	2006	53.57	18.65	5.36	0.00
BW2 4-6 cm	5	2000	52.17	20.16	4.74	0.00
BW2 8-10 cm	9	1995	58.02	13.07	13.47	0.00
BW2 12-14 cm	13	1990	25.94	0.40	17.43	1.39
BW2 14-16 cm	15	1987	45.56	7.69	3.94	2.96
BW2 18-20 cm	19	1982	39.48	3.37	6.15	10.32
BW2 20-22 cm	21	1979	46.61	2.79	6.18	0.00
BW2 24-26 cm	25	1974	53.58	4.26	5.22	0.77
BW2 28-30 cm	29	1968	58.22	6.53	4.55	0.20
BW2 32-34 cm	33	1963	32.29	5.06	3.84	0.35
BW2 36-38 cm	37	1958	25.75	4.99	1.40	0.20
BW2 38-40 cm	39	1955	34.40	2.00	4.60	0.00
BW2 42-44 cm	43	1950	26.53	1.78	2.18	0.40
BW2 46-48 cm	47	1944	27.17	1.52	1.96	0.43
BW2 50-52 cm	51	1939	30.54	5.39	2.59	0.40

Metrics based on van Dam et al. (1994)

Table 14. Diatom Metrics determined from species identification: Churchmans Marsh Core.

Core ID/ Depth Interval (cm)	Mid-Depth (cm)	Year	Eutrophentic	Meso/ eurotrophentic	Mesotrophentic	Oligotrophentic	Oligo/ mesotrophentic
CM1 0-2 cm	1	2005	76.61	4.29	0.97	0.00	76.61
CM1 4-6 cm	5	1999	81.46	2.96	0.59	0.20	81.46
CM1 8-10 cm	9	1992	71.40	6.06	1.14	0.00	71.40
CM1 12-14 cm	13	1985	71.54	2.17	0.99	0.00	71.54
CM1 16-18 cm	17	1979	74.16	2.78	0.00	0.00	74.16
CM1 20-22 cm	21	1972	63.00	3.80	3.00	0.00	63.00
CM! 24-26 cm	25	1965	57.60	6.80	1.20	0.40	57.60
CM1 28-30 cm	29	1959	42.63	10.61	3.34	1.18	42.63
CM1 32-34 cm	33	1952	45.87	7.87	1.57	0.20	45.87
CM1 36-38 cm	37	1945	27.63	8.75	2.58	0.00	27.63
CM1 42-44 cm	43	1935	33.67	7.77	2.19	0.00	33.67
CM1 48-50 cm	49	1925	39.80	8.20	4.20	0.40	39.80
CM1 56-58 cm	57	1912	35.23	7.24	0.78	0.20	35.23
CM1 64-66 cm	65	1899	40.08	9.13	2.38	0.40	40.08
CM1 72-74 cm	73	1885	32.03	3.92	0.87	0.00	32.03
CM1 80-82 cm	81	1872	35.57	4.25	0.22	1.57	35.57

Metrics based on van Dam et al. (1994)

Table 15. Diatom Metrics determined from species identification: Dravo Marsh Core.

Core ID/ Depth Interval (cm)	Mid-Depth (cm)	Year	Eutrophentic	Meso/ eurotrophentic	Mesotrophentic	Oligotrophentic	Oligo/ mesotrophentic
DM2 0-2 cm	1	2006	64.66	7.57	4.47	0.19	64.66
DM2 4-6 cm	5	2000	71.79	3.55	2.37	0.00	71.79
DM 8-10 cm	9	1995	67.13	6.53	4.36	0.20	67.13
DM2 12-14 cm	13	1990	69.41	3.73	4.31	0.78	69.41
DM2 16-18 cm	17	1984	55.45	3.96	1.78	0.40	55.45
DM2 20-22 cm	21	1979	58.27	3.54	3.94	0.20	58.27
DM2 24-26 cm	25	1974	46.22	4.78	0.80	0.20	46.22
DM2 32-34 cm	33	1963	35.39	5.37	0.99	0.20	35.39
DM2 42-44 cm	43	1950	36.67	6.67	1.57	1.57	36.67
DM2 56-58 cm	57	1931	33.27	4.47	2.14	0.58	33.27
DM2 64-66 cm	65	1920	40.59	4.16	2.18	0.20	40.59
DM2 80-82 cm	81	1905	25.84	4.57	5.96	0.00	25.84

Metrics based on van Dam et al. (1994)

Figures

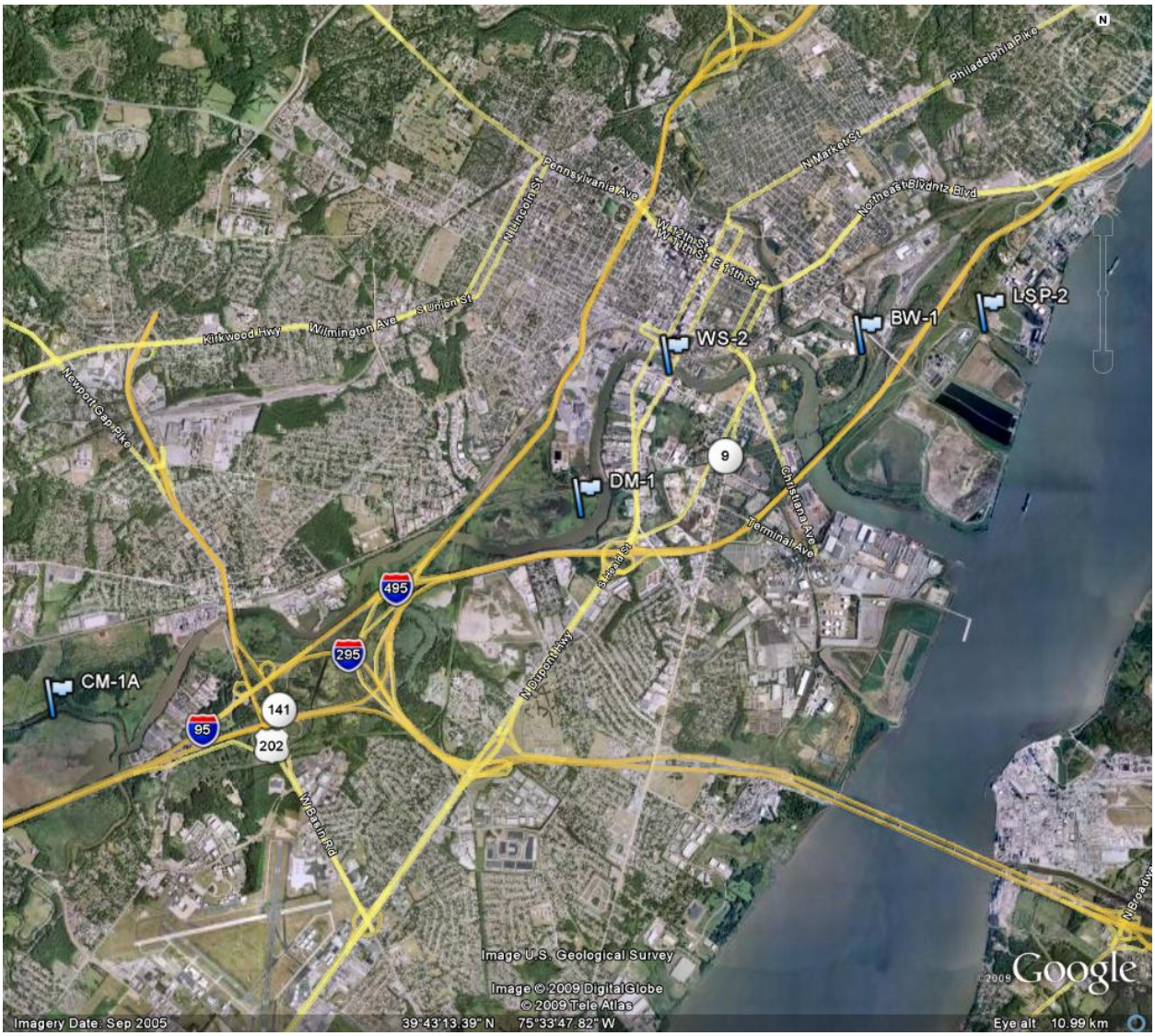

Figure 1. Coring locations within the tidal Christina River system. Key: CM – Churchmans Marsh, DM – Dravo Marsh (Old Wilmington Marsh), WS - Walnut Street embayment, BW-Brandywine wetland, and LSP – Lower Shellpot.

Figure 2. Tripod and pulley system used to retrieve push-piston cores at Dravo Marsh within the tidal Christina River system.

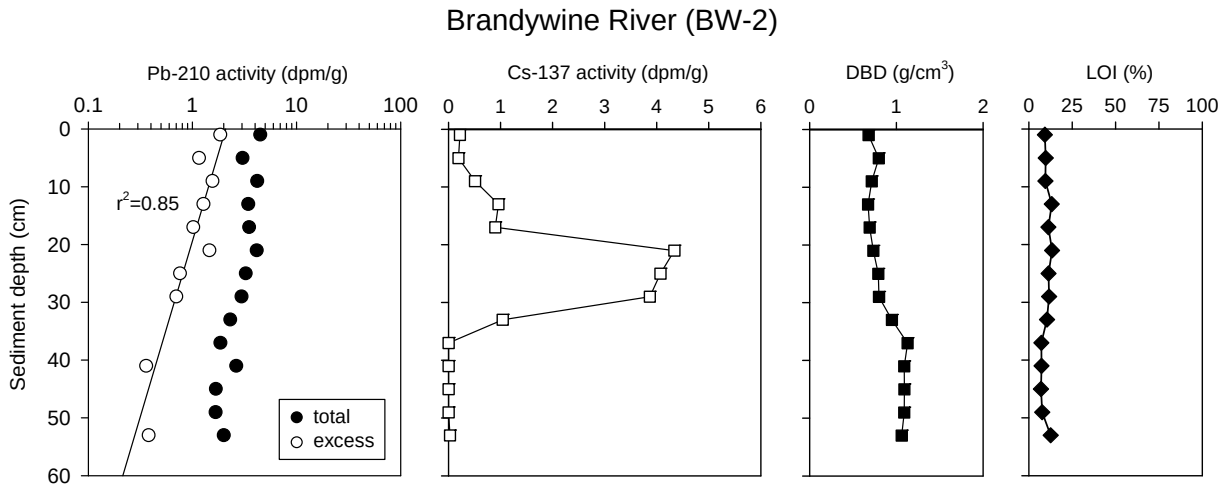

Figure 3. Geochronology for the Brandywine Creek marsh using excess ^{210}Pb and transient fallout ^{137}Cs. The radionuclides give comparable sedimentation rates of 0.80 (constant activity model) and 0.10 cm/yr, respectively. The first occurrence of ^{137}Cs at 36-38 cm is assumed concordant with ca. 1954.

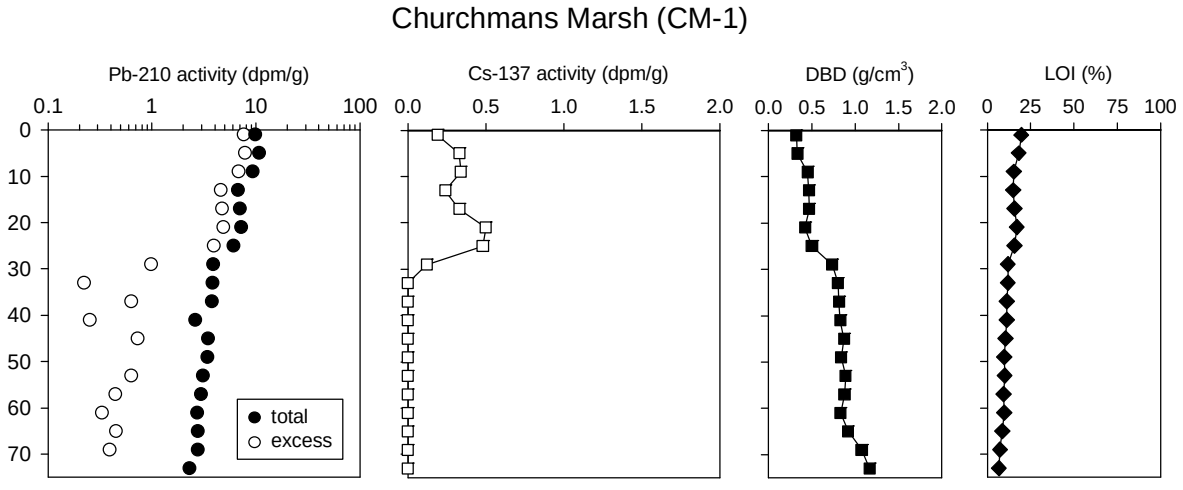

Figure 4. Geochronology for the Churchmans Marsh using excess ^{210}Pb and transient fallout ^{137}Cs. The radionuclides give comparable sedimentation rates of 0.51 (constant flux model) and 0.60 cm/yr, respectively. The first occurrence of ^{137}Cs at 32-34 cm is assumed concordant with ca. 1954.

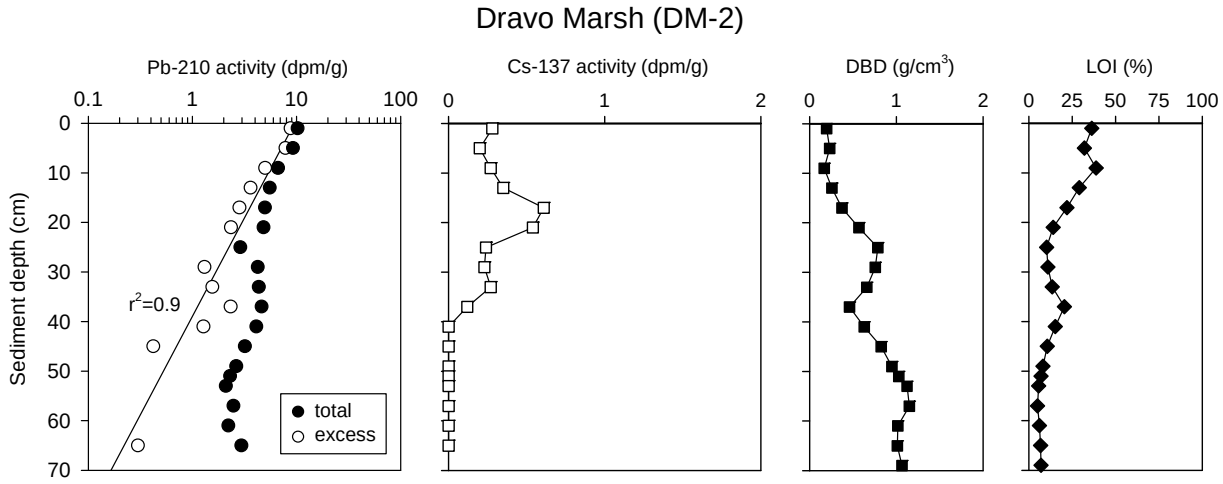

Figure 5. Geochronology for the Dravo Marsh using excess ^{210}Pb and transient fallout ^{137}Cs. The radionuclides give comparable sedimentation rates of 0.56 (constant activity model) and 0.79 cm/yr, respectively. The first occurrence of ^{137}Cs at 38-40 cm is assumed concordant with ca. 1954.

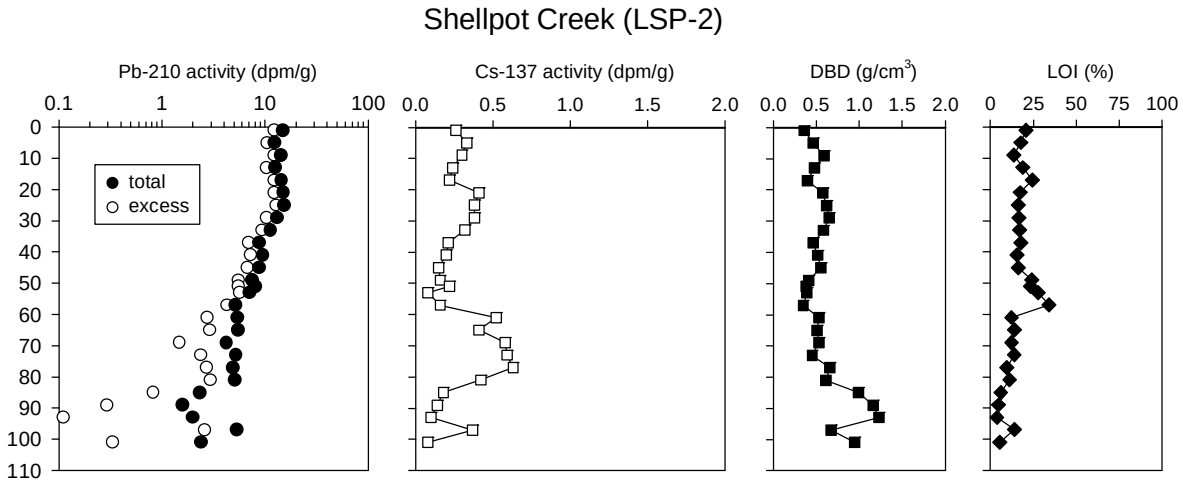

Figure 6. . Geochronology for the Shellpot Creek using excess ^{210}Pb and transient fallout ^{137}Cs. The radionuclides give identical sedimentation rates of 0.19 cm/yr using the constant flux model for ^{210}Pb. The first occurrence of ^{137}Cs at 100-102 cm is assumed concordant with ca. 1954.

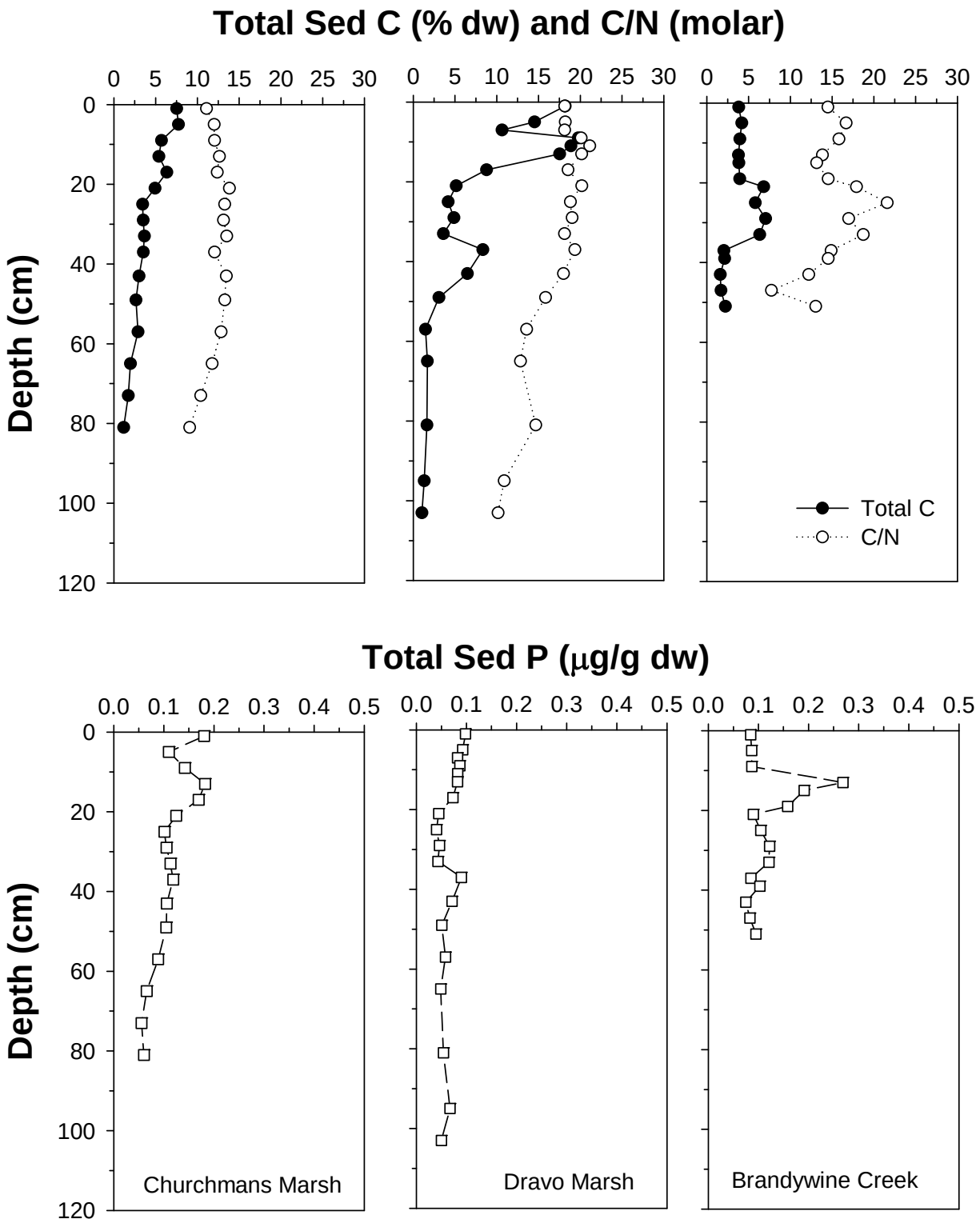

Figure 7a. Sediment organic carbon, C/N and sediment phosphorus distribution with depth for Churchmans, Dravo and Brandywine marshes.

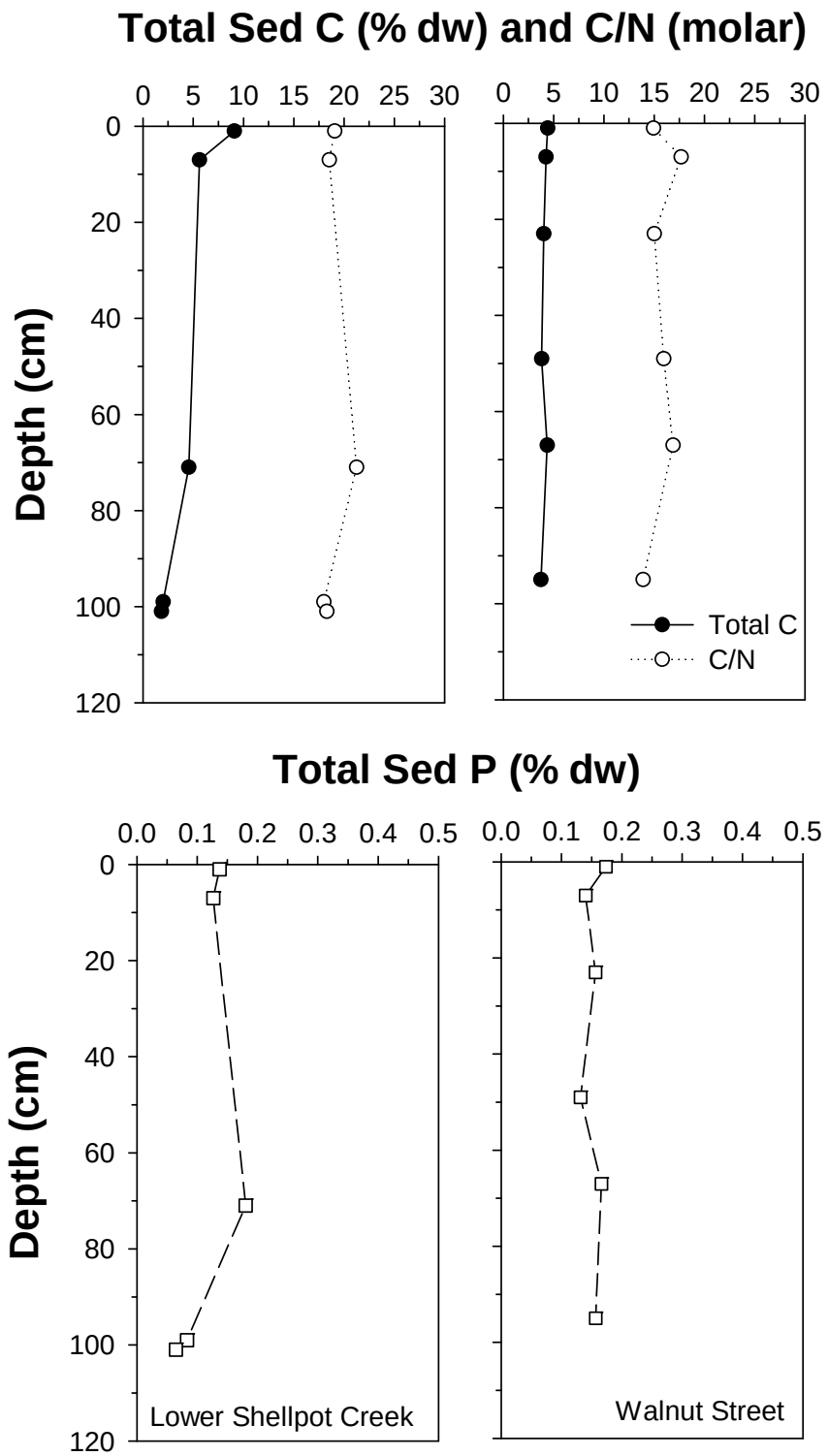

Figure 7b. Sediment organic carbon, C/N and sediment phosphorus distribution with depth for the cores from lower Shellpot Creek and Walnut Street Bridge.

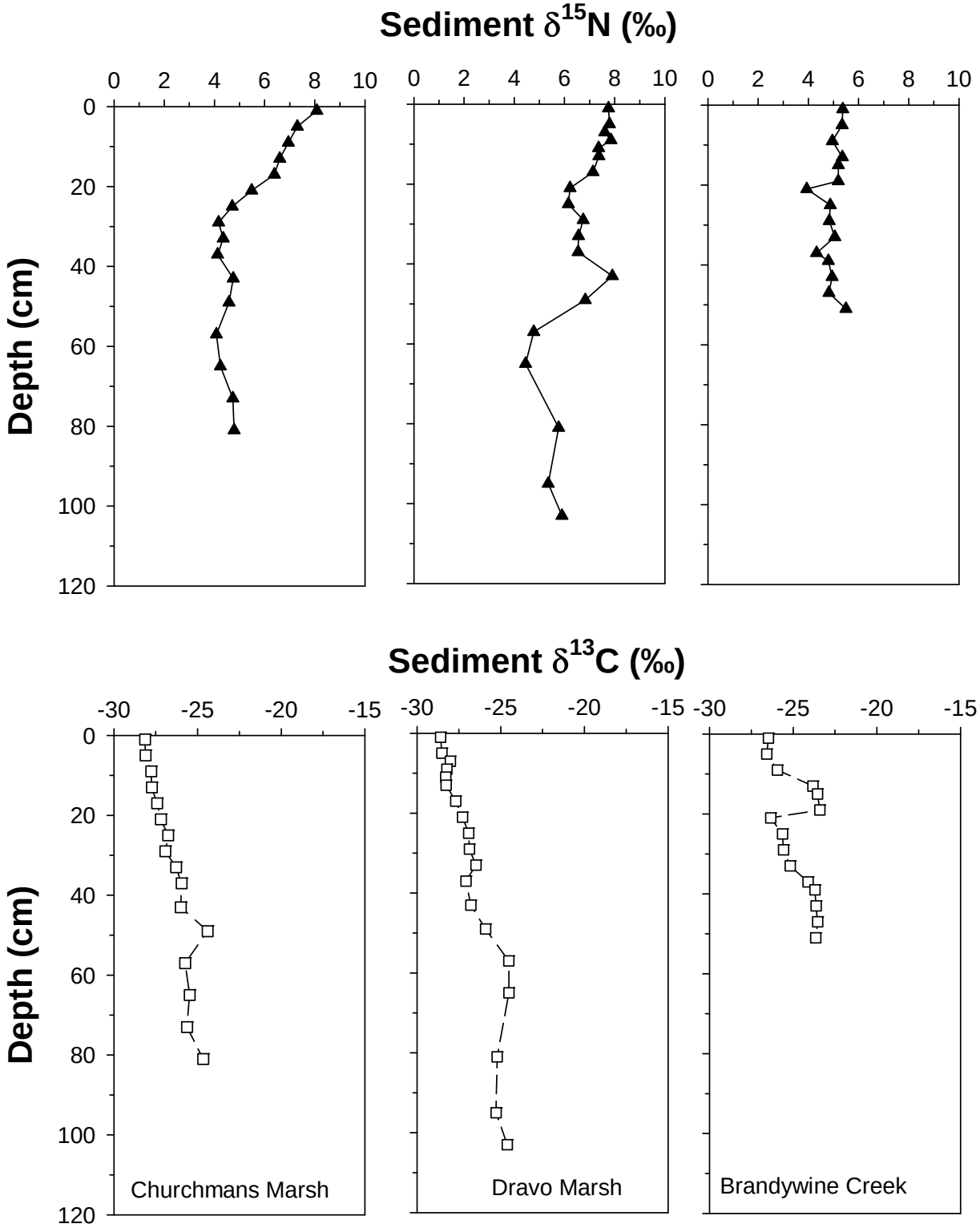

Figure 8. Depth distribution of the isotopic composition sediment N ($\delta^{15}N$) and C ($\delta^{13}C$).

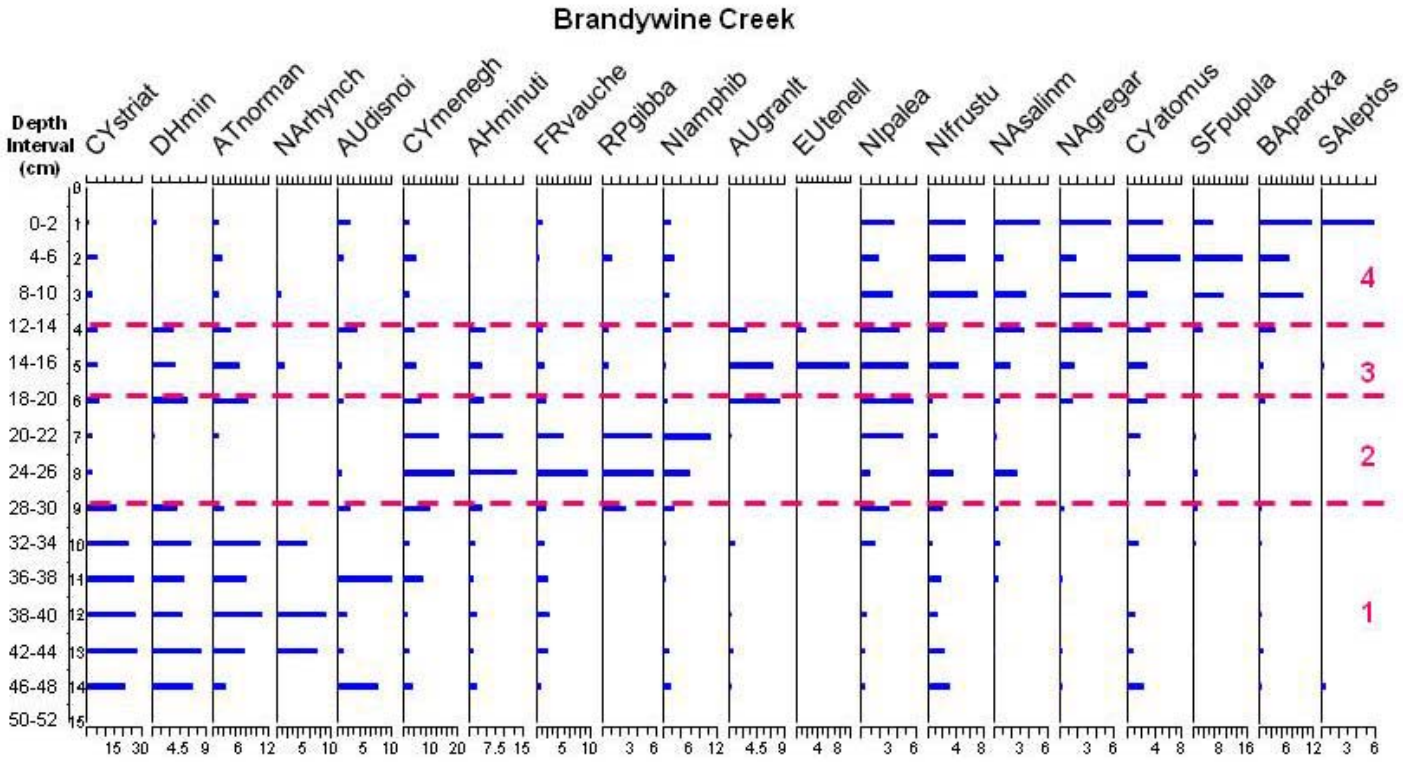

Figure 9a. Distribution of various diatom indicator species with depth in the Brandywine Creek Core.

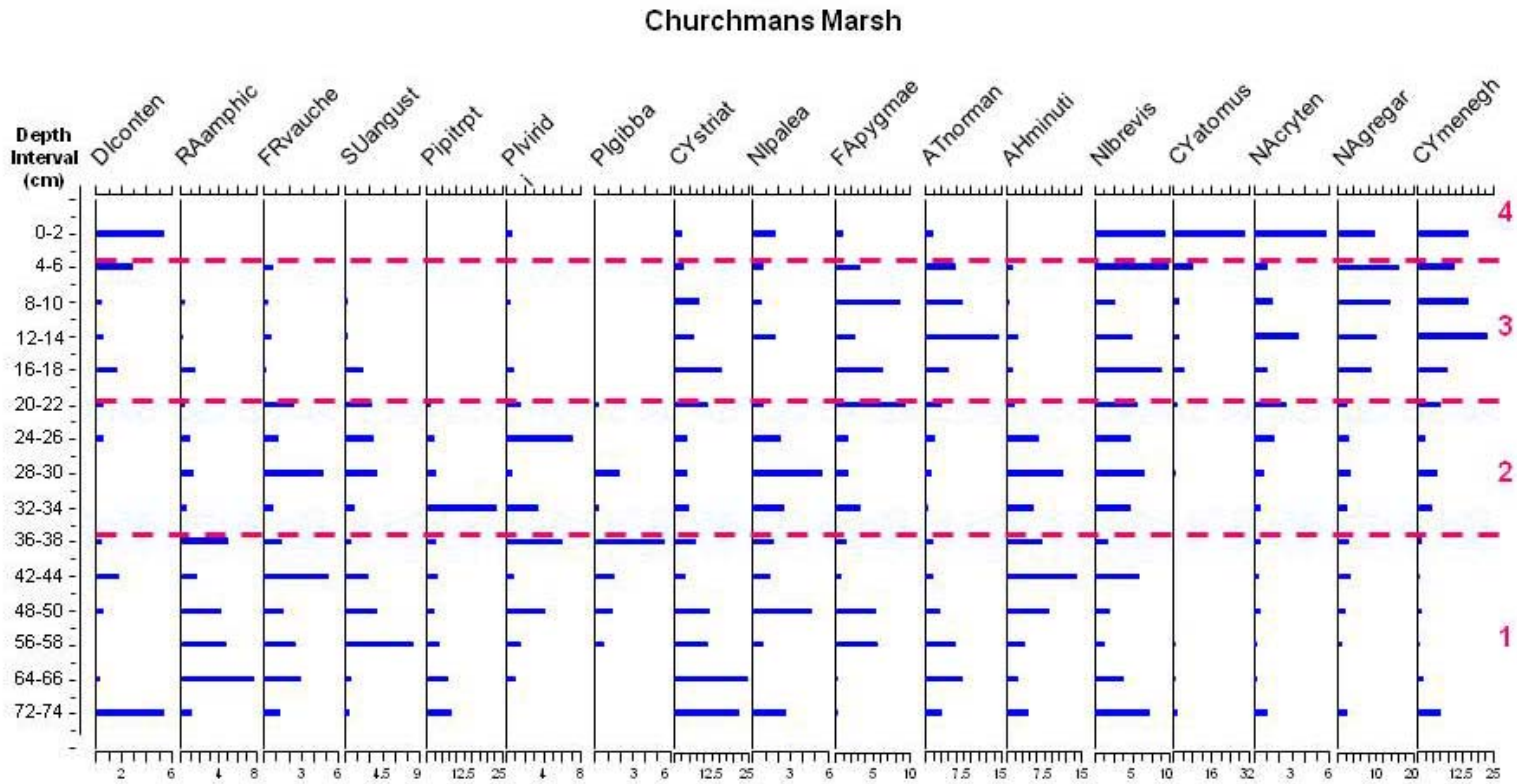

Figure 9b. Distribution of various diatom indicator species with depth in the Churchmans Marsh core.

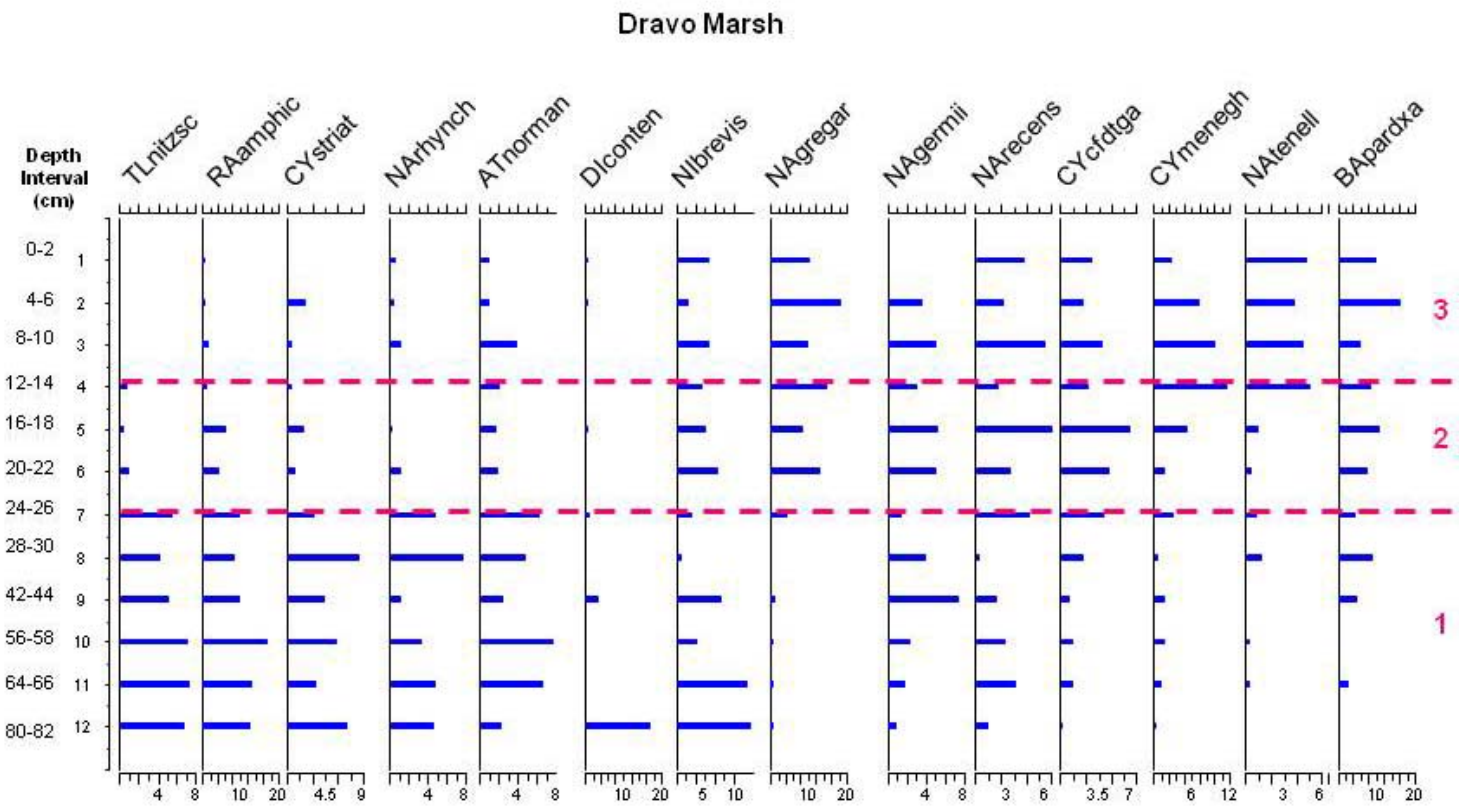

Figure 9c. Distribution of various diatom indicator species with depth in the Dravo Marsh core.

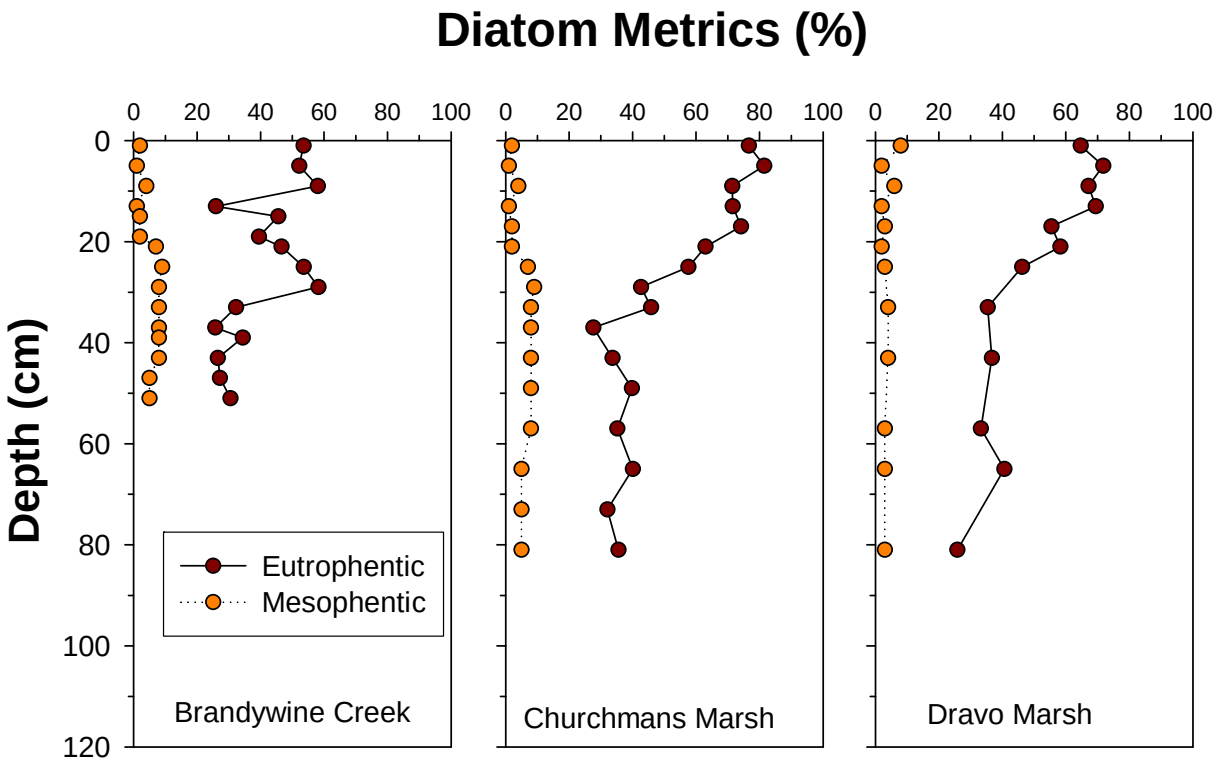

Figure 10. Diatom metrics for the cores of the tidal Christina River using the van Dam et al. (1994).

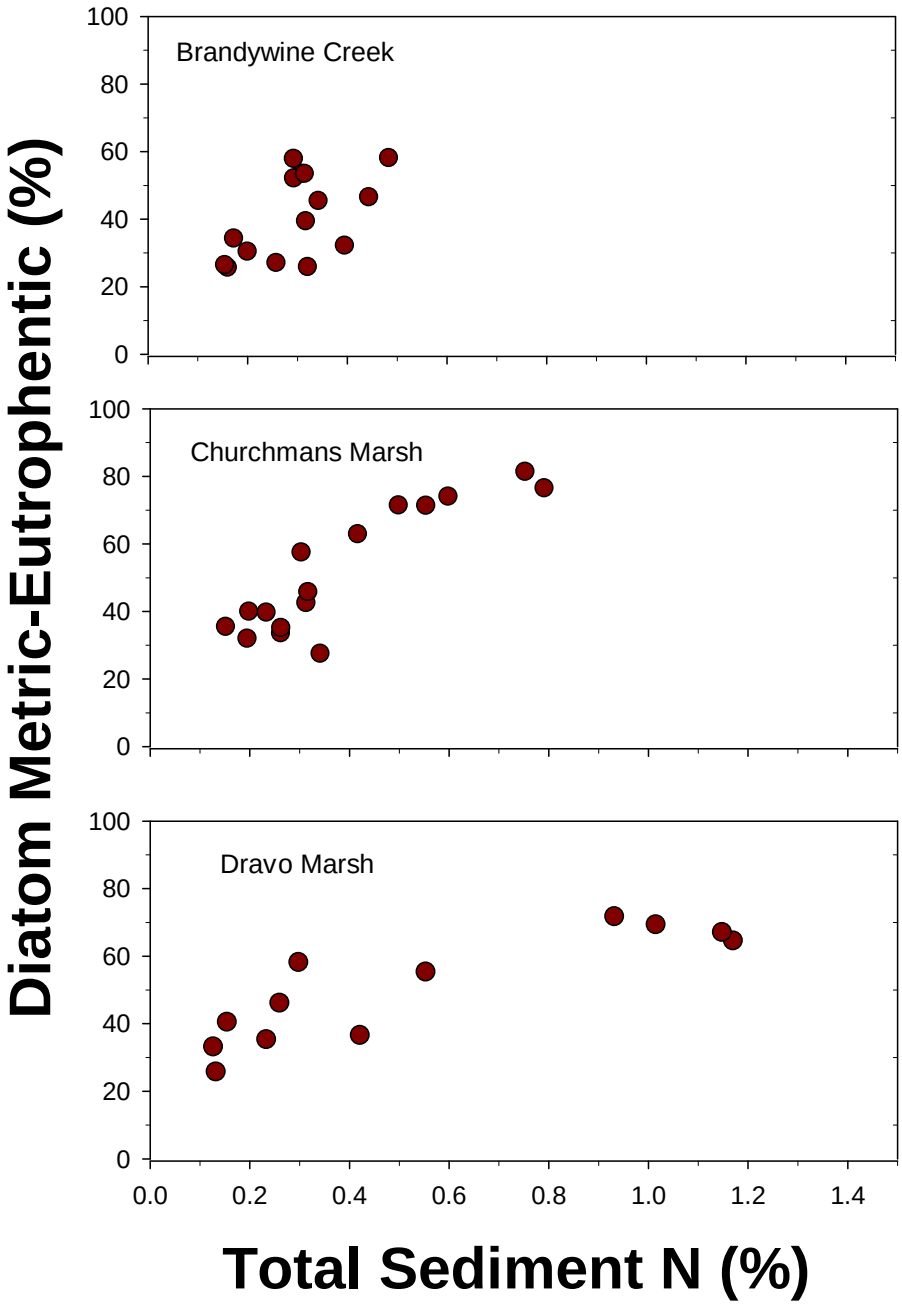

Figure 11. Relationship between total sediment N and the diatom metric for eutrophentic species in each core.

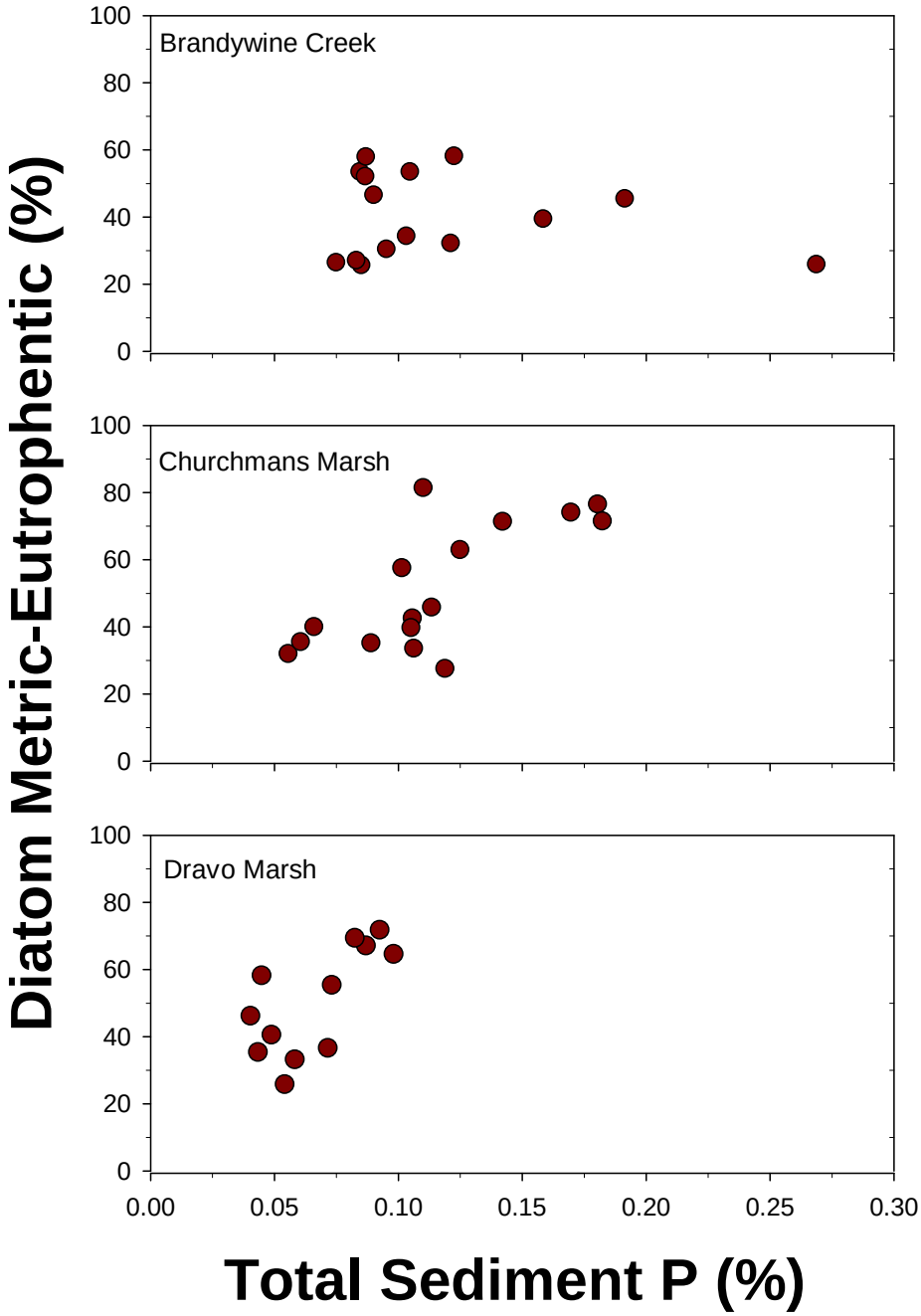

Figure 12. Relationship between total sediment P and the diatom metric for eutrophentic species in each core.

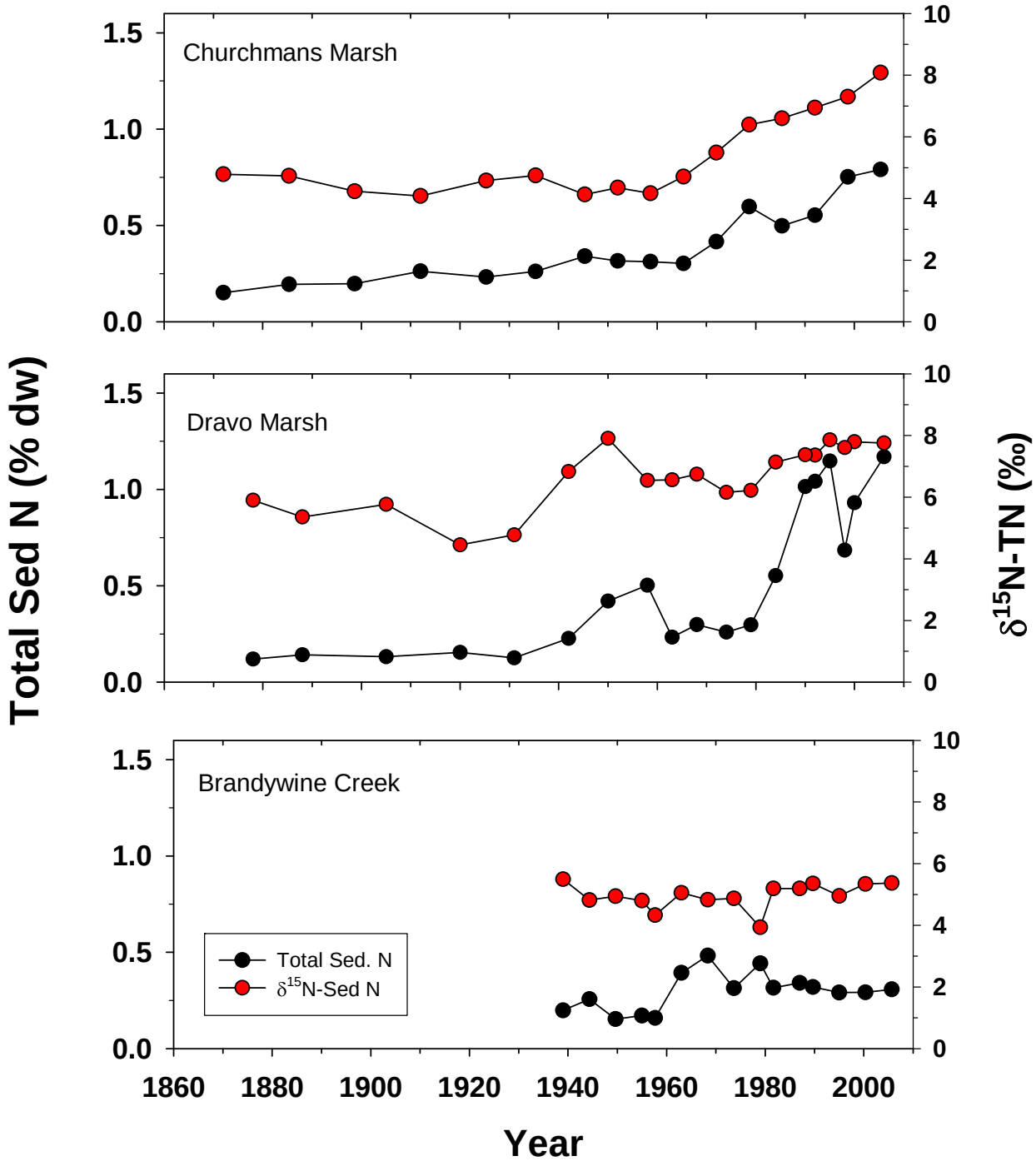

Figure 13. Concentrations of total sediment nitrogen (TN) and the nitrogen isotopic composition of TN (δ^{15}N-TN) from 1860 to 2003.

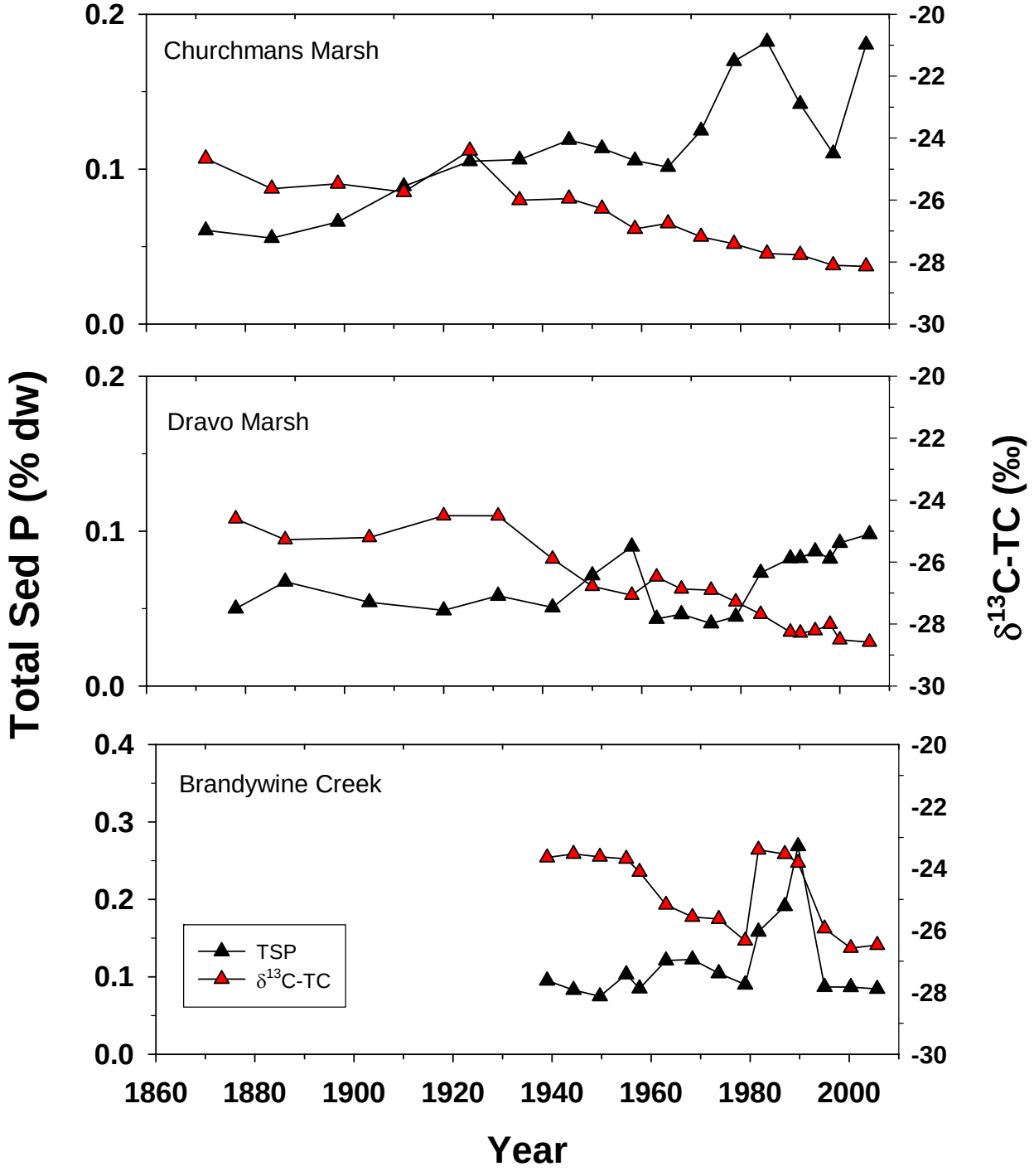

Figure 14. Concentrations of total sediment phosphorus (TSP) and the carbon isotopic composition of total carbon (δ^{13}C-TC) from 1860 to 2003.

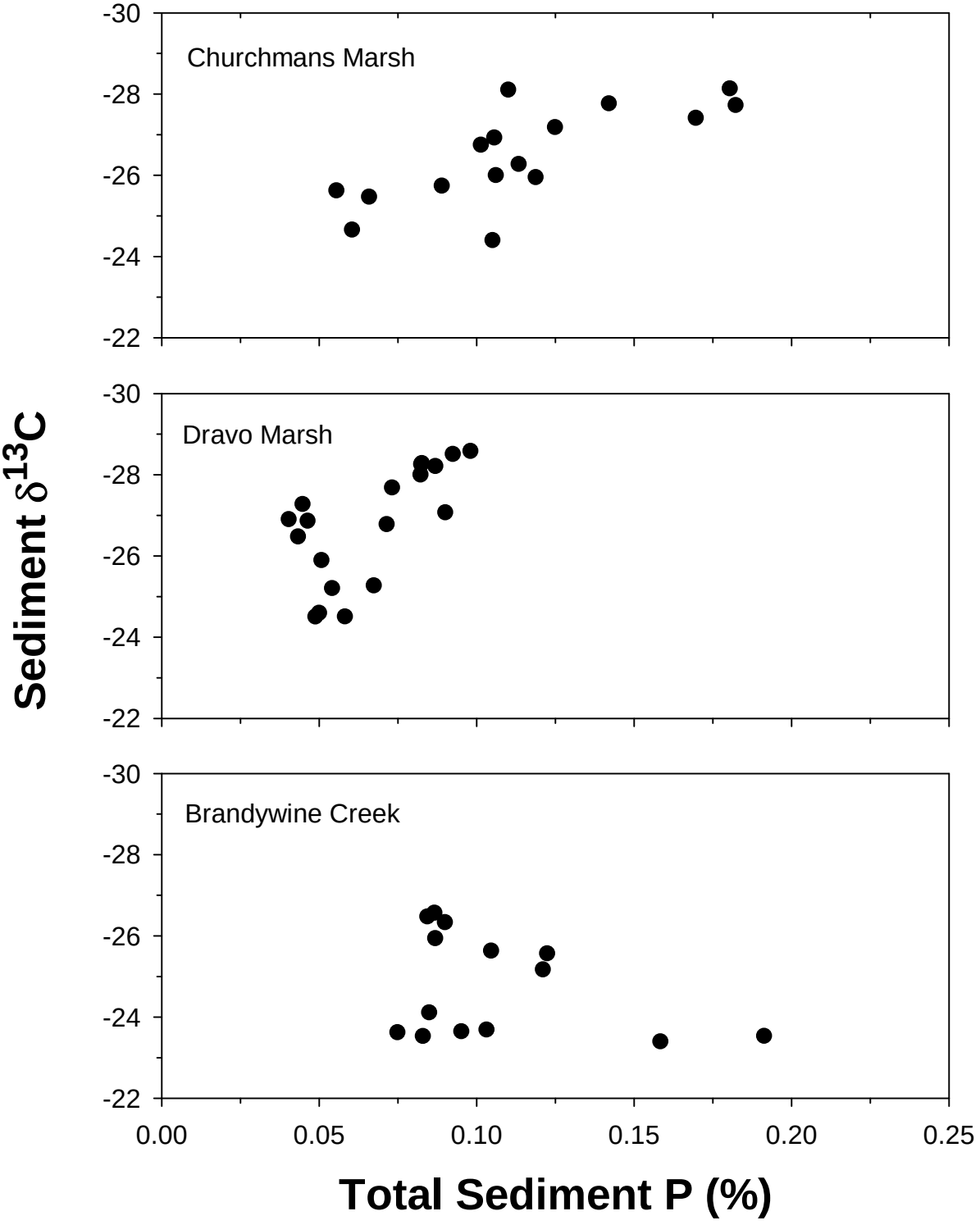

Figure 15. The relationship between total sediment P (TSP) and the carbon isotopic composition of organic matter (δ^{13}C-TC) in Brandywine Creek, Churchmans Marsh, and Dravo Marsh.

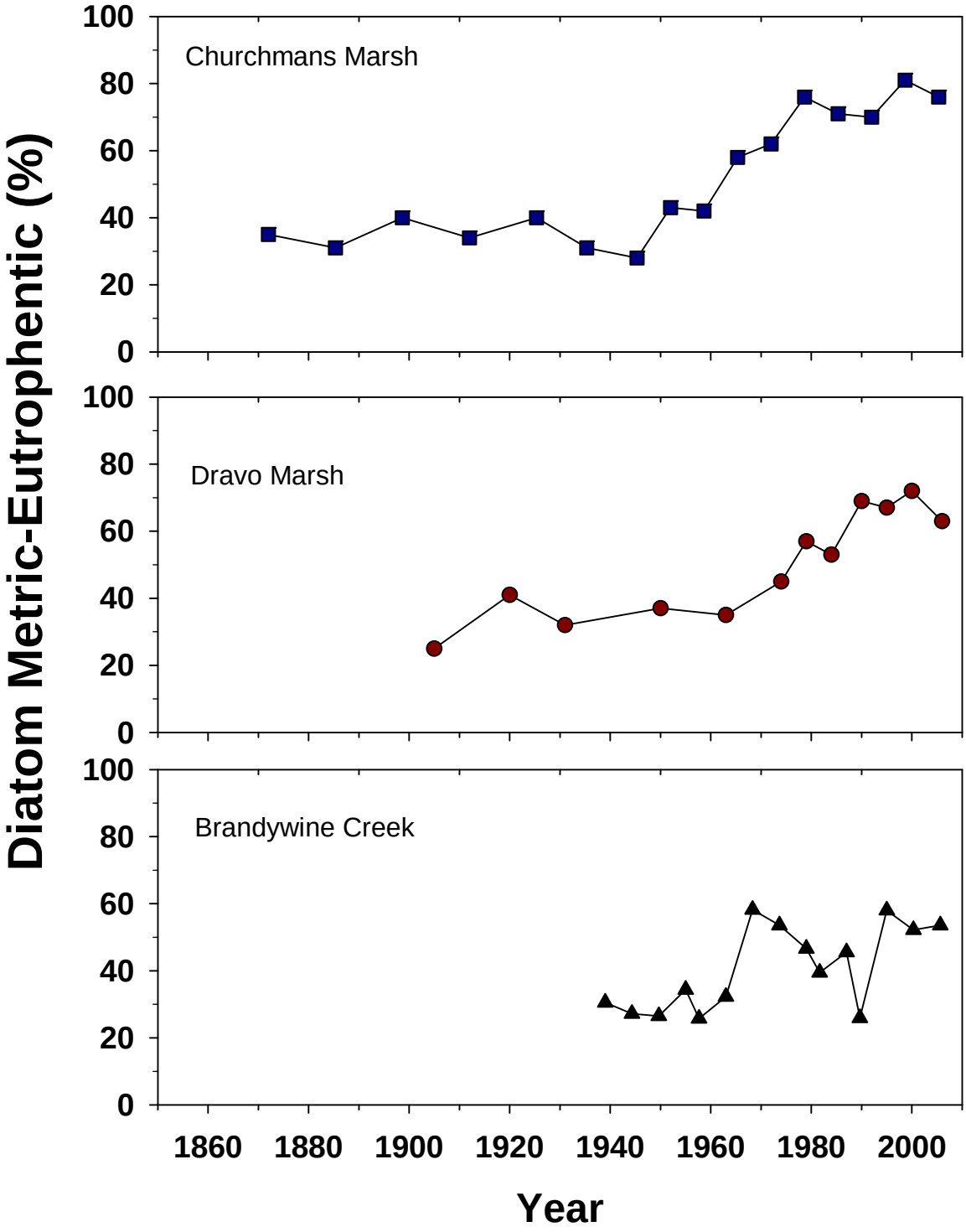

Figure 16. Diatom metric for eutrophentic species from 1860 to 2003.

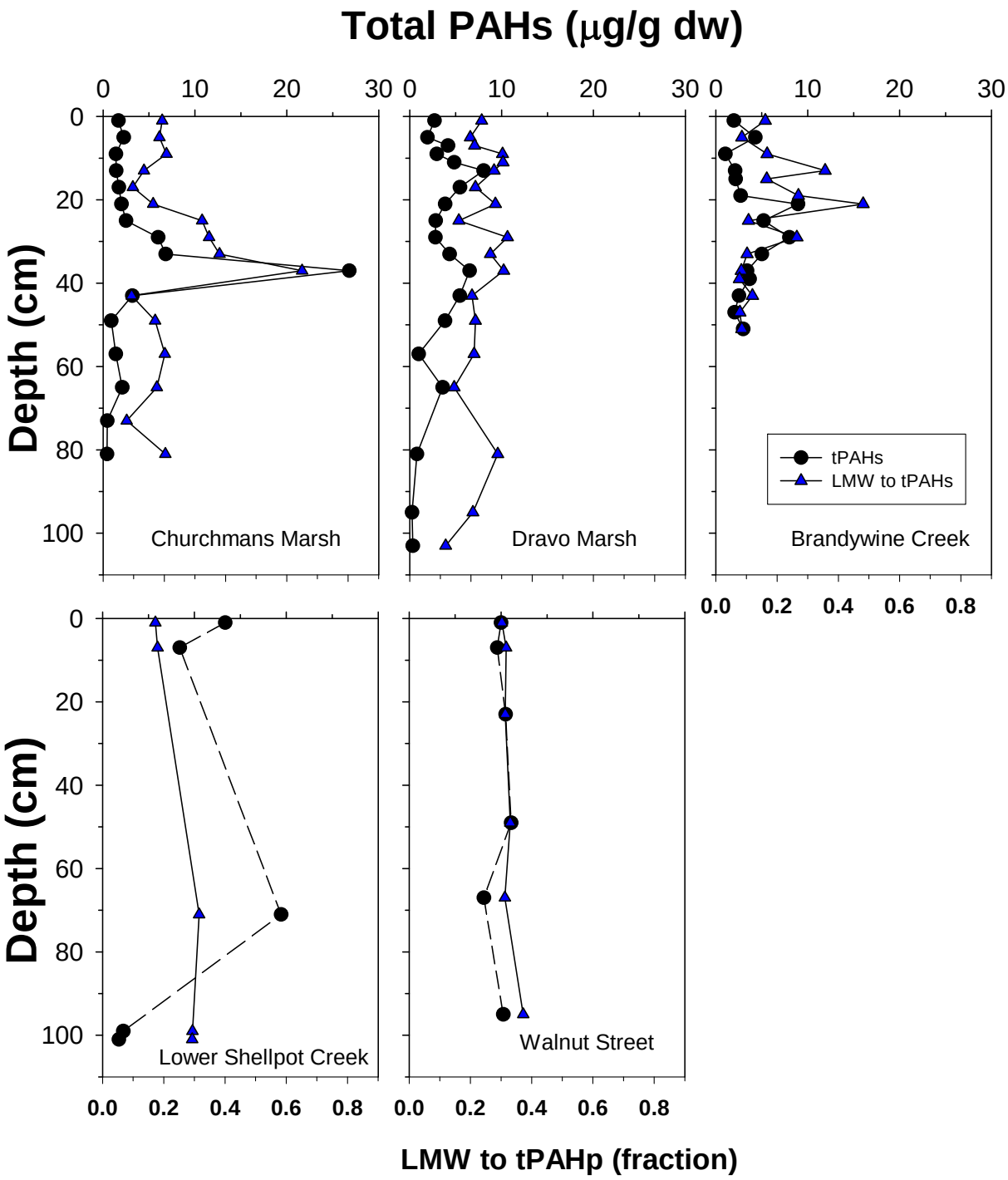

Figure 17. Depth distribution of total polycyclic aromatic hydrocarbons (tPAHs) and the low molecular weight (LMW) to tPAHs in the sediments of the tidal Christina River and Brandywine Creek.

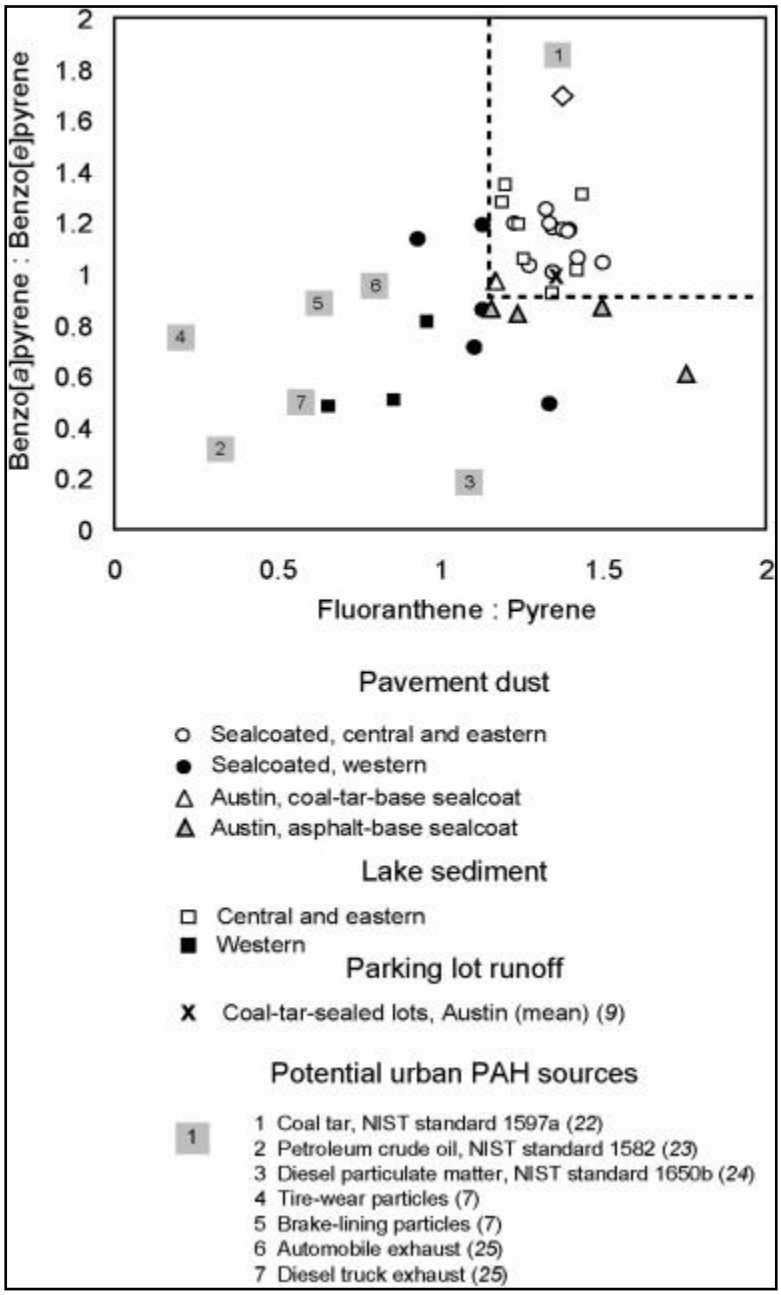

Figure 18. Adapted from Van Metre et al (2009). Comparison of source-indicator ratios of benzo[a]pyrene to benzo[e]pyrene and fluoranthene to pyrene in dust samples, lake samples and seal-coat samples from central and eastern cities (USA). Dashed line indicates approximate separation between samples from central and eastern cities and those from western cities.

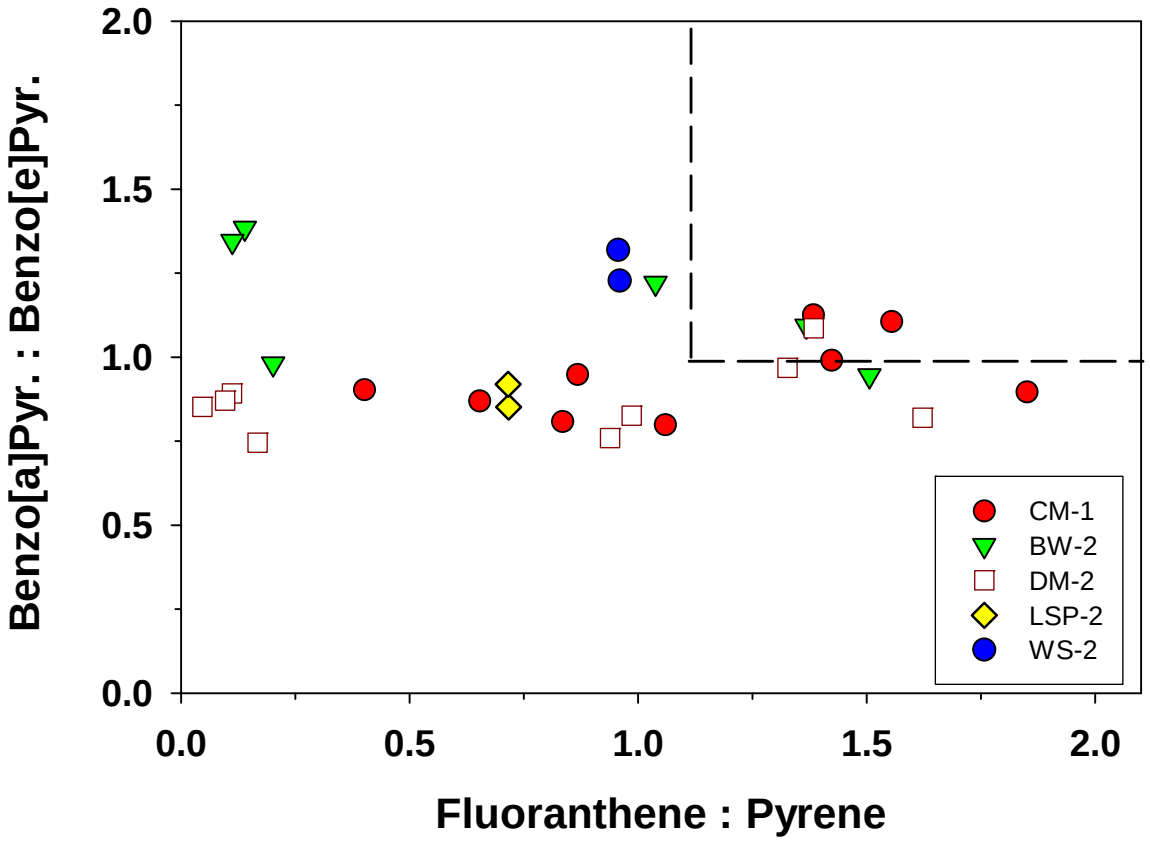

Figure 19. Indicator ratios of benzo[a]pyrene to benzo[e]pyrene and fluoranthene to pyrene in the top sections of all sediment samples collected in the tidal Christina and Brandywine watersheds. The dotted box is related to the area in the van Metre et al. (2009) that suggests high coal tar sealants for parking lots.

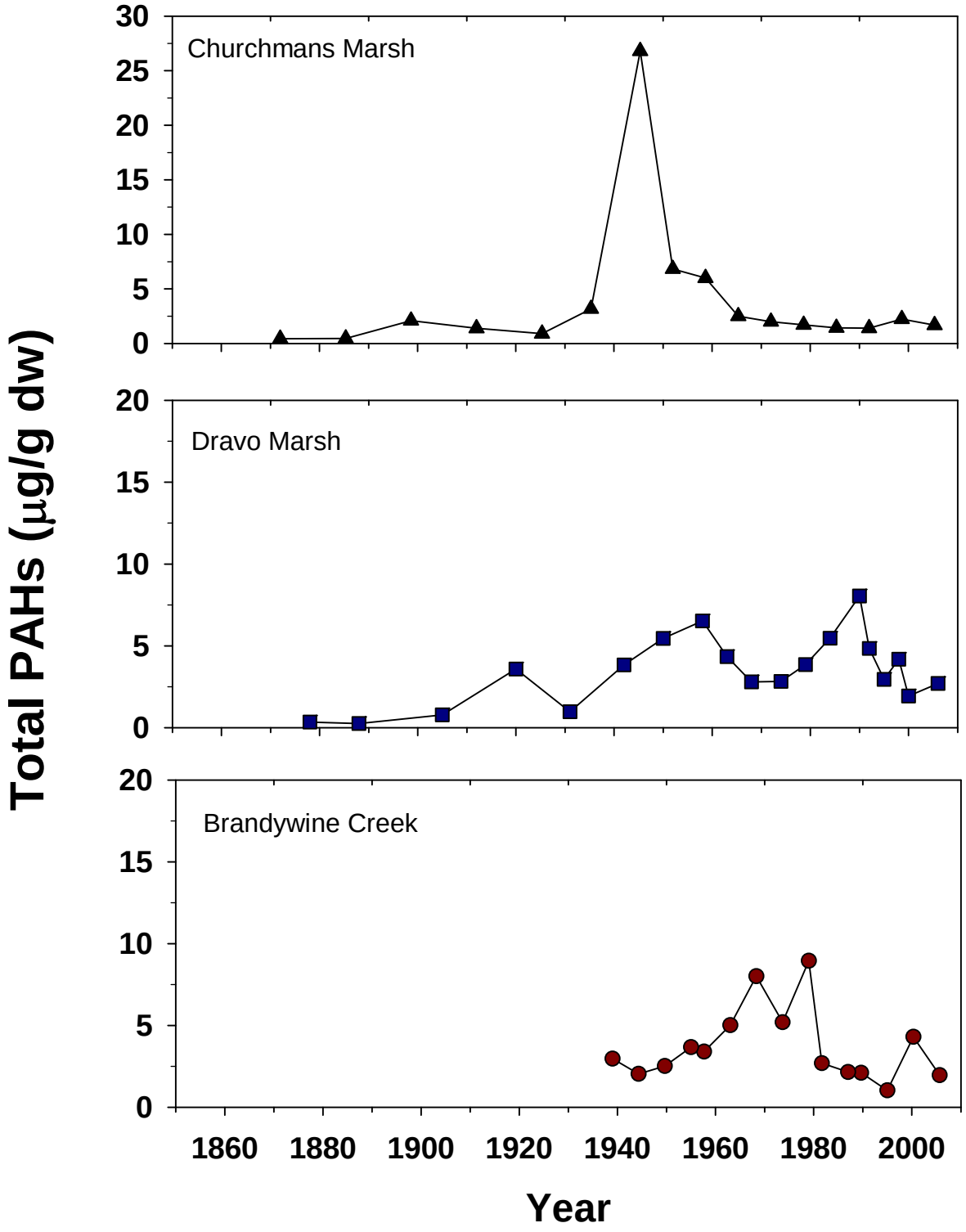

Figure 20. Concentrations of tPAHs from 1860 to 2003 (Note scale change).

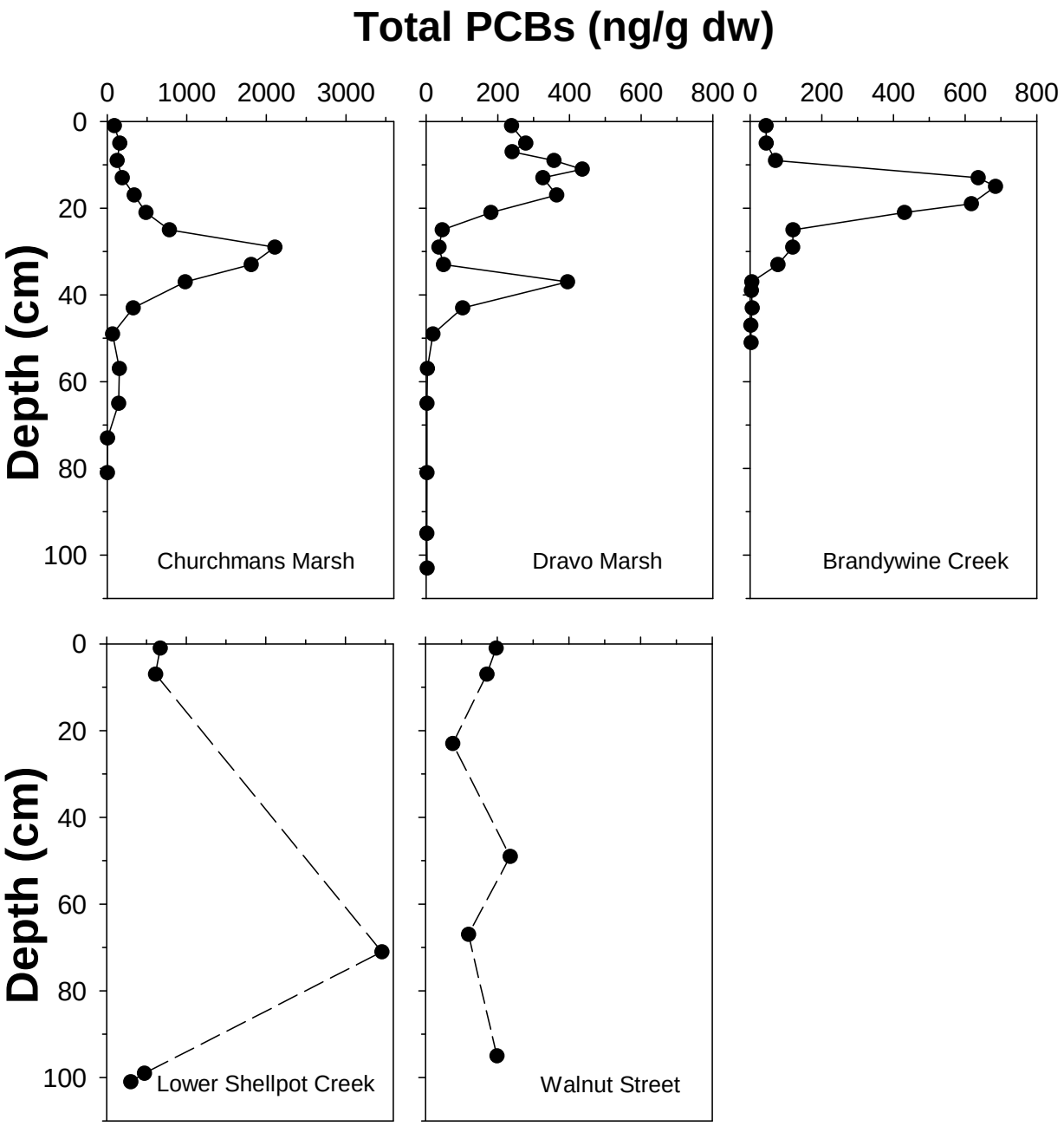

Figure 21. Depth distribution of total PCBs in the five cores in the tidal Christina River and Brandywine Creek.

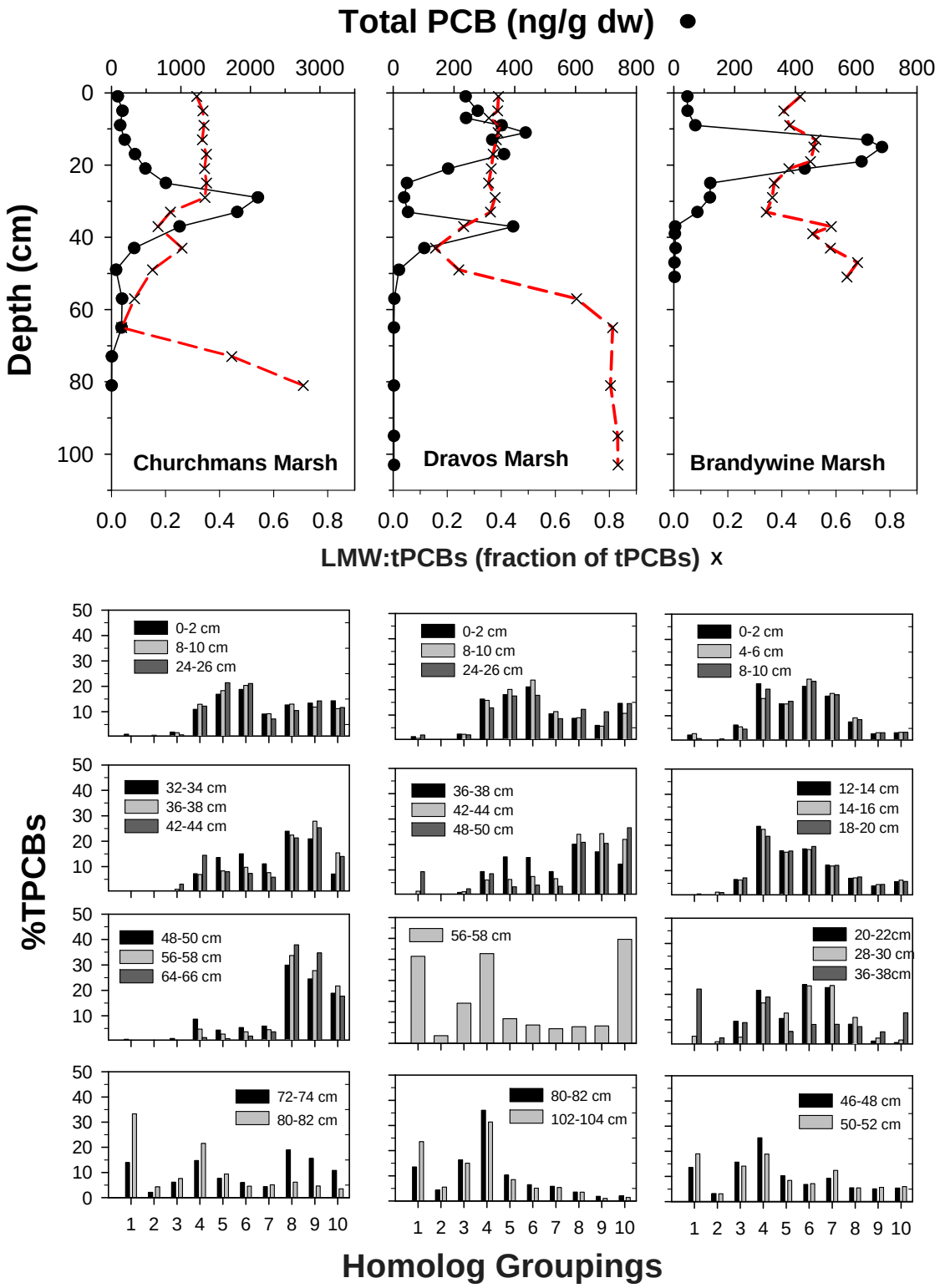

Figure 22a. Depth distribution of total PCBs, LMW to tPCBs ratio and selected homolog distributions with depth.

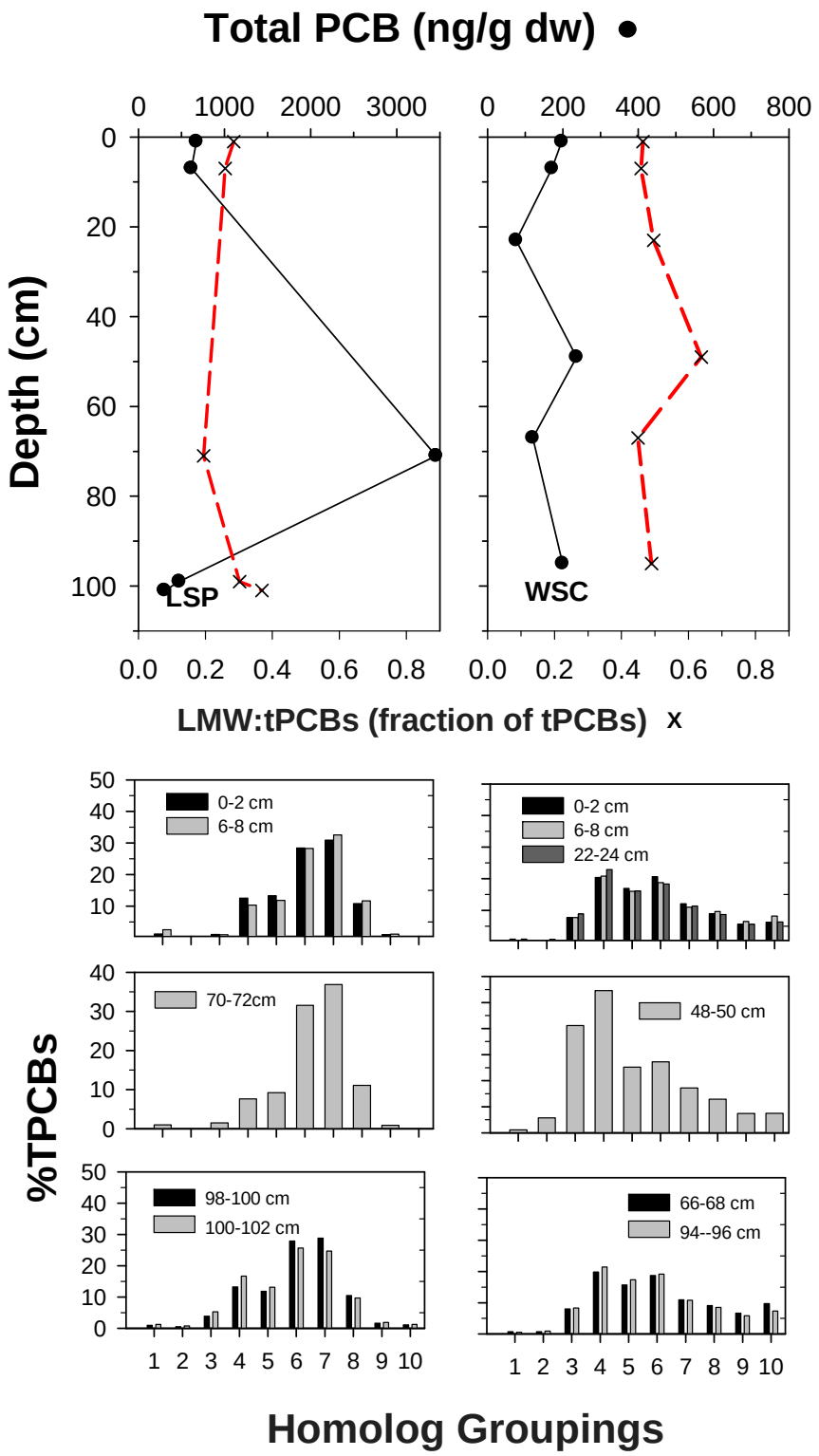

Figure 22b. Depth distribution of total PCBs, LMW to tPCBs ratio and selected homolog distributions with depth

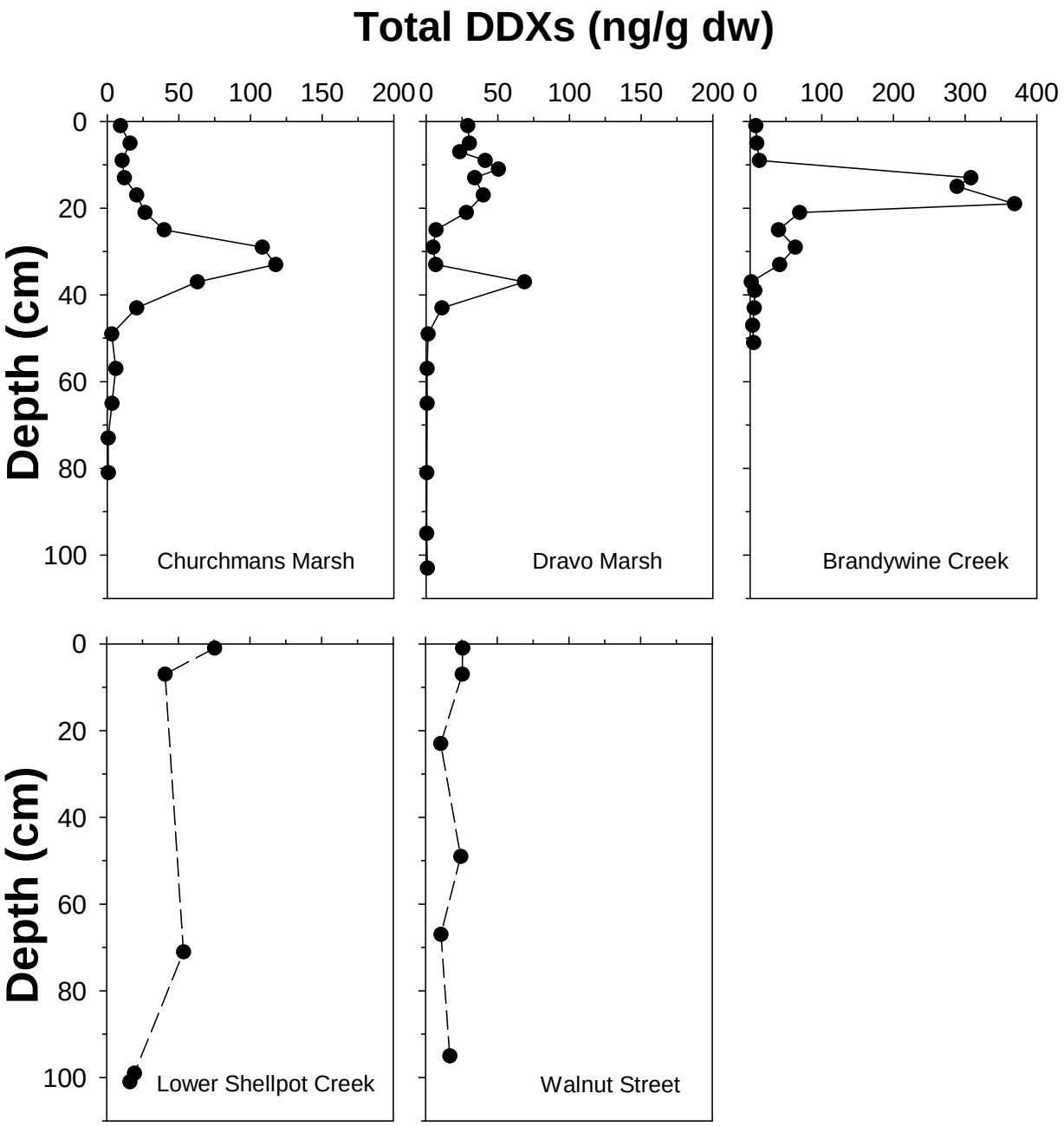

Figure 23. Total DDX (DDT+DDD+DDE all forms) with depth in the tidal Christina River and Brandywine Creek.

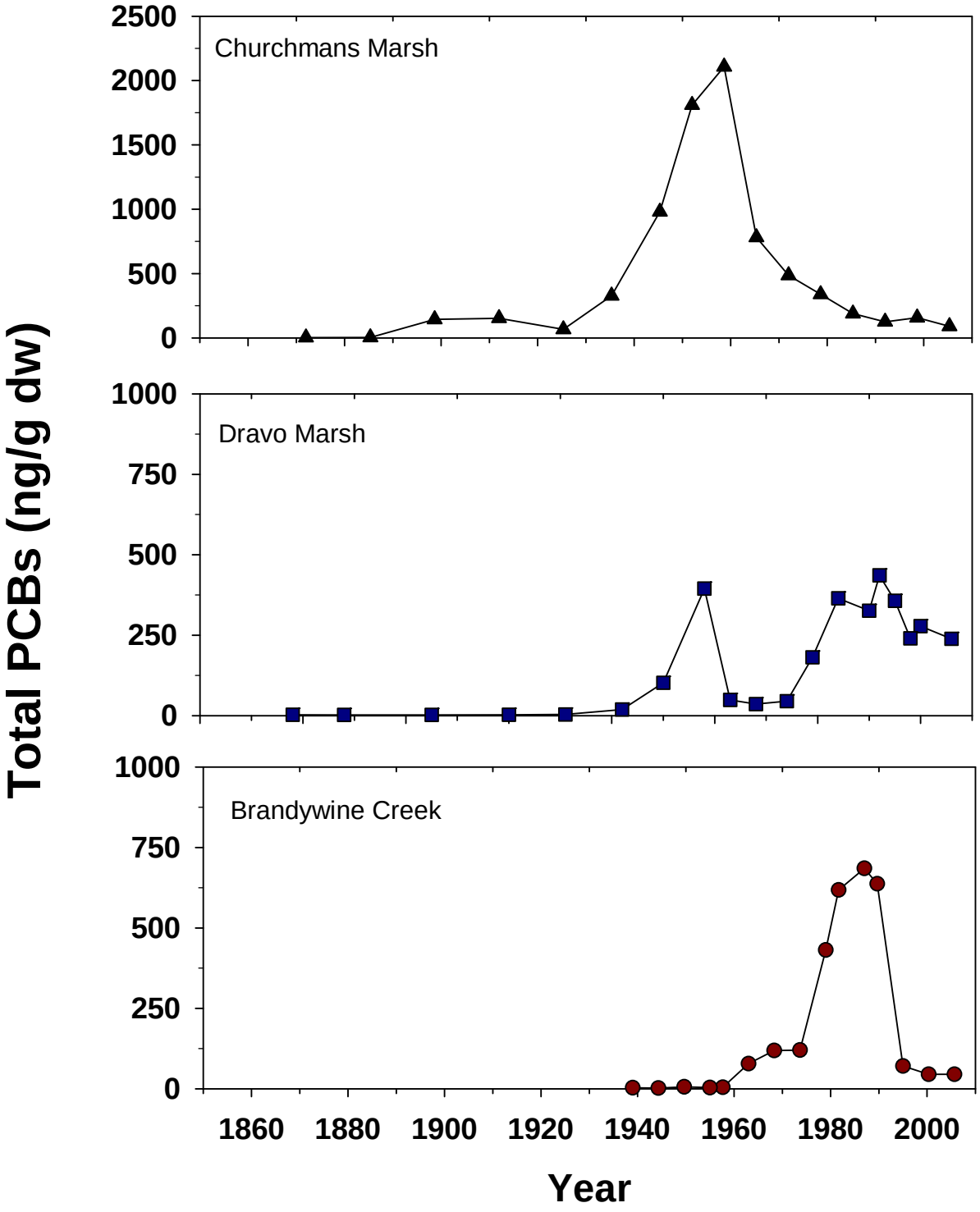

Figure 24. Concentrations of tPCBs from 1860 to 2003 (Note scale change).

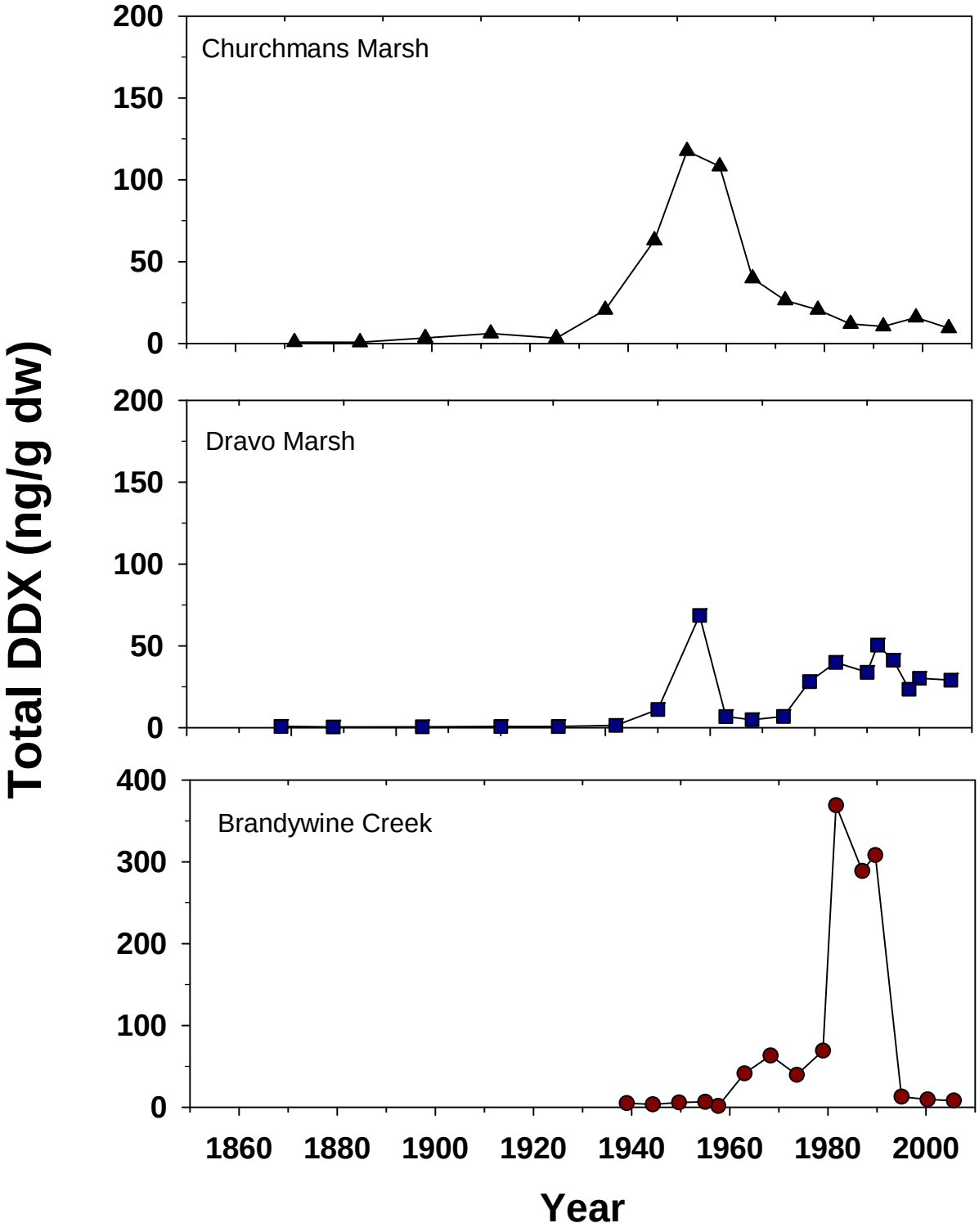

Figure 25. Concentrations of tDDXs from 1860 to 2003 (Note scale change).

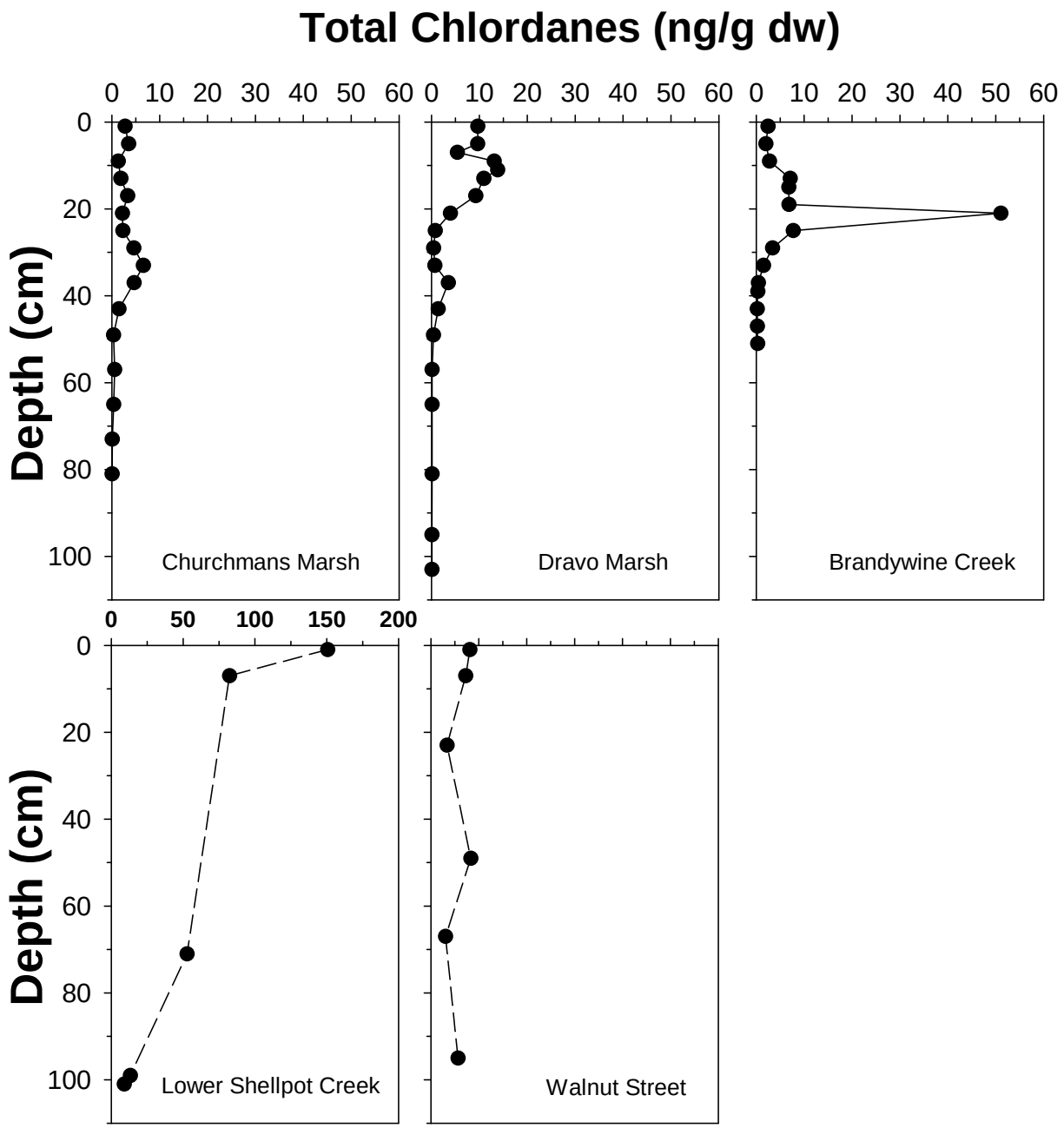

Figure 26. Total chlordane with depth in the tidal Christina River and Brandywine Creek.

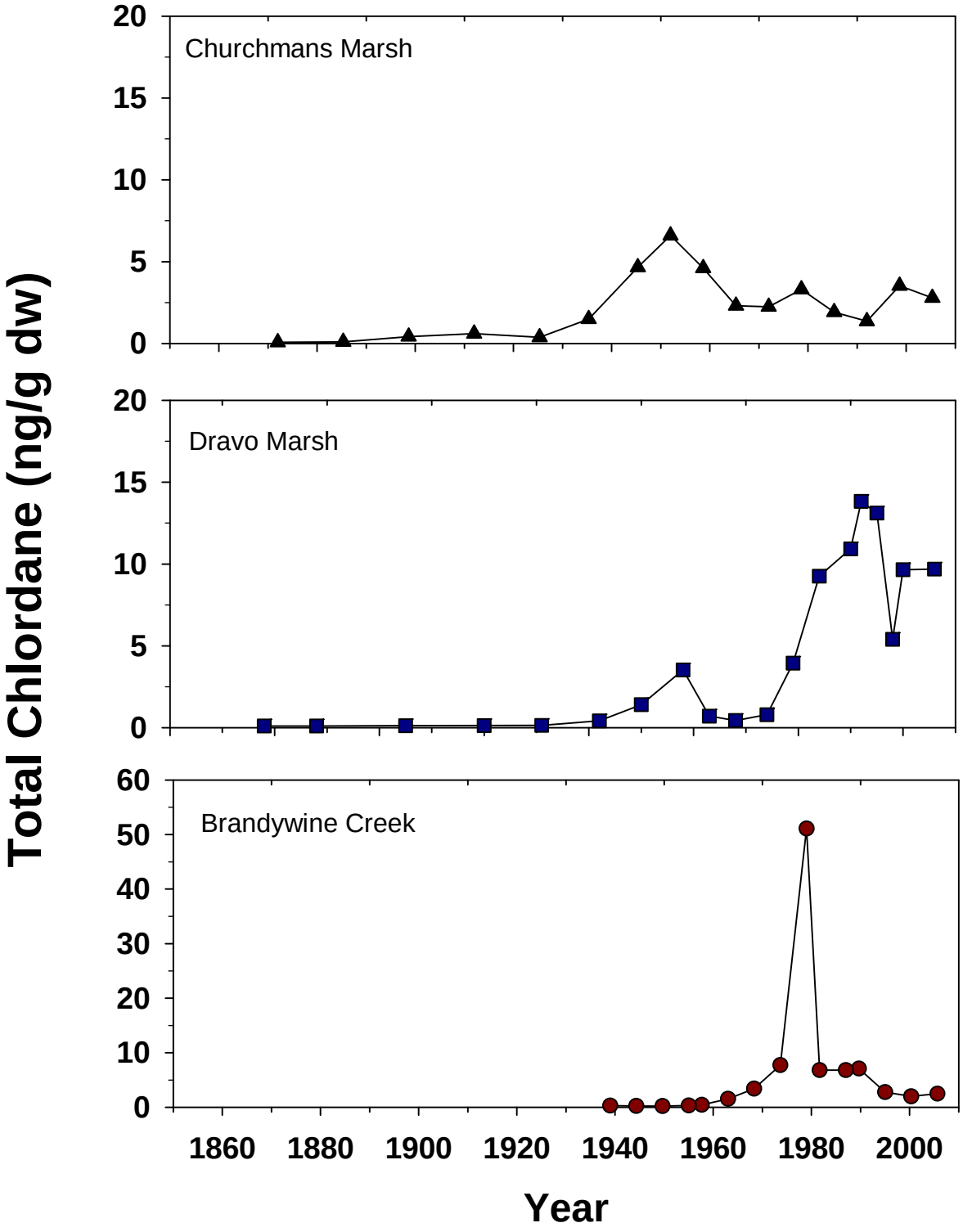

Figure 27. Concentrations of total chlordane from 1860 to 2003 (Note scale change).

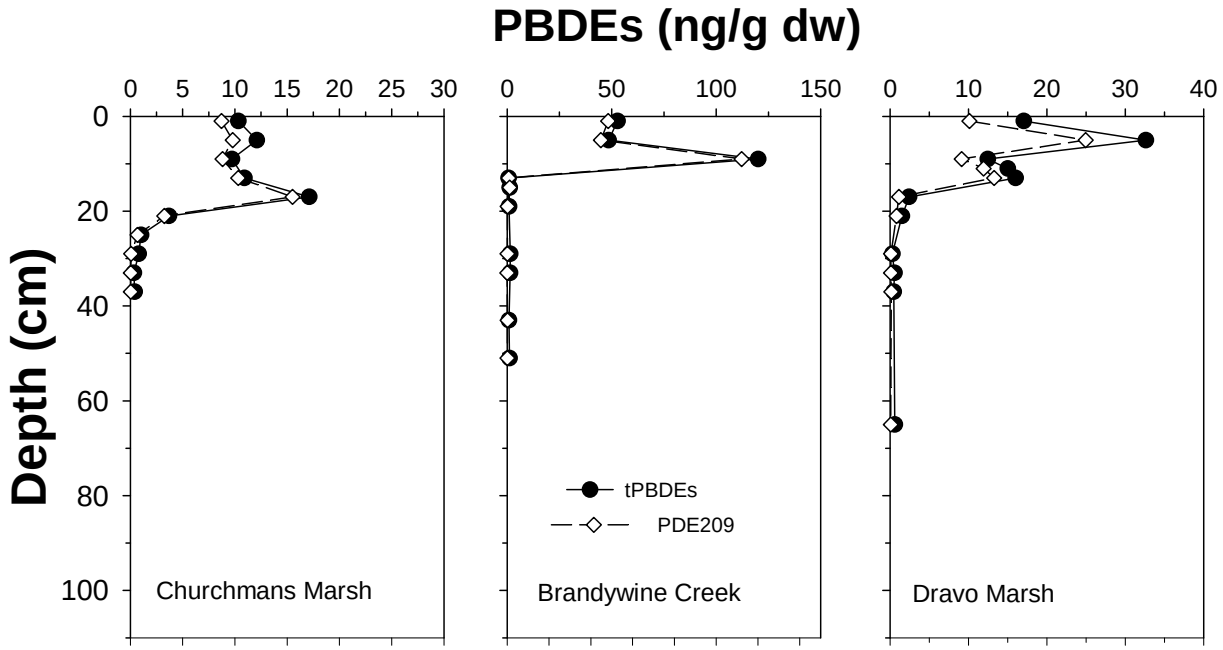

Figure 28. Total PBDEs and the deca congener BDE-209 with depth in the tidal Christina River and Brandywine Creek.

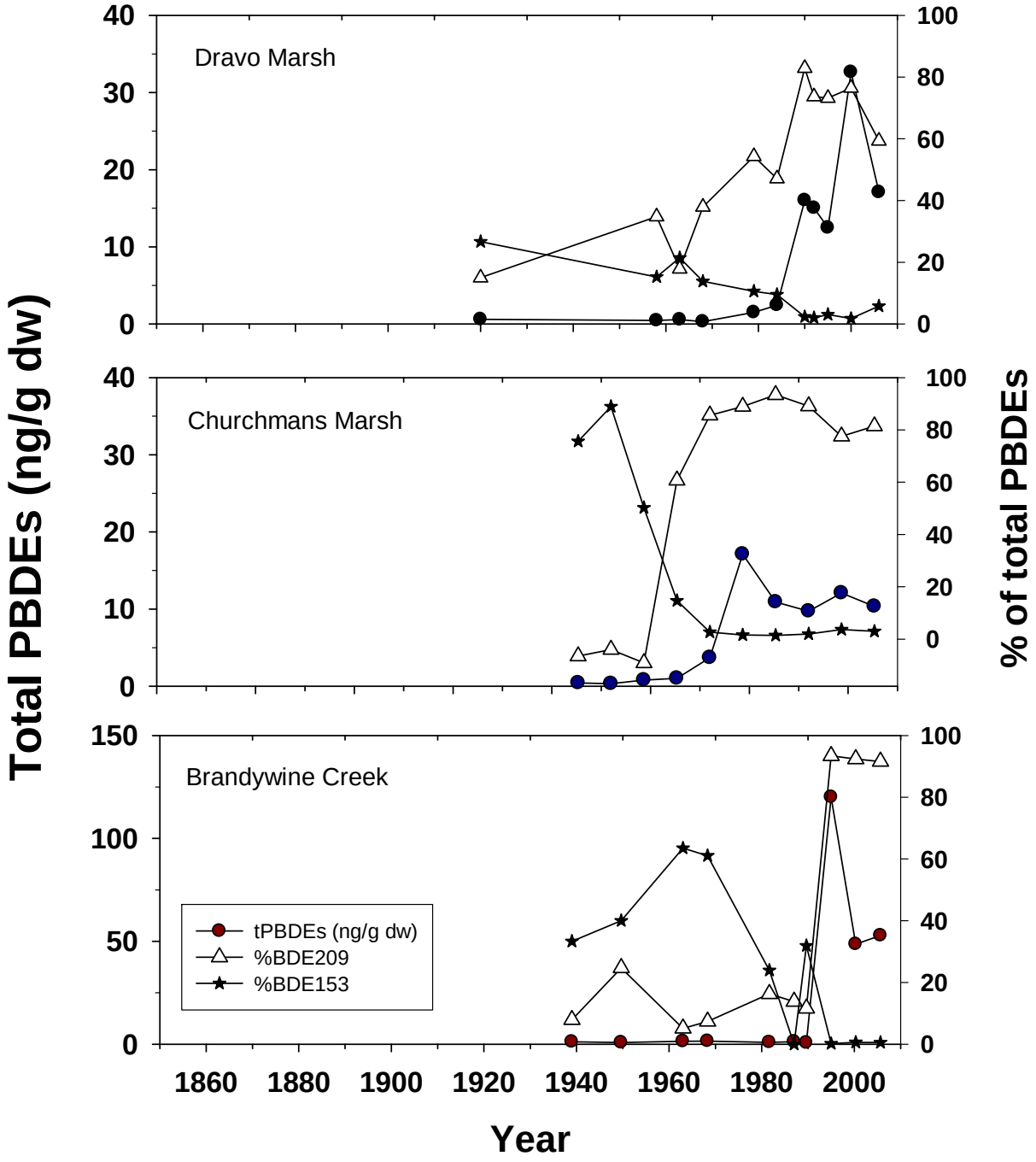

Figure 29. Concentrations of tPBDEs from 1860 to 2003. The circle is for tPBDEs, the triangle is for the percentage of BDE209 and the star is the percentage of BDE 153.

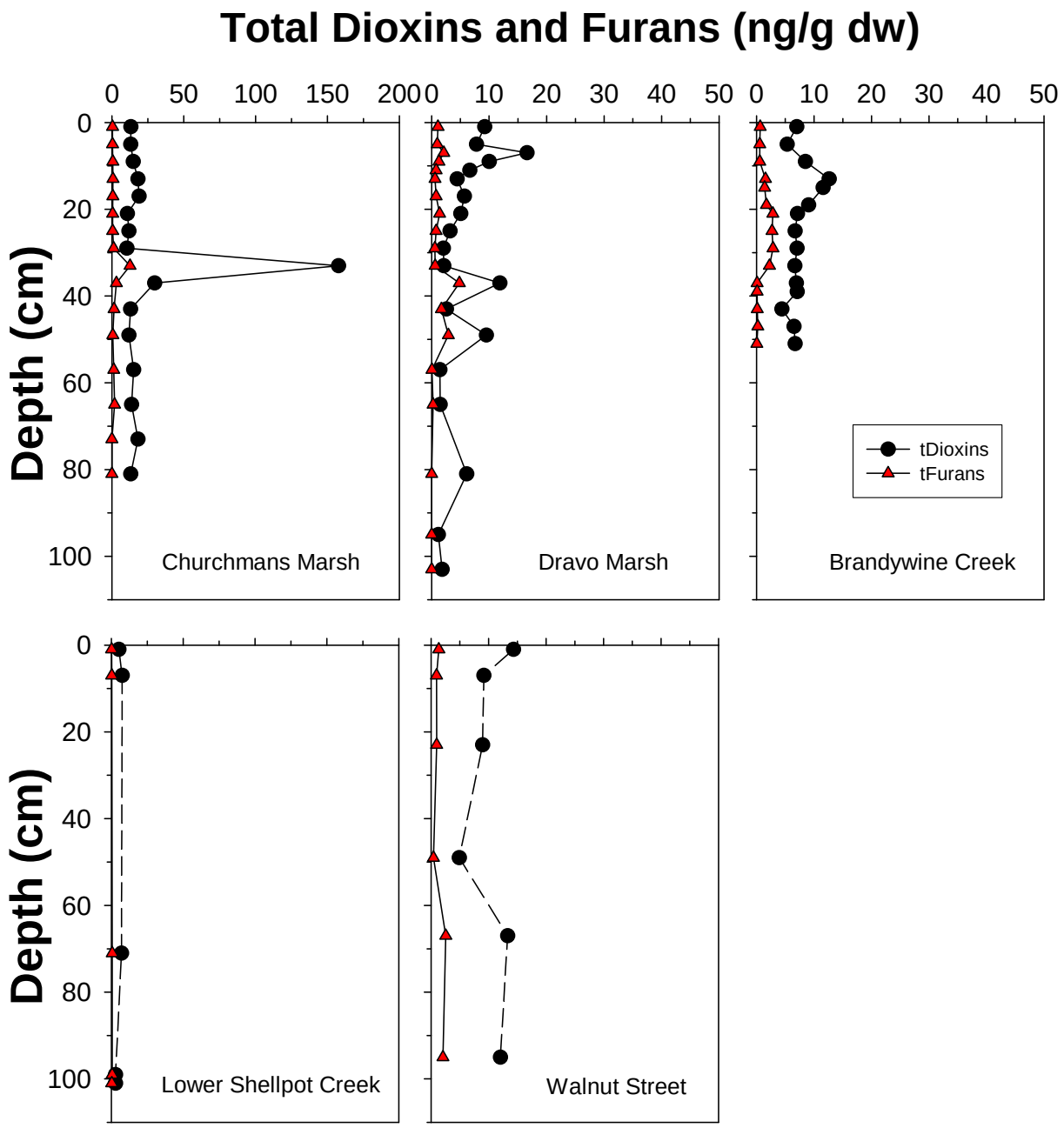

Figure 30. Total dioxins (tPCDD) and furans (tPCDF) with depth in the tidal Christina River and Brandywine Creek.

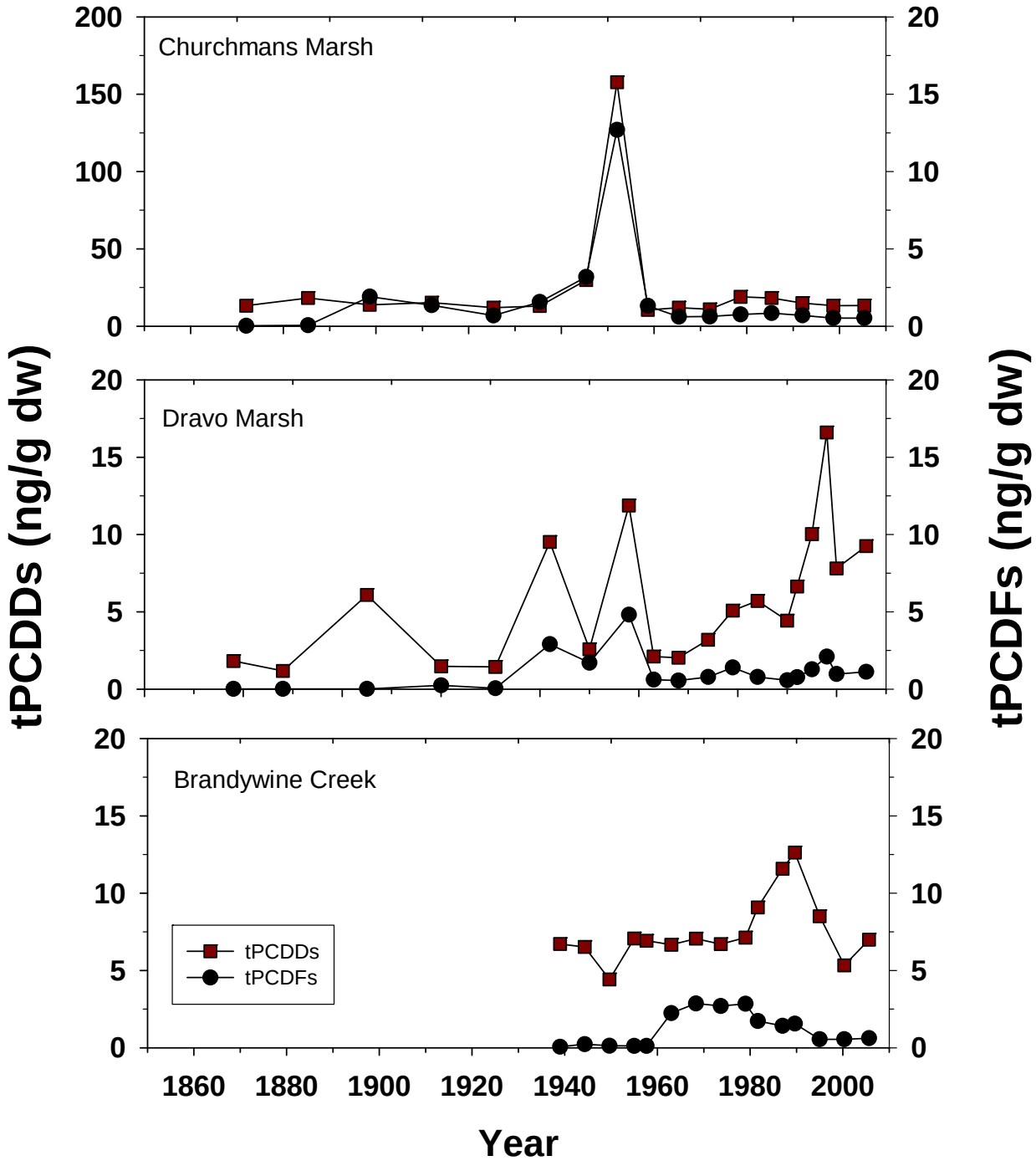

Figure 31. Concentrations of total dioxins and total furans from 1860 to 2003 (Note scale changes).

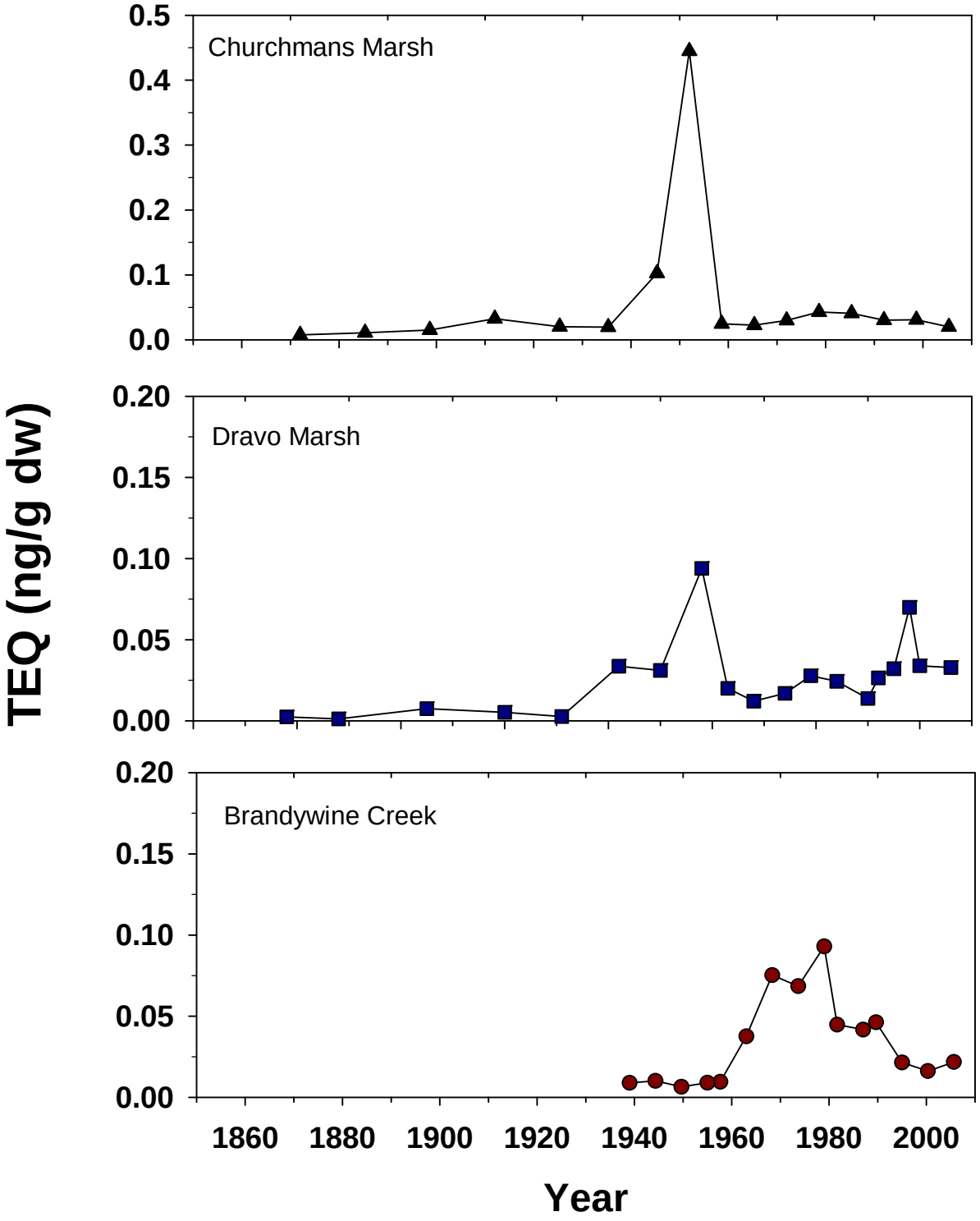

Figure 32. Concentrations of TEQ for dioxins and furans from 1860 to 2003 (Note scale changes).

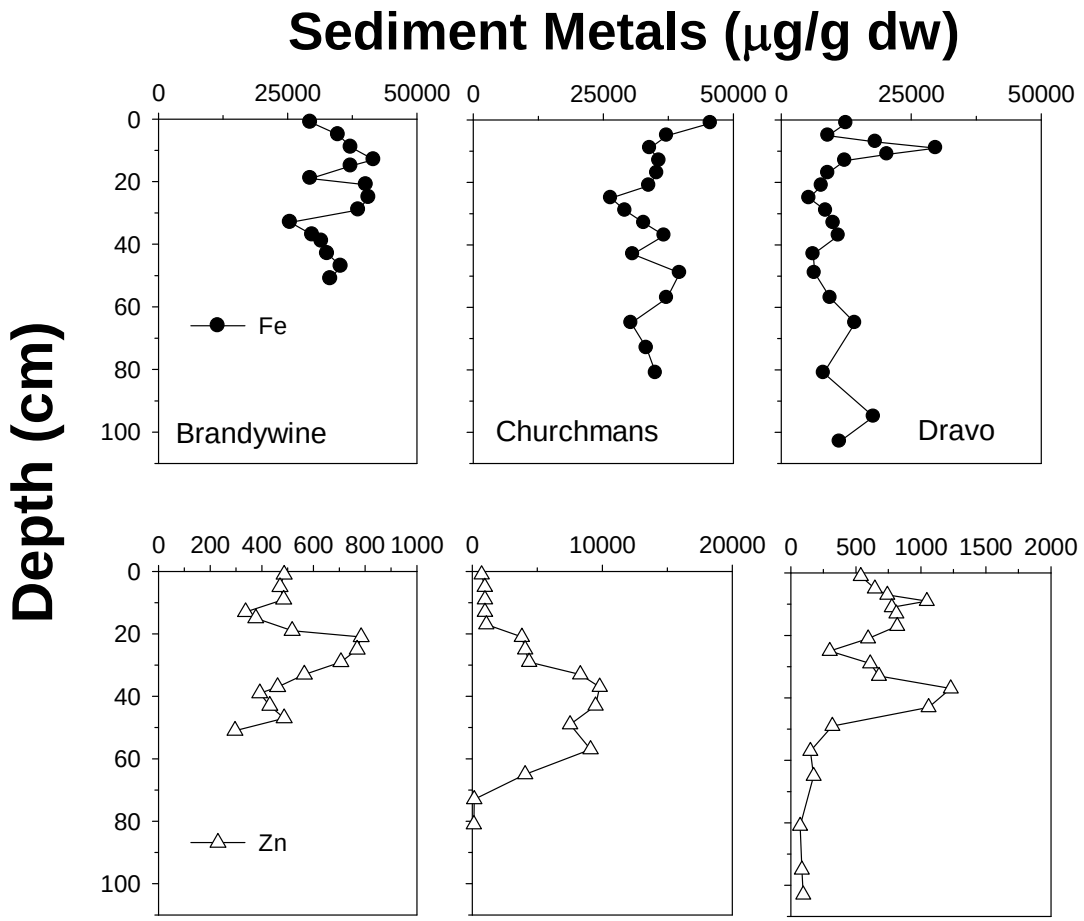

Figure 33. Depth distribution of sediment iron (Fe) and zinc (Zn) in the tidal Brandywine Creek, Churchmans Marsh and Dravo Marsh (Note scale changes).

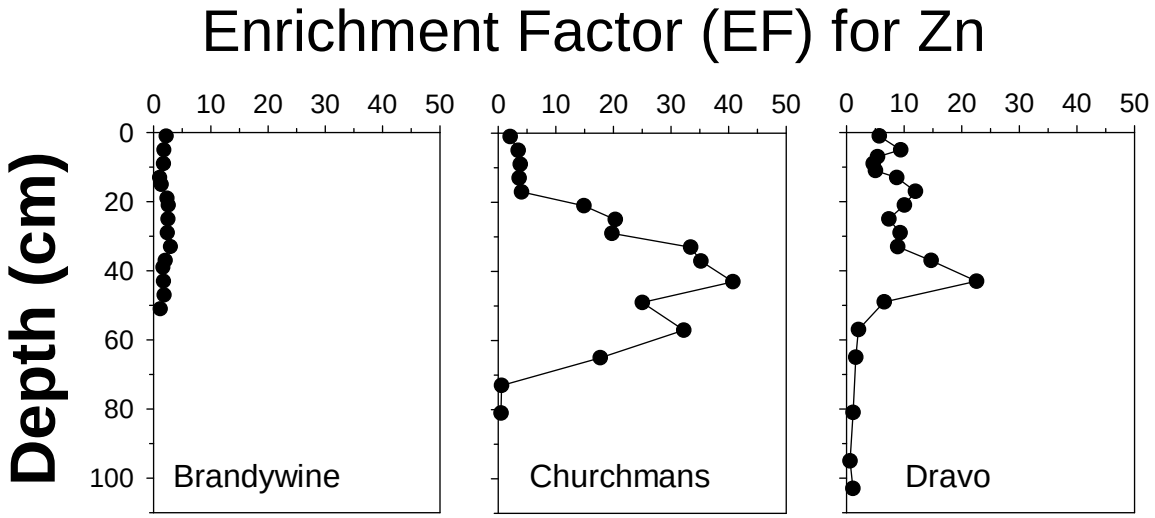

Figure 34. Depth distribution of the Zn enrichment factor (EF) in the tidal Brandywine Creek, Churchmans Marsh and Dravo Marsh.

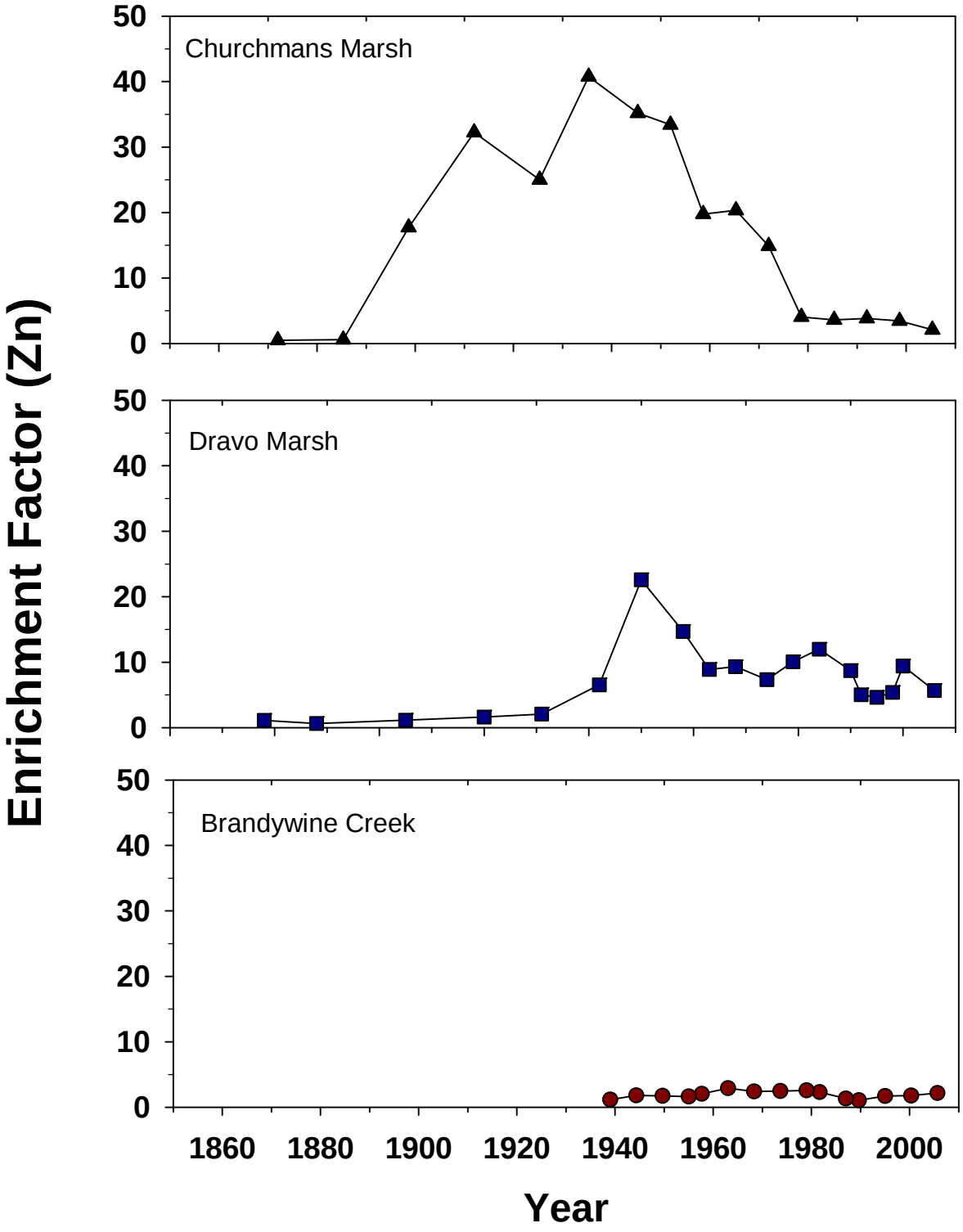

Figure 35. The time distribution of sediment concentrations of zinc (Zn) and the enrichment factor (EF) from 1860 to 2003.

Appendices

Excel File with Data and QA
(Separate Disk; electronic files)